Springer Geography

Dénes Lóczy *Editor*

Geomorphological Impacts of Extreme Weather

Case Studies from Central and Eastern Europe

Springer

Springer Geography

For further volumes:
http://www.springer.com/series/10180

Springer Geography

The Springer Geography series seeks to publish a broad portfolio of scientific books, aiming at researchers, students, and everyone interested in geographical research. The series includes peer-reviewed monographs, edited volumes, textbooks, and conference proceedings. It covers the entire research area of geography including, but not limited to, Economic Geography, Physical Geography, Quantitative Geography, and Regional/Urban Planning.

Dénes Lóczy
Editor

Geomorphological Impacts of Extreme Weather

Case Studies from Central and Eastern Europe

Springer

Editor
Dénes Lóczy
Institute of Environmental Sciences
University of Pécs
Pécs, Hungary

ISBN 978-94-007-6300-5 ISBN 978-94-007-6301-2 (eBook)
DOI 10.1007/978-94-007-6301-2
Springer Dordrecht Heidelberg New York London

Library of Congress Control Number: 2013940178

Foreword

Extreme weather events have always been with us, occupying the attention of scientists and land resource mangers over the years. Today, however, there is a real urgency for understanding such phenomena, for three main reasons. First, the increase in human population and associated rapid growth of fixed assets and infrastructure means the potential for loss and damage from extreme events has increased greatly in recent years. In addition, human modification of natural systems, through urbanisation, land use practices, and river regulation, has dramatically impacted the runoff regime in many catchments. Finally, the increasing evidence for both change and intensification of weather systems as a result of human-induced climate change suggests that we may experience changes to extreme events that we have neither experienced in the past nor made provision for in the future. Thus, this book offers a timely contribution to understanding the hydrological, geomorphological, and human impacts resulting from these rapidly changing processes.

The value of the geomorphological approach offered by this book is that it provides a holistic perspective to the problem. For example, the book demonstrates that an extreme rainfall event is not just an atmospheric phenomenon; rather, it is inevitably linked to earth surface processes (landslides, debris flows, channel degradation, soil erosion) and social process such as resource management, emergency management, and planning. Importantly, this book is a testimony of the geomorphologists of Carpatho–Balkan–Dinaric countries who have risen to the challenge of applying their science to one of the world's most pressing problems. This work sets a benchmark in applied geomorphology that will serve as an excellent example for geomorphologists around the world.

Wellington, New Zealand
10 December 2012

Michael Crozier
President
International Association of Geomorphologists

Contents

Contributors

Gábor Andrási Department of Physical Geography and Geoinformatics, University of Szeged, Szeged, Hungary

László Balatonyi Doctoral School of Earth Sciences, University of Pécs, Pécs, Hungary

Ahinora Baltakova Department of Climatology, Hydrology and Geomorphology, Faculty of Geology and Geography, St. Kliment Ohridski University, Sofia, Bulgaria

Dan Bălteanu Institute of Geography, Romanian Academy of Sciences, Bucharest, Romania

Judit Bartholy Department of Meteorology, Eötvös Loránd University, Budapest, Hungary

Danko Biondić Hrvatske Vode, Zagreb, Croatia

Viktória Blanka Department of Physical Geography and Geoinformatics, University of Szeged, Szeged, Hungary

Martin Boltižiar Institute of Landscape Ecology, Slovak Academy of Sciences, Nitra, Slovakia

Department of Geography and Regional Development, Faculty of Natural Sciences, Constantine the Philosopher University in Nitra, Nitra, Slovakia

Ana Borisavljević Faculty of Forestry, University of Belgrade, Belgrade, Serbia

Szabolcs Czigány Institute of Environmental Sciences, University of Pécs, Pécs, Hungary

Michał Długosz Department of Geoenvironmental Research, Institute of Geography and Spatial Organisation, Polish Academy of Sciences, Cracow, Poland

Slavoljub Dragićević Faculty of Geography, University of Belgrade, Belgrade, Serbia

Andrea Farsang Department of Physical Geography and Geoinformatics, University of Szeged, Szeged, Hungary

Milan Frandofer Department of Physical Geography and Geoecology, Faculty of Natural Sciences, Comenius University, Bratislava, Slovakia

Norbert Gál Department of Physical Geography and Geoinformatics, University of Szeged, Szeged, Hungary

Elżbieta Gorczyca Institute of Geography and Spatial Management, Jagiellonian University, Cracow, Poland

Péter Hernesz Department of Physical Geography and Geoinformatics, University of Szeged, Szeged, Hungary

Danko Holjević Hrvatske Vode, Zagreb, Croatia

Jan Hradecký Department of Physical Geography and Geoecology, Faculty of Science, University of Ostrava, Ostrava, Czech Republic

Milorad Jovanovski Faculty of Civil Engineering, University Ss. Cyril and Methodius, Skopje, Republic of Macedonia

Rositza Kenderova Department of Climatology, Hydrology and Geomorphology, Faculty of Geology and Geography, St. Kliment Ohridski University, Sofia, Bulgaria

Timea Kiss Department of Physical Geography and Geoinformatics, University of Szeged, Szeged, Hungary

Blaž Komac Scientific Research Centre of the Slovenian Academy of Sciences and Arts, Anton-Melik Geographical Institute, Ljubljana, Slovenia

Stanimir Kostadinov Faculty of Forestry, University of Belgrade, Belgrade, Serbia

Adam Kotarba Department of Geoenvironmental Research, Institute of Geography and Spatial Organisation, Polish Academy of Sciences, Cracow, Poland

Ivan Kovalchuk Department of Geodesy and Cartography, Faculty of Land Use, National University of Nature Use and Life Sciences of Ukraine, Kyiv, Ukraine

Kazimierz Krzemień Institute of Geography and Spatial Management, Jagiellonian University, Cracow, Poland

Milan Lehotský Institute of Geography, Slovak Academy of Sciences, Bratislava, Slovakia

Dénes Lóczy Institute of Environmental Sciences, University of Pécs, Pécs, Hungary

Predrag Manojlović Faculty of Geography, University of Belgrade, Belgrade, Serbia

Blagoja Markoski Institute of Geography, Faculty of Natural Sciences, University Ss. Cyril and Methodius, Skopje, Republic of Macedonia

Dana Micu Institute of Geography, Romanian Academy of Sciences, Bucharest, Romania

Mihai Micu Institute of Geography, Romanian Academy of Sciences, Bucharest, Romania

Ivica Milevski Institute of Geography, Faculty of Natural Sciences, University Ss. Cyril and Methodius, Skopje, Republic of Macedonia

Marko V. Milošević Geographical Institute 'Jovan Cvijić' of the Serbian Academy of Sciences and Arts, Belgrade, Serbia

Sanja Mustafić Faculty of Geography, University of Belgrade, Belgrade, Serbia

Andriy Mykhnovych Department of Applied Geography and Cartography, Faculty of Geography, Ivan Franko National University of Lviv, Lviv, Ukraine

Stoyan Nedkov National Institute of Geophysics, Geodesy and Geology, Bulgarian Academy of Sciences, Sofia, Bulgaria

István Németh Department of Physical Geography, University of West-Hungary, Szombathely, Hungary

Valentin Nikolov Institute of Geology, Bulgarian Academy of Sciences, Sofia, Bulgaria

M**ariyana Nikolova** National Institute of Geophysics, Geodesy and Geology, Bulgarian Academy of Sciences, Sofia, Bulgaria

Ivan Novković Faculty of Geography, University of Belgrade, Belgrade, Serbia

Ján Novotný Institute of Geography, Slovak Academy of Sciences, Bratislava, Slovakia

Tomáš Pánek Department of Physical Geography and Geoecology, Faculty of Science, University of Ostrava, Ostrava, Czech Republic

Jovan Br. Papić Faculty of Civil Engineering, University Ss. Cyril and Methodius, Skopje, Republic of Macedonia

Igor Peševski Faculty of Civil Engineering, University Ss. Cyril and Methodius, Skopje, Republic of Macedonia

Josip Petraš Faculty of Civil Engineering, University of Zagreb, Zagreb, Croatia

Ervin Pirkhoffer Institute of Environmental Sciences, University of Pécs, Pécs, Hungary

Rita Pongrácz Department of Meteorology, Eötvös Loránd University, Budapest, Hungary

Olha Pylypovych Department of Applied Geography and Cartography, Faculty of Geography, Ivan Franko National University of Lviv, Lviv, Ukraine

Zofia Rączkowska Department of Geoenvironmental Research, Institute of Geography and Spatial Organisation, Polish Academy of Sciences, Cracow, Poland

Boris Radić Faculty of Forestry, University of Belgrade, Belgrade, Serbia

Ruta Raluca Romanian Waters Company, Buzău-Ialomiţa Branch, Buzău, Romania

Georgi Ratchev Department of Climatology, Hydrology and Geomorphology, Faculty of Geology and Geography, St. Kliment Ohridski University, Sofia, Bulgaria

Ratko Ristić Faculty of Forestry, University of Belgrade, Belgrade, Serbia

Gheorghe Romanescu Department of Geography, Faculty of Geography and Geology, University 'Alexandru Ioan Cuza' of Iaşi, Iaşi, Romania

Levente Ronczyk Institute of Geography, University of Pécs, Pécs, Hungary

Georgiy Rud'ko State Commission of Mineral Resources, Kyiv, Ukraine

Miloš Rusnák Institute of Geography, Slovak Academy of Sciences, Bratislava, Slovakia

Roland Schläffer Department of Physical Geography, University of West-Hungary, Szombathely, Hungary

Karel Šilhán Department of Physical Geography and Geoecology, Faculty of Science, University of Ostrava, Ostrava, Czech Republic

Veronika Smolková Department of Physical Geography and Geoecology, Faculty of Science, University of Ostrava, Ostrava, Czech Republic

Mateusz Sobucki Institute of Geography and Spatial Management, Jagiellonian University, Cracow, Poland

Jacek Bogusław Szmańda Department of Geomorphology and Environmental Management, Institute of Geography, Jan Kochanowski University in Kielce, Kielce, Poland

Radislav Tošić Faculty of Natural Sciences, University of Banja Luka, Banja Luka, Republic of Srpska

Márton Veress Department of Physical Geography, University of West-Hungary, Szombathely, Hungary

Dominika Wrońska-Wałach Institute of Geography and Spatial Management, Jagiellonian University, Cracow, Poland

Răzvan Zarea Romanian Waters Company, Buzău-Ialomiţa Branch, Buzău, Romania

Nenad Živković Faculty of Geography, University of Belgrade, Belgrade, Serbia

Matija Zorn Scientific Research Centre of the Slovenian Academy of Sciences and Arts, Anton-Melik Geographical Institute, Ljubljana, Slovenia

Introduction

This collection of chapters aims at providing an overview of the most recent investigations into the short- and longer-term consequences of weather phenomena of unusual intensity – probably driven by global climate change (IPCC SREX 2012; see also Bartholy, Pongrácz – Chap. 1 in this volume). Although numerous previous events (for instance, those in the years 2002 and 2006) are also treated in the book, the main focus is on the diverse impacts of the 2010 rainfalls which affected most of Europe, particularly the Danubian macroregion and the neighbouring areas (ICPDR 2012 – Fig. 1). On raising the idea and 'screening' interests at a meeting in Ostravice, Czech Republic, in October 2011, first of all the authors of a previous Springer volume (Lóczy et al. 2012) were invited by the editor to explore the opportunities for compiling the most intriguing findings achieved in research in their own countries and summarise them for the international public in a series of selected brief case studies. Positive responses were received from 11 countries of eastern Central Europe, and they resulted in 21 chapters, each including case studies in different numbers (from 1 to 6). The spatial distribution of case studies (Fig. 2) is intended to reflect that of the events with the highest impact.

Starting with the hydrometeorological setting, the material in this book is partly arranged around topics (floods, landslides, and other impacts) and, within that framework, according to areas moving from north to south. Although in 2010 destructive floods were recorded even more to the north, in the Vistula drainage basin, the northernmost region treated in the volume is the Polish Carpathians. Several chapters deal with the only high mountains of Poland, where detailed investigations were launched to assess the impacts from many aspects. In the southernmost countries covered, in Bulgaria and Macedonia, similar research just began and the first inventories of natural hazards have been compiled only recently.

In each chapter the hydrometeorological background to geomorphological processes is assessed against the long-term trends. A reliable assessment, however, is hindered by the observation that the highest-intensity events are also the least frequent. If less data are available on them, these events are less suitable for a sound statistical analysis (Zhang 2011; Zhang et al. 2001). The 'moderate extremes' of higher frequency/probability, which occur in several years or in

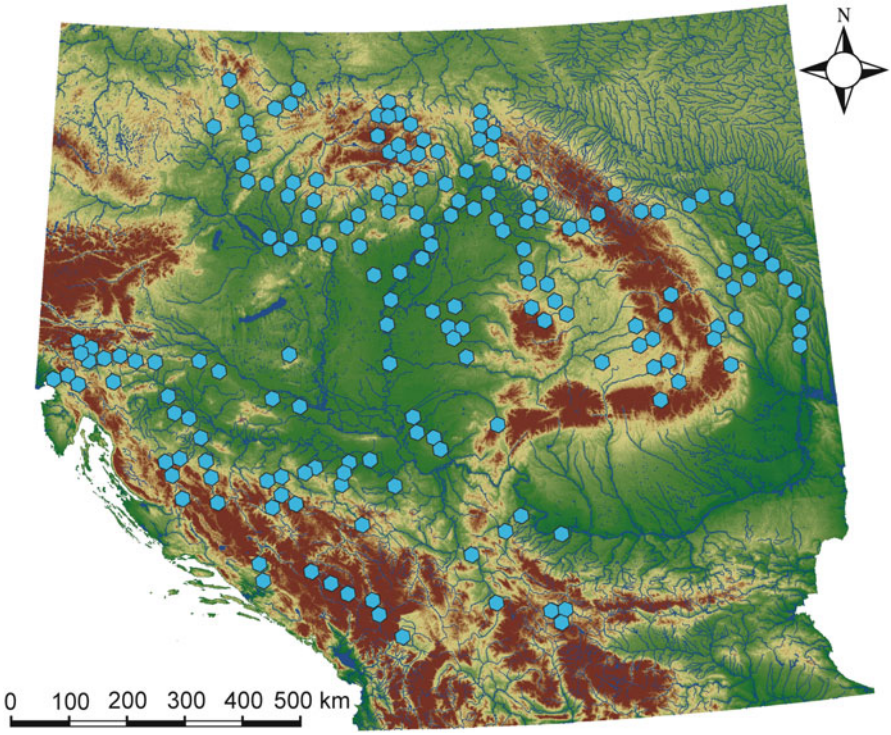

Fig. 1 Geographical distribution of the significant flood events in 2010 (*Source*: ICPDR 2012)

each decade, are easier to tackle statistically. Also their impact on geomorphic evolution is usually more clearly manifested. Notwithstanding, the derived indices of the frequency and intensity of climatic extremes (Frich et al. 2002) are generally suitable for spatial comparisons and pointing out long-term precipitation trends (related to the reference period 1961–1990): RX1D = annual or monthly maximum 1-day precipitation; RX5D = annual/monthly maximum consecutive 5-day precipitation; SDII (Simple Daily Intensity Index) = ratio of annual total precipitation to the number of wet days ($\geq$1 mm); RR1 = annual number of wet days (daily precipitation $\geq$1 mm); RR10 = annual number of days with heavy precipitation ($\geq$10 mm); RR20 = annual number of days with very heavy precipitation ($\geq$20 mm); R95p = very wet days (>95th percentile); and R99p = extremely wet days (>99th percentile). Although the indicators are interpreted slightly differently in the different countries, the editor has tried to make references to the above indices as common denominators of descriptions of precipitation events in the individual chapters. River discharges (and occasionally sediment yields) are described with the parameters routinely used by hydrologists (e.g. Q10, Q50, Q100 return period floods).

The 2009–2010 hydrological year was extraordinarily humid in most of the Danubian countries. Snow depths and rainfall amounts along the Middle and Lower

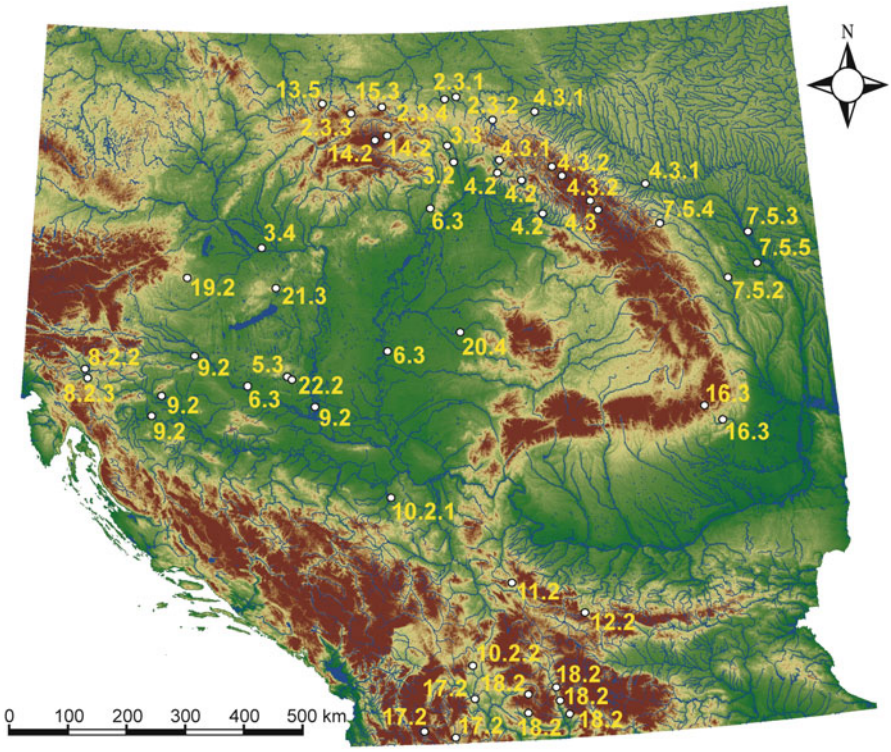

Fig. 2 Location of case studies in the chapters of this volume. The numbers refer to the subchapters where the study areas and the events are presented

Danube River exceeded the multiannual average by 1.5–2.5 times, and maxima never observed since systematic instrumental weather observations have been recorded (Bálint and Liska 2010). The wet period started back in September 2009 and lasted in most of the broader Danubian region for more than a year (with 1 month interruption in March and for some weeks thereafter). The meteorological situation is summarised by Bartholy and Pongrácz (Chap. 1) for this volume.

In the lowlands widespread and lasting flooding was a direct consequence of snowmelt and rainfalls. In May 2010 the most severe damage resulted from *flash floods*, first reported from northern Italy, then from Slovenia (Komac, Zorn – Chap. 8 in this volume). The floods in September 2010 were even more disastrous in Slovenia. They affected 60% of Slovenian municipalities and caused over €240 million damage. The local high water levels accumulated into *riverine floods* on the major rivers of Croatia (see Biondić et al. – Chap. 9). Even the Croatian capital, Zagreb, is endangered by flash floods from Medvednica Mountain, where 52 detention basins are planned to be established (and 19 of them have already been completed – Petráš and Marušić 2009). In 2010 – as well as on previous occasions

(Gilja et al. 2010) – major floods passed on the Sava River. Some parts of Serbia were also heavily affected by riverine and flash floods. The extreme hydrometeorological conditions and the resultant geomorphological processes in two catchments of Serbia, Kolubara and Pcinja River basins, are treated here (Dragićević et al. – Chap. 10). In eastern Serbia, the floods in the Nišava River basin and the suspended load transport of the rivers are presented by Mustafić et al. (Chap. 11). The cyclone soon reached Hungary, where damage was reported from 510 localities (see Czigány et al. – Chap. 5), and Slovakia with more than 900 localities affected. Lateral channel shifts and spatial variability of channel landforms have been studied using sedimentological techniques on the Ondava, Topl'a, and Danube rivers by Lehotský et al. (Chap. 3). Kiss et al. (Chap. 6) surveyed changes along the Hernád and Tisza rivers, where a couple of major flood waves occurred in 2010. On the Hernád River, a new maximum water stage was even recorded, while no significant flood was measured on the Dráva River. The huge cyclone extended over the Carpathians in Poland (Western Tatra, Bieszczady, and Beskid Niski mountains: Gorczyca et al. – Chap. 2) and Ukraine (the Tysa, Borzhava, Latorytsia, and Uzh watersheds: Kovalchuk et al. – Chap. 4) and even beyond that mountain arc. Large areas in Bosnia (where annual precipitation reached 1,836 mm at Bihać; floods on the Una, Sana, Vrbas, and Bosnia rivers – ICPDR 2012), Montenegro (rapid snowmelt as early as December 2009), and Bulgaria (Nikolova et al. – Chap. 12) have not been spared from devastation either. In Romania 3,000 houses, 4,130 km of national and regional roads, and 700 bridges were damaged (Bálint and Liska 2010). Flash floods induced by torrential rainfalls resulted in casualties mainly on the tributaries of the Mureş and Târnava rivers. The high water levels in the Siret and Pruth drainage basins are analysed by Romanescu (Chap. 7). The material damage was severe: the cost estimations of the individual countries affected add up to ca two billion Euros. In addition, the 2010 floods demanded a minimum death toll of 50 people (Bálint and Liska 2010) in the Carpathian (Middle Danube) Basin. (According to the ICPDR report (2010), there were only 34 victims).

As far as the indirect consequences of extreme weather events are concerned, geomorphologists in the eastern half of Europe – or at least the contributors to this volume – focus their attention on some *processes*, both spectacular in appearance and significant for the transformation of topography. Researchers seem to be most concerned with the corollaries of extreme rainfalls on river channel evolution, including *bank retreat* (Kiss et al. – Chap. 6), the influence of *excess water* inundations on soil properties (Gál, Farsang – Chap. 20), *urban flooding* attributed to improper stormwater management (Ronczyk, Czigány – Chap. 22), the various processes of *soil erosion* and *alluvial fan accumulation* generated by storm runoff in middle mountains and their foothills (Veress et al. – Chap. 19), and the modification of the morphometric parameters of *karst depressions* due to repeated extreme rainfalls (Veress – Chap. 21). The primary focus of interest, however, is understandably a wide range of mass movements, including *debris flows* (in the Tatra Massif, Kotarba (1997); Kotarba et al. (Chap. 14); in the Ukrainian

Carpathians, Kovalchuk et al. (Chap. 4); in the Stara planina (Balkan) mountains, Kenderova et al. (Chap. 18)) and *landslides* of different types, sizes, and mechanisms (in the Moravian–Silesian Beskids, Pánek et al. (Chap. 13); in the Polish Carpathians, Gorczyca et al. (Chap. 15); in the Curvature Carpathians of Romania, Micu et al. (Chap. 16); in the low mountains of Hungary, Czigány et al. (Chap. 5); and at much higher elevations in the mountains of the Republic of Macedonia, Jovanovski et al. (Chap. 17)).

Such diverse themes necessarily call for a wide range of *research methods*. Flood-prone areas are identified by geomorphological mapping and detailed land surveying aided by remote sensing image interpretation. River channel features developed during preceding events are described from the analyses of longitudinal profiles and cross sections of channels and valleys. In an optimal situation, data from surveys prior to floods are also available and the impacts are more reliably assessed. Sedimentological evidence (from grain-size distribution analysis) is often useful for the monitoring of hillslope erosion and river channel dynamics. For flow routing and simulations in watershed-scale studies, various hydrologic models are applicable with interface to connect to geographical information systems.

For flash floods *soil saturation* is a major precondition. To disclose its spatial distribution, a number of automated hydrometeorological stations are necessary, each equipped with soil moisture and temperature sensors. To determine soil depth (lower topsoil boundary, important for interflow detection and also to identify slip planes of landslides), vertical electrical sounding (VES) and hydraulic drilling are successfully employed.

Landslides are mapped in detail by GPS, in inaccessible areas; however, slope deformation is better studied on aerial photos. To reconstruct the temporal evolution of such landforms, radiocarbon and dendrogeomorphological datings are used (as in the case of the Girová landslide in the easternmost corner of the Czech Republic: Pánek et al. – Chap. 13). The inventory and monitoring of landslides (which is in Poland the responsibility of the Polish Geological Institute [PGI]) involves various techniques: terrestrial laser scanning (TLS) to create a detailed and accurate digital elevation model (DEM) and to trace landslide motion. Internal deformations can be registered by inclinometers.

The question arises whether the space devoted to the individual countries is proportional to the severity of hazards generated in them by extreme weather events. The answer is naturally not necessarily. A closer correlation can be found between the number of papers and the national traditions of hazards research. In some of the countries (Romania, Poland, and the Czech Republic), such investigations have recently become the leading topics of geomorphology. In Hungary the humid months of May and June, 2010, also provided a unique opportunity to study the impacts of rainfalls not only in fluvial geomorphology but also in other areas (soil science, karst morphology).

By their nature, the selected case studies are restricted to small areas and, consequently, cannot embrace all the consequences of the 2010 events in their entirety and spatial distribution, but, being representative, well illustrate the directions of research followed by hydrologists and geomorphologists in altogether 11 countries of the Carpatho–Balkan–Dinaric Region.

This collection of chapters is intended to be used by professionals specialised in the following theoretical or practical issues: impacts of climate change, geomorphological hazards (landslides), water management (flood and excess water control), and environmental planning. It can be used either as a reference book on the 2010 events or a handbook for research in a wide range of topics.

The spelling of geographical names follows national traditions for mountains (e.g. Beskid in Polish, Beskydy in Czech) and rivers (Tysa in Ukrainian, Tisza in Hungarian, Tisa in Serbian). The differences, however, are not so great that the reader would find it troublesome to identify the same geographical objects with different names in the individual chapters.

Finally, given the sensitivity of any issue concerning the Balkan countries, a remark is due on how political entities appear in the book. The editor has retained map representations and names of countries in the original form used by the contributors of the individual chapters (for instance, Republic of Srpska, Republic of Macedonia, Republic of Serbia incorporating Kosovo). He apologises if it hurt the national feeling of any reader.

References

Bálint G, Liska I (2010) Extreme floods in the Danube Basin. Danube Watch 3, 2010, 3 p. http://www.icpdr.org/main/publications/danube-watch-3-2010-extreme-floods-danube-basin

Frich P, Alexander LV, Della-Marta P, Gleason B, Haylock M, Klein Tank AMG, Peterson T (2002) Observed coherent changes in climatic extremes during the second half of the twentieth century. Clim Res 19:193–212

Gilja G, Oskoruš D, Kuspilić N (2010) Erosion of the Sava riverbed in Croatia and its foreseeable consequences. In: Proceedings of the BALWOIS conference 2010, Ohrid, 25–29 May 2010, 9 p

ICPDR (2012) Preliminary flood risk assessment in the Danube River Basin. Summary report. International Commission for the Protection of the Danube River, Vienna, 37 p. http://www.icpdr.org/main/publications/preliminary-flood-risk-assessment-in-the-danube-river-basin

IPCC SREX (2012) Managing the risks of extreme events and disasters to advance climate change adaptation. Intergovernmental Panel on Climate Change, Special report, Cambridge University Press, Cambridge/New York, 582 p

Kotarba A (1997) Formation of high-mountain talus slopes related to debris-flow activity in the High Tatra Mountains. Permafr Periglac Process 8:191–204

Lóczy D, Stankoviansky M, Kotarba A (eds) (2012) Recent landform evolution: the Carpatho-Balkan-Dinaric Region. Springer Science + Business Media, Dordrecht, 460 p

Petráš J, Marušić J (2009) Flash floods in Croatia. In: Proceedings of the international symposium on water management and hydraulic engineering, Ohrid, 1–5 Sept 2009, pp 647–658

Zhang XB (2011) Indices for monitoring changes of extremes based on daily temperature and precipitation data. WIREs Clim Change 2:851–870

Zhang XB, Hogg WD, Mekis (2001) Spatial and temporal characteristics of heavy precipitation events in Canada. J Clim 14:1923–1936

Part I
Hydrometeorological Background

Chapter 1
Spring and Summer Weather in 2010: Regular or Exceptional?

Judit Bartholy and Rita Pongrácz

Abstract Large rainfall within a relatively short time (a few hours or days) may lead to severe environmental consequences, including floods and landslides. In 2010 numerous precipitation-induced events were reported from Central and Eastern Europe. In order to objectively assess regional precipitation in this particular year, gridded data sets compiled from long-term measurements starting in 1951 are analyzed in this chapter with special focus on the period from May to September 2010. Furthermore, Central/Eastern European extreme values are compared to world records from different geographical regions. In addition to the detected precipitation, projected regional trends for the 21st century are also discussed including precipitation-related climate indices (e.g., number of wet days: when daily precipitation exceeds 1 mm; number of very wet days: when daily precipitation exceeds 20 mm). For this purpose, precipitation outputs from 11 regional climate model simulations are analyzed, taking into account the widely used intermediate global emission scenario (A1B), where the global concentration of carbon dioxide is estimated at 1.9 and 2.6 times the preindustrial atmospheric level by 2050 and 2100, respectively.

Keywords Precipitation distribution • Climate change • Modeling • Wet days • Central and Eastern Europe

J. Bartholy (✉) • R. Pongrácz
Department of Meteorology, Eötvös Loránd University,
Pázmány Péter sétány 1/a, Budapest 1117, Hungary
e-mail: bartholy@caesar.elte.hu; prita@caesar.elte.hu

D. Lóczy (ed.), *Geomorphological impacts of extreme weather: Case studies from central and eastern Europe*, Springer Geography, DOI 10.1007/978-94-007-6301-2_1,

Table 1.1 The highest multiannual average precipitation amounts in different continents

Continent	Precipitation amount (mm)	Geographical location (country)	Elevation (m)	Length of period (years)
Africa	10,287	Debundja (Cameroon)	9	32
Australia	8,636	Bellenden Ker (Queensland)	1,555	9
Asia	11,872	Mawsynram (India)	1,401	38
South America	10,790	Quibdo (Colombia)	37	16
Europe	4,648	Crkvica (Bosnia–Herzegovina)	1,017	22
North America	6,502	Henderson Lake (Canada)	6	14
Oceania	11,684	Mt. Waialeale (Hawaii)	1,569	30

Data source: http://www.satelliten-bilder.de/

1.1 Introduction

Precipitation is among the most variable meteorological elements, both in time and space. Therefore, in order to reliably monitor and analyze its distribution, a much denser network of rain gages is necessary than in the case of temperature measurements. In addition to the global atmospheric circulation, the distance from large water bodies (i.e., ocean, large sea) and the orographic effects determine the geographical distribution of annual precipitation.

Since the beginning of regular precipitation measurements, the highest 1-year precipitation sum (26,461 mm) was observed in the monsoon region of India, in Cherrapunji (elevation: 1,313 m), during the period 1 August 1860–31 July 1861. In the case of four continents (Asia, Oceania, South America, and Africa), precipitation extremes exceed 10,000 mm (Table 1.1), with the lowest of them (4,648 mm) observed in Europe.

In the European regions, however, temporal variability is quite large. In Hungary, for instance, the highest annual precipitation amount (1,554 mm) was observed in 2010 at Jávorkút. It is more than twice as large as the climate normal of the country-wide annual average precipitation (Fig. 1.1). The largest monthly amount (444 mm) was detected in Dobogókő in June 1958. On a finer temporal scale, maximum daily precipitation (203 mm) was observed in Gyömrő on 8 September 1963.

1.2 World Precipitation in 2010

The World Meteorological Organization (WMO) regularly prepares annual statements on the status of the global climate, including globally averaged land *precipitation*. The highest-ever *annual* amount (1,085 mm) occurred in 2010, while for the period 1961–1990, global average was 1,033 mm (WMO 2011). The second and the third highest annual amounts occurred in 1956 and 2000, respectively.

The year 2010 was particularly wet in Central and Southeastern Europe, in the western part of Australia, and in Indonesia (Fig. 1.2). For instance, in Hungary 2010 was the wettest year since 1901, with a spatial average precipitation of

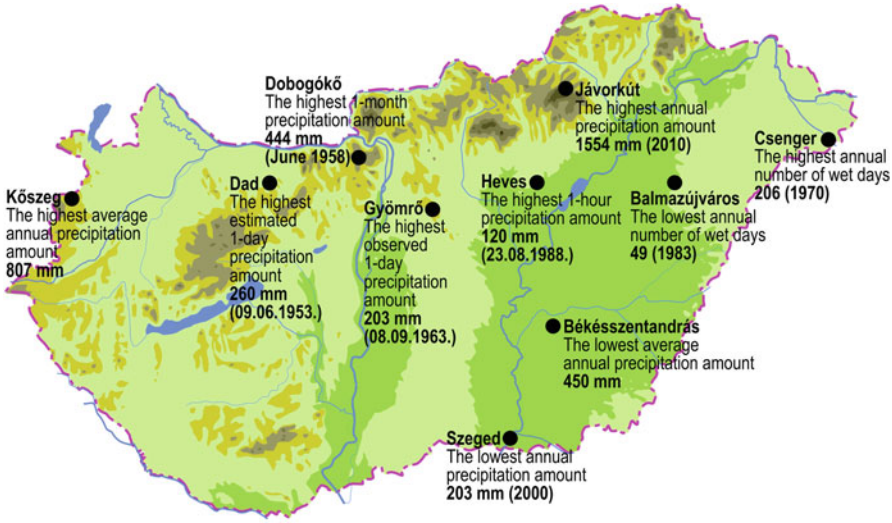

Fig. 1.1 Precipitation-related extremes in Hungary (*Source*: Hungarian Meteorological Service)

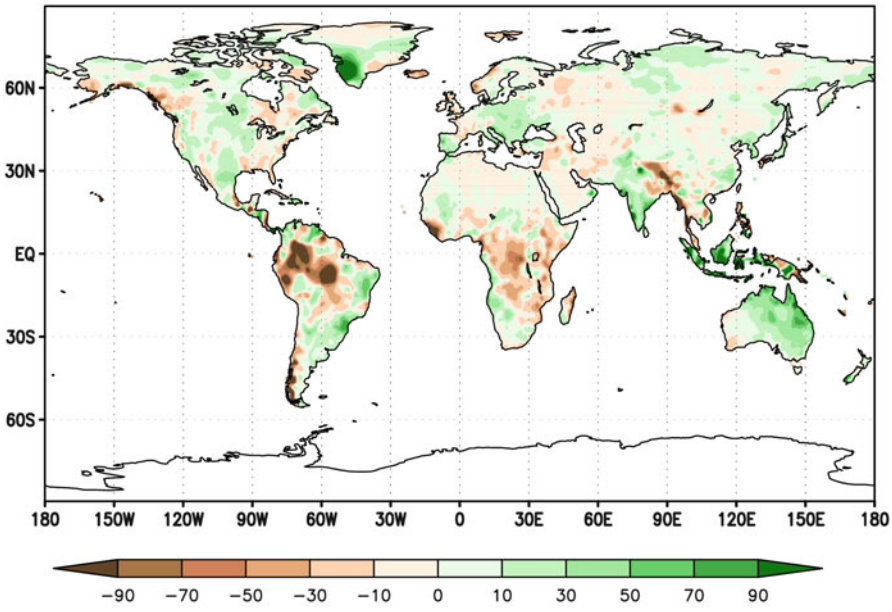

Fig. 1.2 World map of annual precipitation anomaly (mm) in 2010 (reference period: 1979–2000) (*Data source*: Global Precipitation Climatology Centre, Deutscher Wetterdienst (GPCC, DWD))

959 mm (Móring 2011), which is 130 mm more than the previous record (set in 1940). Furthermore, the year 2010 was the most humid on record in Novi Sad, Serbia, and several stations in Moldova (WMO 2011). High precipitation generated intensive runoff processes in Central and Southeastern Europe. Severe *floods* were reported in May–June from southern Poland (IMGW 2010), the Czech Republic, Slovakia, Hungary, Croatia, Bosnia and Herzegovina, Bulgaria, and southern and eastern Germany (Bissolli et al. 2011). In December another series of major floods hit Montenegro, Bosnia and Herzegovina, and Serbia, caused by heavy precipitation in early December when the 3-day precipitation totals reached 100–200 mm (WMO 2011).

1.3 Analysis of Precipitation Time Series for Central/Eastern Europe

The map series of *annual precipitation anomalies* in 2010 for the entire European continent and the Central/Eastern European region (the area between 10°E and 30°E longitudes and between 40°N and 55°N latitudes) compared to the previous 4 years (Fig. 1.3) shows remarkable positive anomalies in Central/Eastern Europe and in the western Iberian Peninsula. For instance, in Portugal and southwestern Spain, the year 2010 was 20 and 50% wetter than normal, respectively (WMO 2011). The spatial extension of the other high positive anomaly is larger for Eastern Europe than in the case of the Iberian Peninsula. The highest annual anomalies occurred near the Adriatic coast; however, annual precipitation was higher than usual in most of Eastern Europe, including Poland, Slovakia, Hungary, and Romania.

For the purpose of the temporal evaluation of precipitation, 60-year *gridded time series* has been analyzed for Central/Eastern Europe with 0.5° horizontal resolution. Maximum, minimum, and spatial average of the annual precipitation grid point anomalies relative to the reference period 1979–2000 have been calculated for the Central/Eastern European region (Fig. 1.4). Also here the record year is undoubtedly 2010, but in the past decade very dry years (2003 and 2000) also occurred in Central/Eastern Europe.

A similar analysis has been accomplished for all countries of the region (Fig. 1.5). The *ranked* country-based *time series* suggests that 2010 was the wettest not only in the broader region but also in the subregions. Spatial mean precipitation *anomalies* were mostly *positive* during the 1951–2010 period in most of the countries, except Hungary and Slovakia. In Slovakia (not shown) the positive and negative anomalies are nearly balanced. Hungary is the only country in the region where negative annual precipitation anomalies dominate the entire period; more specifically, 40 years were drier and 20 years wetter than usual (reference period: 1979–2000).

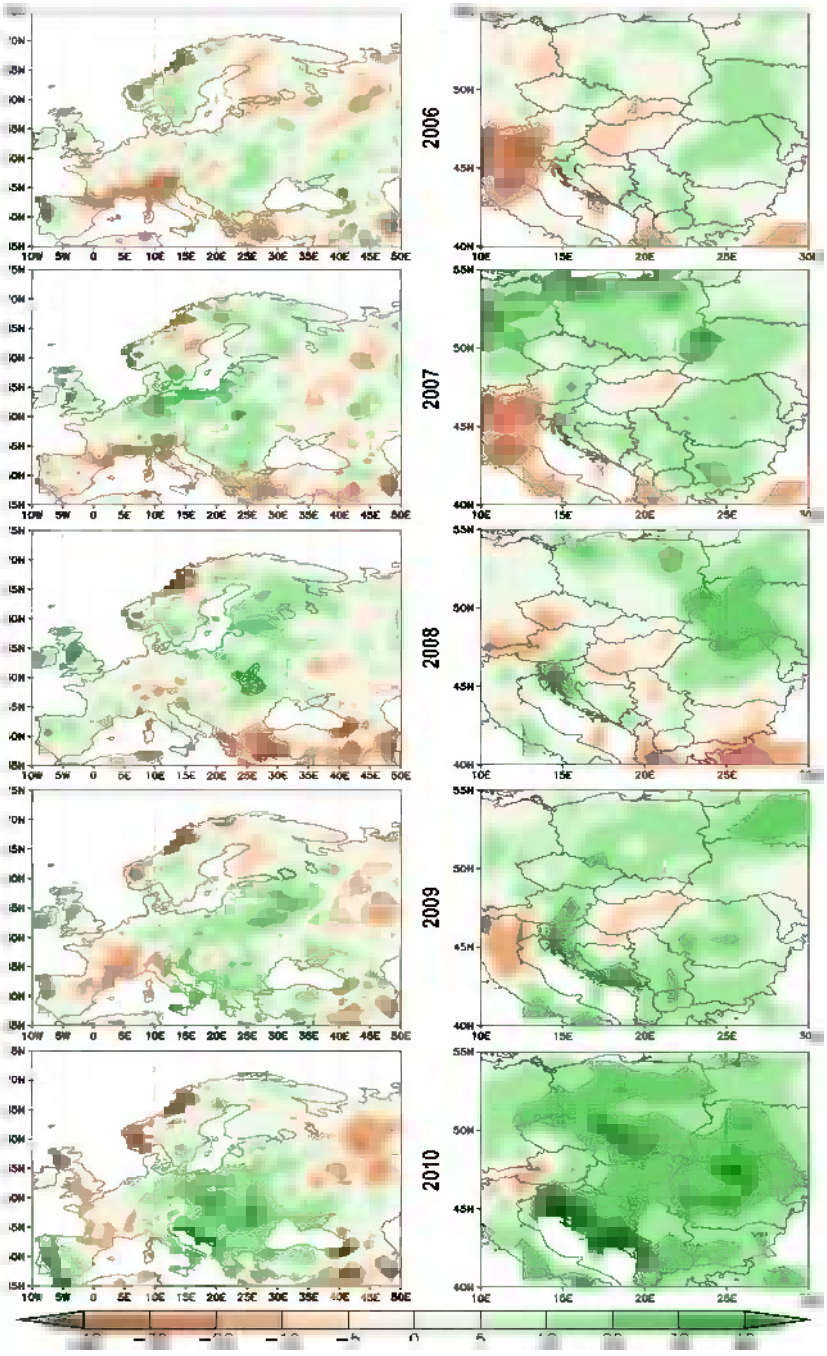

Fig. 1.3 Maps of annual precipitation anomaly (mm) in 2006, 2007, 2008, 2009, and 2010 for the European continent and the Central/Eastern European region (reference period: 1979–2000) (*Data source*: GPCC, DWD)

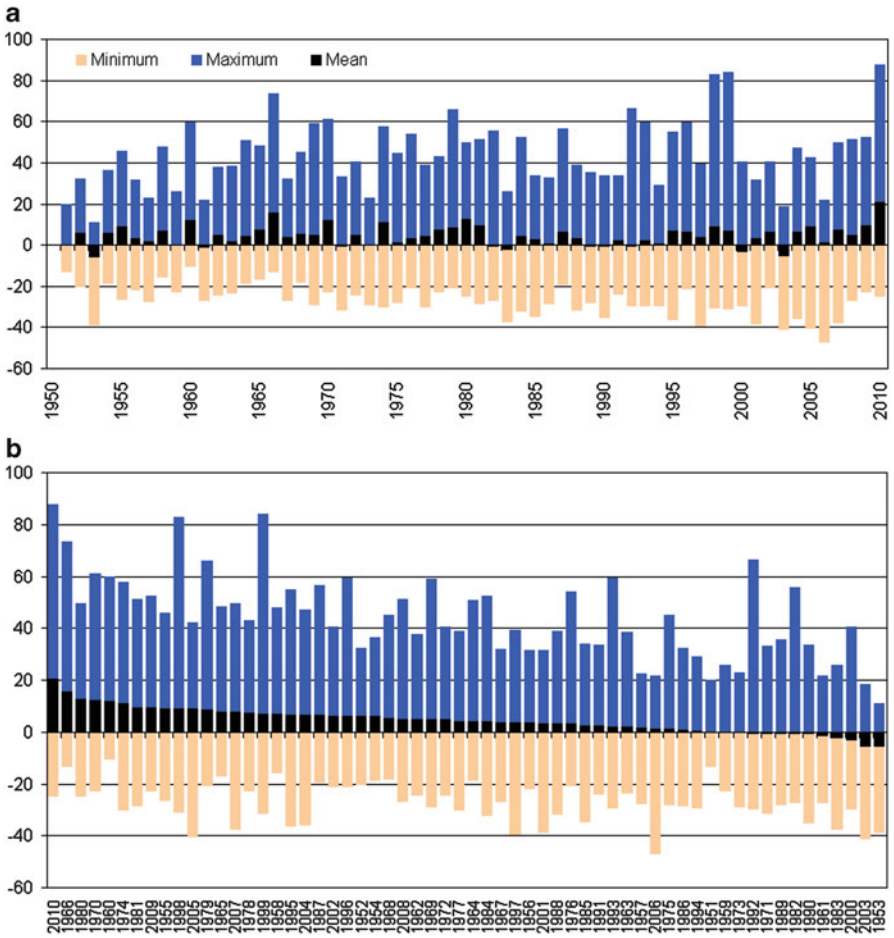

Fig. 1.4 Minimum, mean, and maximum annual precipitation anomalies (mm) for Central/Eastern Europe, 1951–2010 (reference period: 1979–2000. (**a**) Original time series; (**b**) ranked time series based on mean spatial anomalies) (*Data source*: GPCC, DWD)

On the map of *monthly precipitation anomalies* of the Central/Eastern European region for 2010 (Fig. 1.6), remarkably wetter-than-usual conditions can be recognized for May over the entire region with the highest anomalies in southern Poland, northern Slovakia, and the eastern part of the Czech Republic. The high precipitation in May and later in June was caused by two consecutive events resulted from an upper-air low pressure synoptic system over southern Poland, which later became stationary over Southeast Europe (Bissolli et al. 2011).

In most of the months in 2010, *both dry and wet* conditions occurred in different parts of the region. In January, March, and October, the northern subregions were drier than usual, while the southern and southeastern subregions received above-average rainfalls. In July, August, September, November, and December, most of Central/Eastern Europe experienced positive precipitation anomalies, and only

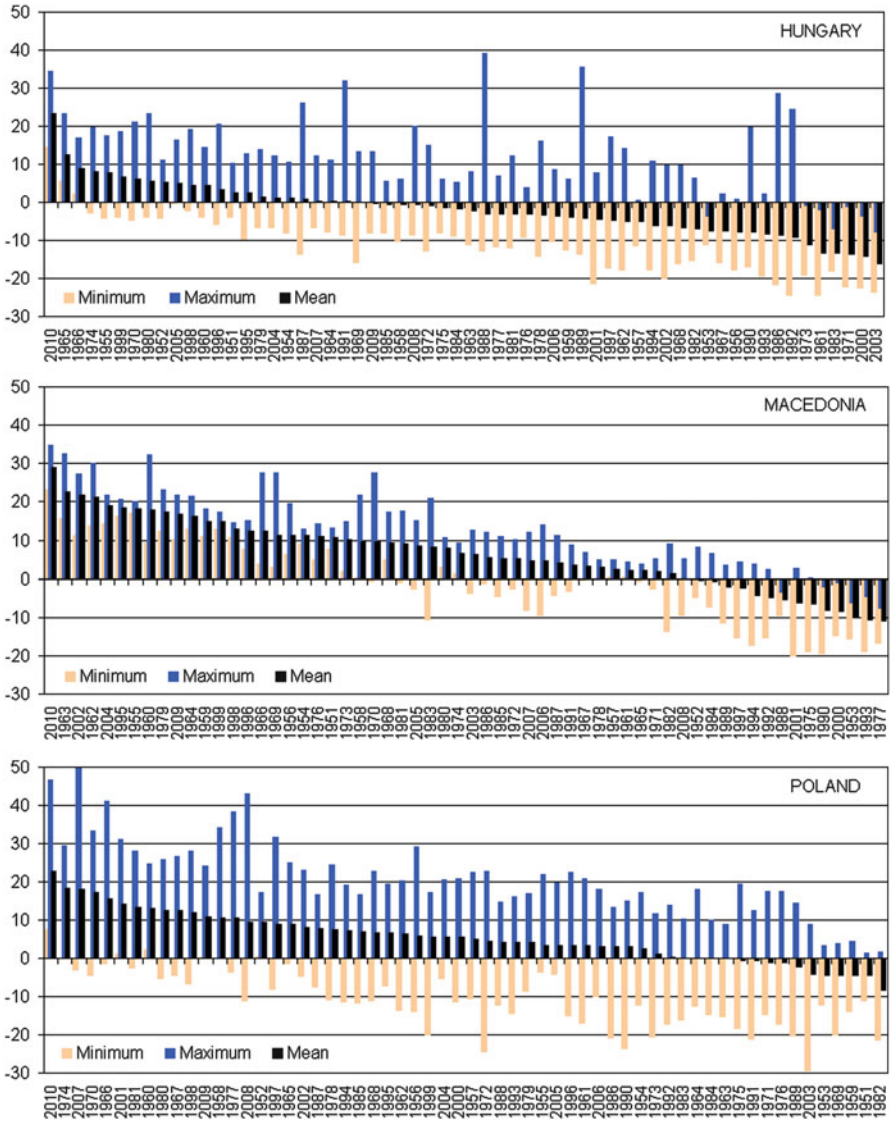

Fig. 1.5 Ranked annual precipitation anomalies (mm) for Poland, Hungary, and Macedonia, 1951–2010 (reference period: 1979–2000) (*Data source*: GPCC, DWD)

small subregions (mostly in the south) were drier than the climate normal. In June, the eastern part of the region was especially wet and the northwest drier than usual.

From the precipitation aspect, the exceptional behavior of year 2010 in the Central/Eastern European region is highlighted in Fig. 1.7, where regional precipitation anomalies for May and an extended summer period (May–September) are

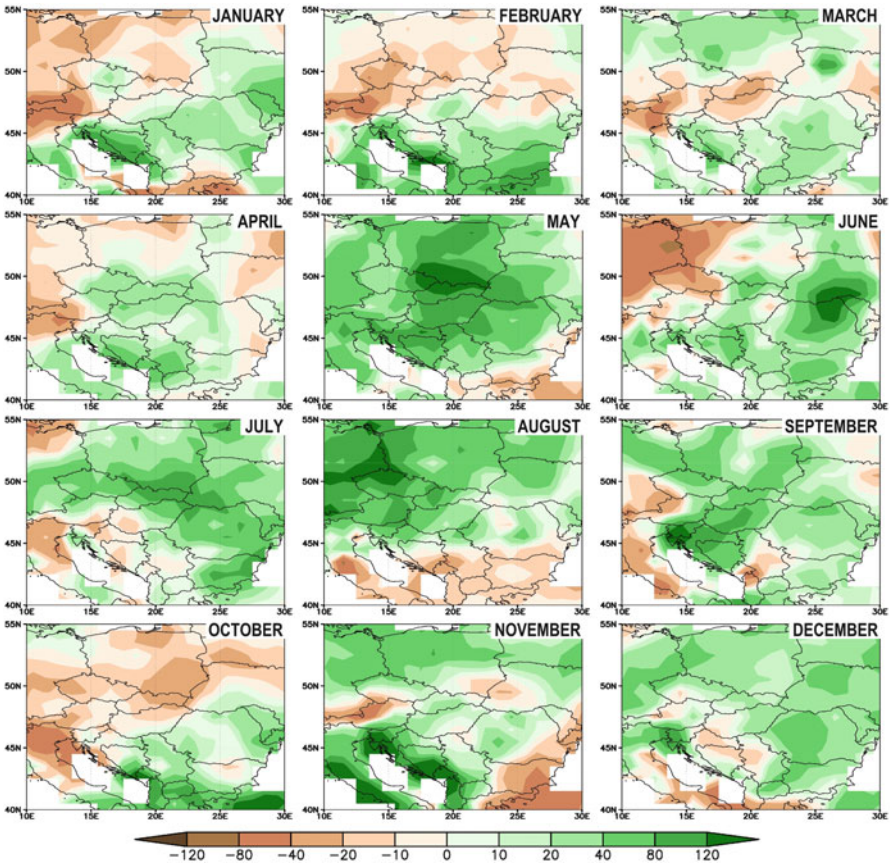

Fig. 1.6 Maps of monthly precipitation anomalies (mm) in 2010 for the Central/Eastern European region (reference period: 1979–2000) (*Data source*: GPCC, DWD)

shown. The anomalies in 2010 are clearly much higher than in any preceding year over 60 years, almost double of the second largest anomalies.

The grid point anomaly values in May and in the extended summer period are used to calculate the distribution for each year (Fig. 1.8). In the entire Central/Eastern European region, the year 2010 (indicated by a thick line) was obviously rather exceptional and extreme in terms of precipitation.

For *Hungary*, located in the center of the region, *monthly precipitations* for 2010 deviated most significantly from the reference period 1971–2000 in May, when the spatially averaged precipitation in the country was 176 mm (Móring 2011) (Fig. 1.9). This is almost three times larger than the monthly mean value. May 2010 was the wettest on record, 50 mm above the previous record (set in 1939). In 2010 monthly precipitation sums were mostly ca 1.5 times higher than usual and only in 2 months (in March and October) below the monthly climate normal. In September the regional average rainfall was 127 mm (Móring 2011), more than 2.5 times above the usual value. In Hungary the September of 1996 (when the highest

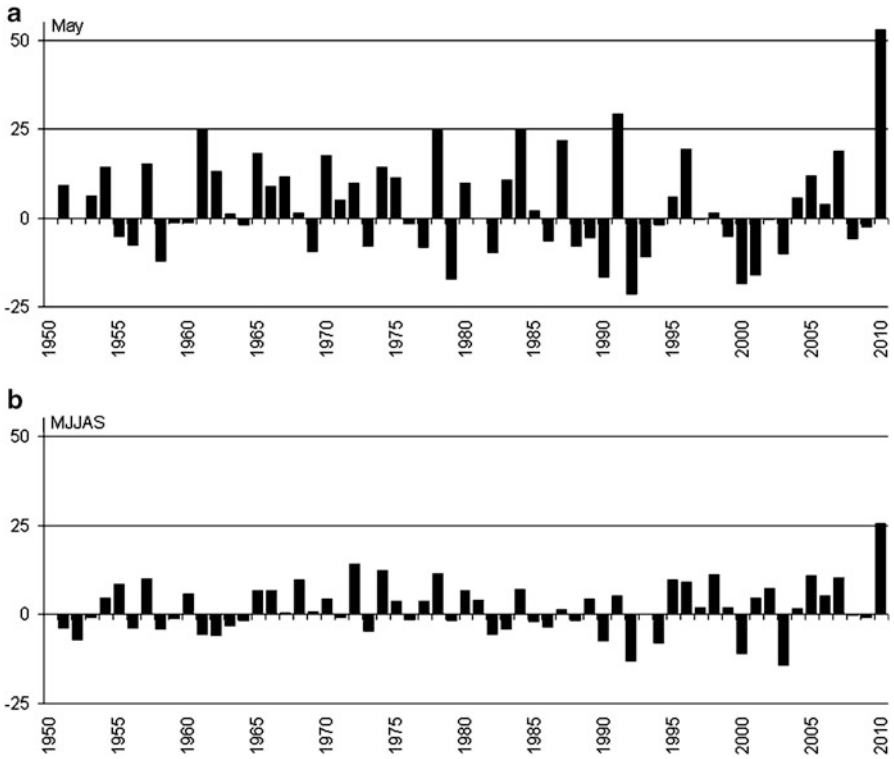

Fig. 1.7 Mean precipitation anomalies (mm) for the Central/Eastern European region in May (**a**) and in May–September period (**b**) (reference period: 1979–2000 (*Data source*: GPCC, DWD)

monthly rainfall amount occurred since 1901) was wetter than that of 2010, but only by 6 mm on average.

Over the entire year, the spatially averaged annual precipitation was 69% above the usual (Fig. 1.9). A new *record annual precipitation* (1,554 mm) was measured at Jávorkút (Bükk Mountains, Northeastern Hungary) (Fig. 1.1). In most of the mountains (Bükk, Mátra, Mecsek, Bakony), annual precipitation was above 1,300 mm, while the long-term averages are around 800 mm for these subregions.

1.4 Future Precipitation Trends

After analyzing past conditions, we assess the prospects for the coming decades of the 21st century in terms of precipitation. Since the industrial revolution, increasing anthropogenic activity has changed the atmospheric concentrations of most of the greenhouse gases, which is very likely to lead to *global climate change* (IPCC 2007). Global warming-induced changes in hydrology-related

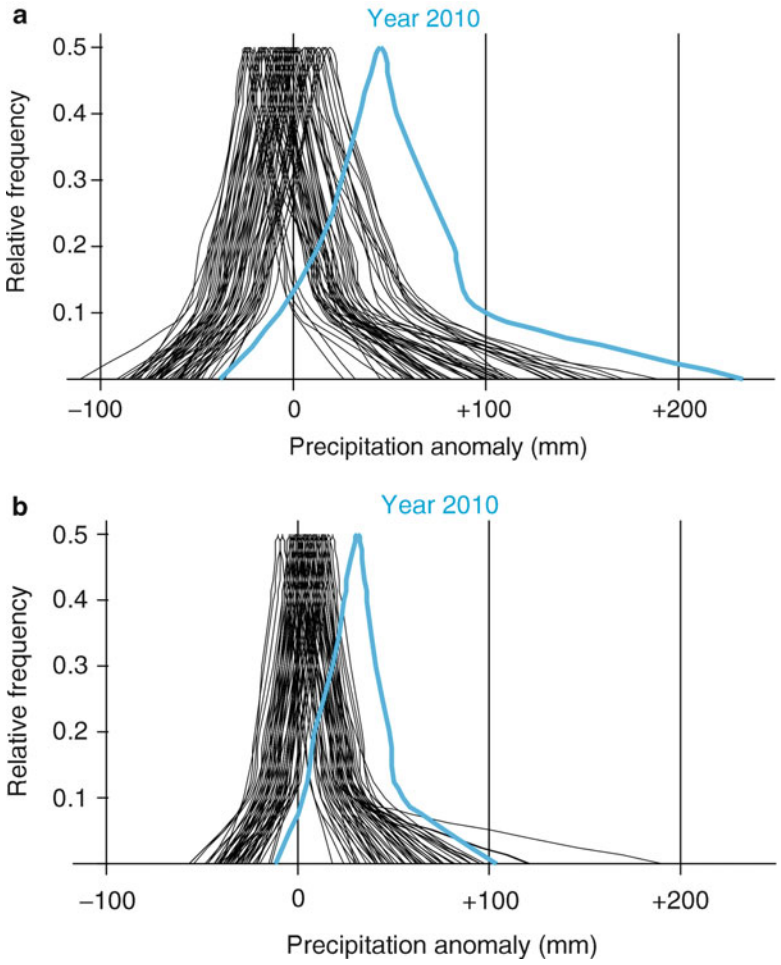

Fig. 1.8 Distribution of precipitation anomalies (mm) averaged for the Central/Eastern European region in May (**a**) and in the May–September period (**b**), for each year between 1951 and 2010 (reference period: 1979–2000) (*Data source*: GPCC, DWD)

environmental conditions are major concerns in every Central/Eastern European country due to the strong potential effects through severe regional drought and flood events. In order to estimate future climate change, *global climate models* (GCM) are applied. However, GCMs are run at spatial resolutions from 150 to 300 km, which makes them unsuitable for projections at a regional scale, particularly in the case of precipitation. Hence, *regional climate models* (RCM) driven by the GCM are used with 5–25 km horizontal resolution, which is a spatial scale where fine-scale climatic processes and resulting climatic conditions might be better described.

In the present analysis, monthly precipitation amounts were used calculated from 1951 to 2100 RCM simulation outputs of the *ENSEMBLES project* (van der Linden and Mitchell 2009). The selected RCMs, their driving GCMs (which

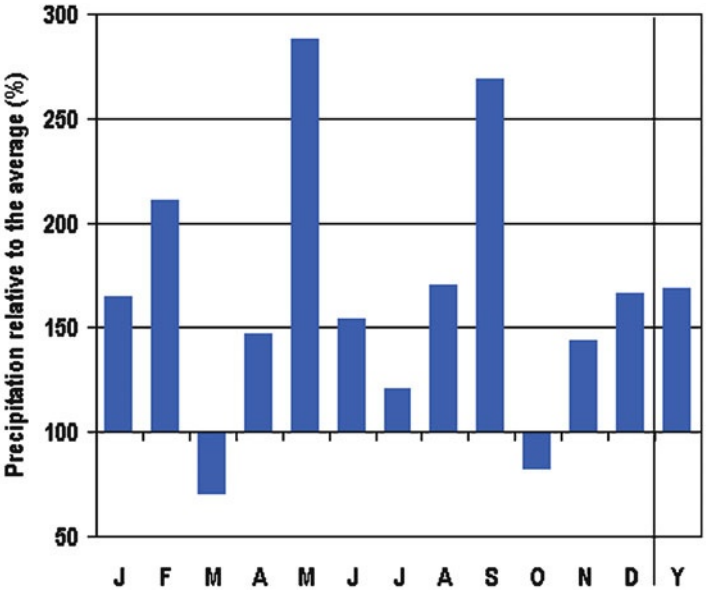

Fig. 1.9 Monthly and annual precipitation in 2010 relative to the 1971–2000 period averaged over Hungary (*Data source*: Hungarian Meteorological Service)

Table 1.2 List of selected regional climate models, their driving global climate models, and the responsible institute

RCM	Driving GCM	Institute	Country
ALADIN	ARPEGE	CNRM	France
RACMO	ECHAM5	KNMI	The Netherlands
RCA	ECHAM5	SMHI	Sweden
RCA	HadCM3Q		
REMO	ECHAM5	MPI	Germany
HadRM3Q0	HadCM3Q	HC	UK
RCA3	HadCM3Q	C4I	Ireland
HIRHAM	ARPEGE	DMI	Denmark
HIRHAM5	ECHAM5		
RegCM	ECHAM5	ICTP	Italy
CLM	HadCM3Q	ETHZ	Switzerland

provide initial and lateral boundary conditions for the regional scale models), and the institutes which accomplished the 150-year-long RCM experiment are summarized in Table 1.2. All these RCM simulations used 25 km horizontal resolution and considered the SRES A1B scenario (Nakicenovic and Swart 2000) for the future, which estimates world population to increase to 9 billion by 2050 but projected to decrease to 7 billion again by 2100. The scenario strikes a balance between the different energy sources (nuclear, renewable, fossil fuels), and it provides a midline scenario for carbon dioxide (532 ppm for 2050 and 717 ppm for 2100).

For Central/Eastern Europe (between 43 and 51°N latitudes and 9–30°E longitudes), 150-year precipitation data sets are available. To evaluate seasonal changes, the 30-year (1961–1990) average amounts calculated for the RCM runs and the future periods (2021–2050, 2071–2100) are compared for all the grid points within the selected domain. For each RCM, seasonal precipitation changes are determined, and then, weighted composite mean values are calculated for each season (Fig. 1.10). On the basis of these maps, the estimated changes for the late century are larger than for the mid-century. More specifically, future winters are very likely to become wetter (and summers drier) than those in the past few decades. The estimated increase of winter precipitation by the last three decades of the twenty-first century exceeds 20% in Slovenia, southern Austria, and north-western Hungary, moreover, in several regions of the Czech Republic, Slovakia, and northern Romania. In most of the southern regions, the projected summer changes by 2071–2100 exceed 20% (including Slovenia, Hungary, and Romania). The largest (20–40%) precipitation decrease in summer is estimated for Romania; consequently, summer drought is especially likely to hit this country. Moderate (10–15%) autumn increases are projected for the entire domain, which is divided into northern (increasing trend) and southern zones (decreasing trend) for spring. The projected changes, however, are almost insignificant.

After analysing the composite maps, a *country-based evaluation* of projected changes may produce more focused information for further impact studies. For this purpose, grid point values of seasonal changes within a given country are averaged in order to determine the *mean seasonal changes* of the country (Fig. 1.11). The six presented graphs illustrate the relationship between the projected precipitation trends by the middle and by the end of the 21st century for selected Central/Eastern European countries. Dashed lines indicate linear changes throughout the century; when the seasonal change is between the dashed line and the y-axis, the projected change during the second part of the century is larger (if between the dashed line and the x-axis, smaller) than in the first part, thus implying accelerating (decelerating or even opposite) precipitation change. Summer drying is projected for both periods in Slovenia, Slovakia, Hungary, and Romania, and likely to accelerate towards the end of the century. In Austria and in the Czech Republic, summers may only become drier in the second part of the 21st century. Winter precipitation is expected to grow somewhat more rapidly in most of the countries (except in Romania), while autumns are estimated to get slightly wetter at a slower pace in all the selected Central/Eastern European countries in the second half of the century.

Regional climatological effects of global warming may be recognized not only in shifts of mean precipitation but also in the *frequency* or *intensity* changes *of* different climatic *extremes*. Detected trends of several climate extreme indices were analysed and compared for the region (Bartholy and Pongrácz 2007) following the guidelines suggested by the joint WMO-CCl/CLIVAR Working Group on climate change detection (Karl et al. 1999). Precipitation indices include the number of wet days (using several threshold values defining extremes), the maximum number of consecutive dry days (CDD), the highest 1-day precipitation amount (RX1D), and the highest 5-day rainfall total (RX5D).

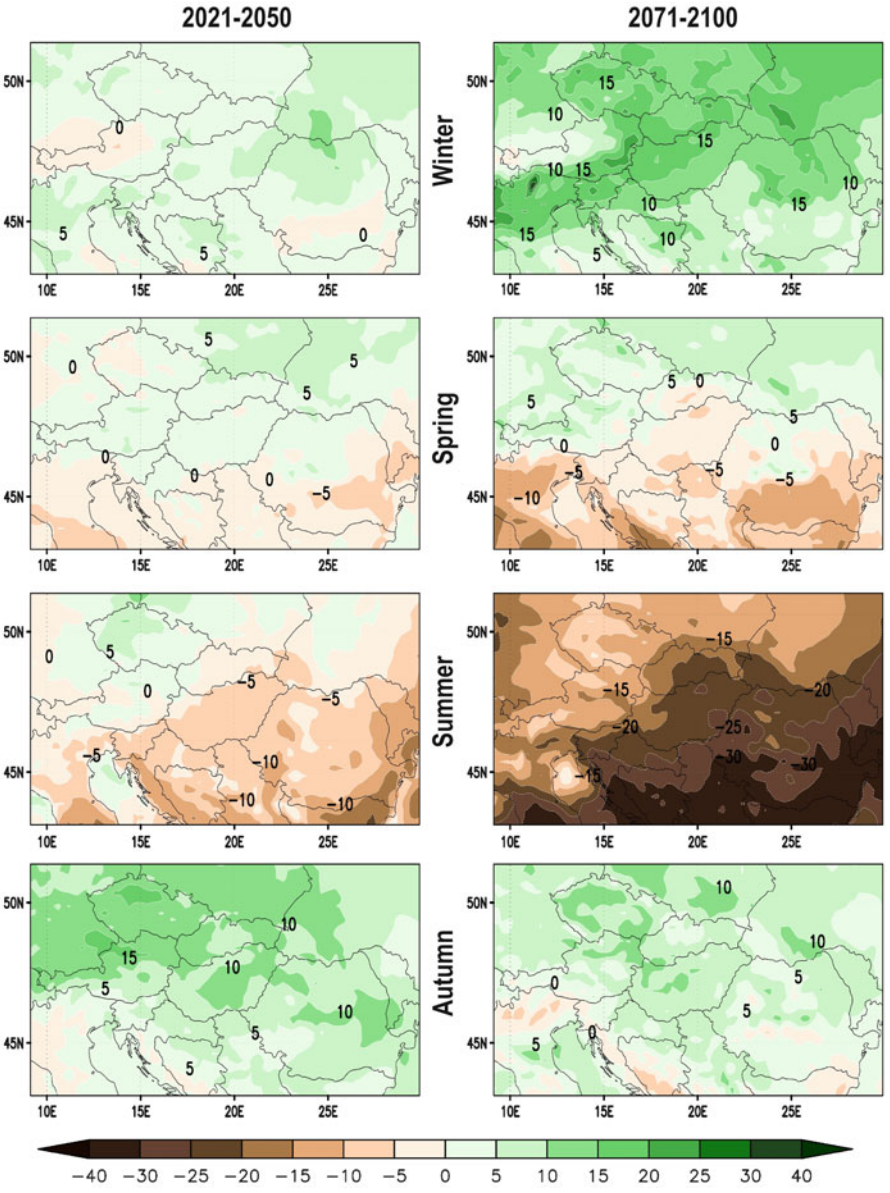

Fig. 1.10 Composite map of the weighted projected seasonal mean precipitation changes (%) by 2021–2050 and 2071–2100 (reference period: 1961–1990)

In order to estimate the bias of the different RCM simulations, outputs from 1951 to 2000 were compared to the E-OBS data sets (Haylock et al. 2008) containing gridded daily precipitation. The validation results suggest that, compared to the observations, the simulated values usually significantly *overestimate* precipitation – except in summer, when underestimations were more characteristic (Pongrácz et al. 2011).

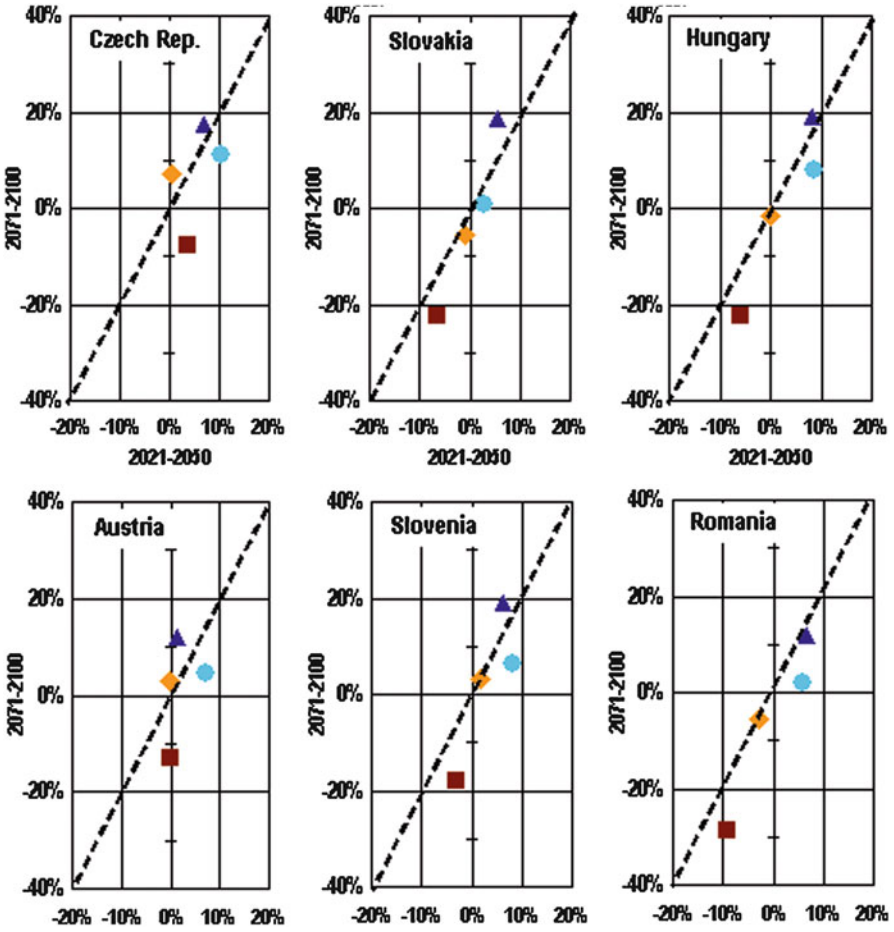

Fig. 1.11 Projected seasonal mean precipitation changes (%) by 2021–2050 and 2071–2100 (reference period: 1961–1990)

These biases of the raw RCM outputs are corrected using monthly empirical distribution functions (Formayer and Haas 2009), and then, precipitation-related climate index time series are calculated from the corrected precipitation data sets for each grid point. Projected seasonal changes by 2071–2100 are determined relative to the 1961–1990 reference period (Figs. 1.12 and 1.13). From these individual seasonal estimations, multi-model average changes are calculated for the selected countries (Tables 1.3 and 1.4).

The results suggest that in general, the seasonal numbers of *wet days* (*RR1*) are likely to decrease by the end of the 21st century (except for winter). Major decrease (23–33%) is predicted for the summer. Estimated changes of all the 11 individual

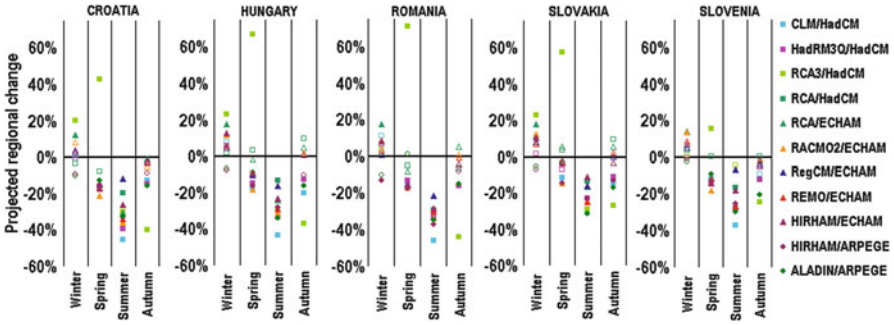

Fig. 1.12 Projected seasonal changes in RR1 by 2071–2100 calculated for Croatia, Hungary, Romania, Slovakia, and Slovenia (reference period: 1961–1990). Filled symbols indicate statistically significant change at 0.05 level

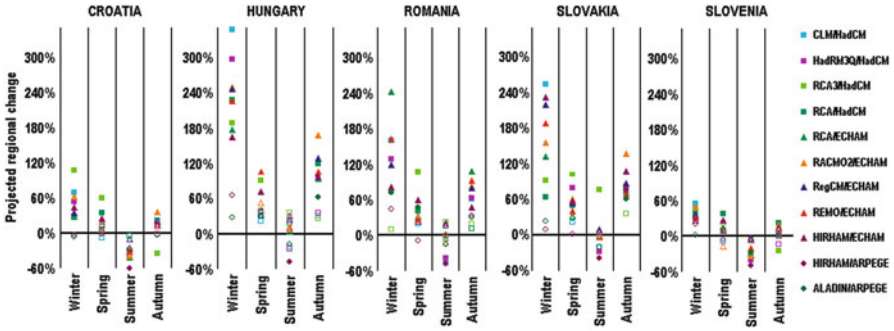

Fig. 1.13 Projected seasonal changes in RR20 by 2071–2100 for Croatia, Hungary, Romania, Slovakia, and Slovenia (reference period: 1961–1990). Filled symbols indicate statistically significant change at 0.05 level

Table 1.3 Multi-model mean projected seasonal changes (in %) in RR1 (number of wet days with precipitation above 1 mm) by 2071–2100 (reference period: 1961–1990) for five Central/Eastern European countries

Country	Winter	Spring	Summer	Autumn
Croatia	0% (2/0)	*-10 % (1/9)*	*-31 % (0/11)*	*-11 % (0/4)*
Hungary	**+4% (4/0)**	*-4% (1/7)*	*-28% (0/11)*	*-9% (0/4)*
Romania	+1% (1/1)	*-4% (1/7)*	*-33% (0/11)*	*-11% (0/4)*
Slovakia	**+6% (4/0)**	-1% (1/3)	*-23% (0/11)*	*-8% (0/5)*
Slovenia	**+3% (2/0)**	*-9% (1/9)*	*-23% (0/11)*	*-10% (0/3)*

Numbers in parentheses indicate the number of model simulations projecting statistically significant increasing (*first number*) and decreasing (*second number*) trends at 0.05 level. **Bold** numbers indicate positive and *italics* negative overall trends

Table 1.4 Multi-model mean projected seasonal changes (%) in RR20 (number of wet days when the precipitation exceeds 20 mm) by 2071–2100 (reference period: 1961–1990) for five Central/Eastern European countries

Country	Winter	Spring	Summer	Autumn
Croatia	**+34% (7/0)**	**+14% (3/0)**	*−34% (0/7)*	**+10% (2/1)**
Hungary	**+175% (9/0)**	**+47% (3/0)**	*−5% (0/1)*	**+84% (8/0)**
Romania	**+102% (9/0)**	**+34% (5/0)**	*−14% (0/3)*	**+51% (7/0)**
Slovakia	**+107% (8/0)**	**+43% (7/0)**	*−6% (1/2)*	**+73% (9/0)**
Slovenia	**+30% (8/0)**	**+9% (2/0)**	*−28% (0/8)*	**+5% (3/1)**

Numbers in parentheses indicate the number of model simulations projecting statistically significant increasing (*first number*) and decreasing (*second number*) trends at 0.05 level. **Bold** numbers indicate positive and *italics* negative overall trends, while **oversize** figures show growths above 50%

RCM simulations are statistically significant at 0.05 level (these are indicated by the filled symbols in Fig. 1.12, and also shown in Table 1.3). Projected changes of RR1 in autumn are around 10%, and only 3–5 simulations out of 11 RCM experiments estimate statistically significant decrease by 2071–2100.

The numbers of *very wet days* (*RR20*) by seasons generally tend to increase in the future, particularly in winter, with significant increase by the late century (in Hungary: 175%; Slovakia: 107%; Romania: 102%). Relatively smaller increase is projected in Slovenia (30%) and Croatia (34%). The comparison of these relative changes can be extended through a similar analysis when changes of index values are expressed in days instead of percentages. Furthermore, in the autumn and spring, regional average values of RR20 are likely to increase by 2071–2100. Similarly to winter, in both equinox seasons, larger changes are projected for the three northeastern countries than the two southwestern countries. Also, more RCM simulations predict statistically significant increase in Hungary, Slovakia, or Romania than in Slovenia or Croatia.

Regional average index values of RR20 are expected to decrease only for the summer, in the northeastern countries; however, the estimated rates are mostly not significant at 0.05 statistical level. In Slovenia and Croatia the projected summer decreases are similar to the projected increases in the winter. In both seasons the estimated changes of RR20 are statistically significant in 7–8 simulations out of the 11 evaluated RCM experiments.

1.5 Conclusions

The analyses of gridded global precipitation data sets suggest that within the past six decades (1951–2010), the year 2010 was remarkably wetter than usual over the entire Central/Eastern European region. Especially in late spring and summer, exceptionally large precipitation occurred in this area. For the future, RCM simulations based on the A1B global emission scenario point to a very likely

decrease (on average) of summer precipitation. This trend is more pronounced in the southern part of the study region than in the northern areas. At the same time, winter and autumn precipitation amounts tend to increase – especially in the northern regions of Central/Eastern Europe. The projected changes may involve an increased frequency of weather extremes. The numbers of days with higher than 20 mm rainfall will generally increase in the future and significantly increase by the end of the century (in Hungary by 175%). If other conditions are also favorable, larger amounts of rainfall may involve remarkable geomorphological impacts.

Acknowledgements The ENSEMBLES data used in this work was funded by the EU FP6 Integrated Project ENSEMBLES (Contract number 505539) whose support is gratefully acknowledged. Furthermore, we acknowledge the E-OBS data set from the EU-FP6 project ENSEMBLES (http://ensembles-eu.metoffice.com) and the data providers in the ECA&D project (http://eca.knmi.nl). Research leading to this chapter has been supported by the Hungarian Science Research Foundation (OTKA, grant no K 78125).

References

Bartholy J, Pongrácz R (2007) Regional analysis of extreme temperature and precipitation indices for the Carpathian Basin from 1946 to 2001. Global Planet Change 57:83–95

Bissolli P, Friedrich K, Rapp J, Ziese M (2011) Flooding in eastern central Europe in May 2010 – reasons, evolution and climatological assessment. Weather 66(6):147–153

Formayer H, Haas P (2009) Correction of RegCM3 model output data using a rank matching approach applied on various meteorological parameters. Deliverable D3.2 RCM output localization methods (BOKU-contribution of the FP 6 CECILIA project). http://www.cecilia-eu.org/

Haylock MR, Hofstra N, Klein Tank AMG, Klok EJ, Jones PD, New M (2008) A European daily high-resolution gridded dataset of surface temperature and precipitation. J Geophys Res Atmos 11:D20119

IMGW (2010) Flooding in Poland – May/June 2010. Institute of Meteorology and Water Management, Warsaw. http://www.wmo.int/pages/mediacentre/news_members/poland_2010_en.html

IPCC (2007) Climate change 2007: the physical science basis. Working group I contribution to the fourth assessment report of the IPCC. In: Solomon S, Qin D, Manning M, Chen Z, Marquis M, Averyt KB, Tignor M, Miller HL (eds) Intergovernmental panel on climate change. Cambridge University Press, New York, 996 p

Karl TR, Nicholls N, Ghazi A (1999) Clivar/GCOS/WMO workshop on indices and indicators for climate extremes workshop summary. Clim Chang 42:3–7

Móring A (2011) 2010 időjárása (weather of 2010). Légkör 56(1):38–42 (in Hungarian)

Nakicenovic N, Swart R (2000) Emissions scenarios. A special report of IPCC working group III. Cambridge University Press, New York, 570 p

Pongrácz R, Bartholy J, Miklós E (2011) Analysis of projected climate change for Hungary using ENSEMBLES simulations. Appl Ecol Environ Res 9:387–398

van der Linden P, Mitchell JFB (eds) (2009) ENSEMBLES: climate change and its impacts: summary of research and results from the ENSEMBLES project. UK MetOffice Hadley Centre, Exeter, 160 p

WMO (2011) WMO statement on the status of the global climate in 2010. World Meteorological Organization Report No. 1074. World Meteorological Organization, Geneva, 15 p. http://www.wmo.int/pages/publications/showcase/documents/1074_en.pdf

Part II
Floods

Chapter 2
Channel Changes due to Extreme Rainfalls in the Polish Carpathians

Elżbieta Gorczyca, Kazimierz Krzemień, Dominika Wrońska-Wałach, and Mateusz Sobucki

Abstract This chapter describes a role of extreme rainfall events in the development and transformation of channels in the Polish Carpathians. An analysis was based on the example of four selected events, which occurred in different parts of Polish Carpathians (Western Tatra, Bieszczady, and Beskid Niski Mountains) during the period 2003–2010. The findings underline that changes of the largest extent follow short and heavy rainfalls. Furthermore, their geomorphic impacts are the most significant in small watersheds. The research showed that the largest transformations of mountain rivers occur in the main channel, while the floodplain is only locally altered. The regularities identified in the study areas are relevant for mountain river channels in forested terrains, where a large supply of woody debris, for example, stems and branches, is ensured.

Keywords Extreme rainfall • Flash flood • Catastrophic events • Channel erosion • Sediment transport • Woody debris • Polish Carpathians

2.1 Introduction

Extreme weather events are undoubtedly the prime driving force behind landform change. They set in motion powerful processes that upset the equilibrium of natural systems such as river channels (Thornes and Brunsden 1978). The three basic types of these extreme events include short but very intense precipitation, heavy long-term precipitation, and rapid snowmelt. They tend to occur infrequently on the long

E. Gorczyca (✉) • K. Krzemień • D. Wrońska-Wałach (✉) • M. Sobucki
Institute of Geography and Spatial Management, Jagiellonian University, ul. Gronostajowa 7, 30-387 Cracow, Poland
e-mail: e.gorczyca@geo.uj.edu.pl; k.krzemien@geo.uj.edu.pl; dominika.wronska-walach@uj.edu.pl; mateusz.sobucki@uj.edu.pl

D. Lóczy (ed.), *Geomorphological impacts of extreme weather: Case studies from central and eastern Europe*, Springer Geography, DOI 10.1007/978-94-007-6301-2_2,

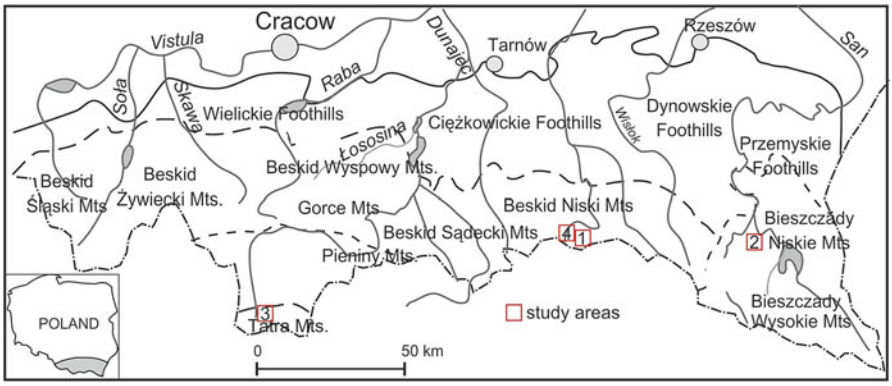

Fig. 2.1 Study areas: *1*, Wisznia basin; *2*, Hoczewka River basin; *3*, Western Tatras; *4*, Upper Wisłoka basin

term but are often clustered with short intervals between them (days, months, or years) (Starkel and Sarkar 2002). The intervals are too short for the system affected to recover after the previous event, and it arrives at a new equilibrium.

During the period 2003–2010, the slopes and valleys of the Carpathian Mountains underwent considerable transformations following intense precipitation and rapid thawing (Gorczyca 2004, 2008; Izmaiłow et al. 2006; Cebulak et al. 2008; Gorczyca and Krzemień 2008; Gorczyca and Wrońska-Wałach 2008; Starkel 2008, 2011; Święchowicz 2008; Kijowska 2011). The areas affected are located in the Beskid Niski, the Bieszczady, and the Western Tatra Mountains (Fig. 2.1).

2.2 Methods

The study involved two main types of fieldwork: (1) geomorphological *mapping* of stream and river *channels* and (2) detailed *land surveying*. Landforms developed during preceding events were identified, and the minimum/maximum grain size of the material transported was measured. Longitudinal and cross sections of selected valleys were also analyzed.

Channels were mapped using a special manual and a set of templates (Kamykowska et al. 1999). Survey maps of the channels and the sets of landforms identified in each of them were used to break down the channels into basic reaches, which were then described. Qualitative and quantitative features were identified, as well as erosion and accumulation – type forms, ruble, and training. Certain areas, for example, the Wisłoka River basin, were mapped both before and after the extreme events.

2.3 Floods and Their Effects

2.3.1 The Wilsznia Basin

A catastrophic flood struck parts of the Wilsznia River basin in the Beskid Niski Mountains range on 18 July 2003. It was triggered by a *downpour* roughly restricted to the river basin itself. Records from a pluviograph at Krosno show that the bulk of the rain fell between 8:00 and 9:00 p.m. (Izmaiłow et al. 2006). Data from precipitation stations located in the area suggest that the largest total daily rainfall was recorded in the upper sections of the basin (88.0 mm at Wisłok Wielki and 98.7 mm at Orzechówka). According to interviews with the local population, the rainfall began around 7:00 p.m. and continued until 10:30 p.m. but was most intense between 8:00 and 9:00 p.m. According to some assessments, more than 100 mm of rain fell in the study area over the course of 1.5 h. An analysis of floodmarks on the rivers and stream suggests that the water levels on the Wilsznia River reached 4 m. The effects in the river valley were devastating. A bridge at Polany was destroyed, and the river current returning through a side channel knocked a car carrying five people off the road. All five perished in the water.

Stream channels in the Wilsznia basin are typical of the Beskid Niski Mountains, as they run through *alternating narrow and broad valley sections*, depending on the underlying geology. In the broader sections, streams converge, which can generate a high flood wave after intensive downpours. The channels, mostly meandering in character, run either askew or parallel to strata with only short reaches perpendicular to the geology. The channels have uneven longitudinal profiles. Bank height normally ranges from 0.5 to 1.5 m, but increases to 3–5 m, and at undercut banks exceptionally up to 20 m.

The mapping resulted in the identification of 17 discrete *reach*es broken down into five *types*. These included (1) straight rocky channels with a tendency to intensive downcutting, (2) rocky and alluvial meandering channels with a tendency to downcutting and local accumulation, (3) rocky and alluvial channels with a tendency to lateral erosion and intensive local accumulation, (4) alluvial channels with small slope and a tendency to intensive accumulation and local lateral erosion, and (5) alluvial channels with a tendency to intensive accumulation.

As a result of the event, the Wilsznia channel changed considerably, especially in reaches nos. 9–11 (Fig. 2.2). There are three reasons for this pattern: (1) the upper section of the basin was where the rainfall was heaviest, (2) this was also where three large streams came together, and (3) the largest amount of large woody debris (logs and branches) carried along these reaches caused channel clogging and avulsion in the valley bottom. Similar patterns emerged from studies of catastrophic floods along other Carpathian rivers and streams (Kaczka 1999; Wyżga et al. 2002–2003).

Despite the scale of change caused by the flood, the channel reach structure remained largely unchanged. Changes that did occur included the *number of landforms*, which decreased in the upper-course reaches and either decreased or slightly increased in the lower reaches (Fig. 2.2). Along most of the narrow reaches,

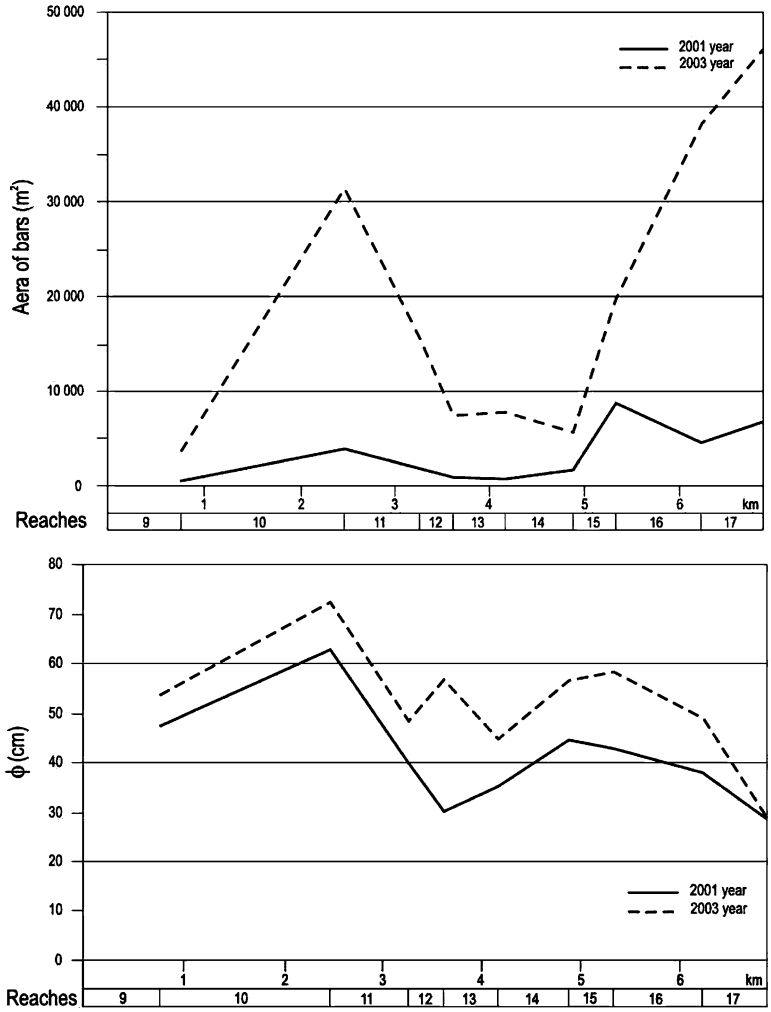

Fig. 2.2 Surface area of channel bars in the Wilsznia channel: (**a**) before and after the flood; (**b**) maximum grain size in the channel long profile (after Izmaiłow et al. 2006)

the number of landforms dropped, but their surface area increased. Indeed, there was a considerable increase in the surface area of mid-channel bars and erosional undercuts along the entire stream channel (Fig. 2.2). The large number of new *rock steps* (knickpoints) suggests an overall increase in downcutting, especially in the middle and lower courses of the stream. The appearance of new rock steps suggests that the alluvial cover is relatively thin even in braiding reaches, as is typical of Carpathian streams and rivers in general (Krzemień 1976, 2003; Wyżga 1992).

During the study period, the maximum *grain size* of sediment in the Wilsznia channel was found to have increased along its entire length (Fig. 2.2). This was due

to higher stream power during the catastrophic flood, when large rocks were carved out of the channel bottom. Now these boulders are either scattered along the channel or form larger clusters, where imbricated specimens can be up to 1 m in size.

The most extensive incision was observed downstream from sites where rubble and woody debris blocked the streams, causing a sudden rise in stream power. Downcutting and lateral erosion were also generated by the accumulation of organic matter and bedload or found at sites of channel avulsion.

Following the extreme event, downcutting and lateral erosion continued along the bedrock reaches of the Wilsznia channel. Increased channel migration was found along the alluvial reaches with instances of avulsion due to channel blocking with large woody debris.

2.3.2 The Hoczewka River Basin

On 26 July 2005 an extreme rainfall event occurred in the Hoczewka River basin and around the Solina Reservoir. A single *thunderstorm* with an intensity of 0.9 mm min^{-1} produced 130.6 mm of rain within 2 h, as measured at the Baligród-Mchawa station. The downpour triggered gravitational processes on slopes and contributed to the formation of torrential flows within mountain stream channels as well as a high flood wave. An analysis of the evidence left by the high water has revealed that the culminations of flood waves were the highest on the streams of Cisowiec (ca 4 m) and Mchawka (ca 3.5 m). An analysis of channel geometry, the size of riverbed features, and maximum grain size of the sediment deposited in them suggests that the water levels were rising rapidly and the event was rather violent.

In the Cisowiec valley, erosion was not limited to the channel, but extended over to the valley floor. In terms of key processes, the Cisowiec channel can be divided into two reaches: the clearly *erosional upper reach* and the mixed erosional-depositional reach below (Fig. 2.3). In the former, *downcutting* alternated with lateral erosion, producing sizable erosion chutes, steps, potholes, side channels, scoured bedrock floors, and undercuts of various sizes. Channel resistance to erosion depended to a large extent on the *underlying geology* and especially on the relationship between channel direction, the tilt of rock strata, and on the cohesion of mineral material. In reaches aligned with the rock beds, large erosion chutes developed. The alluvia were swept clean and the channel bottom consisted of uneven bedrock with isolated boulders greater than 0.5 m in size. Wherever the channel crossed sediment beds, erosion produced steps with evorsion potholes below (0.8 m deep). The channel incised 1.5–2 m, as evidenced by the hanging position of a tributary confluence at ca 2.5 m.

Along the *lower reach* of Cisowiec stream, *erosion alternated with deposition*. Erosion was not confined to the channel itself, but reached existing dirt roads running parallel with the channel. Characteristic of the Cisowiec valley is the *channel walls* consisting of rough material on terraces. This might suggest a very dynamic transport resembling debris flow at some locations.

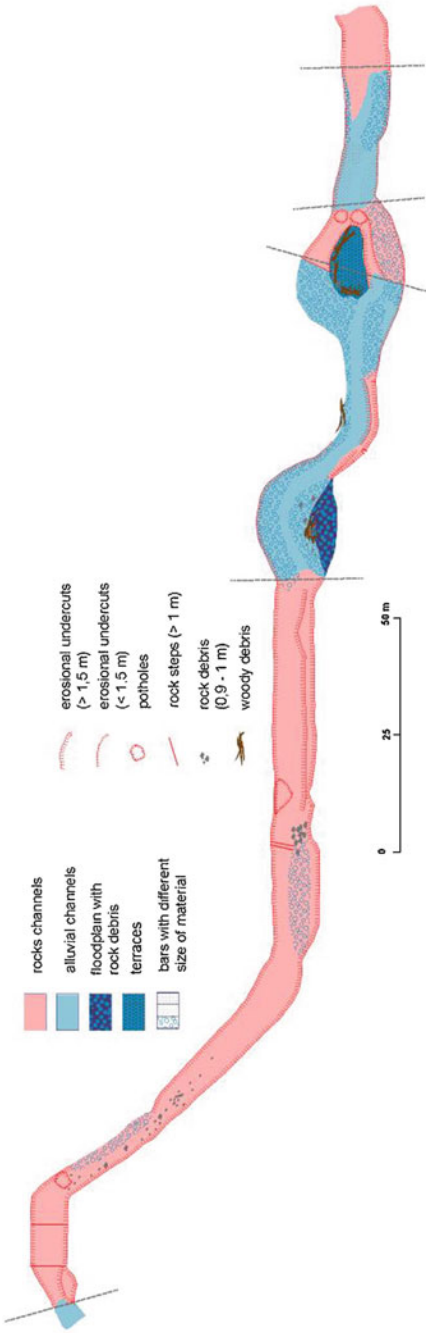

Fig. 2.3 Morphodynamic reaches in the middle course of Cisowiec stream in the Bieszczady (modified after Gorczyca and Wrońska-Wałach 2008)

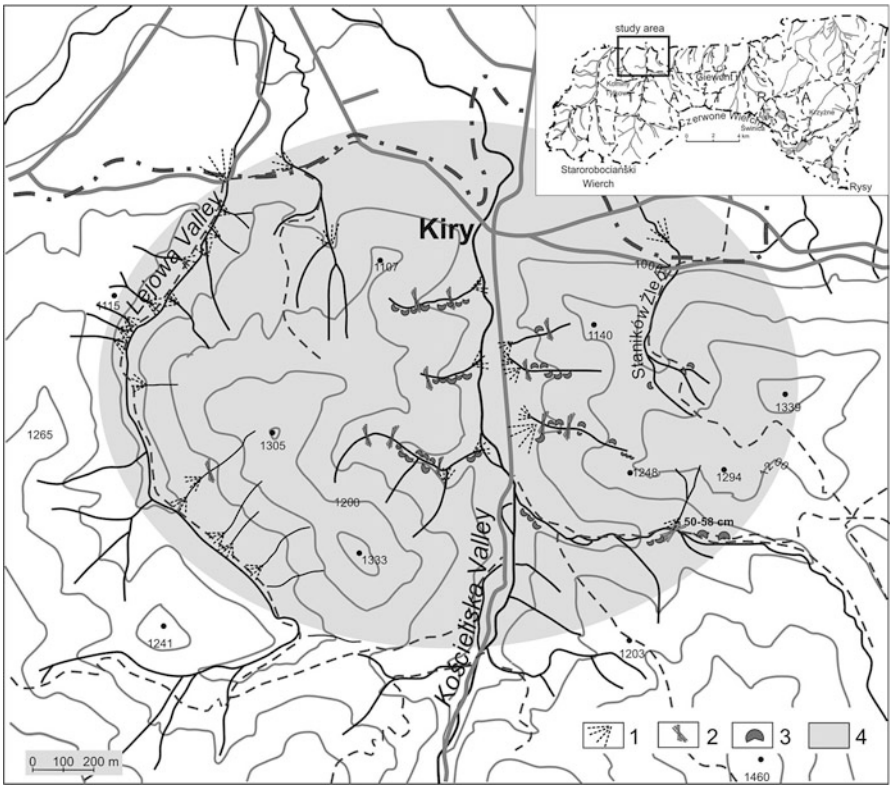

Fig. 2.4 Geomorphological effects of catastrophic rainfall on 5 June 2007 in the Western Tatra Mountains (After Gorczyca and Krzemień 2008); 1 – torrential fan, 2 – woody-debris-dam, 3 – landslide, 4 – area of geomorphological impact of catastrophic rainfall

Large woody debris and stream training were considerable factors during the flood. Perhaps the greatest role, however, was played by the flood wave and destruction of two *fishponds* on one of the tributaries of the Cisowiec. An estimated 3,800 m^3 of water from the ponds would have greatly increased the flood wave, which was indeed found to have reached a level of 3.5–4 m downstream of the ponds. Bridges and road culverts along the stream narrowed down the flow path and were soon clogged with organic debris. The swelling stream rushed over roads, destroying them, while adjacent channel reaches were also considerably transformed.

2.3.3 Mountain Watersheds in the Western Tatras

An extreme rainfall event in June of 2007 affected the montane zone of the Western Tatra Mountains, including the Kościeliska, Lejowa, and Stanikow Żleb Valleys (Fig. 2.4). This middle mountain area is mainly built up of limestones, dolomites,

and marls of Triassic, Jurassic, and Cretaceous age and *Eugenia* limestone, shales, and conglomerates (Bac-Moszaszwili et al. 1979). The event caused major changes primarily in young river valleys, ravines, and V-shaped valleys with narrow floors and uneven longitudinal profiles. The valleys tend to widen on outcrops of softer rocks and narrow down across more resistant limestone and dolomite zones (Klimaszewski 1988). During the Pleistocene and Holocene, periodic water flows transported debris and created *torrential fans* in the main river valleys.

The catastrophic downpour occurred on 5 June 2007, when daily precipitation was 104.2 mm. Much of that amount fell during a thunderstorm that produced 74.1 mm of rain between 2:00 and 5:00 p.m., but its peak intensity of 1 mm min^{-1} lasted for only 1 h (14:30–15:30), totalling 61 mm.

During fieldwork we discovered considerable changes on montane-zone valley floors and accumulation fans. A general *pattern of erosion* emerged in all of the 30.44 km of valleys mapped. In their longitudinal profiles, there were four main types of reaches: the uppermost reaches (*A*) were the least affected (Fig. 2.5), only by the transport of boulders up to 20 cm in size. Channels downstream (*B*) were incised and bed load transported with some deposition of organic and mineral material. There was also a set sequence of *bottom features*: rock and debris steps, erosion chute, and a long stretch of incised bedrock floor. The downstream reaches (*C*) were similar to the *B* reaches, but the valley slopes also showed traces of mass movements (Fig. 2.5). Saturated with water, the thin waste mantle could not hold trees, which were uprooted and fell into the channel. The trunks clogged the streams and caused debris to accumulate, while there were some local accumulation upstream steps in the long section. At the valley mouths, torrential fans, made up primarily of rock boulders with some large woody debris, were either accumulated or cut through (*D*) (Fig. 2.5). An analysis of excavations in the cuts shows their complex structure with alternating layers of fine loam depositions and sandrock beds of 15–30 cm size. This points to two kinds of fan accumulation: medium-power events contributed the deposition of loamy material, while extreme events deposited the coarse fraction.

The size of *bed load transported* within the channels during the event reached 80 cm within the channels and ca 50 cm across the fans. This is much above the sizes identified after the most intense rainfall to date, on 1 July 1973 (Kaszowski and Kotarba 1985).

Perhaps this type of extreme event is more frequent in the history of middle mountains than has been thought before. The considerable rate of changes identified in the montane zone of the Tatras confirms earlier suggestions that local downpours played a significant part in local geomorphic evolution (Jakubowski 1974; Starkel 1996; Gorczyca 2004).

2.3.4 The Upper Wisłoka Basin

In May and June 2010, two floods occurred in the upper Wisłoka River basin as a consequence of continuous rainfall. On 17 May 2010, a flow of 96 m^3 s^{-1} was recorded at the Krempna-Kotań gaging station. It was preceded by 79.6 mm rainfall

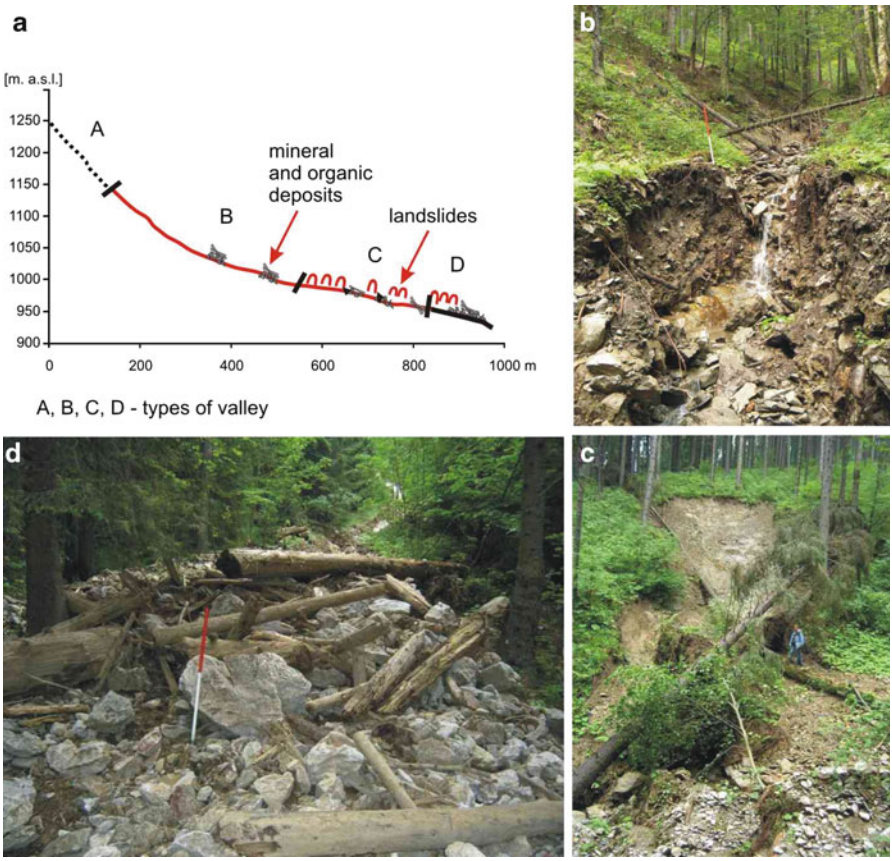

Fig. 2.5 Landform patterns in morphodynamic reaches of the valleys studied in the Western Tatra Mountains; (**a**) longitudinal profile of valley, (**b**) type B of valley, (**c**) type C of valley, (**d**) type D of valley

between 10 and 17 May (with a peak of 35.2 mm on 16 May), recorded at the Wyszowatka station. A second flood on 4 June 2010 had a flow of 85 $m^3\ s^{-1}$, preceded by a 126.6 mm rainfall between 30 May and 4 June (41.3 mm on 3 June). Between 2 May and 4 June, a cumulative rainfall of 303.3 mm was recorded.

The gravel-bed channel of the Wisłoka River runs through the Beskid Niski, a middle mountain range. Also here channel geometry is controlled by the underlying geology, which resulted in a particular *morphological pattern* of parallel ridges and valleys with water gaps across the ridges at almost right angles. This pattern, also found in the Wisłoka river, involves narrow gap segments with intensive erosion and a straight bedrock channel as well as broader segments (embayments) with intensive accumulation and a meandering alluvial channel.

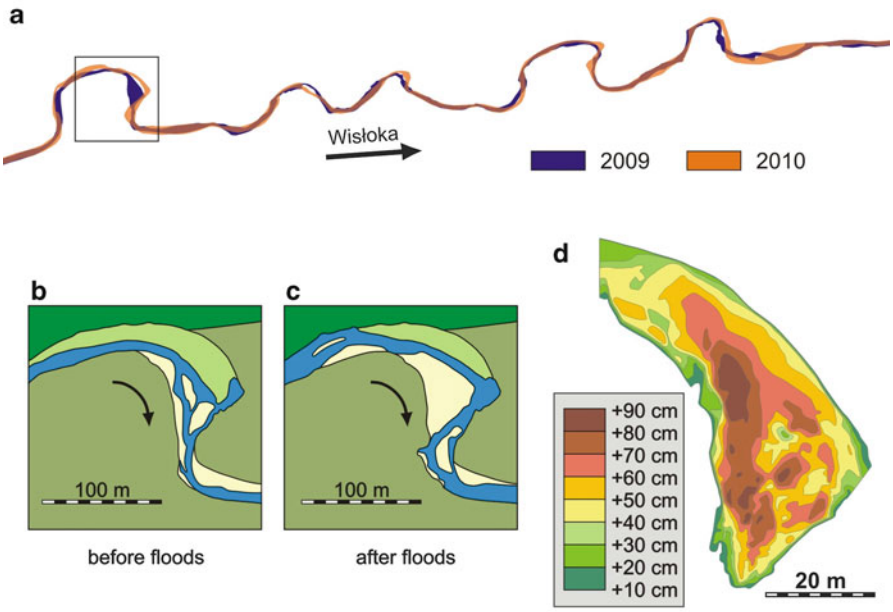

Fig. 2.6 Changes in the studied section of the Wisłoka River channel following floods in May and June 2010: (**a**) Wisłoka channel changes between Nieznajowa and Rozstajne, (**b**, **c**) changes of the undercut reach in Nieznajowa, (**d**) differential surface in the area of developed point bar

During the two floods, the largest scale of change was found in the *broader sections* of the valley. A two-kilometer reach of the river between two adjacent gap sections was selected for a more detailed analysis (Fig. 2.6). The segment involves a 200–400 m wide valley floor, out of which the channel and the lower terrace make up 200 m. Located within the Magura National Park, the meandering channel with braiding migrates freely, without human intervention, over the floodplain.

Analyzing *channel changes* on orthophoto maps from 2009 to 2010, we found that, as a result of the floods, the channel became broader and showed more developed meanders (Fig. 2.6a). Land surveys performed both prior to and following the events showed progressing lateral erosion of both the flood and dry terraces at the site of the undercut reach studied. Maximum channel shift was ca 20 m (Fig. 2.6b, c). This was accompanied by deposition, particularly on the inside of the bend, point bar accumulation providing new land available for the expansion of vegetation. A general overhaul of the pool and riffle pattern attests to a considerable modification of the channel.

The second land survey helped assess the change in bed load volume in the channel. The map shows a segment of the channel at Nieznajowa where a bar has expanded. Isolines connect points of equal vertical debris accumulation (Fig. 2.6d).

The irregularities in the distal section of the bar are a result of a high rate of change in this part of the channel. The deposition of large woody debris induces local

scour and fill. Hanging channel reaches are found within the bar that developed during the descending of the flood wave in supercritical flow conditions. These features are shown as measured during the first and second surveys, and the differential surface reflects the complexity of factors driving the development of this channel system.

In general, during the two springtime floods, *bank undercutting* shaped the Wisłoka channel, particularly across its flood terrace, which resulted in a well-developed meandering channel pattern. Across the flood terrace, the flood destroyed some of the surfaces occupied primarily by pioneer vegetation, making way for large amounts of debris transported. Areas consolidated by older vegetation resisted any major change.

2.4 Conclusions

In a selected study area of the Carpathian Mountains, rainfall with catastrophic consequences is rare. An analysis of the catchments studied shows that disastrous rainfall occurs every 20–30 years on average. The pattern applies to both valley floors and on slopes. The extreme cases studied here suggest that the greatest degree of change follows *short but intensive storms* with a very limited spatial extension. Their geomorphic action is only significant in small watersheds with little impact on larger basins. An exception is when there is a clustering of events in a certain area leading to the triggering of geomorphic processes of extreme intensity.

Due to the considerable channel incision of the Carpathian rivers, a transformation of a mountain river channel system tends to be limited to a deep *chute cutting* into the terraced valley floor. Along bedrock reaches, catastrophic floods lead to local downcutting and lateral erosion. Fresh sediment is brought into the channel, which is clearly seen in the maximum fraction of bed load measured. Along alluvial reaches, there is a significant increase in *channel migration*. Cases of *avulsion* may follow the blocking of the channel with large woody debris or damaged built structures. In 2010 mountain streams were the most affected along their main channels, especially around sites clogged with logs. In general, the floodplain is affected locally by debris accumulation or erosional dissection, which typically happens when the main channel is blocked and the current is deflected onto the floodplain. The patterns identified at the study sites apply mainly to mountain river channels in areas with a high proportion of woodland, which ensures an ample supply of large woody debris.

The study of deposits indicates that *extreme events* occurred repeatedly during the Holocene, as evidenced by the alternating layers of fine and coarse sediments. For this reason, it is likely that such extreme events are *not at all exceptional* in the geomorphic evolution of mountains and their forelands.

References

Bac-Moszaszwili M, Burchart J, Głazek J, Iwanow A, Jaroszewski W, Kotański Z, Lefeld J, Mastella L, Ozimkowski W, Roniewicz P, Skupiński A, Westalewicz-Mogilska E (1979) Geological map of the Polish Tatra, 1:30 000. Wydawnictwa Geologiczne, Warszawa

Cebulak E, Limanówka D, Malota A, Niedbała J, Pyrc R, Starkel L (2008) Przebieg i skutki ulewy w dorzeczu górnego Sanu w dniu 26 lipca 2005 r (The course and the effects of heavy rain in the upper San River basin on July 26, 2005). Materiały badawcze, seria: meteorologia, IMiGW, Warszawa, 56 p (in Polish)

Gorczyca E (2004) Przekształcanie stoków fliszowych przez procesy masowe podczas katastrofalnych opadów (dorzecze Łososiny) (The transformation of flysh slopes by catastrophic rainfall-induced mass-processes (Łososina River catchment basin)). Jagiellonian University, Kraków, 101 p (in Polish)

Gorczyca E (2008) The geomorphological effectiveness of extreme meteorological phenomena on flysch slopes. Landform Anal 6:17–27

Gorczyca E, Krzemień K (2008) Morfologiczne skutki ekstremalnego zdarzenia opadowego w Tatrach reglowych w czerwcu 2007 r (Morphological effects of extreme rainfall event in the Tatra Mountains in June 2007). Landform Anal 8:21–24 (in Polish)

Gorczyca E, Wrońska-Wałach D (2008) Transformacja małych zlewni górskich podczas opadowych zdarzeń ekstremalnych (Bieszczady) (Transformation of small mountain catchments during extreme rainfall events (Bieszczady Mountains)). Landform Anal 8:25–28 (in Polish)

Izmaiłow B, Kamykowska M, Krzemień K (2006) The geomorphological effects of flash floods in mountain river channels. Prace Geograficzne IGiGP UJ, Kraków 116:82–89

Jakubowski K (1974) Współczesne tendencje przekształceń form osuwiskowych w holoceńskim cyklu rozwojowym osuwisk na obszarze Karpat fliszowych (Contemporary trends in the transformation of landslide forms in the Holocene development cycle of landslides in the flysh Carpathians). Prace Muzeum Ziemi 22:169–193 (in Polish)

Kaczka R (1999) The role of coarse woody debris in fluvial processes during the flood of the July 1997, Kamienica Łącka valley, Beskidy Mountains, Poland. Studia Geomorphologica Carpatho-Balcanica 33:117–130

Kamykowska M, Kaszowski L, Krzemień K (1999) River channel mapping instructions: Key to the river bed description. In: Krzemień K (ed), River channels, pattern, structure and dynamics. Prace Geograficzne IGiGP UJ, Kraków 104:9–25

Kaszowski L, Kotarba A (1985) Współczesne procesy geomorfologiczne (Contemporary geomorphological processes). In: Trafas K (ed) Atlas Tatrzańskiego Parku Narodowego. Tatrzański Park Narodowy, Zakopane – Kraków (in Polish)

Kijowska M (2011) The role of downpours in transformation of slopes in the Polish Carpathian foothills. Studia Geomorphologica Carpatho-Balcanica 45:69–87

Klimaszewski M (1988) Rzeźba Tatr Polskich (Relief of Polish Tatra Mountains). PWN, Warszawa, 668 p (in Polish)

Krzemień K (1976) Współczesna dynamika potoku Konina w Gorcach (The recent dynamics of the Konina Stream channel in the Gorce Mountains). Folia Geographica Series Geographica-Physica 10:87–122 (in Polish)

Krzemień K (2003) The Czarny Dunajec River, Poland, as an example of human-induced development tendencies in a mountain river channel. Landform Anal 4:57–64

Starkel L (1996) Geomorphic role of extreme rainfalls in the Polish Carpathians. Studia Geomorphologica Carpatho-Balcanica 30:21–28

Starkel L (2008) Rola ekstremalnych zjawisk meteorologicznych w przekształcaniu rzeźby południowej Polski (Role of extreme meteorological events in the relief transformation of southern Poland). Rozdział 3, Mat. Konf. “Geosfera”, AGH, Kraków, pp 19–30 (in Polish)

Starkel L (2011) Złożoność czasowa i przestrzenna opadów ekstremalnych – ich efekty geomorfologiczne i drogi przeciwdziałania im (Temporal and spatial complexity of extreme rainfalls – their geomorphological effects and ways of counteract them). Landform Anal 15:65–80 (in Polish)

Starkel L, Sarkar S (2002) Different frequency of threshold rainfalls transforming the margin of Sikkimese and Bhutanese Himalayas. Studia Geomorphologica Carpatho-Balcanica 36:51–67

Święchowicz J (2008) Soil erosion on cultivated foothill slopes during extreme rainfall events in Wiśnicz Foothills of southern Poland. Folia Geographica, Series Geographica-Physica 39:79–93

Thornes JB, Brunsden D (1978) Geomorphology and time. Methuen, London, 208 p

Wyżga B (1992) Zmiany w geometrii koryta i układzie facji jako odzwierciedlenie transformacji reżimu hydrologicznego Raby w ciągu ostatnich dwustu lat (Changes in channel geometry and facies system as a reflection of the Raba River hydrological regime transformation over the last two hundred years). Czasopismo Geograficzne 63(3–4):279–294 (in Polish)

Wyżga B, Kaczka R, Zawiejska J (2002–2003) Gruby rumosz drzewny w ciekach górskich – formy występowania, warunki depozycji i znaczenie środowiskowe (Large woody debris in mountain streams – accumulation types, depositional conditions and environmental significance). Folia Geographica, series Geographica-Physica 33–34:117–138 (in Polish)

Chapter 3
Geomorphic/Sedimentary Responses of Rivers to Floods: Case Studies from Slovakia

Milan Lehotský, Milan Frandofer, Ján Novotný, Miloš Rusnák, and Jacek Bogusław Szmańda

Abstract The aim of this study is to outline the geomorphic/sedimentary responses of three Slovak river systems of different character (a non-channelized meandering gravel-bed river, a mixed-bedrock headwater river, and a channelized section of a large alluvial river) to extreme flood events. Lateral channel shifts and the spatial variability of channel landforms as responses of a non-channelized gravel-bed stream to flood events were studied on a 13.2 km long reach of the Ondava River in two time horizons, 2002 and 2009 (reference year: 1987). Two different methods were used to quantify the geomorphic effect of floods on the Topl'a River. First is the analysis of the remotely sensed imagery before (September 2006) and after (October 2009) the July 2008 flood. Second is the analysis of representative cross sections measured on each of the 78 delimited channel reaches. Lithofacies studies of the Danube River overbank deposits were conducted on the right-bank inter-dike inundation area (active floodplain) of 300–600 m width. Case studies prove that the responses of different river systems to floods are governed by a combination of 'global' laws and 'local' spatial and/or temporal factors (different settings and scales).

Keywords Floods • River channels • Cross sections • Lithofacies • Overbank deposition • Remote sensing • Slovakia

M. Lehotský (✉) • J. Novotný • M. Rusnák
Institute of Geography, Slovak Academy of Sciences, Štefánikova, 814 73 Bratislava, Slovakia
e-mail: geogleho@savba.sk; geognovo@savba.sk; geogmilo@savba.sk

M. Frandofer
Department of Physical Geography and Geoecology, Faculty of Natural Sciences, Comenius University, Mlynská dolina 2, 842 105 Bratislava, Slovakia
e-mail: frandofer@nic.fns.uniba.sk

J.B. Szmańda
Department of Geomorphology and Environmental Management, Institute of Geography, Jan Kochanowski University in Kielce, Świętokrzyska 15, 25-406 Kielce, Poland
e-mail: j.szmanda@ujk.edu.pl

D. Lóczy (ed.), *Geomorphological impacts of extreme weather: Case studies from central and eastern Europe*, Springer Geography, DOI 10.1007/978-94-007-6301-2_3,

3.1 Introduction

In the last two decades, when the increasing magnitude and frequency of extreme flood events have generated intense fluvial processes, a number of case studies have dealt with the river morphological response to flood events in Central Europe (e.g. Wyžga 1996, 1997; Hrádek 2000; Klimek et al. 2003; Zielinski 2003; Brázdil and Kirchner 2007; Hauer and Habersack 2009; Bucała 2010).

An increased frequency of floods has also been observed in Slovakia since the second half of the 1990s (Solín 2008). Not only did they cause casualties and considerable material damages but also led to morphological and sedimentary changes in river systems. Extreme flood events increase stream power and the rates of erosion and accumulation in the river channel (Miller 1990; Hrádek 2000). The geomorphological effect of a flood depends on the size of the stream, magnitude, and frequency (distribution in time) of the flood event and on the physical properties of the channel, banks, and floodplain (Miller 1990). Ward (1978) points out that the shorter is the interval between two flood events, the greater the effect of the second flood as the time is not sufficient for the stream to recover from the first event (for instance, through stabilization by vegetation growth). Therefore, the effect of two *consecutive floods* within a short interval is more pronounced and involves more profound geomorphological impacts compared to those of floods more spaced in time. While major floods are rather destructive, normal low-magnitude and high-frequency events are constructive and contribute to the accretion of sediments and stabilization of the system (Corenblit et al. 2007).

This chapter is intended to outline the character of the geomorphic/sedimentary responses to extreme flood events and the controls on changes in three different Slovak river systems (a non-channelized meandering gravel-bed stream, a mixed-bedrock headwater stream, and a channelized reach of a large alluvial stream) (Fig. 3.1).

3.2 Non-channelized Meandering Gravel-Bed River

A change in stream morphology and lateral movements reflect river behavior and mutual effects of bottom aggradation/degradation processes, erosion, and sedimentation of banks (Brierley and Fryirs 2005). Lateral channel shift results from bank erosion and aggradation, which in turn reflects the relationship between erosion processes and bank features (such as point bars).

Lateral channel shifts and the spatial variability of channel landforms in response to flood events on a non-channelized gravel-bed stream were studied on a 13.2 km long reach (Fig. 3.1a) in the middle part of the *Ondava River* in two time horizons of 2002 and 2009 (reference year: 1987). The Ondava springs at 546 m above sea level and crosses the flysch area in north-eastern Slovakia. The Ondava is

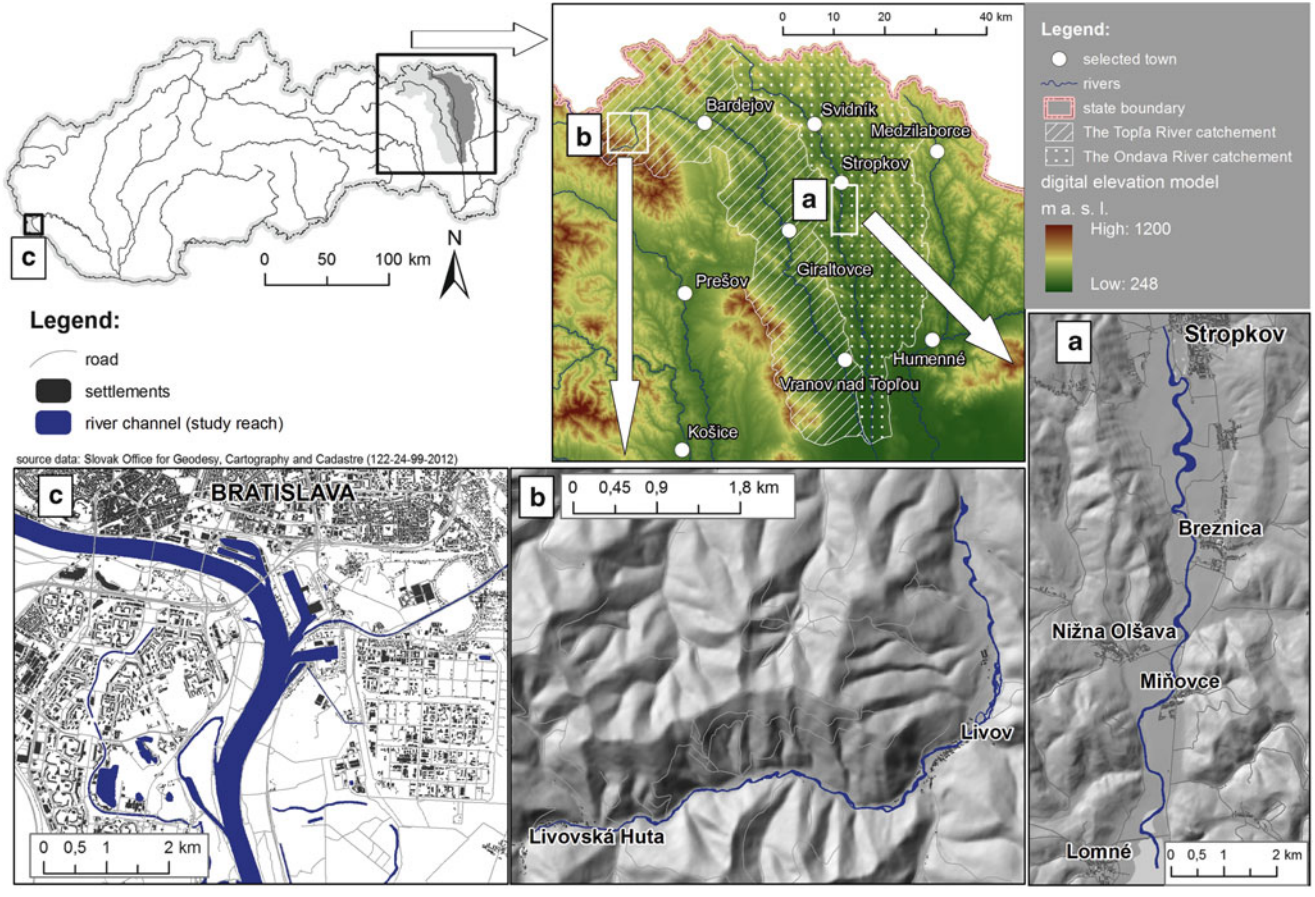

Fig. 3.1 Location of study sections on the Ondava River (a non-channelized meandering gravel-bed river) (**a**); the Topl'a River (a mixed-bedrock headwater) (**b**); and the Danube River (a large alluvial river) (**c**)

Table 3.1 Flood events and flood periods on the Ondava River

Period	N_{5-10} Q_{dmax} (from 285 to 300 m^3 s^{-1})	N_5 Q_{dmax} (235 and 230 m^3 s^{-1})	N_{1-2} Q_{dmax} (from 141 to 210 m^3 s^{-1})
First (1987–2002)	1987, 1989, 1992		1993, 1995, 1996, 1998, 1999, 2000
Second (2002–2009)	2006	2001, 2004	2005, 2008

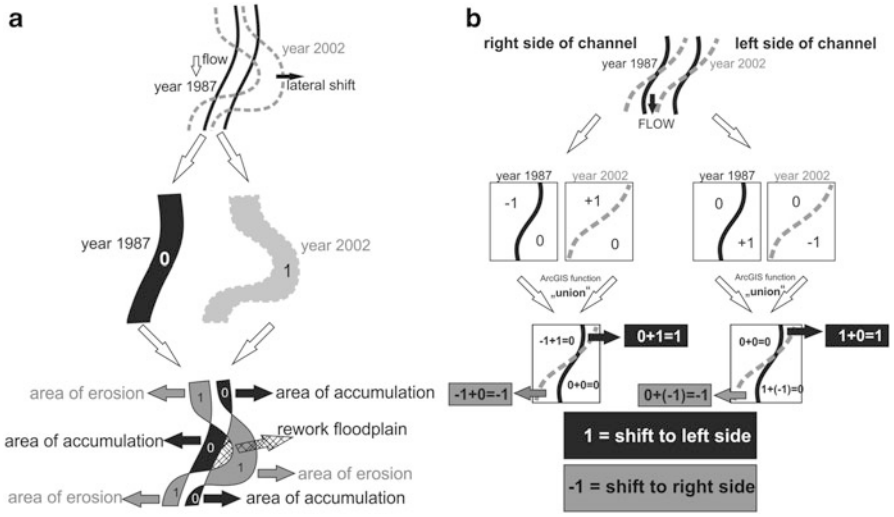

Fig. 3.2 Stages of assessment of lateral channel shift from aerial photos: identification of floodplain areas with accumulation, erosion, and reworking in GIS environment (**a**) and calculation of bank shift with definition of direction (**b**)

characterized by a high range of water regime: the long-term annual discharge at the gage of Stropkov oscillates around 5,730 m^3 s^{-1}, while during floods, it amounts to as much as 95-fold of the long-term mean (absolute maximum discharge: 550 m^3 s^{-1} on 19 July 1974) or in the study period 52-fold (300 m^3 s^{-1}). The choice of time horizons was based on an effort to capture morphological changes that followed two flood periods distinguished by analyses of flood hydrographs (Table 3.1).

Black-and-white aerial images were used as the basic information source for the assessment of stream morphology in the reference year of 1987. Color orthophoto images of two time horizons (2002 and 2009) were analyzed in ArcGIS software, channel morphology identified, and bars classified from the background grid to establish response to flood events. Lateral channel shift was observed based on the overlay of channel polygons in ArcGIS. Pursuing the assigned attribute values, erosion and accumulation areas and the reworked floodplain (floodplain eroded and then remodeled by sedimentation) were identified (Fig. 3.2a). Another method

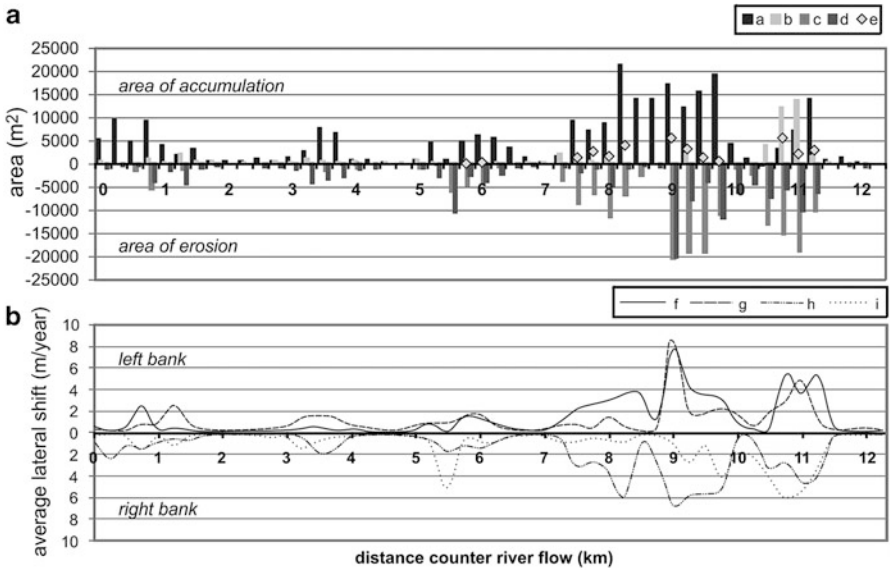

Fig. 3.3 Area of accumulation (**a**) in 1987–2002 (*a*) and 2002–2009 (*b*); area of erosion in 1987–2002 (*c*) and 2002–2009 (*d*); area of reworked floodplain in 1987–2002 (*e*) and lateral shift per year (**b**) of the left bank in 1987–2002 (*f*) and 2002–2009 (*g*); and of the right bank in 1987–2002 (*h*) and 2002–2009 (*i*) for the Ondava River

(Fig. 3.2b) was used for the computation of channel and bank changes in *m* ($m^2 = m \cdot m$). Four types of gravel bars as defined by Brierley and Fryirs (2005) (lateral bars, point bars, mid-channel bars, and islands) were identified within the channel.

The flood response of the Ondava river systems clearly manifests itself by *lateral instability* and changes in pattern of channel landforms. In the years from 1987 to 2009, the river eroded 35.6 ha of the floodplain and accumulated 31.6 ha in the form of gravel bars attached again to the floodplain. Another 5.3 ha is the area of reworked floodplain eroded by the stream in this period and then again accumulated and stabilized by vegetation (Fig. 3.3a). Mean channel shift of the river in that period was 25.7 m (1987–2009), but maximum bank retreat amounts to as much as 217 m, as a result of local meander shift at higher water stages. Average bank retreat is 1.07 m $year^{-1}$ (for the left bank) and 1.27 m $year^{-1}$ (for the right bank), but in meander loops it is above 4 m $year^{-1}$ (Fig. 3.3b).

Regarding the changes in distribution and rate of flooding, the area of *accumulation* decreased from 17,351 m^2 $year^{-1}$ (for 1987–2002) to 7,952 m^2 $year^{-1}$ (2002–2009) and the *erosion* area increased from 13,619 to 21,740 m^2 $year^{-1}$. The first period is characterized by the stabilization of meandering after the floods in the late 1980s and early 1990s, while in the second, this pattern was destroyed, the stream was *straightened*, and channel morphology was modified by repeated

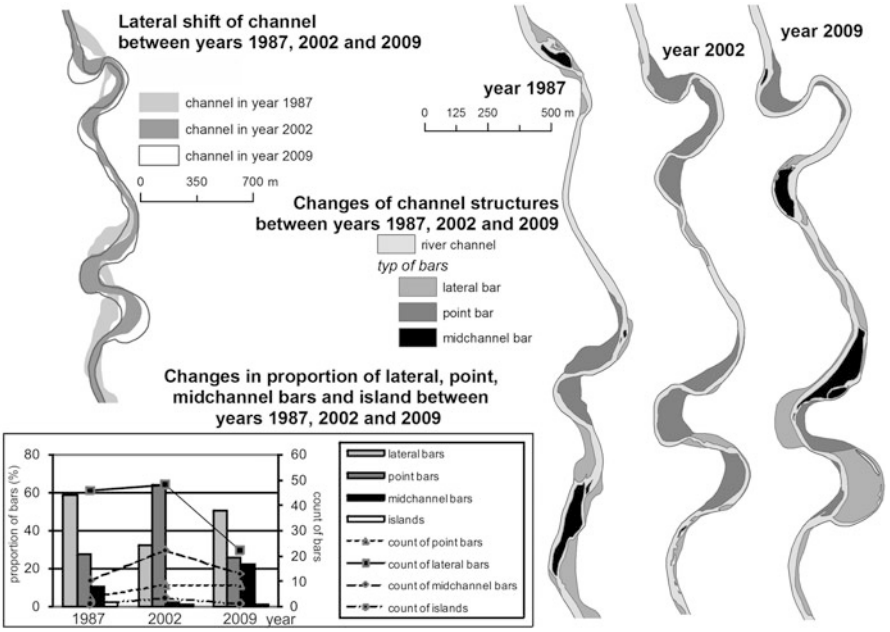

Fig. 3.4 Changes of channel planform of the Ondava River in 1987, 2002, and 2009 from 7 to 11.5 km of the study reach and changes in percentage of lateral, point, and mid-channel bars and islands in 1987, 2002, and 2009

floods after 2002 (first of all in 2004, 2006, and 2008) also due to high rates of erosion. In the first period (1987–2002), under the effect of meandering, a *progressive lateral shift* (marked erosion of the concave banks and accumulation of extensive point bars) pointed to balanced accumulation and erosion areas on the left and right banks (erosion at 8,485 m^2 $year^{-1}$ and accumulation at 6,928 m^2 $year^{-1}$ for the right bank; erosion of 7,295 m^2 $year^{-1}$ and accumulation of 12,584 m^2 $year^{-1}$ for the left bank). In the second period (2002–2009) under the effects of flood events, erosion processes prevailed and the rate of erosion increased to 11,431 m^2 $year^{-1}$ or 10,305 m^2 $year^{-1}$ and that of accumulation dropped to 3,127 m^2 $year^{-1}$ or 4,823 m^2 $year^{-1}$ for the respective banks.

The changes in the channel *landform types* and their areas indicate another kind of stream response to flooding. Gravel bars of the Ondava in 1987, 2002, and 2009 occupied areas of 21.1, 17.8, and 19.7 ha, respectively. The largest area (up to 12.4 ha in 1987, 5.8 ha in 2002, and 10.0 ha in 2009) of the monitored bar types is occupied by *lateral attached bars*. *Point bars* had 5.9, 11.4, and 5.1 ha of area, while the areas of *mid-channel bars* were 2.2, 0.4, and 4.5 ha, and those of *islands* were 0.6, 0.2, and 0.2 ha in the mentioned years. A pronounced decrease in the areas of lateral bars was observed in 2002 in favor of point bars, and a renewed areal expansion is seen since 2009 (Fig. 3.4). The growth of sinuosity from 1.34 to 1.57 was followed by a decrease of meander areas attributed to cutting off and straightening of the channel during flood events, while the resulting effect was an increase

in the areas of lateral and the mid-channel bars. The most extensive bars are found at the sites of maximum lateral shift.

The Ondava River has recently shown a very dynamic behavior with pronounced lateral instability and bank erosion. Instead of causing destruction, the high-frequency and low-magnitude floods on the Ondava by the end of the 1990s led to the stabilization of the system, erosion of the concave banks, and formation of a meandering planform. In contrast, the repeated high-magnitude floods of the last decade has changed channel planform, straightened the stream, created gravel bars, and remodeled fluvial landforms.

As a laterally unstable system, not only has the Ondava River eroded riparian forests, arable land, and grassland, but also pioneer vegetation has appeared on the newly emerged bars, and succession has started. As a consequence, the share of forest areas has grown, and the percentage of other land cover classes has dropped in the riparian zone.

3.3 Mixed Bedrock–Alluvial Mountain River

The behavior of mixed bedrock–alluvial mountain rivers is exemplified by an 8.7 km long reach of the *Topl'a River* (Fig. 3.1b), in the Čergov Mountains (highest peak: Minčol, 1,157 m), which issues at 1,015 m elevation. The mountain range is built of the flysch of the Magura nappe, i.e. more resistant coarse-grained sandstones, less resistant sandy claystones, and sandstones containing claystone galls (Nemčok 1990). In the Čergov average annual precipitation is 830 mm at the station Livovská Huta, and 822 mm at Kríže station, and drops to 700 mm at the piedmont station of Malcov. The study reach begins at 3.7 km from the spring, at 675 m elevation, and ends at the foot of the Čergov, 12.4 km from the spring, at 460 m.

Channel morphology is strongly affected by the intramountain setting, with narrow valley bottom varying in width from 35 to 180 m, *partial lateral confinement* between bedrock outcrops, and thin discontinuous coarse-grained alluvial beds.

Heavy precipitations in July 2008 and June 2010 caused extreme discharges extending the active river channel enlarged both in width and depth. The flood of July 2008 was caused by a series of extraordinary *precipitation events*. Three days of abundant precipitation (on 14, 17 and 20 July 2008), each totaling from 20 to 40 mm, led to complete saturation of soils on the watershed. Another extreme precipitation event occurred on 23 July (97 mm day^{-1} at Livovská Huta station), located at the upper end of the study reach. The resultant flood wave caused extensive damage to the road along the river (Fig. 3.5). Peak discharge at nearest gaging station (Gerlachov) set a new record of 90.09 m^3 s^{-1}, while further downstream (at Bardejov), the maximum discharge was 169 m^3 s^{-1}, assessed as a 20-year flood. The June 2010 flood on the majority of the eastern Slovakian rivers was generated by excessive rains over an extensive area. In the study area, daily precipitation measured at Livovská Huta was 23.6 mm on 31 May, 59.8 mm on 1

Fig. 3.5 Damaged road passing the Topľa River during flood, on 23 July 2008 (photo by M. Frandofer)

June, and the most abundant on 3 June, 63.6 mm. Similarly to the July 2008 flood, the crucial rainfall followed previous wet days. At Gerlachov station, the maximum discharge of 79 m^3 s^{-1} did not exceed the record of 2 years before, while at Bardejov, with a larger contributing watershed upstream in combination with precipitation over a larger area, a new record discharge was achieved ($Q_{max} = 350$ m^3 s^{-1}, assessed as over the 100-year flood).

The Topľa River channel was analyzed using ArcGIS. The study section was unevenly divided into 78 reaches. Two different methods were used to quantify the geomorphic effect of the floods. First is the analysis of the remotely sensed imagery before (September 2006) and after (October 2009) the July 2008 flood (No images available from the time after the June 2010 flood). Secondly, representative cross sections across each of the 78 delimited channel reaches were analyzed.

The results show that the active *channel* of the Topl'a River *expanded* significantly during the July 2008 flood. The main features which can be clearly identifiable on remote sensed imagery of this relatively narrow stream with mostly forested riparian zone are *channel bars* in the active channel. Provided that in the image taken before the extreme event no such bar or only small bars were visible and in the image taken after the event distinct bar areas are detected, it is assumed that *bank erosion* occurred. The presence of bars in the eroded area is associated with a drop in stream power and subsequent sedimentation after the passing of the flood wave (Fonstad 2003).

The total area eroded in the study reach during the flood of July 2008 was 3.43 ha (Fig. 3.6). Average *bank retreat* along reaches with floodplain pockets was 7 m (maximum: 39 m). This means that the channel of 8.5 m mean width widened by 80% on average and up to fourfold in some locations (Fig. 3.7). When comparing the channel with the pre-flood state, total *bar area* is a parameter of high reliability. A total 4.74 ha of new bars emerged after the July 2008 flood (30-fold growth).

With lower discharge on the study reach, the flood of June 2010 did not produce comparable extents of horizontal channel change. Based on field observations, channel narrowing and significant incision resulted in majority of reaches. Removing the material aggraded by previous events, the June 2010 flood predominantly had a vertical effect. The resultant bank shape is a distinct *flood bench*, recognizable

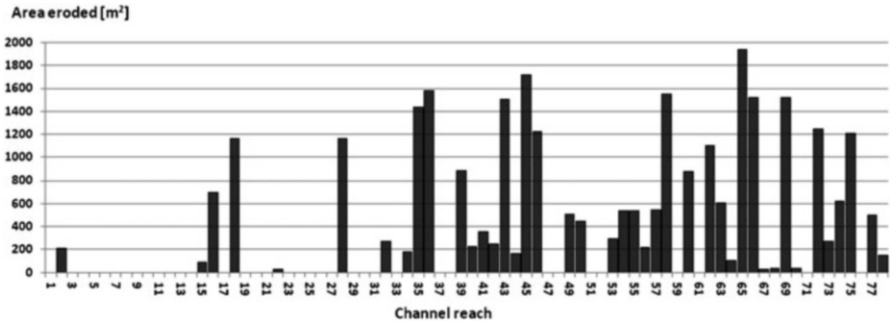

Fig. 3.6 Weighted areas affected by bank erosion at channel reach during the July 2008 flood event

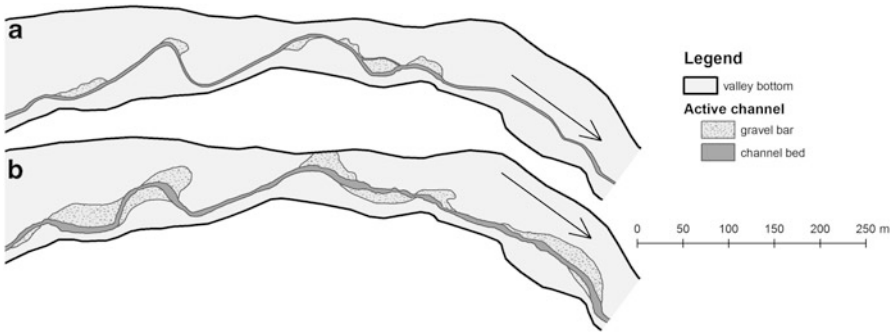

Fig. 3.7 A section of the study reach with channel floor and bars before (**a**, 2006 imagery) and after (**b**, 2009 imagery) the July 2008 flood

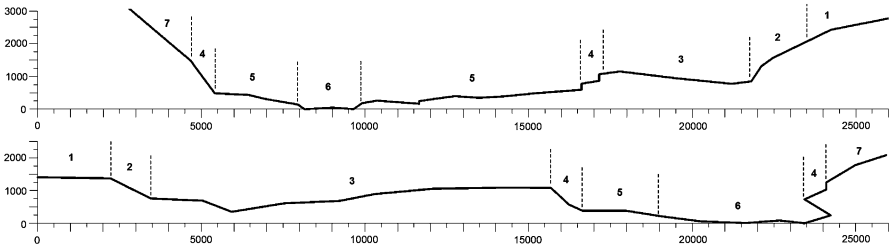

Fig. 3.8 Two examples of the 78 cross sections surveyed after the June 2010 flood. *1*, floodplain; *2*, bank eroded by the July 2008 flood; *3*, gravel bar aggraded by the July 2008 flood; *4*, bank eroded by the June 2010 flood; *5*, flood bench of June 2010 flood, level of pre-event channel bottom; *6*, present channel bottom; *7*, slope. The axes are in mm

in the majority of cross sections (Fig. 3.8). We estimated the extent of *channel incision* during the last flood from the height difference between the flood bench level and a new channel bottom level: average vertical channel erosion during the June 2010 flood was 0.33 m, and the maximum was 0.87 m.

At locations, where narrow channels favored incision, the *bedrock* was exposed on the bottom, but where the *channel* was wide, the bottom was alluvial. Unfavorable channel morphometric conditions for vertical erosion were compensated by the presence of sediments relatively easy to entrain, and, conversely, favorable morphometric conditions were constrained by the bedrock channel. Thus, the process of vertical bed erosion was strongly affected by the local influence of bedrock channel.

The channel morphology of the investigated reach of the Topľa River still carries legacies of both extreme flood events. Combined, these flood processes evacuated large amounts of floodplain sediments into piedmont reaches, where the channel approaches a braided style. Within the Čergov reach studied, bedrock channel prevails with *wagrams* or new terrace levels that are being colonized by pioneer riparian vegetation.

3.4 Channelized Reach of a Large Alluvial River

A lithofacies study was conducted on the Danube River (Fig. 3.1c) overbank deposits in the right-side inter-dike inundation area (active floodplain) of 300–600 m width. It is a unique, tectonically preformed bench of ca 5 km length and 1.5 km radius, part of an extensive alluvial fan. Previous geomorphological and sedimentological research (Novotný et al. 2007; Lehotský et al. 2010) has shown that the old Danube channel formed an *anabranching pattern*. The present valley floor has been strongly affected by human impact in the past. In the eighteenth to nineteenth centuries, the river system was reduced to a single main channel with the floodplain limited by dikes in order to protect the city against floods (Pišút 2002). The width of the Danube River channel adjacent to the study floodplain is ca 350–400 m; average annual discharge is 2,045 $m^3\ s^{-1}$ and the computed 100-year discharge (Q_{100}) equals ca 10,000 $m^3\ s^{-1}$ (Svoboda et al. 2000).

Sediment structures and textures as a response to three flood events (24 March 2002 – Q_{max} = 8,474 $m^3\ s^{-1}$; 16 August 2002 – Q_{max} = 10,370 $m^3\ s^{-1}$; 8 September 2007 – Q_{max} = 7,238 $m^3\ s^{-1}$; all data from the Devín gage) were interpreted; deposition rates and sediment transport were investigated. Borings (from 10 localities) and pits (20 localities) served as sampling points to determine the processes and rates of vertical accretion employing an allostratigraphic approach classified on the basis of the fluvial style (Miall 1996), and 132 samples were taken for granulometric analysis. Ten types of *lithofacies* and two subtypes were identified in the flood alluvia of the Danube (Table 3.2) by grain-size distribution. We set the granular characteristics of samples representing the gravel-sand fraction in 1-phi intervals. The same characteristics were assessed for the sand–silt fraction with an interval of 0.25 phi by laser method. We have sorted out analyzed samples into individual classes (Friedman and Sanders 1978) and computed textural parameters (Folk and Ward 1957) and the values of the first percentile (C) using the Gradistat computer software (Blott and Pye 2001).

Table 3.2 Results and interpretation of grain-size analyses

Lithofacies	Proportion (%)	Parameters after Folk and Ward (1957)				Average velocity (cm^{-1})	Traction (%)	Saltation (%)	Suspension (%)	CT (phi)	FT (phi)
		M_z (phi)	σ_1	Sk	K_G						
Fm	13.5	6.2	1.5	0.3	1.1	4.0	0	60	40	–	6
FSm	38.1	5.1	1.8	0.3	1.1	5.2	0.2	33.8	34	0	5.5
FSm (H)	1.6	4.3	2.6	−0.1	1.1	6.6	38	40	22	3.7	6
SFm	25.4	3.7	1.6	0.4	1.2	7.6	0	64	36	–	4
SFh	2.4	3.3	1.3	0.4	1.5	8.6	0	78	22	–	3.8
SFmi (L)	5.6	3.2	1.4	0.5	1.5	8.7	0	89	11	–	3.5
SFmi (H)		2.5	1.3	0.4	1.7	10.6	0	92	8	–	3.2
Sm	2.4	2.4	0.9	0.4	2.0	10.9	0	76	24	–	3.7
Sr	0.8	1.9	0.9	0.3	1.4	12.2	0	87	13	–	3.7
GSm	5.6	−1.1	2.4	0.3	0.6	26.6	70	29.5	0.5	1	5
Dm	2.0	−1.7	2.8	0.7	1.0	32.2	89	19	1	2	5
Gm	3.0	−3.5	1.1	0.4	1.8	52.0	85	93	7	From 0 to 1	From −2 to 0

Lithofacies types/subtypes: 1, massive mud (*Fm*); 2, massive sandy mud (*FSm*); 3, massive muddy sand (*SFm*); 4, horizontally laminated muddy sand (*SFh*); 5, massive muddy sand with inversed grading (*SFmi*); 6, massive sand (*Sm*); 7, sand with diagonal ripple cross-lamination (*Sr*); 8, massive gravelly sand (*GSm*); 9, gravel with compact granular structure (*Gm*); 10, massive diamicton (*Dm*)

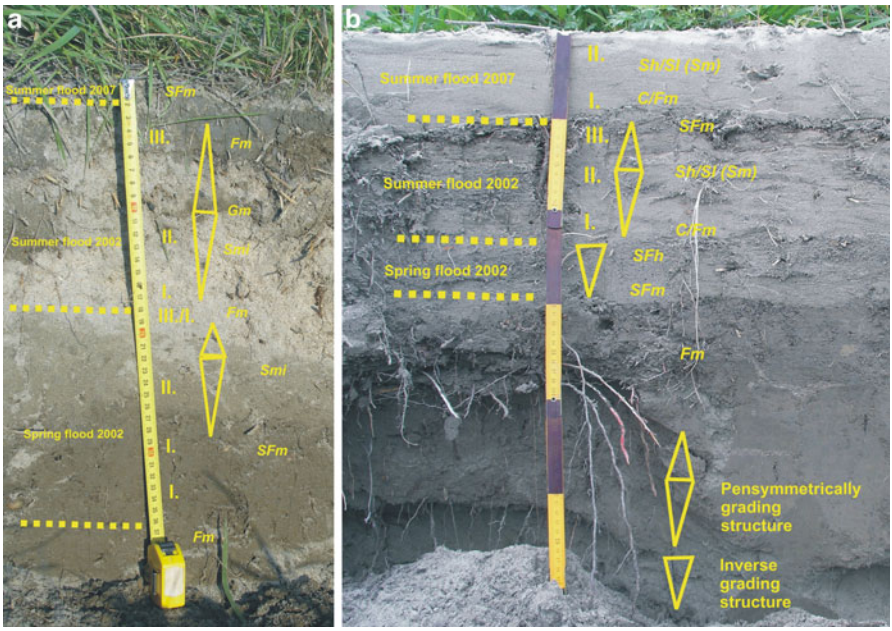

Fig. 3.9 Profile of lithofacies in overbank alluvia of the Danube River, on the natural levee (**a**) and in the channel bank (**b**)

The analyses showed a great variety of deposition conditions. *Vertical accretion* during floods dominates floodplain evolution. Our study suggests that levee formation proceeds, albeit unusually, in the convex bank of the Danube's bend, explained by limited lateral migration due to the embankment of the left concave bank, which heavily influenced flow direction during floods. Although the convex bankline was shifted (naturally and also by human action, i.e. channel widening) by 70 m into the floodplain after the 1997 flood (Q_{10}), an approximately 50 m wide strip of overbank sediments was deposited forming a new *levee* in the vicinity of the new bankline after the floods of 2002, 3 m above the average annual water level. The base of the bank consists of gravel horizons overlain by fine sand fractions of the new levee. The transition between the channel (gravel) and the floodplain (finer) facies is sharp. The thickness of levee sand deposits in the upper portion of the bank profile is about 1 m. The present situation is due to dramatic *human influence* over the last 60 years (e.g. channel widening and deepening, upstream dam constructions, floodplain terrain plantation).

It is possible to observe the *sedimentary records* of the flood events from 2002 to 2007 in the profile of overbank alluvia next to the riverbank (Fig. 3.9a). We recognized two three-unit sequences making up the record of three flood phases. They are deposited above massive silt with isolated pebbles. The similar *flood cyclothem* of

overbank deposits was found on the bank profile (Fig. 3.9b). It is possible to identify three units of different lithofacial features in each of these layer sets:

- The *lower unit* represents the initial, rising phase of flood wave, with the lithofacies (representing this unit): (1) 5 cm thick massive sandy silts (lithofacies SFm) (Fig. 3.9a); (2) 2–3 cm thick massive, inversely graded, fine sands (Smi fragment) (Fig. 3.9a); and (3) organic matter layer with massive silt admixture (C/Fm) of a few millimeters of thickness (Fig. 3.9b).
- The *middle unit* reflects the stage of widespread water cover (Allen 1970; Klimek 1974) or 'floodplain inundation and initial deposition' and 'flood peak and widespread transport and deposition' after Zwoliński (1992) that corresponds with the lithofacies of middle unit. The middle unit of the cyclothem is represented by (1) 3–8 cm thick, inversely graded massive fine and coarse sand lithofacies (Smi) and 4 cm thick inversely graded massive coarse sand lithofacies (Smi) overlain by the matrix-supported gravel lithofacies (Gm) on the levee sedimentary profile (Fig. 3.9a) and (2) 15 cm thick subhorizontally and low-angle cross-laminated medium-sand lithofacies (Sh/Sl) (Fig. 3.9b).
- The *top unit* of flood cyclothem is recording the decline of the flood wave and clearing of flood basins (Allen 1970; Klimek 1974) or two final phases of flood recognized by Zwoliński (1992). The top unit is represented by (1) a few cm thick layer of the massive mud lithofacies (Fm) (Fig. 3.9a) and (2) a few cm thick layer of the massive muddy sand (SFm) in the bank wall (Fig. 3.9b).

The lithofacies can be correlated with flood events in the following way:

- The *2002 spring flood* corresponds to the three-unit flood cyclothem SFm–Smi–Fm of the levee profile (Fig. 3.9a) and the two-unit inversely graded sequence SFm–SFh in the bank wall (Fig. 3.9b).
- During the *2002 summer flood*, the three-unit flood cyclothem Fm–Smi (Gm)–Fm (Fig. 3.9a) and the three-unit series C/Fm–Sh/Sl–SFm (Fig. 3.9b) were deposited. It should be underlined that this sequence is the closest to the three-unit flood cyclothem described by Klimek (1974).
- The massive mud (Fm) with organic matter (grass) was accumulated in the rising stage of the *2007 summer flood*. The horizontally laminated and low-angle laminated sands (Sh/Sl) were deposited in the peak phase of the flood (Fig. 3.9b). Moreover, during this flood a thin massive muddy sand (SFm) bed was deposited on the natural levee (Fig. 3.9a).

The 2002 spring flood had a lesser effect on the riverbank (deposited up to 10 cm of mainly silt) than on the natural levee (up to 30 cm of silt and sand). The 2002 summer flood had a more balanced effect (up to 20 cm of sediments on the bank as well as on the natural levee), on the bank mainly horizontally laminated sand, on levee a complete flood cyclothem (silt–sand–silt) deposited. On the bank sands are mainly subhorizontally laminated, and on the levee, a complete flood cyclothem is found. The last flood event (in 2007) afflicted sedimentation mostly in the close vicinity of the bank (up to 10 cm of sand), and only veneers of finer sediment further away.

The grain-size analysis showed that the composition of the mud, sand, and gravel lithofacies is unimodal, while that of the mud–sand, sand–gravel, and diamictic ones is bimodal, indicating a relatively high variability of sedimentation during floods (Table 3.2). The total amount of new sediments, their texture, and spatial distribution do not only depend on flood discharge but also on the sources of floodwater and sediments in the river system. Independently from the energy of flood flow, overbank alluvia had been mainly transported by *saltation* and to a much lesser extent by suspension. It was also confirmed that the lithofacies of massive sandy mud (FSm), and also gravels with the clast-supported texture (Gm), had been moved by traction alternating with saltation. Traction could only be traced in 4 subtypes of lithofacies of the 12 those studied on the Danube floodplain.

3.5 Conclusions

The behavior of the three rivers studied is governed by a combination of the 'global' laws of floods largely (if not wholly) independent of time and place and of 'local' place and/or time-contingent factors of settings and scales.

The flood response of the Ondava River is manifested in lateral instability and changes in the pattern of channel landforms. In the period 1987–2009, both bank erosion and gravel bar development were intensive, and the maximum channel shift amounted to 217 m. The shares of the individual bar types have been rearranged by floods: in 2002, the lateral bar areas shrank in favor of point bars but increased their areas again in 2009.

For the Topľa River, two flood events (2008 and 2010) caused growth both in channel width and depth. During the flood of 2008, new bars emerged, and total bar area grew 30-fold. The 2010 flood caused lesser transformation compared to the 2008 flood, but predominantly generated channel incision (average extent: 0.33 m; maximum: 0.87 m).

Floodplain vertical accretion (including levee formation) during the flood events 2002 and 2007 dominates the evolution of the Danube floodplain. Two three-unit sequences were correlated with three flood stages. Grain-size analysis helped reconstruct the sediment transport mechanisms of the river during floods. Alluvia with various lithofacies attest to distinctly different shares of transport types, predominantly saltation, traction alternating with saltation, or (for four subtypes of lithofacies) traction.

Acknowledgement This chapter was supported by the Science Grant Agency (VEGA) of the Ministry of Education of the Slovak Republic and the Slovak Academy of Sciences (grant No. 2/0106/12).

References

Allen JRL (1970) Physical processes of sedimentation. G. Allen & Unwin University Books, London, 248 p

Blott SJ, Pye K (2001) GRADISTAT: a grain size distribution and statistics package for the analysis of unconsolidated sediments. Earth Surf Process Land 26(11):1237–1248

Brázdil R, Kirchner K (eds) (2007) Vybrané přírodní extrémy a jejich dopady na Moravě a ve Slezsku (Selected natural extremes and their impacts in Moravia and Silesia). Masarykova univerzita – Český hydrometeorologický ústav – Ústav Geoniky AV ČR, v.v.i., Brno – Praha – Ostrava, 432 p (in Czech with English summary)

Brierley GJ, Fryirs K (2005) Geomorphology and river management. Applications of river styles framework. Blackwell Publishing, Malden, 398 p

Bucała A (2010) Morphological role of floods in the shaping of stream channels in the Gorce mountains (exemplified by Jaszcze and Jamne stream valleys). Geomorphologia Slovaca et Bohemica 10(1):45–54

Corenblit D, Tabacchi E, Steiger J, Gurnell AM (2007) Reciprocal interactions and adjustments between fluvial landforms and vegetation dynamics in river corridors: a review of complementary approaches. Earth Sci Rev 84:56–86

Folk RL, Ward WC (1957) Brazos river bar (Texas); a study in the significance of grain size parameters. J Sediment Petrol/J Sediment Res 27(1):3–26

Fonstad MA (2003) Spatial variation in the power of mountain streams in the Sangre de Cristo Mountains, New Mexico. Geomorphology 55(1–4):75–96

Friedman GM, Sanders JE (1978) Principles of sedimentology. Wiley, New York, 792 p

Hauer C, Habersack H (2009) Morphodynamics of a 1000-year flood in the Kamp River, Austria, and impacts on floodplain morphology. Earth Surf Process Land 34(5):654–682

Hrádek M (2000) Geomorfologické účinky povodně v červenci 1997 na území severní Moravy a Slezska (Geomorphic effects of the July 1997 flood in the North Moravia and Silesia (Czech Republic)). Geografický Časopis 52(4):303–321

Klimek K (1974) The structure and mode of sedimentation of the floodplain deposits in the Wisłoka valley (South Poland). Studia Geomorphologica Carpatho-Balcanica 8:136–151

Klimek K, Malik I, Owczarek P, Zygmunt E (2003) Climatic and human impact on episodic alluviation in small mountain valleys, the Sudetes. Geographia Polonica 76(2):55–64

Lehotský M, Novotný J, Szmańda JB, Grešková A (2010) A suburban inter-dike river reach of a large river: modern morphological and sedimentary changes (the Bratislava reach of the Danube river, Slovakia). Geomorphology 117(3–4):298–308

Miall AD (1996) The geology of fluvial deposits. Springer, Berlin/Heidelberg/New York, 582 p

Miller AJ (1990) Flood hydrology and geomorphic effectiveness in the central Appalachians. Earth Surf Process Landforms 15(2):119–134

Nemčok J (1990) Geological map of the Pieniny, Čergov, Ľubovniansky and Ondavsky Mountains (1:50,000). Dionýz Štúr Geological Institute, Bratislava

Novotný J, Lehotský M, Grešková A (2007) Súčasný morfologický vývoj medzihrádzového priestoru (Dunaj, Bratislava) (Morphological development of the inter-dike space (Danube, Bratislava)). Geomorphologia Slovaca et Bohemica 7(2):72–78

Pišút P (2002) Channel evolution of the pre-channelized Danube River in Bratislava, Slovakia (1712–1886). Earth Surf Process Landforms 27(4):369–390

Solín Ľ (2008) Analýza výskytu povodňových situácií na Slovensku v období rokov 1996–2006 (Analysis of floods occurrence in Slovakia in the period 1996–2006). J Hydrol Hydromech 56 (2):95–115

Svoboda A, Pekárová P, Miklánek P (2000) Flood hydrology of Danube between Devín and Nagymaros. Institute of Hydrology, Slovak Academy of Sciences, Bratislava, 96 p

Ward R (1978) Floods – a geographical perspective. Macmillan, London, 244 p

Wyżga B (1996) Changes in the magnitude and transformation of flood waves subsequent to the channelization of the Raba River, Polish Carpathians. Earth Surf Process Landforms 21(8):749–763

Wyżga B (1997) Methods for studying the response of flood flows to channel change. J Hydrol 198 (1–4):271–288

Zielinski T (2003) Catastrophic flood effects in alpine/foothill fluvial system (a case study from the Sudetes Mountains, SW-Poland). Geomorphology 54(3–4):293–306

Zwoliński Z (1992) Sedimentology and geomorphology of overbank flows on meandering river floodplains. Geomorphology 4(6):367–379

Chapter 4
Extreme Exogenous Processes in the Ukrainian Carpathians

Ivan Kovalchuk, Andriy Mykhnovych, Olha Pylypovych, and Georgiy Rud'ko

Abstract In the Ukrainian Carpathians hydrometeorological and topographical conditions jointly control the geographical distribution of exogenous geomorphic processes. In the region, channel-forming floods occur at daily precipitation intensities of 40–60 mm. Maximum daily amount of precipitation reached 160 mm in 1992 and caused rapid water level rises up to 8.5 m. Similar floods with catastrophic effects happened in 1947, 1957, 1969, 1970, 1980, 1998, and 2001. The main causes of the November 1998 and March 2001 floods were natural hydrometeorological factors reinforced by considerable human impact over the last decades. For landslides 5-year cycles and for mudflows 11-year cycles are observed. Seismic activity also influences landsliding in the Ukrainian Carpathians. The risk of extreme devastation by mudflows is also very high. For dangerous mudflows the precipitation threshold is 30 mm day^{-1}, while disasters only ensue from rainfalls above 100 mm day^{-1} intensity. Types and drivers of movements are identified. During extreme flash floods, significant changes in riverbed morphology have been observed (bank erosion, channel incision, and sediment accumulation). Bank retreat along the Tysa River, particularly at the confluences of major tributaries, reaches rates of 1 m year^{-1} (for the Tereblia confluence even 5 m year^{-1}).

I. Kovalchuk
Department of Geodesy and Cartography, Faculty of Land Use, National University of Nature Use and Life Sciences of Ukraine, Vasylkivs'ka Str. 17/114, 03040 Kyiv, Ukraine
e-mail: kovalchukip@ukr.net

A. Mykhnovych (✉) • O. Pylypovych
Department of Applied Geography and Cartography, Faculty of Geography, Ivan Franko National University of Lviv, Doroshenko Str. 41, 79000 Lviv, Ukraine
e-mail: 2andira@ukr.net; olha@tdb.com.ua

G. Rud'ko
State Commission of Mineral Resources, Kutuzova Str. 18/7, 01133 Kyiv, Ukraine
e-mail: scmr@dkz.gov.ua

D. Lóczy (ed.), *Geomorphological impacts of extreme weather: Case studies from central and eastern Europe*, Springer Geography, DOI 10.1007/978-94-007-6301-2_4,

Keywords Floods • Landslides • Mudflows • Riverbed erosion • Damage • Ukrainian carpathians

4.1 Introduction

The diversity and regional distribution of geomorphic processes active in the Ukrainian Carpathians have been described in several papers recently (Aizenberg et al. 1976; Slyvka 1994, 2001; Holoyad et al. 1995; Kovalchuk 1997; Rud'ko et al. 1997; Kravchuk 1999, 2005, 2008; Kyryliuk 2001; Obodovs'kyi 2000; Kovalchuk and Mykhnovych 2004; Romashchenko and Savchuk 2002; Lymans'ka 2001; Hoshovs'kyi et al. 2002; Rud'ko and Kravchuk 2002; Kovalchuk and Mykhnovych 2004; Problems... 2004; Dubis et al. 2006; Oliferov 2007; Budz and Kovalchuk 2008; Stetsiuk 2010; Kravchuk and Khomyn 2011; Kovalchuk et al. 2008, 2012). Less attention has been paid so far to extreme weather events in the region and their geomorphological impacts (Hoshovs'kyi et al. 2002). This issue would require long-term observations on the intensity of extreme processes in representative areas of different geological environments and basin geosystems (the Precarpathian depression along the southwestern margin of the Eastern European Platform, the Carpathian Mountains, and the Transcarpathian internal depressions).

4.2 Extreme Floods

In the region there is a close relationship between *hydrometeorological* and *topographical conditions*. With 100 m increase of average altitude of the watershed, annual average precipitation grows 68 mm and the coefficient of surface runoff by 0.1; 5% increase in slope angle adds 77.5 mm to surface runoff. The interactions between factors induce dangerous exogenous processes in river basins. Heavy precipitation results in 10- to 100-fold increases in water discharge and flooding. Due to considerable channel slope, flow velocity increases and destruction ensues. Flood flows can move coarse sediments; remodel river beds; destroy buildings, engineering structures, recreation facilities, and communication lines; and trigger landslides, mudflows, rockfalls, and erosion processes on slopes. Heavy rains combined with floods lead to landslides and mudflows of different genetic types and sizes. For instance, the landslide at the village Vilkhivs'ki Lazy with a volume of 40 million m^3 destroyed the village and a mudflow of 12 million m^3 demanded death tolls – among others – in the village Rus'ka Mokra.

In the region floods with significant influence on stream channel morphology occur at *threshold* rainfall *intensities* of 40–60 mm day^{-1}. The maximum daily amount of precipitation (RX1D) reached 160 mm in 1992 and caused rapid water level rises up to 8.5 m. Similar floods with catastrophic effects happened in 1947, 1957, 1969, 1970, 1980, 1998, and 2001 (Lymans'ka et al. 2001).

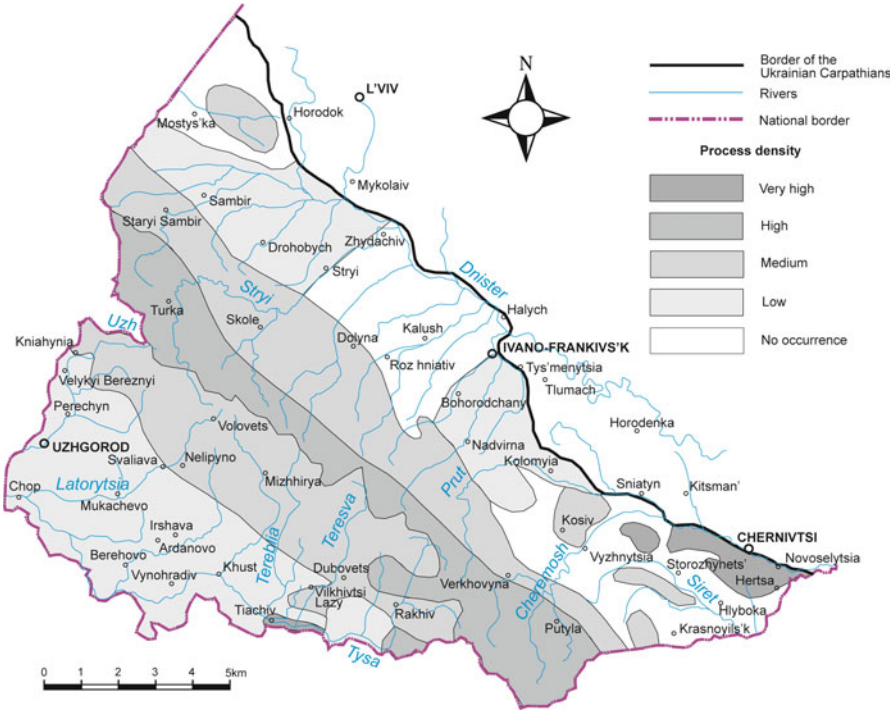

Fig. 4.1 Location of the sites mentioned in the text

In 1992, the Latorytsia River has flooded the city of Mukachevo and destroyed roads, railway, power supply lines, and hydro-engineering structures. The highest flood on the Uzh River near Uzhgorod (452 cm above normal stage) formed under the influence of additional factors: river islands overgrown by trees and bushes have hindered water flow and induced additional water level rise. Water covered the floodplain with buildings, roads, arable lands, and residential houses at 0.5–1.9 m depth. More than 100 settlements and large tracts of agricultural land were flooded, 150 km of roads and more than 2,000 hydro-engineering objects; 250 bridges have been completely or partly destroyed in the Rakhiv, Tiachiv, Khust, Irshava, and Mezhyhirya districts of the Transcarpathian region between Uzhgorod and Rakhiv (Lymans'ka et al. 2001 – Fig. 4.1). After snowmelt and rainfalls, highly saturated soils and rapid water flow have provided excellent conditions for the renewed activity of old mudflows and landslides and generated new ones.

During 1995 in the Tiachiv, Khust, Irshava, and Mezhyhirya districts, large amounts of surface water runoff were generated and caused inundations, damaging 63 houses in the towns of Khust and Irshava (Fig. 4.1). The Tysa (Tisza) and Latorytsia River valleys were inundated at 0.9–3 m depths. This flood resulted in intensive incision, bank erosion, and changes in the topography of the floodplain (Lymans'ka 2001).

The 1998 and 2001 floods produced the highest long-term water levels and geomorphological impacts as a consequence of hydrometeorological conditions (Table 4.1). A weather front and *microcyclones* passing through the Carpathians

Table 4.1 Maximum water levels of the 1998 and 2001 floods compared to the absolute maxima for the period of observation (Boyko and Kul'bida 2001)

	March 2001		November 1998			Long-term period	
River (settlement)	H_{max}, cm	Precipitation on 3–5 March, mm	H_{max}, cm	Precipitation on 3–8 October, mm	Difference between maxima in 1998 and 2001	H_{max}, cm	Date
Latorytsia (Pidpolozzia)	263	110	320	109	−57	388	14 December 1957
Latorytsia (Svaliava)	252	157	304	109	−52	416	1 March 1967
Latorytsia (Mukachevo)	580	72	687	84	−107	687	5 November 1998
Latorytsia (Chop)	750	48	746	44	4	746	6 November 1998
Vecha (Nelipyno)	168	157	239	109	−71	308	14 December 1957
Uzh (Zhornava)	188	63	246	68	−58	296	14 December 1957
Uzh (V. Bereznyi)	425	44	433	49	−8	527	14 December 1957
Uzh (Zarichevo)	422	72	442	73	−20	446	29 January 1979
Uzh (Uzhgorod)	207	42	295	45	−88	350	17 November 1992
Luta (Chornoholova)	149	64	275	–	−126	275	5 August 1998
Turya (Turya Poliana)	270	76	348	–	−78	348	5 November 1998
Turya (Simer)	260	62	320	66	−60	332	23 July 1980

brought heavy rains to the Transcarpathian region on 4–5 November 1998. Over two days, 40–120 mm of precipitation (10% of the annual average) was measured, and the resultant local water runoff generated a very high flood wave. Water levels have exceeded the historical maximum for the Tysa River by 2–25 cm and by 22–68 cm on its tributaries. During the flood of 1998, the floodplains were mostly inundated, and riverbeds were transformed in many places of river valleys due to flow velocities of ca 4–4.5 m s^{-1}.

On 4–9 March 2001, the main driver of flood formation was the large amount and high intensity of precipitation on recently deforested mountain slopes. Then the hydrometeorological situation in the Transcarpathian region was very different from the flood in early November 1998. The summer–autumn season in 2000 was characterized by *precipitation deficit* and lowest water levels. Only after the short- and medium-level winter rains did river flow reach the mean long-term value. Water storage in snowpack during the winter 2000–2001 was 20–30% lower than usual. Soils were wet and did not freeze deeply. On 3–5 March, very heavy and prolonged rains were observed in the Ukrainian Carpathians (110–296 mm precipitation, 15–20% of the annual average). Compared to 3–5 November 1998, this precipitation was 23–90 mm higher almost everywhere in the region. From the intense snowmelt on 3–4 March, watersheds received additional 20–40 mm of water (Boyko and Kul'bida 2001). According to government information, 40,793 buildings were flooded, 2002 destroyed, 21,256 persons evacuated, and 3.57 km of dykes damaged. During the flood, 18 water intake stations stopped to operate; 43.6 km of roads, 0.4 km of railway, and 30 bridges were destroyed; 514.2 km of main national roads and 206.8 km of regional roads and large tracts of agricultural land were flooded; and 18 people were killed (Kyryliuk 2001). Flood levels have 16–38 cm exceeded historical maxima in November 1998 (Boyko and Kul'bida 2001). In 255 settlements, 33,569 buildings were flooded, 1925 were completely destroyed, and 107 settlements were left without power supply. After the flood event 338 landslides, 81 mudflows, and 102 sectors of bank erosion have been detected.

The floods of combined (primarily rainfall) origin, like in March 2001, are typical for the winter hydrological regime of the Tysa River. This flood, however, was characterised by absolute discharge maxima (Boyko and Kul'bida 2001).

The main causes of the March 2001 flood as well as the November 1998 flood were natural hydrometeorological factors *reinforced by* considerable *human impact* over the last decades. Such catastrophic floods are often result from uncontrolled economic activities (especially complete deforestation of slopes) and even channelisation and floodplain development in mountain watersheds over the last 10 years.

The significance of human impact and changes in flood regime can also be confirmed on example of the 1947 flood in the Transcarpathian region. But in spite of similar rainfall intensity and amount, peak discharges were lower in 1947 compared to 1998. Flooded zones and destruction in 1947 were also considerable, but floodwater returned into the rivers parallel with dropping water levels (Boyko and Kul'bida 2001).

4.3 Extreme Landslides

There are ca 6,000 landslides with long history of the alternation of active and inactive periods in the Ukrainian Carpathians. For example, in 1969, a landslide of a volume of 40 million m^3 became active with a catastrophic intensity in the village of Verkhniy Yaseniv (Chornyi Cheremosh River basin – Fig. 4.1). In April 1979, many old landslides were observed to move again in the Precarpathians, destroying more than 500 buildings and engineering structures. They were also triggered by the extreme floods in November 1998 and March 1999. In the Transcarpathian region, more than 400 landslides are active at present.

4.3.1 Landslides within the Precarpathian and Transcarpathian Regions

Within the Precarpathian and Transcarpathian depressions, landslides developed in *molasse* formations, mostly of carbonates and *clays*. The Precarpathians present folded structures replaced by step-block structures in the zone of contact with the platform. In weakness zones the clay masses change their character and become plastic (hydromicas become montmorillonites). Clay beds are potential slip planes for *plastic*, *structural-plastic*, and *structural landslides*. In the decomposed molasse, sediments of the Transcarpathian region salt stocks also occur and salt karst processes operate.

In the southwestern part of the Eastern European platform, terrigenous-carbonate formations appear with karst, gravitational, and erosion processes. Tectonic conditions are defined by block and circular mega- and macrostructures with local earthquakes. Landslides are formed in Neogene clays and karst processes prevail in sulfates and carbonates.

In the Upper Dnister River basin, structural landslides are active on the slopes of high terraces in the Neogene sediments, structural-plastic landslides on the slopes of the Dnister River valley in upper Proterozoic argillites and siltstones, and plastic landslides almost everywhere in deluvial sediments. A representative site is Konivka, on the right bank of the Dnister (Fig. 4.1), with a landslide of $500 \cdot 800$ m area and a volume of moving mass of more than 1.5 million m^3, which became active in 1979–1980. The main trigger of such flow-type landslides is precipitation of extreme intensity following 4–5 years of high moisture content or saturation of sediments (in this particular case 1996–1997 and 2001–2002), raising the groundwater table. Surveying testified that maximum rate of movement occurs along the lower section in spring (15–22 cm $year^{-1}$).

In the Prut (Pruth) River basin, three *types of erosion regime* for hillslope–channel systems have been defined: *erosion damping*, *stable erosion regime*, and *increasing erosion rate*. The first type is presented by the left tributaries of the Prut River with typical flow-type plastic landslides, developed under moist

conditions of clays in the decay zone. Development and activity are controlled by precipitation intensity. The second type is represented by the terrace complexes of the steep right-bank slope of the Prut Valley. Here block-type landslides dominate which are activated at disastrous rate to the influence of multiple groundwater horizons and remarkable human impact (for instance, at Sniatyn, activated at a catastrophic rate in 1977).

In the Precarpathians *man-induced landslides* are especially dangerous. A good example is found in the valley of a left-bank tributary of the Rybnytsia River (between Verkhovyna and Kosiv – Fig. 4.1). Construction activities undercut the slope and upset the gravitational equilibrium. A landslide developed with extrusion of plastic clays, which served as a slip plane, destroyed the road and damaged buildings. On the right-bank slope of the Rybnytsia River valley, sliding and clay extraction led to intensive river bank erosion. The size of the landslide is 500 · 250 m and the depth of deformed sediments is 8–10 m. The rate of movement in the upper part of the slope is 10–15 cm year^{-1}, in the northwestern section 150–200 cm year^{-1}, and in the southeastern (open pit zone) 300 cm year^{-1}. The movement is caused by enduring soil saturation. Maximum activity was observed in 1978–1980.

In the Transcarpathian, internal depression landslides are derived from the decomposition of volcanic rocks. For instance, the old landslide on the left slope of the Uzh Valley near the village of Onkivtsi became active in 1985–1986 and has maintained movement until now. Its length is 750 m, width 950 m, depth 15 m, and total area 500,000 m^2; the height of failure is 5–6 m and the rate of movement is 20–30 cm month^{-1}.

Another example of active man-induced movement is the Kamenets' plastic landslide of ca 15 million m^3 in the piled-up spoil of a gravel pit. It dates from 1974, when, triggered by heavy rainfalls, 300,000 m^3 of too steeply dumped material began to move. In 1988 movement was reactivated due to strong vibration in the open pit. Damage was caused to a road and railway.

One of the largest block-type landslide occurred near the village of Vilkhivtsi (30 million m^3) in autumn–winter 1998 and the largest plastic landslide in the village of Ardanovo (ca one million m^3) in spring 1999 (Fig. 4.1). Another group of major landslides in 1998–1999 was associated with the decay of volcanic rocks in the Vyhorlat-Huta ridge (with volumes of 1.2–1.5 million m^3).

In the Transcarpathian region, ca 850 landslides were active between 1998 and 1999, and 200 more were in the stage of critical equilibrium. When mobilized, slides destroyed more than 200 buildings and threatened more than 300 others. Twelve sections of public roads, two sectors of railway, and one of water pipeline have been damaged (Hoshovs'kyi et al. 2002). The landslides developed in bentonite clays were particularly active. Their length amounted to 1,000 m, width was 300–350 m, and volume 1.5–2 million m^3. Many active landslides in the region are located within the area of Neogene swelling clays and formed under the influence of river undercutting. Deformations usually happen at very slow rates.

4.3.2 Landslides in the Carpathian Mountains

The Carpathian *flysch* is prone to gravitational processes like landslides, rockfalls, and mudflows (see also Chap. 2 by Gorczyca et al., this volume). Here nappes, tectonic zones, and a complicated system of the transversal and diagonal faults with ca 70% of landslides (of 1–70 million m^3 volume) and rockfalls are observed. In the contact zone of sandstones and argillites by loosening and moistening of flysch clay layers of 0.4–4 m thickness are slip planes for structural-plastic landslides. From the 6,000 mapped landslides in the Carpathians, ca 4,000 are located in the high mountains.

A typical example is the landslide on the right bank of the Tereblia River, generated in a *road cut* near the village of Kushnytsia (Fig. 4.1). In the period 1983–1986, there was 473 mm displacement (average intensity: 70–140 mm $year^{-1}$) increasing proportionately to the amount of the precipitation fallen on saturated ground. The loamy sliding mass has a volume of 360,000 m^3.

An example of old stabilized landslides reactivated by *human impact* is in a small river valley west of Kniahynia village (Fig. 4.1). In the period of activity the rate of movement is 5–10 cm $month^{-1}$. The displaced and deformed beds here are 5–20 m thick eluvial, deluvial, and proluvial sediments (mostly clays). The extreme activity of the landslide resulted from snowmelt and rainfalls on 20–22 March 1992. The length of the landslide is 330 m, width is 175 m, average depth 8 m, and volume more than 0.5 million m^3. The rate of the widening of cracks in the upper part of the landslide was 35 mm day^{-1} (between 25 and 30 of March 1992).

A common reason for landslide formation is the *deforestation* of mountain slopes and construction of forest roads for timber transportation. This is exemplified by a landslide near the village of V. Kopania in the Vynohradiv district (Fig. 4.1), where an asphalt road with road cuts was constructed in 1972. A minor depression with a groundwater spring below the road was buried. In autumn 1974, prolonged rains washed 1.5 m deep sediment out from the upper part of the buried depression; the road was flooded by 1.2 m deep water and the depression extended 12–20 m downslope. Road-transport workers have started to build a new road at the distance of 10–15 m removed from the damaged section. Undercutting the slope displaced to the depressed sector increased the pressure on the slide slope, and, consequently, the landslide became active again.

The last period of mass activation of different types of landslides in the region was between autumn 1998 and spring 2001. For instance, during 1998–1999 in the Teresva River basin, three landslides activated in Quaternary sediments in the lower slopes with depth of 1 m and ca 1 ha area each. In 1998, in the watersheds of the right-bank tributaries of the (Velykyi and Sukhyi) Teresva River (Fig. 4.1), eight landslides became active with an overall area of 18 ha and 2–4 m depth. In the Mokrianka River, a set of old slides renewed at the footslopes, and 18 new slides formed with 2–5 m average depth and 0.3–2.0 ha area. Also 22 new and four remobilised old slides have been recorded in the upper part of the Hlybokiy

Potik Stream catchment. Their areas range from 0.12 to 45 ha and depth between 1 and 5 m.

The *largest active landslides* are situated in the Vilkhivchyk River basin (Solotvyno depression – Fig. 4.1). Two of these landslide systems exceed the volume of ten million m^3: one on the right bank of the Vilkhivchyk River with a depth of 30–45 m and a second near Tyshevo village, a large flow slide of smaller depth. The interfluve slides simultaneously in opposite directions. Such landslide systems can only develop in tectonically active zones. There are numerous active landslides in the eastern part of the Solotvyno depression: first of all flow-type movements of in ca $1{,}400 \cdot 500$ m area of deforested and saturated deluvial sediments.

In addition to hydrometeorological conditions, *seismic activity* also influences mass movements in the Ukrainian Carpathians – particularly in the zone of contact between the Pannonian Plate and the Carpathian Mountains or the Carpathians and the Transcarpathian depression. Monitoring testifies that every seismic shock can make stabilised but saturated slide masses to move downslope up to 1–5 mm per event. For instance, 2 years after the 6 M earthquake on March 1977, in April 1979 intensive precipitation (50 mm day^{-1}) coupled with high moisture contents of sediments generated more than 560 slides in the southeastern Precarpathians (Hoshovs'kyi et al. 2002).

4.4 Extreme Mudflows

Intensive rainfalls (above 50 mm day^{-1}) extremely enhance water turbidity in rivers. The water brings much erosion products. *Sediment loads* range from 1,700 g m^{-3} (April 1996) to 2,400 g m^{-3} (May 1993) as opposed to the average turbidity of Carpathian rivers of 3 g m^{-3} in winter and 130 g m^{-3} in spring. The fast-flowing mountain rivers can carry up to 10,000 m^3 of sediments and turn to *mudflows*. The daily sum and distribution area of precipitation are the most significant parameters for mudflow formation. The dangerous *threshold* in the Ukrainian Carpathians is 30 mm day^{-1} and disasters ensue from rainfalls above 100 mm day^{-1} intensity (Lymans'ka 2002). In 2005 a rainfall event of 42 mm (Skole town) and 25 mm (Slavs'ke) induced mudflows in the Butyvlia River basin.

Water–stone mudflows with volumes around 5,000 m^3 are predominant. According to the classification scheme by B. Ivanov (Lymans'ka 2001), three main types are distinguished in the Ukrainian Carpathians: *denudational*, *gravitational*, and *water-accumulational mudflows*. The first type dominates the deforested areas, while the third type mudflows are observed in riverbeds. Gravitational mudflows are rather rare processes in this part of the Carpathians.

By the conditions of their development, they are referred into three classes: *slope*, *riverbed*, *and ravine–gully mudflows*, the first and second classes being predominant (Table 4.2). Third class mudflows are formed under the conditions

Table 4.2 Morphometric parameters of some typical mudflow watersheds within the National Park Skole Beskydy

Catchment name	Dominating types of mudflow forming	Length, m	Area, km^2	Altitude, m		Declination, m
				Source	Mouth	
Butyvlia	Slope and river bed mudflows	16	80	954	560	394
Krasnyi	Riverbed mudflows	3.3	36.3	1,105	607.4	497.6
Gullies and streams	Gully–ravine mudflows	0.45	0.15	710	532	178

of very high-intensity rains. The main source of sediment is erosion in ravines and on tributary gully fans. Such mudflows are formed on 25–35° slopes.

As far as the spatial distribution of mudflows is concerned, most of them are associated with zones of *fault lines* from where over 600–3,400 m^3 km^{-2} year^{-1} of sediment are dislodged. More than 220 mudflow catchments have been identified in the region. Mudflows are triggered by prolonged heavy rains with intensities of ca 0.85–1.25 mm min^{-1}. Usually the volume of solid fraction is 10,000–25,000 m^3, while for 10% of all events, it ranges from 25,000 to 100,000 m^3.

Mudflows are particularly dangerous if they destroy the dams of millponds (e.g., in a left-bank tributary valley of the Teresva River, near Rus'ka Mokra), where three buildings were destroyed by the transport of 25,000 m^3 of clay mixed with large blocks of the deposits.

Today the risk of extreme devastation by mudflows is very high in the region. Extreme mudflows are very often generated by plastic landslides, creating ponds which are the usual source of the liquid fraction of mudflows. After the natural dam is breached, the mudflow has sufficient power to destroy railways, roads, power lines, and buildings.

One of the most representative watersheds for mudflow formation is Svydovets' (north of Rakhiv), built up of medium rhythmic *flysch* with sandstone strata of up to 2 m thickness and the lower of dark gray sandstones. In the valley two colluvial fans are known. In the periods of heavy rainfalls and intensive erosion, rockfalls and other mass movements are active. Heavy rains cause flash floods in the basins with stones carried along the channels, river bed remodeled, and new colluvial fans formed in the valleys.

Mudflows are also induced by the complete *deforestation* of steep slopes, removal of soil cover, undercutting footslopes, and other human activities. In the periods of prolonged rainfalls or snowmelt on the slopes with 35° inclination, soils of 1 m depth are moving slowly (together with the vegetation) towards the river channels and act as sources of material for additional mudflows. Many new mudflow cones are discovered in slope sections used for timber transportation (Figs. 4.2 and 4.3), where turbulent water–stone mudflows dominate with 30% of stone fraction and large woody debris. Mudflows on cleared surfaces are usually observed a year after tree felling. For instance, a destructive mudflow in 1969 in the valley of the right-bank tributary of the Opir River reached a velocity of 3.98 m s^{-1}

Fig. 4.2 The road for timber transport in the deforested Krasnyi watershed on 16 July 2004 (photo by O. Pylypovych)

Fig. 4.3 The fan of the mudflow activated by deforestation of slopes in summer 2004 and a heavy rainfall event on 10 June 2005 (an intensity of 56 mm·day^{-1} recorded at the meteorological station in Oriava) (photo by O. Pylypovych)

and maximum discharge of 44.1 $m^3 s^{-1}$ and built a fan 212 m wide and 36,268 m^3 in volume (Lymans'ka 2001).

During the flood of 1998 on the right-bank slope of the Dubovets' River valley (Fig. 4.1), three mudflows partly destroyed a few buildings and accumulated 1 m of sediment layer over an area of 0.5–0.6 ha. In the Mokrianka and Brusturanka watersheds, 12 mudflows damaged buildings, engineering structures, and also involved a death toll.

4.5 Extreme Riverbed Erosion

During extreme *flash floods* in the Ukrainian Carpathians, significant changes in riverbed morphology have been observed (bank erosion, channel incision, and sediment accumulation). The rates of river *bank retreat* have locally reached 3–5 m $year^{-1}$. One of the most dynamic is the sector of Tysa River between Rakhiv and Khust at the confluences of major tributaries with bank retreat rates of 1 m $year^{-1}$ (for the Tereblia confluence even 5 m $year^{-1}$). Intense bank erosion along the Teresva River has damaged ca 850 m of roads and some buildings.

The length of sections with catastrophic bank erosion sometimes reaches 200–250 m along the Mokrianka River (between Neresnytsia and Pidplesha) and the Tersva, Luzhanka, Tereshul, Bila Tysa, Chorna Tysa, Lazeshchyna, Kosivka, Shopurka, Apshytsia, and other rivers. The width of the eroded zones varies from 2 to 5 m in the headwaters to 10–30 m in the lower river reaches. In the Precarpathian foothills, the Dnister River and its tributaries also show very intensive channel processes. For example, during the high flash flood in 2009 along the Upper Dnister, extreme river bank erosion near Staryi Sambir city completely destroyed ca 200 m of railway line.

4.6 Conclusions

Natural conditions (tectonic and geological structure, relief, precipitation) define the zones and periods of extreme activity of geomorphic processes in the Ukrainian Carpathians. For landslides 5-year cycles and for mudflows 11-year cycles are observed. The most significant triggers of geomorphic processes are human activities in the river basins, often coupled with high seismicity.

Three *landslide types* are defined: structural-plastic (typical for the whole region, developed in decayed and jointed sediment strata intercalated by clay beds as slip planes (volumes are from 40 to 100,000 m^3, rates up to 10 m day^{-1})); structural landslides (on slopes built of (sub)horizontal sediment strata mainly in the contact zone between the Precarpathians and the Eastern European platform, typical is a long preparatory period (up to 70 years) and very sudden activity (rates of

movement up to 15 m day^{-1}; volumes: maximum 30 million m^3)); and plastic landslides (in deluvial deposits (maximum volume: one million m^3)).

For *triggering* effects the following types are defined: (1) undercutting of footslopes and saturation of sediments, (2) saturation and rapid changes in the hydrogeological conditions in unstable tectonic zones, (3) water saturation of sediments on unstable slopes with old landslides, (4) oversaturation of deluvial deposits, and (5) generation of mudflows on steep slopes.

The three main *types of* the *mudflows* are (1) denudational (generated by weathering and sheet wash), (2) gravitational (generated by rockfalls and other mass movements), and (3) accumulational (generated by fan formation, deluvial, proluvial, and colluvial fans).

The most dynamic period of the geomorphic processes in the region was between autumn 1998 and spring 1999, when mudflows and landslides of different origin, volume, intensity, and extent of destruction occurred.

References

Aizenberg M, Ignatenko S, Khloeva E, Yablonskiy V (1976) Mudflows in the Tysa river basin and their quantitative characteristics. Sci Pap Ukr Sci Hydro Meteorol Inst 143:155–161 (in Ukrainian)

Boyko V, Kul'bida M (2001) Hydrologic analysis of the extreme thawing-rain flood in the Transcarpathians on March 2001 and the problems of operative prediction. Hydrol Hydrochem Hydroecol 2:272–278 (in Ukrainian)

Budz M, Kovalchuk I (2008) Geologic-geomorphological classification of mud-flows. Bull Lviv Univ Series Geogr 35:28–33 (in Ukrainian)

Dubis L, Kovalchuk I, Mykhnovych A (2006) Extreme geomorphic processes in the Eastern Carpathians: spectrum, causes, development, activization and intensity. Studia Geomorph Carp Balcan 40:93–106

Holoyad B, Slyvka R, Panevnyk V (1995) Erosion-denudation processes in Ukrainian Carpathians. Ivan Franko University, Ivano-Frankivs'k, 114 p (in Ukrainian)

Hoshovs'kyi S, Rud'ko G, Presner B (2002) Environmental security of technogenous-natural geosystems and catastrophic development of geological processes. Nichlava Publishers, Kyiv, 624 p (in Ukrainian)

Kovalchuk I (1997) Regional ecological-geomorphologic analysis. Institute of Ukraine Studies, Lviv, 440 p (in Ukrainian)

Kovalchuk I, Mykhnovych A (2004) Recent morphodynamical processes in the forested landscapes of Ukrainian Carpathians. Sci Bull Forest Eng Tech Technol Environ State Forestry Univ Lviv 14(3):273–285 (in Ukrainian)

Kovalchuk I, Mykhnovych A, Quast J, Steidl J, Ehlert V (2008) Concepts of the sustainable water use and flood protection in the Upper Dnister Floodplain. In: Roth M, Nobis R, Stetsiuk V, Kruhlov I (eds) Transformation processes in the Western Ukraine – concepts for a sustainable land use. Weißensee Verlag, Berlin, pp 435–444

Kovalchuk I, Kravchuk Y, Mykhnovych A, Pylypovych O (2012) Recent landform evolution in the Ukrainian Carpathians. In: Lóczy D, Stankoviansky M, Kotarba A (eds) Recent landform evolution: the Carpatho-Balkan-Dinaric region, Springer Science+Business Media, Dordrecht, pp 177–204

Kravchuk Y (1999) Geomorphology of the Precarpathians. Merkator, Lviv, 188 p (in Ukrainian)

Kravchuk Y (2005) Geomorphology of the Lump Carpathians. University Publishers, Lviv, 232 p (in Ukrainian)
Kravchuk Y (2008) Geomorphology of the Polonyna-Chornohora Carpathians. University Publishers, Lviv, 188 p (in Ukrainian)
Kravchuk Y, Khomyn Y (2011) Relief of the volcanic bridge of the Ukrainian Carpathians. University Publishers, Lviv, 188 p (in Ukrainian)
Kyryliuk M (2001) Historical floods forming regime in the Ukrainian Carpathians. Hydrol Hydrochem Hydroecol 2:163–167 (in Ukrainian)
Lymans'ka I (2001) Extremely high floods on the Transcarpathian rivers, their types and consequences. Phys Geogr Geomorphol 41:144–149 (in Ukrainian)
Lymans'ka I (2002) Evaluation of the flood-forming rains impact upon the water levels of the Transcarpathians rivers. Hydrol Hydrochem Hydroecol 3:91–97 (in Ukrainian)
Lymans'ka I, Obodovs'kyi O, Kobzystyi S (2001) Synoptic conditions of flood-forming rains in the Transcarpathians. Bull Kyiv Nat Univ Series Geogr 47:41–45 (in Ukrainian)
Obodovs'kyi O (2000) River beds stability evaluation and floods classification of the mountain rivers. Ukraine and the global processes: geographic dimension, vol 2. Luts'k, Kyiv, pp 205–209 (in Ukrainian)
Oliferov A (2007) Mudflows in the Crimea and Carpathians. Tavria, Simferopil, 176 p (in Ukrainian)
Problems... (2004) Problems of the geomorphology and paleogeography of the Ukrainian Carpathians and adjoining areas, Scientific papers. University Publishers, Lviv, 329 p (in Ukrainian)
Romashchenko M, Savchuk D (2002) Water disasters. Carpathian floods. Statistics, causes, regulations. Agrarian Science, Kyiv, 304 p (in Ukrainian)
Rud'ko G, Kravchuk Y (2002) Engineering-geomorphologic analysis of the Ukrainian Carpathians. University Publishers, Lviv, 172 p (in Ukrainian)
Rud'ko G, Yakovliev Y, Ragozin O (1997) Monitoring of the areas of geological processes and natural-technogenous disasters risks calculations. Znannia, Kyiv, 80 p (in Ukrainian)
Slyvka R (1994) Mudflows in the Ukrainian Carpathians and the methods of their regulation. Bull Lviv Univ Series Geogr 19:131–155 (in Ukrainian)
Slyvka R (2001) Geomorphology of the dividing Verkhovyna Carpathians. University Publishers, Lviv, 152 p (in Ukrainian)
Stetsiuk V (ed) (2010) Relief of Ukraine. Slovo Publishers, Kyiv, 689 p (in Ukrainian)

Chapter 5
Flash Flood Analysis for Southwest-Hungary

Szabolcs Czigány, Ervin Pirkhoffer, Dénes Lóczy, and László Balatonyi

Abstract The 15–18 May 2010 flood events on the watershed of the Bükkösd Stream, SW Hungary, are described, their general topographic and hydrologic characteristics are analyzed using the HEC-HMS numeric runoff model, and geomorphological impacts are surveyed. In addition to extreme rainfall volumes, the major reasons found to contribute to extreme impoundment were the fluctuating and locally reduced width of the valley, the confluence of tributaries, which create intermittent bottlenecks for drainage, and high soil moisture contents, which also caused slope instability in deeper soil mantle. Flash flood hazard is closely associated with landslide hazard in upland valleys.

Keywords Extreme rainfall • Flash flood • Numeric modeling • Topographic analysis • Soil depth • Landslides • Hungary

5.1 Introduction

Flash floods are localized phenomena that occur in streams and small river basins with a drainage area of few hundred square kilometers or less usually triggered by extreme rainfall events (Georgakakos 1987; Reid 2004; Lóczy et al. 2011). Flash floods are generated on small temporal and spatial scales. Under favorable environmental conditions, their sudden development and high flow energy make them an efficient geomorphic agent (see, e.g., Gutiérrez et al. 1998).

S. Czigány (✉) • E. Pirkhoffer • D. Lóczy
Institute of Environmental Sciences, University of Pécs, Ifjúság útja 6, 7624 Pécs, Hungary
e-mail: sczigany@gamma.ttk.pte.hu; pirkhoff@gamma.ttk.pte.hu; loczyd@gamma.ttk.pte.hu

L. Balatonyi
Doctoral School of Earth Sciences, University of Pécs, Ifjúság útja 6, 7624 Pécs, Hungary
e-mail: Laszlo.Balatonyi@gmail.com

D. Lóczy (ed.), *Geomorphological impacts of extreme weather: Case studies from central and eastern Europe*, Springer Geography, DOI 10.1007/978-94-007-6301-2_5,

Whereas warning systems for riverine flooding are widely applied all around the world (Davis 2001), flash floods still represent prediction and detection challenges because a successful method for flash flood warning is the *Flash Flood Guidance* (FFG) system, which is operating in the United States since the 1970s (Georgakakos 2006). It is based on the depth of rainfall of a given duration distributed uniformly over a small catchment that is just enough to cause minor flooding at the outlet of the draining stream. The FFG approach is focused on the representation of initial soil moisture contents in a network of small-size catchments. Based on soil moisture estimates, the rainfall depth of a given duration which is able to generate flooding is computed. In other regions, where flash floods are also common (Gaume et al. 2009), there are also numerous efforts implementing FFG (for instance, in the Black Sea and Middle East regions).

Although FFG provides a useful concept that simplifies communication between hydrologists to meteorologists as well as promotes mitigation, it does not predict flash flood timing (Collier 2007). The need for a better prediction in Hungary was also underlined by the May 2010 events (Czigány et al. 2010).

5.2 Objectives

The major goal of our investigations was to describe and analyze the hydrologic characteristics of the flood events of 15–18 May 2010 on the Bükkösd watershed using the HEC-HMS numeric runoff model (USACE 2005) and GIS (Carpenter et al. 1999) to study the significance of topographical setting and soil properties in flood generation and in modifying geomorphic processes. Being flooded several times over the past decades, the Bükkösd Stream is an optimal pilot watershed for hydrometeorological as well as geomorphological studies (Pirkhoffer et al. 2009a, b). The long-term objective of the project, however, is the construction of a real-time operational FFG system for Hungary.

5.3 Study Area

The selected catchment is located in SW Hungary in the western corner of the Mecsek Mountains (Fig. 5.1), in the drainage area of the Drava River (Fig. 5.2). Downstream from the confluence with the Fekete-víz Stream at the village of Bükkösd, the Bükkösd Stream is a typical lowland watercourse, but upstream the western side has hilly and the eastern side low-mountain topography, with locally steep slopes and V-shape valleys – usually the primary contributors to intense runoff and flash floods (Schmittner and Giresse 1996). Upstream of Bükkösd, the stream is fed by five tributaries: the Sormás, Gorica, Kán, Sás, and Megyefa Streams (Fig. 5.1). The total length of the watercourses is 111.26 km, and drainage density is 0.99 km km^{-2} (Table 5.1).

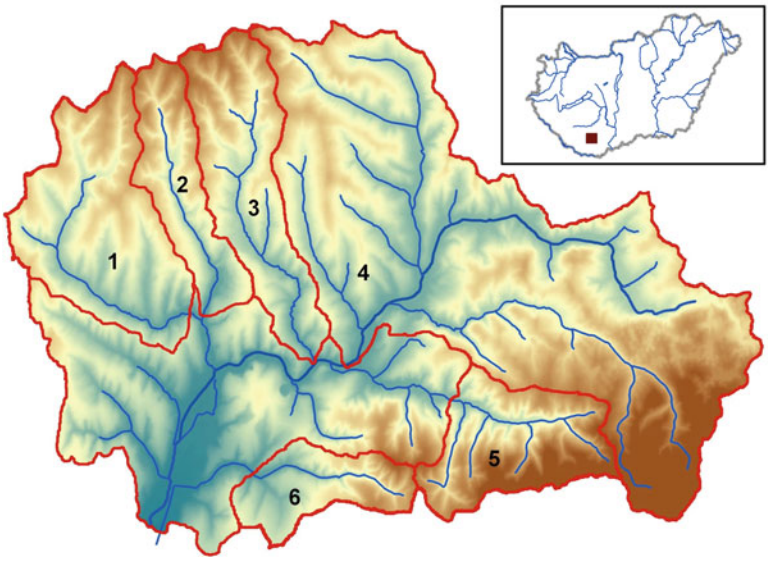

Fig. 5.1 Location and DEM of the Bükkösd Stream watershed with tributaries. *1*, Sormás stream; *2*, Gorica stream; *3*, Kán stream; *4*, trunk stream; *5*, Sás stream; *6*, Megyefa stream

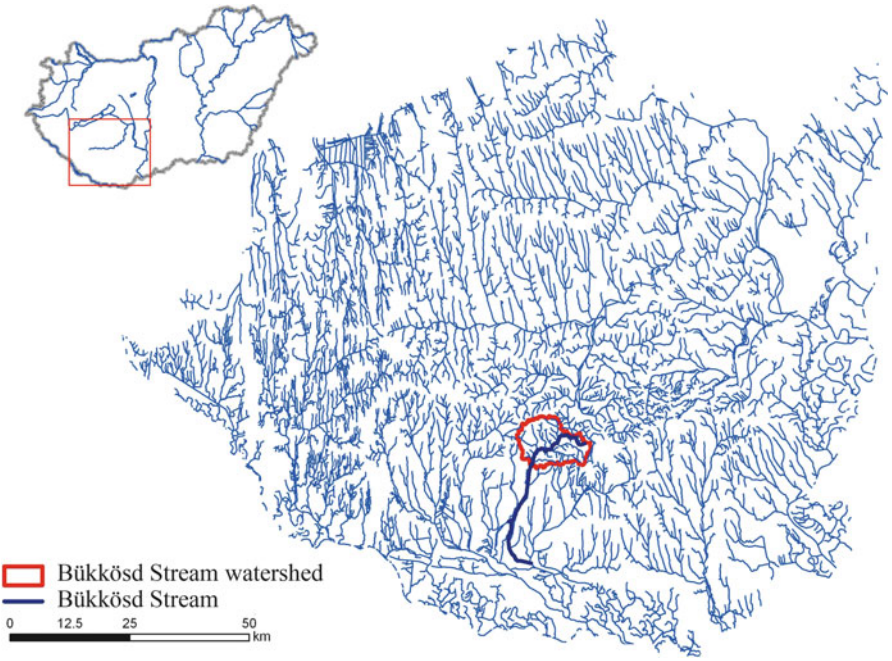

Fig. 5.2 Location of the Bükkösd Stream within the drainage network of Southern Transdanubia (SW Hungary)

Table 5.1 Elevation, stream length, and slope of the tributaries of the Bükkösd Stream

	Bükkösd stream (Bükkösd)	Bükkösd stream (Hetvehely)	Sormás stream	Megyefa stream	Sás stream	Gorica stream	Kán stream
Elevation of source (m)	235	235	221	276	288	247	240
Elevation of confluence (m)	135	157	191	150	181	151	154
Length (m)	13,583	10,751	1,841	3,406	3,182	4,816	6,800
Slope (m/m)	0.0074	0.0073	0.0167	0.0371	0.0336	0.0199	0.0126

Table 5.2 Physical soil types from the AGROTOPO map and our own investigations

	Area (km^2)	
Soil textural type	AGROTOPO map	Corrected from field survey
Sand	None	0.56
Sandy loam	None	8.00
Loam	75.83	81.71
Clay loam	12.35	17.58
Clay	22.96	3.06

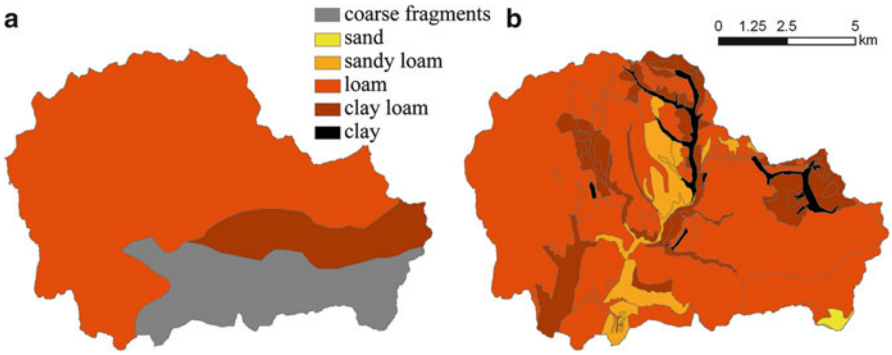

Fig. 5.3 Physical soil types of the Bükkösd Stream catchment based on the AGROTOPO map (soil types: loam; clay-loam; coarse fragments) (**a**) and our own field survey (soil types: sand; sandy loam; loam; clay loam; clay) (**b**)

For flash floods we only studied the upper section of the watershed, an area of 112 km^2 with a perimeter of 69 km and elevations ranging from 127 m (the outflow point) to 609 m (the highest point – Table 5.1). Slope angles range between 0° and 53°. The Mecsek Mountains are built up of sandstones, limestones (in the highest regions of intense infiltration), granite, sands and gravels formations, and loess deposits.

The physical soil type is primarily loam and clayey loam, and soils are classified as Luvisols in the WRB nomenclature (Table 5.2 and Fig. 5.3). To determine runoff/infiltration ratio, we estimated soil depth from the AGROTOPO Hungarian

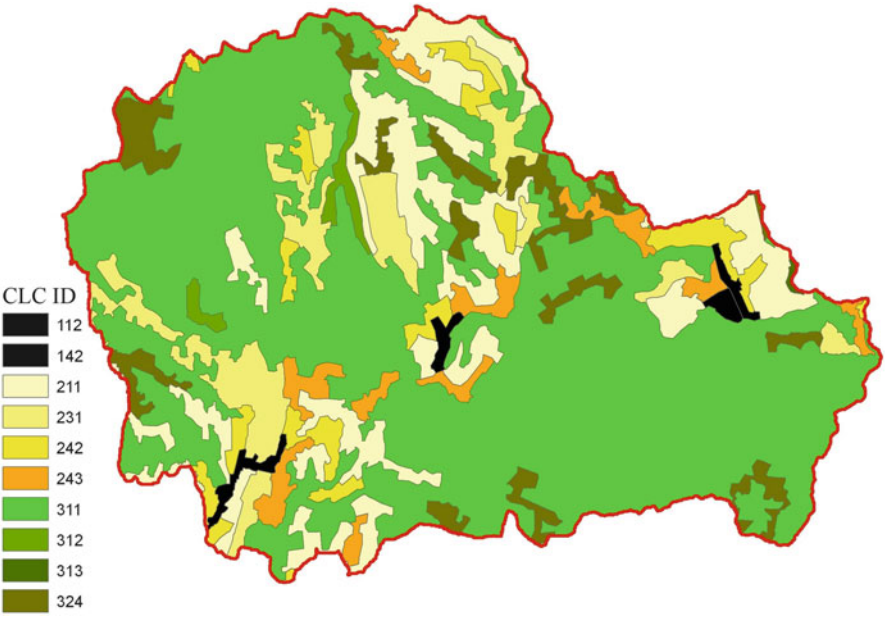

Fig. 5.4 Land use on the Bükkösd Stream catchment (CORINE classes: *112*, discontinuous urban fabric; *142*, sport and leisure facilities; *211*, nonirrigated croplands; *231*, pastures; *242*, complex cultivation patterns; *243*, agricultural land; *311*, deciduous forest; *312*, coniferous forest; *313*, mixed forest; *324*, bush-forest transition)

soil database, developed by the Research Institute for Soil Science and Agricultural Chemistry (RISSAC), Budapest. However, the spatial resolution of the AGROTOPO is insufficient. To improve resolution, we performed detailed soil depth measurement using VES (Vertical Electric Sounding), geoelectric soil resistance, and auger drilling.

The upper catchment of the Bükkösd Stream is heavily forested (68.9%), predominantly by beech (*Fagus sylvatica*) woods. Agricultural land occupies 28.6% and built-up areas 2.3% (Fig. 5.4).

5.4 Flash Flood History

The Bükkösd riverbed incises 2–3 m into its floodplain along most of its length, but locally depth is reduced to less than 1 m. Vegetation in the riverbed (mostly willows) frequently hinder flow. Damages by flash floods have been common, already mentioned in documents from 1733 to 1840 (when one-third of the village Hetvehely was inundated). Streamflow has been measured regularly since 1951 at the Hetvehely automated stream gage. Since then seven notable flood events happened on 1 July 1954, 31 July 1959, 10 July 1967, 6 May 1987, 27 June 1987, and 16 May 1996.

All floods were generated by extremely intense, *convective rainfall* coupled with relatively *high soil moisture* contents (Vass 1997). In all cases, the measured daily precipitation exceeded 60 mm, although estimated rainfall duration ranged between 1 and 3 h for the six flood events. Times of concentration (1–5 h) were relatively short in all cases, allowing a very limited time for prevention and evacuation. Due to their environmental settings, floodwater was the deepest at Hetvehely and Bükkösd. Two major reasons contribute to extreme impoundment there: (1) reduced and fluctuating valley width and (2) the confluence of the Bükkösd Stream and the Hétméhevölgy, Nyáras, and Okorvölgy Streams. Valley width ranges between a few meters to 200 m upstream of Bükkösd, where it broadens to 800–900 m.

For the two aforementioned reasons, flood levels increase very rapidly at Hetvehely: for instance, in 1996 the rising limb of the hydrograph lasted for a mere 6 min, while the falling limb lasted for 3–3.5 h. Over the 27 June 2007 flood event, flood level increased by 1 m in 10 min. In at least two cases, at peak discharge values, water level was about 4 m above the stream bed (as on 10 July 1967 and 27 June 1987). Locally the riverbed in the village lies 2.5–3 m below the surrounding floodplain (or bordered by manmade levees of about the same height). In the past decades, floods of increased frequency were reported for the Bükkösd catchment, explained by (1) the increasing frequency of extreme rainfall events and (2) increasing urban development in the study area. With a growing area of sealed surfaces (which implies enhanced runoff and depleted infiltration), springing from increased development of the floodplain and low terraces, the potential impacts of flash floods are expected to be even more serious in the future.

5.5 Collection of Field Data

5.5.1 Hydrometeorological Monitoring

The Bükkösd Watershed has been relatively extensively monitored, primarily hydrologically, and to a lesser degree meteorologically, since 2000 (Fig. 5.5). Detailed meteorological data are provided by an automated meteorological station located at the outflow point of the Sás Stream.

The aftermath of the 2010 rainfalls were studied along the Sás Stream, located in the SE section of the Bükkösd catchment (Fig. 5.1) since September 2010. One section (the Pósa Valley) with an area of 1.7 km^2 is currently monitored by 11 *hydrometeorological stations* (Fig. 5.6). Each station is equipped with soil moisture and temperature sensors, a rain gage, and a data logger. Data are collected in 10 min intervals, but during thunderstorms in every minute. The Pósa Valley is also equipped with a stream gage at the outflow point (Fig. 5.6).

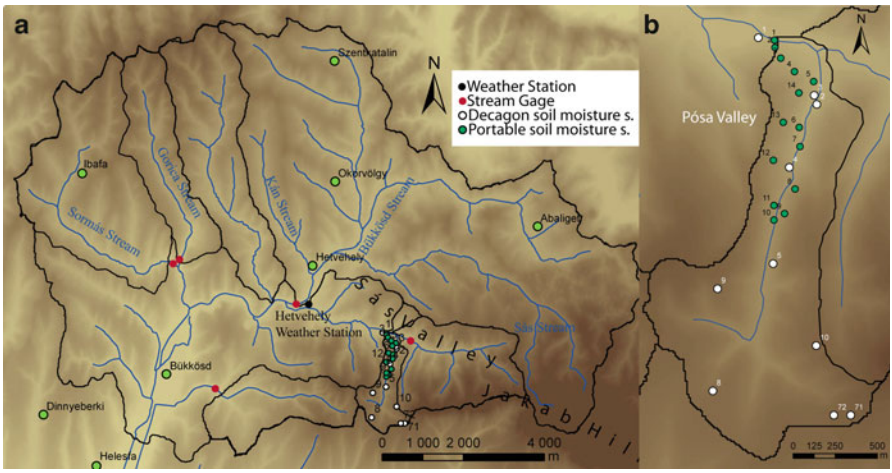

Fig. 5.5 Location of stream gages, the met station and soil moisture measurement sites in the Bükkösd Watershed

5.5.2 *Measuring Soil Depth*

To determine soil depth, we used one-dimensional *vertical electrical sounding* (*VES*) (RESP-12 geoelectrical system with Schlumberger electrode arrangement). Where the current reaches the bedrock, a major drop in resistivity is expected. VES measurements were taken at 190 points in a 50 · 50 m grid (Fig. 5.7), supplemented with 9 borehole drillings to allow detailed soil depth mapping The deepest soil profiles are found in the accumulation zones (Fig. 5.8). To obtain soil depth data, we also applied KUBOTA KCR121R type hydraulic drilling with 125 mm diameter spiral auger or a manual Stihl BT 360 auger with 60 mm diameter spiral drill. The VES and the drilling data show a relatively good correspondence (Table 5.3). The VES results clearly indicate a marked lower topsoil boundary, important for flash flood contributing interflow as well as for the formation of landslide slip planes (Fig. 5.9).

According to the AGROTOPO database, topsoil depth on the Bükkösd catchment ranges between 0 and 40 cm. Our field survey, however, indicates much deeper soil profiles locally, pointing to higher rainwater retention capacity and, at the same time, higher landslide hazard.

5.5.3 *Soil Particle Size Distribution*

Soil particle size distribution was determined by *static light scattering*; analyses were using a Fritsch Analysette Pro22 instrument. Silt content ranges between 75 and 90% without major fluctuations.

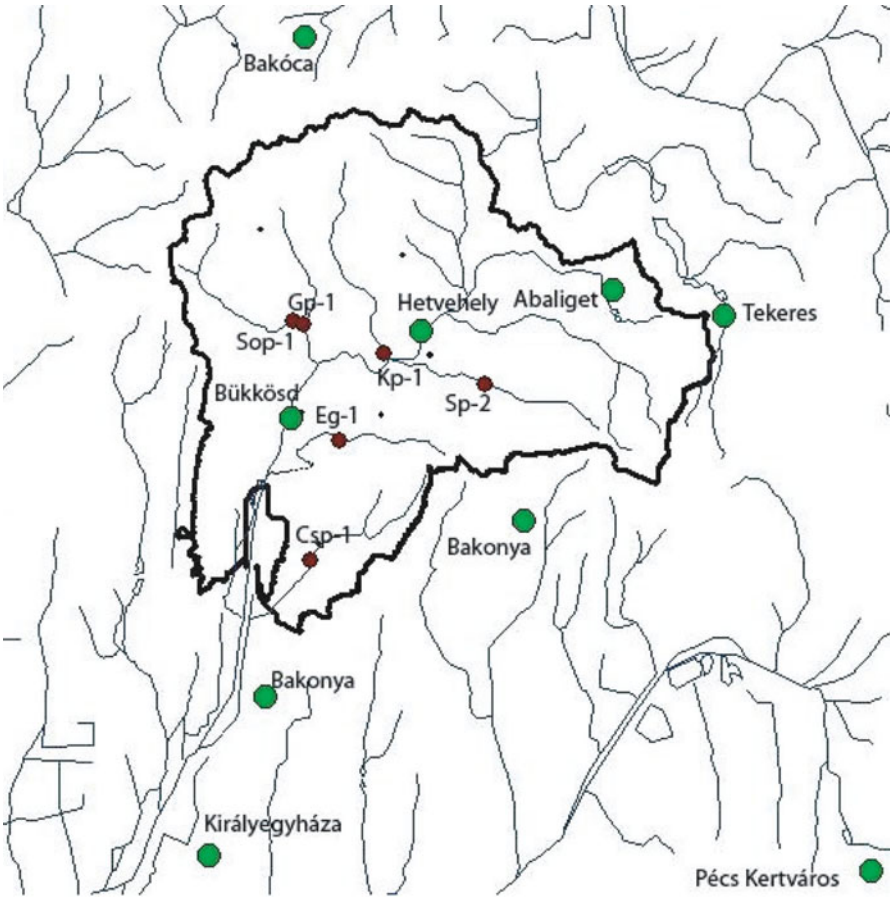

Fig. 5.6 Monitoring sites in the Pósa valley as of 30 September 2011

5.6 Analysis of the May 2010 Event

Annual rainfall in the region indicates high annual variability, as a typical consequence of continental climate. The Bükkösd Stream also has a variable, primarily rainfall-affected flow regime with a highest discharge of 8.8 $m^3\ s^{-1}$ at Hetvehely between 1 January 2000 and 31 December 2010 and increasing temporal frequency of high stages in the second half of the observation period (DDKÖVIZIG 2010).

The precipitation observed in May 2010 considerably exceeded the long-term mean value (Fig. 5.10). Extreme daily precipitations were observed on 16 and 17 May, triggered by a Mediterranean cyclone, while for 7 days equaled or exceeded the long-term daily average during the period of 10–31 May. Cumulative rainfall in this period reached 155.7 mm at Hetvehely. Compared to torrential thunderstorms, however, mean rainfall intensity remained relatively low, 0.33 mm h^{-1}.

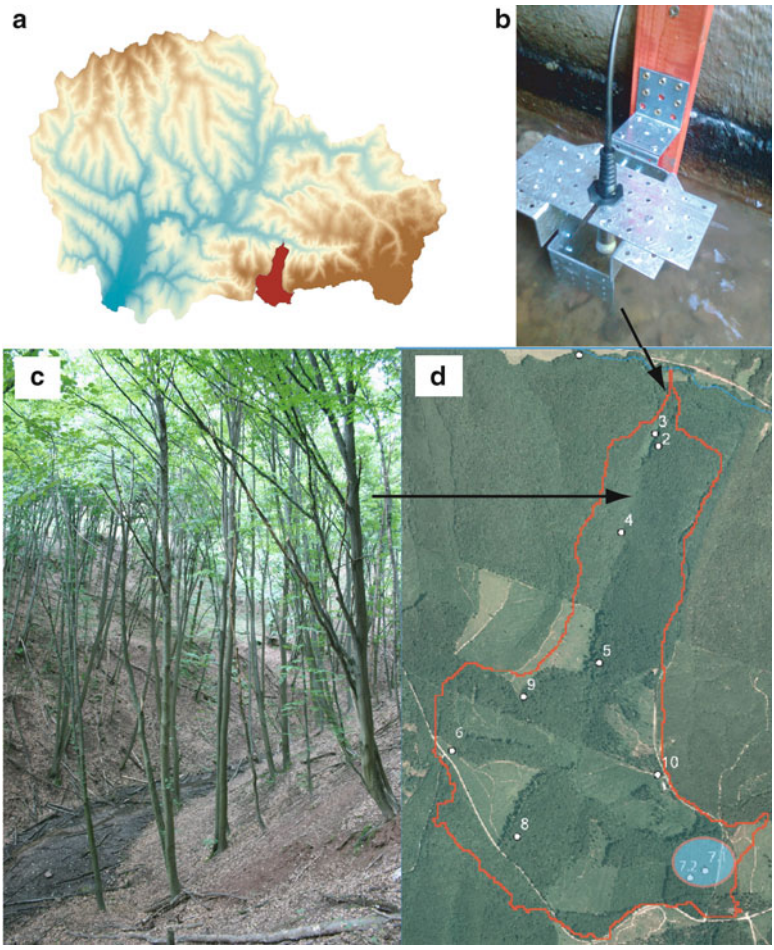

Fig. 5.7 VES soil depth and resistivity results in the southern corner of the Pósa valley (**a**) with instrument (**b**), valley view (**c**) and measurement sites (**d**)

The second highest and most prolonged flood wave for the period 2001–2010 (only surpassed in 2005) was generated on the stream (Fig. 5.11). The first peak was shortly followed by a second, somewhat higher (8.3 $m^3 s^{-1}$) on 1 June 2010, due to the high soil moisture content. The daily range of discharge was also at its observed maximum.

As part of the hydrologic modeling, the first flood peak (of 16 May) was selected for the separation of *baseflow* from *direct runoff* (Fig. 5.12). The inflection point at the rising limb of the hydrograph marks the start, while that at the falling limb the end of direct runoff. In between baseflow was estimated through linear interpolation (Fig. 5.12). Times of concentration were established for the tributary streams (Table 5.4). The parameters length (L) and slope (S) were calculated from the DEM.

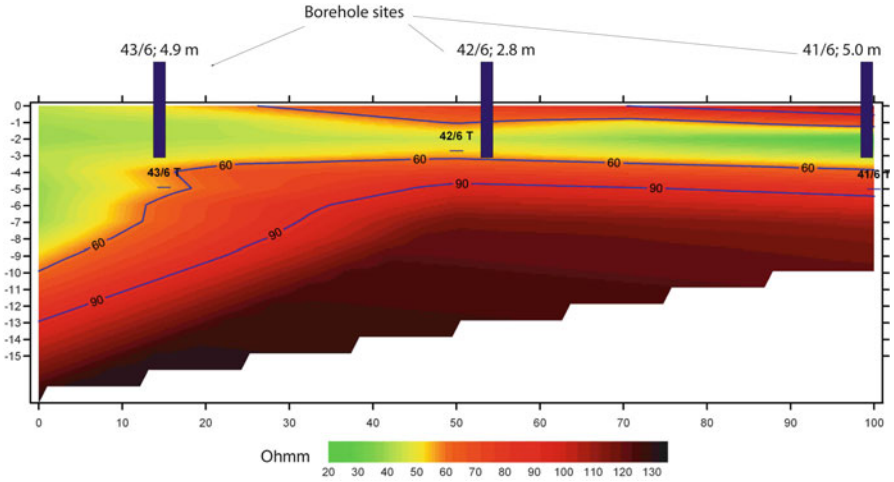

Fig. 5.8 Soil depth map with the sites of VES measurements in the Pósa valley

Table 5.3 VES and drilling based soil and unconsolidated sediment depths measured in the Pósa valley

Borehole ID	Borehole diameter (mm)	Soil depth from drilling (m)	Soil depth from VES (m)
MÉV 5056	n.a.	8	n.a.
MÉV 5043	n.a.	9.8	n.a.
MÉV 5026	n.a.	8.9	n.a.
V41/6	125	5.0	4.9
V42/6	125	2.8	3.1
V43/6	125	4.9	5.7
S1/1	60	2.0	2.1
S1/2	60	1.4	1.6
S1/3	60	2.2	2.1
S1/5	60	1.2	1.5
S1/6	125	1.2	1.0
S1/7	125	3.3	2.9
	Mean:	2.66/4.231	2.76

As actual soil moisture is a decisive factor in flash flood generation (Norbiato et al. 2008), we have defined four pre-event soil moisture wetness classes (very dry, dry, wet, very wet) that correspond to four different initial soil conditions, based on the length of the dry (rainless) period prior the selected precipitation/flood event (Fig. 5.13). The influence of initial soil moisture conditions is evident from Fig. 5.14, too.

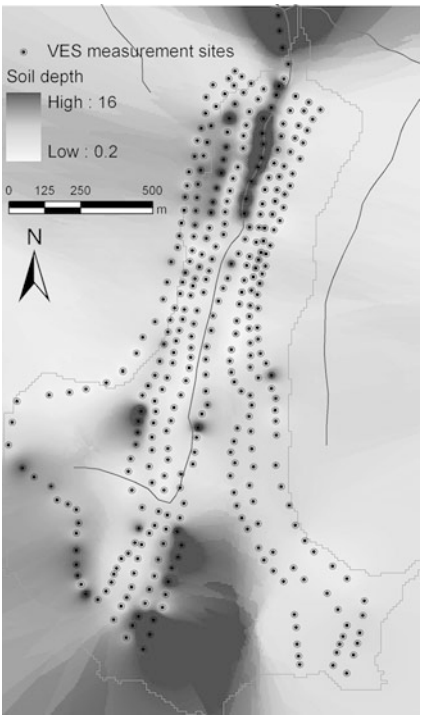

Fig. 5.9 Soil depth as depicted by the VES measurement

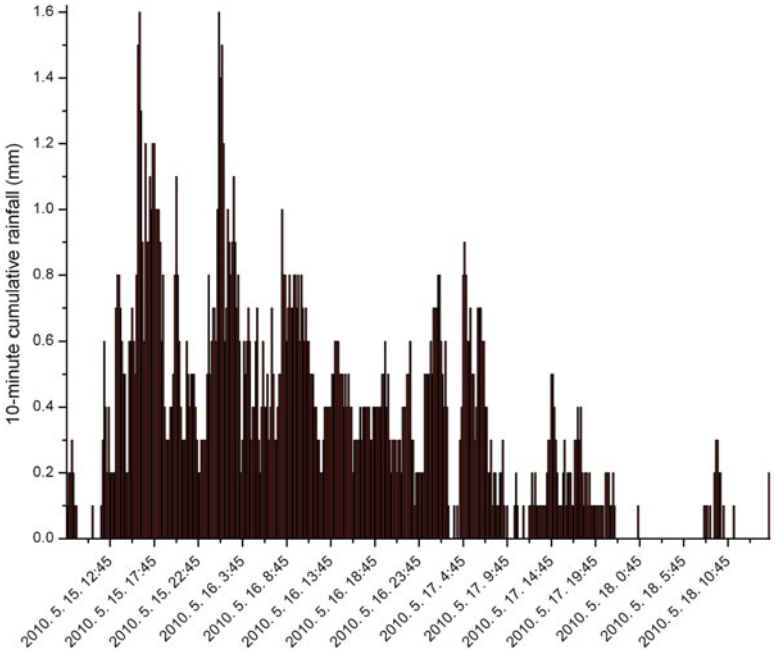

Fig. 5.10 10-min cumulative rainfall totals observed between 15 and 18 May 2010

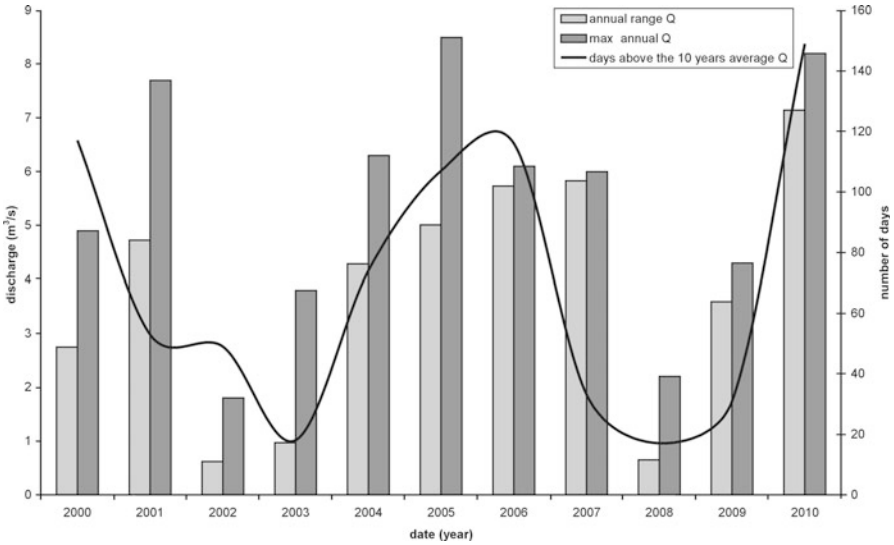

Fig. 5.11 Annual discharge, its range, and number of days when peak flow exceeded the mean flow of the period between 2000 and 2010. *Line* indicates daily variation (the difference between daily minimum and maximum flow)

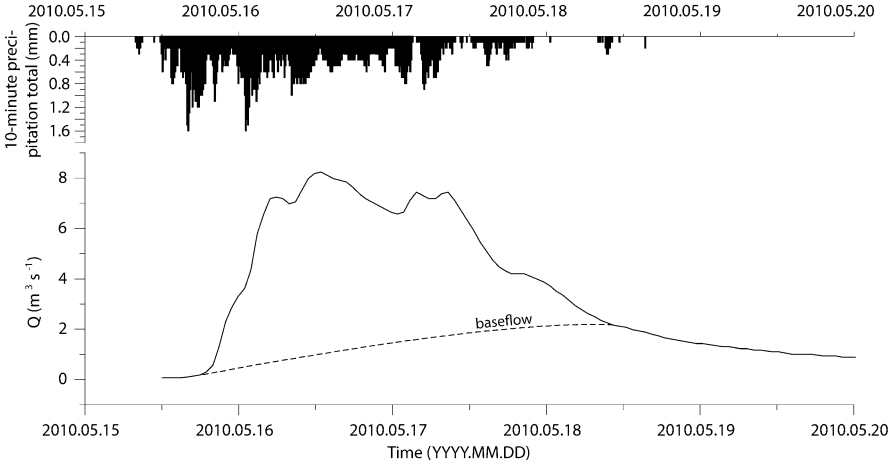

Fig. 5.12 10-min cumulative precipitation and stream discharge at Hetvehely between 15 and 20 May 2010

Table 5.4 Measured and calculated topographic data and time of concentrations for the subcatchments of the Bükkösd stream

Streams	L	h_{max} (m)	h_{min} (m)	Distance (m)	S	T_c (h)
Gorica	1,550	340	156	4,816	0.034074	2.728997
Sormás	2,250	336	156	4,518	0.025899	4.54383
Kán	2,250	338	159	6,800	0.025645	4.566328
Bükkösd (Hetvehely)	4,600	600	159	10,751	0.046915	6.902173
Sás	1,300	437	196	3,182	0.066944	1.632937
Megyefa	1,150	360	158	3,406	0.055041	1.593084

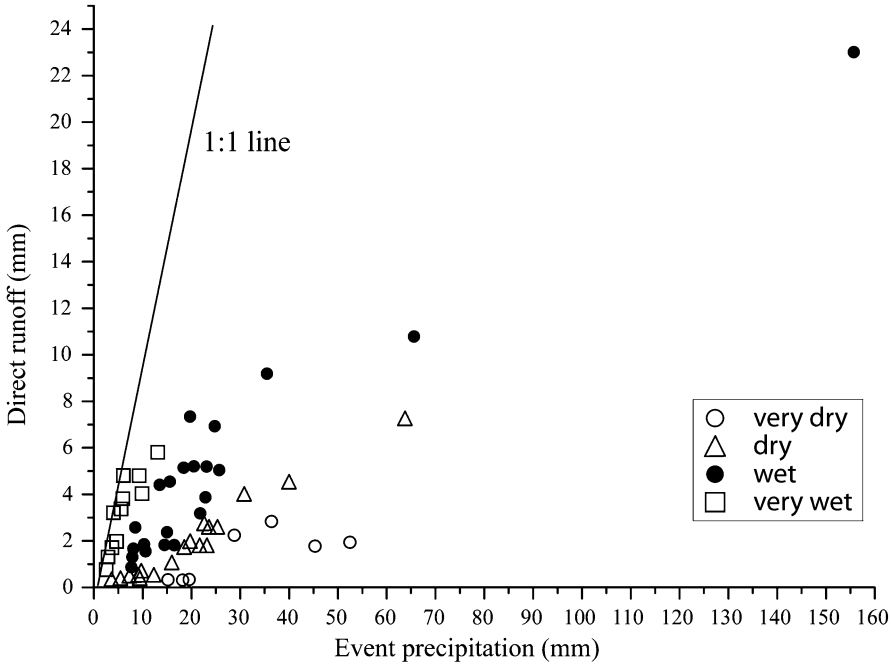

Fig. 5.13 Precipitation/direct runoff relationship for data measured at Hetvehely. Symbols indicate soil moisture conditions prior to the flood events

5.7 Geomorphological Impacts

The detailed Digital Elevation Model and the valley cross sections constructed for the HEC-RAS model (the quasi-natural thalweg determined from them) can also be used for the identification of landslide-prone sites. Superimposed with the map of soil depths, the map of slope angle classes indicates sufficient relief for landsliding. On the Bükkösd Stream watershed, the probability of *slope instability* is highest in the Sás Valley, where at least one actually occurred during the wet period of

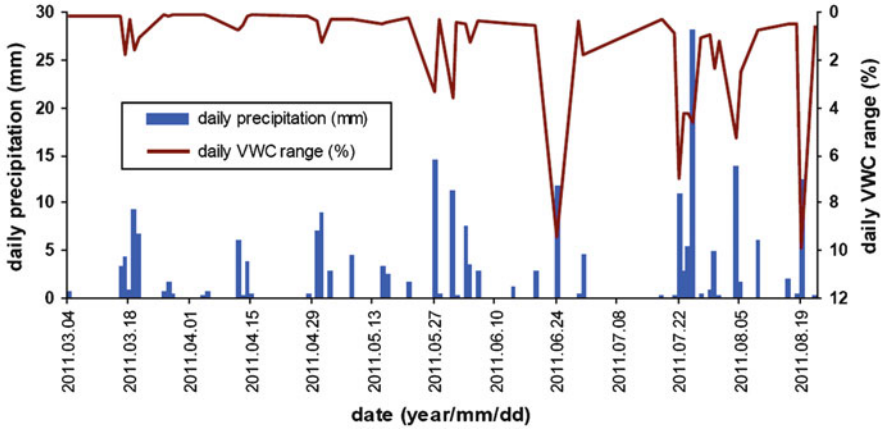

Fig. 5.14 Changes in the daily range of volumetric soil moisture contents (VWC) as a function of daily cumulative precipitation

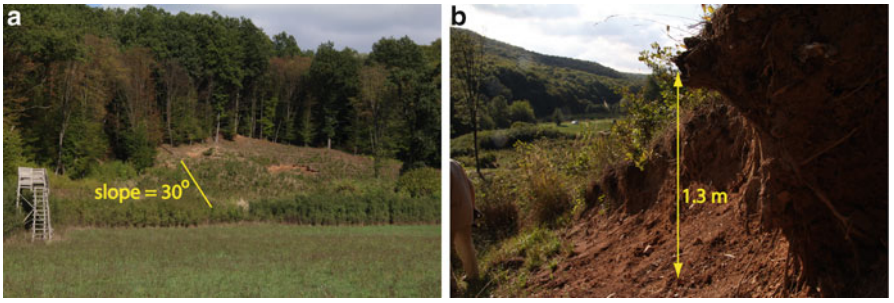

Fig. 5.15 The Pósa Valley landslide. (**a**) Downhill slope gradient in the immediate vicinity of the landslide; (**b**) lateral height on the eastern side of the landslide (Photos by L. Balatonyi taken on 3 October 2012)

May–June 2010. The head scarp of the *slump* is 12 m wide and 1.3 m high, its length is 40 m, maximum depth is estimated at 4.5 m, and its tongue rises 1.5–3 m above the neighboring terrain (Fig. 5.15). The main factors responsible for landslide development here may be (a) high rainfall totals in a short period of time, (b) clay-rich subsurface horizons, (c) steep slopes, (d) lack of slope-stabilizing tree root system, and (e) stream incision and undercutting.

Precipitation totals in the valley reached, about 154.5 and 106.7 mm during 15–18 May and 29 May to 4 June 2010, respectively. *Rainfall* data were recorded at the automated weather station 600 m to the west at western tip of the Pósa Valley. The mean rainfall intensity however remained low throughout the 3-day precipitation event, averaging 0.302 and 0.115 mm in 10 min, respectively. Due to lack of interception, however, the excess amount of water infiltrated into the subsurface

triggered mass movement. The most probable date of occurrence for the slump is 24 June or 22 July, when, after a dry spell, soil pores were filled up again with rainwater and, at the same time, river undercutting became more intense.

The landslide developed on Luvisols (forest soils with clay illuviation). Thirteen borehole drillings were deepened ca 1.5 km to the SE from the site of the landslide, under similar topographical and vegetation conditions to that of the landslide. Silty loam texture prevails in 12 A-horizon soil samples, while one sample falls into the clayey loam category. Silt (2–63 μm) is the predominant particles size in all A-horizon samples. Clay contents in the A-horizon (0–40 cm) are usually less than 10% by mass, while sand fraction present at 10% or slightly higher as a weathering product of the local parent material of sandstone. However, significant *clay illuviation* is observed in the B horizons of the borehole soil samples, at a depth of about 1.2–1.6 m, where clay percentage reaches 20% by mass.

The landslide evolved on a 30° *slope* at a relatively new clear-cut site downhill from a densely forested part of the valley, dominated by hornbeam and beech. The rapidly *incising* Sás Stream, which drains the Pósa Valley ca 20 m to the south of the terminus of the landslide toe, may have also contributed to the generation of the landslide. In general it can be claimed that the increasing development areas with sealed surfaces (implying enhanced runoff and depleted infiltration) on the floodplain and low terraces, the potential impacts of flash floods are expected to be more serious.

Acknowledgement The project was financed within the framework of the Integrated Approach to Flood Risk Management (INARMA) program for Central Europe (European Union Regional Development Fund). The research was also supported by the grant of Developing Competitiveness of Universities in the South Transdanubian Region (SROP-4.2.1.B-10/2/KONV-2010-0002).

References

Carpenter TM, Sperfslage JA, Georgakakos KP, Sweeney T, Fread DL (1999) National threshold runoff estimation utilizing GIS is support of operational flash flood warning systems. J Hydrol 224(1):21–44

Collier C (2007) Flash flood forecasting: what are the limits of predictability? Q J R Meteorol Soc 133(622A):3–23

Czigány S, Pirkhoffer E, Fábián SÁ, Ilisics N (2010) Flash floods as natural hazards in Hungary, with special focus on SW Hungary. Riscuri şi catastrofe (Cluj-Napoca, Romania) 9(8):131–152

Davis RS (2001) Flash flood forecast and detection methods. Meteorol Monogr Am Meteorol Soc 28:481–526

DDKÖVIZIG (2010) Az esőzések miatt kialakult helyzet Dél-Dunántúlon (The situation caused by heavy rainfall in Southern Transdanubia). South-Transdanubian Directorate for Environmental Protection and Water Management, Pécs. http://www.ddkovizig.hu/magyar/hirek/az_esozesek_miatt_kialakult_helyzet_del-dunantulon (in Hungarian)

Gaume E, Bain V, Bernardara P, Newinger O, Barbuc M, Bateman A, Blaškovičova L, Bloschl G, Borga M, Dumitrescu A, Daliakopoulos I, Garcia J, Irimescu A, Kohnova S, Koutroulis A, Marchi L, Matreata S, Medina V, Preciso E, Sempere-Torres D, Stancalie G, Szolgay J, Tsanis

I, Velascom D, Viglione A (2009) A compilation of data on European flash floods. J Hydrol 367(1):70–78
Georgakakos KP (1987) Real-time flash flood prediction. J Geophys Res 92(D8):9615–9629
Georgakakos KP (2006) Analytical results for operational flash flood guidance. J Hydrol 317 (1–2):81–103
Gutiérrez F, Gutiérrez M, Sancho C (1998) Geomorphological and sedimentological analysis of a catastrophic flash flood in the Arás drainage basin (Central Pyrenees, Spain). Geomorphology 22(3–4):265–283
Lóczy D, Czigány Sz, Pirkhoffer E (2011) Flash flood hazards. In: Kumarasamy M (ed) Studies on water management issues. InTech Publications, Rijeka, pp 27–52
Norbiato D, Borga M, Degli Esposti S, Gaume E, Anquetin S (2008) Flash flood warning based on rainfall thresholds and soil moisture conditions: an assessment for gauged and ungauged basins. J Hydrol 362(3–4):274–290
Pirkhoffer E, Czigány Sz, Geresdi I (2009a) Impact of rainfall pattern on the occurrence of flash floods in Hungary. Zeitschrift für Geomorphologie 53(2):139–157
Pirkhoffer E, Czigány Sz, Geresdi I, Lovász Gy (2009b) Environmental hazards in small watersheds: flash floods – impact of soil moisture and canopy cover on flash flood generation. Riscuri şi catastrofe (Cluj-Napoca, Romania) 7(5):117–129
Reid I (2004) Flash flood. In: Goudie AS (ed) Encyclopedia of geomorphology, vol 1. Routledge, London, pp 376–378
Schmittner KE, Giresse P (1996) Modelling and application of the geomorphic and environmental controls on flash flood flow. Geomorphology 16(4):337–347. doi:10.1016/0169-555X(96)00002-5
USACE (2005) Hydrologic modeling system HEC-HMS. User's manual, version 3.0.0. US Army Corps of Engineers Hydrologic Engineering Center, Davis
Vass P (1997) Árvizek a Bükkösdi-patak felső szakaszán (Floods in the headwaters of the Bükkösd stream). In: Tésits R, Tóth J (eds) Földrajzi tanulmányok a pécsi doktoriskolából I. Bornus Nyomda, Pécs, pp 261–285 (in Hungarian with English summary)

Chapter 6
Extreme Weather and the Rivers of Hungary: Rates of Bank Retreat

Timea Kiss, Viktória Blanka, Gábor Andrási, and Péter Hernesz

Abstract In 2010, extreme flood events occurred on several rivers of the Carpathian Basin, especially on catchments which are open to the south. On the studied Hernád and Tisza Rivers, a couple of significant flood waves occurred; on the Hernád River, a new maximum water stage was even recorded. In contrast, no significant flood was measured on the Dráva River, which has a catchment opening towards the east and where several reservoirs impede flow. Consequently, on the Hernád and Tisza Rivers bank retreat was intensive, two or three times larger in 2010 than in the previous or in the following years. Floods particularly accelerated bank retreat along sections where bank height is low and bank material has low resistance. In the case of high bluffs, mass failure also contributes to bank erosion, and thus, the process of undercutting and the removal of the toe material during medium- and low-stage periods are influential in bank retreat.

Keywords Extreme precipitation • Flood wave • Bank retreat • Rate of erosion • Hernád River • Tisza River • Dráva River • Hungary

6.1 Introduction

Bank erosion is a complex process controlled by the interaction of several factors, including hydrological parameters and mechanical properties of bank material. Vegetation also influences the stability and resistance of banks.

The variability of water level and the time elapsed between *floods* significantly affect the rate of bank erosion. Hughes (1977) found that, although sediment

T. Kiss (✉) • V. Blanka • G. Andrási • P. Hernesz
Department of Physical Geography and Geoinformatics, University of Szeged,
Egyetem u. 2-6, 6722 Szeged, Hungary
e-mail: kisstimi@gmail.com; blankav@gmail.com; andgab86@gmail.com;
herneszpeti@gmail.com

D. Lóczy (ed.), *Geomorphological impacts of extreme weather: Case studies from central and eastern Europe*, Springer Geography, DOI 10.1007/978-94-007-6301-2_6,

removal and bank retreat also take place during monthly moderate flows, the most intensive bank erosion and channel changes are associated with peak floods with a 1.5-year return period. Fluvial entrainment and bank collapse are also influenced by the antecedent precipitation conditions. The most critical conditions of strength reduction are prolonged precipitation events, snowmelt and rapid drawdown after a high flow stage, because cohesive materials become more erodible when wet. The increased *saturation* causes strength reduction and increased unit weight. However, according to Luppi et al. (2009), the duration of moderate erosive flows, rather than peak discharge, is decisive for fluvial erosion.

The stability of composite *bank*s (coarse-grained beds overlain by fine-grain *material*) is controlled by the stability of the less cohesive basal layer (Brierley and Fryirs 2005). Desiccation plays a role in the erosion of banks of high clay content. When the bank material dries out and becomes cracked and loose, aggregated material falls from the bank (Thorne 1982).

The type, spatial structure, health and age of the *vegetation* also influence bank erosion (Hickin 1984; Simon and Collison 2002). Dense vegetation and roots can reduce sediment entrainment by one or two orders of magnitude. However, Mastermann and Thorne (1992) observed that the effect of vegetation is only significant if the channel width/depth ratio is less than 12. The spacing and pattern of trees control the impact on flow resistance. Although trees can increase flow velocity and cause heavy turbulence, they most often hinder flow in the bank zone. In addition, the weight of the biomass and the power impulses of wind on trees can decrease the stability of the bank (Mastermann and Thorne 1992, 1994). Hickin and Nanson (1975) recognised that the rate of bank erosion is generally decreasing with increasing *bank height*, because a larger amount of material must be eroded and transported per unit time to maintain the rate of bank retreat.

The aim of this research was to analyse the rates of bank retreat for some rivers in Hungary in an extremely wet year of 2010, compared to long-term rates, to reveal regional variations and local influencing factors.

6.2 Precipitation Conditions in 2010

In the whole Carpathian Basin, 2010 was an extremely wet year, with annual precipitation 69% higher than the long-term average (www.met.hu/eghajlat/visszatekinto/elmult_evek/2010/csapadek/). In March and October, rainfall was less than the monthly, in all the remaining months; however, precipitation was 20–180% above the long-term average. The rainfall in May and June (Fig. 6.1) was the highest since the beginning of observations in 1901 (Ujváry 2010).

Between 15 and 18 May, 2010, a *cyclone* transported wet air from the *Mediterranean* region towards north (Ujváry 2010; Chap. 1, Bartholy and Pongrácz, this volume). In the catchments of the Hernád and Bodrog Rivers, North Hungary, rainfall amounts exceeded 100 mm (Horváth et al. 2010a). Two weeks later, on 31 May, another cyclone had arrived into the Carpathian Basin causing also notable

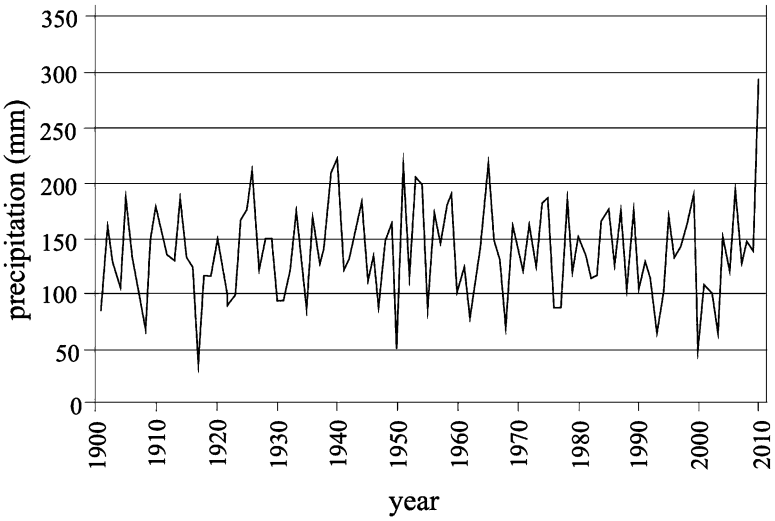

Fig. 6.1 Precipitation totals for May and June in Hungary, 1901–2010 (after Ujváry 2010)

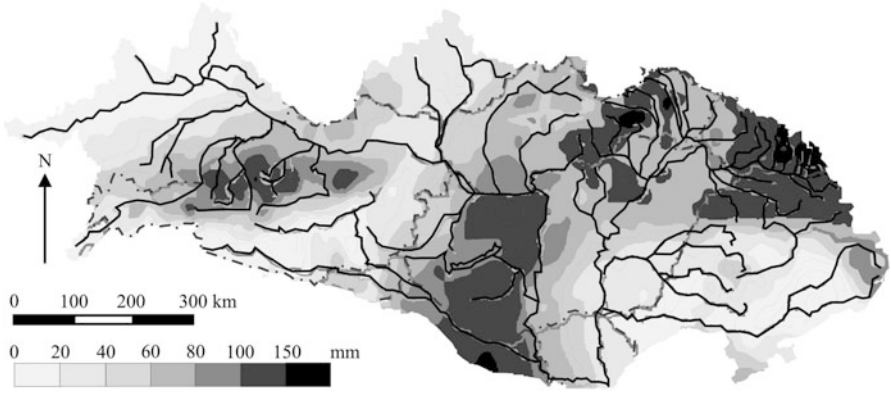

Fig. 6.2 Precipitation pattern of the second cyclone (1–7 June 2010) in the northern Danube catchment (*Source*: www.hydroinfo.hu)

precipitation (Fig. 6.2), especially in Southern Transdanubia and in the northern part of the catchment of the Tisza River (80–140 mm) (Ujváry 2010). During the second event the amount of rainfall exceeded 50 mm in the northeastern Carpathian Basin, where serious flood problems already emerged in the wake of the first cyclone (Horváth et al. 2010b).

Most of the precipitation was transported by southerly winds. Therefore, largest rainfall amounts were observed on catchments opening to the south. Recorded maximum flood levels were measured on several rivers (e.g. Zagyva, Sajó, Hernád), while the previous record was exceeded by 138 cm on the Ipoly River (Fig. 6.3).

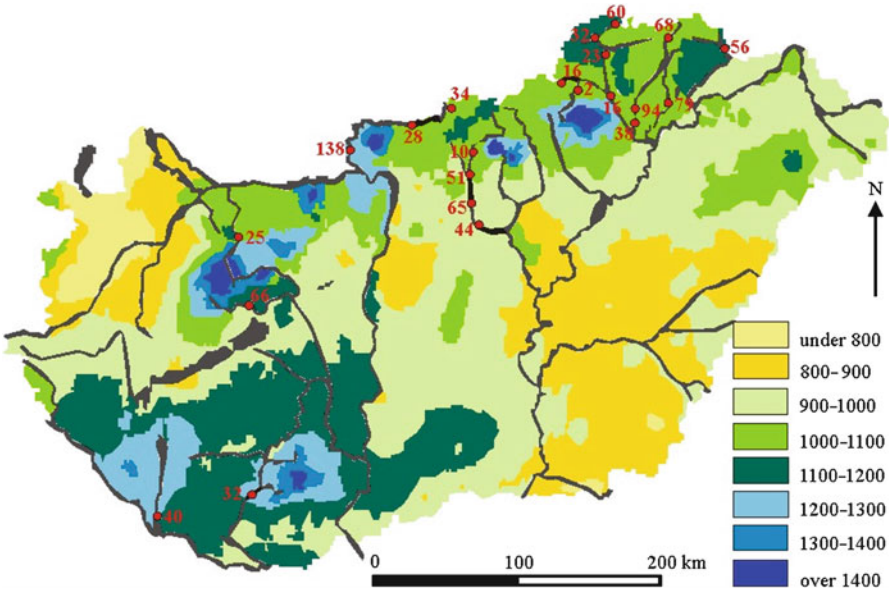

Fig. 6.3 Rainfall pattern in Hungary in 2010 and the gaging stations where a new maximum water stage was measured (the increase of flood level in cm is indicated by numbers) (*Source*: www.met.hu/eghajlat/visszatekinto/elmult_evek/2010/csapadek/ and http://www.vizugy.hu/)

6.3 Study Areas

Three rivers were studied for bank erosion (Fig. 6.4). The Hernád River in the northern part of the Carpathian Basin exemplifies the effect of high and rapid floods on bank evolution. The study area on the Tisza River, located in the centre of the Basin, presents the geomorphic consequences of smaller but prolonged floods (Tímár 2005). In the Dráva River catchment, the floods were impeded by several dams on the upper sections of the river.

The catchment of the *Hernád River* (5,436 km^2) is open towards the south. Also getting narrower, no significant tributary joins the river in Hungary. As the result of the highly fluctuating regime and high sediment discharge (Table 6.1), natural channel diversions are frequent, especially during major floods (Bendefy 1973). The range of water stages is 631 cm (based on daily data for 1901–2011). The average duration of a single flood was 59.2 h in the period of 1950–1995 (Reimann et al. 2001). On the Hungarian section of the river, three unregulated *meanders* were studied (near Alsódobsza, 36–42.5 river km). At the meanders *A* and *C*, the bank height is 2–3 m over mean low water, while at the apex of meander *B*, bank height is 8–10 m. Although locally arable lands reach down to the edge of the floodplain, the top of the banks is mostly with herbaceous vegetation. Bank material changes vertically, with decreasing proportions of silt and clay and increase of sand content downwards. Thus, in the level of mean low stage (−50 cm) the sand contents in the

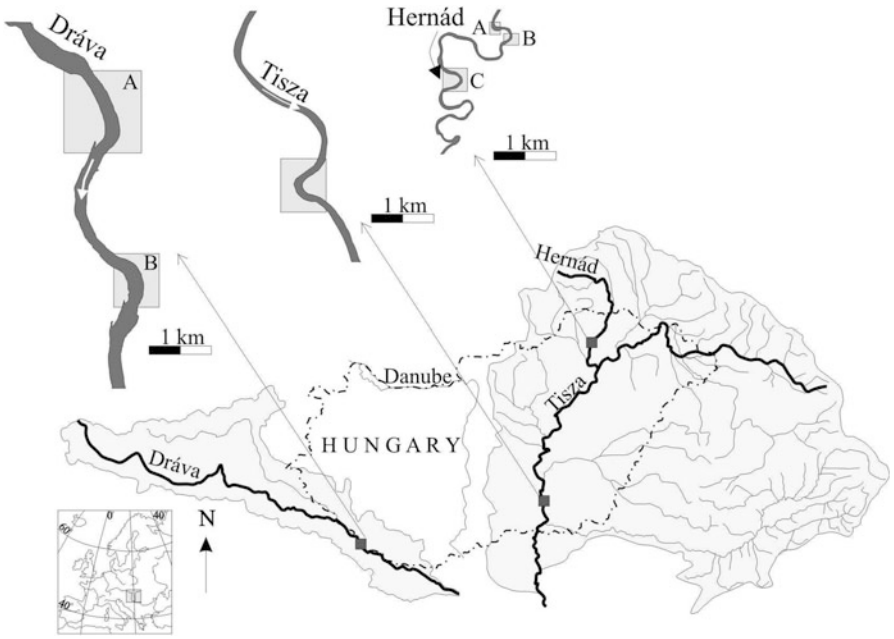

Fig. 6.4 The studied bends on the Dráva, Tisza, and Hernád Rivers

Table 6.1 Hydrological features of the studied rivers

River (gaging station)	Q_{min} ($m^3\ s^{-1}$)	Q_{mean} ($m^3\ s^{-1}$)	Q_{max} ($m^3\ s^{-1}$)	Slope	Mean grain size of bank material (mm)	Average bedload transport ($t\ year^{-1}$)
Hernád (Hidasnémeti)	2.8	27	685	0.000474	0.04–0.09	6,000
Tisza (Csongrád)	115	550	3,630	0.000029	0.003–0.03	9,000
Dráva (Barcs)	115	496	3,070	0.000175	1.3–1.15	83,167

Data source: Csoma (1973), Bogárdi (1971)

bank material are above 80% (Blanka 2010), except in meander *B*, where the whole bank is composed of silt and clay. The *A* and *C* meanders migrate freely, while at the apex of meander *B*, the river reaches an escarpment, and meander development is highly restricted on the downstream half of the bend.

The catchment of the *Tisza River* (157,200 km^2) is also open towards the south. Floods are regularly caused by rapid snowmelt and early summer rainfall, and overbank floods have a 2-year return period on average (Kiss et al. 2008). Due to low gradient and large amounts of suspended sediment, the Tisza used to be a highly sinuous river in its natural state (Table 6.1). At the end of the nineteenth century, numerous meanders were cut off artificially, and bank protection was built between 1930 and 1960 in almost each meander to protect the levees (Kiss et al. 2008). The studied meander is located on the lower section of the Hungarian reach,

south of Mindszent (at 216 rkm). Being among the few meanders with no bank protection, it could migrate downwards by 165 m between 1842 and 1999 with more or less constant meander parameters (Kiss et al. 2008). The bank material of the studied meander is silt and clay, sandy layers appear only in the upper part of the ca 9 m high bank. Planted poplar forest with dense bushes grows on the floodplain.

The third studied site is on the *Dráva River* (Table 6.1), the elongated catchment area (40,489 km^2) of which opens towards the east (Lovász 1972). Before *dam constructions* floods usually occurred in summer and autumn (October to November). After reservoir constructions (1975–1989), however, flood levels dropped significantly, and overbank flows ceased. Due to the peak operation method of the dams daily, water-level fluctuations (0.5–0.7 m) became characteristic. On the Dráva River, two bends were analysed near Heresznye (at rkm 187.5–185). The bank height on the upstream half of bend *A* is 20–22 m, while on its southern it is only 2.5–3 m, and bend *B* has a 6–7 m high bank. The upper parts of the banks consist of silty clayey sediments, but their lower parts are built of sands and gravels on both studied sites. Arable lands occupy the overbank areas on both sites.

6.4 Methods

The rate of bank erosion was measured based on the geographic location of the outer bankline surveyed several times. To assess bank erosion in 2010, its rate was repeatedly determined in the previous years. Because of different data sources, the applied methods slightly vary with study sites (Table 6.2).

On the Hernád and Tisza Rivers, investigations started earlier; thus, bankline survey data are available since 2007. These surveys were carried out by *high precision GPS* and digital total station. In case of the Dráva River, topographical maps and aerial photos were available for the period before 2010. The rate of bank erosion in 2010 was measured by RTK GPS after the extreme flood: in August of 2010 on the Hernád River and in the autumn of 2011 on the Tisza and Dráva Rivers. The banklines were surveyed and the data were georeferenced and analysed using ArcGIS 10 software.

The average rate of bank erosion (m $year^{-1}$) was calculated by dividing the area of the polygon of the eroded surface between two surveys by the centreline of the polygon (Lawler 2008; Lawler et al. 1997). The maximum annual rate of bank erosion (measured perpendicularly to the last bankline) and the spatial change of the location of the maximum bank erosion were also computed. On the Hernád River, two surveys were made in 2008 (in March and August), and consequently, in this case, bank erosion was calculated for a half-year. To assess the effect of floods on bank erosion, the rates of bank retreat and the hydrography of the studied periods were compared.

Table 6.2 Bankline survey dates and methods

	Source and type of data					
River	Before 2007	2007	2008	2009	2010	2011
Hernád	No data	No data	March and August– GPS/ total station	August – GPS/ total station	August – GPS/ total station	Dec. – GPS
Tisza		Oct. – GPS	No data	Oct. – GPS	No data	Dec. – GPS
Dráva	2003: topo maps 2005: aerial photo	No data	No data	No data	No data	Dec. – GPS

6.5 Results and Discussion

6.5.1 Hydrographical Characteristics of the Studied Periods

The hydrography of the *Hernád River* was assessed using the data of the river gauge at Hidasnémeti (97 river km), located 55 km upstream of the studied meanders. At the gauge, overbank floods appear if the water level is higher than 225 cm.

Before the first field survey (January 2007–March 2008), mostly low stages were typical (Fig. 6.5). In the next period, between the first and second surveys (March–August 2008) an overbank flood (386 cm) occurred; thus, these months represent the effect of a single, normal flood on bank retreat. In the following period (August 2008 – August 2009), water regime was more pronounced, though no flood occurred. The next period (August 2009 – August 2010) could be considered as extreme from the hydrological point of view: *four overbank flows* happened, two of them with extremely high water stages. The first flood (17 April 2010) was moderately high with 261 cm maximum (slightly above bankfull stage). The next two floods occurred within a short time. The first (17 May 2010 – 23 May 2010) brought a 402-cm high water level – close to the recorded highest water stage (434 cm). Then, a new flood record was set (2 May 2010 – 10 June 2010), which peaked at 503 cm, exceeding the former record water stage by 69 cm. At the end of this wet period, another moderate flood wave (28–31 July 2010) occurred, barely above bankfull level (232 cm). In the last measurement period (August 2010 – November 2011), medium and low water stages were typical, and, especially in the second half, mainly low water stages were recorded.

On the *Tisza River*, the gaging station at Mindszent (217.8 river km) is located only 4 km upstream of the study site. In the studied period (1 January 2007 – 1 December 2011), early spring floods and the low water periods at summer and autumn alternated, except in 2010, when four flood waves developed (Fig. 6.6).

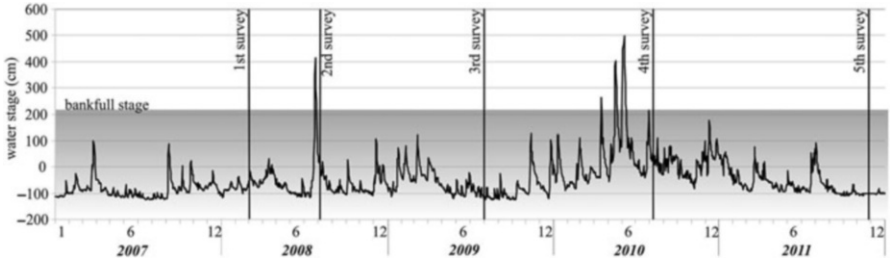

Fig. 6.5 Water regime of the Hernád River at the gaging station of Hidasnémeti, 2007–2011. The bankline was surveyed on the days indicated

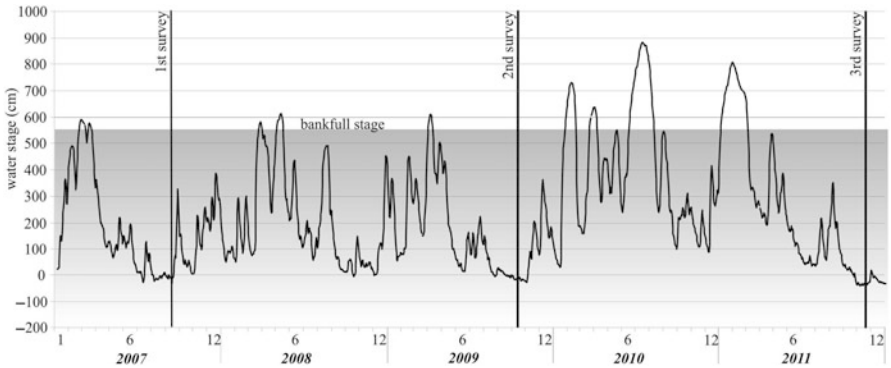

Fig. 6.6 Water regime of the Tisza River at Mindszent gauge, 2007–2011. The bankline was surveyed on the days indicated

Before the first survey (January 2007 – September 2007), a minor bankfull flood wave (550 cm) occurred, followed by low stages. Between the first and the second survey (September 2007 – October 2009), moderate spring floods (height around 600 cm) were recorded. In the long-lasting low water period between April 2007 and May 2008, water levels never exceeded 400 cm. Until the third survey (October 2009 – December 2011), four significant flood waves were observed on the Tisza River caused by the extreme precipitation on the catchment. The water stages exceeded the bankfull level in 20% (151 days) of the period. The first flood occurred unusually as early as January in 2010 and another flood wave followed in late February. The third flood developed in the middle of May with a high water stage (879 cm) and long duration (2 months). At the end of the year, another flood took place (December 2010 – February 2011), reaching 803 cm at its peak and drifting ice. The year of 2011 was quite dry; thus, a 9-month-long low water (below 400 cm) period was recorded before the third survey.

The hydrography of the *Dráva River* was assessed using the data of the gaging station at Barcs (154 river km), located 30 km upstream of the study sites. On the studied bend *A*, the river inundates its floodplain if the water level is higher than 300 cm at the gauge, but along higher banks, overbank flow never occurs.

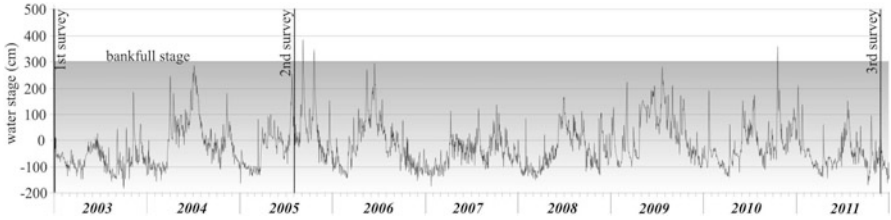

Fig. 6.7 Water stage changes of the Dráva River between 1 January 2003 and 1 December 2011 at the Barcs gauge. The bankline was mapped on the days indicated

Between the first and second surveys (January 2003 – July 2005) bankfull flow was experienced just for one day (28 June 2004; 301 cm), and the duration of water stages around channel-forming discharge (above 200 cm) was just only 2.7% of time (Fig. 6.7). Low stages were frequent, below −100 cm occurred for 6% of the period. The second period (August 2005 – November 2011) started with two moderate flood waves (heights: 397 and 358 cm) resulting in the highest water stages of the studied period. In the year 2006, a typical summer flood developed, while low stages were characteristic in the winter and spring months. In 2007 and 2008, water stages dropped, and they did not exceed the 200-cm water level. The year of 2009 was similar to 2006. In 2010, as opposed to other study sites, the *effect* of extreme precipitation on water stages *could hardly be detected* (a minor overbank flow only lasted for two days). This was probably due to the continuous sedimentation in the reservoirs upstream. Similarly to 2007 and 2008, in 2011 low stages were typical. Overall, the water stages exceeded the bankfull level in only 0.4% of the whole studied period (January 2003 – November 2011), while extremely low waters (below −100 cm) occurred in 4.5% of time.

6.5.2 Rates of Bank Retreat Along the Studied Sections

For the *Hernád River* (2008–2011), the rate of *bank retreat* considerably varied with time and the studied meanders (Fig. 6.8, Table 6.3). The highest rate was measured on meander *A*, downstream of its apex. Between the first and the second surveys, one flood occurred, and the rate of bank erosion was 9.8 m for half a year, which was almost three times higher than in the second period (6.2 m year^{-1}). The highest rate of bank retreat (16.7 m year^{-1}) was measured when extreme floods developed on the river. In the last period (August 2010 – November 2011), when low water stages were dominant, it was only 5 m year^{-1}, similar to the long-term (1975–2007) average (4.5 m year^{-1}) (Blanka and Kiss 2011). Average bank retreat (12.6 m year^{-1}) in the meander was also the highest during the period of extreme floods in 2010, transporting large amounts (over 12,000 m^3) of sediment into the river.

The upstream section of meander *B* confines with an *escarpment*, thus the height of the bank is 6–7 m higher than on the downstream section. The highest bank erosion rate was measured where the escarpment terminates, but its extent was

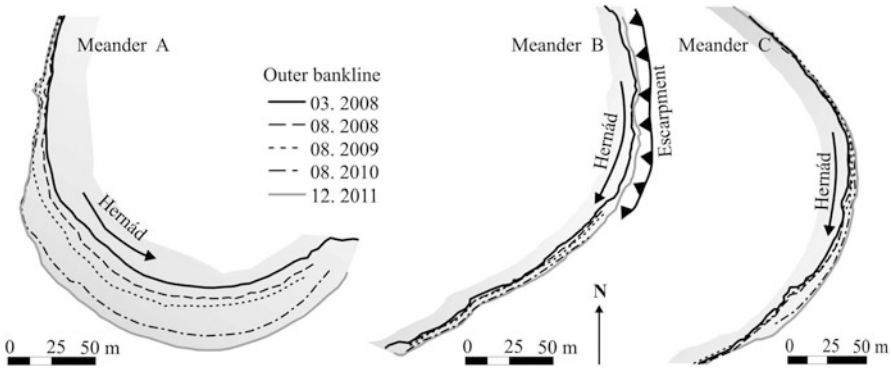

Fig. 6.8 Bank retreat pattern on the Hernád River

much lower than on the freely migrating meander *A*. In meander *B*, during the first measurement period, maximum bank retreat rate was 2.2 m within half a year, while in the second 4 m year^{-1}. With the extreme floods, bank retreat slightly intensified (5.7 m year^{-1}), while in the last period, it slowed down (to 1.2 m year^{-1}) but still remained around the multiannual average (established for 1975–2007 as 1.7 m year^{-1} – Blanka and Kiss 2011). As only the lower section of the meander eroded intensively, and, therefore, a small amount of sediment reached the channel, mean bank retreat was much slower than the maximum for this meander.

In the case of meander *C*, the rate varied similarly to the other meanders. In the first period (with one flood), maximum bank retreat was 3.2 m in half a year, while in the second period, it dropped to 1.6 m year^{-1}. Maximum bank retreat during floods was much higher (10.6 m year^{-1}) than in the previous periods. The lowest rate (1.3 m year^{-1}) was recorded in the last period. Thus, the temporal pattern of the bank retreat was similar to the other meanders, since in 2010 it 3.6-fold surpassed the rate in other periods.

On the Hungarian section of the *Tisza River* (studied between 2007 and 2011), the freely migrating meanders almost entirely disappeared due to *bank stabilisation* works; thus, only one meander was suitable for the analysis of bank retreat. Average bank erosion between 2007 and 2009 was 0.6 m year^{-1}, and maximum rates were 3.3–5 m year^{-1}. The *retreat* was spatially *not uniform*, as zero erosion was measured in the middle section of the analysed bank (survey points 7–9). In the period of 2009–2011, both the average rate of bank retreat (1.7 m year^{-1}) and the maximum value (5.7–7.4 m year^{-1}) were almost doubled, and the location of the maximum bank retreat shifted downstream (Fig. 6.9).

In the studied meander, close connection could be established between bank retreat and the different water stages. The extreme flood events of 2010 caused increased bank erosion. In the first period, the territory of the eroded forest was only 574 m^2 (equal with 12,600 m^3 eroded sediment), while in the period of 2009–2011, the eroded area almost tripled (1,490 m^2), resulting in 32,700 m^3 sediment input

Table 6.3 Rates of bank retreat in the studied meanders of the Hernád River

Period	Meander *A*				Meander *B*				Meander *C*			
	March – August 2008	August 2008 – August 2009	August 2009 – August 2010	August 2010 – November 2011	March – August 2008	August 2008 – August 2009	August 2009 – August 2010	August 2010 – November 2011	March – August 2008	August 2008 – August 2009	August 2009 – August 2010	August 2010 – November 2011
Maximum bank retreat (m year^{-1})	9.8 m/0.5 y	6.2	**17.6**	5	2.2 m/0.5 y	4	**5.2**	1.2	3.2 m/0.5 y	1.6	**10.6**	1.3
Average bank retreat (m year^{-1})	7.4 m/0.5 y	4.8	**12.6**	3.6	1.3 m/0.5 y	0.7	**1.9**	0.5	1.9 m/0.5 y	0.8	**3.5**	1.0
Eroded material (m^3 year^{-1})	6,305 m^3/0.5 y	4313	**1,2645**	3,996	1,330 m/0.5 y	726	**1,947**	556	1,568 m/0.5 y	702	3,009	854

Extreme values are shown bold

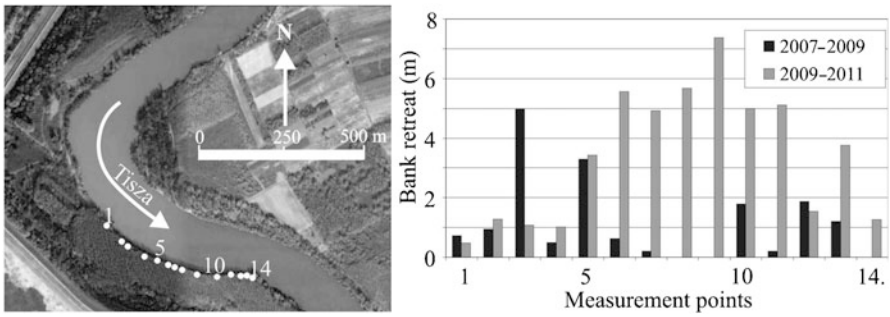

Fig. 6.9 Bank retreat pattern on the Tisza River

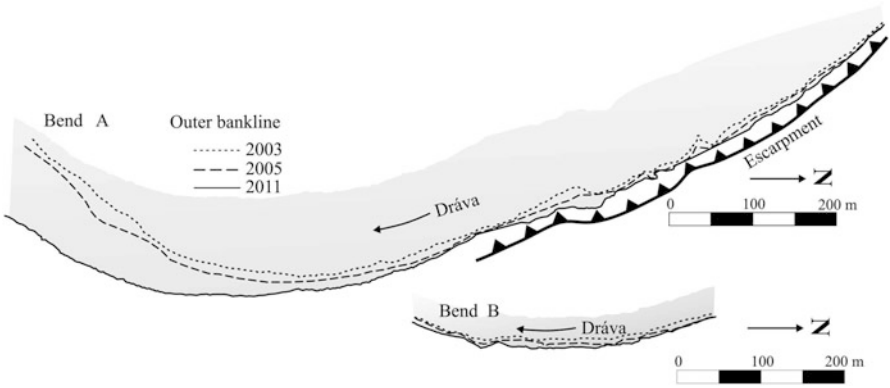

Fig. 6.10 Bank retreat pattern on the Dráva River

into the river. In the studied meander, *mass failure* is the governing process of bank retreat. The slumped material is removed from the base of the bank mainly during low stages.

On the *Dráva River* (studied over the period 2003–2011), the two studied bends differ in their bank height; therefore, the rate and location of maximum bank erosion were also different. The bank height structure of bend *A* is similar to meander *B* on the Hernád River, since the upper section of the bend contacts the escarpment; thus, the bank is 20–22 m high, while on the downstream section of the bend, it is only 2.5–3 m high. In the first period (January 2003 – July 2005), the rate of bank retreat on the upper section was 1.8 m year^{-1} and on the lower section 3.9 m year^{-1} (Fig. 6.10, Table 6.4). On the upper section with particularly high bank, large amounts of sediment were transported into the river (20,800 m^3 year^{-1}, as opposed to only 19.5 m^3 year^{-1} on the lower section). In the second period (July 2005 – November 2011), bank retreat slowed down to 0.7 m year^{-1} on the upper section but increased to 4.7 m year^{-1} on the lower section, and the eroded area grew ca threefold (23,800 m^3 year^{-1}) compared to the previous period. The location of

Table 6.4 The rate of bank retreat in the studied meanders of the Dráva River

	Bend A upstream section		Bend A downstream section		Bend B	
Period	2003–2005	2005–2011	2003–2005	2005–2011	2003–2005	2005–2011
Maximum bank retreat (m year^{-1})	5.4	2.6	9.6	15.0	3.0	1.4
Average bank retreat (m year^{-1})	1.8	0.7	3.9	4.7	1.6	0.6
Eroded material (m^3 year^{-1})	20,815	8,093	19,510	23,806	5,670	2,037

maximum bank retreat shifted 120 m downstream. The spatial and temporal differences in bank retreat could be explained by the different bank erosion processes and hydrograph characteristics. On the lower section, where the bank is lower, moderate but frequent flood waves resulted in intensive bank erosion, though where the bank is high mass failure controlled the processes.

Bend *B* is similar to the upper section of bend *A*, bank height is 6–8 m, and thus, overbank floods could not influence its development. During the first measurement period (January 2003 – July 2005), the average rate of bank retreat was 1.6 m year^{-1}, and maximum bank retreat was 3.0 m year^{-1}. During this period, 1,573 m^2 arable land was eroded by the river, which resulted in 14,600 m^3 sediment input into the river. In the second period (July 2005 – November 2011), bank retreat became slower (average rate: 0.6 m year^{-1}). Comparing these changes with the hydrological variations, it could be observed that in this case – similar to the upper section of bend *A* – mass failures played an important part in bank retreat. Rates are higher during low water stages, as they promote bluff *undercutting*. It is supported by the duration of extremely low waters (stages below −100 cm): 6.0% of time in the first period and 4.8% in the second period.

6.6 Conclusions

As the result of extreme precipitations in 2010, floods with high magnitude and frequency had developed, especially in catchments which are open towards the south, because the rainfall was the result of cyclones arriving from the Mediterranean region. On the Hernád and Tisza Rivers, more than one significant flood waves occurred, and on the Hernád River, even a new record maximum water stage was recorded. Simultaneously, on the Dráva River, no significant flood developed, because its catchment is narrow and open towards the east, and several dams impeded flow. Thus, even though extremely high precipitations were recorded over the entire Carpathian Basin, floods did not affect every catchment, just mostly those which are open towards the south.

As in some regions, extremely high records of floods developed, while on other catchments no flood at all, the resultant bank retreat could vary significantly. Consequently, among the studied rivers, bank retreat on the Hernád and Tisza Rivers was 2–3 times more rapid in 2010 than in the previous or the following years. However, in lack of floods, on the Dráva River the rate of bank retreat has not changed considerably. The results also revealed that probably smaller rivers (e.g. Hernád River) respond more sensitively to extreme events, since their floods could acquire higher magnitudes, and therefore, the rate of bank erosion could be multiplied. In contrast, on larger rivers the height of the flood waves could be reduced by lower slope (e.g. Tisza River) or by upstream reservoirs on the river (e.g. Dráva River). As flood waves are more subdued and bank erosion is also less intensive on these rivers.

Floods had great importance in the increased bank retreat on sections, where the bank material has low resistance and banks are low. Therefore, in periods when medium and low stages dominate, the rate of bank retreat is much slower, since the flow energy is not large enough to erode particles directly from the bank; the toes of landslides and debris falls, however, could be removed during these low stages. In the case of escarpments, mass failure processes are dominant in bank retreat; thus, in these cases, not only the frequency of floods are important but that of low water periods too, as during low stages, the undercutting of the banks and the removal of the eroded material could proceed.

Comparing the results with other researches in the Carpathian Basin, it could be ascertained that bank erosion in 2010 was certainly extreme. On the Hernád River, Kozma (2008) recorded 1–5.5 m year^{-1} bank retreat in the period of 2007–2008, though in 2010 it was 1.9–16.7 m year^{-1} according to the presented survey. On the Tisza and Maros Rivers, the long-term mean bank retreat is 0.9–1.7 m year^{-1} (Sipos 2006; Nagy et al. 2006), and in 2010, mean bank retreat was almost the same (1.7 m year^{-1}) on the Tisza River; however, the maximum rate was 7.4 m year^{-1}.

As a result of bank erosion, considerable tracts of agricultural, mostly arable, lands were destroyed at the study sites. Consequently, extreme floods cause *agricultural losses* not only to crops through inundation but through destroying lands along the banks. The large amount of extra sediment input increases the sediment discharge, especially on the sections next to an escarpment (for instance, on the Dráva and Hernád Rivers).

Acknowledgements Research was supported by the Hungarian Research Foundation (OTKA, contract no. K 100761). Special thanks to Zsuzsanna Knyihár and several other students for taking part in field surveys and preliminary data processing.

References

Bendefy L (1973) A Hernád geomorfológiája (Geomorphology of the River Hernád). In: Vízrajzi Atlasz 16, VITUKI, Budapest, pp 16–19 (in Hungarian)

Blanka V (2010) Kanyarulatfejlődés dinamikájának vizsgálata természeti és antropogén hatások tükrében. Dynamics of meander development in response to natural and human impacts. Manuscript Ph.D. thesis, University of Szeged, Szeged, 144 p (in Hungarian)
Blanka V, Kiss T (2011) Effect of different water stages on bank erosion: case study on River Hernád, Hungary. Carp J of Earth and Env Sci 6(2):101–103
Bogárdi J (1971) Vízfolyások hordalékszállítása (Sediment transport of streams). Akadémiai Kiadó, Budapest, 755 p (in Hungarian)
Brierley GJ, Fryirs KA (2005) Geomorphology and river management: applications of the river styles framework. Blackwell Publishing, Malden, pp 93–103
Csoma J (1973). Hernád. Hidrológia (Hydrology of the River Hernád). In: Vízrajzi Atlasz, VITUKI, Budapest, pp 7–15 (in Hungarian)
Hickin EJ (1984) Vegetation and river channel dynamics. Can Geogr 28:11–126
Hickin EJ, Nanson GC (1975) The character of channel migration on the Beatton River, Northeast British Columbia, Canada. Geol Soc Am Bull 86:487–494
Horváth Á, Zsikla Á, Hadvári M (2010a) A "Zsófia" ciklon meteorológiai leírása (Meteorological description of the "Zsófia" cylone). www.met.hu/pages/Zsofia_ciklon_20100515-18.php (in Hungarian)
Horváth Á, Zsikla Á, Kovács A (2010b) Az "Angéla" ciklon meteorológiai leírása (Meteorological description of the "Angéla" cylone). www.met.hu/pages/Angela_ciklon_20100531-0604.php (in Hungarian)
Hughes DJ (1977) Rates of erosion on meander arcs. In: Gregory KJ (ed) River channel changes. Wiley, Chichester, pp 193–205
Kiss T, Fiala K, Sipos Gy (2008) Altered meander parameters due to river regulation works, Lower Tisza, Hungary. Geomorphology 98(1–2):96–110
Kozma K (2008) Recens folyóvízi fejlődés néhány kérdése a Hernád Alsódobsza–Gesztely közötti szakaszán (Recent fluvial development of the Hernád River between Alsódobsza and Gesztely). In: Geographica generalis et specialis. University of Debrecen, Debrecen, pp 155–161 (in Hungarian)
Lawler DM (2008) Advances in the continuous monitoring of erosion and deposition dynamics: developments and applications of the new PEEP-3T system. Geomorphology 93:17–39
Lawler DM, Thorne CR, Hooke JM (1997) Bank erosion and instability. In: Throne CR (ed) Applied fluvial geomorphology for river engineering and management. Wiley, Chichester, pp 137–173
Lovász G (1972) A Dráva–Mura vízrendszer vízjárási és lefolyási viszonyai (Hydrology of the Dráva and Mura river system). Akadémiai Kiadó, Budapest, 158 p (in Hungarian)
Luppi L, Rinaldi M, Teruggi LB, Darby SE, Nardi L (2009) Monitoring and numerical modelling of riverbank erosion processes: a case study along the Cecina River (Central Italy). Earth Surf Process Land 34(4):530–546
Mastermann R, Thorne CR (1992) Predicting the influence of bank vegetation on channel capacity. Proc Am Soc Civ Eng 118:1052–1059
Mastermann R, Thorne CR (1994) Analytical approach to predicting vegetation effects on flow resistance. In: Kirkby MJ (ed) Process models and theoretical geomorphology, BGRG special publication series. Wiley, Chichester, pp 201–218
Nagy ÁT, Tóth T, Sztanó O (2006) Új, kombinált módszerek a Közép-Tisza jelenkori mederképződményeinek jellemzésére (New combined methods to study channel forms of the Middle Tisza). Földtani Közlöny 136(1):121–138 (in Hungarian)
Reimann J, Fehér J, Gáspár J (2001) A Hernád árvizeinek statisztikai elemzése (Statistical analysis of the floods of the River Hernád). Vízügyi Közlemények 83(4):581–600 (in Hungarian)
Simon A, Collison AJC (2002) Quantifying the mechanical and hydrologic effects of vegetation on streambank stability. Earth Surf Process Land 27:527–546
Sipos Gy (2006) A meder dinamikájának vizsgálata a Maros magyarországi szakaszán (Channel dynamics on the Hungarian section of the Maros River). Manuscript Ph.D. thesis, University of Szeged, Szeged, 138 p (in Hungarian)

Thorne CR (1982) Processes and mechanisms of river bank erosion. In: Thomas CR, Bathurst JC, Hey RD (eds) Gravel bed rivers. Wiley, Chichester, pp 227–271

Tímár G (2005) Az alluviális folyók alaktípusai és a típusok kialakulásának feltételei (Planform types of alluvial rives and the conditions of their occurrence). Hidrológiai Közlöny 85(1):1–10 (in Hungarian)

Ujváry K (2010) "Zsófia" és "Angéla" ciklon csapadék-szinoptikai közelítése és előrejelezhetősége (Precipitation-synoptic approximation and predictability of the "Zsófia" and "Angéla" cyclones). http://www.met.hu/pages/Zsofia-Angela_ciklon_20100515-0604.php (in Hungarian)

Chapter 7
Floods in the Siret and Pruth Basins

Gheorghe Romanescu

Abstract The greatest floods on Romanian territory occurred in the past 20 years (1990–2010), and in 2005 the highest peak discharge (4,650 $m^3\ s^{-1}$, exceedance probability 0.5%) was recorded on the Siret River and its tributaries (Suceava, Trotuş, Tazlău, Buhai, and others). In 2008, it was the turn of the Pruth River to beat the record for Romanian territory (7,146 $m^3\ s^{-1}$, exceedance probability 0.1% at Oroftiana, upstream from the Stânca–Costeşti reservoir). One of the most interesting floods occurred on the Buhai Stream, direct tributary of Jijia (tributary of the Pruth River). The waters of the Buhai Stream rose upstream on the Jijia River penetrated through the high dam of the Ezer reservoir. In this case, the waters had to climb the walls of the dam ("spider flow"). The analyses of major floods on Romanian rivers underline that there have been more extreme hydrologic events lately, as a direct response to global climate change. Since massive deforestation within the past 20 years intensified the emergence and impacts of heavy rains in Eastern Romania, record discharges and water levels mostly occur there.

Keywords Floods • Global climate change • Flood hazard • Record discharges • Water management • Siret • Pruth

7.1 Introduction

Although cannot be confirmed by data, in the beginning of the twenty-first century, the occurrences of extreme natural phenomena have multiplied with ever more intense consequences (Romanescu 2003, 2005, 2006, 2009; Romanescu and Nistor 2011; Romanescu et al. 2011a, b). Disastrous floods are more frequent under

G. Romanescu (✉)
Department of Geography, Faculty of Geography and Geology,
University 'Alexandru Ioan Cuza' of Iaşi, Bd. Carol I, 20A, 700505 Iaşi, Romania
e-mail: romanescugheorghe@gmail.com

D. Lóczy (ed.), *Geomorphological impacts of extreme weather: Case studies from central and eastern Europe*, Springer Geography, DOI 10.1007/978-94-007-6301-2_7,

continental than under equable climates (Diaconu 1988; Bravard and Petit 2000). Extreme discharges were recorded on the Danube: 15,100 m^3 s^{-1} at Orşova (on 13 April 1940), 15,900 m^3 s^{-1} (in May 1942), and 15,500 m^3 s^{-1} at Ceatalul Ismail (5 June 1970). The highest ever discharge 35,000 m^3 s^{-1} seems to have occurred in 1897 at the entrance to the delta.

The Romanian territory is not properly protected against floods, and *flood hazard* remains to be high. In the watershed of the Bahlui River, for instance, after defense works ended, heavy rains still endanger the city of Iaşi (Romanescu and Lasserre 2006).

In recent decades, large *forests* have been simply *cut*, in both mountain and lowland areas, mostly in regions with no other sources of fuel (on the Moldavian Plateau, Romanian Plain, or Transylvanian Plateau) (Diaconu 1999; Podani and Zavoianu 1992). The remaining tree stumps carried away by waters can block streams and cause floods, both downstream (as backwater effect) and upstream (after dam breaches). Stumps are also a serious danger to hydrotechnical structures.

Increasing *housing development* and the elimination of wetlands on floodplains have a special influence on floods. Floodplain restoration is a major step towards better nature conservation and environmental protection (Romanescu et al. 2011a, b). The first floodplain management projects started as early as the beginning of the twentieth century, along the Timiş River and by damming certain enclosures within the Danube Delta and floodplain (Romanescu and Nistor 2011; Romanescu et al. 2011a). The first mentions of establishing reservoirs in Moldavia date back to 1450–1550, when ponds were established for water supply after a prolonged drought (Cantemir 1716). However, the construction of modern *reservoirs* – multiple-purpose or only for flood control – began after 1960. Currently, there are 1,270 artificial lakes in Romania, with a total surface of 1,150 km^2 (one-third of total lake surface). Most reservoirs have complex purposes, but their main function is electricity generation and flow regulation.

7.2 Objectives

As floods occurred in 2004, 2005, 2006, 2008, and 2010, they have almost become the "norm" in Romania over the past decade. This chapter aims to survey the conditions leading to major floods and their environmental impacts in Eastern Romania and to draw attention to the predictable impacts on local or regional economy. After the catastrophic floods of 2005, the Siret River has benefited from a special attention and was equipped with an automated monitoring system of flood hazard (Siret Water Basin Administration 2010).

Although floods are very well studied at national and international levels, proper conclusions and measures are still missing at times. The topic is well represented in *Romanian literature* (Podani and Zavoianu 1992; Mustaţea 2005; Jolin et al. 2009; Pleşoianu and Olariu 2010; Romanescu et al. 2011a, b). At the same time, most of the data of general or local significance have been extracted from the international hydrologic literature (e.g., Dalrymple 1960; Blynth and Biggin 1993; Schumann

and Geyer 1997; Smith and Ward 1998; National Employee Development 1999; Tockner et al. 2000; Berz et al. 2001; Glade et al. 2005; Konecsny 2005; Barroca et al. 2006; Büchele et al. 2006; Pinter et al. 2006; Strupczewski et al. 2006; Chen et al. 2007; Gabitsinashvili et al. 2007; Jaber and Shukla 2007; Komma et al. 2007; Dorner et al. 2008; Förster et al. 2008; Sudhaus et al. 2008; WMO 2008; Portela and Delgado 2009; Kuhlicke 2010).

7.3 Study Areas

The drainage basins of Siret and Pruth Rivers are situated in Eastern Romania, in the historical province of Moldavia (Fig. 7.1) with sources in Ukraine and confluence with the Danube near Galaţi.

The *Siret River* issues in the Wooded Carpathians (Ukraine). Its middle course crosses the Suceava Plateau and then the boundary between the Moldavian Sub-Carpathians and the Bârlad Plateau, while the lower is of lowland character. Its total length in Romania is 559 km. The drainage network of 1,013 watercourses is the richest in Romania (length: 15,157 km – 19.2% of the total in Romania; drainage density: of 0.35 km km^{-2}, well above the national average of 0.33 km km^{-2}). The watershed (42,890 km$^{2)}$ represents 18.1% of Romanian territory. Forests

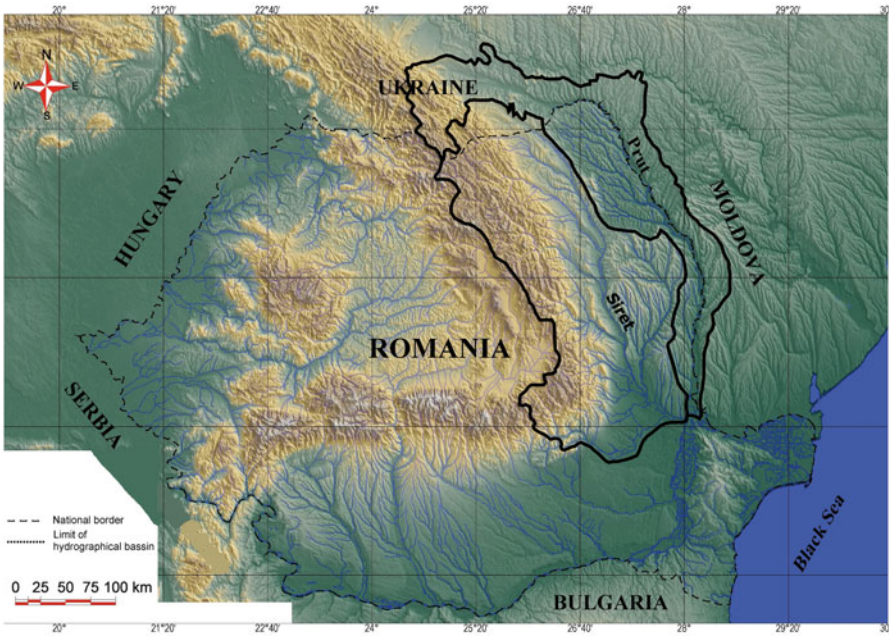

Fig. 7.1 Location of the Siret and Pruth Rivers

(15,882 km^2) cover 37% of the watershed (Atlas of the Waters Survey Romania 1992; Romanescu and Nistor 2011).

The discharge of the Siret River is the highest of all rivers issuing on the territory of Romania: the multiannual average is 210 $m^3 s^{-1}$ at the confluence with the Danube River. The contributions of tributaries to river discharge from the Moldavian Plateau of continental climate are low (e.g., the left-bank tributary Bârlad River: 1–2 L s km^{-2}) compared to those of the Eastern Carpathians tributaries (e.g., Bistriţa River watershed: 14–15 L s km^{-2}) (Romanescu and Nistor 2011).

The *Pruth River*, on the border between Ukraine and Romania for a length of 31 km and between Romania and the Republic of Moldova for 711 km, is the second longest and the last important tributary of the Danube (952.9 km) (Romanescu et al. 2011b). Mean elevation of the drainage basin varies between 130 m in the central part and 2 m at the confluence. Average slope is ca 0.2%. The watershed of elongated shape includes 248 tributaries, 11,000 km total length of watercourses, 3,000 km (33%) of which are permanent and 8,000 km (67%) are of intermittent character, drainage density is 0.41 km km^{-2} (Pruth-Bârlad Water Basin Administration 2010; Romanescu et al. 2011b).

In the drainage basin, there are 26 large reservoirs, including Stânca–Costeşti (1,400,000,000 m^3) (Romanescu 2006). Land use in the Pruth drainage basin includes 54.7% arable land, 21.4% forests, 13.3% perennial crops, and 1.19% water surfaces (Pruth–Bârlad Water Basin Administration 2010). Mean annual air temperature is 9 °C, and annual average precipitation is 550 mm. Average discharge in the upstream section is 78.1 $m^3 s^{-1}$ (at Radauti Pruth), downstream 86.7 $m^3 s^{-1}$ (at Ungheni), and 93.8 $m^3 s^{-1}$ (for the period 1950–2008) at the river mouth (at Oancea).

7.4 Methods

To accurately assess recent major floods, we analysed hydrologic data and *satellite images* from the Siret Water Headquarters in Băcau, the Pruth Water Headquarters in Iaşi and the National Institute of Hydrology in Bucharest, the Romanian Space Agency, or from the Internet (http://sertit.u-strasbg.fr/). The areas affected by floods were identified from the interpretation of Landsat TM images using the FAO-LCCS classification. Data processing was performed in the ASR-CRUTA (2008, 2010) remote sensing laboratory (Romanian Space Agency 2005, 2008, 2010). Data were collected from communal and municipal authorities on site, from local residents, from ministries (on damage to infrastructure, especially to roads and railways).

The data on torrential downpours is based on 24-h monitoring according to the Berg scale of intensity. That data is derived from measurements at the river gages and from the automated meteorological stations of the national monitoring system in the Siret and Pruth basins.

The data on river levels and flow rates only included the daily recordings during floods. Average monthly and multiannual river levels and flow rates were used for comparison. Histograms were drawn to show changes in river levels before and during floods, the threshold of dangerous levels, daily and monthly outflow, and finally, hourly variations in bank overflow during the flood.

Observations and field measurements were made from 22 to 27 July 2005 (on the Siret and Suceava Rivers), 21–27 July 2008 (Pruth), and 27 June to 2 July 2010 (Buhai). At the most important hydrologic stations, daily flows were monitored and topographic measurements were made upstream and downstream from the confluence. The Siret and Pruth Rivers have an adequate network of hydrometric stations, with systematic observations starting in 1886.

7.5 A Brief History of Floods

The information on major floods in Romania falls into three categories (Mustaţea 2005):

- Certain, but subjective data (occasional notes, chronicles, old documents, etc.)
- Certain and objective meteorological data (visual observations and instrumental measurements noted in yearbooks, scientific works, and monographs)
- Certain and objective hydrologic data (written documents, specialized papers, monographs)

7.5.1 Major Floods in the 20th Century

In March, there is usually a deep snowpack and frequent rainfalls occur. The spring of 1932 brought floods affecting most of Romania (Table 7.1) and bringing new water-stage records at 70 out of the 229 hydrometric stations (Mustaţea 2005; Romanescu 2006). At the Barboş station, on the Siret, a peak level of 410 cm was recorded.

In 1970, catastrophic floods were registered on all Romanian streams (Table 7.2). On the rivers in Moldavia, peak flow was significantly higher than in other years (Table 7.3). The floods were caused by high amounts of precipitations fallen on saturated soils. Maximum discharge on the Siret was 3,189 $m^3\ s^{-1}$ on 19 May 1970 and, a record valid until 2008, on the Pruth: 2,960 $m^3\ s^{-1}$ at Rădăuţi Pruth (not influenced by the Stânca–Costeşti reservoir) on 26 July 1974.

In July 1975, heavy rainfalls affected ca 60,000 km^2 in the drainage basins of the Siret, Pruth, Ialomiţa, Argeş, Olt, and Mureş Rivers. The rainfalls in the Siret Basin resulted from a thermobaric blockage created by the Black Sea basin and atmospheric perturbation, which persisted for 24 h east of Moldavia. Preceding soil saturation also contributed to extreme discharges. Monthly rainfall amounts peaked

Table 7.1 Maximum water levels (H_{max}) during the 1932 floods on several rivers of Romania

No.	River	Hydrometric station	Founding year	H_{max}, cm	Exceedance of previous H_{max}, cm
1	Someş	Satu Mare	1868	613	0
2	Someşul Mic	Cluj-Napoca	1927	394	164
3	Lăpuş	Răzoare	1927	332	82
4	Crişul Negru	Zerind	1872	776	25
5	Crişul Alb	Chişineu Criş	1872	763	47
6	Mureş	Alba Iulia	1870	461	63
7	Mureş	Brănişca	1870	610	88
8	Mureş	Arad	1861	604	57
9	Târnava Mare	Mediaş	1898	537	97
10	Bega Veche	Beregsău	1881	390	62
11	Timiş	Teregova	1902	240	40
12	Olt	Feldioara	1898	460	19
13	Olt	Făgăraş	1898	430	18
14	Argeş	Budeşti	1914	296	14
15	Ialomiţa	Slobozia	1928	486	106
16	Siret	Barboş	1926	410	40
17	Moldova	Gura Humorului	1886	338	3
18	Pruth	Fălciu	1927	500	60

Table 7.2 Peak flows (Q_{max}) registered on several rivers during the floods of 1970

No.	River	Hydrometric station	F, km^2	Q_{max}, m^3 s^{-1}	Avoidance probability, %	Date
1	Bistriţa	Dorna Giumalău	740	310	10	13 May
2	Bistriţa	Dorna Arini	1,656	580	5–10	13 May
3	Bistriţa	Frumosu	2,816	772	5–10	13 May
4	Trotuş	Târgu Ocna	2,084	503	10	24 May
5	Trotuş	Vrânceni	4,077	1,213	10	25 May
6	Oituz	Ferăstrău	263	129	10	19 May
7	Putna	Colacu	1,100	860	5	18 May
8	Putna	Boţârlău	2,518	1,250	5	18 May
9	Milcov	Goleşti	395	560	5	18 May
10	Râmna	Groapa Tufei	164	307	5–10	18 May
11	Râmnicul Sărat	Tătaru	992	274	5–10	18 May
12	Siret	Lungoci	36,030	3,186	2–5	19 May
13	Olt	Rm.Vâlcea	15,292	1,715	5–10	25 May
14	Timiş	Ciavoş	5,790	765	10	27 May
15	Crişul Repede	Oradea	2,198	576	10	11 June
16	Crişul Negru	Tinca	2,216	626	5–10	11 June
17	Crişul Negru	Zerind	3,750	517	10	13 June
18	Crişul Alb	Bocsig	2,376	466	10	13 June

F, watershed area

Table 7.3 Peak discharges (Q_{max}) on several rivers and highest specific runoff values (q_{max}) on their watersheds (area: F) during the 1970 floods in the Siret Basin

No.	River	Hydrometric station	F, km^2	Q_{max}, m^3 s^{-1}	Avoidance probability, %	q_{max}, L s km^{-2}
1	Buzău	Sita Buzăului	360	390	5–10	1,115
2	Bâsca Mare	Comandău	111	204	5–10	1,840
3	Bâsca Mare	Varlaam	424	600	2–5	1,415
4	Bâsca Mică	Varlaam	235	390	2–5	1,665
5	Bâsca Unită	Bâsca Roziliei	759	980	1–2	1,290
6	Buzău	Nehoiu	1,549	1,400	2	903
7	Bâsca Chiojd	Chiojd	114	300	1–2	2,630
8	Buzău	Măgura	2,273	2,100	1–2	925
9	Slănic	Lopătari	85	215	1	2,530
10	Buzău	Baniţa	3,980	2,200	2–5	553
11	Buzău	Racoviţa	5,240	1,600	2–5	306
12	Ramnicu Sărat	Tulburea	170	220	5–10	1,295
13	Zăbala	Nereju	244	360	5–10	1,475
14	Năruja	Herăstrău	137	244	5–10	1,780
15	Oituz	Fierăstrău	263	417	0.5–1	1,585
16	Trotuş	Vrânceni	4,077	2,020	2–5	495
17	Cracău	Slobozia	399	438	1–2	1,100

Table 7.4 Maximum discharges (Q_{max}) and historical water levels (H_{max}) registered on several small rivers (of F watershed area) during the floods of July 1991

No.	River	Flow section	F, km^2	H_{max}, m	Q_{max}, m^3 s^{-1}	Avoidance probability, %
1	Calu	Piatra Şoimului	67	622	168	–
2	Iapa	Luminiş	58	745	82	0.5–1
3	Mesteacăn	Ruseni	24	374	127	–
4	Nechitu	Borleşti	58	644	67	–
5	Şuşiţa	Ciuruc	179	588	582	1
6	Răcăciuni	–	78	325	435	–

at 232 mm at Întorsura Buzăului, 211 mm at Chichiran, 188 mm at Zăbrătău, and 173 mm at Comandău.

Aggravated by soil wetting, heavy rains in May and June 1988 (exceeding 146 mm between 1 and 11 June at Haloş) generated high waters on the Siret, Trotuş, and Bârlad Rivers with a peak discharge of 2,700 m^3 s^{-1} at Lungoci on 5 June 1988. From 3 June to 19 August 1991, serious floods occurred on many rivers situated in the Siret Basin (Table 7.4), on both small and large watersheds (Table 7.5).

The most spectacular flood affected the Tazlău watershed on 28–29 July 1991, where the Belci dam breached. A peak discharge of 460 m^3 s^{-1} was recorded at the gage of Lucăceşti ($F = 123$ km^2) and 1,500 m^3 s^{-1} at the Helegiu station ($F = 984$ km^2). When inaugurated, the Belci reservoir had a useful capacity of 12.5 million m^3,

Table 7.5 Peak discharges (Q_{max}) registered on several small rivers during the floods of July 1991

No.	River	F, km^2	Q_{max}, m^3 s^{-1}
1	Strâmba	21	194
2	Helegiu	27	273
3	Bârsăneşti	22	150
4	Brătila	13.2	206
5	Moreni	52	275
6	Valea Rea	11	145
7	Cernu	63	537

F, watershed area

but by the date of the flood it had been reduced to 2 million m^3. Theoretical exceedance probability for the Tazlău River was assessed as 0.8–1% and for some minor tributaries 0.1–1%. During this disaster, in Bacău County alone, 97 people died, 806 dwellings were destroyed, another 4,377 were damaged, 69 bridges and footbridges were ruined, and around 20 km of local roads suffered damage. In addition, 15 electricity lines and 10 telephone cables were interrupted; 25 torrent management facilities and ca 8 km of bank revetments were damaged (Podani and Zavoianu 1992). Losses also included 4,603 large animals and 5,732 heads of poultry; crop harvest was destroyed on 4,860 ha of land completely and on 6,900 ha partially.

7.5.2 Floods on the Siret River Between 2001 and 2010

The disastrous flood in the summer of 2005 on the Siret River resulted from extreme rainfall in the basins of the Moldova and Suceava Rivers, which supply the northern sector (Table 7.6). The flood wave on Siret unfolded in two phases, depending on the spatial distribution and temporal intensity of precipitation. Locally, over 200 mm of rainfall was registered in 3 days. The 6-day maximum was 377.9 mm (half of the multiannual average) at Vicovu de Sus, on the Suceava River (Table 7.6).

Dangerous levels were exceeded at all hydrometric stations on the Siret River before 2005, too. Peak discharges had a 2–5% (Table 7.7), the 4,650 m^3 s^{-1} peak flow of 2005 at Lungoci 0.5% probability. Reconstructed flow for Cosmeşti was 5,500 m^3 s^{-1}. The prognoses estimated over 6,600 m^3 s^{-1}, but the local authorities ordered the opening of several dams and intentional flooding of inhabited enclosures to reduce the flow downstream (Fig. 7.2). Only due to these measures did the discharge of the Siret not exceed that of the Danube.

High flow breached flood-control dykes and filled abandoned channels (Fig. 7.3), thus enlarging the areas where alluvia accumulated and also significantly eroded the concave banks. At Cosmeşti village, more than 50 m of the concave bank were eroded (Fig. 7.4), while at Piscu, a new accumulation strip of 100 m length emerged (Romanescu and Nistor 2011) (Fig. 7.5).

Table 7.6 The situation of the precipitations that generated the two floods in the Moldova (the upper sector) and Suceava catchment basins and the upper half of the Siret River (mm)

			First flood, mm				Second flood, mm				Sum
No.	River	Hydro/meteo station	22 July	23 July	24 July	Total	25 July	26 July	27 July	Total	total, mm
1	Siret	Siret	–	13.5	36.6	**50.1**	37.9	16.3	71.6	**125.8**	**175.9**
2		Zvoristea	–	11.2	2.9	**14.1**	11.6	12.8	10.7	**35.8**	**49.2**
3		Hutani	–	11.9	42.3	**54.2**	15.6	22.7	3.5	**41.8**	**96.0**
4		Lespezi	–	9.5	90.3	**99.8**	15.6	14.5	0.4	**30.5**	**130.3**
5		Nicolae Balcescu	3.0	20.0	68.5	**88.5**	8.5	0.5	6.5	**15.5**	**104.0**
6		Dragesti	10.8	6.6	27.1	**44.5**	–	–	–	**–**	**44.5**
7	Suceava	Brodina	–	8.4	55.2	**63.6**	102.3	107.7	10.2	**220.2**	**283.8**
8		Vicovu de Jos	–	8.5	33.4	**41.9**	113.0	135.0	88.0	**336**	**377.9**
9		Tibeni	–	8.9	58.1	**67.0**	55.6	23.2	27.6	**106.4**	**173.4**
10		Itcani	0.1	8.6	51.1	**59.8**	74.4	19.8	–	**94.2**	**154.0**
11		Suceava	7.1	1.6	58.1	**66.8**	77.8	5.2	19.2	**102.2**	**169.0**
12		Radauti	5.2	7.4	65.0	**77.6**	75.4	45.8	3.8	**125.0**	**202.6**
13	Putna	Putna	2.5	7.2	55.4	**65.1**	26.6	5.0	33.9	**64.9**	**130.6**
14	Pozen	Horodnic	–	8.3	73.2	**81.5**	90.0	81.7	37.2	**208.9**	**290.4**
15	Sucevita	Sucevita	0.4	13.7	54.8	**68.9**	115.9	73.7	7.3	**196.9**	**265.8**
15	Solonet	Parhauti	–	10.8	51.3	**62.1**	85.5	13.0	16.8	**115.3**	**177.4**
17	Somuzu Mare	Dolhesti	0.2	10.5	28.2	**38.9**	73.6	27.5	3.8	**104.9**	**143.8**
18	Moldova	Fundu Moldovei	0.7	8.6	64.8	**74.1**	6.4	6.7	16.2	**29.3**	**103.4**
19		Campulung Moldovenesc	0.5	9.7	98.2	**108.4**	7.9	6.8	26.3	**41.0**	**149.4**
20		Prisaca Dornei	1.1	7.4	56.3	**64.8**	14.2	4.0	47.8	**66.0**	**130.8**
21		Gura Humorului	–	5.9	62.4	**69.3**	33.5	1.6	37.8	**72.9**	**142.2**
22		Tupilati	–	10.7	37.1	**47.8**	9.5	–	5.5	**15.0**	**62.8**
23		Roman	3.0	20.0	63.5	**86.5**	8.5	0.6	5.5	**14.6**	**101.1**
24	Putna	Pojorata	2.5	7.2	78.1	**87.8**	2.9	5.0	33.9	**41.8**	**129.6**
25	Moldovita	Lungulet	0.4	9.1	57.3	**66.8**	30.0	16.2	56.4	**56.4**	**169.4**
26		Dragosa	0.2	9.4	73.6	**83.2**	36.5	4.2	–	–	**123.9**
27	Suha	Stulpicani	3.5	7.4	74.9	**85.8**	–	8.1	19.9	**19.9**	**113.8**
28	Humor	Gura Humorului	–	5.9	62.4	**69.3**	33.5	1.6	37.8	**37.8**	**142.2**
29	Rasca	Bogdanesti	–	10.0	42.0	**52.0**	36.0	9.8	2.5	**2.5**	**100.3**

7.5.3 Floods on the Pruth River Between 2001 and 2010

The Pruth River, on the border of Romania and the Republic of Moldova, experienced frequent floods in the period 1930–1975. In 1978, the Stânca–Costeşti reservoir was inaugurated and ever since has effectively reduced flood hazard downstream. On the Upper Pruth, upstream of the reservoir, however, flood hazard remains to be an important issue.

Before 2008, maximum discharge of the Pruth River, upstream of the Stânca–Costeşti reservoir, was 5,200 $m^3\ s^{-1}$ at Chernivtsi (Ukraine) and

Table 7.7 Comparative discharges registered in the Siret Basin before 2005

No.	River	Hydrometric station (founding year)	Q_{max} before 2005, $m^3\ s^{-1}$	Avoidance probability, %
1	Siret	Siret (1950)	1,193 (July 1969)	1–2
2		Hutani (1950)	866 (July 1969)	2
3		Lespezi (1950)	1,133 (July 1969)	5
4		Nicolae Balcescu (1986)	919 (August 2005)	5–10
5		Dragesti (1950)	1,948 (August 2005)	2–5
6		**Lungoci (2005)**	**4,650 (July 2005)**	**0.5**
7	Suceava	Brodina (1950)	365 (June 1969)	2–5
8		Tibeni (1981)	520 (June 1995)	10
9		Itcani (1948)	1,354.0 (June 1969)	2
10	Solonet	Parhauti (1950)	309 (July 2006)	2
11	Moldova	Gura Humorului (1972)	694 (August 2002)	2–5

Fig. 7.2 Dam breach at Condrea village

3,900 $m^3\ s^{-1}$ at Rădăuţi Pruth (Romania) (Table 7.8). The catastrophic floods in the summer of 2008 were caused, in the first phase, by heavy rainfalls on Ukrainian territory and, in the second phase, in Romania (Table 7.9). During the 2008 flood record, water levels were reached, and huge land surfaces were covered by water (Table 7.10, Figs. 7.6 and 7.7). The record water level was 1,130 cm at Rădăuţi Pruth, while the 7,146 $m^3\ s^{-1}$ peak discharge (of 0.1% probability) has not yet been surpassed ever since neither in Romania nor in Ukraine or the Republic of Moldova (Romanescu et al. 2011b). Extensive tracts of arable land (173,916 ha), permanent

Fig. 7.3 Flooding of Năneşti village and of the abandoned channels on the Siret floodplain

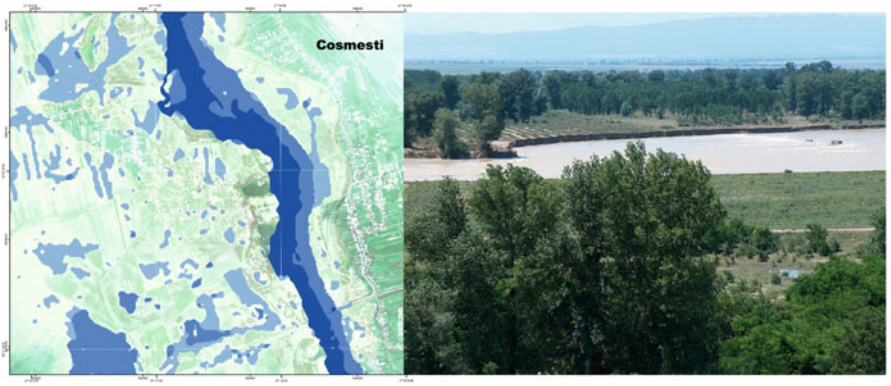

Fig. 7.4 Erosion of the right bank of the Siret at Cosmeşti village (maximum reconstructed flow: 5,500 $m^3\ s^{-1}$)

Fig. 7.5 Alluvial accumulation at Piscu village (downstream of Lungoci)

Table 7.8 Peak discharges (Q_{max}) and water transport (V) of the Pruth at the gages Chernivtsi (Ukraine) and Rădăuţi Pruth (Romania) during floods before 2008

	Chernivtsi (Ukraine)		Rădăuţi Pruth (Romania)	
Date	Q_{max}, $m^3\ s^{-1}$	V, million m^3	Q_{max}, $m^3\ s^{-1}$	V, million m^3
3–8 July 1964	2,170	175	1,400	185
8–14 July 1969	**5,200**	472	**3,900**	590
13–18 May 1970	3,050	324	2,450	330
21–26 July 1974	3,880	360	2,960	371

pastures (163,360 ha), forests (104,307 ha), and 2,835 ha of built of areas were inundated (Romanian Space Agency 2005, 2008, 2010).

The Pruth *flood* between the end of July and the end of August, the *longest* in Romanian history, was aggravated by backwater effect. In the first phase the sector upstream of the Stânca–Costeşti reservoir was flooded, while later reservoir overflow and the rains along the river section between the Stânca–Costeşti reservoir and the mouth have generated floods on the Lower Pruth.

7.5.4 Floods on the Suceava River

The Suceava River is a major tributary of the Lower Siret, where it enters Romanian territory. In July 2008, heavy rainfalls all over its watershed (in 6 days 431.9 mm at Vicovu de Jos, over half of the multiannual average) generated a catastrophic flood on this river (Table 7.11). On this relatively small river, a *colossal historical*

Table 7.9 Rainfall amounts at several stream gages in the Pruth Basin during the 2008 floods

	Hydrometric station					
Date	Darabani	Botoşani	Stânca–Costeşti	Cotnari	Iaşi	Bârnova
21 July	–	–	9.9	–	–	–
22 July	4.3	3.8	2.2	4.3	7.2	19.6
23 July	5.5	0.6	15.8	–	2.5	–
24 July	32.2	34.9	9.0	42.5	28.7	35.9
25 July	7.1	34.8	15.5	84.2	51.6	29.1
26 July	49.1	–	10.2	1.6	–	2.4
27 July	6.4	19.6	10.0	15.2	12.0	27.3
28 July	0.5	–	0.1	–	0.5	0.2
29 July	3.2	1.6	0.5	–	–	–
30 July	1.0	–	–	–	–	–
4 August	0.2	–	–	–	–	–
5 August	0.5	18.6	0.9	4.4	31.8	7.5
6 August	2.2	0.2	–	–	–	–
9 August	0.6	1.2	0.8	14.6	3.7	0.8
10 August	0.6	9.1	3.4	5.8	2.6	18.9
18 August	5.7	10.8	11.6	11.1	2.0	2.1
24 August	21.8	21.2	10.7	13.2	–	–
25 August	13.2	8.8	18.8	2.8	16.4	23.0
29 August	1.7	3.4	–	–	–	0.9
30 August	4.6	9.4	5.0	9.4	2.9	3.0
Total	160.4	178.0	124.4	209.1	161.9	170.7

Table 7.10 Historical water levels (H_{max}) before and during the floods in the summer of 2008

Hydrometric station	H_{max} in 2008, cm	H_{max} before 2008, cm
Oroftiana	**867**	703
Rădăuţi Pruth	**1,130**	964
Stanca Aval	**512**	403
Trifeşti	**702**	563
Sculeni	**605**	503
Ungheni	633	654
Prisăcani	619	622
Grozeşti	**658**	615
Drânceni	710	718
Pogăneşti	**546**	518
Sărata	**634**	600
Broscoşeşti	**579**	551
Bumbata	**525**	485
Berezeni	**550**	538
Doniceasa	**365**	336
Fălciu	**650**	631
Oancea	**640**	622

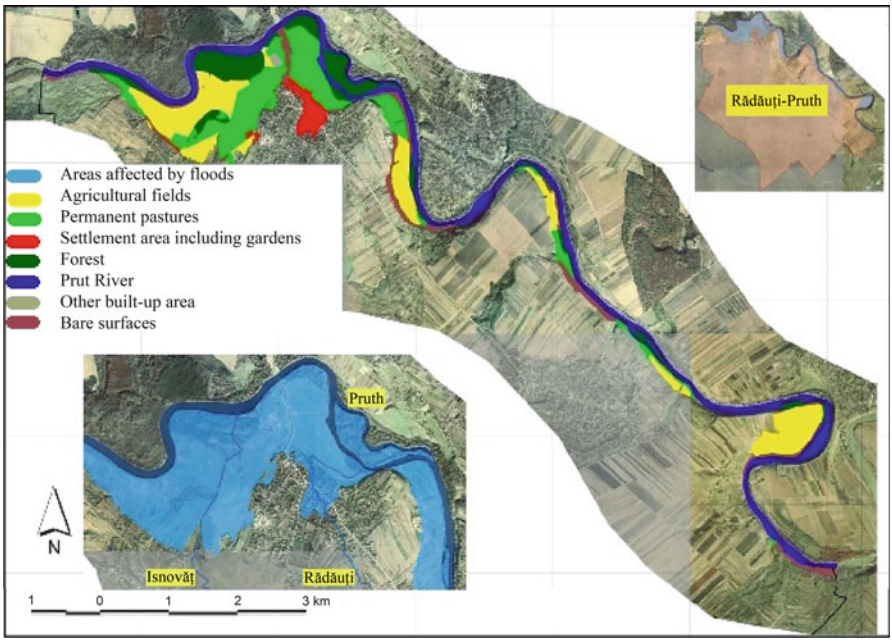

Fig. 7.6 The Rădăuţi Pruth area affected by floods (contour lines at scale 1:5.000; orthophoto images) (modified from Romanian Space Agency 2005, 2008, 2010)

Fig. 7.7 The area affected by the floods on Pruth at Rădăuţi Pruth on 29 July 2008, 3 m resolution (scale 1:25,000) (Source: http://sigur.rosa.ro 2008)

discharge (1,946 m^3 s^{-1} at Iţcani) was measured on 27 July 2008. For the upper section, the absolute maximum discharge was 465 m^3 s^{-1} at Brodina and for the middle was 966 m^3 s^{-1} at Ţibeni in July 2008. The water flow of the Suceava

Table 7.11 Precipitation totals (mm) for 22–27 July 2008 at the meteorological stations in the Suceava Basin

	Daily precipitation, mm						
Hydrometric station	22 July	23 July	24 July	25 July	26 July	27 July	Total, mm
Brodina	3.2	23.8	52.7	102.3	107.7	10.2	299.9
Vicovu de Jos	6.0	32.7	56.2	**145.5**	99.5	92.0	**431.9**
Ţibeni	–	8.9	58.1	55.6	23.2	27.6	173.4
Iţcani	0.1	8.6	51.1	74.4	19.8	–	154.0
Suceava	7.1	1.6	58.1	77.8	5.2	19.2	169.0
Horodnic	–	8.3	73.4	85.0	24.1	1.2	192.0
Rădăuţi	5.2	7.4	65.0	75.4	45.4	3.8	202.2
Cacica	3.5	15.8	50.8	80.0	7.5	13.0	170.6
Pârhăuţi	–	10.8	51.3	85.5	13.0	16.8	177.4

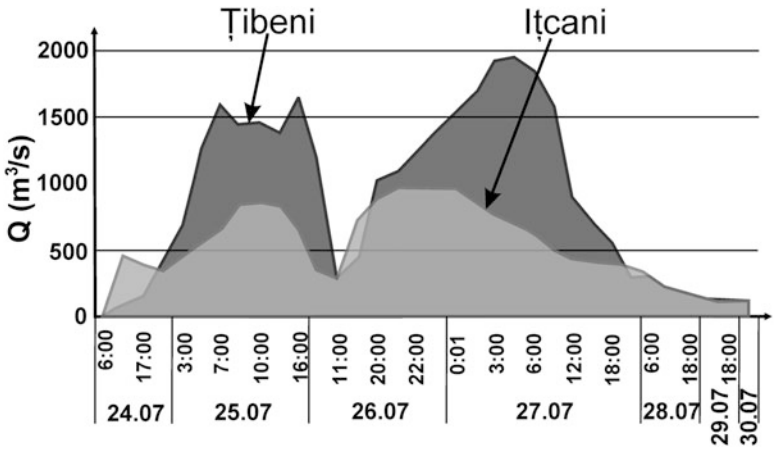

Fig. 7.8 Flood hydrograph for the period 24–30 July 2008 on the Suceava River at the hydrometric stations of Ţibeni and Iţcani

(and Moldova) River contributed substantially to peak discharges on the Middle Siret (2,930 $m^3\ s^{-1}$ at Drăgeşti, a historical high for this station).

Between July 23 and 7 August 2008, high flood waves passed on the upper (465 $m^3\ s^{-1}$ at Brodina on 26 July), middle (966 $m^3\ s^{-1}$ at Ţibeni on 26 July), and lower Suceava (1,946 $m^3\ s^{-1}$ at Iţcani on 27 July) (Fig. 7.8). Most material damage was registered in the city of Suceava, where plants and residential homes had been built in the floodplain.

7.5.5 Floods on the Buhai Stream

The Buhai Stream is a *small* direct *tributary* of the Jijia River, a member of the Pruth river system (Fig. 7.1). The confluence is near Dorohoi town. The source of the Buhai is in Ukraine, but its 134 km^2 watershed lies almost entirely on Romanian

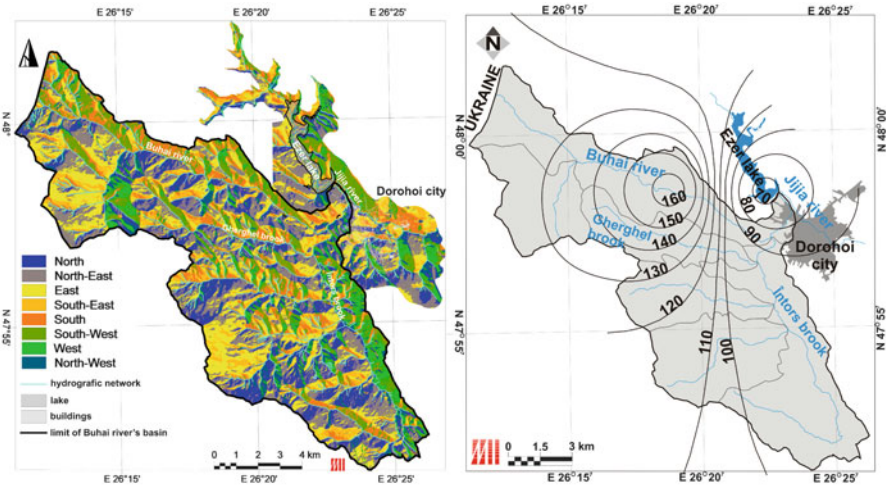

Fig. 7.9 Drainage network of the Buhai watershed and the confluence area with the Jijia River (**a**) with the location of the Ezer reservoir on the Jijia River. Core areas of heavy rains in the Buhai Basin and around the Ezer reservoir (**b**)

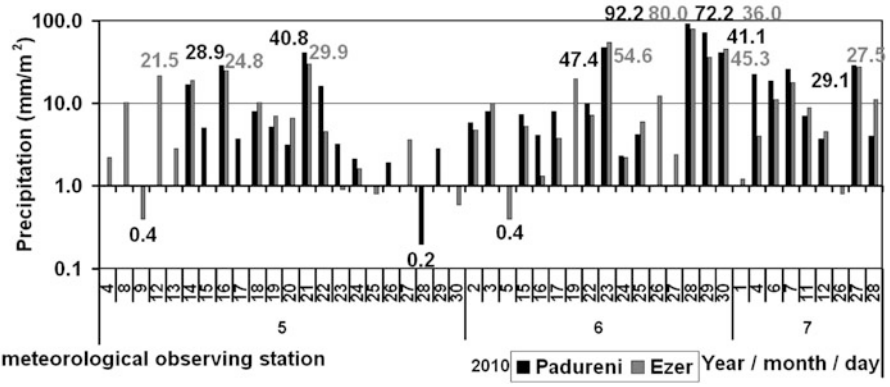

Fig. 7.10 Rainfall amounts on the Buhai watershed (at the rain-gage of Pădureni) and around the Ezer reservoir in May, June, and July

territory (Fig. 7.9). In the summer of 2010, one of the most bizarre floods on Earth occurred here. Heavy rains (184 mm in 24 h) with two core areas, along the upper Buhai and over the Ezer Lake (on the Jijia River – Fig. 7.9), induced a flood wave with 85 $m^3 s^{-1}$ peak discharge. Rainfall events in the previous 2 months made the soils saturated (Fig. 7.10). Therefore, the rainfall in the night of 28 June 2010 generated the runoff of huge amounts of water on the watershed carried by the stream towards the confluence with the Jijia River. On the Jijia, downstream of the confluence, the Ezer reservoir reduces flood levels and protects the town of Dorohoi from flooding. During the night of 28 June, between eleven o'clock and midnight,

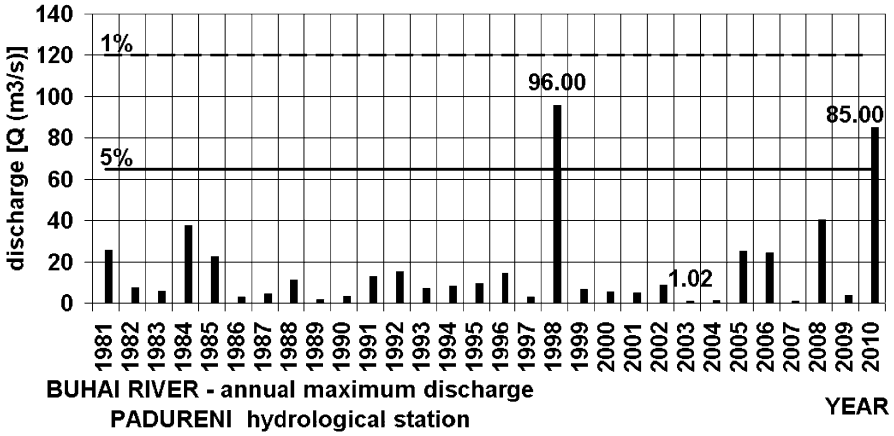

Fig. 7.11 Peak annual discharges of the Buhai Stream in 1981–2010 with the historical discharges of 1998 and 2010 (error: 2%)

an 85 m^3 s^{-1} high wave caused material damage and took a death toll in two rounds (Fig. 7.11). At first, areas on the Buhai watershed were flooded to the backwater effect (oversized bridges did not allow the water to flow through). After the major riverbed filled up and the water passed over the bridges, a second wave followed. Then the common floodplain of the two streams was flooded and the flood wave from the Buhai Stream moving at full speed managed to 'climb' the dam of the Ezer reservoir (Fig. 7.12). The waters penetrated the lake through the high-water spillway, situated at an altitude of 153 m. The high-water wave reached 153.5 m in height and spilled over in 50 cm depth. As this phenomenon was noticed and analysed for the first time in the literature, it was named '*spider flow*', referring to the fact that the water climbed the walls. Since the rainfall event occurred at night, the hydrologic warning came with delay. The consequences were devastating: six deaths, public buildings destroyed, and over 1,500 dwellings damaged (Fig. 7.13).

7.6 Flood Control

Reservoirs and other *engineering structures* could not retain high discharges which were registered in 2005, 2008, and 2010. Within the area supervised by the Siret Water Basin Administration, there are 249.63 km of flood-control dikes, 321.59 km of regulation structures, 104.15 km of (consolidated) embankments, eight permanent reservoirs (Poiana Uzului, Bucecea, Rogojeşti, Dragomirna, Şomuz II, Solca, Lac Bacău, and Şerbăuţi), three non-permanent reservoirs (Horodnic 1, 2, and 3), four water-intake dams (Mihoveni, Paşcani, Trotuş, and Călimăneşti), and seven pumping plants (Siret Water Basin Administration 2010). Within the Pruth–Bârlad Water Basin Administration, there are 417 watercourses with watersheds of more

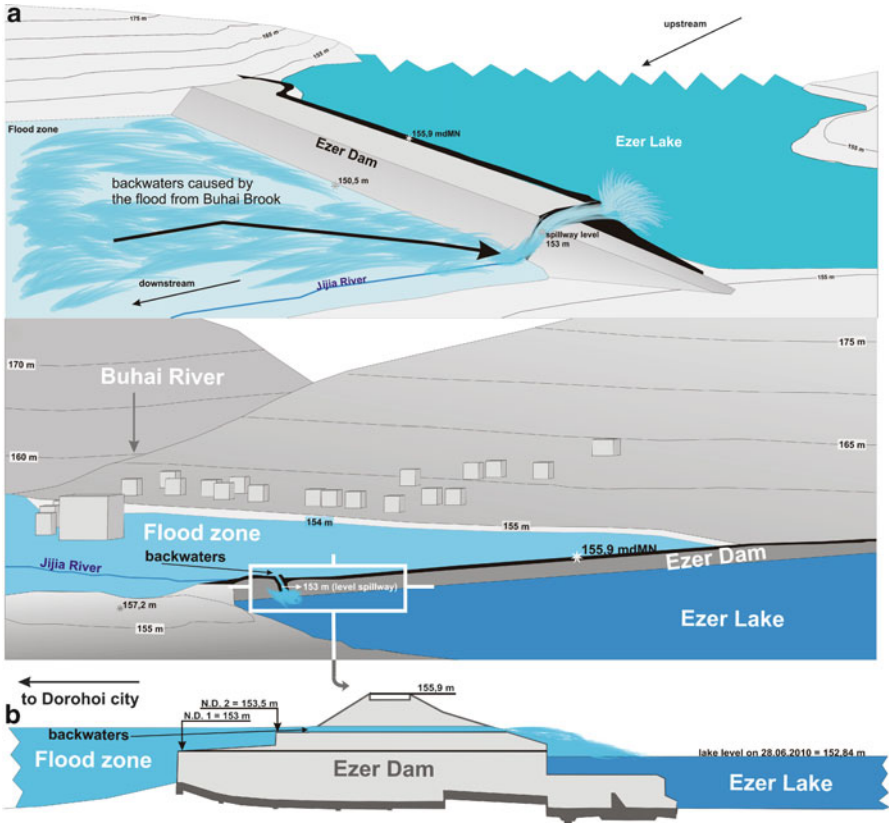

Fig. 7.12 The climbing of the spider flow waters over the flood spillway of the Ezer reservoir (**a**). Stages of backwater accumulation on the Buhai Stream and penetration ('spider flow') into the Ezer reservoir (**b**), 'inverted waterfall' and the rise of water level in the Ezer reservoir

Fig. 7.13 Barriers (railway and road bridges) at Dorohoi town

than 10 km^2 area, channelised along 1,173 km, regulated along 1,084 km. In addition, 262 fish ponds were established (Pruth–Bârlad Water Basin Administration 2010).

The floods on the Pruth River have been controlled by the Stânca–Costeşti reservoir. Major floods only occur on its tributaries and in the sector downstream from Stânca–Costeşti (examples are the floods of 2008 and the 'spider flow' flood on the Buhai Stream at Dorohoi). In order to reduce flow to warning or danger levels, certain dams were breached intentionally as a precaution. Flooded surfaces increased significantly, but the damage downstream diminished.

In order to increase the protection from floods, according to an agreement signed with Romania in Washington, Lockheed Martin LMT, a US company, will develop an advanced *hydrologic prognostic system* in Romania within the '*Destructive Waters*' (*DESWAT*) *Program.* To improve flood monitoring and modelling capacities, Lockheed will install over 600 hydrologic stations with sensors in 11 basins, including the Siret and the Pruth Basins. The hydrologic data obtained, together with the meteorological information offered by the SIMIN radar, will be transmitted to the National Office for Hydrologic Services in Bucharest. The service identifies the phenomena that might turn into floods, issue warnings, and hydrologic alerts and contacts the authorities responsible for flood defense.

7.7 Conclusions

Most of the floods in Eastern Romania were induced by *human activities*, among which the most important is deforestation. After 1990, some forests in the 'hands' of irresponsible owners were cut irrationally. There have also been massive deforestations in the southern, mountainous part of the Siret Basin, mostly in the watersheds of the Trotuş, Tazlău, Putna, and other rivers. Deforestation led to the *alteration of climate* in the drainage basins of the Siret and Pruth Rivers: intensified the torrential character of streams as well as desiccation. The annual *frequency of extreme precipitation events* (above amounts of 100 mm in 24 h) increased from 1.7% before 1900 to 47.9% in the period 1981–2000. After data homogenisation (adjusting the values according to increased number of stations), the percentages have altered: from 7.7% before 1900 to 35.9% in the period 1981–2000 (Fig. 7.14). After 2000, there have been frequent daily values exceeding 200 mm, mostly during the floods of 2004, 2005, 2006, 2008, and 2010 (Pleşoianu and Olariu 2010). The most conclusive cases of massive, uncontrolled deforestation occurred precisely in the basins (of the Suceava, Moldova, Moldoviţa, Suceviţa, Soloneţ, and other rivers) most affected by the floods of 2005, 2008, and 2010.

In addition to the material damage caused by floods, *geomorphological impacts* also have to be mentioned, such as the emergence and disappearance of channel bars, the accumulation of alluvia in the bank zone, and the retreat of concave banks, channel widening, direction changes of watercourses through spilling, re-flooding

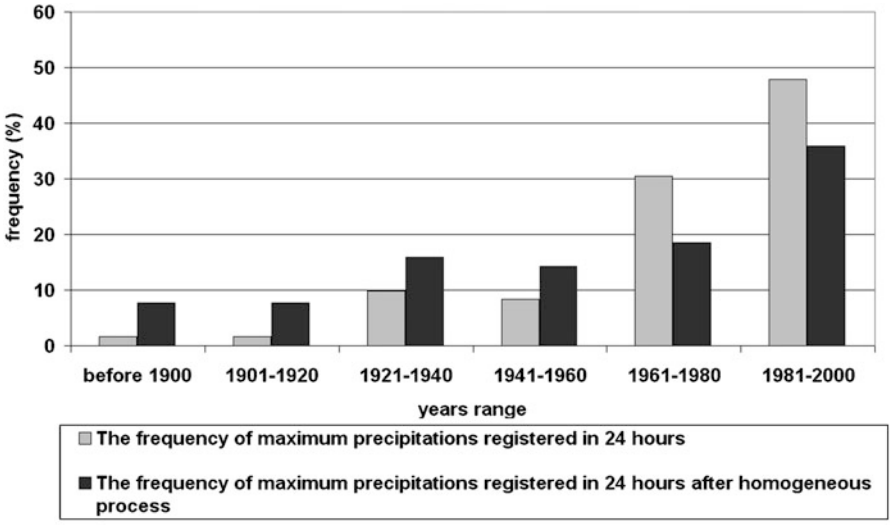

Fig. 7.14 Frequency of peak precipitation above the threshold of 100 mm in 24 h

of abandoned meanders, sedimentation of polders, and emergence of new surfaces for soil formation.

The flood on the Siret River in July 2005 pointed to the fact that most rural (and rarely even urban) settlements are situated in river floodplains or floodways. The lack of general national development planning of drainage basins, with maps illustrating hydrologic or geomorphologic hazards, allows poor management of extreme hydrologic phenomena.

For an optimal development of watersheds, certain *flood prevention* and mitigation *tasks* should be fulfilled:

- Short-term planning is necessary for areas with high flood hazard.
- Long-term planning for the improvement of hydromorphological conditions.
- Protection of densely populated areas by minor hydrotechnical structures.
- Modernisation of the warning/alarm system.
- Improving the application and observation of legislation on land use in flood-prone areas.
- Proper training of the population for measures to be taken in case of floods.

Acknowledgements We would like to thank the Siret Water Headquarters in Băcau for facilitating data collection regarding flow rates, water levels, and precipitation amounts. We also appreciate the assistance we received from the team of the Geo-archaeology Laboratory, Faculty of Geography and Geology, who analyzed and interpreted some of the data. With the analysis of satellite images, the Romanian Space Agency (ROSA) and the National Institute of Hydrology and Water Management (INHGA) helped. Data processing was performed in the ASR-CRUTA remote sensing laboratory using the images provided in the framework of the international CHARTER (Call ID-98), SIGUR project, and SAFER project (FP7 funding, agreement no. 218802).

References

Atlas of Water Cadastral Survey in Romania (1992) Date morfohidrografice cu privire la reteaua hidrografica a Romaniei (Morpho-hydrographic data on the surface hydrographic network). Ministry of Environment, Bucharest (in Romanian)

Barroca B, Bernardara P, Mouchel JM (2006) Indicators for identification of urban flooding vulnerability. In: Glade T, Kelman I, Hollenstein K, Kienholz H (eds) Vulnerability assessment in natural hazard and risk analysis for management and civil defence application. Nat Hazards Earth Syst Sci 6:553–561, special issue

Berz G, Kron W, Loster T, Rauch E, Schimetschek J, Schmieder J, Siebert A, Smolka A, Wirtz A (2001) World map of natural hazards – a global view of the distribution and intensity of significant exposures. Nat Hazards 23(2–3):443–465

Blynth K, Biggin DS (1993) Monitoring floodwater inundation with ERS-1 SAR. Earth Obs Q 42:6–8

Bravard JP, Petit F (2000) Les cours d'eau. Dynamique du système fluvial. Armand Colin, Paris, 222 p

Büchele B, Kreibich H, Kron A, Thieken A, Ihringer J, Oberle P, Merz B, Nestmann F (2006) Flood-risk mapping: contributions towards an enhanced assessment of extreme events and associated risks. Nat Hazards Earth Syst Sci 6(4):485–503

Cantemir D (1716) Descriptio Moldaviae. Berlin

Chen CN, Tsai CH, Tsai CT (2007) Reduction of discharge hydrograph and flood stage resulted from upstream detention pounds. Hydrol Process 21(25):3492–3506

Dalrymple T (1960) Flood-frequency analyses. U.S. Government Printing Office, Washington, DC, 80 p

Diaconu C (1988) Raurile – de la inundatii la seceta (Rivers – from floods to droughts). Technical Publishing House, Bucharest, 128 p

Diaconu S (1999) Cursuri de apa – Amenajare, Impact, Reabilitare (Water courses – development, impact, rehabilitation). HGA Publishing House, Bucharest, 189 p

Dorner W, Porter M, Metzka R (2008) Are floods in part a form of land use externality? Nat Hazards Earth Syst Sci 8(3):523–532

Förster S, Kuhlmann B, Lindenschmidt KE, Bronster A (2008) Assessing flood risk for a rural detention area. Nat Hazards Earth Syst Sci 8:311–322

Gabitsinashvili G, Namgaladze D, Uvo CB (2007) Evolution of artificial neutral network techniques for river flow forecasting. Environ Eng Manag J 6(1):37–43

Glade T, Anderson M, Crozier MJ (eds) (2005) Landslide hazard and risk. Wiley, Singapore, 824 p

Jaber FH, Shukla S (2007) Accuracy of hydrodynamic modeling of flood detention reservoirs. J Hydrol Eng 12(2):225–230

Jolin C, Diaconescu D, Neagoe M, Saulescu R (2009) The eco-impact of small hydro implementation. Environ Eng Manag J 8(4):837–841

Komma J, Reszler C, Blöschl G, Haiden T (2007) Ensemble prediction of floods – catchment non-linearity and forecast probabilities. Nat Hazards Earth Syst Sci 7(4):431–444

Konecsny K (2005) Reducerea gradului de impadurire ca factor de risc in formarea inundatiilor in bazinul hidrografic Tisa superioara (The decrease in forestation as a risk factor for the formation of floods in the upper Tisa hydrographical basin). Riscuri şi Catastrofe 4(2):165–174

Kuhlicke C (2010) The dynamics of vulnerability: some preliminary thoughts about the occurrence of radical surprises and a case study on the 2002 flood (Germany). Nat Hazards 55(3):671–688

Mustaţea A (2005) Viituri exceptionale pe teritoriul Romaniei (Exceptional flash-floods on Romanian territory). National Institute of Hydrology and Water Management Publishing House, Bucharest, 409 p

National Employee Development Center (1999) Module 211 reservoir flood routing. Engineering hydrology training series, Bucharest, 49 p

Pinter N, van der Ploeg RR, Schweigert P, Hoefer G (2006) Flood magnification on the River Rhine. Hydrol Process 20(1):147–164. doi:10.1002/hyp. 5908
Pleşoianu D, Olariu P (2010) Cateva observatii privind inundatiile produse in anul 2008 in bazinul Siretului (Some observation concerning the 2008 floods in the Siret basin). Ann Stefan cel Mare Univ Suceava Geogr Sect 19:69–80
Podani M, Zavoianu I (1992) Cauzele si efectele inundatiilor produse in luna iulie 1991 in Moldova (The causes and effects of the floods that occurred in July 1991 in Moldova). Geogr Stud Res 39:71–78
Portela MM, Delgado JM (2009) A new plotting position concept to evaluate peak flood discharges based on short samples. Water Resources Manag 5:415–428, WIT Press
Pruth-Bârlad Water Basin Administration (2010) General data. Iaşi
Romanescu G (2003) Inundatiile – intre natural si accidental (Floods – between natural and accidental). Riscuri şi Catastrofe 2:130–138
Romanescu G (2005) Riscul inundatiilor in amonte de lacul Izvorul Muntelui si efectul imediat asupra trasaturilor geomorfologice ale albiei (The flood risk upstream of the Izvorul Muntelui Lake, and the immediate effect on the geomorphological features of the riverbed). Riscuri şi Catastrofe 4:117–124
Romanescu G (2006) Inundatiile ca factor de risc. Studiu de caz pentru viiturile Siretului din iunie 2005 (Floods as a risk factor. Case study: the flash-floods on the Siret from June 2005). Terra Nostra Publishing House, Iaşi, 88 p
Romanescu G (2009) Siret river basin planning (Romania) and the role of wetlands in diminishing the floods. WIT Trans Ecol Environ 125:439–453
Romanescu G, Lasserre F (2006) Le potentiel hydraulique et sa mise en valeur en Moldavie Roumaine. In: Brun A, Lasserre F (eds) Politiques de l'eau. Grands principes et realites locales. Presses de l'Université de Québec, Québec, pp 325–346
Romanescu G, Nistor I (2011) The effect of the July 2005 catastrophic inundations in the Siret River's Lower Watershed, Romania. Nat Hazards 57(2):345–368
Romanescu G, Jora I, Stoleriu C (2011a) The most important high floods in Vaslui river basin – causes and consequences. Carpath J Earth Environ Sci 6(1):119–132
Romanescu G, Stoleriu C, Romanescu AM (2011b) Water reservoirs and the risk of accidental flood occurrence. Case study: Stanca–Costesti reservoir and the historical floods of the Pruth river in the period July–August 2008, Romania. Hydrol Process 25:2056–2070
Romanian Space Agency (2005, 2008, 2010) ROSA, Bucharest
Schumann AH, Geyer J (1997) Hydrological design of flood reservoirs by utilization of GIS and remote sensing. Proc Rabat Symp S3(242):173–180
Siret Water Basin Administration (2010) General data. Bacău
Smith K, Ward R (1998) Floods: physical processes and human impacts. Wiley, Chichester, 382 p
Strupczewski WG, Sing VP, Weglarczyk S, Kochanek K, Mitosek HT (2006) Complementary aspects of linear flood routing modelling and flood frequency analysis. Hydrol Process 20(16):3525–3554
Sudhaus D, Seidel J, Burger K, Dostal P, Imbery F, Mayer H, Glaser R, Konold W (2008) Discharges of past flood events based on historical river profiles. Hydrol Earth Syst Sci 12:1201–1209
Tockner K, Malard F, Ward JV (2000) An extension of the flood pulse concept. Hydrol Process 14:2861–2883
WMO (2008) Reservoir operations and management flows. A tool for integrated flood management. Associated programme on flood management. World Meteorological Organization, Geneva. http://www.apfm.info/pdf/ifm_tools/Tools_Reservoir_Operations_and_Managed_Flows.pdf

Chapter 8
Extreme Floods in Slovenia in September 2010

Blaž Komac and Matija Zorn

Abstract Slovenia was struck by big floods in September 2010, which affected large parts of the country. This chapter presents a geographical analysis of the event through identifying the main causes, types, and consequences of floods. The floods were characterized by exceptionally high water levels, long duration, and great variety of flash floods, lowland (riverine) floods, karst floods, and urban flooding. Case studies are presented from the Ljubljana Marsh and Dobrepolje karst polje in central Slovenia. The legislative framework for flood risk protection in Slovenia is also presented along with text analyses of newspaper articles about the 2010 floods.

Keywords Extreme rainfall • Flood types • Damage • Landslides • Spatial planning • Slovenia

8.1 Introduction

The great landscape diversity of Slovenia also involves remarkable *hydrogeographical diversity*, which is seen in discharge regimes (Hrvatin 1998; Frantar and Hrvatin 2005), characterized by changes in the influence of rainfall and snowfall, surface karstification, and morphological variations of Slovenian rivers (Repnik Mah et al. 2010). Because of the terrain of high relief, most Slovenian rivers are less than 20 km long, and a full third of them are flashy streams (Mikoš 1995, 2007).

"High water appears every year in Slovenia and is common. It can appear in any season, but most often in the fall. . . . Over the past century, not even a decade has been without major floods. They have appeared across all of Slovenia" (Polajnar 2002, p. 247). This has also been the case in the last two decades (Fig. 8.1), when

B. Komac (✉) • M. Zorn
Scientific Research Centre of the Slovenian Academy of Sciences and Arts, Anton-Melik Geographical Institute, Novi trg 2, 1000 Ljubljana, Slovenia
e-mail: blaz.komac@zrc-sazu.si; matija.zorn@zrc-sazu.si

D. Lóczy (ed.), *Geomorphological impacts of extreme weather: Case studies from central and eastern Europe*, Springer Geography, DOI 10.1007/978-94-007-6301-2_8,

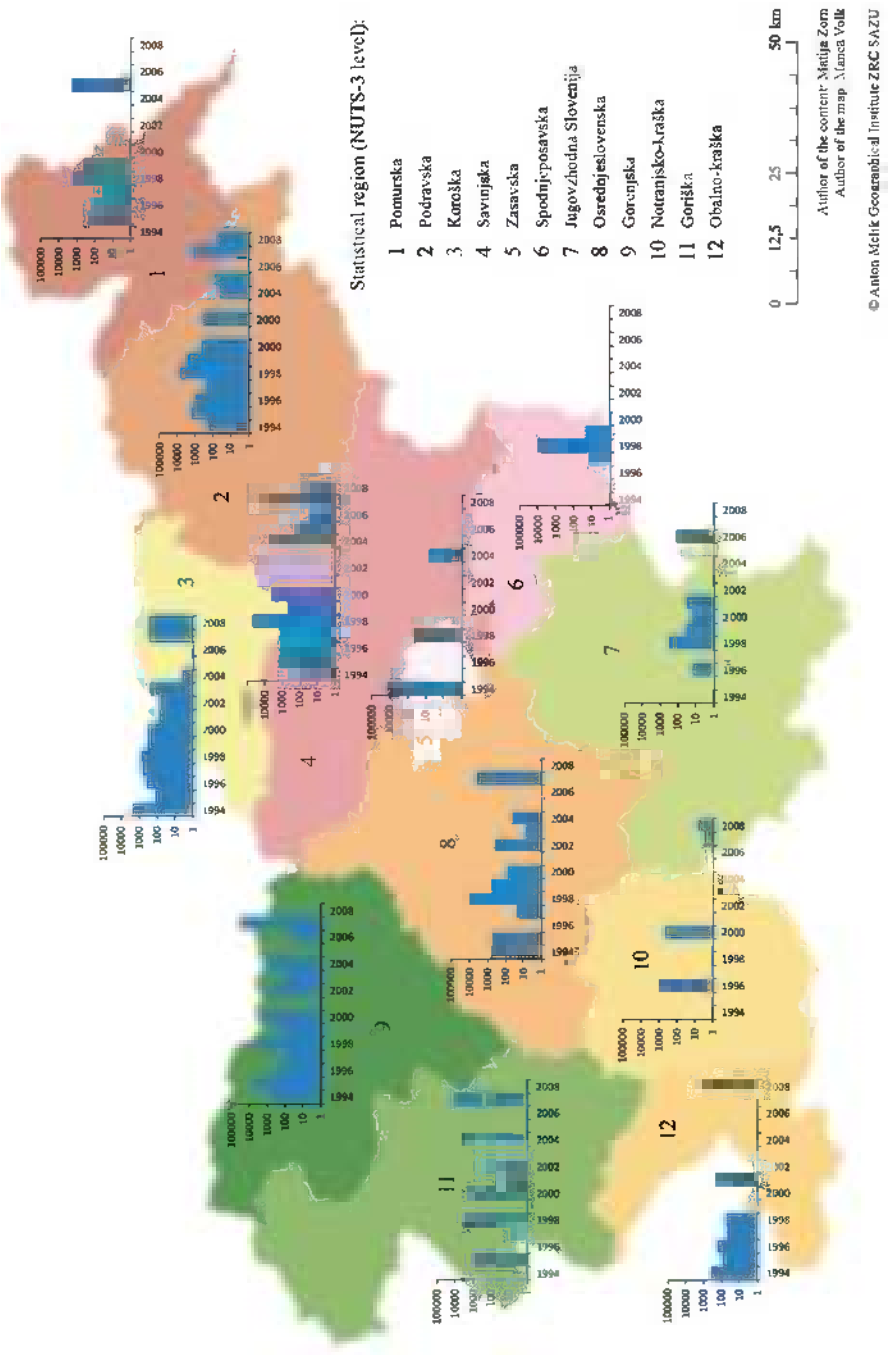

Fig. 8.1 Damage (€000) due to floods in Slovenia by statistical region, 1994–2008 (Zorn and Komac 2011)

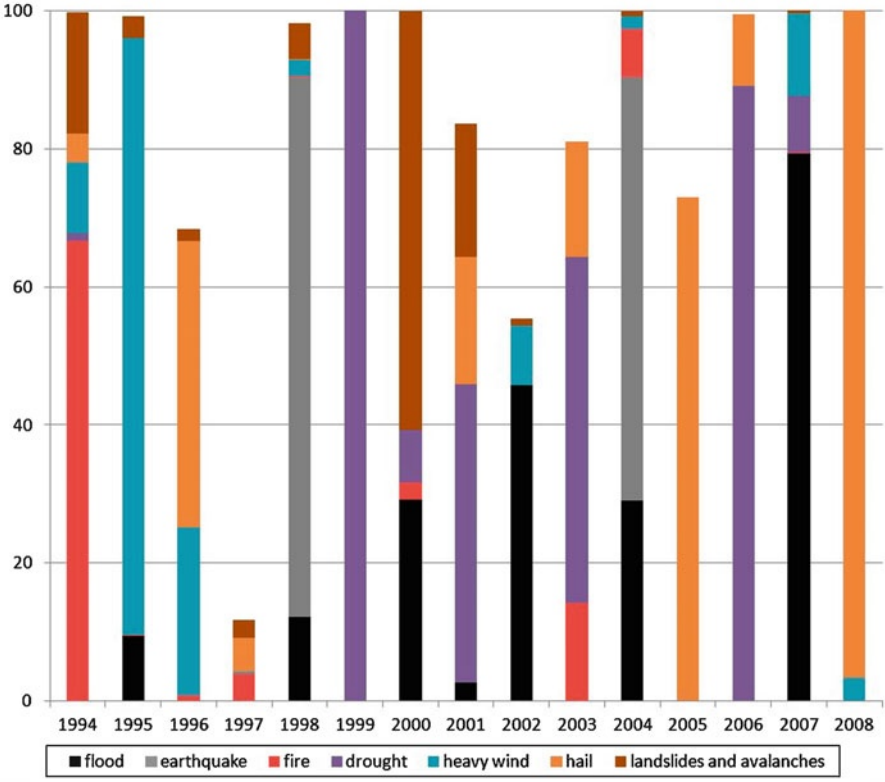

Fig. 8.2 Share of direct damage in Slovenia by selected natural disasters, 1994–2008 (Zorn and Komac 2011)

floods have been responsible for 15% of the total damage due to natural disasters in the country (Fig. 8.2). Before the floods in 2010, the following years have stood out in this regard: 1994 (31.3% of total damage from natural disasters), 1995 (18.1%), 1998 (51.9%), 1999 (12.1%), 2004 (15.2%), and 2007 (64.8%) (Zorn and Komac 2011).

These hydrogeographical factors influence the main types of floods. Landscapes are most affected by flash floods and lowland (riverine) flooding, whereas floods on some karst poljes constitute another distinct type. From the perspective of flood risk, areas with infrequent but major floods are of special interest. In karst poljes, ordinary and extreme floods nearly overlap. Because of the slow inflow of water, these floods are usually less dangerous; being frequent and regularly recurring, people have adapted to them and have located their settlements, fields, and main traffic routes on terrains above their levels. With lowland flooding, the outer boundary of flood areas in the landscape is often clearly visible in the string of settlements that are more or less safely set back from the flood

Fig. 8.3 Adaptation of the location of settlements and traffic routes to lowland floods, example from the Pannonian Basin (*izmera Slavonska vojna krajina* "survey of the Slavonian Military Frontier," 1780–1782), section 4 map of the military survey from the end of the eighteenth century (Zorn 2007). The map bears the text: *Bis hieher ist die Uberschvemmung alljärlich 3 bis 4 Mahl* ("floods extend to this point three or four times per year"). The *arrow* shows the extent of annual floods. Current urbanization in Slovenia too often does not consider past knowledge about the landscape (Komac et al. 2008b; Komac 2009), which considerably increases damage during lowland floods

area (Fig. 8.3). This is not the case for flash floods (Fig. 8.4). Buildings are often right alongside the beds of small streams of gentle flow but with flash flood hazard (Komac et al. 2008a).

8.2 The Floods of September 2010

The *floods* in September 2010 were among the greatest natural disasters in the past decades in Slovenia. They affected 137 Slovenian municipalities (60%), and the *damage* (including VAT) was estimated at over €240 million. For the sake of comparison, the damage of the most costly flooding prior to this event was

Fig. 8.4 Consequences of flash floods in the Davča Valley (western Slovenia) during the 2007 floods (photo by M. Zorn)

estimated at over €500 million in 1990. Considerable damage was also caused by floods in September 2007 (€233 million), which affected 50 municipalities, the 1998 floods (€170 million; Mikoš et al. 2004), and the November 2012 floods (over €200 million).

The damage in the September 2010 floods exceeded 0.3‰ of the planned revenues for the 2010 national budget (Komac and Zorn 2011a). In addition to its large spatial dimensions and effects on the landscape, the flooding was characterized by great diversity. The majority of flood-prone areas in Slovenia were flooded, in some places the flow rates of rivers and streams were the highest ever recorded (Strojan et al. 2010, p. 10), and many watercourses reached or exceeded their 100-year return period. The extent of the damage from the September 2010 floods was particularly influenced by the rapid spread of dense settlement over floodplains (Gašperič 2004; Komac et al. 2008b).

8.2.1 Causes and Types of Floods

The floods were the result of *heavy rainfalls* from 16 to 19 September 2010. In 48 h (from 17 to 19 September), an average of 175 mm of precipitation fell – "the greatest amount during such a time period in the past 60 years" (Poročilo … 2010, p. 5).

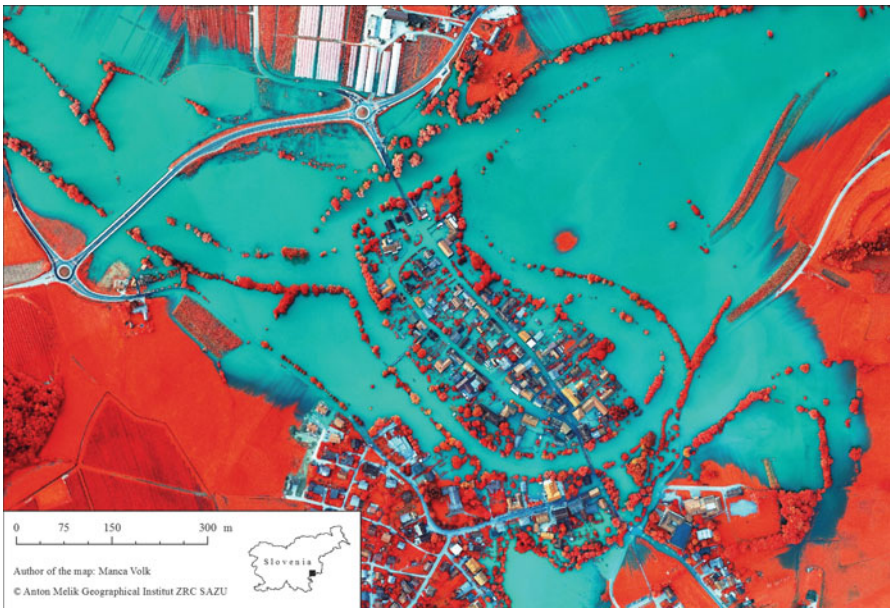

Fig. 8.5 Lowland floods along the Krka River (southeastern Slovenia) during the September 2007 floods – the settlement Kostanjevica na Krki (photo: GEOIN d.o.o.)

In southern, central, and western Slovenia, the precipitation reached or exceeded the value of 100-year return period for 2 days. In Ljubljana (in central Slovenia), more rain fell (271 mm between 17 and 20 September 2010) than during the extensive floods of 1926 (125 mm) and 1933 (259 mm) (Strojan et al. 2010). At Otlica above Ajdovščina (in western Slovenia), in only 3 days, between 17 and 20 September 2010, 539 mm of precipitation fell, which is one-fourth of the average annual precipitation. Elsewhere in western and central Slovenia, between one-fifth and one-fourth of the average annual precipitation fell (Globevnik and Vidmar 2010; Poročilo . . . 2010).

Based on the main features of floods and the flood-prone areas of Slovenia, Natek (2005) distinguished five *types of floods* (partially taken from Gams 1973): flash floods, lowland floods (Fig. 8.5), karst polje floods (Fig. 8.6), coastal floods (Kolega 2006), and urban floods. Among these, only coastal floods did not occur in September 2010. In addition to their great diversity, the progress of floods in time is also interesting. First to appear were *flash floods* on the morning of 17 September, primarily in western Slovenia. During the middle of the day, urban floods appeared in central Slovenia; underpasses in Ljubljana were flooded. Soon after, flashy steams such as the Gradaščica, Sora, Savinja, Ložnica, Dravinja, Rižana, and Dragonja flooded, leading to *lowland floods* along the larger Krka (Fig. 8.5) and Sava Rivers. Because of karst water retention, this finally led to *karst polje floods*. Flash floods severely affected Zagorje, and a day later the southwestern part of the capital city was inundated. Dozens of *landslides* were triggered, especially in the hilly regions of Posavsko hribovje and Idrijsko-Cerkljanskem hribovje and also in

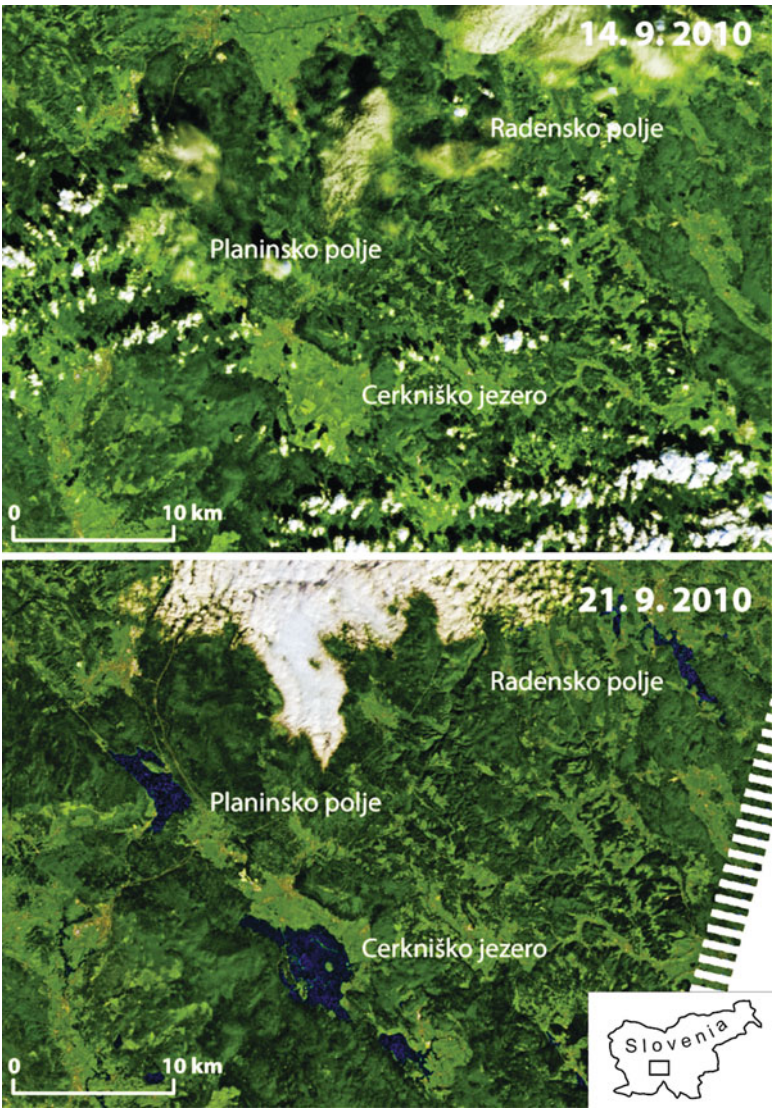

Fig. 8.6 Floods on karst poljes in Landsat TM5 satellite images (*top*, 14 September 2010 before the floods; *bottom*, 21 September 2010 after the floods). The *dark blue* areas are floods in karst poljes: the Radensko, Planinsko, and Cerkniško karst polje (Veljanovski et al. 2011)

the coastal area around Koper, the Vipava Valley, and the Pohorje Massif. Nearly 100 landslides were triggered in the municipality of Laško (in eastern Slovenia) alone, of which 15 threatened residential structures. The Stogovce landslide (Petkovšek et al. 2011) near Col destroyed a kilometer of the road between Ajdovščina and Predmeja (Fig. 8.7). Sediments from floodwaters were visible in the Gulf of Trieste (in the northern Adriatic) (Fig. 8.8).

Fig. 8.7 During extensive precipitation in September 2010, the Stogovce landslide was triggered, which destroyed a kilometer of the road between Ajdovščina and Predmeja (photo by M. Zorn)

Fig. 8.8 Sediments from floodwaters visible in the Gulf of Trieste (in the northern Adriatic) (© NASA Landsat TM5, 21 September 2010)

Fig. 8.9 Flood in the Ljubljana Marsh, 23 September 2010, 3:30 p.m.; nearly a week after the floods started, the settlements Lipe and Črna vas (southwest of Ljubljana) were still flooded (photo by M. Pavšek)

8.2.2 Floods in the Ljubljana Marsh

In the flood zone along the Ljubljanica River, *karst-type floods* are common because they occur two to three times a year, but with a limited extension. They develop gradually and last from a few days to several weeks. Normal or regular floods do not cause damage – precisely because of their frequency: settlements, farmland, and transportation routes are located on somewhat higher edges, on embankments, or on isolated hills. In addition to karst floods, the Ljubljana Marsh is also threatened by flash floods from streams in the hilly region of Polhograjsko hribovje. The floods are the most destructive when the water from flashy streams becomes trapped in low-lying areas by influent karst water sources of the Ljubljanica River.

The central, lowest part of the Ljubljana Marsh between Vrhnika and Ljubljana is often inundated and, with the exception of the settlements of Lipe and Črna vas (Fig. 8.9), is completely uninhabited. The first settlement of this area was made possible only with drainage work at the end of the eighteenth century, when ditches and canals were excavated alongside rivers and streams, and the Ljubljanica River was dredged in 1825. This measure lowered the groundwater table sufficiently for agriculture and settlement in some areas (Melik 1963; Natek 2005; Zorn and Šmid Hribar 2012). In the period between 1885 and 1933, there were *five major floods* in the Ljubljana Marsh: 3 November 1885 (Fig. 8.10), 18–19 March 1888, the end of

Fig. 8.10 The Ljubljana Marsh flooded in 1895. View from Ljubljana Castle toward the south. Bottom part of image today: the southern part of Ljubljana with population of several ten thousands of people (GIAM ZRC SAZU Archive)

March 1895, 27 September 1926, and 23–24 September 1933. There had been no major floods until the 1970s, and a somewhat larger one on 5 November 1998. This undoubtedly contributed to the fact that the current residents of the Vič neighborhood in Ljubljana (in the southern part of the capital) were unaware of their exposure to flood risk. A survey just a few years before the flood showed that 72% of people in the area did not know that catastrophic floods are possible there and 59% did not know that the area had previously been flooded (Gašperič 2004). The presented flood in the Ljubljana Marsh started on 18 September 2010, and it reached its greatest extent on 20 September 2010 (Fig. 8.11), when 76.8 km^2 of land was flooded, and the volume of floodwater is estimated at 34 million m^3. The likelihood of such an extensive flood was 1%. The water levels were almost the same as those in 1933, and in places the water was up to 95 cm deep (Globevnik and Vidmar 2010).

8.2.3 Flood in the Dobrepolje Karst Polje

The Rašica drainage basin, in which surface watercourses predominate, and the Dobrepolje karst polje in the region of Suha krajina are connected by a dry valley between Ponikve and Predstruge that shows hydrological activity only during exceptionally high water levels. Flooding both in the Rašica drainage basin and the northwestern Dobrepolje karst polje is of the lowland type. Karst flooding occurs in the southeastern part. In the Dobrepolje karst polje, floods are frequent in the southern and southeastern areas, near the settlement of Pri Cerkvi–Struge (Figs. 8.12 and 8.13). *Extreme flooding* occurs in Dobrepolje because of high water

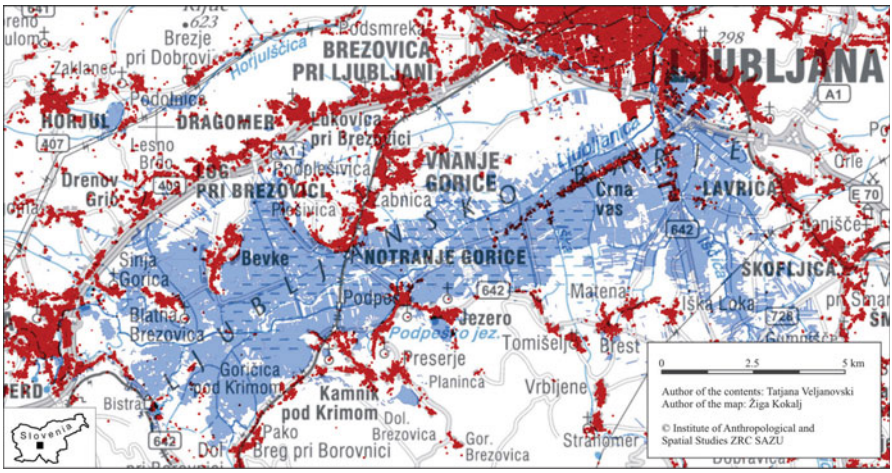

Fig. 8.11 Flood in the Ljubljana Marsh, 20 September 2010. *Blue*, flooded areas; *red*, built-up areas (Veljanovski and Kokalj 2012)

Fig. 8.12 Flooded karst mosaic in the Dobrepolje karst polje between the villages of Podtabor (*left*) and Paka (*right*), 23 September 2010; an example of extreme karst flooding. *Bottom* of the picture: flooded dolines (photo by M. Zorn)

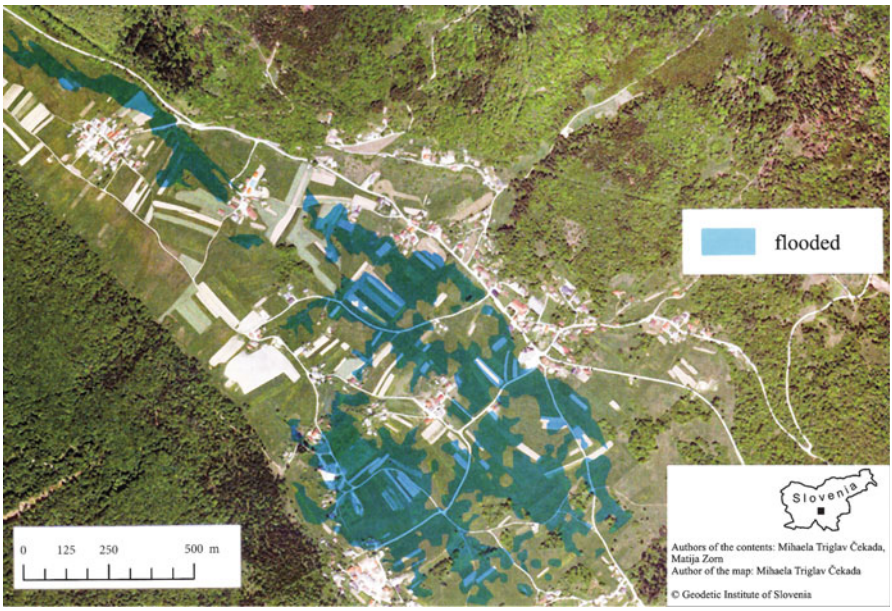

Fig. 8.13 Up to 50 ha of Dobrepolje karst polje were flooded after heavy rains (Triglav Čekada and Zorn 2012)

outflow from karst caves (Potiskavec Cave, Kompolje Cave, and Podpeč Cave). Sometimes, this karst water is joined by floodwater from Rašica, which happened in 1933 and 2010. In 1933 the parish church in Struge was submerged to the top of the main entrance. At that time the water was rising very fast, "in 3 h a full 5 m," and took approximately 14 days to drain away (Meze 1983, pp. 29–30). Kranjc (1981) writes that the floods of 1882, 1917, 1933, 1939, and 1973 were "destructive."

8.3 Legislative Framework for Flood Hazard and Risk in Slovenia

In recent decades, progress has been made in the study of natural disasters, their effects, and the threat they represent. Nonetheless, damage is increasing (Zorn and Komac 2011). The *legal provisions* for natural-disaster areas are also satisfactory in principle, but in many countries "there has been an inadequate focusing of disaster risk management effort and resources where they are most clearly needed. Obviously, insufficient progress has been made in converting theoretical research findings into concrete actions in practical disaster management" (Weichselgartner and Obersteiner 2002).

In spite of clear legislation, in Slovenia hundreds of cases of new construction of residential, business, and other buildings have been approved in flood-risk areas.

In addition, every year the Slovenian Environment Agency issues over a 1,000 *building permits* (there are approximately 6,000 settlements in Slovenia) for development in areas that affect the water regime of rivers, and through decrees the government allows construction in riparian areas, where it is supposedly forbidden by the Water Act (Komac et al. 2008a).

For the postcommunist countries of central and eastern Europe in social and economic transition (Pallagast and Mercies 2007; Stanilov 2007), it is characteristic that the ever-increasing pressure from investment and construction in flood areas shows no regard for the threat of future floods or their predicted intensification due to global climate change. The most important *legislation* defining Slovenian society's relationship to natural disasters includes:

- The Protection Against Natural and Other Disasters Act (Zakon o varstvu . . . 1994),
- The Strategy for the Spatial Development of Slovenia (Strategija . . . 2004),
- The National Program for Protection Against Natural and Other Disasters (Nacionalni . . . 2006),
- The Resolution on the National Program for Protection against Natural and Other Disasters from 2009 to 2015 (Resolucija . . . 2009),
- The Water Act (Zakon o vodah 2002),
- The Spatial Planning Act (Zakon o prostorskem . . . 2007),
- National development programs,
- Regional development programs,
- The EU Floods Directive (2007).

References that only pay lip service to the paradigm of sustainable development are frequent. In Slovenia, a corresponding approach to "coexistence" with nature appears in the *Strategy for the Spatial Development of Slovenia* (Strategija . . . 2004); however, due to different development priorities, its provisions are not realized in practice. The strategy clearly states that "Natural processes that can threaten settlement and human activity must be respected as limitations in planning uses and activities in space" (Strategija . . . 2004, p. 30). In connecting the measures for attaining sustainable development, it is clearly stated that it is necessary to "ensure that vulnerability to natural and other disasters is consistently taken into account in maintaining the settlement and development of landscapes" (p. 41).

The *Water Act* (Zakon o vodah 2002) is also quite clear: "For the use of and other activities in water, riparian, or coastal land areas and land in protected or threatened areas . . . it is necessary to program, plan, and execute these so as . . . to provide safety from the damaging activity of water, and to preserve natural processes and the natural balance of water and river ecosystems" (Article 5). Article 83 states that the minister responsible for this area "shall, with the agreement of the minister responsible for protection against natural and other disasters, prescribe a detailed methodology for defining threatened areas and a manner for categorizing land into threat categories." A suitable directive for floods, taking into account the EU Floods Directive (2007), was issued in 2007 (Pravilnik . . . 2007), and in 2012 a methodology for defining flood-risk areas was published (Đurović 2012).

Unfortunately, these statements are all too often true more in word than in deed, because in practice things are often different. This is often the result of informal

planning practices by various stakeholders trying to achieve their legitimate (political, economic, ideological) goals through lobbying, clientelism, or even corruption (Kušar 2010). An example is the case of the expansion of the Laško Spa (in eastern Slovenia). Although the natural conditions in Laško make major preventive measures impossible, the government issued a decree allowing expansion of the health spa on land subject to river flooding. The consequences were predictable: during the floods of September 2007, the new buildings suffered €1.8 million in damage. In addition, the government also provided financial help to the spa after the flood, although this completely contradicts the standards of sustainable development and applicable legislation (Komac et al. 2008a). In the case of flood-prone areas, this would mean that spatial planning would permanently ensure their primary functions (floodwater drainage and retention) and prescribe land-use regulations (forest, meadows, and pastures) which do not affect them.

8.4 Society and the Perception of Floods

In the recent past in most European countries, society still overtook the majority of responsibility for preventive measures and damages associated with natural disasters, although in recent years this burden has increasingly shifted toward the individual. This is leading to a process of individualization. The reason for this is inconsistency and lack of explicitness in legislation as well as an inert insurance system, on the one hand, and on the other, according to Walker et al. (2010), growing consciousness among people about responsible citizenship. In addition to other long-term activities, such as the implementation of regulations and spatial planning, education has contributed much to the *consciousness* of responsible citizenship (Kuhlicke et al. 2011; Komac et al. 2011). With a comprehensive, long-term approach to regulating space and informing society, we can expect a change in the understanding of natural disasters and perhaps also a change in behavior with appropriate effects on the landscape (Komac 2009). Understanding natural disasters is connected with knowledge, even though logical knowledge most often does not have a direct impact on behavior.

Unfortunately, the current understanding of the landscape is shaped considerably by the *media*. Even though it is difficult to quantitatively define the significance of the media, an analysis of the texts that journalists use in their work provides insight into how modern society understands natural disasters. An analysis of articles from the Slovenian leading newspaper *Delo* from the month following the September 2010 floods shows that the articles most often used expressions connected with the damage caused by natural disasters (Figs. 8.14 and 8.15 – Komac and Zorn 2011b). In addition to the expression *voda* "water" (550 occurrences) and *poplava* "flood" (368), the most frequent expressions referred to money (*evro* "euro" 255, *denar* "money" 75), followed by *občina* "municipality" (191) and *cesta* "road" (221). The writers of the articles were also interested in which areas were affected by floods and landslides (177 mentions) and the state response to the floods (135). It is

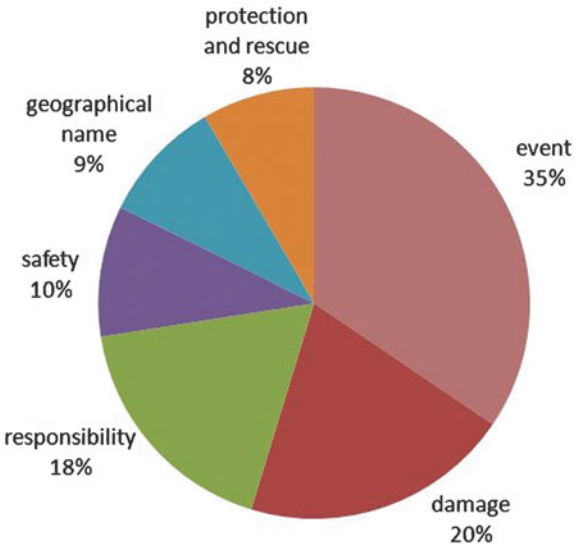

Fig. 8.14 Shares of mention of expressions connected with the September 2010 floods in the leading Slovenian newspaper *Delo* a month after the event (Komac and Zorn 2011b)

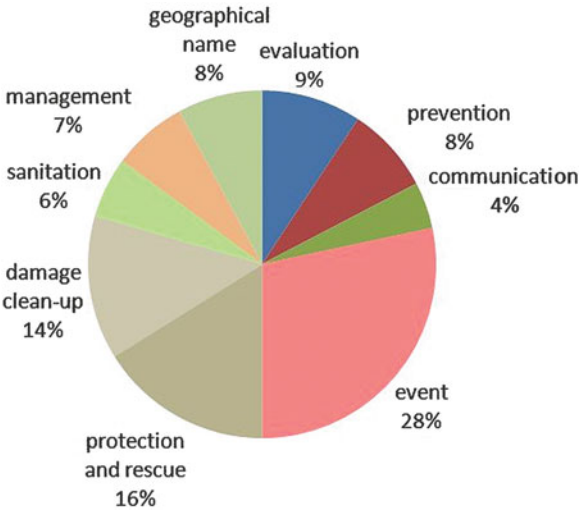

Fig. 8.15 Shares of mention of expressions concerning the management of natural disasters by area in the leading Slovenian newspaper *Delo* (Komac and Zorn 2011b)

understandable that the newspaper reports dedicated special attention to spatially defining the incidents. Thus, *Ljubljana* (150), together with the expressions *mesto* "city" (70) and *Vič* (11), was mentioned a full 231 times. This indicates the exceptional nature of the phenomenon in Ljubljana and at the same time the centralized perspective of the newspaper reporters. The name *Ljubljana* was followed in terms of frequency of mention by *Celje* (59), *Barje* "Ljubljana Marsh" (51), *Laško* (43), *Dragonja* (25), *Posavje* "Lower Sava Valley" (22), *Savinja* (21), *Koper* (13), *Zagorje* (11), and *Ljubljanica* River and *Štore* (10 each).

These are followed by words that apply to more detailed descriptions of damage to houses (134) and descriptions of events (*nesreča* "disaster" 91 times, *ljudje* "people" 90, *gasilci* "firefighters" 75), descriptions of *prizadeti* "flood victims" and *sanacija* "cleanup" (62 each), and *ukrepi* "measures" and *zavarovalnica* "insurance company" (59 each). This is followed in frequency by the expressions *vlada* "government" (50) or *premier* "prime minister" (49), *varnost* "safety" (47), *minister za okolje* "minister of the environment" (46), *deževje* "extended rainfall" (46), *sklad* "fund" (43), etc.

One-third of the words in the articles were dedicated to describing the phenomena, one-fifth each to presenting damage and responsibility, and one-tenth each to safety, the flooded areas, and protection and rescue. The division of expressions by area of managing natural disasters is also interesting. Evaluation (i.e., research-based assessment of natural disasters, in this case floods) accounted for one-tenth of the vocabulary, as did preventive measures. Less than 5% of the words described communication before or during the event, and nearly one-third of the words were directly related to the event itself (Fig. 8.15).

8.5 Conclusions

According to the findings of psychologists, in some particularly risk areas of Slovenia, one may speak of a subculture of natural disasters, which means that the population is already somewhat adapted to natural processes (Komac and Zorn 2011a). However, a *culture* of avoiding natural disasters is nonetheless underdeveloped in Slovenia. Most resources are used to post-event cleanup instead of for prevention; investing only one-third of the resources used for cleanup into prevention would have the same effect (Siegel 1996).

The culture of "putting out fires," which is characteristic for a transitional period of development, has not yet been replaced by a "culture of prevention" or a "culture of risk." So long as natural disasters affect the countryside or occur at regional level, few are affected, and the damage is slight, society is capable of dealing with the inconveniences accompanying rescue, assistance, and cleanup. However, it is different if something happens in an urban area, as happened in Slovenia in September 2010, when, among other things, the southern part of the capital, Ljubljana, was flooded (Fig. 8.11, Komac and Zorn 2011a). Those affected seek to find someone to blame for the resulting damage at any cost, preferring to forget about their own irresponsibility.

In recent decades in Slovenia, various interests have resulted in increasingly frequent *development of unsafe areas*, due to which the question of responsibility for possible damage in the face of natural disasters has repeatedly been raised. This unsustainable "evolution" may be connected to a transitional (postcommunist) society where various stakeholders are trying to achieve their legitimate (political, economic, ideological) goals, with no regard to increasing vulnerability due to their actions.

In Slovenia the national government still assumes the majority of *responsibility* for preventing natural disasters and for the damage resulting from them, but in some European countries in recent years, the weight of responsibility is increasingly shifting toward the individual.

In Slovenia it is typical that after a natural disaster people intensively exploit their rights, whereas before the disaster they partially or completely disregard their civic responsibilities. The overall solution to the issue of natural disasters is characterized by the "NIMBY (not in my backyard) syndrome." It is here that the government and professional community must intervene, usually through appropriate *spatial planning* supported by *legislation*. In transition countries, various illegal informal planning practices are rather frequent. In such cases even an independent and expert approach cannot ensure sustainable and balanced development.

In Slovenia *flood damage potential* was estimated as at least €3.5 billion. This is equivalent to 11% of the GDP or approximately €1,700 per resident of Slovenia. The damage potential is least in frequently flooded areas (€20 million), greater in rarely flooded areas (€544 million), and greatest in very rarely flooded areas (€2.9 billion). Although these are only approximate figures, the data are worrisome because floods are also an expected natural phenomenon in areas where they are very rare. This is confirmed by the *ratio* between the *area* of *flooded* regions with various *flood frequencies* and the *damage potential* in these areas. The ratio between areas with frequent, rare, and very rare floods is 1:14:25; however, the ratio of the potential damage in these areas is two- to fivefold: 1:26:139. Between 1994 and 2006, the average annual flood damage was €12 million, which is 58% of the damage that may result from regular flooding (Ocenjena … 2008). A large amount of damage during this period occurred during the 1998 flood year, amounting to €88 million. At that time the damage was four times greater than the calculated value of damage potential in Slovenia due to regular flooding. The flooding of September 2007, which also affected only regularly flooded areas, caused damage exceeding €200 million, which is nearly ten times greater than the calculation for damage potential caused by regular flooding.

References

Đurović B (2012) Določitev in razvrstitev poplavno ogroženih območij v Sloveniji (Identification and classification of flood risk areas in Slovenia). Inštitut za vode Republike Slovenije, Ljubljana, 103 p (in Slovenian)

EU Floods Directive (2007) Official Journal of the European Union L 288/27/2007. http://ec.europa.eu/environment/water/flood_risk/index.htm

Frantar P, Hrvatin M (2005) Pretočni režimi v Sloveniji med letoma 1971 in 2000 (Discharge regimes in Slovenia from 1971 to 2000). Geografski Vestnik 77(2):115–127 (in Slovenian)

Gams I (1973) Prispevek h klasifikaciji poplav v Sloveniji (Contribution to the classification of floods in Slovenia). Geografski Obzornik 20(1–2):8–13 (in Slovenian)

Gašperič P (2004) The expansion of Ljubljana onto the Ljubljansko barje moor. Acta Geographica Slovenica 44(2):7–33

Globevnik L, Vidmar A (2010) Poplave na Ljubljanskem barju v septembru 2010 (Floods on the Ljubljana moor in September 2010). Mišičev vodarki dan 21:24–29 (in Slovenian)

Hrvatin M (1998) Discharge regimes in Slovenia. Geografski Zbornik 38:59–87
Kolega N (2006) Slovenian coast sea floods risk. Acta Geographica Slovenica 46(2):143–167
Komac B (2009) Social memory and geographical memory of natural disasters. Acta Geographica Slovenica 49(1):199–226
Komac B, Zorn M (2011a) Geografija poplav v Sloveniji septembra 2010 (Geography of September 2010 floods in Slovenia). In: Zorn M, Komac B, Ciglič R, Pavšek M (eds) Neodgovorna odgovornost. Naravne nesreče 2. Založba ZRC, Ljubljana, pp 59–80 (in Slovenian)
Komac B, Zorn M (2011b) Dojemanje ogroženosti zaradi poplav na primeru iz leta 2010 (Flood risk perception – 2010 flood case study). Ujma 25:157–162 (in Slovenian)
Komac B, Natek K, Zorn M (2008a) Geografski vidiki poplav v Sloveniji (Geographical aspects of floods in Slovenia). Geografija Slovenije 20. Založba ZRC, Ljubljana, 180 p (in Slovenian)
Komac B, Natek K, Zorn M (2008b) Influence of spreading urbanization in flood areas on flood damage in Slovenia. In: IOP conference series: Earth and environmental science 4(1):1–9
Komac B, Zorn M, Ciglič R (2011) Izobraževanje o naravnih nesrečah v Evropi (Natural-disaster education in Europe). Georitem 18. Založba ZRC, Ljubljana, 110 p (in Slovenian)
Kranjc A (1981) Prispevek k poznavanju razvoja krasa v Ribniški Mali gori (The Karst development in 'Ribniška Mala gora' (Slovenia). Acta Carsologica 9:27–85 (in Slovenian)
Kuhlicke C, Steinführer A, Begg C, Bianchizza C, Bründl M, Buchecker M, De Marchi B, Di Masso TM, Höppner C, Komac B, Lemkow L, Luther J, McCarthy S, Pellizzoni L, Renn O, Scolobig A, Supramaniam M, Tapsell S, Wachinger G, Walker G, Whittle R, Zorn M, Faulkner H (2011) Perspectives on social capacity building for natural hazards: Outlining an emerging field of research and practice in Europe. Environ Sci Policy 14(7):804–814
Kušar S (2010) Informal planning practices: some evidence from Slovenia. J Land Stud 3:159–165
Melik A (1963) Ob dvestoletnici prvih osuševalnih del na Barju (A l'occasion du deux-centenaire des premiers travaux de desséchement du Barje (Marais du Ljubljana)). Geografski Zbornik 8:5–64 (in Slovenian)
Meze D (1983) Poplavna področja v porečju Rašice z Dobrepoljami (Flood areas in the Riverbasin of Rašica with Dobrepolje). Geografski Zbornik 22:5–37 (in Slovenian)
Mikoš M (1995) Soodvisnost erozijskih pojavov v prostoru (Interdependence of erosion processes in environment). Gozdarski Vestnik 53(2):342–351 (in Slovenian)
Mikoš M (2007) Rizični menedžment na področju naravnih nesreč (Risk management in natural disasters). In: Problemi in perspektive upravljanja z vodami v Sloveniji. Svet za varstvo okolja Republike Slovenije, Ljubljana (in Slovenian)
Mikoš M, Brilly M, Ribičič M (2004) Floods and landslides in Slovenia. Acta Hydrotechnica 22 (37):113–133
Nacionalni program varstva pred naravnimi in drugimi nesrečami (The national program for protection against natural and other disasters) (2006) Official Gazette of the Republic of Slovenia 51/2006 (in Slovenian)
Natek K (2005) Poplavna območja v Sloveniji (The flood areas of Slovenia). Geografski Obzornik 52(1):13–18 (in Slovenian)
Ocenjena škoda, ki so jo povzročile elementarne nesreče (Estimated damage caused by natural disasters) (2008). Statistični urad Republike Slovenije, Ljubljana (in Slovenian)
Pallagast K, Mercies G (2007) Urban and regional planning in Central and Eastern European countries – from EU requirements to innovative practices. In: Stanilov K (ed) The post-socialist city: urban form and space transformations in central and eastern Europe after socialism. Springer, Dordrecht, pp 473–490
Petkovšek A, Fazarinc R, Kočevar M, Maček M, Majes B, Mikoš M (2011) The Stogovce landslide in SW Slovenia triggered during the September 2010 extreme rainfall event. Landslides 8(4):499–506
Polajnar J (2002) Visoke vode (High waters). In: Ušeničnik B (ed) Nesreče in varstvo pred njimi. Uprava RS za zaščito in reševanje, Ljubljana, pp 246–251 (in Slovenian)
Poročilo o izjemno obilnih padavinah od 16. do 19. septembra 2010 (Report on the extremely heavy rainfall from 16 to 19 September 2010) (2010) Agencija Republike Slovenije za okolje, Ljubljana, 16 p (in Slovenian)

Pravilnik o metodologiji za določanje območij, ogroženih zaradi poplav in z njimi povezane erozije celinskih voda in morja, ter o načinu razvrščanja zemljišč v razrede ogroženosti (2007) Official Gazette of the Republic of Slovenia 60/2007 (in Slovenian)

Repnik Mah P, Mikoš M, Bizjak A (2010) Hydromorphological classification of Slovenian rivers. Acta Geographica Slovenica 50(2):201–229

Resolucija o nacionalnem programu varstva pred naravnimi in drugimi nesrečami v letih 2009 do 2015 (The resolution on the national program for protection against natural and other disasters from 2009 to 2015) (2009) Official Gazette of the Republic of Slovenia 57/2009 (in Slovenian)

Siegel FR (1996) Natural and anthropogenic hazards in development planning. Academic, San Diego, 300 p

Stanilov K (ed) (2007) The post-socialist city: urban form and space transformations in central and eastern Europe after socialism. Springer, Dordrecht, 496 p

Strategija prostorskega razvoja Slovenije (The strategy for the spatial development of Slovenia) (2004) Official Gazette of the Republic of Slovenia 76/2004 (in Slovenian)

Strojan I, Kobold M, Polajnar J, Šupek M, Pogačnik N, Jeromel M, Petan S, Lalić B, Trček R (2010) Poplave v dneh od 17. do 21. septembra 2010 (Floods from 17 to 21 September 2010). Mišičev vodarki dan 21:1–11 (in Slovenian)

Triglav Čekada M, Zorn M (2012) Uporabnost nemerskih fotografij za preučevanje poplav – primer poplav na Dobrepolju septembra 2010 (Non-metric images as a tool for floods research – the example of floods on Dobrepolje in September 2010). In: Ciglič R, Perko D, Zorn M (eds) Geografski informacijski sistemi v Sloveniji 2011–2012. Založba ZRC, Ljubljana, pp 55–62 (in Slovenian)

Veljanovski T, Kokalj Ž (2012) Objektno usmerjeno kartiranje poplav in njihova vloga v poselitvi osrednjega dela Ljubljanskega barja (Object-oriented mapping of floods and their role in the settlement in the central part of Ljubljana moor). In: Ciglič R, Perko D, Zorn M (eds) Geografski informacijski sistemi v Sloveniji 2011–2012. Založba ZRC, Ljubljana, pp 63–72 (in Slovenian)

Veljanovski T, Pehani P, Kokalj Ž, Oštir K (2011) Zaznavanje poplav s časovno vrsto radarskih satelitskih posnetkov ENVISAT in RADARSAT-2 (Detection of flooding with the time series of radar satellite images ENVISAT and RADARSAT-2). In: Zorn M, Komac B, Ciglič R, Pavšek M (eds) Neodgovorna odgovornost. Naravne nesreče 2. Založba ZRC, Ljubljana, pp 81–89 (in Slovenian)

Walker G, Whittle R, Medd W, Watson N (2010) Risk governance and natural hazards. CapHaz-Net WP2 report. Lancaster Environment Centre, Lancaster, 62 p

Zakon o prostorskem načrtovanju (Law on Spatial Planning) (2007) Official Gazette of the Republic of Slovenia 33/2007 (in Slovenian)

Zakon o varstvu pred naravnimi in drugimi nesrečami (Protection Against Natural and Other Disasters) (1994) Official Gazette of the Republic of Slovenia 64/1994 (in Slovenian)

Zakon o vodah (Act on Water) (2002) Official Gazette of the Republic of Slovenia 67/2002 (in Slovenian)

Weichselgartner J, Obersteiner M (2002) Knowing sufficient and applying more: challenges in hazards management. Environ Hazards 4:73–77

Zorn M (2007) Jožefinski vojaški zemljevid kot geografski vir (The Joseph II military land survey as a geographical source). Geografski Vestnik 79(2):129–140 (in Slovenian)

Zorn M, Komac B (2011) Damage caused by natural disasters in Slovenia and globally between 1995 and 2010. Acta Geographica Slovenica 51(1):7–41

Zorn M, Šmid Hribar M (2012) A landscape altered by man as a protected area: a case study of the Ljubljana marsh (Ljubljansko barje). Ekonomska i ekohistorija 8(1):45–61

Chapter 9
Floods in the Danube River Basin in Croatia in 2010

Danko Biondić, Danko Holjević, and Josip Petraš

Abstract The recent decades have witnessed very intensive rainfalls throughout Europe which resulted in flood waves in rivers that reached or sometimes even exceeded the maximum water levels recorded to date. In the Danube River basin in Croatia, such a year was 2010, which was defined in terms of precipitation as an extremely wet, very wet, or wet year in 99% of the territory. Between 30 May and 2 June, precipitation reached record quantities of up to 180 mm over most of Slavonia, and again, between 20 June and 23 June additional 90–100 mm of rain fell (the highest daily precipitation, 107.2 mm, was measured in Osijek). Snow melting due to sudden warming at the end of December 2009 and beginning of January 2010 also contributed to the formation of two large water waves not only on the Danube, Sava, and Drava Rivers but also on their numerous minor tributaries. Despite timely undertaken defence measures, embankments were breached at some critical locations, with water uncontrollably flooding the floodplains and causing heavy damages. This chapter presents key flood events and the lessons learned from them.

Keywords Precipitation • Floods • River water levels • Organization of defence • Flood control tasks • Slavonia

9.1 Hydrometeorological Situation

The year 2010 in Croatia was, in view of precipitation, an extremely wet, very wet, or wet year in 99% of the territory (CMHS 2011 – Fig. 9.1). In the Danube River basin, January, February, May, August, October, November, and December were

D. Biondić (✉) • D. Holjević
Hrvatske vode, Ulica grada Vukovara 220, 10000 Zagreb, Croatia
e-mail: Danko.Biondic@voda.hr; danko.holjevic@voda.hr

J. Petraš
Faculty of Civil Engineering, University of Zagreb, ul. Kačićeva 26, 10000 Zagreb, Croatia
e-mail: jpetras@grad.hr

D. Lóczy (ed.), *Geomorphological impacts of extreme weather: Case studies from central and eastern Europe*, Springer Geography, DOI 10.1007/978-94-007-6301-2_9,

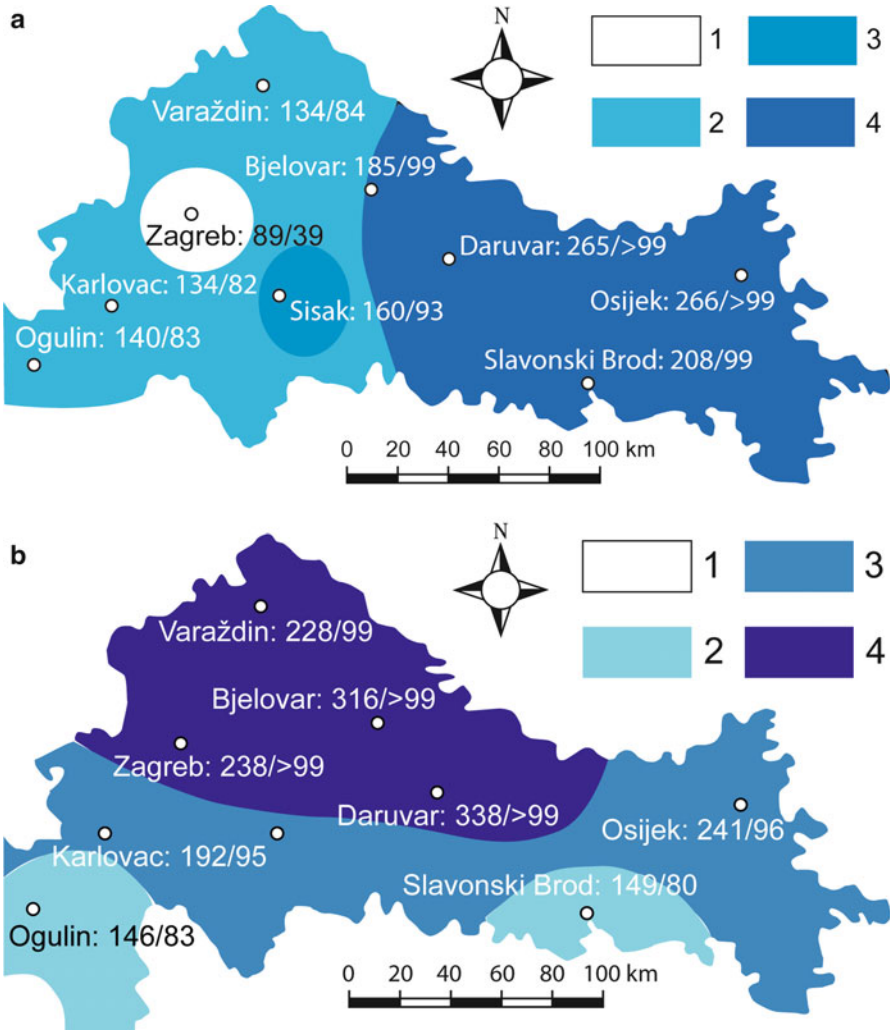

Fig. 9.1 Precipitations for the meteorological stations in Slavonia for June (**a**) and September 2010 (**b**). In numerator: monthly precipitation amount (mm); in denominator: percentage of climatic normal for the period 1961–1990. 1, average (25–75% of climatic normal); 2, wet (75–91%); 3, very wet (91–98%); 4, extremely wet (≥99%) (*Source*: Hydrometeorological Service of Croatia)

wet to *very wet*, and June and September *extremely wet* months. In June, precipitation was restricted to the eastern part of the river basin, while during September it was centred in the northwestern regions (Fig. 9.1).

The hydrometeorological conditions were particularly unfavourable between 30 May and 2 June 2010 (ICPDR 2012). In most of Slavonia, cumulative precipitation (RX4D) reached *record amounts* of up to 180 mm. In the period between 20 and 23

June 2010, additional 90–100 mm of rain fell in Slavonia. On 22 June, recorded daily precipitation (RX1D) of 107.2 mm, the highest daily value of the available time series (1899–2010), was measured in Osijek. In the period from 16 to 19 September, 89 mm of rain fell within 2 days at the meteorological station Zagreb–Maksimir and exceeded the long-term monthly average for September (ca 86 mm). In the same period, the following quantities were recorded at the meteorological stations in the upper stretches of the Sava and Drava River basins: at Krapina (north of Zagreb): 98 mm, Parg (in the Rijeka hinterland): 193 mm, Križevci (between Zagreb and Bjelovar): 122 mm, and Varaždin: 104 mm. Apart from heavy rainfalls, *snowmelt* due to sudden warming at the end of December 2009 and beginning of January 2010 played a significant role in the formation of two major flood waves.

9.2 Key Flood Events

The meteorological conditions in Croatia described above generated large *flood waves* on the tributaries of the Sava and Drava Rivers in Croatia, while large waves on the Croatian sections of the Sava, Drava, and Danube Rivers were formed due to the large inflow from the upstream sections of the river basin in Slovenia, Germany, Austria, Slovakia, and Hungary (ICPDR 2012).

In the period from the end of 2009 and during 2010, a particularly large number of high water events were registered in the Sava River basin, some of which were characterised by unprecedented floods with disastrous consequences. In the Danube River basin, floods occurred in January, February, March, May, June, September, November, and December, while the most damages were caused by the floods in June, September, and December 2010 (Figs. 9.1, 9.2, 9.3 9.4, 9.5, 9.6, and 9.7).

At many hydrological stations, *maximum water levels* which occurred during 2010 exceeded or were only slightly below those recorded in the previous 35 years, from 1975 to 2009. This period was chosen because it was the period when flood relief structures for the Sava and Kupa Rivers (the Jankomir Weir and the Sava–Odra Canal; the Prevlaka Sluice and the Lonja–Strug Canal in Lonjsko polje and the Kupa–Kupa Canal) were either constructed or put into operation, which significantly changed the high water regime (Fig. 9.8).

In the Sava River section upstream of Sisak and in the western left-bank Sava tributaries, extremes occurred during the large flood wave of September 2010. The eastern left-bank tributaries reached their maximum stages in June of the same year, while the largest right-bank tributaries, the Kupa and the Una, during December 2010. Table 9.1 provides an overview of selected hydrological stations, their maximum water levels recorded in 2010, and the corresponding ranks for the period 1975–2010. The table also shows the absolute maxima at the stations until 2009, which were, even at some stations with long time series, exceeded in 2010.

Fig. 9.2 The Sava at its entrance into Zagreb, 19 September 2010 (*Source*: Hrvatske vode)

Fig. 9.3 Overflow of the right-bank Sava embankment downstream of Zagreb, 20 September 2010 (*Source*: Hrvatske vode)

Fig. 9.4 Flood defence in the broader Zagreb region, 19 September 2010 (*Source*: Hrvatske vode)

Preliminary statistical analyses showed that the large flood wave along the upper section of the Sava River basin in September was an event of 100-year return period. The flood maxima in June were occurrences between 25- and 100-year return periods and those in December between 10- and 50-year return period (Table 9.2).

Operative flood control is carried out according to the Water Act (2009) and State Flood Defence Plan (2010). In 2010, flood defence measures lasted for a total of 136 days in the Sava River basin and 96 days in the Drava and Danube River basins.

The highest level of flood control alert was reported on as many as 20 watercourses – *serious emergency flood defence* (Sava, Orljava, Londža, Western Lateral Canal of Bić polje, Eastern Lateral Canal of Jelas polje, Glogovica, Bić, Poganovačko–Kravički Canal, Karašica Stream, Marjanac, Zdenačka Rijeka, Vuka, Našička Rijeka, Gornja Jasenovica, Travnik Stream, Hatvan Canal, Borza Stream, Velika Osatin Canal, Podgorački Dubovik) and *emergency flood defence* measures on 18 watercourses (Kupa, Česma, Ilova, Krapina, Lonja–Strug Canal, Dunav, Vučica, Karašica River, Iskrica, Lapovac, Breznica, Čađavica, Voćinska River, Klokočevac, Krajna, Vučja Jama, Bistra). On other watercourses, regular flood defence measures and preparatory activities were carried out.

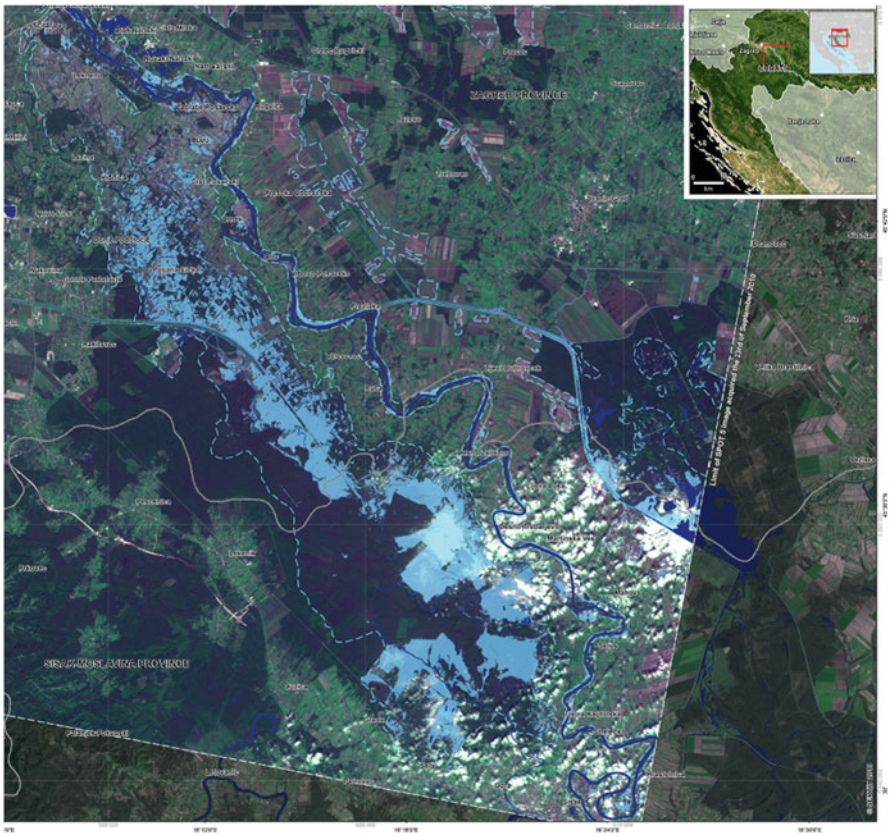

Fig. 9.5 A satellite image of the flooded area along the Sava River downstream of Zagreb, 23 September 2010 (*Source*: SERTIT)

9.3 Flood Warning and Monitoring

9.3.1 National Systems of Organization

At the level of the Republic of Croatia, the *Main Flood Control Centre* was established as the central organizational unit of Croatian Waters (Hrvatske vode) for the purpose of management, coordination, and information on flood defence status (Water Management Strategy 2008). In the case of disasters, all measures necessary for the organization of management are carried out by the *National Protection and Rescue Directorate*. The *protocol* regarding the way of communication between National Protection and Rescue Directorate and Hrvatske vode prescribes the procedure to be followed in the case of notifications about the threat and occurrence of floods in the Republic of Croatia (Husarić et al. 2011). The protocol designates Hrvatske vode as the expert, competent body for management

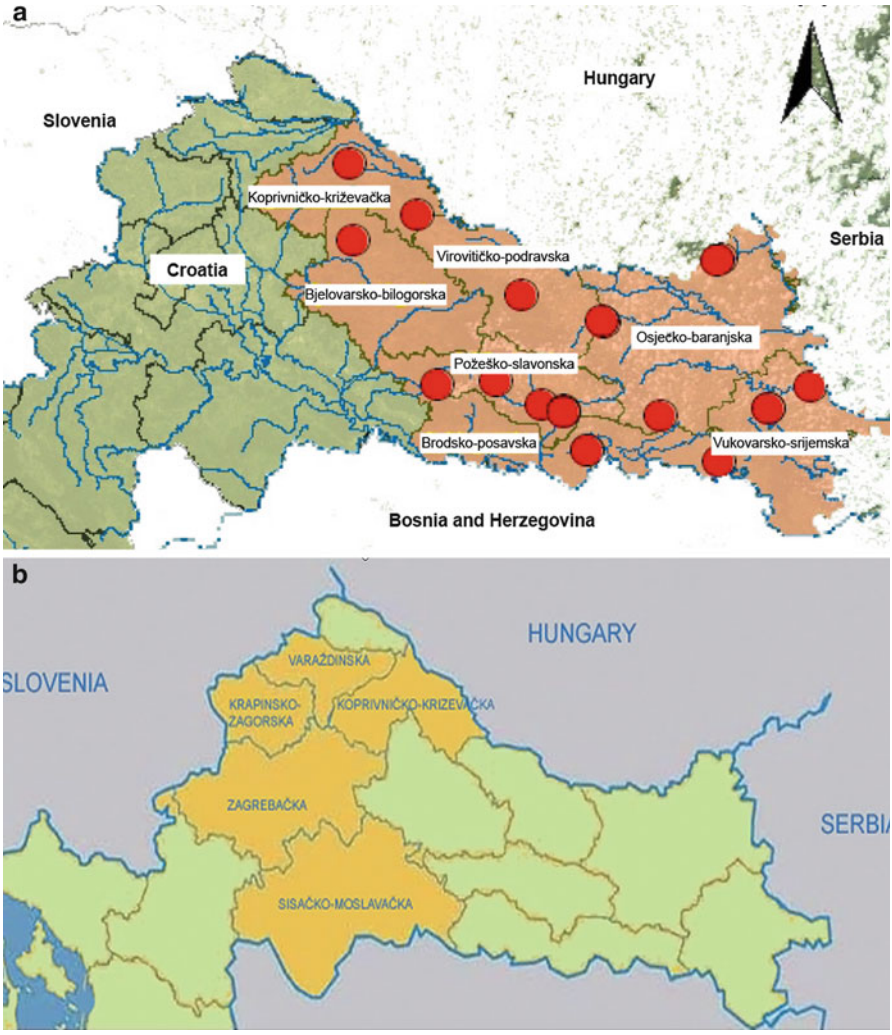

Fig. 9.6 Map of flood-stricken counties in May/June (**a**) and in September (**b**)

and interpretation of flood defence status, whereas 112 centres function as communication units which connect Hrvatske vode with all other participants in the protection and rescue system.

The Main Flood Defence Centre continuously collects and systemizes all relevant data and information necessary for flood defence management. It is in direct contact with the State Meteorological and Hydrological Service which prepares reports on the quantity and type of precipitation as well as weather forecasts (ALADIN (1997) and ECMWF models (Woods 2005)). The Main Flood Defence Centre disposes of an established system for up-to-date *monitoring* of the hydrological regime on watercourses and other waters in the Republic of Croatia. In the Danube River basin, water level is monitored at more than 140 automated gages and

Fig. 9.7 Flooded village Čičkova Poljana along the Sava River downstream of Zagreb, 20 September 2010 (*Source*: Hrvatske vode)

Fig. 9.8 Flood protection system in the Central Sava region (Srednje Posavlje)

Table 9.1 Maximum water levels at hydrological stations in the Sava River basin

	Maximum in 2010			Maximum for 1975–2009		Absolute maximum until 2009		
River, station	Water level (cm)	Date	Rank	Water level (cm)	Year	Available period	Water level (cm)	Year
Sava, Jesenice	580	19 September	1	578	1990	1948–2009	578	1990
Sava, Zagreb	**464**	19 September	1	**441**	1979	1900–2009	514	1964
Sava, Rugvica	980	20 September	1	944	1998	1924–2009	944	1998
Sava, Dubrovčak	**872**	20 September	1	**854**	1998	1926–2009	**854**	1998
Sutla, Zelenjak	450	19 September	1	437	1989	1967–2009	448	1974
Krapina, Kupljenovo	557	19 September	5	648	1989	1964–2009	648	1989
Česma, Čazma	615	20 September	2	616	1993	1962–2009	616	1993
Kupa, Karlovac	**809**	10 December	1	**802**	1995	1926–2009	872	1939
Kupa, J. Kiselica	707	11 December	1	686	1979	1970–2009	740	1974
Una, H. Kostajnica	431	4 December	5	483	1982	1939–2009	537	1955
Ilova, V. Vukovje	541	3 June	2	546	1999	1958–2009	623	1972
Lonđa, Pleternica	484	2 June	1	414	2004	1972–2009	414	2004
Bić, Vrpolje	473	3 June	1	463	1996	1978–2009	463	1996
Bosut, Vinkovci	267	3 June	1	217	1998	1988–2009	217	1998

other hydrological stations relevant for immediate flood defence with data collected in real time. Via the internet and phone communication, hydrometeorological conditions and forecasts are monitored also in parts of the basin which are located in the neighbouring countries. When hydrometeorological conditions and forecasts indicate flood hazard, *warnings* are issued to all county flood defence centres, competent Hrvatske vode services, and chief flood defence managers, and 24-h duty is established at the Main Centre as it happened during the 2010 events. Through the 112 National Centres, the Main Centre regularly informed the National Protection and Rescue Directorate on the development of the status and forecast situation as well as the undertaken flood defence measures. During regular flood defence, *daily reports* were prepared on the situation and the flood defence measures and also forecasts regarding the magnitude and timing of the arrival of the flood wave. During higher flood protection levels, reports were prepared several times a day. The general public was officially informed through mass media and the Hrvatske vode web page.

Table 9.2 Maximum water levels at hydrological stations in the Drava and Danube River basins

	Maximum in 2010			Maximum for 1975–2009		Absolute maximum until 2009		
River, station	Water level (cm)	Date	Rank	Water level (cm)	Year	Available period	Water level (cm)	Year
Danube, Batina[a]	737	12 June	2	751	2006	2001–2010	751 (**795**[b])	2006 (**1965**[b])
Danube, CS Tikveš	710	13 June	2	738	2006	2001–2010	738 (**776**[b])	2006 (**1965**[b])
Danube, Aljmaš	773	13 June	2	808	2006	1923–2010	820	1965
Danube, Dalj	911	13 June	2	932	2006	1985–2010	932 (**958**[b])	2006 (**1965**[b])
Danube, Vukovar	690	14 June	2	720	2006	1900–2010	769	1965
Danube, Ilok	713	14 June	2	750	2006	1900–2010	790	1965
Drava, Botovo	485	20 September	6	526	1998	1926–2010	582	1972
Drava, Terezino Polje	160	22 September	7	364	1975	1876–2010[c]	403	1972
Drava, Vrbovka	567	22 September	2	573	1998	1997–2010	573	1998
Drava, Moslavina Podravska	410	23 September	5	532	1975	1968–2010[c]	565	1972
Drava, Donji Miholjac	411	23 September	4	454	1975	1900–2010[c]	482	1972
Drava, Belišće	446	24 September	14	604	1975	1962–2010	627	1972
Drava, Osijek	471	13 June	2	503	2006	1900–2010[c]	542	1965

[a]The automated hydrological station Batina was established in January 2001 and has performed continuous monitoring since 23 March 2001. In this period, the highest water level was recorded on 10 April 2006.

[b]Since the absolute maxima on the Danube were recorded in 1965, this is the calculated maximum water level from the water gages Bezdan, which already existed at that time. The maximum water level from 1965 would be ca. +795 cm at the present water gages Batina! The absolute maxima after 1965 for the CS Tikveš and the automated hydrological station Dalj were also calculated.

[c]Discontinuous time series

9.3.2 The Danube EFAS Response

Heavy rains in large parts of Slovenia and northwestern Croatia from 17 to 20 September 2010 caused significant flooding on the Sava and its tributaries. Although the *European Flood Alert System* (*EFAS*) forecasts indicated as early as 13 September a very low probability of flooding in the Sava River, the subsequent forecasts were not persistent enough to send out an the EFAS alert. It was not until the forecast on 16 September at 12:00 UTC, which clearly indicated a high probability of flooding starting on 18–19 that an EFAS alert was sent to competent authorities for the Sava (Slovenia, Croatia, and Serbia) and Drava (Croatia, Serbia, and Hungary) River basins covering the period between September and October 2010.

9.4 Flood Defence Interventions and the Area Affected

Pursuant to the Water Act and the State Flood Defence Plan, Hrvatske vode carried out flood defence measures with the aid of companies licensed for works in water management. In the case of a higher level of hazard (Fig. 9.4) identified according to the protocol on cooperation with the National Protection and Rescue Directorate and county emergency centres, they coordinated the deployment of Croatian army units, police, fire fighters, and civil protection units of local self-governments.

In addition to works aimed at the superelevation and stabilization of *protective structures* and raising temporary embankments (in the total length of ca 50 km), sand bags were used for protection of family residences and industrial facilities in endangered areas. In several places, new counter-pressure wells were constructed, and planks were driven to strengthen embankments. Simultaneously, sluices were operated to relieve and strengthen individual culverts, protective walls and revetments, plugs were closed, discharge profiles were cleaned, cutoffs were built, pipe culverts removed, and for drainage of hinterland, seepage and flood waters all active pumping stations were used, with additional mobile pumps of higher capacities, which prevented larger damages on hydrotechnical facilities and possibly greater damages and suffering of the population in the defended area. The top of the large flood wave was relieved several times through the Prevlaka Sluice into the Lonja–Strug Canal and the retention areas of Lonjsko polje.

In total, for the purposes of flood defence 750,000 bags were used as well as 60,000 m^3 of materials such as sand, gravel, earth, and stone. At the same time, almost all capacities and equipment of licensed companies were used for works in water management, and, if necessary, also those belonging to utility companies and other companies from the endangered areas. In total, 200 excavators, 40 bulldozers, and 250 other machines for transportation and installation of materials (trucks, tractors, loaders, etc.) were employed.

Both large flood events in 2010 (floods in May/June and flood in September) caused large-scale damages in 11 of the 13 counties of the Croatian Danube River basin: in the counties of Koprivnica–Križevci, Virovitica, Podravina, Bjelovar–-Bilogora and Požega in Slavonia; Brod–Posavina, Osijek–Baranja, Vukovar–Srijem, Krapina–Zagorje, Zagreb County with the City of Zagreb, Sisak–Moslavina, and Varaždin (Fig. 9.6). Of the remaining two counties, floods in November and December also affected the Karlovac County severely.

9.5 Flood Damage and Geomorphological Impacts

Due to successful emergency operations, there were no casualties. However, the catastrophic floods in May/June caused severe damages to agriculture (arable fields, orchards, and vegetable gardens), livestock breeding, infrastructure, personal, and local government property in the eastern and central parts of Croatia. The economy of an area, and of the country as a whole, depends on the proceeds from farming, including livestock production, and fruit growing. Since floods, hail, and thunderstorms destroyed most crops and pastures, it was estimated that financial consequences would be felt more than a year afterwards. Four hundred and twenty-seven houses, cellars, and yards were flooded; 682 houses were directly threatened and damaged; 112 families were evacuated, and, where appropriate, also movables and domestic animals (poultry, pigs, cattle). The evacuated population (and animals) were looked after and provided with temporary accommodation. Wells and other water sources were polluted, so potable water had to be delivered by water trucks. Floods blocked road traffic on county and local roads, which impeded the delivery of food and other livelihood products and provision of health service and potable water, as well as public transport.

The *repercussions* of floods that occurred in September were the following: 900 residential buildings were flooded and 257 people were evacuated from flood-affected areas and, where appropriate, movables and domestic animals as well (poultry, pigs, cattle, and horses). From the area of the Nature Park Lonjsko polje, 600 animals were evacuated, mostly native horse species. Municipality water wells and other water sources were polluted, so water trucks delivered potable water. Many roads were closed. Since Zagreb is one of the nodes of heavy traffic in the country, closing down the roads caused enormous material losses and great reparation costs.

The total damage from flooding in May/June has been estimated at almost €153.1 million and for the September floods at almost €32 million.

The 2010 floods in the Danube River basin in Croatia had no significant geomorphological impacts on river channels, banks, and floodplains – or, at least, no detailed studies have revealed such impacts. Damages to embankments were repaired soon after waters had receded in order to make them ready to withstand future flood waves. Several collapses in critical locations with concave river banks were also repaired.

9.6 Lessons Learned

Numerous flood events in the Danube River basin during 2010, two of which had catastrophic consequences and damages, indicated the necessity of:

- Construction, extension, and reconstruction of the flood defence system at critical locations
- Analyses of hydrological and hydraulic aspects of the flood and estimates of impact of climate changes on these events
- Analyses of relief structures operation, preparation of regulations on adoptation of defined goals and criteria
- Development of new forecasting models and updating of the existing ones
- Development of forecasting models for precipitation–water levels
- Development of flooded area maps, with estimates of water depth
- Determination of existing safety levels in individual areas
- Evaluation of embankment quality in all sections, with proposals of necessary rehabilitation, extension, or construction of new embankments
- Preparation of uniform criteria for facility design/sizing
- Preparation of flood hazard and flood risk maps
- Proposal of stations for monitoring of status and discharges of watercourses
- Geodetic survey of the present state of all defensive embankments according to a certain annual dynamics (embankment register)
- Development of a dynamic plan for preparation and implementation of design documents
- Improvement of international cooperation, particularly with hydrometeorological services of the neighbouring countries
- Implementation of permanent education of junior engineers on flood defence systems

References

ALADIN (1997) The ALADIN project: mesoscale modelling seen as a basic tool for weather forecasting and atmospheric research. WMO Bull 46(4):317–324

CMHS (2011) Reviews N°21. Climate monitoring and assessment for 2010. Croatian Meteorological and Hydrological Service, Zagreb, 14 p

Husarić J, Đuroković Z, Biondić D, Obrdalj M (2011) Flood protection in Croatia. In: Proceedings of the 5th Croatian water conference 'Croatian waters facing the challenge of climate changes', Opatija, 2011, pp 39–51

ICPDR (2012) 2010 floods in the Danube river basin: brief overview of key events and lessons learned. International Commission for the Protection of the Danube River, Vienna, 20 p. http://www.icpdr.org/main/publications

State Flood Defence Plan (2010) Republic of Croatia, OG 84/2010

Water Act (2009) Republic of Croatia, OG 153/2009 and 130/2011

Water Management Strategy (2008) Republic of Croatia, OG 91/2008

Woods A (2005) Medium-range weather prediction: the European approach. Springer, New York, 270 p

Chapter 10
Floods in Serbia in 2010 – Case Study: The Kolubara and Pcinja River Basins

Slavoljub Dragićević, Ratko Ristić, Nenad Živković, Stanimir Kostadinov, Radislav Tošić, Ivan Novković, Ana Borisavljević, and Boris Radić

Abstract Riverine and torrential floods are the most significant natural hazards on the territory of Serbia. The potentially flooded area in Serbia with a 100-year return period is 15,198.07 km^2 (17.2% of total area). Serbia is mostly threatened by the floods of small to medium-size torrential rivers mostly in late spring (from May to the end of June), a period characterised by intensive rainfalls of a few-hour duration. In the Pcinja River Basin, the town of Trgoviste was struck by a flood in May 2010. Two people were killed, almost 170 ha of land and 27 buildings were flooded (including 12 severely damaged), roads damaged or blocked, and 230 inhabitants evacuated. The flood in the Kolubara River Basin of late June 2010 affected 500 ha with 230 flooded households. Total damage was estimated at €370,000. In the watersheds studied, the 2010 floods were natural occurrences, but human action significantly aggravated the disasters. The messages to be learned help improve the system of prevention and the organisation of mitigation of flood damages, in order to reduce it to an acceptable level.

Keywords Natural hazards • Floods • Intensive rainfall • Maximum discharge • Sediment transport • Bank erosion • Serbia

S. Dragićević (✉) • N. Živković • I. Novković
Faculty of Geography, University of Belgrade, Studentski trg 3/3, 11000 Belgrade, Serbia
e-mail: slavoljubdragicevic@eunet.rs; ocaha@eunet.rs; novkovic.ivan@gmail.com

R. Ristić • S. Kostadinov • A. Borisavljević • B. Radić
Faculty of Forestry, University of Belgrade, Kneza Višeslava 1, 11030 Belgrade, Serbia
e-mail: ratko.risticc@gmail.com; kost@eunet.rs; borisavljevic.ana@gmail.com; boris.radic@gmail.com

R.I. Tošić
Faculty of Natural Sciences, University of Banja Luka, M. Stojanovića 2, 78000 Banja Luka, Republic of Srpska
e-mail: rtosic@blic.net

D. Lóczy (ed.), *Geomorphological impacts of extreme weather: Case studies from central and eastern Europe*, Springer Geography, DOI 10.1007/978-94-007-6301-2_10,

10.1 Introduction

The first multihazard map of the Serbian territory indicates that this area is vulnerable to natural hazards (Dragićević et al. 2011), which include seismic hazards, landslides, rockfalls, floods, torrential floods, accelerated soil erosion, droughts, and forest fires. The risk is not uniform for the whole territory but varies with the type of hazard and potential damage.

Floods of all kinds are the most frequent natural catastrophic events worldwide (Berz et al. 2001). Recent studies on floods in Europe have not encompassed the territory of Serbia (Barredo 2007; de Moel et al. 2009; Bissolli et al. 2011), where riverine and torrential floods are the most common natural hazards. Through frequency, intensity, and spatial distribution, they present a permanent threat for the ecological conditions, economic, and social life (Kostadinov 1988; Dragićević et al. 2010a).

The *potentially inundated area* in Serbia during 100-year floods is 15,198.07 km^2 (17.2% of total area) (Dragićević et al. 2011), affecting 500 larger settlements, 515 industrial facilities, 680 km of railroads, and about 4,000 km of roads (Petkovic and Kostadinov 2008). The most vulnerable part is northern Serbia (Vojvodina) with ca 12,900 km^2 of potentially flooded land along the Danube River and tributaries (Tisa/Tisza, Tamiš/Timiş, and Sava). In the 20th century, the largest flood in Serbia affected the Danube region in May and June 1965, when more than 2,500 km^2 was flooded and 16,000 households and 214 km of roads affected. The second largest area of flood hazard is the right bank of the Sava River, followed by certain areas of the Morava basin, the right bank of the Drina River, and smaller watersheds (the Beli Drim, Kolubara, Sitnica, Timok, Binacka Morava, and Lepenica).

Flood control in the Republic of Serbia is at a satisfactory level on larger rivers (the Danube, Sava, Drina, Velika Morava, Veliki Timok, and others) with 29 major reservoirs, more than 3,550 km of embankments, and numerous river regulation structures (RASP 2010). The lower sections of small rivers with a potential risk of inundation of arable land, infrastructural systems, and residential objects are also protected. In the last couple of decades, defence systems have been completed for the major rivers, but some medium-size rivers (like the Kolubara) are still frequently exposed to floods.

Recently, Serbia is most threatened by floods on small to medium *torrential rivers*. The attribute 'torrential' refers to any watershed with a sudden appearance of maximal discharge with a high concentration of sediment, regardless of size and stream category (Ristić et al. 2011a). A total of 9,260 torrential watersheds were inventoried in Serbia from 1930 to 1974 (Gavrilović 1975), and their peak discharges were studied by processing the data from 128 control profiles equipped with automatic water-level recorders (Ristić et al. 2011a). The spatial distribution of the most destructive torrential floods over the last 60 years has been mapped. Historical torrential floods were reconstructed using the 'hydraulic flood traces' method (Ristić et al. 2011b). In the past 60 years, the death toll by floods was 70 people in Serbia, and material damage is estimated to more than €8 billion (Ristić et al. 2012). Between 1994 and 2010, 17 people died in floods.

The *critical periods* for floods in Serbia are late spring (from May to the end of June) – when intensive rainfalls of a few-hour duration (Ristić et al. 2009; Živković 2005, 2009) and maximum daily and monthly precipitations occur – and late winter (from February to the first half of March).

The main aim of this chapter is to present the extreme hydrometeorological conditions and the resultant geomorphological processes in spring 2010 for two basins in Serbia (the Kolubara and Pcinja River basins). The material damage points out many oversights detected in flood defence.

10.2 Study Area

10.2.1 The Kolubara River Basin

The Kolubara River, in the western part of Serbia, is the last large right-bank tributary of the Sava River and classified by its length (86.4 km) and watershed size (3,641 km^2) as a medium-size river (Dragićević et al. 2012a). It drains 4.12% of Serbia's surface area (Fig. 10.1), average elevation of its watershed is 272 m, with the highest point at 1,346 m and the lowest at 73 m. The Kolubara River flows through landscapes of different geological structure, age (Palaeozoic metamorphics, Mesozoic/Cenozoic igneous, and sedimentary rocks), and geotectonic complexity.

The basin has a continental climate (mean annual temperature is 11 °C, average annual precipitation was 822 mm for the period 1925–2000). Maximum rainfall occurs in June at 25 of the 27 meteorological stations and in May at only two stations. The average discharge of the Kolubara River (at Draževac gauging station) was 21.8 $m^3\ s^{-1}$ for the period 1961–2005.

The Kolubara River has all the necessary *conditions for* frequent and large-scale *floods*: watershed shape coefficient (0.79 – very rare in nature), position and orography (in the path of wet air masses from the northwest), considerable deforestation and torrential properties of many tributaries, rock and soil properties in the lower section, weak retention capacity of runoff, and human activities (coal mining, river course changes). Excessive runoff generates sudden and short-lived flooding, while the periods of low flow (close to *environmental flow*) are long and every year they are approaching the ecological minimum. At Beli Brod, there is a ca 1,200-fold difference between maximum (more than 700 $m^3\ s^{-1}$) and minimum discharge (ca 0.6 $m^3\ s^{-1}$), and at Valjevo it is even higher, 3,400-fold. With reducing low flow to 0.3 $m^3\ s^{-1}$ and doubling the highest flow to 1,400 $m^3\ s^{-1}$ (which is not improbable at all), the ratio grows to 2,400 (Dragićević et al. 2007).

In the lower part of the Kolubara valley (Obrenovac municipality), once (or sometimes twice) a year the Kolubara River overflows its banks and the lower basin is endangered by flood. During a major flood from March to May 1937, the river and its tributaries inundated this area. Floods also occurred in 1965, 1975, and 1981. After the construction and improvement of several small dams on the tributaries in the 1980s, no major floods happened, but high flood waves passed on the river in 1996, 1998, 1999, 2001, 2004, 2006, 2008, and 2010 (Dragićević et al. 2012b).

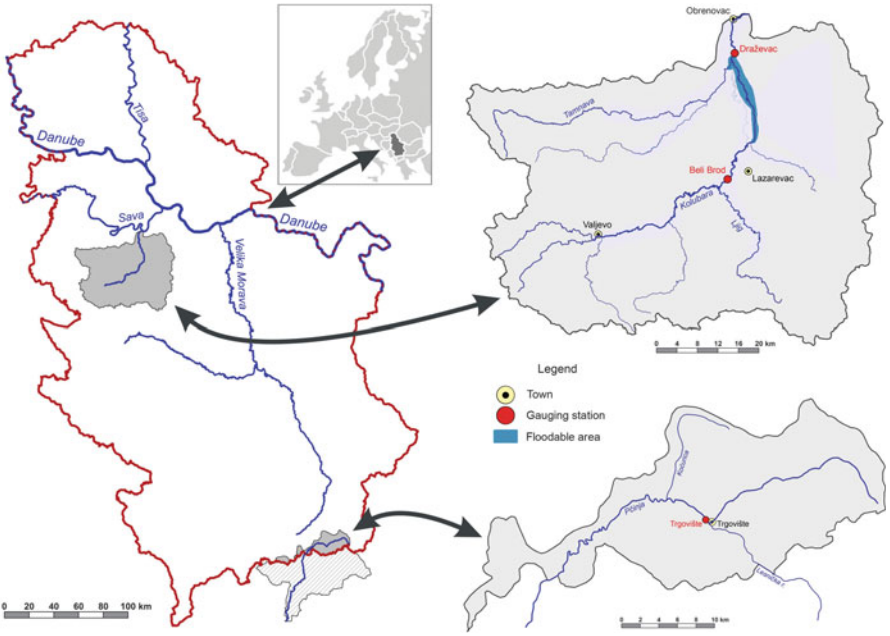

Fig. 10.1 Location of the Kolubara and the Pcinja River basins in Serbia (Designed by Ivan Novkovic)

10.2.2 The Pcinja River Basin

The Pcinja is one of the largest left-bank tributaries of the Vardar River, which drains southeastern Serbia and northeastern Macedonia. River length is 135 km, and watershed area is 2,877.3 km^2 with divides 366 km long. The recorded sediment yield, geomorphology of the catchment (Milevski 2005; Milevski et al. 2007), the map of erosion (Lazarevic 1983; Djordjevic et al. 1993), and multihazard map (Dragićević et al. 2010b) all point to the *great erosive power* of the Pcinja River. Although control measures in the last three decades of the twentieth century have significantly reduced the rate of erosion in its basin, rills and gullies are still active in many areas.

Flood risk assessment at watershed level is based on a historical overview of torrential (flash) floods. At the town of Trgoviste (Fig. 10.1), the most destructive torrential flood happened on 15 May 2010.

10.3 Methods

Daily data series of precipitation, discharge, and suspended load concentration for the Kolubara River Basin were obtained from Hydrometeorological Office of Serbia (RHMOS 2010). For the gauging station of Beli Brod, mean daily flow

(Q in $m^3\ s^{-1}$) and suspended load concentration (C in mg L^{-1}) can be calculated. The assessment of *sediment yield* is based on daily measurements of suspended load concentration during the period 1985–2007 and also for the year 2010. At the Draževac gauging station, daily flow rates are available since 1950, and sediment yield for 2010 was estimated by regression (Dragićević 2007):

$$\text{Sediment yield}_{2010} = 1.192^{*}Q^{1.6188};\ R^2 = 0.8627$$

To determine the lateral migration of the Kolubara riverbed, topographic maps, aerial photos, and orthophotos have been analysed in previous research. *Bank erosion* has been *monitored* using topographic maps (scale: 1:50,000), cadastral maps (at 1:2,500, dating from 1967), aerial photos from 1981, and orthophotos from 2004 and 2010. Comparing the data from different dates, we determined the evolution of the river course over three intervals: 1967–1981, 1981–2004, and 2004–2010. The rate of bank erosion was calculated using GeoMedia Professional 5.0 software.

On-site measurements were conducted at location 1 (Fig. 10.3) using Trimble 5800 GPS receiver system (accuracy ± 1.5 cm). The difference between river bank positions before and after the flood was determined for river profiles upstream of the bridge, and total riverbed migration was calculated as the average deviation between the two positions of the banks. From the data on extreme discharges, we drew a probability curve of maximum discharges for the Kolubara River and its tributaries in order to estimate the impact of future floods on bank erosion.

The *historical maximum discharge* for the Pcinja River ($Q_{\text{maxHFT-2010}}$) was reconstructed by the method of 'hydraulic flood traces' (Ristić and Malošević 2011), for control profile P in Fig. 10.1 (the town of Trgoviste). Maximum discharge was computed by the *combined method* using the DM software (Malošević 1995) and combining the synthetic unit hydrograph theory (maximum ordinate of unit runoff, $q_{\max}$) and the Soil Conservation Service (SCS 1979) methodology (deriving effective rainfall, P_e, from total precipitation, P_b). The computation was performed for AMC III (Antecedent Moisture Conditions III – high soil moisture content and reduced infiltration capacity). Synthetic triangular unit hydrographs were transformed to *synthetic* (computed) *curvilinear hydrographs* of total direct runoff using the SCS basic dimensionless hydrograph (Chang 2003). Daily precipitation data were provided from the records of neighbouring rain-gauge stations Trgoviste (600 m elevation), Radovnica (925 m), Dukat (1,100 m), Kalovo (950 m), Siroka Planina (1,160 m), and radar weather reports (RHMOS 2010). A regional analysis of time lag (Ristić 2003), internal daily distribution of precipitation (Janković 1994), and soil hydrological classification of groups to determine CN-runoff curve number (Djorović 1984) were also performed.

Land use in the Pcinja River Basin was analysed from documentation, field survey, remote sensing images, topographic, geologic, soil maps, and Corine Land Cover database for 2006. Land use classification relied on the CORINE methodology (EEA 1995) using the MapInfo software. Since the Pcinja River has an ungauged basins, the sediment yield during the 2010 flood and the *rate of erosion* were estimated using the *Erosion Potential Method* (EPM), developed and calibrated in Serbia (Gavrilović 1972), and it is still in use in the successor countries

of the former Yugoslavia. Its input parameters are Z, erosion coefficient according to Gavrilović; h, the level of average annual torrential rain (m); Y_n, density of sediment (t m^{-3}); e, coefficient of torrential stream saturation by sediment; Q_{maxav}, maximum water discharge in an average year (m^3 s^{-1}); Q_n, total sediment transport (m^3 s^{-1}); T_b, duration of the flood wave (h); and G, total sediment transport by the flood wave (m^3).

10.4 Results

10.4.1 Hydrometeorological Situation in the Kolubara Watershed in June 2010

The data series for 1961–1990 shows that in the lower Kolubara basin, June is the rainiest (108.5 mm), while February is the driest month (40 mm). Prior to 2010, extreme hydrometeorological conditions in the Kolubara basin occurred in 1996, when in June *absolute maximum discharge* was measured at the stations Beli Brod on the Kolubara (638 m^3 s^{-1}), at Pastric (on the Ribnica River), and at Bogovadja (on the Ljig River). Downstream, at Draževac station, discharge was considerably lower (270 m^3 s^{-1}) than the all-time maximum (646 m^3 s^{-1}). The difference in discharges is explained by the high *retention capacity* of the Kolubara floodplain. On 13 June 1996, the Kolubara basin received a downpour with precipitation amount (174 mm recorded at the Lazarevac station) representing the highest daily value (RX1D) in the Kolubara basin, the fourth in whole Serbia. The return period of 3-h rainfall at some stations was 1,000 years (Dragićević et al. 2007). Rainfall intensity was estimated from the record for the Valjevo station: 39 mm in 30 min.

Downstream, two floods occurred in the Kolubara River at Obrenovac. The first on 26 February, 2010, did not have extraordinary proportions as 40–50 mm rainfall on 25 February (without significant precipitation on the previous or the following days) generated a maximum daily discharge of 324 m^3 s^{-1} at Beli Brod (considerably lower than the absolute maximum on 23 June: 767 m^3 s^{-1}) and 223 m^3 s^{-1} at Draževac. However, floods also occurred on 24 and 25 June, following 7 days of 2.0–41.2 mm precipitation. Extremely high precipitation was recorded on many stations in the following 2 days: 29 mm on 22 June at Lazarevac and 58 mm on the 23th – together almost equalling the monthly average (97 mm). Monthly values reached 251 mm at Lukovac and 216.8 mm at Valjevo (30–40% of the average annual precipitation for the period 1961–1990) (Fig. 10.2).

10.4.2 Floods on the Kolubara River and Geomorphic Processes

The highest discharge of the Kolubara River in the period of 1959–2010 was 767 m^3 s^{-1} (on 23 June 2010), at Beli Brod. (The previous record was 672 m^3 s^{-1}

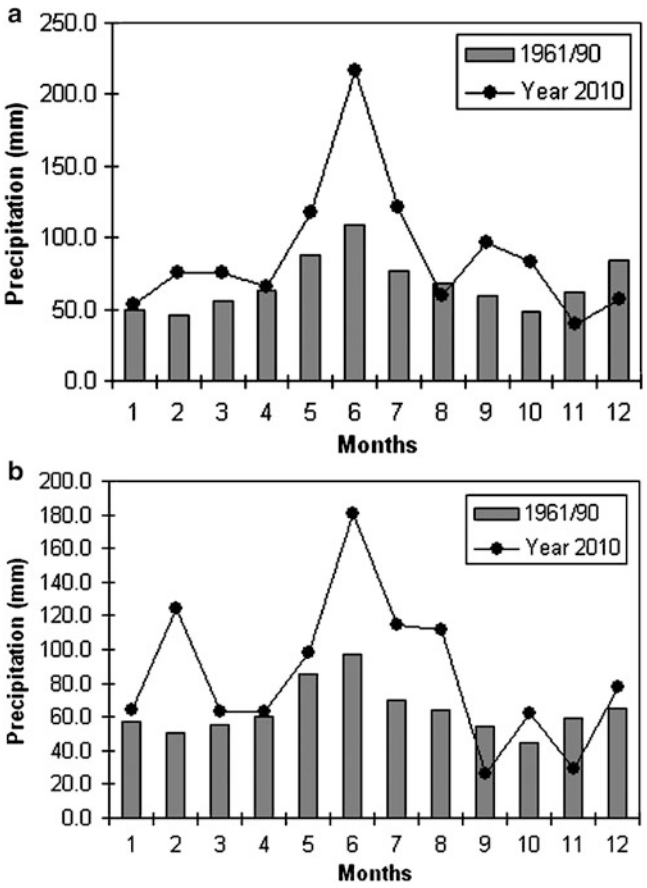

Fig. 10.2 Monthly values of precipitation at Valjevo station (**a**) and Lazarevac (**b**) for the period 1961–1990 and 2010

on 22 June, 2001 and at Drazevac 646 $m^3 s^{-1}$ on 30 March, 1962.) According to the probability curve, 646 $m^3 s^{-1}$ may occur once in 46 years. The lowest annual maximum discharge is ca 25 $m^3 s^{-1}$; the highest discharge of 100-year return period, 740 $m^3 s^{-1}$; and of 1,000-year return period, 960 $m^3 s^{-1}$ (Dragićević et al. 2012b). The *torrential* properties of the Kolubara River are also indicated by the ratio of absolute maximum (767 $m^3 s^{-1}$) to absolute minimum discharge (0.60 $m^3 s^{-1}$) at Beli Brod for 1959–2010: 1–1,280! Maximum monthly discharges above the annual mean maximum discharge ($Q_{max} > Q_{srmax}$, 1961–1990) were most common during spring months and in early summer (April, May, June), in 25 out of 600 cases. For the period 1983–2007, Ristić et al. (2009) point out that maximum discharges most commonly occur in May and June followed by February and March (at four sites in May, three in June, and one in June and February).

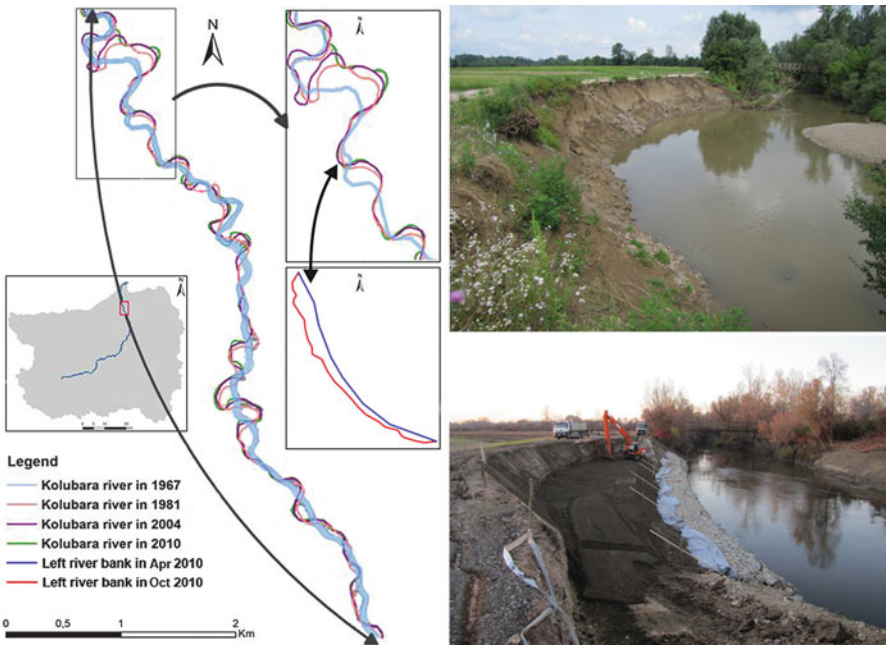

Fig. 10.3 The Kolubara riverbed lateral migration, 1967–2010, endangering river bank after the flood wave, construction of the bank revetment (Figure and photos made by Slavoljub Dragićević)

The predominant processes of *erosion* and their intensity in the Kolubara River basin were analysed in a previous project (Dragićević 2007). The findings pointed to intense lateral dynamics of the river channels. Bank erosion (Roksandić et al. 2011; Dragićević et al. 2012b), sediment yield and accumulation (Dragićević 2002), floods and landslides (Dragićević et al. 2012a, b), and soil and water pollution are the major environmental problems in the basin. The largest mean *sediment yield* for 1985–1992 was observed at Beli Brod and Draževac in May and June (Dragićević 2001). The floods are directly related to bank erosion and sediment yield.

In the studied section (Fig. 10.3), river length was 7.5 km in 1925, 8.2 km in 1967, 9.6 km in 1981, 10.06 km in 2004, and 10.14 km in 2010 (Roksandić 2012). Between 1967 and 1981, the total channel shift amounted to 50 m (27 m to the left and 23 m to the right, rate: 3.6 m year^{-1}). Between 1981 and 2004, the *migration rate* was 1.1 m year^{-1}, and between 2004 and 2010, 2 m year^{-1}. In 2010, intense bank erosion and meander shifts along the Kolubara slowed down river flow and caused flooding and sediment accumulation. At the bridge of Draževac, average channel shift induced by the 2010 flood wave was 3.06 m (in the most endangered area even 6.16 m) and a loss of 0.235 ha of land resulted. In December 2010, the emergency construction of a bank revetment had to start. At this location the rate of bank erosion in a single season equalled that of 3 years between 2004 and 2010.

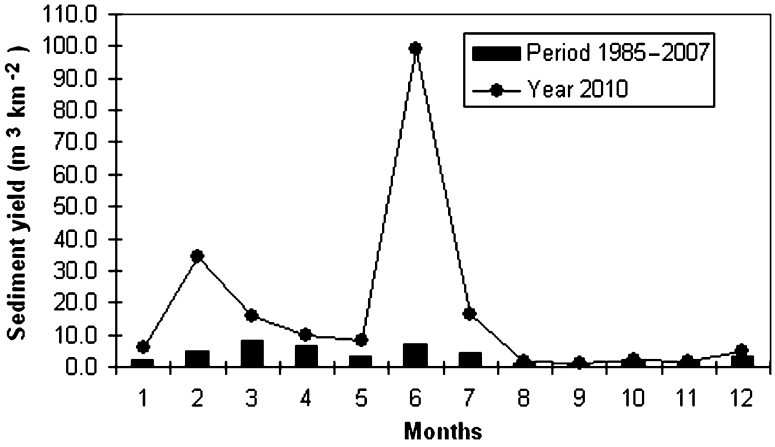

Fig. 10.4 Specific sediment yield for the period 1985–2007 and for 2010

The changes in sediment regime are associated with bank erosion. In the period 1985–2007, specific sediment yield ranged from 1.55 m^3 km^{-2} (in 1990) to 146 m^3 km^{-2} (in 1999) (Fig. 10.4). *Specific sediment transport* was 201.5 m^3 km^{-2} at Beli Brod in 2010 (in June 99.1 m^3 km^{-2}, 49.2 of total), and 58.9 m^3 km^{-2} at Draževac. On 24 June, specific sediment transport at Beli Brod was 54 m^3 km^{-2} (54.5% of the monthly total) and 78 m^3 km^{-2} on 23 and 24 June, considerably higher than at Draževac for the whole year of 2010 (58.9 m^3 km^{-2}). Since the flood area is located between Beli Brod and Draževac, the analysis confirms the preliminary assumption that most sedimentation took place between these two sites.

10.4.3 Hydrometeorological Situation and River Discharge in the Pcinja Basin in May 2010

On 15 of May 2010, 39–110 mm rainfall was registered in the watershed of Pcinja River (Table 10.1). The headwater was under anticyclone field, with convection and cumulonimbus formation. The mean intensity of *radar* reflexivity (weather radar Mitsubishi RC34A) was 47–61 dB, which corresponds to intensities between 32 and 237 mm h^{-1}. The velocity of convective cells was 12–37 km h^{-1}. The water of the Pcinja River level rose from 30 cm to 3.7 m and the discharge 411-fold, from $Q = 0.81$ m^3 s^{-1} to $Q_{\text{maxHFT-2010}} = 333.3$ m^3 s^{-1}.

From 5 to 15 of May, before the extreme rainfall event, 12.3–156.2 mm of precipitation was recorded. Soil water storage capacity was reduced, especially in skeletal soils at 0.2–0.4 m depth on steep slopes, and fast surface runoff resulted.

Table 10.1 Main hydrographic properties of the Pcinja experimental watershed

Parameter	Code	Unit	Pcinja river
Area	A	km^2	339.1
Perimeter	P	km	91.94
Highest point	Hp	m a.s.l.	1,805
Confluence point	Cp	m a.s.l.	615
Mean altitude	Am	m a.s.l.	1,169.5
Length of the main river	L	km	27.26
Maximum channel slope	Sa	%	4.37
Mean channel slope	Sm	%	2.37
Mean slope of the watershed	Smt	%	27.48
Drainage density	D	$km\ km^{-2}$	2.36

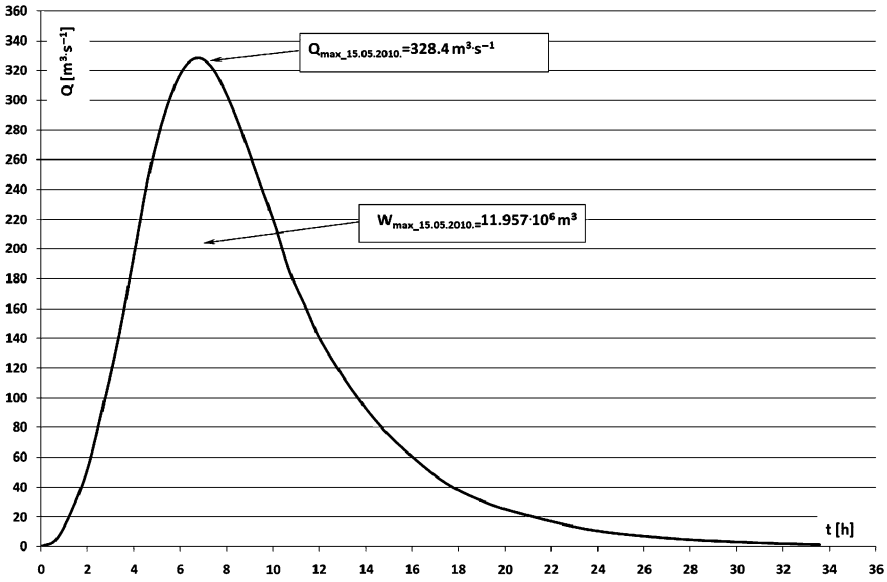

Fig. 10.5 Computed hydrograph of maximum discharge for the Pcinja River, profile Trgoviste (15 May 2010)

Maximum discharge ($Q_{\text{maxHFT-2010}}$) on 15 May 2010 (Fig. 10.5), was reconstructed using the *hydraulic flood traces* method (Table 10.2) and, from input data of radar weather reports, the combined method ($Q_{\text{maxC-2010}}$) (Table 10.3, Fig. 10.6).

In lack of measured data, sediment transport during the flood wave was estimated applying Gavrilović's method (Gavrilović 1972) (Table 10.4). Bank erosion was also intensive in the Pcinja basin, but its intensity was not measured. Bank revetments caved in at several sites in Trgoviste.

Table 10.2 Outputs of computations using the 'hydraulic flood traces' method

Parameter	Code	Unit	15 May 2010, 17 h
Mean cross-section area	A_m	m^2	72.0
Mean wetted perimeter	χ_m	m	40.0
Mean hydraulic radius	R_m	m	1.8
Slope of water surface	S	%	1.5
Manning's roughness coefficient	η	$m^{-1/3}$ s	0.039
Mean current velocity	V_m	m s^{-1}	4.63
Maximum discharge	$Q_{maxHFT\text{-}2010}$	m^3 s^{-1}	333.3
Specific maximum discharge	$q_{maxspHFT\text{-}2010}$	m^3 s^{-1} km^{-2}	0.983

Table 10.3 Outputs of computations using the combined method

Parameter	Code	Unit	Value
Maximum ordinate of unit runoff	q_{max}	m^3 s^{-1} mm^{-1}	9.314
Runoff curve number for saturated soil, low infiltration capacity	CN_{sr}	III	88
Total precipitation	P_{br}	mm	92
Effective rainfall	P_e	mm	35.26
Lag time	t_p	h	4.293
Rising limb of hydrograph	Tp	h	6.71
Falling limb of hydrograph	Tr	h	13.68
Time base of hydrograph	T_b	h	20.39
Specific maximum discharge	$Q_{maxC\text{-}2010}$	m^3 s^{-1}	328.4

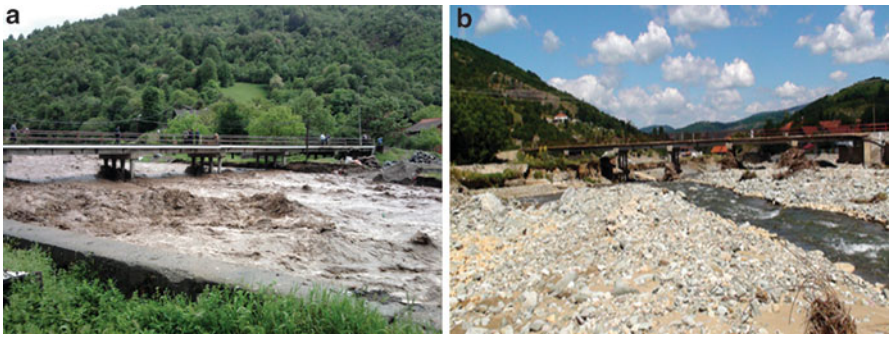

Fig. 10.6 Pcinja River bed during (**a**) and after (**b**) the flood wave of 15 May, 2010 (Photo by Ratko Ristić)

Table 10.4 Calculated sediment transport during the flood wave

Parameter	Code	Unit	
Coefficient of erosion	Z		0.62
Average value of precipitation	h	m	0.04
Density of sediment	γ_n	t m^{-3}	1.8
Coefficient of torrential stream saturation by sediment	e		0.189
Maximum discharge in average year	Q_{maxav}	m^3 s^{-1}	35.0
Sediment transport in the wave	Q_n	m^3 s^{-1}	4.101
Time base of hydrograph	T_b	h	20.39
Total sediment transport in the flood wave	G	m^3	301,030

10.5 Conclusions

Rapid runoff and floods in Serbia are generated by short intensive rainfalls, prolonged but less intensive rainfalls, snowmelt, or the combination of rainfall and snowmelt. By the data of the Hydrometeorological Office of Serbia, annual precipitation amounts in 2010 exceeded the maximum values over the last 60 years at five main meteorological stations. Monthly precipitation for June 2010 at Valjevo was 216.8 mm as opposed to the previous maximum of 193.3 mm in 1979.

The 2010 flood in the Kolubara basin affected an area of 500 ha and 230 households. Total damage was estimated at €370,000, including agricultural (€190,000), infrastructure (€130,000), and residential damages (€54,000). Traffic on a bridge, vital for Draževac, was jeopardised as a consequence of bank erosion. The construction of a bank revetment became necessary for the protection of the bridge (costing €60,000). In the Pcinja River basin, in the town of Trgoviste, the flood killed two people, almost 170 ha of land and 27 buildings were flooded (12 of which was severely damaged), roads damaged or blocked, and 230 inhabitants evacuated. The flood triggered several landslides, the largest with a volume of ca 250,000 m^3, affecting the riverbed and threatening with the impoundment of a lake of millions of cubic metres volume. Fortunately, it did not happen, and a few months later a protective concrete dam for water and sediment retention was completed. Water and electricity supply and telecommunication systems were badly damaged or destroyed.

Damages by the floods of June 2010 in the Kolubara basin, and mainly the Pcinja basin, were the result of extremely *poor coordination* between responsible authorities, particularly local governments. According to the *Law on Waters* of the Republic of Serbia, each municipality is obliged to adopt two basic documents on flood control: the *Plan of Identifying Erosion Regions* and the *Plan of Torrential Flood Control*. The Plan of Identifying Erosion Regions identifies the areas with soil erosion hazard, present and future. Proper management is to be adopted by landowners. The plan also defines action for torrential flood control.

The Plan for Torrential Flood Control defines four stages of defence: Phase I – preparation for torrential floods control (the most important stage as only a short time is available to react to torrential rainfall); Phase II – extraordinary (emergency) flood control; Phase III – state of emergency; and Phase IV – clearing the detrimental impacts (Kostadinov et al. 2012).

For effective coordination and cooperation (important principles of natural hazard mitigation), *public participation* is required. Informing the local inhabitants on potential risks, timely information in the case of emergency, as well as active public participation in the defence or rescue actions are vital tasks, covered by Phase III.

10.6 Future Tasks

Although the 2010 floods were natural occurrences, the human factor also significantly contributed to the disasters. The following measures of flood control and mitigation seem appropriate:

1. The implementation of a *Decision Support System* (DSS) for the optimal coordination of all flood prevention or mitigation activities and a telecommunication system to enable rapid response in the case of flood emergency
2. The preparation of an inventory on risks for spatial and urban planning which identifies acceptable levels of risk
3. The compilation of a new erosion map of Serbia based on the scientific analyses of rates of erosion
4. Regular and continuous torrent erosion and complex of erosion control measures in watersheds (Kostadinov 2007, 2010)
5. The preparation of Plans of Identifying Erosion Regions for each municipality in Serbia
6. The preparation of Plans of Torrential Flood Control
7. The compilation of an inventory of torrents for each watershed of Serbia
8. The documentation of performed erosion and torrential flood control activities performed
9. Real-time monitoring of rainfall and river discharge and to establish forecasting and early warning systems

Acknowledgement This study was supported by the Ministry of Education and Science of the Republic of Serbia within Project 43007 ('Studying climate change and its influence on the environment: impacts, adaptation and mitigation – subproject: Frequency of torrential floods and degradation of soil and water as a consequence of global changes') and by the Ministry of Environment and Spatial Planning within the project 'Influence of geological and hydrogeological conditions on the occurrence of destructive erosion processes and torrential floods in Serbia'.

References

Barredo JI (2007) Major flood disasters in Europe: 1950–2005. Nat Hazards 42:125–148

Berz G, Kron W, Loster T, Rauch E, Schimtschek J, Schmieder J, Siebert A, Smolka A, Wirtz A (2001) World map of natural hazards – a global view of the distribution and intensity of significant exposures. Nat Hazards 23:443–465 (Kluwer Academic Publishers)

Bissolli P, Friedrich K, Rapp J, Ziese M (2011) Flooding in eastern central Europe in May 2010 – reasons, evolution and climatological assessment. Weather 66:147–153. doi:10.1002/wea.759

Chang M (2003) Forest hydrology. CRC Press, Washington, DC, 373 p

de Moel H, van Alphen J, Aerts JCJH (2009) Flood maps in Europe – methods, availability and use. Nat Hazards Earth Syst Sci 9:289–301

Djordjevic M, Trendafilov A, Jelic D, Georgievski S, Popovski A (1993) Erosion map of the Republic of Macedonia-textual part. Water Development Institute, Skopje, 89 p (in Macedonian)

Djorović M (1984) Determination of soil hydrologic class. J Water Resour Manag 87:57–60

Dragićević S (2001) Pluviometric regime and its influence on erosive processes in the Kolubara river basin. Bull Serbian Geogr Soc 78(2):27–36 (in Serbian with summary in English)
Dragićević S (2002) Sediment load balance in the Kolubara Basin. Faculty of Geography, Belgrade, 184 p (in Serbian with summary in English)
Dragićević S (2007) Dominant processes of erosion in the Kolubara Basin. Faculty of Geography, Jantar grupa, Belgrade, 245 p (in Serbian with summary in English)
Dragićević S, Živković N, Ducić V (2007) Factors of flooding on the territory of the Obrenovac Municipality. Collection of the papers, Faculty of Geography 55:39–54
Dragićević S, Filipović D, Kostadinov S, Novković I (2010a) Protection from natural disasters. Spatial Plan of the Republic of Serbia. Faculty of Geography, Funded by Ministry of Environment and Spatial Planning, Belgrade (in Serbian)
Dragićević S, Milevski I, Blinkov I, Novković I, Luković J (2010b) Natural hazard assessment in the Pcinja catchment. In: BALWOIS conference, Ohrid, May 2010, pp 25–29
Dragićević S, Filipović D, Kostadinov S, Ristić R, Novković I, Živković N, Andjelković G, Abolmasov B, Šećerov V, Djurdjić S (2011) Natural hazard assessment for land-use planning in Serbia. Int J Environ Res 5(2):371–380
Dragićević S, Carević I, Kostadinov S, Novković I, Abolmasov B, Milojković B, Simić D (2012a) Landslide susceptibility zonation in the Kolubara river basin (western Serbia) – analysis of input data. Carpathian J Earth Environ Sci 7(2):37–47
Dragićević S, Zivković N, Roksandić M, Kostadinov S, Novković I, Tosić R, Stepić M, Dragićević M, Blagojević B (2012b) Land Use changes and environmental problems caused by bank erosion: a case study of Kolubara river basin in Serbia. In: Appiah-Opoku S (ed) Environmental land use planning. InTech, Rijeka. ISBN 979-953-307-943-0
EEA (European Environmental Agency) (1995) Coordination of information on the Environment (CORINE)-Land Cover. Commission of the European Communities, 163 pp
Gavrilović S (1972) Engineering of torrents and erosion. J Constr (special issue), Belgrade, 292 p (in Serbian)
Gavrilović S (1975) Torrents in Serbia. Republic Water Fund and Faculty of Forestry, Belgrade, 149 p (in Serbian)
Janković D (1994) Characteristics of intensive rainfall for territory of Serbia. Civil Engineering Almanac, Belgrade, pp 248–268 (in Serbian)
Kostadinov S (1988) Hydrological properties of a torrential flood wave. J Fac Forest 70:37–49 (in Serbian)
Kostadinov S (2007) Erosion and torrent control in Serbia: hundred years of experiences. In: International conference "Erosion and torrent control as a factor in sustainable river basin management", Belgrade, 25–27 Sept 2007, Proceedings (CD)
Kostadinov S (2010) Torrential floods and torrent control in Serbia. Croatia – Japan project on risk identification and land use planning for disaster mitigation of landslides and floods in Croatia: 1st project workshop "international experience", Dubrovnik, 22–24 Nov 2010
Kostadinov S, Borisavljević A, Mladjan D (2012) Torrents and torrential floods in Serbia: characteristics and possibilities of its control. In: LANDCON international conference, Abstract Book, Belgrade – Donji Milanovac, Sept 2012, Full paper on CD
Lazarevic R (1983) The erosion map of Serbia, 1:500000. Institute of Forestry and Wood Industry, Belgrade (in Serbian)
Malošević D (1995) DM-runoff model for ungaged watersheds. Belgrade (in Serbian)
Milevski I (2005) Characteristics of recent erosion in the Kumanovo basin. Bull Phys Geogr Skopje 2:25–45 (in Macedonian)
Milevski I, Dragićević S, Kostadinov S (2007) Digital elevation model and satellite images in assessment of soil erosion potential in the Pcinja catchment. Bull Serbian Geogr Soc 87 (2):11–20
Petkovic S, Kostadinov S (2008) Modern approach to managing risks from natural disasters. Faculty of Forestry, Belgrade, 37 p

RASP (2010) Draft of spatial plan of the Republic of Serbia. Republic Agency for Spatial Planning, Belgrade, 266 p (in Serbian)

Republic Hydrometeorological Office of Serbia (RHMOS) (1946–2007) Hydrologic annual reports-surface water, Belgrade, Serbia (in Serbian)

RHMOS (2010) Daily data precipitation records and weather radar reports for torrential flood in Trgoviste on 15 May 2010. Republic Hydrometeorological Office of Serbia, Belgrade (in Serbian)

Ristić R (2003) Runoff lag time on torrential watersheds in Serbia. J Fac Forest 87:51–65 (in Serbian)

Ristić R, Malošević D (2011) Torrent hydrology. Faculty of Forestry, University of Belgrade, Belgrade, 221 p (in Serbian)

Ristić R, Radić B, Vasiljević N (2009) Characteristics of maximal discharges on torrential watersheds in Serbia. Bull Serbian Geogr Soc 89(4):161–189

Ristić R, Radić B, Nikić Z, Trivan G, Vasiljević N, Dragićević S, Živković N, Radosavljević Z (2011a) Erosion control and protection from torrential floods in Serbia – spatial aspects. Spatium 25:1–6. doi:10.2298/SPAT1125001R

Ristić R, Radić B, Vasiljević N (2011b) Characteristics of maximum discharges on torrential watersheds in Serbia. J Environ Prot Ecol 12(2):471–487

Ristić R, Kostadinov S, Abolmasov B, Dragićević S, Trivan G, Radić B, Trifunović M, Radosavljević Z (2012) Torrential floods and town and country planning in Serbia. Nat Hazards Earth Syst Sci 1(12):23–35

Roksandić M (2012) Causes and consequences of changes of hydrographic network in Donjokolubarski basin. Manuscript Ph.D. thesis, Faculty of Geography, University of Belgrade, Belgrade, 197 p (in Serbian with summary in English)

Roksandić M, Dragićević S, Živković N, Kostadinov S, Zlatić M, Martinović M (2011) Bank erosion as a factor of soil loss and land use changes in the Kolubara River basin, Serbia. Afr J Agric Res 6(32):6604–6608. doi:10.5897/AJAR 11.736

Soil Conservation Service (SCS) (1979) National engineering handbook, Section 4, hydrology. US Department Agriculture, Washington, DC, 364 p

Živković N (2005) The impact of physical-geographical factors on the level of discharge in Serbia. Special editions of the Faculty of Geography, Belgrade No. 6 (in Serbian with summary in English)

Živković N (2009) Average annual and seasonal river discharges in Serbia. The Faculty of Geography, Belgrade, 174 p (in Serbian with summary in English)

Chapter 11
Extreme Erosion Rates in the Nišava River Basin (Eastern Serbia) in 2010

Sanja Mustafić, Predrag Manojlović, and Marko V. Milošević

Abstract In the last decade several major floods have been registered on the territory of Serbia. The floods that affected the Nišava River Basin in spring 2010 have been the most severe in the last 50 years. During 2010 daily measurements of suspended sediment were carried out at the last hydrologic profile of Niš along the river. In the study period, mean annual specific runoff was 12.3 L s^{-1} km^{-2} and mean annual suspended load concentration was 0.1272 g L^{-1}. A maximum mean monthly concentration of suspended load of 0.3806 g L^{-1} was recorded in May, when the mean monthly specific runoff was 24 L s^{-1} km^2, and minimum 0.0118 g L^{-1} in September (2.7 L s^{-1} km^{-2}). Total suspended load transport was 475,792.2 t (specific yield, 122.9 t km^{-2} $year^{-1}$). The suspended transport over the year was 2.1 times higher than the average for the period of 50 years. Out of total annual sediment, 90.7% was moved in the period February to May. On a monthly level, the highest transport was observed in May (31% of the annual transport).

Keywords Floods • Erosion hazard • Suspended load • Hysteresis loops • Nišava River • Serbia

11.1 Introduction

Torrential floods are the most common natural hazard in Serbia (Ristić et al. 2012) and among the most severe consequences of erosion processes (Dragićević 2007). Maximum discharge in the torrential basins occurs seasonally, in the periods of

S. Mustafić (✉) • P. Manojlović
Faculty of Geography, University of Belgrade, Studentski trg 3/3, Belgrade, Serbia
e-mail: sanjam@gef.bg.ac.rs; peca@gef.bg.ac.rs

M.V. Milošević
Geographical Institute 'Jovan Cvijić' of the Serbian Academy of Sciences and Arts, Djure Jakšića 9/3, Belgrade, Serbia
e-mail: m.milosevic@gi.sanu.ac.rs

D. Lóczy (ed.), *Geomorphological impacts of extreme weather: Case studies from central and eastern Europe*, Springer Geography, DOI 10.1007/978-94-007-6301-2_11,

cyclonic activity (Gavrilović et al. 2012). The *critical periods* in Serbia are the end of spring (from May to the first half of June) and the end of winter (from February to the first half of March) (Ristić et al. 2012). Daily and monthly *maximum precipitations* were recorded at almost all rain gages in Serbia from May to June (Živković 2009), whereas the period from February to the first half of March was the secondary maximum of precipitation (Ducić and Radovanović 2005). In the 20th century disastrous floods in Serbia occurred every fourth or fifth year on average (Gavrilović 1981), and some of them were classified as historical: on the Vlasina River in June 1988, the Zapadna Morava River in May 1965, the Ibar River in 1979, and the Ribnica River in April 1996 (Prohaska et al. 2010). Also in the first decade of the twenty-first century, numerous severe floods were recorded (Milanović et al. 2010).

The dynamics of river sediment transport are also controlled by the variability of precipitation. Studies in Central Europe (Scholz et al. 2008) have shown that there is a *redistribution of precipitation* from summer/autumn to winter/spring, when extreme events are on the increase: 12% growth per decade as opposed to 8% of decrease per decade in the summer period (Zolina et al. 2008). Recent studies point out that in the last 70 years there has been a noticeable increase in precipitations with intensities able to induce soil erosion. A growing trend of rainfall intensities higher than 20 mm h^{-1} is particularly expressed over the last 35 years (Mueller and Pfister 2011). The redistribution of precipitation and its intensity are manifested in the increased rates of erosion process in spring (March, April, and May) and during winter, mostly in February (Scholz et al. 2008). These seasonal changes and trends have also been observed in the Nišava River Basin, where the floods from February to the end of May 2010 were among the largest in Serbia. High discharges caused suspended sediment transport 2.1 times higher in that year than the average for the period of 50 years.

According to the Map of Natural Hazards for Serbia (Dragićević et al. 2011a), the Nišava River Basin is vulnerable to all kinds of natural hazards, among which potentially flooded areas and excessively eroding terrains are widespread. Flood-prone areas are widespread along the whole length of the Nišava River from its entrance from Bulgaria into Serbia, until it joins the Južna Morava River. Two areas of high *erosion hazard* are identified in the Nišava River Basin: (1) the upper mountainous section with the largest tributaries (the Visočica and Jerma Rivers) and (2) the lower section with the most extensive area in the Kutinska River Basin (Dragićević et al. 2011b), which has torrential characteristics. Historically, *major floods* were recorded in the basin in December 1952, February 1955, April 1958, February 1963, February 1966, February 1969, June 1976, April 1987, June 1988, and November 2007 (Stefanović et al. 2010).

11.2 Study Area

The Nišava River Basin is located in the southern part of Eastern Serbia (Fig. 11.1), and it encompasses an area of 4,068 km^2, shared between the Republic of Bulgaria (27%) and the Republic of Serbia (73%). Total length with the headwater Ginska is

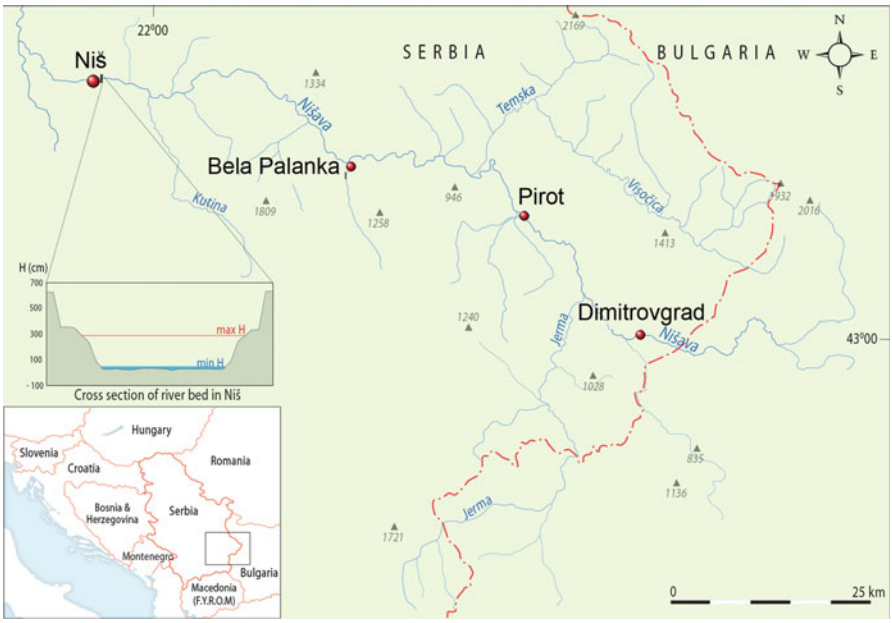

Fig. 11.1 Location of the Nišava River Basin

202 km (151 km on the territory of Serbia). The average elevation of the basin is 739 m (highest point 2,186 m and the lowest 200 m). Hilly area up to 500 m covers 26.7%, while the major portion (50.9%) is low mountains (between 500 and 1,000 m elevation), and areas above 1,000 m is occupying 22.5% of the basin.

The Nišava River Basin is formed on diverse metamorphic, igneous, and sedimentary rocks of different ages. Three almost evenly spread rock complexes dominate the basin: limestones and dolomites (28.4% of total area), alluvial and Neogene sediments (25.1%), and flysch (22.1%) and sandstones (16.5%). The most widespread metamorphic rocks are schists (3.9%), and the most common igneous rock is andesite (2.2%).

The basin is characterized by high inclinations: the major portion (28.5%) is below 5°; slopes 5–10° occupy 19.6%, 10–15°, 18.9%; 15–30°, 27.4%; while slopes steeper than 30° make up 5.6% of the area.

The average annual *precipitation* in the basin is 731 mm, close to the national average (739 mm – Bajat et al. 2012), but with uneven spatial distribution, the Nišava valley is one of the driest regions in Serbia (586 mm – Petrović 1998, 1999). The mountainous frame makes the lowlands relatively isolated (Milovanović 2010). The highest parts of the Stara Planina (Balkan) Mountains receive about 1,200 mm of precipitation annually (Mustafić 2006; Ducić and Radovanović 2005) – relatively low given their elevation. The reason for this lies in the fact that precipitation in Eastern Serbia decreases in the northwest-southeastern direction (Živković 2005) as well as by its position in the rain shadow of parallel mountain ranges

(Milovanović 2010). According to Živković (2009), the precipitation in the Nišava River Basin rises on average 26 mm with 100 m increase of altitude, while in some parts of the basin (Suva Planina and Stara Planina), the lapse rate is 55–59 mm per 100 m (Živković and Andjelković 2004; Živković 2005). In the summer half year (April to September), precipitation is ca 10–12% higher than in the winter half year (October to March). The highest precipitation is observed in June and the lowest in September and October.

Mean annual air *temperature* in the basin is 8.3 °C, but in the lowest-lying Niš basin, it is 11.8 °C (Ivanović et al. 2011). The 1 °C isotherm (at 2,045 m elevation) encircles the highest summits of Stara Planina, and the lapse rate is 0.58 °C per 100 m (Živković and Smiljanić 2005).

11.3 Methods

Suspended sediment concentration was measured daily at Niš data by the Republic Hydrometeorological Office of Serbia (RHMOS) between 1961 and 2008 supplemented with personal observations for 2009–2010. The concentration was established by filtration of liter samples using vacuum pump (Sartorius) and measuring weight of filter paper (Albet) using digital scales after drying in dry section at the temperature of 105 °C and on desiccators before and after filtering.

Air temperature, precipitation, and discharge were also obtained from the RHMOS for the whole study period. Mean monthly and annual precipitation totals were derived from 22 rain gages. The data from two meteorological stations (Dimitrovgrad and Niš) were employed for the analysis of daily precipitation and air temperature. To identify extreme precipitation events, mean maximum daily precipitation totals for the period 1961–2010 were considered. Analysing the impact of air temperature on erosion, daily maximum air temperatures and mean monthly and absolute maxima were regarded. Data were processed using the programs STATISTICA and ORIGIN.

11.4 Results

11.4.1 Hydrometeorological Conditions in 2010

In 2010 precipitation in the study area was 20% above average. The monthly distribution of precipitation in 2010 was extremely uneven. In winter and spring months (February, March, April, and May), it was 20–100% higher (347 mm, 41% of the annual total) than the monthly averages. In contrast, in July, August, and September, the basin received below-average amounts, while in autumn above-average

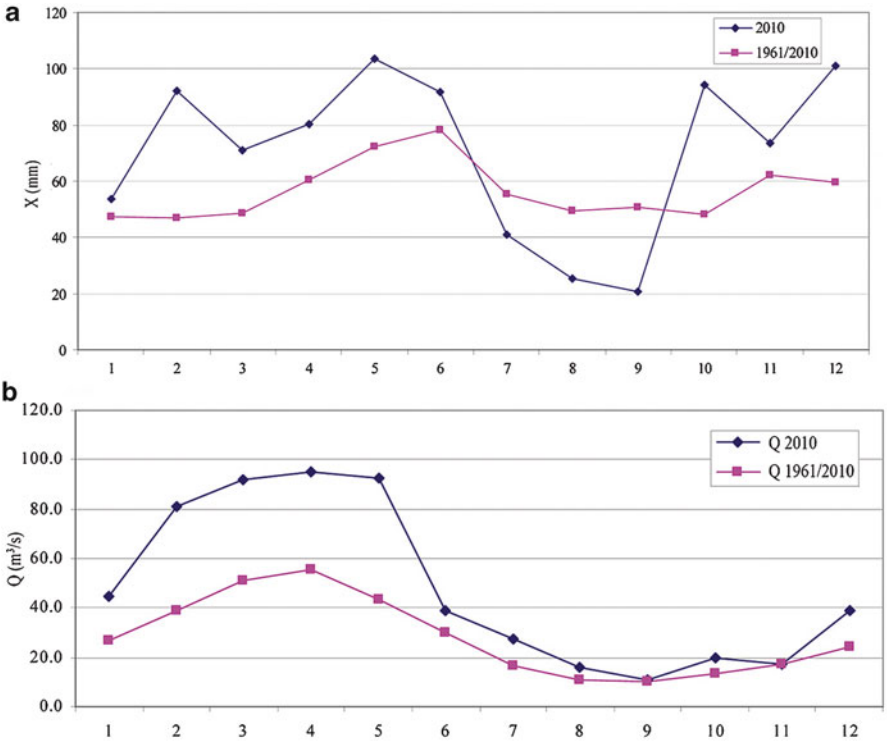

Fig. 11.2 Average monthly precipitation (**a**) and average monthly discharge (**b**) at Niš in 2010 and in the period 1961–2010

rainfalls. The best indicator of extreme precipitation values during 2010 is the annual *coefficient of variability*, which was 41.1 (as opposed to the average of 18.1).

Maximum *discharges* on the Nišava occur in April and March, with secondary maxima in May and February. However, in 2010 the hydrologic regime was different: maximum discharge was recorded in May (Fig. 11.2). Mean specific runoff at Niš is 7.3 L s^{-1} km^{-2} (close to the national average of 7.06 L s^{-1} km^{-2} (Manojlović and Živković 1997)), but in 2010 it amounted to 12.3 L s^{-1} km^{-2} (69% above the 50-year average). Pearson III distribution showed that the year 2010 saw the largest water masses in the last 50 years (in February and March 1.7–2.2 times the average, in 4 months 62% of the annual runoff).

11.4.2 Runoff and Suspended Load in 2010

Mean annual concentration of *suspended load* in 2010 was 0.1272 g L^{-1}. Maximum mean monthly concentration of suspended load was registered in May (0.3806 g L^{-1}), with a discharge of $Q = 92.8$ m^3 s^{-1}, which corresponds to a

Table 11.1 Mean monthly concentrations of suspended load (g L^{-1}) in 2010 compared to the period 1961–2010

	J	F	M	A	M	J	J	A	S	O	N	D
C_s 2010	0.0326	0.3457	0.2021	0.2181	0.3806	0.0797	0.0529	0.0188	0.0118	0.0448	0.0418	0.1137
C_s 1961/2010	0.0831	0.1516	0.1744	0.1358	0.1397	0.2203	0.1384	0.1123	0.0559	0.1304	0.1543	0.1107
Ratio	0.39	**2.28**	**1.16**	**1.61**	**2.72**	0.36	0.38	0.17	0.21	0.34	0.27	**1.03**

Bold numbers indicate extreme values

Table 11.2 Mean monthly specific discharge of suspended load (t km^{-2}) in 2010 compared to the period 1961–2010

	J	F	M	A	M	J	J	A	S	O	N	D
Q_s 2010	1.6	30.9	14.9	27.7	38.1	2.3	1.1	0.2	0.09	0.8	0.6	4.7
Q_s 1961/2010	2.9	8.9	10.9	8.4	6.9	7.9	2.7	1.3	0.5	1.7	3.1	3.4
Ratio	0.53	**3.50**	**1.37**	**3.31**	**5.52**	0.29	0.42	0.19	0.16	0.48	0.18	**1.38**

Bold numbers indicate extreme values

specific runoff of $q = 24.0$ L s^{-1} km^{-2}. Minimum mean monthly concentration of 0.0118 g L^{-1} occurred in September ($Q = 10.6$ m^3 s^{-1}; $q = 2.7$ L s^{-1} km^{-2}). The ratio of extreme mean monthly concentrations was 1–8.5. A maximum daily concentration of suspended load of 2.8166 g/L was recorded on 20 February 2010 ($Q = 169$ m^3 s^{-1}; $q = 43.7$ L s^{-1} km^{-2}), while – in this exceptional year – its minimum (0.0018 g L^{-1}) was in the same month, on 1 February ($Q = 20.0$ m^3 s^{-1}; $q = 5.2$ L s^{-1} km^{-2}). The ratio between the extremes was as high as 1 to 1565.

Related to the monthly averages for 1961–2010, the deviations of monthly values of suspended load concentrations in 2010 are huge and mostly peak in the period from February to May (Table 11.1). Consequently, the concentrations of suspended load in May were 2.72, in February 2.28, in April 1.61, and in March 1.6 times higher than their 1961–2010 mean values.

The Nišava River transported 475,792.2 t of suspended load (122.9 t km^{-2} $year^{-1}$) at Niš in 2010. The extreme conditions are best illustrated by the fact that specific suspended load in that year was 2.1 times higher than the 50-year average (58.6 t km^{-2} $year^{-1}$). The annual distribution of suspended load also had an extreme range: from 342.2 t in August to 147,307.3 t in May (monthly specific sediment yields in the range from 0.1 to 38.1 t km^2). It is noteworthy that the highest daily sediment yield of 50220.8 t (12.9 t km^{-2} day^{-1}) was not recorded during the maximum daily concentration in February, but on 21 April 2010 with the highest discharge ($Q = 311$ m^3 s^{-1}; $q = 80.4$ L s^{-1} km^{-2}) and suspended load concentration of 1.8690 g L. Minimum daily of suspended load transport was 2.1 t (0.001 t km^{-2} day^{-1}) on 22 August 2010 with suspended load concentration of 0.0026 g L^{-1} ($Q = 9.2$ m^3 s^{-1}; $q = 2.4$ L s^{-1} km^{-2}) and the ratio between extremes: 1 to 24,221. From February to May, 90.7% of the annual amount of suspended load was transported. May is the month with the highest erodibility (147,307 t suspended load; 31% of the annual value). The extremes are even more emphasized if we compare the mean monthly values in 2010 with mean monthly values for 1961–2010. The value for May was 5.52-fold, in February 3.5-fold, and in April 3.3-fold higher than the monthly average (Table 11.2).

The *frequency distribution* of suspended sediment concentration is skewed to the left, while that of suspended sediment transport leans towards F-distribution with a strong right *skewness*. This can be explained by the annual distribution of discharge. Low and medium water levels with low concentrations of suspended load dominate over most of the year, while the short spells of high water show high concentrations and large-scale transport of suspended load. In 2010, for 142 days (39% of time), suspended load concentration was 0.01–0.05 g L^{-1}, exceeded 1 g L^{-1} on several occasions (1.9% of time). The dominant class of transport of suspended sediment was 200–500 t day^{-1} (19% of the year) (Fig. 11.3).

This distribution of transport does not provide a detailed insight into how sediment transport is related to *specific runoff*. To reveal this relationship, specific runoff has been grouped into eight classes (Table 11.3). Runoff up to 20 L s^{-1} km^{-2} (81.4% of time) dominated in 2010 with mean suspended load concentration of 0.048 g L^{-1} and made up only 10.3% of annual sediment transport. On the other hand, during the period of high water levels ($q > 30$ L s^{-1} km^{-2}; 8.2% of time), 75.6% of suspended load was transported (concentration, 0.7914 g L^{-1}).

Figure 11.4 best illustrates the extent to which the year 2010 deviates from the average. While distribution of specific erosion shows normal distribution according to the classes of runoff in the 50-year period, the distribution of sediment transport in 2010 has a character of F-distribution with the dominance of transport in higher discharge classes (Fig. 11.4). Deviation from the average distribution is found in the classes of runoff above 20 L s^{-1} km^{-2}.

The relationship between cumulative percentage of time on one hand and cumulative percentage of runoff and suspended sediment transport on the other is represented in the form of a *Lorenz curve* (Fig. 11.5). The curve deviation from a hypothetically even distribution indicates the excessiveness of the erosion process. Great variability of transport is represented by sharp bends on the sediment transport curve within its annual distribution. In 2010 2.3% of the annual amount of sediment was carried by the Nišava River during 50% of time corresponding to 20% of annual runoff. On the other hand, during 90% of time, 70% of the annual runoff transported only 20% of sediment.

The close relationship between specific runoff/discharge and suspended sediment concentration is best illustrated by the regression model of exponential type with a coefficient of 0.72 (Fig. 11.6). For the determination of the intra-annual distribution of this relationship, *hysteresis loops* are employed. The different types of hysteresis loops point to different events which determine the relationship between runoff and suspended load concentration and indicate the location of the source of material, the conditions and dominant factors which activate the sedimentation source (Seeger et al. 2004), and the modes of transport to the watercourses (Jansson 2002). The relationship between precipitation conditions, runoff, concentration of suspended material, and sediment transport can be illustrated by a hysteresis loop for the period of perennial flow (Grenfell and Ellery 2009). The analysis of mean monthly concentration of suspended sediment and specific runoff has shown the existence of a long-term hysteresis effect (Fig. 11.7). From the established five types of hysteresis loops (Williams 1989), one was found

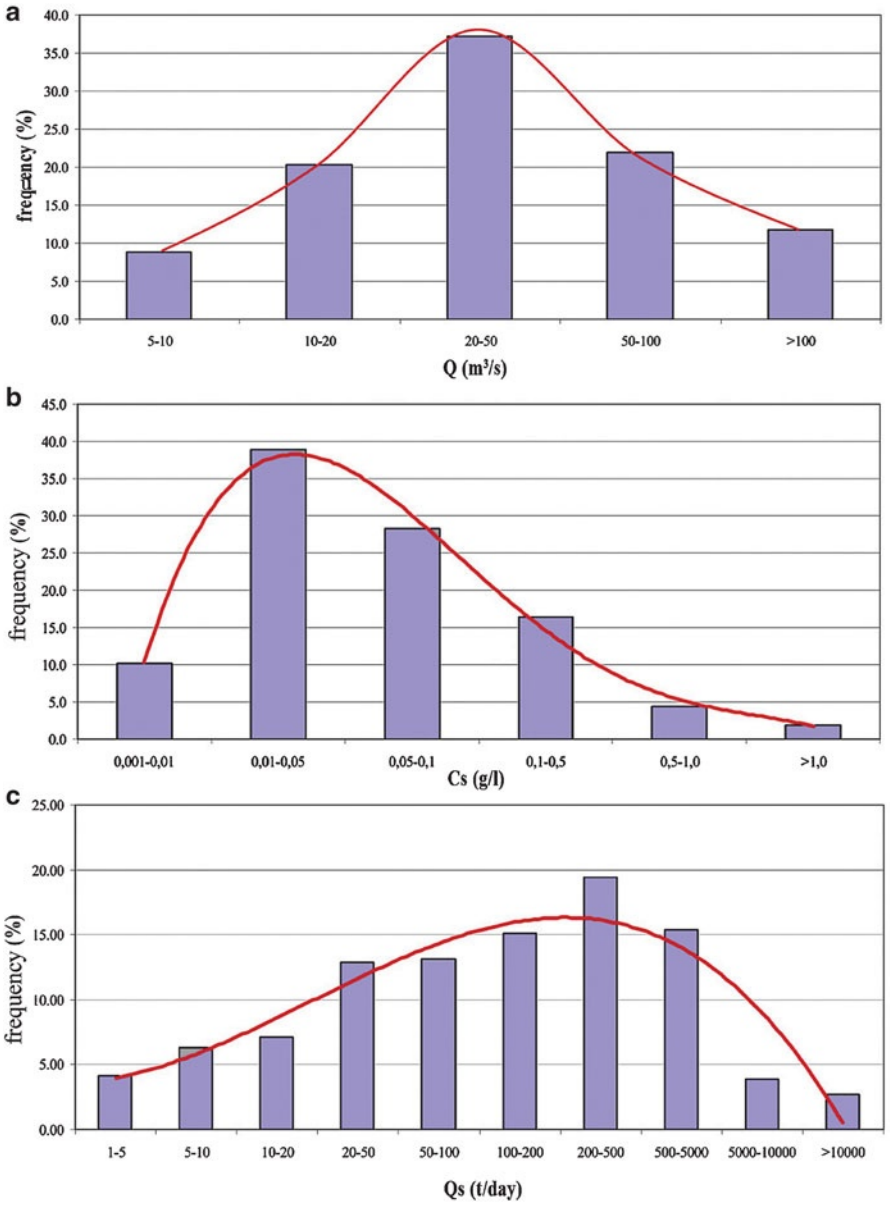

Fig. 11.3 Frequency distribution of discharge (**a**) suspended load concentration (**b**) and transport of suspended load (**c**)

typical for the lowermost section of the Nišava River (Fig. 11.8), which means that complex events are linked and occur after dry conditions (Soler et al. 2008). Thus, *soil moisture* is a very important factor (Klein 1984; Seeger et al. 2004) also in the case of the lowland area of the Nišava Basin, which is, according to the Map of

Table 11.3 Suspended sediment transport related to the frequency distribution of runoff

	2010						1961–2010
Classes of q (L s^{-1} km^{-2})	q (frequency)	q (%)	C_s (g L^{-1})	Q_s (t)	Q_s (%)	Q_s (t km^{-2} year^{-1})	Q_s (t km^{-2} year^{-1})
>3	45	12.3	0.0152	518.4	0.1	0.1	1.3
3.01–5.00	54	14.8	0.0243	1750.9	0.4	0.5	2.8
5.01–10.00	102	**27.9**	0.0485	12602.0	2.6	3.3	8.0
10.01–20.00	96	26.3	0.0762	34284.6	7.2	8.9	**12.4**
20.01–30.00	38	10.4	0.2077	66872.5	14.1	17.3	10.4
30.01–40.00	19	5.2	0.5092	112881.3	23.7	29.2	9.1
40.01–50.00	8	2.2	1.2194	143260.9	**30.1**	**37.0**	5.6
50.01–60.00	3	0.8	1.6157	103621.5	21.8	26.8	3.1

Bold numbers indicate extreme values

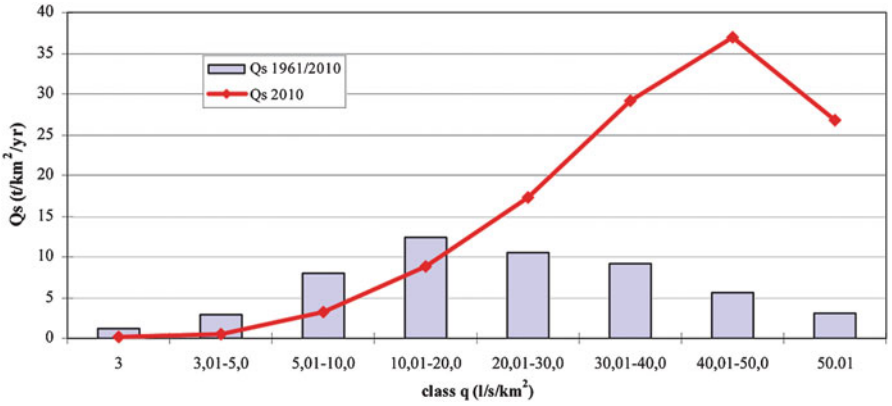

Fig. 11.4 Distribution of specific sediment transport according to the classes of specific runoff during 2010 and in the period 1961–2010

Natural Hazards for Serbia (Dragićević et al. 2011a), one of the driest regions in Serbia. The summer season lasts 15 days more than the calendar summer, and dry season is continued during the autumn, which is warmer than spring. Maximum mean air temperature is considerably high (22.3 °C), and hot days are frequent (Ivanović et al. 2011).

This type of loop indicates complex sediment transport dynamics. In the first phase (from February to April or May), the loop is oriented in clockwise direction. In the Nišava Basin, the first phase follows summer–autumn drought and stable winter conditions. Due to snowmelt and spring precipitation, in this phase the soil is wet, its water retention capacity is reduced, and runoff intensifies. From May to September, the loop has an opposite character. Maximum suspended load concentration occurs after maximum discharge, followed by a decline and minimum in September. In the second phase (counterclockwise direction), there is a situation in which precipitation of high intensity dominates (June). That means that the

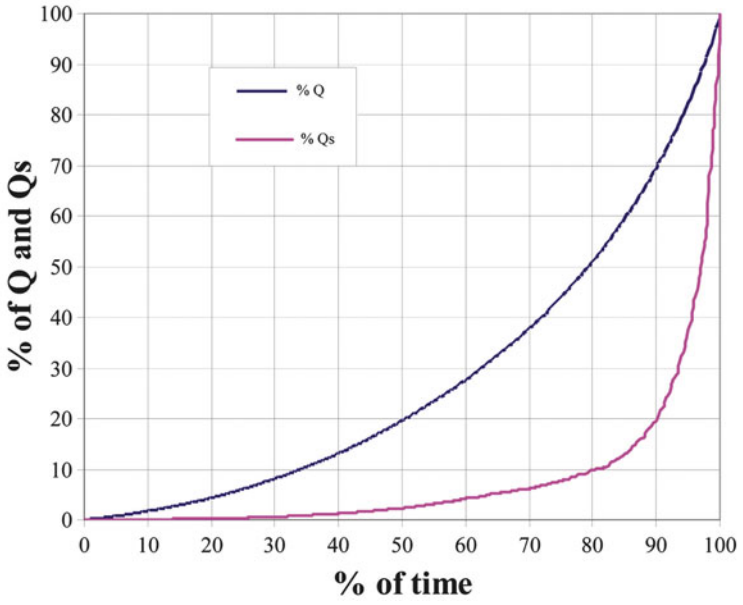

Fig. 11.5 Cumulative annual distribution of discharge and transport of suspended load in 2010

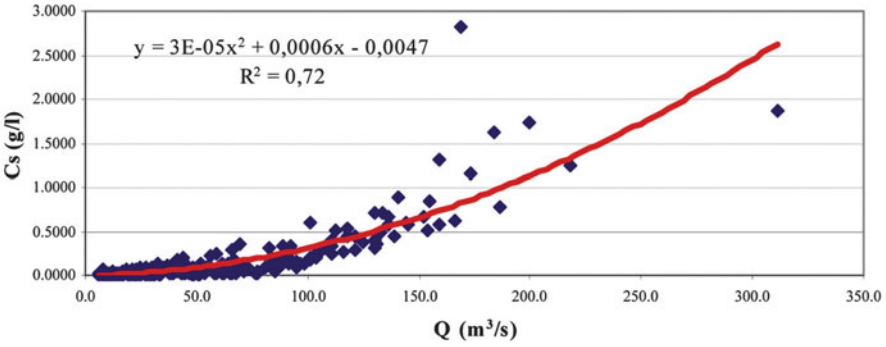

Fig. 11.6 Ratio between the runoff and suspended load concentration in 2010

sediment source can be activated over a larger area. From September the orientation of the loop changes again for a clockwise direction.

The relationship of concentrations of suspended load and runoff in 2010 closely follows the trend line (Fig. 11.8), which proves the dependence of suspended load concentrations on water discharge. Generally speaking, increased concentrations of suspended load follow the increase of runoff with a maximum in May, when the discharge is also the highest, while high values of suspended load concentrations in February indicate that stable winter conditions are over.

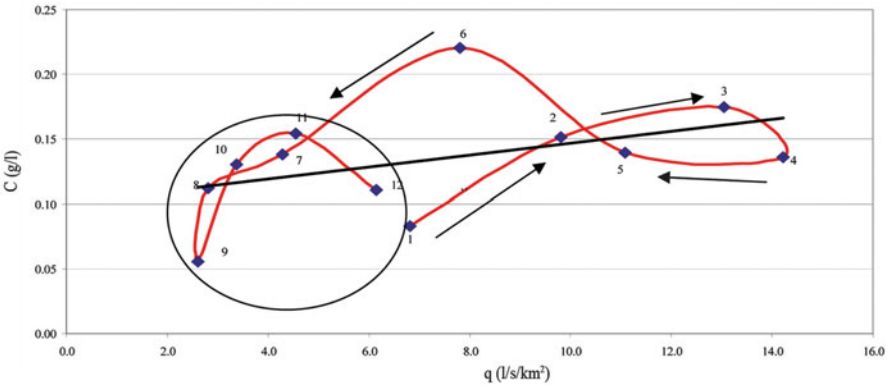

Fig. 11.7 Mean annual hysteresis loop for the Niš profile (1961–2010)

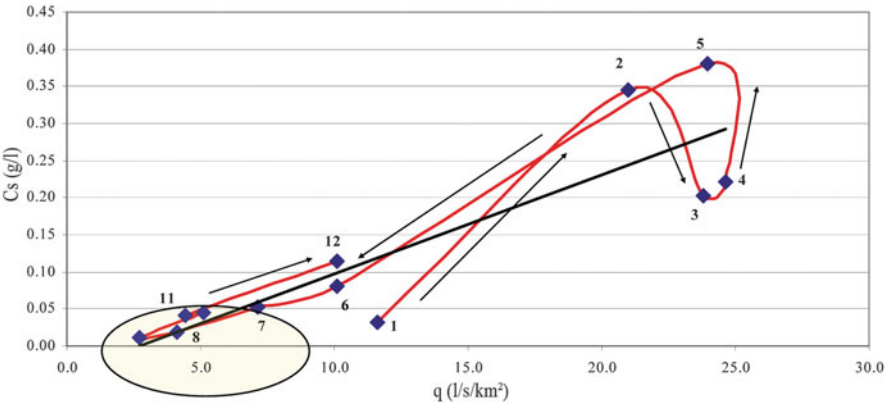

Fig. 11.8 Mean annual hysteresis loop for the Niš profile (2010)

11.4.3 The Influence of Precipitation and Air Temperature On Excessive Erosion

The extreme character of maximum concentrations of suspended load in February and May can be best seen if their values are compared to the long-term (1961–2010) average (Fig. 11.9). Suspended load concentrations in January and in the June to November period are below the multiannual average, while in December they are relatively close to the average. May and February show the largest deviations: 2.84- or 2.58-fold higher concentrations than the average, respectively (Fig. 11.10). The most extreme month was May with 7.59-fold sediment transport followed by February (6.82-fold), April (5.7-fold), and May (2.96-fold the long-term average) – adjusted to periods of intensive surface runoff caused by intensive rain or snowmelt or by the coincidence of both.

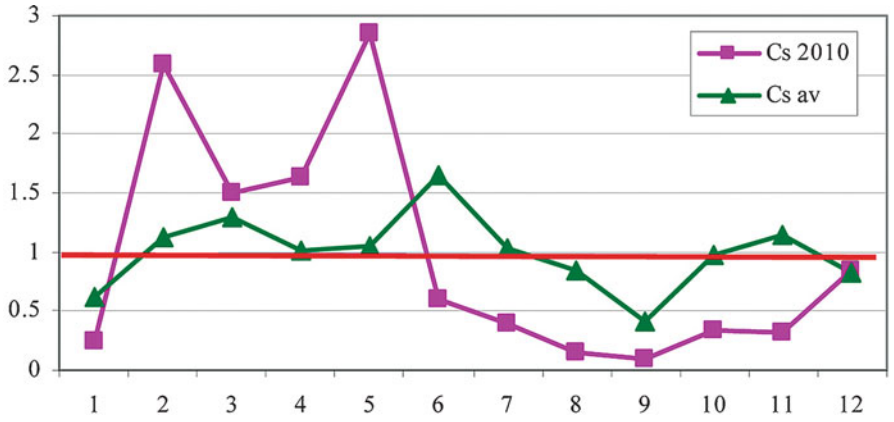

Fig. 11.9 Module values of suspended load concentration (C_s) (mean monthly/mean long term)

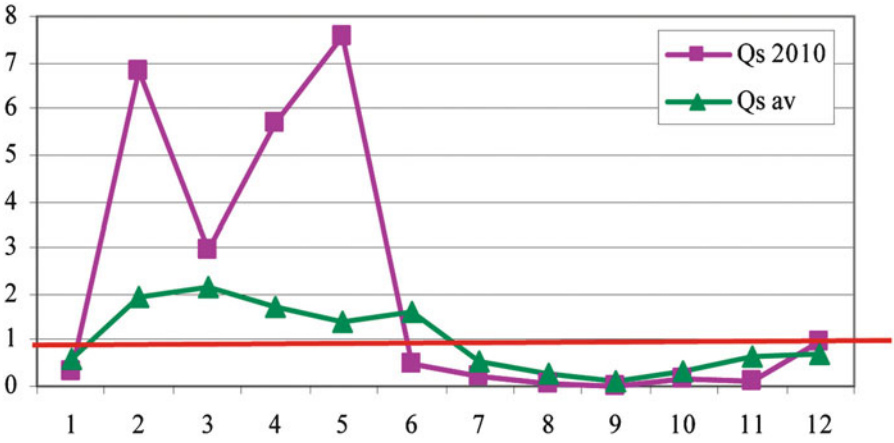

Fig. 11.10 Module values of suspended sediment transport (Q_s) (mean monthly/mean long term)

In 2010 two large flood waves occurred with extreme suspended load concentrations and transport: the first in February and the other in May. Extremely high transport of suspended sediment in 2010 was determined by high runoff generated by high precipitation. However, studies in Serbia have shown that every increase of precipitation does not exclusively accelerate the rate of erosion (Dragićević 2002, 2007). Therefore, the question arises as to what amount of precipitation can be considered sufficient to cause excessive erosion. *Erosion thresholds* are different in various studies throughout Europe: 10 mm h^{-1} in England, 6 mm h^{-1} in Germany, or 1 mm h^{-1} in Belgium (Morgan 1995). Some research in Serbia has pointed out that river flooding occurs when precipitation intensity is 25 mm day^{-1} (Milanović 2006), whereas daily precipitation above 30 mm has been regarded as a threshold for excessive erosion (Dragićević 2007). *Maximum daily precipitation* was considered as the key factor in excessive erosion

Table 11.4 Maximum daily precipitation (X, mm) in 2010 and thresholds for intensive precipitation

	1	2	3	4	5	6	7	8	9	10	11	12
Dimitrovgrad												
X 2010	8.9	9.5	**22.7**	**20.4**	**35.7**	21.6	12.6	12.9	6.6	18.1	29.9	29.7
X_{dmax}	12.5	13.2	14.7	14.8	21.0	25.5	25.3	20.0	18.4	17.3	17.7	13.8
Niš												
X 2010	12.8	**14.2**	**19.9**	**23.5**	16.9	16.9	13.2	12.9	3.4	19.0	15.8	18.4
X_{dmax}[a]	11.3	12.0	13.3	16.3	19.1	22.2	16.3	18.9	18.0	15.7	16.3	14.3

Bold numbers indicate extreme values

[a]X_{dmax} is average maximum daily precipitation in mm (1961–2010) as threshold for erosive rainfall

Table 11.5 Mean monthly maximum air temperatures t (°C) in 2010 and average maximum air temperatures t_{dmax} (°C) for the period 1961–2010

	1	2	3	4	5	6	7	8	9	10	11	12
Dimitrovgrad												
t 2010	**4.0**	**6.6**	**12.0**	16.6	21.9	25.3	27.7	30.0	23.8	14.5	17.0	6.1
t_{dmax}	3.4	6.0	11.1	16.7	21.6	24.9	27.3	27.6	23.3	17.7	10.8	4.8
Niš												
t 2010	**5.1**	**7.9**	**13.2**	18.5	23.3	27.2	29.6	31.4	25.2	15.4	18.9	7.7
t_{dmax}	4.4	7.4	12.6	18.2	23.4	26.7	28.9	29.3	24.7	19.0	12.1	5.7

Bold numbers indicate extreme values

(Andjelković 2009). On the other hand, in some cases even low precipitation amounts coupled with high temperatures can induce excessive erosion (Tables 11.4 and 11.5).

The *first flood wave* started on 18 February as a result of a warm front and lasted until the end of February. Although the precipitation in February (88.3 mm) was double the average for this month, the decisive factor for high concentrations and transport of suspended load was air temperature (Figs. 11.11 and 11.12). The relationship between air temperature and discharge on the one hand and air temperature and suspended load on the other hand is best illustrated by exponential regression with coefficients of 0.79 or 0.77. In the upper part of the basin (represented by the meteorological station Dimitrovgrad), mean maximum temperature was 10% above the monthly average, and an absolute maximum temperature of 19.2 °C was also measured. In addition, in the last decade of this month, all days had maximum daily temperatures above 6 °C and for 5 days above 12 °C. In the lowermost basin section (represented by the meteorological station Niš), the air temperature surpassed the average by 6.1%, absolute maximum temperature was 18.7 °C, and daily maxima were positive in the whole month. The peak of flood wave was on 21 February with $Q = 186.0\ m^3\ s^{-1}$ and $q = 48.1\ L\ s^{-1}\ km^{-2}$. Such a high discharge was the result of high mean air temperature of the previous day (12.7 °C) and maximum 18.7 °C, which generated the highest concentration of suspended load over the whole 2010 (daily maximum, 2.8166 g L^{-1} – 34.4% of monthly sediment transport).

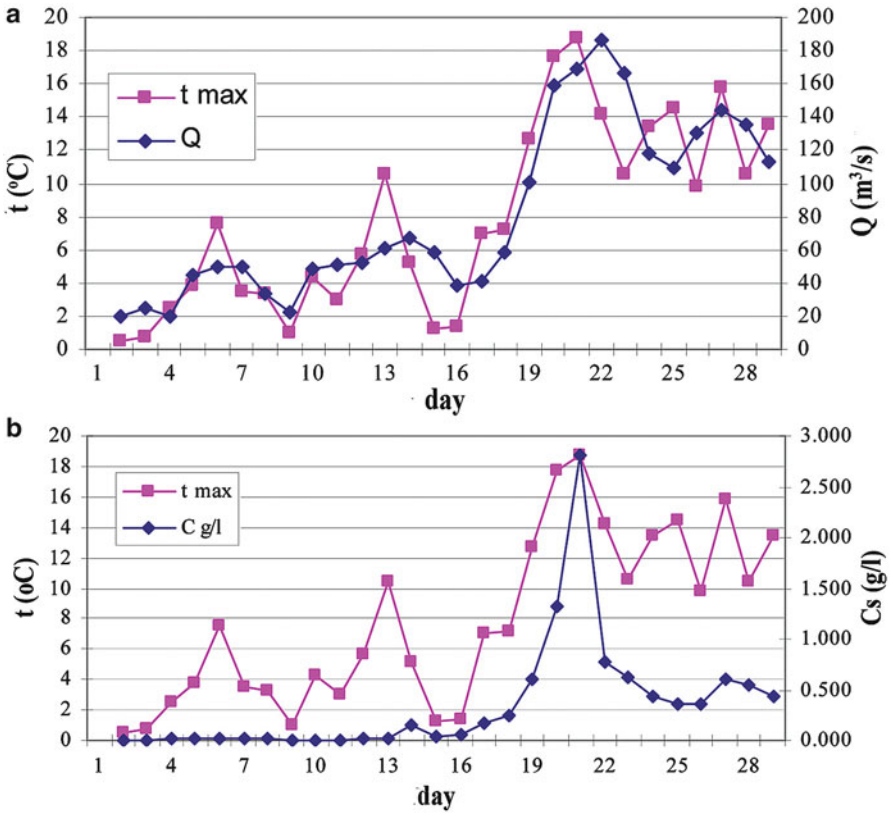

Fig. 11.11 Daily discharge and maximum air temperature change (**a**) and daily suspended load concentration and maximal air temperature change (**b**) on February 2010 at the Niš profile

The *second flood wave* occurred from 16 to 26 May, when 61.2% of the monthly runoff and 92.2% of suspended load transport were observed. The peak of the flood wave was on 19 May, when the discharge reached its maximum ($Q = 200\ \mathrm{m^3\ s^{-1}}$; $q = 51.6\ \mathrm{L\ s^{-1}\ km^{-2}}$), and the concentration of suspended load was $1.73\ \mathrm{g\ L^{-1}}$. On this day 20.3% of the monthly sediment transport was realized. The reason for the May flood wave was precipitation conditions in the mountainous part of the basin. At the highest-lying stations on the Stara Planina, 66.7% more precipitation fell than the long-term monthly average (the maximum was 75%): Dojkinci (elevation, 880 m) 152 mm, Visočka Ržana (700 m) 144 mm, and Topli Do (770 m) 140.2 mm. The influence of precipitation on intensified erosion can also be seen in maximum daily precipitation: at Dimitrovgrad 70% higher than the threshold. Daily maxima above 20 mm in May were also registered at the valley stations: in Pirot 43.5 mm and in Bela Palanka 20.4 mm.

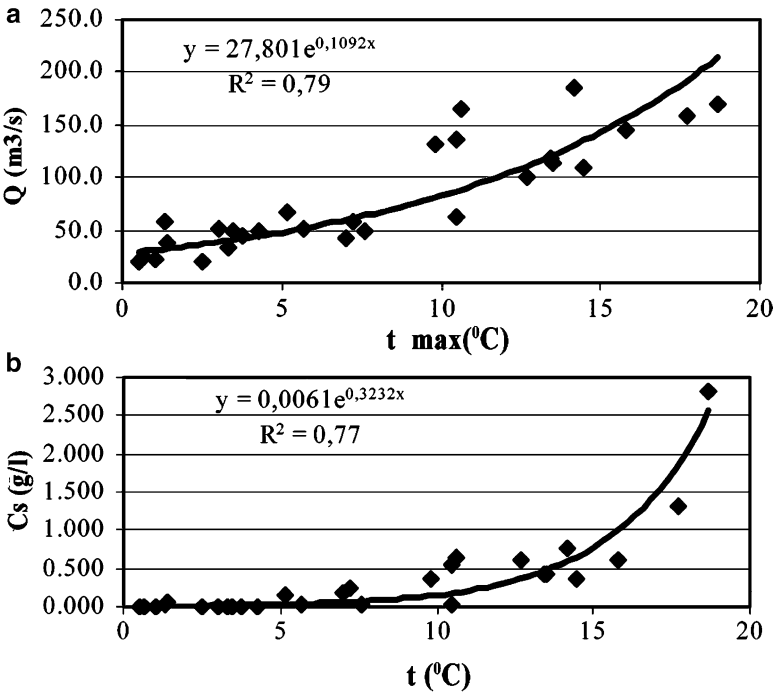

Fig. 11.12 Ratio between maximum daily air temperatures and discharge (**a**) and maximum daily air temperatures and sediment concentration (**b**) in February 2010 at the Niš profile

11.5 Conclusions

The 2010 European floods also affected the territory of Serbia. In the southeast, in the Nišava River Basin, they were disastrous, damaging settlements, traffic routes, and infrastructure and also causing human casualties. Floods are common on the tributaries of the Nišava River, but in that year torrential floods were observed on the whole course of the main river from its entrance into Serbia to its confluence. Extreme precipitation and temperature conditions generated extraordinarily high runoff and intensive erosion.

Extreme conditions in the basin are best expressed by the specific transport of suspended load (122.9 t km^{-2} $year^{-1}$) – 2.1-fold higher in 2010 than the average for the period 1961–2010 (58.6 t km^{-2} $year^{-1}$). The reason for intense erosion lies in the extreme hydrometeorological conditions of the period from February to May 2010, with 41% of annual precipitation, 62% of annual runoff, and 92% of annual sediment transport. May is the month that stands out in terms of erosivity (31% of annual sediment transport). The second month with extremely large transport was February (maximum daily concentration of suspended load, −2,8166 g, 34.4% of the monthly sediment transport), when the high concentration of suspended load and transport is explained by unusually high air temperatures.

Complex sediment dynamics springs from the rapid alternation of dry and wet periods. The analysis of the relationship between mean monthly concentration of suspended load and specific runoff has shown a long-term hysteresis effect. It is typical for Nišava River Basin that peak discharge is followed by the peak of suspended load with a certain lag time. However, the example of 2010 does not fit into this pattern. In May 2010 extreme precipitations and river flow overlapped, so the maximum of suspended load occurred coincided with peak discharge.

Acknowledgements This chapter is part of the project "The Research on Climate Change Influences on Environment: Influence Monitoring, Adaptation and Mitigation" (43007), subproject No. 9 "Torrential Floods Frequency, Soil and Water Degradation as the Consequence of Global Changes," financed by the Ministry of Education and Science of the Republic of Serbia.

References

Andjelković G (2009) Extreme climate events in Serbia. Manuscript Ph.D. thesis. Faculty of Geography, University of Belgrade, Belgrade, 251 p

Bajat B, Pejović M, Luković J, Manojlović P, Ducić V, Mustafić S (2012) Mapping average annual precipitation in Serbia (1961–1990) by regression kriging. Theor Appl Climatol. doi:10.1007/s00704-012-0702-2

Dragićević S (2002) Sediment load balance in the Kolubara Basin. Faculty of Geography, Belgrade, 184 p (in Serbian with English summary)

Dragićević S (2007) Dominant processes of erosion in the Kolubara Basin. Jantar Grupa, Beograd, 245 p (in Serbian with English summary)

Dragićević S, Filipović D, Kostadinov S, Ristić R, Novković I, Živković N, Andjelković G, Abolmasov B, Šećerov V, Djurdjić S (2011a) Natural hazard assessment for land-use planning in Serbia. Int J Environ Res 5(2):371–380

Dragićević S, Novković I, Carević I, Živković N, Tošić R (2011b) Geohazard assessment in the Eastern Serbia. Forum Geogr 10(1):10–19

Ducić V, Radovanović M (2005) Klima Srbije (Climate of Serbia), Zavod za udžbenike i nastavna sredstva, Beograd, 212 p (in Serbian)

Gavrilović Lj (1981) Poplave u Srbiji u XX veku – uzroci i posledice (Floods in Serbia in the 20th century – causes and consequences). Srpsko geografsko društvo, Beograd 52. 137 p (in Serbian)

Gavrilović L, Milanović-Pešić A, Urošev M (2012) A hydrological analysis of the greatest floods in Serbia in the 1960–2010 period. Carpathian J Environ Sci 7(4):107–116

Grenfell SE, Ellery WN (2009) Hydrology, sediment transport dynamics and geomorphology of a variable flow river: the Mfolozi River, South Africa. Water SA 35(3):271–282

Ivanović R, Martić-Bursać N, Ivanović M, Nikolić M (2011) Thermal characteristics of air of the Nis for the purpose of quicker economic development. Bull Serbian Geogr Soc 91(2):83–98

Jansson MB (2002) Determining sediment source areas in a tropical river basin, Costa Rica. Catena 47:63–84

Klein M (1984) Anti-clockwise hysteresis in suspended sediment concentration during individual storms. Catena 11:251–257

Manojlović P, Živković N (1997) The map of Runoff in Serbia. Collection of the papers Faculty of Geography University of Belgrade 48:15–25 (in Serbian)

Milanović A (2006) Hydrological forecast of maximal water level in Lepenica river basin and flood control measures. Bull Serbian Geogr Soc 86(1):47–54

Milanović A, Urošev M, Milijašević D (2010) Floods in Serbia in the 1999–2009 period – Hydrological analysis and flood protection measures. Bull Serbian Geogr Soc 90(1):93–121

Milovanović B (2010) Climate of the mountain Stara planina. Geographical Institute 'Jovan Cvijić', Serbian Academy of Science and Arts 75:1–135

Mueller EN, Pfister A (2011) Increasing occurrence of high-intensity rainstorm events relevant for the generation of soil erosion in a temperate lowland region in Central Europe. J Hydrol 411:266–278

Mustafić S (2006) Spatial distribution of Runoff in Temstica River Basin. Bull Serbian Geogr Soc 86(2):45–52 (in Serbian)

Petrović J (1998) Natural features of Bela Palanka and Central Ponisavlje region. Institute of Geography, Faculty of Natural Sciences, University of Novi Sad, Novi Sad, 112 p (in Serbian)

Petrović J (1999) Natural features of the Pirot valley and upper parts of Ponisavlje Region. Institute of Geography, Faculty of Natural Sciences, University of Novi Sad, Novi Sad, 144 p (in Serbian)

Prohaska S, Ilić A, Miloradović B, Petković T (2010) Identification and classification of Serbia's historic floods. Bull Serbian Geogr Soc 89(4):191–199

Ristić R, Kostadinov S, Abolmasov B, Dragićević S, Trivan G, Radić B, Trifunović M, Radosavljević Z (2012) Torrential floods and town and country planning in Serbia. Nat Hazard Earth Syst Sci 12:23–35

Scholz G, Quinton JN, Strauss P (2008) Soil erosion from sugar beet in Central Europe in response to climate change induced seasonal precipitation variations. Catena 72:91–105

Seeger M, Errea MP, Begueria S, Arnaez J, Marti C, Garcia-Ruiz JM (2004) Catchment soil moisture and rainfall characteristics as determinant factors for discharge/suspended sediment hysteretic loops in a small headwater catchment in the Spanish Pyrenees. J Hydrol 288:299–311

Soler M, Latron J, Gallart F (2008) Relationships between suspended sediment concentrations and discharge in two small research basins in a mountainous Mediterranean area (Vellcebre, Eastern Pyrenees). Geomorphology 98:143–152

Stefanović M, Gavrilović S, Milovanović I, Milojević M, Jurišić S (2010) Vlasina river and Nišava river floods. J Torrent Eros Control 35:55–62

Williams GP (1989) Sediment concentration versus water discharge during single hydrologic events in rivers. J Hydrol 111:89–106

Živković N (2005) Precipitation in Eastern Serbia in the period 1961–1990. In: Gavrilović Lj (ed) Physico-geographical problems of Carpatoho-Balkanic Mountains in Serbia. Faculty of Geography, University of Belgrade, Belgrade 2:45–58 (in Serbian with summary in English)

Živković N (2009) Average annual and seasonal river discharge in Serbia. Faculty of Geography, University of Belgrade, Belgrade, 174 p (in Serbian)

Živković N, Andjelković G (2004) Altitude precipitation gradient in Serbia. Bull Serbian Geogr Soc 84(2):31–36 (in Serbian)

Živković N, Smiljanić S (2005) The isotherm map of eastern Serbia. Bull Serbian Geogr Soc 85 (1):31–38 (in Serbian)

Zolina O, Simmer C, Bachner S, Gulev S, Maechel H (2008) Seasonally dependent changes of precipitation extremes over Germany since 1950 from a very dense observational network. J Geophys Res 113:1–17

Chapter 12
Flood Hazard in Bulgaria: Case Study of Etropolska Stara Planina

Mariyana Nikolova, Stoyan Nedkov, and Valentin Nikolov

Abstract Climate change in Europe is often manifested in the increasing frequency of extreme weather phenomena like storms, intensive rains, and floods. For the period 2000–2009, the highest number of severe floods in Southeastern Europe was registered in Romania (30), Greece (14), and Bulgaria (11). The EM-DAT database (CRED 2012) includes 13 major floods in Bulgaria for 1900–2011. Eleven of them occurred between 2000 and 2009, 1.2 cases per year, a significant increase compared to the average number of 0.1 cases for the past 111 years, mainly due to the extremely wet year 2005. A typical mountain area strongly affected by extreme weather is the upper Malki Iskar River basin on the northern slopes of the Etropolska Stara Planina. The chapter analyses the influence of intense rainfalls (on the examples of events between 1995–2005 and in 2007) on peak river flows and flood hazard, the role of topography in the spatial distribution of rainfall in the basin, and the passage rate of flood waves; identifies critical areas and settlements; and recommends risk mitigation measures. The kinematic runoff and erosion model (KINEROS) was used to simulate the influence of rainfall of different intensity and quantity on peak flow during storm events. The findings allow us to assess flood hazard in the river basin for possible future climate and land use/cover changes and propose management measures directed at reducing flood risk.

Keywords Climate change • Extreme rainfall • Flood • Hydrologic modeling • Bulgaria

M. Nikolova (✉) • S. Nedkov
National Institute of Geophysics, Geodesy and Geology, Bulgarian Academy of Sciences, "Acad. Georgi Bonchev" Str., Bl.3, 1113 Sofia, Bulgaria
e-mail: mn@bas.bg; snedkov@abv.bg

V. Nikolov
Institute of Geology, Bulgarian Academy of Sciences, "Acad. Georgi Bonchev" Str., Bl.24, 1113 Sofia, Bulgaria
e-mail: valnvaln97@gmail.com

D. Lóczy (ed.), *Geomorphological impacts of extreme weather: Case studies from central and eastern Europe*, Springer Geography, DOI 10.1007/978-94-007-6301-2_12,

12.1 Introduction

The regional and local dimensions of climate change vary with regions. This is especially valid for precipitation regime and distribution. Even for a country of relatively small like Bulgaria, there are opposite trends in different regions (CRED 2012). Torrential rains, however, show an undoubtedly increasing trend for most of the territory (Velev 2005; Bocheva et al. 2009). In mountainous areas, the amount of precipitation is normally higher and the topography also favors rapid formation of *flash floods* (Nikolova and Nikolov 2011). Torrential rains are concentrated on certain sections of river basins and only exceptionally affect simultaneously all the tributaries of a river system as it happened in the upper Malki Iskar basin (Nikolova 2007). Therefore, it is necessary to investigate in detail the influence of the physical environment of small mountain subbasins on the formation of peak flow and the impact of an increased occurrences and intensity of torrential rains (Precipitations in Bulgaria 1990).

No universal hydrological model exists that would yield equally reliable results for all river basins. For the present study, the *KINEROS model* (kinematic runoff and erosion model) was chosen (Semmens et al. 2005), because it gives the opportunity to simulate runoff from relatively small basins for a particular storm event as well as to assess the influence of various landscape parameters on this process under the conditions of future climate change.

12.2 Study Area

The basin of the Malki Iskar River above the town of Etropole (Fig. 12.1) was selected as representative for the Etropolska Stara Planina mountains. Numerous steep ridges stretch out from the central Stara Planina ridge, which contribute to the increased share of surface runoff in recharging the rivers. The development of the stream network, collecting most surface runoff from the slopes of the mountains, leads to intensive incision, lateral and gully erosion (Fig. 12.2). *Dissection* is reduced in the valley embayments near the town of Etropole and Boykovets village, where sedimentation prevails (Fig. 12.3). In combination with the gorge sections of the valleys, the prerequisites exist at these local base levels for intensive sediment accumulation, especially during flood time. The total Malki Iskar basin above Etropole (Fig. 12.1) occupies an area of 196 km^2 with an average altitude of 1,164 m. The area of the Malki Iskar watershed above the Etropole gage station (No. 108) is 54.3 km^2 and that the Ravna Stream above the Boykovets gage station (No. 107) is 21.2 km^2 (Hydrologic Reference Book 1981).

The rugged mountain *relief* and *slope exposure* relative to the prevailing north–northwestern winds ensure intensive precipitation during the inrush of moist air masses in the warm half year and sudden snowmelt and thawing due to the strong foehn effect along the northern mountain slopes through air masses

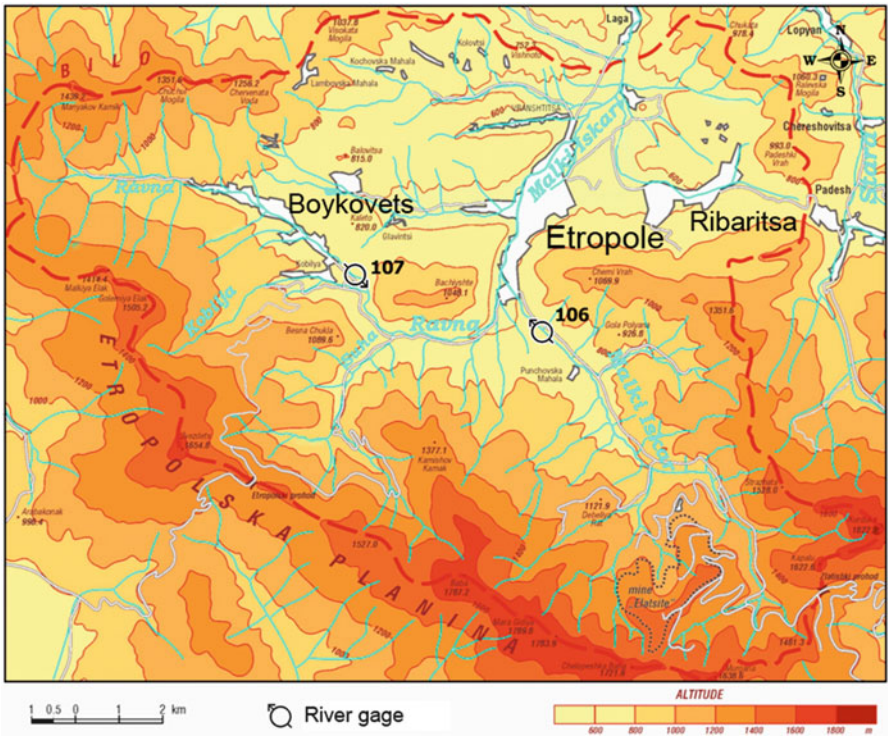

Fig. 12.1 The Malki Iskar basin above Etropole

Fig. 12.2 Erosion in the basin of the Ravna Stream

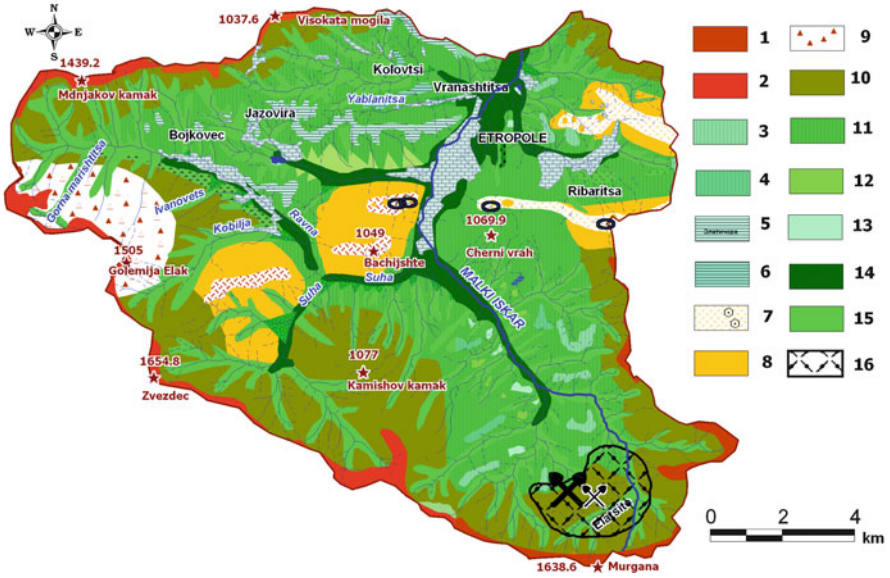

Fig. 12.3 Geomorphological map of the Malki Iskar basin above the town of Etropole. *1*, remodeled peneplain; *2*, initial peneplain; *3*, high pediment; *4*, middle and lower pediment; *5*, interfluvial ridges; *6*, river terrace; *7*, karst plateau with karren and potholes; *8*, karst slopes; *9*, colluvial features; *10*, hillslopes shaped from the Paleogene to the Holocene; *11*, hillslopes shaped in the Pleistocene–Holocene; *12*, diluvial–proluvial deposits; *13*, alluvial–proluvial fans; *14*, floodplain; *15*, stream valley; *16*, anthropogenically modified (mining) surfaces

arriving from the south to southeast during the cold season. In both cases, favorable conditions are created for increased surface runoff, which is capable of swelling rivers to floods within a very short time.

The synoptic conditions for abundant precipitation and flood wave formation are most often observed during orographic *occlusion* along a cold front and the passing of Mediterranean cyclones over the south of the country (Nikolova 2007). At the Etropole meteorological station, maximum temperature is recorded in July and maximum precipitations in May (Fig. 12.4). In May and June falls 14–15% of the annual precipitation (879 mm).

Peak runoff on the Malki Iskar River is registered in April and May and on its tributary, the Ravna River, in August (Figs. 12.5 and 12.6). A record daily amount of precipitation (105 mm) for the Etropole station and extreme runoff on the Suha (Ravna) Stream (94.8 m^3 s^{-1}) were observed on 5 August 2005. The number of heavy rainfalls and their intensity in the region shows a rising trend over the last decades (Fig. 12.7).

Due to the mountainous character of the region, intensive *rainfalls* are often *concentrated* in certain parts of the watershed. Therefore, flood waves do not occur at the same time. The Malki Iskar River threatens Etropole because it receives the water of the Suha Stream immediately upstream of the town and within the town

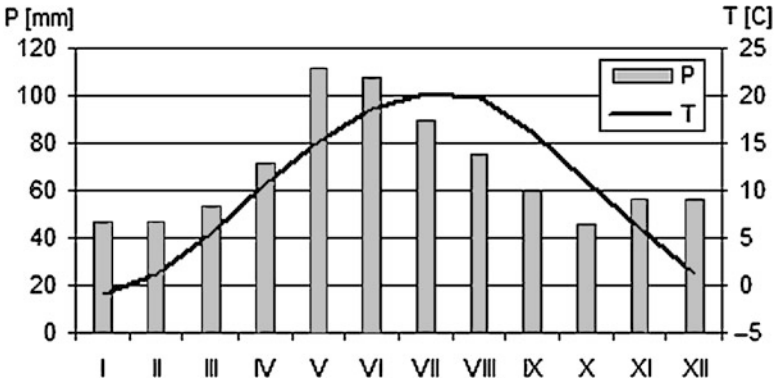

Fig. 12.4 Monthly mean temperatures (*T*) and precipitations (*P*) for the Etropole meteorological station, 1961–2005 (After Genev 2007)

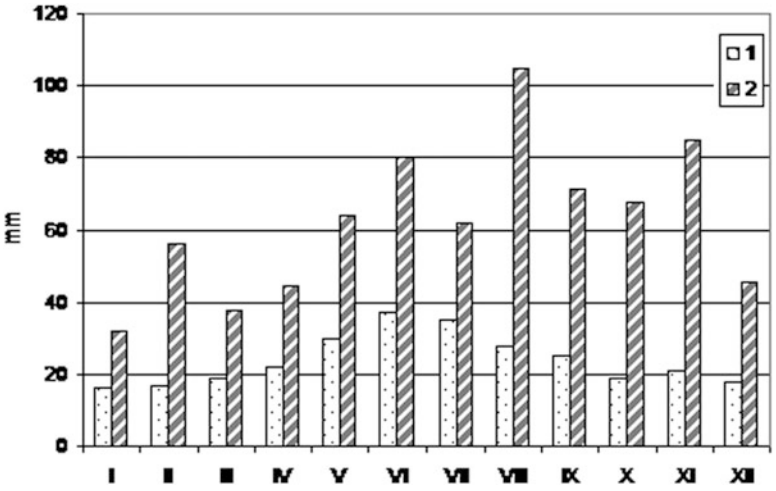

Fig. 12.5 Maximum monthly precipitations (*1*) and maximum daily precipitations (*2*) at Etropole, 1931–2005

boundaries it is joined by the Yablanitsa Stream. Even without flood wave formation, this fact enhances flood hazard there. The rainfall thresholds which cause high river stages and flash floods in the subbasins had to be established.

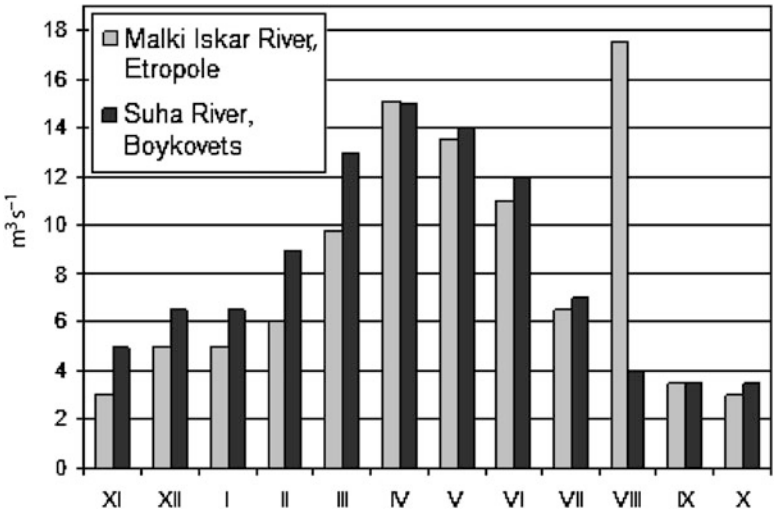

Fig. 12.6 Monthly runoff distribution (%) on the Mali Iskar and Suha Rivers, 1950/1951–1982/1983 (After Hristova 2004)

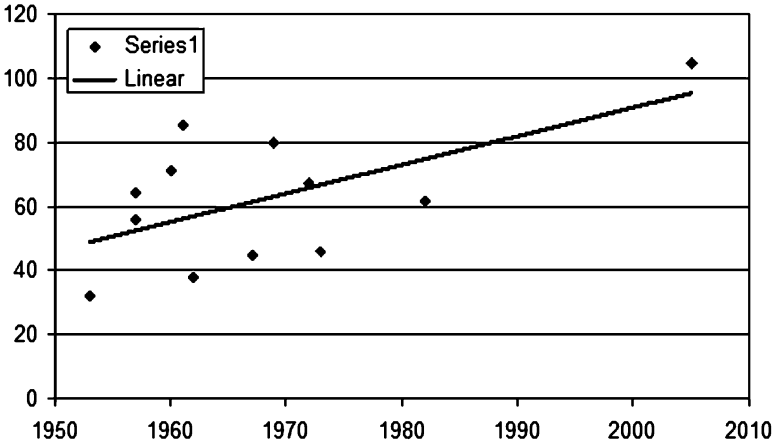

Fig. 12.7 Trend of maximum daily precipitations (mm) at Etropole, 1951–2005

12.3 Methods

A complex geographical (mathematical modeling, remote sensing, cartographic and statistic) analysis was performed to estimate the relationships between *environmental factors* which lead to peak flow formation. *KINEROS* is a distributed, physically based, event *model* describing the processes of interception, dynamic infiltration, surface runoff, and erosion predominantly by overland flow. The watershed is conceptualized as a cascade and channels, over which flow is routed

Table 12.1 The storm events used for model calibration

Data	Data from NIMH		
Event	23 May 1995	9 February 2001	26 May 2005
Rainfall (mm)	38	25	59
Peak flow ($m^3\ s^{-1}$)	4.7	2.7	7.6

in a top-down approach using a finite difference solution of the one-dimensional kinematic wave equations (Semmens et al. 2005). The *five main components* of the model are overland flow, channel routing, infiltration, erosion and sediment load, and rainfall and interception.

Excess rainwater, which leads to runoff, is defined as the difference between precipitation amount and interception + infiltration depth. The rate of infiltration depends on rainfall intensity and cumulative infiltrated water (soil moisture content). Rainfall data are entered as time-accumulated depth or time-intensity breakpoint pairs. Interception is controlled by interception depth and the percentage of vegetation cover.

A geographic information system user interface, the *Automated Geospatial Assessment Tool* (AGWA) compatible with ArcGIS 9x, facilitates KINEROS modeling (Miller et al. 2002). AGWA *inputs* included a digital elevation model (DEM) extracted from 1:50,000 topographic maps, CORINE land cover, soil map of the area from Bulgarian Research Institute of Soil Science database in FAO/UNESCO soil classification (Nedkov 2007; Nikolova 2009), rainfall amounts for at least one rain gage within the basin, and detailed meteorological information for calibration.

Modeling in AGWA GIS begins with the delineation of the basin using flow direction and flow accumulation DEM derivatives. Then the basin is subdivided into surfaces with overland flow and elements of channel flow, intersected with soil and land cover data. The stage of 'writing precipitation files' is as follows: the parameters of the modeled storm event are set. There are three options: selection from editable database file of predefined rainfall events, constructing our own rainfall file using the AGWA module, or using return period depth grids. We could only choose the second option as the AGWA dataset only includes US events. A saturation coefficient representing pre-event soil moisture is set at this stage. The next stage is the model execution, where AGWA automatically imports model results for all surfaces and channels to generate output parameters for the simulated event, and the final task is to visualize results. Modeling was implemented for the Ravna, Kobilya, Suha, and Yablanitsa watersheds (Fig. 12.1).

The calibration was carried out for the Ravna watershed (Fig. 12.1) using runoff and precipitation data measured in the National Institute for Meteorology and Hydrology (NIMH) stations for the years 1995–2005 and by our team in the summer of 2007. A satisfactory correlation between simulated and measured values was achieved (Nedkov 2007 – Table 12.1). Initial soil moisture, saturated hydraulic conductivity, and channel and surface roughness remained the same for all simulations, only the precipitation amount and intensity changed with events.

12.4 Results and Discussion

After the overview of relevant literature, precipitation intensity generating flash floods was assumed to be 30 mm day^{-1}. Five *classes of daily rainfall* had been suggested by Bocheva et al. (2009): light (A), <4.9 mm; light to moderate (B), 5.0–14.9 mm; moderate to heavy (C1), 15.0–29.9 mm; heavy (C2) 30.0–59.9 mm; and torrential (D), >60.0 mm. Alternatively, daily precipitation higher than 5 and 10% of the annual total is also proposed (Fukui 1970). An increase of the number of days with precipitations above 10% of the annual total is observed in Bulgaria for the period 1901–2004 with summer and autumn maxima (Velev 2005). Our understanding is that the critical *threshold* of daily precipitation causing river swelling and floods *differs with geographical units and watersheds*. Data show that the number of days with precipitation above 20 mm at Etropole is growing (Fig. 12.8), recorded in every month from April to August with a maximum in May (15 out of 22 cases). In the same period, precipitation events up to 10 mm daily amount swelled rivers on 18 occasions, half of them in May. Two extremes (of the total 3 cases) over 50 mm were observed in August and one in May, including the *extreme precipitation* of 107 mm at the Etropole gage on 5 August 2005. The data show that, in addition to precipitation, flood hazard heavily depends on landscape factors (Table 12.2).

A number of *landscape parameters* were included in hydrologic modeling: slope inclination, Manning's roughness coefficient, interception, physical soil type, and hydraulic conductivity (Table 12.3). River flow begins to increase gradually when a

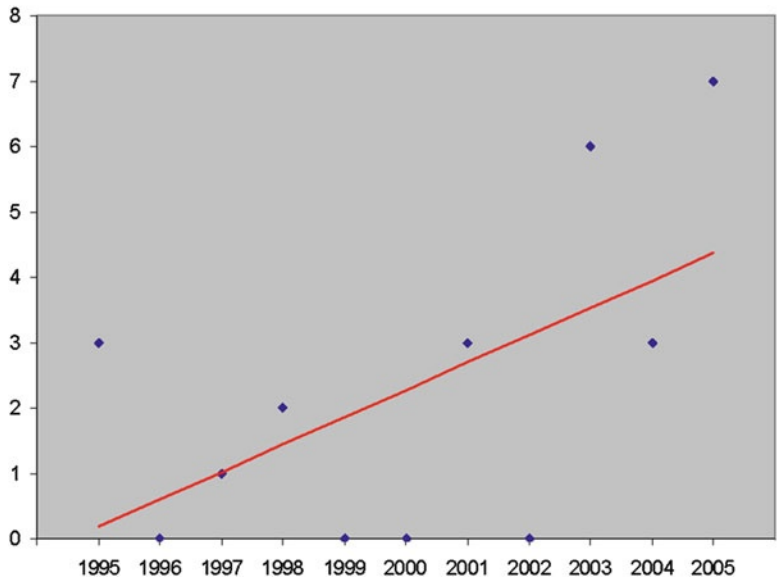

Fig. 12.8 Number of days with precipitation above 20 mm at Etropole, 1995–2005

Table 12.2 Monthly distribution of torrential rains which swelled rivers, 1995–2005

Month							
P (mm)	February	April	May	June	July	August	Annual
>10	3	2	9	0	0	4	18
>20	0	1	15	3	2	1	22
>50	0	0	1	0	0	2	3
Total	3	3	25	3	2	7	43

Table 12.3 Average values of the main parameters calculated for the subbasins

	Slope (°)	Interception (mm)	Roughness coefficient	Saturation coefficient	Sand fraction (%)	Silt fraction (%)	Clay fraction (%)
Ravna	26.5	1.11	0.027	16.6	34	39	27
Kobilya	31.4	1.19	0.016	22.4	42	32	25
Yablanitsa	19.2	0.84	0.047	12.8	39	36	25
Suha	36.3	1.22	0.016	26.7	49	27	22

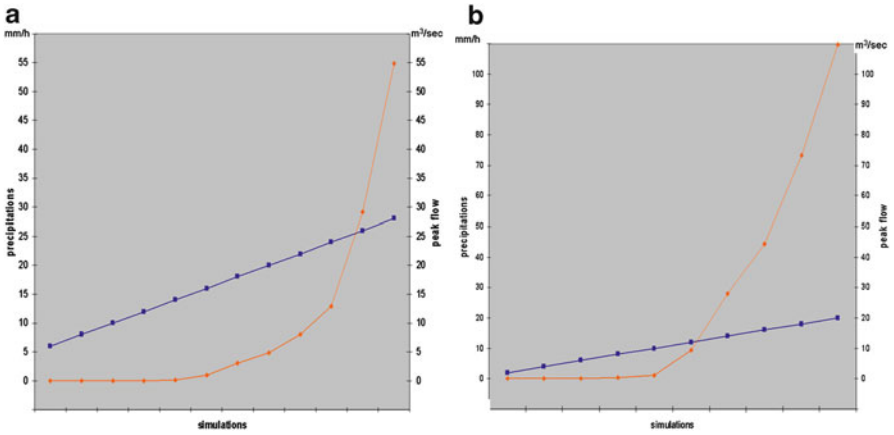

Fig. 12.9 Change of the peak flow on the watershed as a result of the increase of the rainfall intensity using the model adjustment for the calibrated events on 9 May 2001 (**a**) and 4 June 2007 (**b**)

particular intensity of the rainfall is reached (Fig. 12.9). The intensity threshold is strongly dependent on preceding soil moisture content: 12 mm h^{-1} for the event on 4 June 2007 (Fig. 12.9b), 16 mm h^{-1} for 9 May 2001 (Fig. 12.9a), and 28 mm h^{-1} for 11 July 2007. *Peak flow response* to rising rainfall intensity takes place in three stages: (1) phase of no increase, when the landscape 'absorbs' almost the whole amount of received water; (2) phase of gradual increase, when part of the water induces surface runoff; and (3) phase of rapid growth, when almost all the water feeds surface runoff. The boundary between the second and third phase is the crucial point, estimated between 18 and 38 mm h^{-1}.

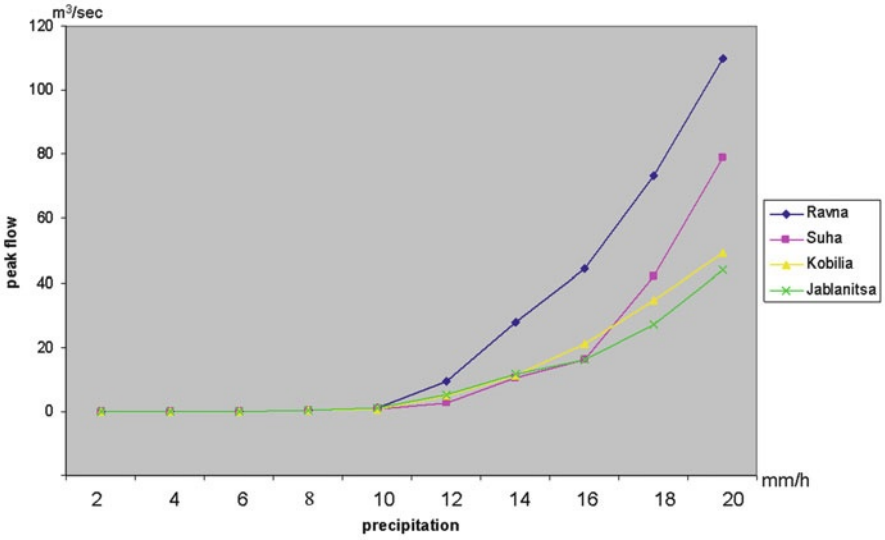

Fig. 12.10 Precipitation and peak flow in the subbasins for the calibrated event on 4 June 2007

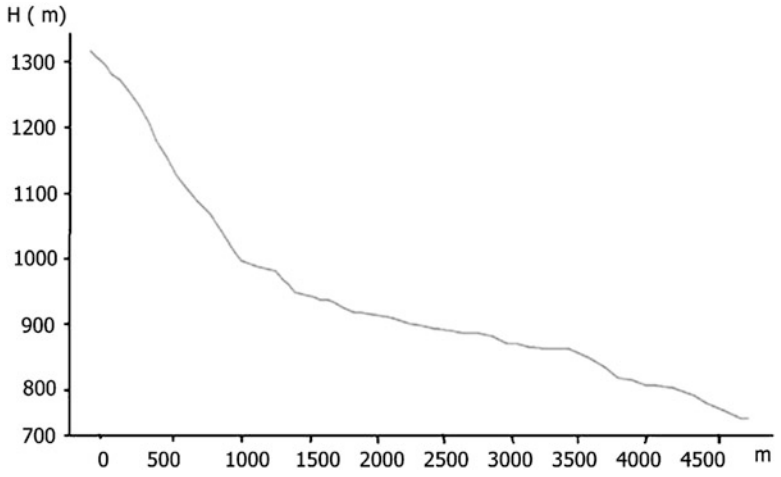

Fig. 12.11 Longitudinal profile of the Ravna Stream upstream of Boykovets

The *hydrographs* simulated for the event of 4 June 2007 *differ with* the modeled *subbasins* (Fig. 12.10). Peak flow increases most rapidly on the Ravna River, for the Suha rise is slow in the second stage, but speeds up in the third, while the opposite behavior is observed for the Kobilya and Yablanitsa. The critical point also varies to some extent with subbasins: in the Ravna basin, 14 mm h^{-1}; for the Suha, 16 mm h^{-1}; and for the Kobilya and Yablanitsa, 18 mm h^{-1}.

River *longitudinal profiles* and *cross sections* of tributaries (Figs. 12.11, 12.12, 12.13 and 12.14) are considered to be synthetic geomorphological parameters

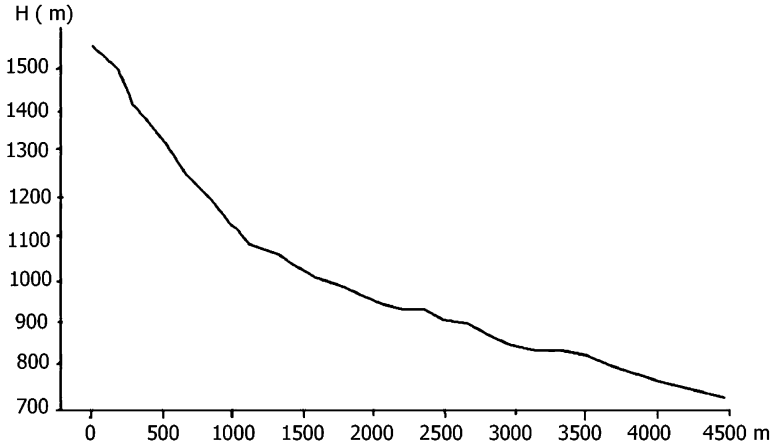

Fig. 12.12 Longitudinal profile of Kobilya Stream

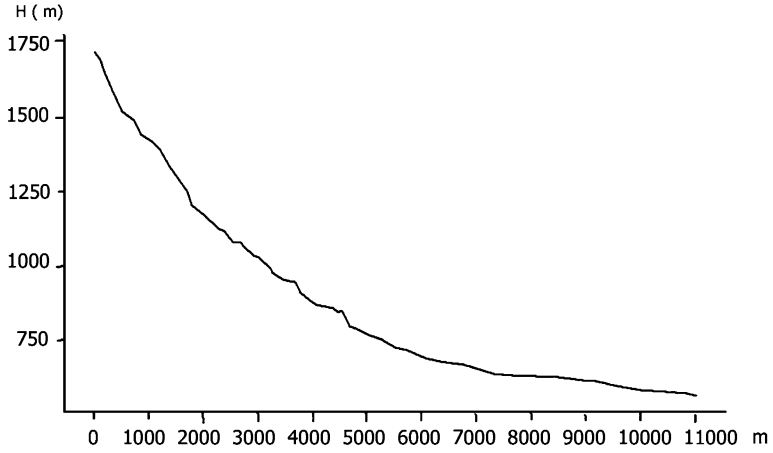

Fig. 12.13 Longitudinal profile of the Suha Stream

representative of the three basic measures of the catchment: mean elevation per unit area, elevation of the local base level, and watershed area (Nikolov 2009).

The local distribution and intensity of precipitation also depend on the specific *orographic effect*: the aspect of slopes towards the air movement. Abundant precipitation and flood wave formation are most often observed in the case of orographic occlusion along a cold front and passing of Mediterranean cyclone over southern Bulgaria in summer (Nikolova 2007).

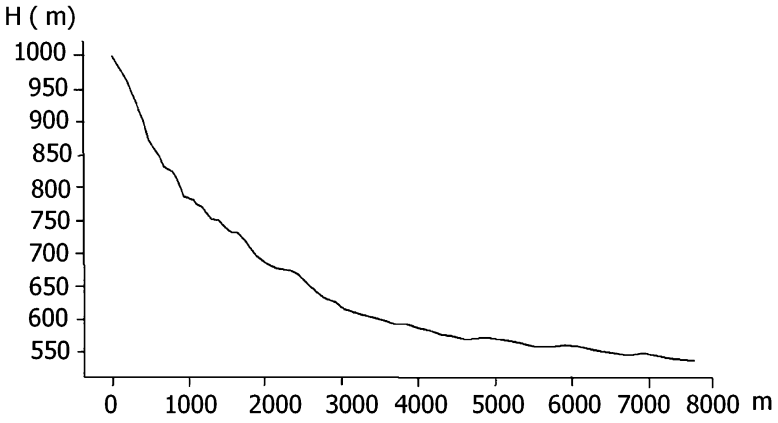

Fig. 12.14 Longitudinal profile of Yablanitsa Stream

12.5 Conclusions and Recommendations

There has been a significant increase in the number and amount of torrential rains on the northern slopes of Etropolska Stara Planina during the last decade, which corresponds to a similar trend observed for the rest of the country. The simulations using the KINEROS model show even more significant growth in the peak flows of the rivers on the watershed of the Malki Iskar as a result of the increased rainfalls. Due to the mountainous character of the region, extreme *precipitation* has a *localized* ('spot') character, being most often concentrated in restricted segments of the watershed. A simultaneous effect on the runoff of all the tributaries is seldom observed. The simulations show significant variations by subbasins even if rainfall intensity and soil moisture contents are uniform all over the region.

The implementation of the KINEROS model provides an opportunity for the simulation of the changes in river runoff depending on the amount of precipitation and human modification of land cover (deforestation). The findings may be useful for the management of flood risk and accompanying hazards (soil erosion) in relatively small catchments, which are representative for other mountains in the country.

Etropole town is particularly endangered by floods as the confluences of the Suha and Yablanitsa Streams into the Malki Iskar River are located in the urban area. Urban planning and land use on the territory of the municipality have to cope with maximum flash flood hazard, and no construction should be permitted in the danger zones.

Establishing a *complex monitoring* system for precipitation, runoff, and erosion in the torrential sections of the river basins will provide the necessary information for modeling and the preparation of hazard maps with the purpose of more effective management and damage mitigation. Through the preservation of existing forests and the *afforestation* of barren slopes, a beneficial measure from a landscape ecological aspect too and the rate of surface runoff and, consequently, of erosion processes can be reduced on the watersheds of the Malki Iskar and Suha, and the collateral damages (sedimentation of channels, destruction of bridges) can also be avoided.

We have to emphasize that flood hazard can be reduced, but cannot be entirely eliminated. Therefore, the environmental awareness of the local population has to be increased; economic activities adjusted to the objective natural conditions, including the corollaries of climatic change; and adaptation has to be supported by various insurance solutions.

Acknowledgements This investigation was carried out in the framework of the research project 'Implementation of the KINEROS model for estimation of the flood-prone territories in the Malki Iskar River Basin,' funded by the Ministry of Crisis Management.

References

Bocheva L, Marinova T, Simeonov P, Gospodinov I (2009) Variability and trends of extreme precipitation events over Bulgaria (1961–2005). Atmos Res 93:490–497

CRED (2012) EM-DAT. The international disaster database. Centre for Research on the Epidemiology of Disasters, Université catholique de Louvain, Louvain http://www.emdat.be

Fukui E (1970) Distribution of extraordinarily heavy rainfalls in Japan. Geogr Rev Jpn 43:10

Genev M (2007) Hydrologic characteristic of the Malki Iskar River basin above town of Etropole. In: Nikolova M et al. (ed) Implementation of the KINEROS model for estimation of the flood-prone territories in the Malki Iskar River basin. Info Secur 24:89–103

Hristova N (2004) Typification drainage regime in Bulgaria. Sofia University "st. Kliment Ohridski" Yearbook 296:129–152 (in Bulgarian)

Hydrologic Reference Book (1981) National Institute for Meteorology and Hydrology (NIMH), Sofia

Miller SN, Semmens DJ, Miller RC, Hernandez M, Goodrich DC, Miller WP, Kepner WG, Ebert DW (2002) GIS-based hydrologic modeling: the Automated Geospatial Watershed Assessment Tool. In: Proceedings of the second federal interagency hydrologic modeling conference, Las Vegas, 28 July–1 Aug 2002

Nedkov S (2007) Modeling of river discharge in small watersheds in cases of flood events. In: Proceedings of the second national research conference on emergency management and protection of the population, Sofia, 9 Nov 2007, pp 299–308 (in Bulgarian)

Nikolov V (2009) Geomorphologic methods for estimating the flood hazard in mountain catchments. Info Secur 24:89–103

Nikolova M (2007) Climatic conditions for high waves and floods in the basin of Malki Iskar River above the town of Etropole. In: Proceedings of the second national research conference on emergency management and protection of the population, Sofia, 9 Nov 2007. Bulgarian Academy of Sciences, Sofia, pp 309–319 (in Bulgarian)

Nikolova M (2009) Implementation of the KINEROS model for estimation of the flood-prone territories in the Malki Iskar River basin. Info Secur 24:89–103

Nikolova M, Nikolov V (2011) Assessment of the impact of geomorphologic and hydroclimatic factors on the flood hazard in river basins. Studia Geomorphol Carpath Balcanic 45:121–135

Precipitations in Bulgaria (1990) Reference book. Bulgarian Academy of Sciences, Sofia

Semmens D, Goodrich D, Uncrich C, Smith R, Woolliser D, Miller S (2005) KINEROS2 and the AGWA modeling framework. In: International G-WADI modeling workshop, Roorkee, 2005. http://gwadi.org/shortcourses/chapters/Semmens_L6.pdf

Velev S (2005) Torrential rains in Bulgaria during the 20th century. Probl Geogr 2005 (1–2):169–172 (in Bulgarian)

Part III
Landslides

Chapter 13
The May 2010 Landslide Event in the Eastern Czech Republic

Tomáš Pánek, Veronika Smolková, Karel Šilhán, and Jan Hradecký

Abstract In May 2010 intensive rainfalls and consequent floods affected Central Europe, including the eastern part of the Czech Republic. In the period 15–25 May 2010, more than 150 landslides originated in the Outer Western Carpathians and their foredeep. In the case of the Girová rockslide, the May 2010 rainfall event only supplied the final triggering push. The main preconditions of slope failure were long-term, internal changes within the rock mass. As evidenced by dendrogeomorphological dating, rock strength weakening was connected to long-term (decennial-scale) creep leading to the final catastrophic movement. Many trees from the upper section of the landslide do not reveal any year of reaction wood. It could be explained by a translational, blocklike character of movement.

Keywords Rockslide • Translational landslide • Dendrogeomorphology • Radiocarbon dating • Reaction wood analysis • Czech Republic

13.1 Introduction

Due to specific lithological and structural conditions, landslides repeatedly activate in the Outer Western Carpathians (OWC), usually triggered by meteorological events: intensive and/or long-lasting rainfalls in combination with snowmelt. From last decades, the most significant (and well-documented) events in the eastern part of the Czech Republic were the 1997 and 2006 landslide activations (Rybář and Stemberk 2000; Krejčí et al. 2002; Bíl and Müller 2008; Klimeš et al. 2009). In July 1997, 257 mm of precipitation fell within 5 days in the study area (Kirchner 2001).

T. Pánek • V. Smolková • K. Šilhán • J. Hradecký (✉)
Department of Physical Geography and Geoecology, Faculty of Science, University of Ostrava, Chittussiho 10, 71000 Ostrava, Czech Republic
e-mail: tomas.panek@osu.cz; veronika.smolkova@osu.cz; karel.silhan@osu.cz; Jan.Hradecky@osu.cz

D. Lóczy (ed.), *Geomorphological impacts of extreme weather: Case studies from central and eastern Europe*, Springer Geography, DOI 10.1007/978-94-007-6301-2_13,

More than 1,500 landslides of different types originated causing extensive damage (€31 million) to buildings and infrastructure (Krejčí et al. 2002). At the turn of March and April 2006, rapid snowmelt and intense precipitation triggered and reactivated more than 80 (mostly shallow) landslides in the study area (Bíl and Müller 2008). During both events, a notable share of the active landslides were associated with previous slope failures.

In May 2010, intensive rainfalls and consequent floods affected Central Europe, including eastern part of the Czech Republic. During the period 15–25 May 2010, more than 150 landslides originated in the Outer Western Carpathians and their foredeep (Fig. 13.1a), which brought significant economic losses (damage to houses, infrastructure, and forests) (see also Chap. 2, Gorczyca et al. in this volume). The financial costs of mitigation works exceeded €5 million.

In this chapter, we describe the May 2010 landslide through (1) the distribution of landslides in relation to rainfall patterns, (2) the delineation of the spatial relationships between activated landslides, geological settings, and antecedent landslides, and (3) the demonstration of the most pronounced slope failure reactivated during the May 2010 event.

13.2 Regional and Hydrometeorological Settings

Most of the landslides are concentrated in the OWC and their foredeep (Fig. 13.1). The area is built of Cretaceous–Oligocene flysch bedrock thrust onto the Subsilesian, Silesian, and Magura Nappes of NW vergency during the Miocene (Menčík et al. 1983). Predominantly thick-bedded flysch complexes prevail in the southern Silesian Nappe and within the Magura Nappe and form the highest parts of the Beskydy region (1,323 m). Weaker thin-bedded flysch complexes of the northern part of the Silesian and Subsilesian Nappes form a rather subdued hilly landscape covered by Neogene and Quaternary deposits in the western and northern sections of the region (Fig. 13.1a). Mean annual precipitation totals (for 1961–2000) in the study area range from ca. 650 mm in lower-lying areas to more than 1,200 mm at the highest elevations (Tolasz et al. 2007).

Extremely high precipitations were recorded in the northeastern part of the Czech OWC on 16–18 May 2010 (Fig. 13.2). Shallow subsurface saturation can be documented by the antecedent precipitation index (API_{30}), the precipitation totals for the previous 30 days:

$$\mathrm{API}_{30}(\mathrm{d}) = \sum \mathrm{S_n} \cdot 0.93^{\mathrm{n}},$$

where S_n (mm) stands for daily precipitation totals of n days ($n = 1, 2, \ldots, 30$) before the day d and 0.93 is the evaporation constant (Hladný 1962). For the study region and for 16 May, higher than 100 mm was calculated (Fig. 13.2a): in the mountain areas 20–30 mm fell on 15 May, and, in the following 2 days, even much

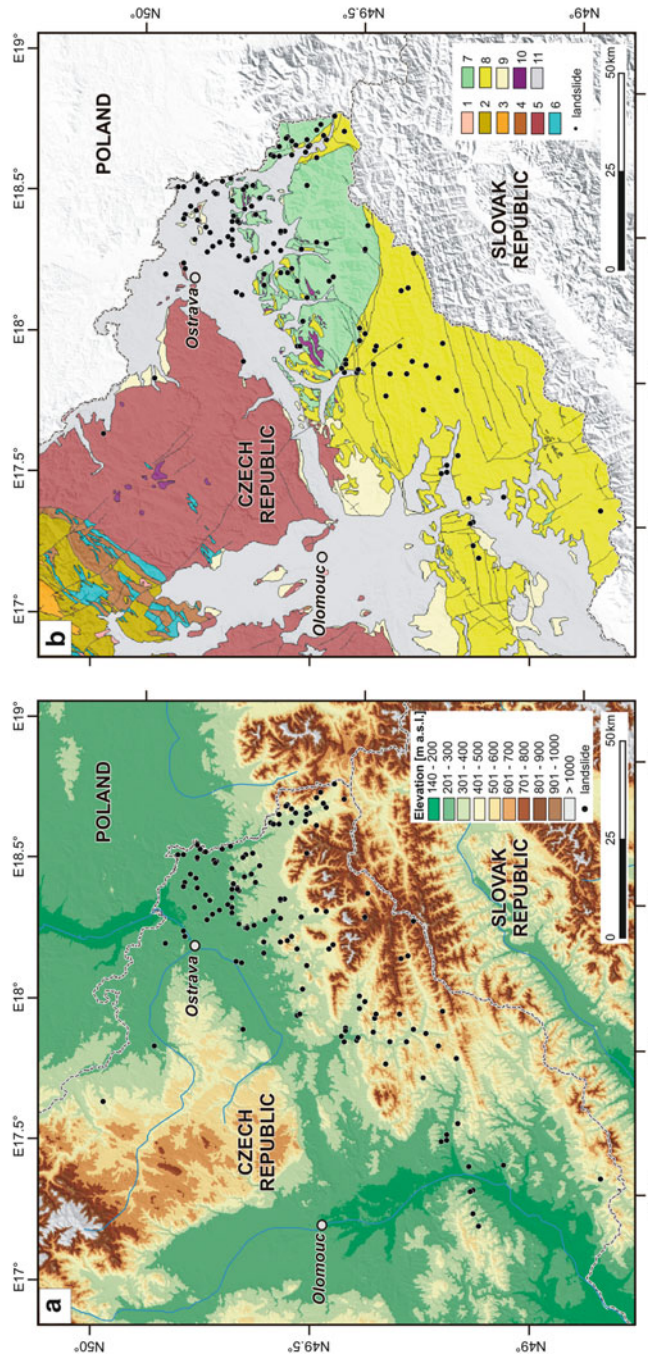

Fig. 13.1 Location of the study area and spatial distribution of the May 2010 landslides in the eastern part of the Czech Republic. (**a**) Distribution of the landslides in the context of topography and hypsometrical conditions (Source of elevation data: SRTM3v2). (**b**) Geological setting: *1–6*, Proterozoic–Mesozoic rocks of the Bohemian Massif; *7*, Mesozoic flysch deformed by the Alpine orogeny; *8*, Tertiary flysch deformed by the Alpine orogeny; *9*, Tertiary unconsolidated deposits; *10*, Tertiary volcanic rocks; *11*, Quaternary unconsolidated deposits. (Reprinted with kind permission from Springer Science+Business Media: Landslides, Rainfall-induced landslide event of May 2010 in the eastern part of the Czech Republic, 8, 2011, 507–516, Pánek T et al.)

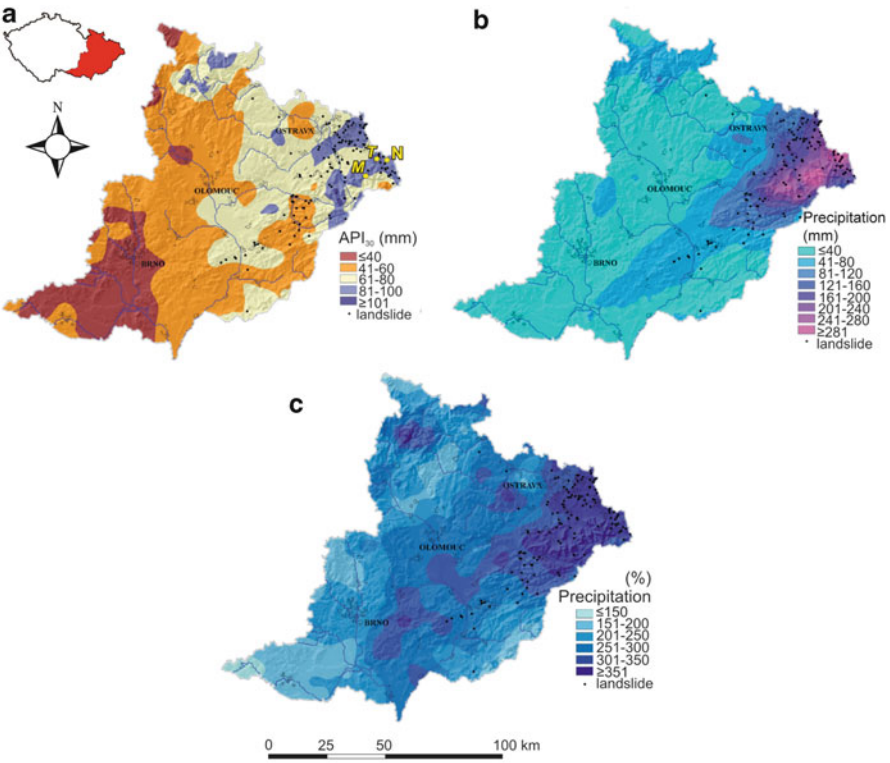

Fig. 13.2 Spatial distribution of precipitation in the eastern Czech Republic in May 2010 (meteorological stations: *M* Morávka dam, *T* Třinec, *N* Nýdek). (**a**) Antecedent Precipitation Index API_{30} (mm) for 16 May. (**b**) Precipitation totals (mm) on 16–18 May. (**c**) Precipitations of May 2010 as percentage of the 1961–2000 mean May precipitation (Reprinted with kind permission from Springer Science+Business Media: Landslides, Rainfall-induced landslide event of May 2010 in the eastern part of the Czech Republic, 8, 2011, 507–516, Pánek T et al.)

higher values were recorded in the Beskydy Mountains and in the adjacent areas. On 16 May, daily totals above 100 mm were recorded at 33 stations of the Czech Hydrometeorological Institute (maximum in Třinec, at 340 m elevation, 179.8 mm). On the following day, 17 May, only 5 stations recorded more than 100 mm (Morávka dam, 500 m, 115.0 mm), but at 37 other stations more than 50 mm was measured. On 18 May, only 4 stations recorded more than 60 mm (Nýdek, 400 m, 71.0 mm), and 17 stations measured $\geq$30.0 mm. Three-day precipitation totals (16–18 May) made up more than 300 mm at six stations (at Třinec, 327.6 mm) and more than 250 mm at five stations in the study area (Fig. 13.2b). Thus, precipitation totals for May were in many locations more than three times higher than the corresponding monthly means for 1961–2000 (Fig. 13.2c). Extreme daily precipitations induced not only extensive landslides but also floods: peak river flows corresponded to discharges of 50–100 years return period.

13.3 Methods

Slope deformations activated in May 2010 were studied by field *geomorphological survey*: extraction of geological and topographical information from topographical (10 m-resolution DEM) and geological sources (Menčík et al. 1983) using GIS to reveal the spatial distribution of all activated landslides. The dimensions of 134 landslides were measured directly in the field. The 150 landslides reported to local authorities can only be considered a minimum number. This dataset was enlarged by an aerial survey performed in the Beskydy Mountains at the beginning of July 2010.

The largest studied landslide (Girová) was mapped by GPS in detail (Pánek et al. 2011a, b). Inaccessible corners and overall context of this slope deformation were studied on *aerial photos*. Radiocarbon and dendrogeomorphological dating was used to study the chronological evolution of mass movements within the area of the Girová landslide. Conventional and AMS *radiocarbon* (^{14}C) *dating* was provided by the Beta Analytics (Miami, USA) and Gliwice Radiocarbon Laboratory of the Institute of Physics, Silesian University of Technology (Poland). Historical chronology of landslide movements for the past few decades was derived using *dendrogeomorphological dating*. The analysis was performed using 152 increment cores coming from 76 individuals of common spruce (*Picea abies*). All inclined trees that did not fall during the May 2010 catastrophic failure were sampled (56 trees; 112 increment cores); other samples were taken from 20 undisturbed trees (40 increment cores) growing completely outside the landslide area for reference. Two increment cores were taken from each sampled tree using Pressler increment borer (one on the upper side and the other one on the lower site of the trunk) (Stoffel and Bollschweiler 2008). All samples were cross-dated with reference chronology in order to identify and correct false/missing rings. Historical events were dated through the identification of the first years of reaction (compression) wood occurrence (i.e., growth reactions of conifers to tilting). Results of the *reaction wood analysis* are presented by the *It index* expressing the percentage of trees containing geomorphic signal (reaction wood) from all sampled trees alive in year *t* (Shroder 1978).

13.4 The May 2010 Landslide Events

The first landslides happened on 15 May, whereas the last of them were reported on 25 May 2010. The majority of movements started on 18 May just after the most intensive 3-day rainfall episode (Fig. 13.2). The event was accompanied by numerous small failures, 88% of which reached 10^4 m^2 area (Fig. 13.3) and only 12% of the measured landslides affected areas larger than 1 ha. The size range of observed landslides is dominated by the giant Girová landslide with 20 ha area and ca. 2–3 million m^3 volume. Most slope failures were *incipient landslides* (mainly in the

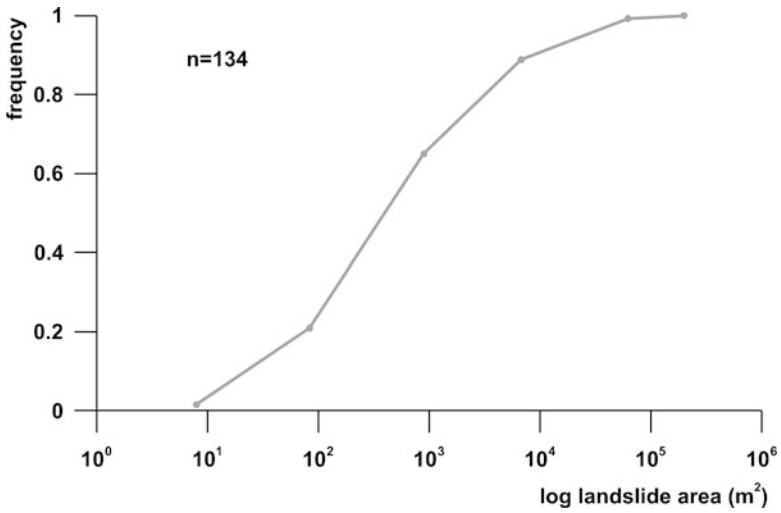

Fig. 13.3 Cumulative size frequency distribution of the May 2010 landslides in the eastern Czech Republic ($n = 134$ landslides with measured area). (Reprinted with kind permission from Springer Science+Business Media: Landslides, Rainfall-induced landslide event of May 2010 in the eastern part of the Czech Republic, 8, 2011, 507–516, Pánek T et al.)

stage of tension cracks), *shallow translational debris slides*, and *soil slips* (Fig. 13.4). Except for the isolated case of the Mt. Girová deep-seated rockslide, slope failures showed shear surfaces at medium (10–30 m) to shallow (less than 10 m) depths.

Most of the 150 reported landslides (67%) affected unconsolidated Quaternary colluvial, fluvial, aeolian, and glacial deposits. Thin-bedded flysch bedrock characterized by the dominance of clay stones/mudstones was involved in 16% of the cases (Fig. 13.5a). Most of the instabilities (67%) occurred in hilly (local relief up to 100 m), urbanized, or agricultural landscapes. They are mainly clustered on steep slopes (>25°) undercut by stream erosion (Fig. 13.5b, d). A very important aspect of the May 2010 landslide event was that 70% of instabilities developed on older (Holocene or historic) landslide terrains (Fig. 13.5c). Some of these landslides have experienced *multiple activation* over the past few decades (e.g., in 1972, 1995, 1997, 2005, and 2006; see, e.g., Krejčí et al. 2002; Hradecký and Pánek 2008; Pánek et al. 2009).

There is a quite *uniform spatial distribution* of the studied landslides in areas with different precipitation totals (16–18 May 2010, Fig. 13.2b), which were their main trigger. Four precipitation intervals (81–120, 121–160, 161–200, and 201–240 mm) involve 19, 15, 19, and 18% of all investigated landslides, respectively. On the other hand, 65% of the recorded landslides are limited to areas where May totals are more than three times higher than the monthly mean for 1961–2000 (Fig. 13.2c). Moreover, 50% of the landslides are situated in the region with API_{30} between 80 and 100 mm (Fig. 13.2a). The relative absence of landslides in the highest parts of the Beskydy Mountains (despite highest precipitations) is most likely explained by rather rigid sandstone-dominated flysch and dense forest cover.

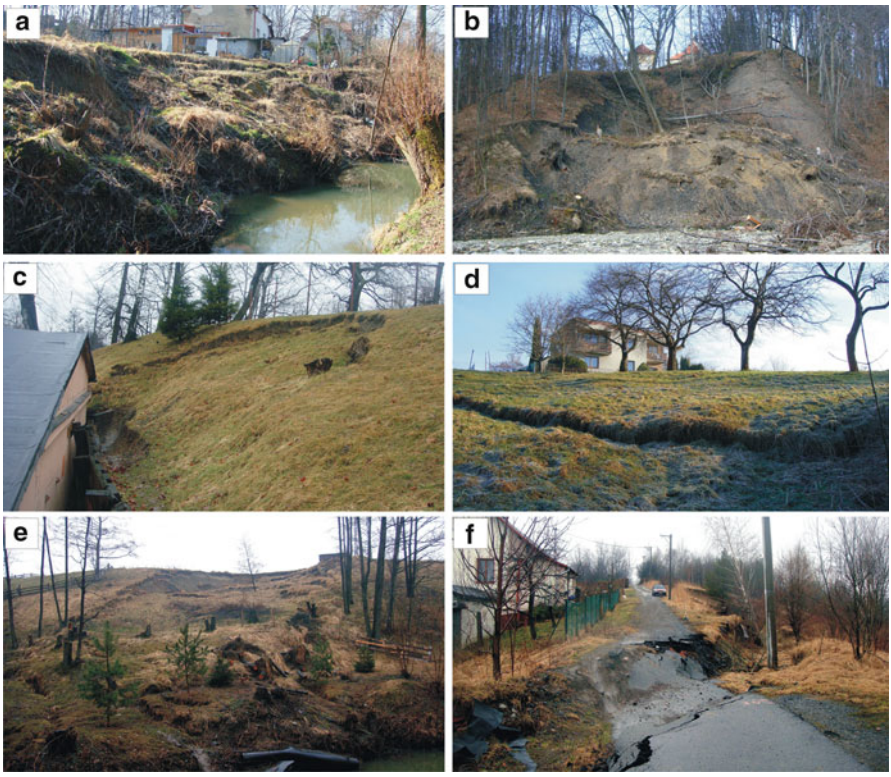

Fig. 13.4 Examples of typical landslides of the May 2010 event. (**a**) Right bank of the Horní Datyňka River is affected by translational landslides along a length of 100 m due to lateral erosion (Horní Datyně village). (**b**) A debris slide situated below the church in Skalice village formed due to lateral erosion of the Morávka River. (**c**) Incipient translational landslide in Orlová town. (**d**) Tension cracks in the upper part of a shallow translational landslide, Horní Bludovice village. (**e**) Rotational landslide in the Quaternary deposits, endangering two houses in Stonava village. (**f**) Large rotational landslide in Doubrava village. Two houses suffered structural damage and had to be demolished (Photos by L. Kubiszová)

13.5 Case Study: The Girová Landslide

The largest catastrophic landslide (area, ca. 20 ha; length, 1,150 m; volume, 2–3 million m^3) associated with the May 2010 rainfall event affected the southern slope of Girová Mountain (839 m) in the vicinity of Jablunkov town (Pánek et al. 2011a, b). It is the largest long-runout landslide in the Czech Republic over the past few decades. The landslide destroyed ca. 18 ha of forests and caused economic losses exceeding €0.5 million.

The whole SW slope of the Girová Mountain is occupied by a *complex slope deformation* (sensu Dikau et al. 1996) of dimensions of 1.5 × 1.0 km. The geomorphological mapping performed in the western part of the slope deformation in

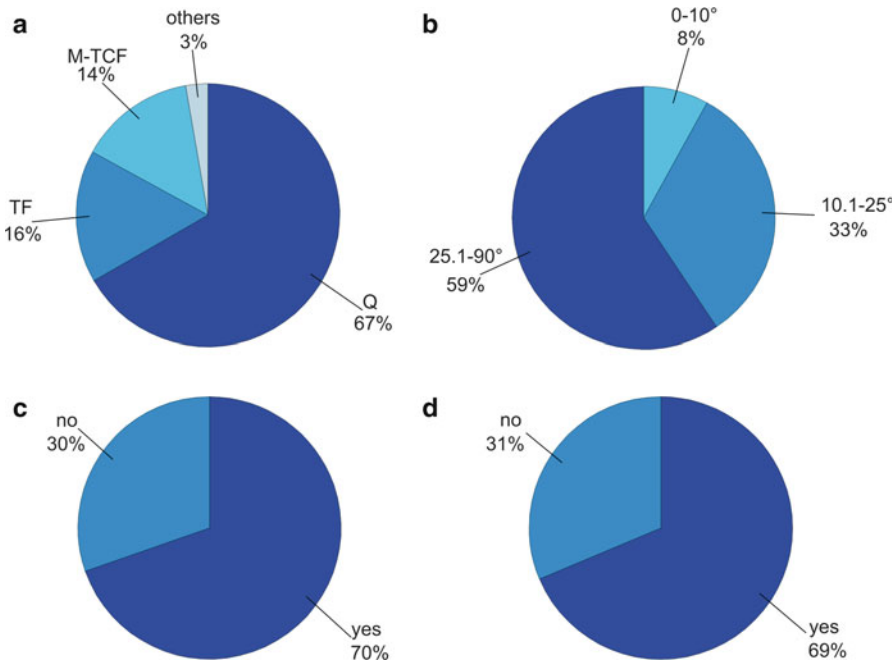

Fig. 13.5 Selected properties of the May 2010 landslide event ($n = 150$). (**a**) Landslide distribution in different lithological units (*Q* Quaternary deposits, *TF* thin-bedded flysch, *M-TCF* medium to thick-bedded flysch). (**b**) Landslide distribution within hillslope gradient classes. (**c**) Percentage of landslides that originated within old landslide terrains. (**d**) Percentage of landslides situated on slopes actively undercut by stream erosion. (Reprinted with kind permission from Springer Science+Business Media: Landslides, Rainfall-induced landslide event of May 2010 in the eastern part of the Czech Republic, 8, 2011, 507–516, Pánek T et al.)

2005 revealed a trough-like source area with 10 m high, soil-mantled, head scarps, peat bogs and the extremely long (1,500 m), eroded accumulation lobe of an ancient long-runout landslide (Fig. 13.6). Due to regression, this slope segment collapsed again in the night from 18 to 19 May 2010 and formed a wedge-like, *translational rockslide*. The movement started just below the mountain ridge and affected deeply weathered clay stone/mudstone flysch of the Magura Unit in the intersection zone of two normal faults dipping 250°/50° and 110°/55°, respectively. The translational displacement of this deep-seated block significantly destabilized the slope by (1) unloading the remaining mass upslope – particularly in the western part of the head scarp – and by (2) overloading the central part of the slope. Subsequent collapse of the frontal part of the rockslide toe lasted until 22 May.

The main properties of the May 2010 Girová rockslide are shown in Table 13.1, and its typical features in Figs. 13.6 and 13.7. The translational character is evidenced by terrain morphology and similar strike/dip between bedding planes outcropping in the main head scarp and gravitationally dislodged blocks. The upper part of the landslide (just below the wedge-like head scarp) experienced ca. 80 m of horizontal movement, whereas the middle section of the slope failure shifted ca. 270 m downslope. The rockslide front is a 550-m-long distal lobe partly overlying

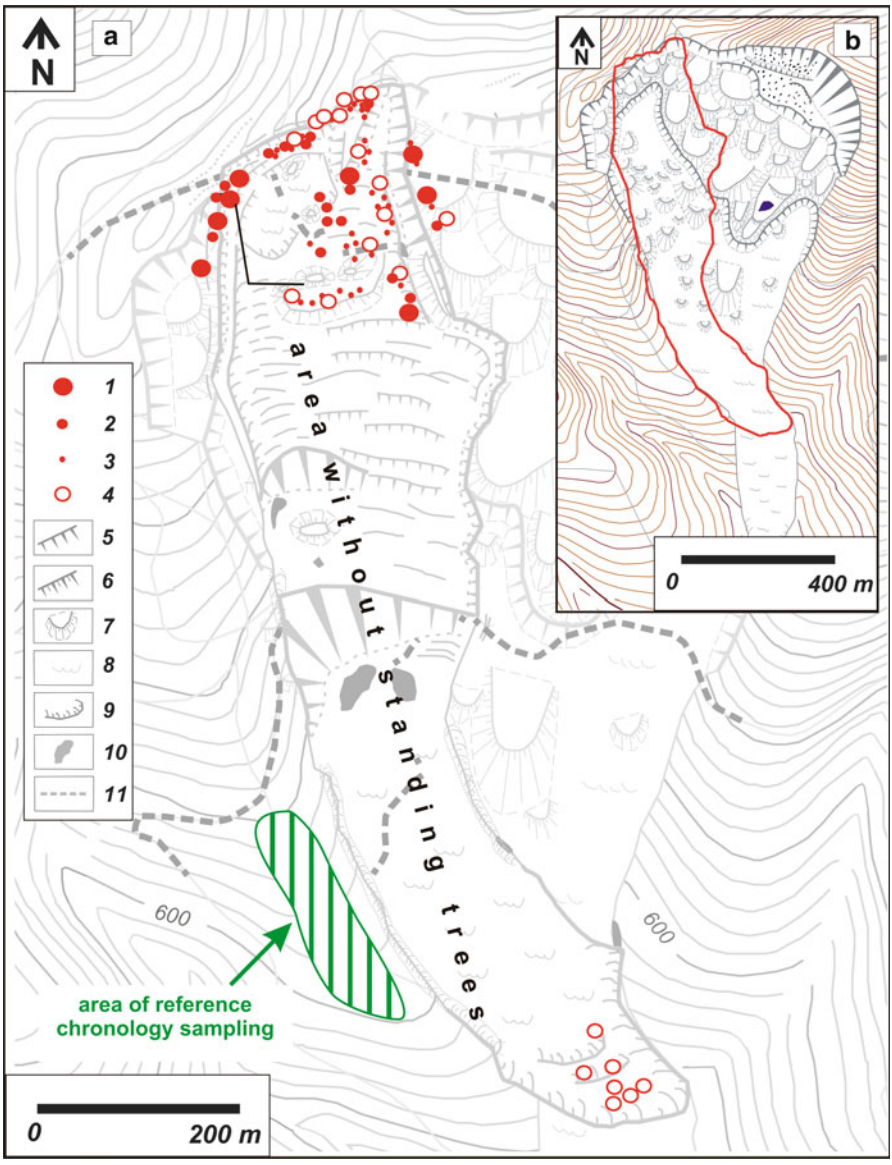

Fig. 13.6 Geomorphological map of the Girová Mountain slope deformation and localization of trees (*Picea abies*) sampled for dendrogeomorphological dating. (**a**) Reaction wood related to the May 2010 event is excluded. *1*, trees with ≥3 occurrences of reaction wood; *2*, trees with two occurrences of reaction wood; *3*, trees with one occurrence of reaction wood; *4*, trees without occurrence of reaction wood; *5*, head scarps of old landslides within DSGSD; *6*, counterslope scarps; *7*, landslide blocks; *8*, accumulation surfaces; *9*, accumulation toes; *10*, ponds within the May 2010 landslide; *11*, damaged roads. (**b**) Outline of the May 2010 failure in the context of older slope failures. (Reprinted from Geomorphology, 130/3–4, Pánek T et al., Catastrophic slope failure and its origins: Case of the May 2010 Girová Mountain long-runout rockslide (Czech Republic), pp. 352–364, Copyright (2012), with permission from Elsevier.)

Table 13.1 Main properties of the May 2010 Girová Mountain rockslide. (Reprinted from Geomorphology, 130/3–4, Pánek T et al., Catastrophic slope failure and its origins: Case of the May 2010 Girová Mountain long-runout rockslide (Czech Republic), pp. 352–364, Copyright (2012), with permission from Elsevier.)

Parameter	
Landslide area	20 ha
Landslide volume (approximate)	2–3 $\times$ 10^6 m^3
Landslide runout L (maximum)	1,150 m
Maximum landslide width	300 m
Elevation of head scarp	718–743 m
Elevation of terminal point	572 m
Landslide height (H)	171 m
H/L	0.15
Excess travel distance (Le)	891 m
Le/L	0.77

the older generation of long-runout landslide(s). Several ponds have survived on the surface of the distal lobe for the rest of the year 2010.

Radiocarbon dating revealed at least *three generations* of major landslides which preceded the May 2010 disastrous failure. A tree trunk incorporated in landslide accumulation underlying the recent lobe (upthrust in front of the recent failure) was dated at 7,420 $\pm$ 60 cal BP (Beta-288258) and reflects the age of the long-runout lobe (first-time landslide?) continuing ca. 500 m below the end of the May 2010 rockslide (Fig. 13.7). Another two dated samples indicate minimum ages of younger, rather short-distance movements. Dating of the basal part of the peat bog situated in the upper axis of contemporary rockslide returned the age of 1,540 $\pm$ 40 cal BP. It means that the upper part of the May 2010 rockslide has not been affected by displacements for at least the last 1,500 years. The youngest sample dated 600 $\pm$ 30 cal BP marks the onset of bog formation disturbed on the eastern margin of the catastrophic landslide in May 2010.

Dendrogeomorphological dating helped to determine the dynamics of minor, accelerated *creep*-like movements within the landslide body for 1930–2010 (Fig. 13.8). Trees in the reactivated slope section revealed 34 years with tree trunk tilting. The area of the reactivated rockslide points to an increasing frequency of years with tree tilting since the mid-1970s with the culmination in the late 1990s. Sliding/creep was triggered by an extreme hydrometeorological event in July 1997. The spatial distribution of disturbed trees is presented in Fig. 13.6. The majority of sampled trees with more than two dated disturbances indicated by reaction wood in the last 80 years are concentrated in the vicinity of the May 2010 head scarp. On the other hand, the zone of the contemporary lobe lacks any evidence of previous slope movement. The first event indicated by reaction wood in this domain comes from 2010; its origin is undoubtedly connected with the May rockslide.

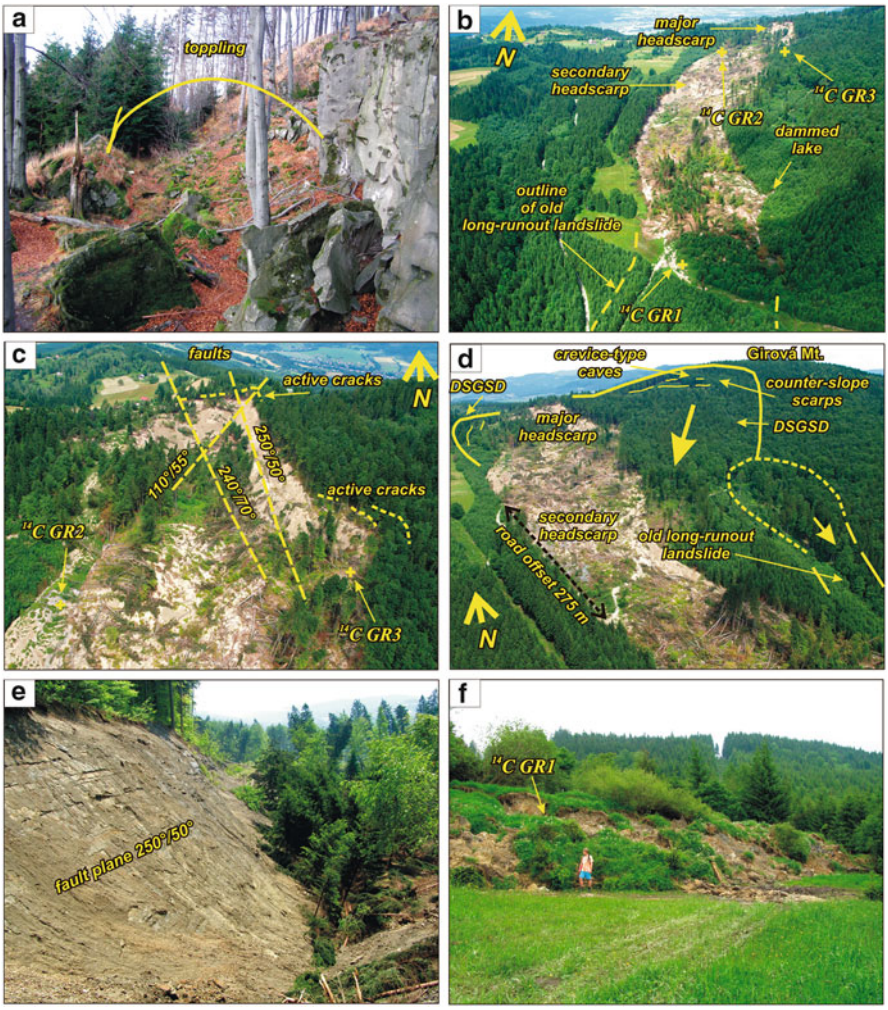

Fig. 13.7 Typical morphological features within the Girová Mountain slope deformation. (**a**) Toppling-related head scarp area of the DSGSD within sandstone-dominated flysch (Lukov Member). (**b**) Overall aerial view of the May 2010 catastrophic rockslide. (**c**) Detailed aerial view of the wedge-like depletion zone of the rockslide with marked main tectonic elements of the slope and position of dated peat bogs. (**d**) Aerial view of the upper half of the rockslide displaying relations to older slope deformations and displacement markers (destroyed road). (**e**) Main fault-predisposed head scarp of the May 2010 catastrophic rockslide. (**f**) Frontal part of the May 2010 long-runout lobe (upthrust of a precedent landslide) with a marked position of a dated buried trunk. (Reprinted from Geomorphology, 130/3–4, Pánek T et al., Catastrophic slope failure and its origins: Case of the May 2010 Girová Mountain long-runout rockslide (Czech Republic), pp. 352–364, Copyright (2012), with permission from Elsevier.)

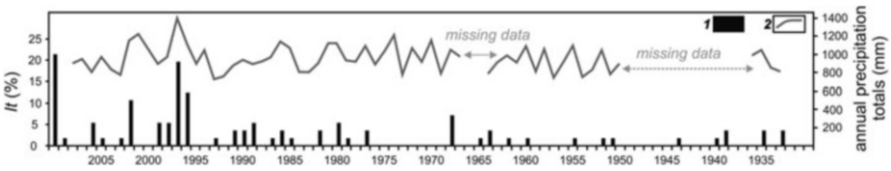

Fig. 13.8 Results of dendrogeomorphological analysis (initial occurrence of reaction wood expressed by the anomaly index). *1*, It index; *2*, annual precipitation totals. (Reprinted from Geomorphology, 130/3–4, Pánek T et al., Catastrophic slope failure and its origins: Case of the May 2010 Girová Mountain long-runout rockslide (Czech Republic), pp. 352–364, Copyright (2012), with permission from Elsevier.)

13.6 Discussion

Along with well-saturated soil by antecedent rainfalls, extremely high precipitations (locally above 300 mm during 3 days) on 16–18 May 2010 generated more than 150 slope failures within the lithologically weak domain of the OWC and their foredeep. A strong lithological predisposition of the landslide event in May 2010 is evident from the clustering of May 2010 landslides on Quaternary deposits and/or thin-bedded flysch bedrock and the relative lack of new landslides within the highest, flysch, parts of the OWC (although heavily affected by older deep-seated landslides – see Hradecký and Pánek 2008). Apart from this, the distribution of landslides seems to be rather more closely related to that of extreme rainfalls in May 2010 and the API_{30} index than to the precipitations in 16–18 May. The majority of the landslides show characteristics of rather small reactivations of older, recurring slope instabilities. Similar situation has also been described in other flysch regions (Sabatakakis et al. 2005; Borgatti et al. 2006; Mikoš et al. 2009). The landslides typically originated on steep eroded slopes, where – besides rainfall-generated pore pressures – the role of increased shear stress due to lateral erosion of rivers at bank-full discharge was decisive (for comparison see Kim et al. 2010). The predominance of incipient failures (short-travel landslides, tension cracks) and shallow debris slides or soil slips supports the fact that the duration and intensity of the May 2010 rainfall were insufficient (except for the Girová rockslide) for the occurrence of major landslides, as compared with the situation in July 1997 (Krejčí et al. 2002). In spite of the fact that the May 2010 landslide event in the OWC was only moderately destructive, it left many initial slope failures behind with a high potential for future reactivation (for comparison, see Saba et al. 2010).

Although recently the medium-height mountains of Central Europe have only rarely been affected by such long-runout landslides (Němčok 1982; Rybář and Stemberk 2000; Migoń et al. 2002; Klimeš et al. 2009), the May 2010 Girová Mountain rockslide demonstrates that they still might evolve under specific circumstances also in settings characterized by relatively gentle hillslopes (20°) and local relief (200 m). The combination of preparatory factors within the zone of the Girová Mountain slope deformation has produced several recurrent Holocene collapses especially in its fault-preconditioned, wedge-like western margin of clay stone. At least one of these

collapses dated to the *Atlantic* chronozone (~7.4 cal ka BP) evolved into a *long-runout landslide*, whose lobe length exceeded that of the May 2010 landslide by several hundreds of meters. The age of this major failure can be correlated with numerous slope failures and flood deposits in the nearby Polish Carpathians, also dated to the very humid Atlantic chronozone (Margielewski 2006). The dating of landslide-related peat bogs within these blocks suggests that the *recurrence interval* of major slope failures within the rockslide zone is on the order of ~1 ka, presumably correlated with bedrock *relaxation time*, i.e., a period necessary for shear strength reduction as a result of weathering along wedge-like fault planes (Hartvich and Mentlík 2010).

13.7 Conclusions

Although unusual in Central Europe, merely the duration and intensity of the May 2010 rainfall event were probably insufficient for generating failures of extraordinary dimensions, such as the Girová rockslide, which remained a site-specific, isolated failure. Furthermore, even more extreme rainfall episodes of several last decades (e.g., three- to six-day precipitation amounts of 537 and 625 mm at the Šance station on 4–9 July 1997 – see Štekl et al. 2001) activated slope failures which reached at most half of the size of the May 2010 Girová Mountain rockslide (Krejčí et al. 2002). Therefore, the May 2010 rainfall event was only the final (but important) incremental change leading to the collapse of the Girová Mountain slope.

The main preconditions of slope failure were long-term, internal changes within the rock mass. As evidenced by dendrogeomorphological dating, rock strength weakening was connected to long-term (decennial-scale) creep leading to the final catastrophic movement. This creep was accelerated several times over the 1930–2010 period, mostly as a consequence of the growing rate of strain induced by hydrometeorological conditions which increased pore pressure. A similar behavior of recent disastrous deep-seated landslides was described by Petley and Allison (1997).

Dendrogeomorphological data support an assumption that the May 2010 long-runout landslide was initiated in its upper part with concentrated creeping (with some periods of accelerations) for at least 80 years before the catastrophic collapse. However, many trees from the upper part of the landslide do not reveal any year of reaction wood. It could be explained by a translational, blocklike character of movement. Some trees (e.g., standing on the boundary of sliding blocks) represent a good dendrogeomorphological signal of past failures, while trees within the internally non-deformed sliding blocks do not react to slope movements.

Acknowledgements The research was supported by a project of the Czech Science Foundation no. P209/10/0309: "The effect of historical climatic and hydrometeorological extremes on slope and fluvial processes in the Western Beskydy Mountains and their forefield" and by the University of Ostrava Foundation SGS/PrF/2013.

References

Bíl M, Müller I (2008) The origin of shallow landslides in Moravia (Czech Republic) in the spring 2006. Geomorphology 99:246–253

Borgatti L, Corsini A, Barbieri M, Sartini G, Truffelli G, Caputo G, Puglisi C (2006) Large reactivated landslides in weak rock masses: a case study from the Northern Apennines (Italy). Landslides 3:115–124

Dikau R, Brunsden D, Schrott D, Ibsen ML (eds) (1996) Landslide recognition: identification, movement and causes. Wiley, Chichester

Hartvich F, Mentlík P (2010) Slope development reconstruction at two sites in the Bohemian Forest Mountains. Earth Surf Process Landf 35:373–389

Hladný J (1962) Some remarks on the problematics of parameters of precipitation–runoff relationships. Sborník mezinárodní hydrologické konference, Slovenské akademie věd a Ústavu hydrologie a hydrauliky, Bratislava, pp 1–11 (in Czech)

Hradecký J, Pánek T (2008) Deep-seated gravitational slope deformations and their influence on consequent mass movements (case studies from the highest part of the Czech Carpathians). Nat Hazards 45:235–253

Kim HT, Cruden DM, Martin CD, Froese CR (2010) The 2007 Fox Creek landslide, Peace River Lowland, Alberta, Canada. Landslides 7:89–98

Kirchner K (2001) Klimatologie. In: Příroda Valašska (okres Vsetín), ČSOP ZO 76/06 Orchidea. Vsetín, Czech Republic, pp 61–66 (in Czech)

Klimeš J, Baroň I, Pánek T, Kosačík T, Burda J, Kresta F, Hradecký J (2009) Investigation of recent catastrophic landslides in the flysch belt of Outer Western Carpathians (Czech Republic): progress towards better hazard assessment. Nat Hazards Earth Syst Sci 9:119–128

Krejčí O, Baroň I, Bíl M, Jurová Z, Hubatka F, Kirchner K (2002) Slope movements in the Flysch Carpathians of Eastern Czech Republic triggered by extreme rainfalls in 1997: a case study. Phys Chem Earth 27:1567–1576

Margielewski W (2006) Records of the Late Glacial–Holocene palaeoenvironmental changes in landslide forms and deposits of the Beskid Makowski and Beskyd Wyspowy Mts. Area (Polish Outer Carpathians). Folia Quat 76:1–149

Menčík E, Adamová M, Dvořák J, Dudek A, Jetel J, Jurková A, Hanzlíková E, Houša V, Peslová H, Rybářová L, Šmíd B, Šebesta J, Tyráček J, Vašíček Z (1983) Geology of the Moravskoslezské Beskydy Mountains and Podbeskydská pahorkatina upland. Ústřední ústav geologický, Praha (in Czech with English abstract)

Migoń P, Hrádek M, Parzóch K (2002) Extreme events in the Sudetes Mountains. Their long-term geomorphic impact and possible controlling factors. Studia Geomorphol Carpath Balcanic 36:29–49

Mikoš M, Petkovšek A, Majes B (2009) Mechanisms of landslides in over consolidated clay and flysch. Landslides 6:367–371

Němčok A (1982) Zosuvy v slovenskych Karpatoch Publ (Landslides in the Slovak Carpathians). VEDA, Bratislava, 318 p

Pánek T, Hradecký J, Šilhán K (2009) Geomorphic evidence of ancient catastrophic flow type landslides in the mid-mountain ridges of the Western Flysch Carpathian Mountains (Czech Republic). Int J Sedim Res 24:88–98

Pánek T, Brázdil R, Klimeš J, Smolková V, Hradecký J, Zahradníček P (2011a) Rainfall-induced landslide event of May 2010 in the eastern part of the Czech Republic. Landslides 8:507–516

Pánek T, Šilhán K, Tábořík P, Hradecký J, Smolková V, Lenárt J, Brázdil R, Kašičková L, Pazdur A (2011b) Catastrophic slope failure and its origins. Case study of the May 2010 Girová Mountain long-runout rockslide (Czech Republic). Geomorphology 130:352–364

Petley DN, Allison RJ (1997) The mechanics of deep-seated landslides. Earth Surf Process Landf 22:747–758

Rybář J, Stemberk J (2000) Avalanche-like occurrences of slope deformations in the Czech Republic and coping with their consequences. Landslide News 13:28–33

Saba SB, Van der Meide M, Van der Werff H (2010) Spatiotemporal landslide detection for the 2005 Kashmir earthquake region. Geomorphology 124:17–25

Sabatakakis N, Koukis G, Mourtas D (2005) Composite landslides induced by heavy rainfalls in suburban areas: city of Patras and surrounding area, Western Greece. Landslides 2:202–211

Shroder JF (1978) Dendrogeomorphological analysis of mass movements on Table Cliffs Plateau, Utah. Quat Res 9:168–185

Štekl J, Brázdil R, Kakos V, Jež J, Tolasz R, Sokol Z (2001) Extrémní denní srážkové úhrny na území ČR v období 1879–2000 a jejich synoptické příčiny (Extreme daily precipitation totals over the Czech Republic territory in the 1879–2000 period and their synoptic reasons). Národní klimatický program České republiky, Praha, 140 p

Stoffel M, Bollschweiler M (2008) Tree-ring analysis in natural hazards research – an overview. Nat Hazards Earth Syst Sci 8:187–202

Tolasz R, Brázdil R, Bulíř O, Dobrovolný P, Dubrovský M, Hájková L, Halásová O, Hostýnek J, Janouch M, Kohut M, Krška K, Křivancová S, Květoň V, Lepka Z, Lipina P, Macková J, Metelka L, Míková T, Mrkvica Z, Možný M, Nekovář J, Němec L, Pokorný J, Reitschläger JD, Richterová D, Rožnovský J, Řepka M, Semerádová D, Sosna V, Stříž M, Šercl P, Škáchová H, Štěpánek P, Štěpánková P, Trnka M, Valeriánová A, Valter J, Vaníček K, Vavruška F, Voženílek V, Vráblík T, Vysoudil M, Zahradníček J, Zusková I, Žák M, Žalud Z (2007) Climate Atlas of Czechia. Czech Hydrometeorological Institute, Prague – Palacký University, Olomouc (in Czech and English)

Chapter 14
Recent Debris Flows in the Tatra Mountains

Adam Kotarba, Zofia Rączkowska, Michał Długosz, and Martin Boltižiar

Abstract This chapter results from the interpretation of the data collected by field studies of debris flow events including geomorphological effects, of an Ikonos satellite image from 2004, and the DEM prepared for the entire Tatra massif. Based on about 20-year-long field observations, the rainfall thresholds necessary to trigger debris flows have been identified. Such thresholds, however, vary with lithology and relief. As it is illustrated by the lack of debris flows associated with the extreme weather events in May and June of 2010 in the Tatras, there is no clear relationship between periods of high daily precipitations and the triggering of this type of mass movement. The most spectacular topographic impacts of debris flows are observed in the middle section of the vertical profile of the mountains. Debris flow activity is strongly conditioned by relief (topography and substrate properties) that resulted from Pleistocene glacial and periglacial morphogenesis.

Keywords Debris flow • Typology • Geoecological and morphodynamic zones • Rainstorms • Tatra Mountains

A. Kotarba • Z. Rączkowska (✉) • M. Długosz
Department of Geoenvironmental Research, Institute of Geography and Spatial Organisation, Polish Academy of Sciences, str. Św. Jana 22, 31-018 Cracow, Poland
e-mail: kotarba@zg.pan.krakow.pl; raczk@zg.pan.krakow.pl; dlugosz@zg.pan.krakow.pl

M. Boltižiar
Institute of Landscape Ecology, Slovak Academy of Sciences, Branch in Nitra, str. Akademická 2, 949 01 Nitra, Slovakia

Department of Geography and Regional Development, Faculty of Natural Sciences, Constantine the Philosopher University in Nitra, Trieda A. Hlinku 1, 949 74 Nitra, Slovakia
e-mail: martin.boltiziar@savba.sk; mboltiziar@ukf.sk

D. Lóczy (ed.), *Geomorphological impacts of extreme weather: Case studies from central and eastern Europe*, Springer Geography, DOI 10.1007/978-94-007-6301-2_14,

14.1 Introduction

Debris flows belong to most important geomorphic processes in the Tatra massif, south Poland, evidenced by numerous debris flow tracks formed or renewed in recent years. Similarly to other alpine regions, we assume a relationship between debris flow triggering and observed changes in rainfall intensities. In the high-mountain environment of the Tatras, rapid mass movements are favored by direct and indirect causes. Steep slopes and unconsolidated weathering mantles of glacial and periglacial origin promote erosion, while specific hydrometeorological conditions – intensive rainstorms or several-days-long precipitation followed by an intensive, short-lasting rainfall event – are direct triggers of debris flows. In recent years the frequency of debris flow incidents has increased in the Carpathians. In order to assess a role of debris flows in the present-day modeling of the Tatra relief, monitoring has been launched at several research stations on both the Polish and Slovakian side (Kotarba 2004; Hreško et al. 2008; Kapusta et al. 2010). Ikonos satellite images of 2004 have been interpreted, and a Digital Elevation Model (DEM) has been prepared for the entire Tatra massif.

14.2 Relief Features and Geoecological Zones

The Tatras (of 785 km^2 area and 53 km length) are the highest mountain group in the whole Carpathian arc. This region of diverse *relief* is traditionally divided into three landscape units: the High (Eastern) Tatra, Western Tatra, and Belianske Tatry (the smallest area of ca 70 km^2) (Fig. 14.1). In the High Tatra several summits rise above 2,500 m elevation (Gerlachovský štit 2654.4 m), the Western Tatra is ca 400 m lower (the highest point is Bystra, 2,248 m), while the Belianske Tatry also has some summits rising above 2,000 m (Havran 2151.5 m). The Tatra landscape is controlled by various rocks, tectonic features, and differentiated relief remodeled by Pleistocene glaciers (Nemčok et al. 1994).

The most resistant granite occurs in the crystalline core of the High Tatra *batholith*, while the less competent pegmatite-aplite granite is present in a marginal zone. The granite core is densely dissected by joints and faults. The Tatra horst of east–west strike is built up of crystalline rocks. Mylonites, which promote formation of deep troughs and passes (Grochocka-Piotrowska 1970), occur in dislocation zones. Metamorphic rocks – gneisses, amphibolites, and biotite schists – predominate, and white granites (alaskites) also occur in the Western Tatras. The entire Belianske Tatry is built up of *nappes* of Mesozoic sedimentary rocks, which are also present on the northern slopes of the Tatras (Nemčok et al. 1994).

Geologic structures, climatic conditions, and vegetation are differentiated both vertically and horizontally. A characteristic feature of the Tatras, high mountains not glaciated at present, is the *vertical zonation* of climate and vegetation with the accompanying geomorphic processes. Determined by elevation above sea level, particular parts of the Tatras are subjected to various climatic conditions: nival,

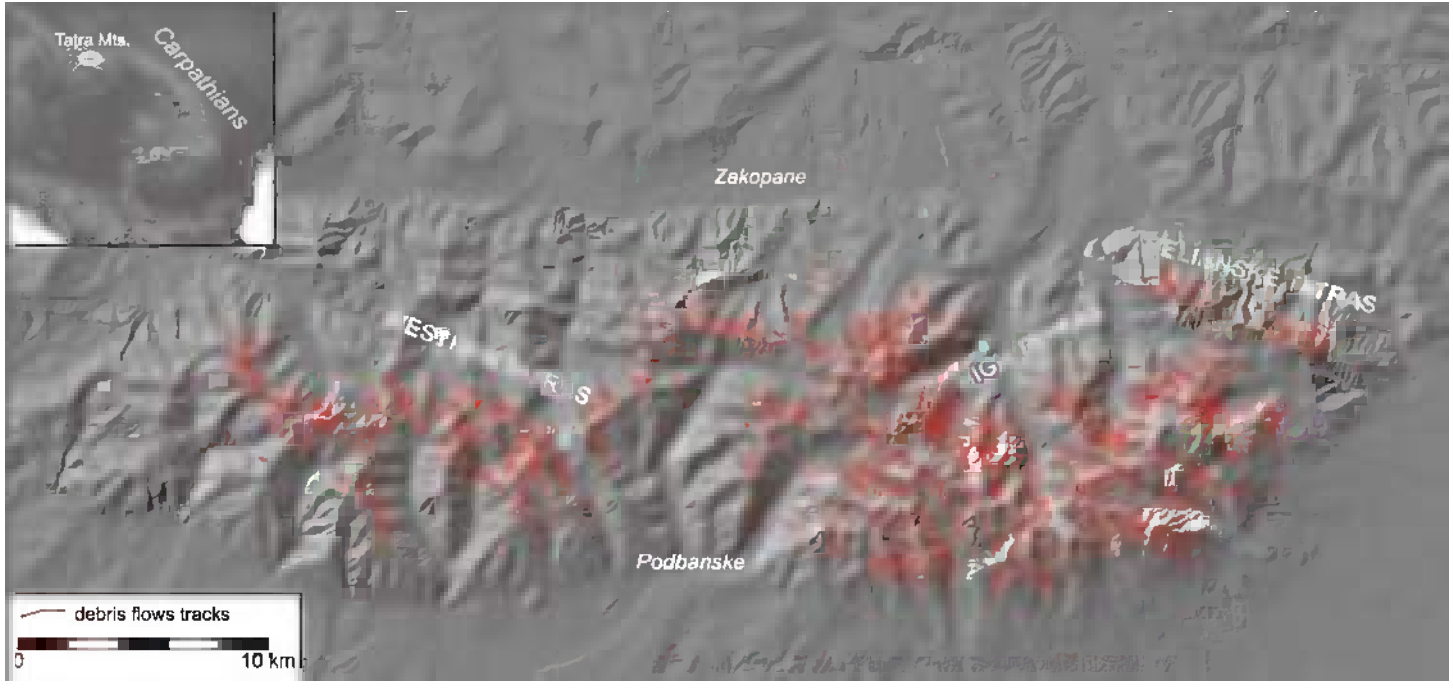

Fig. 14.1 Map of debris flow tracks in the Tatra Mountains (By M Dlugosz)

from 2,200 m to the summits; nival-pluvial (1,550–2,200 m); and pluvial-nival, below 1,550 m (Hess 1965). So water retention in the form of snow lasts for long, snow patches are found above 1,800 m (Wiśliński 1996), and abundant supply of water originates from rainfalls and snowfalls.

The recharge of water resources as well as water circulation is mainly driven by rainfalls (75% of annual precipitation – Łajczak 1966). The highest totals and intensities of rainfalls are recorded in the summer season, i.e., from June to August. The Tatra Mountains receive high annual precipitation (1,100–1,900 mm), with the highest amounts (1,600–1,900 mm) observed on northerly slopes at 1,400–2,000 m elevation (Niedźwiedź 1992, 2003).

The unique features of high mountains are their rise above the present-day timberline and the presence of numerous glacial, nival, and periglacial landform complexes. From a geoecological viewpoint, two geomorphological domains are distinguished (Kotarba and Starkel 1972): the *cryonival* or periglacial (Jahn 1958) zone and the *temperate forest* zone, separated by an upper timberline at 1,500 m elevation. There are two *morphogenetic zones* in the cryonival domain: the lower zone with congelifluction processes and the upper zone, reaching to the permanent snow line, where frost sorting processes are observed (Starkel 1980). Small periglacial features clearly actively develop also at present (Rączkowska 2007).

Being the most important geomorphic process, *debris flows* transport weathered material from the rock crests to the bottoms of glacial cirques or troughs. By the end of glaciations, under paraglacial conditions, rapid mass movements dissected the slopes below melting glaciers and formed systems of rock chutes. At present, slopes are still being remodeled by debris flows and avalanches.

Debris flows occur in all physical-geographic units and geoecological vertical zones of the Tatras (Table 14.1, Fig. 14.1), but they differ with respect to type, frequency, and magnitude. The necessary condition for a debris flow formation is favorable terrain configuration: steep slopes and unconsolidated regolith. If these conditions are fulfilled, flow of regolith is possible provided satisfactory hydrometeorological triggers are available. Following Brunsden's classification (1979), we distinguish *hillslope debris flows* and *valley-confined debris flows* in the Tatras (Kotarba 1992). The longest valley-confined debris flows reach the maximum length of over 1,000 m; they amount to 9.3 and 5% of all debris flows in the High and Western Tatras, respectively (Midriak 1984), and transfer the weathering products across geoecological vertical zones.

The size, number, and distribution of debris flows depend mainly on topography and substrate properties. The spatial differentiation of the topography of the Tatras results from diverse impacts of Pleistocene *glaciations*. The High Tatra was subjected to the most profound transformation (Fig. 14.2). Within the relief between the highest summits and mountain footslopes of the order of 1,500 m, a vertically distributed system of hanging cirques and glacial troughs has formed. According to Klimaszewski (1988), in the Polish part of the High Tatra, glaciation covered 50% of the area, 21.5% in the Western Tatra, while only minor fragments of the northern slopes of the Belianske Tatry were glaciated.

Table 14.1 Description of debris flows in the Western Tatra, High Tatra and Belianske Tatry Mountains

Region	Lithologhy	Highest summit (m a.s.l.)	Area (km^2)	Number of debris flows	Elevation of debris flow starting zone (m a.s.l.)			Elevation of debris flow frontal zone (m a.s.l.)			Height difference (m)			Debris flow length (m)			Distribution of debris flows by slope aspect (%)				Distribution of debris flows by slope inclination (%)		
					Max.	Min.	Mean	Max.	Min.	Mean	Max.	Min.	Mean	Max.	Min.	Mean	N	E	S	W	15–25	26–36	37–55
Western Tatra	Gneisses, granitoids, limestone, dolomites	2,248	379	1,127	2,217	1,293	1,817	2,095	1,213	1,711	519	15	106	966	38	200	34	31	8.7	26.3	15	47	35
High Tatra	Granitoids,	2,654	341	2,300	2,396	1,291	1,936	2,350	1,044	1,828	633	11	111	1,410	36	212	21	30	20	29	15	45	33
Belianske Tatry	Limestone, dolomits, sandstones	2,152	67.5	153	2,101	1,449	1,786	1,906	1,260	1,622	638	27	163	1,163	47	274	40	31	6	21	5.5	29	60

Fig. 14.2 View of the Medena Dolinka valley, Slovakian High Tatra, with hanging cirque and glacial trough, a suitable setting for the development of gullies and levees of valley-confined debris flows, which transport material from ridge to valley bottom through subnival, alpine to subalpine belts (Photo by B. Gądek)

The varied influence of glacial and periglacial action in the Pleistocene differentiated *slope morphology*. In the High Tatra, granite narrow crests, slopes, and rockwalls inclined above 40° predominate. The latter are strongly dissected by rocky chutes (8–17 km km^{-2} density) along their entire lengths (Klimaszewski 1988). At footslopes, heaps and debris taluses were formed, so the slope profile consists of two sections (Fig. 14.2). In the Western Tatra, less remodeled by glaciers, the slopes consist of three or four segments (Fig. 14.3). Ridge culminations, gradually change from gently inclined near-ridge slope segments, remodeled by Pleistocene periglacial processes, into rocky slopes dissected by chutes (density of chutes ca. 6 km km^{-2}), which vary in size depending on the properties of metamorphic rocks and on slope aspect. Talus heaps rarely occur, but footslopes are formed by alluvial fans or alluvial-avalanche fans.

The Belianske Tatry has a shape of a huge mountain ridge of *crête* type, enclosed with subsequent valleys of the Biela voda and the Medodolský potok streams. A fundamental feature of this sloping morphostructure is a north–south *asymmetry*, alternatively with southeastern slopes. Consequent valleys on the north face were initially carved by glaciers. In addition, the longitudinal profile of valleys contains several rock bars and steps. The northern slopes are rockwalls, while the southern side of the main ridge combines smooth slopes with horizontal intersection belts of walls and towers of compact quartzites and limestones (Fig. 14.4 – Lukniš 1973).

Fig. 14.3 View of the Staroroboci̇ański glacial cirque, Western Tatra. Three-partite slope composed of (from ridge crest to valley bottom) periglacial slope, rocky slope dissected by chutes, and alluvial slope. The active valley-confined debris flows begin in the subnival or alpine belts and continue to the subalpine belt (Photo by Z. Rączkowska)

14.3 Debris Flow Characteristics

Debris flows might differ in shape, size, and mode of movement, depending on their setting, relief, and type of slope cover. Therefore, Krzemień (1988, 1989) distinguished three *morphodynamic zones*: source area of debris and water, track zone, and accumulation zone (zone of debris deposition), which form a system of debris flow. He distinguished three fundamental patterns (types) in the Western Tatras:

- Type *A* – scar → chute → track → lobe
- Type *B* – scar → track → lobe
- Type *C* – chute → track → lobe

These systems were identified in the part of the Western Tatras, where preglacial relief was only slightly remodeled by the Pleistocene glaciers. Glaciers on the interfluve of the Western Tatras did not cover entire valleys. The *interfluvial crests*, under the influence of periglacial and perinival processes during glaciations (Klimaszewski 1988), protruded above the glaciers. It is the reason why they are mantled with debris often showing pattern ground (Jahn 1958; Rączkowska 2007).

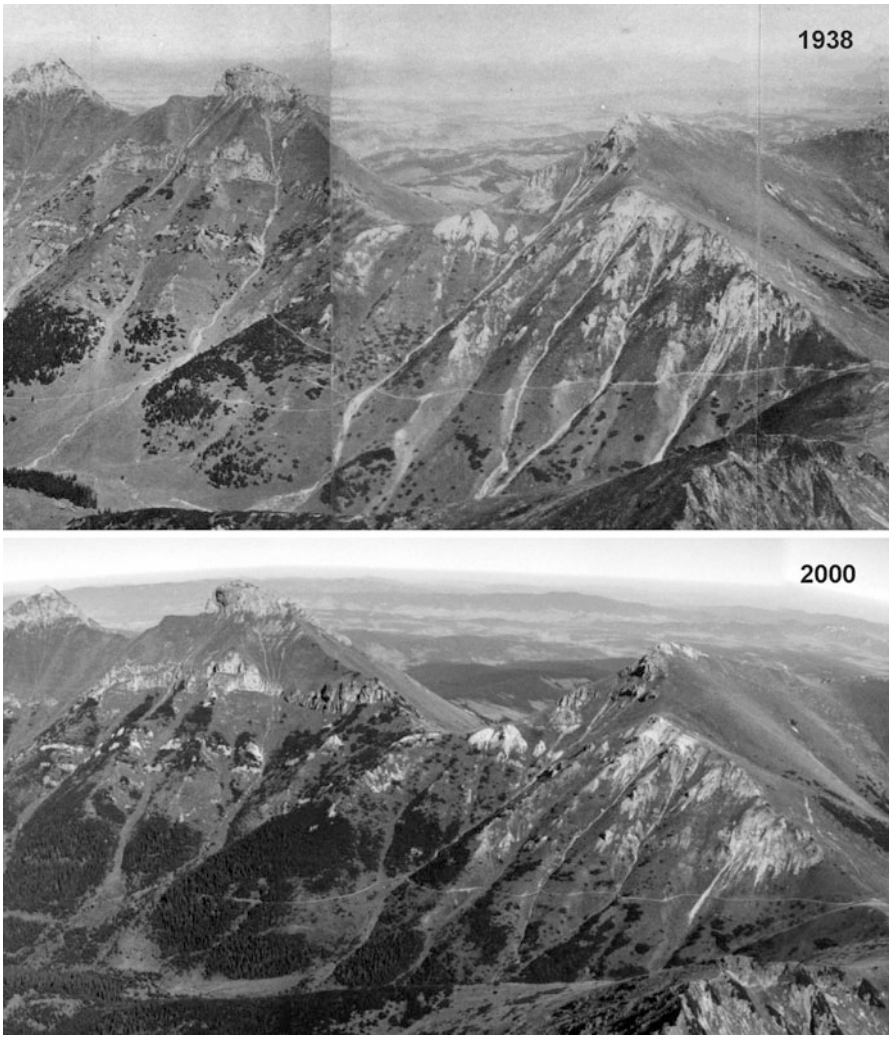

Fig. 14.4 Gullies of long valley-confined debris flows in the Belianske Tatry, documented in 1938, probably formed during a wet period in the 1930s. Recently some gullies are modeled by debris flows, while the majority by avalanches (Photo by M. Boltižiar)

In the *interfluve* zone, singular or, more often, complex rock-debris niches developed, which initiated *chutes* formation *on rocky slopes* after glacier melting. Huge talus heaps, with gullies, levees, and tongues, formed at the foot of rocky slopes. Such system, named type *A* by Krzemień (1988, 1989), reaches up to 1,000 m. The type *B* system occurs on rocky slopes and reaches up 750 m in length. It starts with gullies incised in relatively thin (ca up to 1.5 m thick) weathering mantles of the rocky slopes. The type *C* system comprises three elements – chutes, gullies (tracks), and tongues – and, without possessing a niche, its lengths vary from 100 to 700 m (Krzemień 1989).

Fig. 14.5 Overland flow on the rockwall of Maly Kežmarský štit peak on 17 July 2001, triggering a debris flow which affected the whole length of debris slopes. Rainfall intensity was 64 mm in 6 h (Photo by G. Bugár)

In the High Tatra, the systems of debris flows are more complicated. The Pleistocene glaciers formed classical, alpine-type valleys. In the highest regions, a debris flow is triggered by rainwater concentrated in chutes which flows rapidly onto gravitational talus heaps and talus cones (Fig. 14.5), forming typical *hillslope debris slopes*. As rock steps and exaration depressions with tarns occur, the longitudinal profiles of the main valleys are graded. In the High Tatra, debris flows start in the highest located cirques and continue downvalley. During extreme precipitation events in summer months, debris flows are set into motion, producing a complex system (Fig. 14.2), and weathered material is transferred across two or three vertical climatic zones (Kotarba and Strömquist 1984).

The basic condition of debris flow generation in the Belianske Tatry is a sufficient amount of clastic material detached from rockwalls, eventually from the denuded rocky slopes (e.g., on southern slopes below Hlúpy peak, 2,061 m). Historically grazing has accelerated debris flows in the Zadné Meďodoly and the Predné Meďodoly valleys.

Debris flow generation is evident in *gullies* or in upper sections of north-oriented valleys (the Nový potok, the Tristárska dolina valleys, and the north kettle below

the Jatky peak) permanently supplied with clastic material by gravitational and fluvio-gravitational processes. Resultant from debris flows, gullies erode the bedrock or incise in their own deposits. The *bifurcation furrows* with marked lateral mounds were formed in the accumulation zone (Fig. 14.4).

Similarly to other high mountains, debris flow tracks in the Tatra formed directly after glacier melting as outcomes of *paraglacial processes*. Considering the paraglacial environment at the end of the last glaciation, physical weathering (block disintegration and fragmentation of inclined surfaces, formation of tors and minor valleys) was a crucial process (Lukniš 1973; Klimaszewski 1988). The nival niches, which had developed at that time, became areas of melt- and rainwater concentration and promoted the formation of corrasion gullies, which functioned as paths for valley-confined debris flows in the Holocene.

As shown on the map drawn from the interpretation of 2004 *Ikonos satellite images* and the *DEM* (Fig. 14.1), debris flows are not evenly distributed in the Tatras. All forms with clearly noticeable boundaries along the whole longitudinal profiles of the debris flows are depicted on the map. The pixel size of the Ikonos image was 1 m for panchromatic images and 4 m for multispectral images (Guzik et al. 2006), while the grid size of the DEM was $10 \cdot 10$ m. The precise terrain model allowed to determine relative and absolute heights of the identified forms and to define their aspects. Based on the DEM, maps of slope gradients and aspects of the Tatras were prepared. All the maps and analyses were made using ILWIS 3.6 GIS software.

This way more than 3,500 features were identified. (For comparison, Midriak (1984) marked 830 debris flow paths in the Slovak Tatras). The majority of debris flows were registered in the High Tatra (2,300), and only half of that number (1,127) were recorded in the Western Tatras. Nevertheless, despite differences in lithology and the Pleistocene remodeling of relief, *debris flow densities* are similar. The smallest number of debris flows (153) with 2.27 flows km^{-2} is registered in the Belianske Tatry. This can be attributed to karst-driven water outflow.

More variation is observed in *debris flow lengths*: 200–300 m on the average and up to 1.5 or 2 km on the northern and eastern slopes of the High Tatras (Lukniš 1973; Nemčok 1982). Debris flows in the lowest number are recorded on south-facing slopes, explained by a faster development and more moderate dissection of such slopes. Such regularity is observable in the whole Tatras. The landforms, located near valley outlets, where denudation processes were initiated shortly after deglaciation, are usually larger in size, for instance, on eastern and western slopes of valleys on the southern side of the Tatra massif. The forms located higher, within the area of cirques, are definitely much smaller in size. It does not apply to north-facing slopes, where the largest debris flows developed in glacial cirque walls.

The debris flows form at elevations of 2,390–1,290 m and their source areas often reach the crests. Midriak (1995) is also of opinion that majority (65%) of debris flows begin at 1,900 m or higher, in the alpine or subnival zones, and continue within rocky chutes on slopes inclined at 26–36 or 37–55°. They end in debris flow gullies and *debris flow levees* developed on debris slopes and alluvial fans with their base at 1,260–1,906 m elevation. The difference in altitude between source and end zones of debris flows vary in the different parts of the Tatras.

As field surveys show, the gullies of recent debris flow tracks are from 3–4 to over 10–20 m wide and at most a few or a dozen meters deep (Kotarba 1989, 1995; Krzemień et al. 1995; Rączkowska 2006). The dimensions depend on slope morphology and substrate properties as well as triggering precipitation amounts and intensities. Debris flow gullies developed during a particular event can also form a complex interconnected network.

Debris flow transport can reach 100 to maximum 25,000 m^3 of material during a singular event (Midriak 1984; Kotarba et al. 1987; Krzemień 1991; Kotarba 1995), and, thus, they can be assigned to the second and third categories in Innes' classification (1983).

14.4 Precipitation and Debris Flow Triggering

In the Tatras, debris flows are mainly *trigger*ed by rainfalls. Snowmelt is almost insignificant because of a high permeability of the slope deposits. Not even a minor debris flow below snow patches has been recorded to date (Rączkowska 1999). The *amount of rainfall* necessary to trigger a debris flow varies with lithology and relief, but it is also different for the debris flow types. Hillslope debris flows, which are bound to the upper part of the debris slope, can be triggered by 30 mm rainfall in the High Tatra (Kotarba 1995) and 20 mm rainfall in the Western Tatra (Janačik 1971). The probability of such precipitation is 5–25% (Cebulak 1983). According to Krzemień (1988), such debris flows can occur at the same spot in the Western Tatra several times in a year.

Based on about 20-year-long observations in the High Tatras, the debris flows which extend over the full length of the debris slope are triggered by *rainfall*s of 35–40 mm h^{-1} *intensity* of or at least 80–100 mm day^{-1} (Kotarba 1992, 1997) with instantaneous intensity of 1.3–1.7 mm min^{-1} (Kotarba 1995) and 10% probability (Niedźwiedź 2003). The majority of the flows occur on the slopes of the subalpine and alpine zones, whereas stimulating runoff comes from a zone of bare rock (Figs. 14.2 and 14.5). Long-lasting precipitation below 1 mm min^{-1} intensity triggers mud-debris flows or rill erosion the forest belt close to the upper timberline and on subalpine slopes (Kotarba 1998; Rączkowska 2006).

Debris flows can be either generated by local rainstorms, often confined to a single small valley, or by *prolonged rainfalls* over the Tatra massif or the entire Carpathians as it was the case *in 2010*. In June and July of that year, long-lasting cyclone activity produced high precipitation: in both of the months, 5-day precipitation amounted to 220 and 200 mm in the Polish Tatras, respectively (Fig. 14.6). The automated gaging station located at 1,900 m elevation in Slovakian Western Tatras (Jalovecka Valley) recorded 157 mm rain for the second 5-day period. Nevertheless, debris flow activity did not intensify in response to the high precipitation in May and June 2010, which brought about many changes in the relief of the Polish Flysch Carpathians (see, e.g., Kijowska 2011; Bajgier-Kowalska 2011). Debris flows were not observed even in such locations as the region of the Morskie

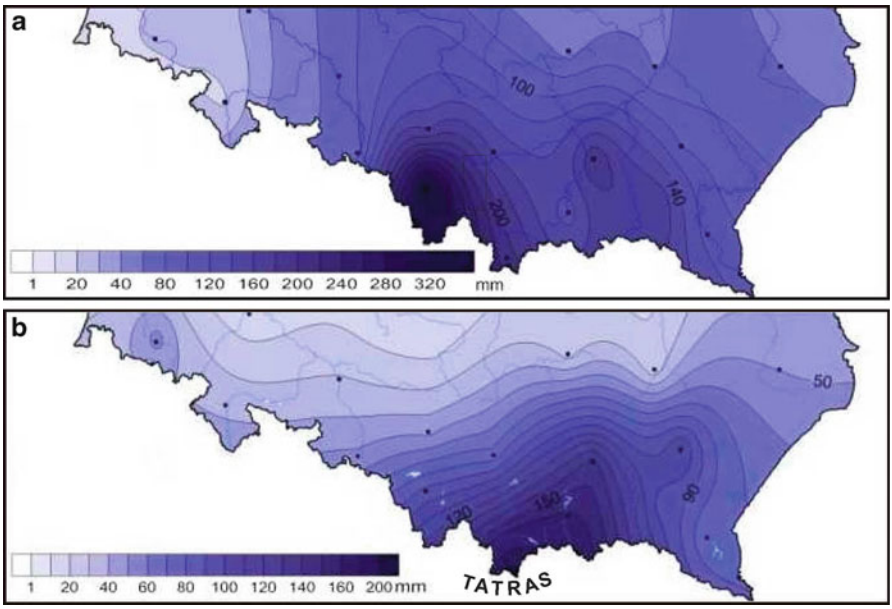

Fig. 14.6 Cumulative totals of precipitation in the Polish Carpathians during spring 2010, for the period 15–20 May 2010 (**a**) and for the period 31 May to 4 June (**b**) (After Miętus et al. 2010a, b)

Oko lake, where numerous debris flow gullies evidence that such processes are common (for instance, on the debris slopes of Szeroki Piarg and Zielony Piarg). Three photos, depicting the entire slope, provide evidence for the occurrence of new hillslope debris flows at least once per 10 years. At the same time the photos show that the slope surface was not changed in 2010 (Fig. 14.7). Debris flows were triggered by the 41.4 mm rain lasting 1.5 h on 23 August 2011. Precipitation as high as that was recorded at the valley bottom in 1 km distance from the emerged forms. At the crests, precipitation amounts might have been even higher and intensity above 1 mm min^{-1}.

Precipitation in the Tatras in 2010 was high but mostly in the form of *snow* and happened in a period with almost continuous snow cover particularly at higher elevations. That is the reason why apparent geomorphological effects are lacking.

14.5 Conclusions

1. Debris flows belong to the predominant gravitational processes which model the present-day slopes of the Tatra Mountains. They may develop in any geoecological zone, although their geomorphic role is most apparent *in the cryonival domain above the upper forest line*. The performed inventory showed that over 3.5 thousand modern tracks occur in that relatively small mountain

Fig. 14.7 Hillslope debris flows at the Szeroki Piarg and the Zielony Piarg above the Morskie Oko lake, where fresh gullies evidence frequent debris flow activity in 2001, 2010, and 2011, but no geomorphological impact of the high precipitation in 2010 (2001, photo by T. Ferber; 2010 and 2011, photo by Z. Rączkowska)

massif, and the most (2,300) and the largest of them are in the High Tatra. Their size, number, and distribution mainly depend on local topography and substrate properties.

2. Extreme summer rainfalls (short-term storms with very intensive convection) confined to small areas are the main trigger of debris flows. Therefore, there is *no clear relationship* between periods of high *daily precipitation* and the *triggering of rapid mass movements* in the Tatras. It is exemplified by the lack of debris flows in May and June 2010. The long-lasting precipitation which resulted in catastrophic landslides observed in the Flysch Carpathians did not generate debris flows in the Tatras. At that time, the snow cover of the last winter was still present in the Tatras and prevented rapid runoff.
3. The zone of the highest precipitation on the northern side of the Tatra massif (1,400–2,000 m elevation) overlaps with the zone where *debris flows start* (1,290–2,390 m). This fact underlines the role of precipitation in the present-day relief evolution of the Tatras.

References

Bajgier-Kowalska M (2011) Procesy osuwiskowe w gminie Lanckorona na Pogórzu Wielickim jako efekt rozlewnych opadów w maju 2010 roku (Landslide processes in the Lanckorona district of the Wielickie Foothills as a result of extreme rainfall events in May 2010). Probl Zagospod Ziem Górskich 58:27–39 (in Polish)

Brunsden D (1979) Mass movements. In: Embleton C, Thornes J (eds) Process in geomorphology. Edward Arnold, London, pp 130–186

Cebulak E (1983) Maximum daily rainfalls in the Tatra Mountains and Podhale Basin. Zesz Nauk UJ Pr Geogr 57:337–343

Grochocka-Piotrowska K (1970) Fotointerpretacja i geneza struktur nieciągłych w masywie granitowym polskiej części Tatr Wysokich (Photointerpretation and genesis of the disjunctive structures in the granite massif of the Polish Tatra Mts). Acta Geol Pol 20(2):365–411 (in Polish with English summary)

Guzik M, Struś P, Celer S, Borowski M (2006) Ortofotomapa satelitarna Tatr (The satellite orthophotomap of the Tatra Mountains). In: Tatrzański Park Narodowy na tle innych górskich terenów chronionych I, pp 131–134 (in Polish)

Hess M (1965) Piętra klimatyczne w polskich Karpatach Zachodnich (Vertical climatic zones in the Polish Western Carpathians). Zesz Nauk UJ Pr Geogr 11:1–267 (in Polish with English summary)

Hreško J, Bugár G, Boltižiar M, Kohút K (2008) The dynamics of recent geomorphic processes in the alpine zone of the Tatra Mountains. Geogr Pol 81(1):53–65

Innes JL (1983) Debris flows. Prog Phys Geogr 7(4):469–501

Jahn A (1958) Mikrorelief peryglacjalny Tatr i Babiej Góry (Periglacial microrelief of the Tatras and Babia Góra Massif) Biul Peryglac 4:227–249 (in Polish)

Janačik (1971) Niektoré poznatky z inventarizačneho výskumu v chránenej krajinej oblasti Malé Fatra (Some piece of knowledge of the inventory research and investigation in the protected landscape region of Malá Fatra Krivánská). Geogr čas 23(2):186–191 (in Slovak with English summary)

Kapusta J, Stankoviansky M, Boltižiar M (2010) Changes in activity and geomorphic effectiveness of debris flows in the High Tatra Mts within the last six decades (on the example of the Velická Dolina and Dolina Zeleného plesa valleys). Studia Geomorphol Carpath Balcanic 44:3–34

Kijowska M (2011) The role of downpours in transformation of slopes in the Polish Carpathian foothills. Studia Geomorphol Carpath Balcanic 45:69–87
Klimaszewski M (1988) Relief of the Polish Tatra Mountains. PWN, Warszawa, 668 p (in Polish)
Kotarba A (1989) On the age of debris flows in the Tatra Mountains. Studia Geomorphol Carpath-Balcanic 23:139–152
Kotarba A (1992) High-energy geomorphic events in the polish Tatra Mountains. Geogr Ann 74A (2–3):123–131
Kotarba A (1995) Rapid mass wasting over the last 500 years in the High Tatra Mountains. Quaest Geogr Spec 4:177–183
Kotarba A (1997) Formation of high-mountain talus slopes related to debris-flow activity in the High Tatra Mountains. Permafr Periglac Process 8:191–204
Kotarba A (1998) Morfogenetyczna rola opadów deszczowych w modelowaniu rzeźby Tatr podczas letniej powodzi w roku 1997 (Morphological role of rainfalls in modeling of Tatra relief during summer flood of 1997). Dok Geogr 12:9–23 (in Polish)
Kotarba A (2004) Zdarzenia geomorfologiczne w Tatrach Wysokich podczas małej epoki lodowej (Geomorphic events in the High Tatra Mountains during the Little Ice Age). Pr Geogr Inst Geogr Przestrz Zagospod PAN 197:9–55 (in Polish)
Kotarba A, Starkel L (1972) Holocene morphogenetic altitudinal zones in the Carpathians. Studia Geomorphol Carpath Balcanic 6:21–35
Kotarba A, Strömquist L (1984) Transport, sorting and deposition processes of alpine debris slope deposits in the Polish Tatra Mountains. Geogr Ann 66A(4):285–294
Kotarba A, Kaszowski L, Krzemień K (1987) High-mountain denudational system in the Polish Tatra Mountains. Pr Geogr Inst Geogr Przestrz Zagospod PAN, Special Issue 3, 106 p
Krzemień K (1988) The dynamics of debris flows in the upper part of the Staroroboci ańska Valley (Western Tatra Mts.). Studia Geomorphol Carpath Balcanic 22:123–144
Krzemień K (1989) Struktura i dynamika spływów gruzowych w krystalicznej części Tatr Zachodnich (Structure and dynamics of debris flows in cristalline part of Western Tatra Mts). Zesz Nauk UJ Pr Geogr 73:149–171 (in Polish)
Krzemień K (1991) Dynamika wysokogórskiego systemu fluwialnego na przykładzie Tatr Zachodnich [Dynamics of the high-mountain fluvial system with the Western Tatra Mts. as example]. Rozprawy habilitacyjne UJ 215:1–160, (in Polish, with an English summary)
Krzemień K, Libelt P, Mączka T (1995) Geomorphological conditions on the timberline in the Western Tatra Mountains. Zesz Nauk UJ Pr Geogr 98:155–170
Łajczak A (1966) Hydrologia (Hydrology). In: Przyroda Tatrzańskiego Parku Narodowego (Nature of the Tatra National Park). Zakopane – Kraków, pp 169–196 (in Polish)
Lukniš M (1973) Relief Vysokých Tatier a ich predpolia (Relief of the High Tatra and their foreland). Bratislava, 375 p (in Slovak)
Midriak R (1984) Debris flows and their occurrence in the Czechoslovak Carpathians. Studia Geomorphol Carpath Balcanic 18:135–149
Midriak R (1995) Natural hazard of the surface in the Tatras Biosphere. Ekol Bratisl 14(4):433–444
Miętus M, Ustrnul Z, Marosz M, Owczarek M, Biernacik D, Czekierda D, Kilar P, Czernecki B (2010a) Biuletyn monitoringu klimatu Polski. Maj 2010 (Monthly climate monitoring bulletin. May 2010). Warszawa, http://www.imgw.pl/ (in Polish)
Miętus M, Ustrnul Z, Marosz M, Owczarek M, Biernacik D, Czekierda D, Kilar P, Czernecki B (2010b) Biuletyn monitoringu klimatu Polski. Czerwiec 2010 (Monthly climate monitoring bulletin. June 2010). Warszawa, http://www.imgw.pl/ (in Polish)
Nemčok A (1982) Zosuvy v slovenských Karpatoch (Landslides in the Slovak Carpathians). Veda, Bratislava, 319 p (in Slovak)
Nemčok J, Bezák V, Biely A, Gorek A, Gross P, Halouzka R, Janák M, Kahan Š, Kotański Z, Lefeld J, Mello J, Reichwalder P, Rączkowski W, Roniewicz P, Ryka W, Wieczorek J, Zelman J (1994) Geologická mapa Tatier 1:50 000 (Geological map of the Tatra Mts, 1:50 000). Geologicky ústav Dionyza Štúra, Bratislava

Niedźwiedź T (1992) Climate of the Tatra Mountains. Mt Res Dev 12(2):131–146
Niedźwiedź T (2003) Extreme precipitation events on the northern side of the Tatra mountains. Geogr Pol 76(2):15–23
Rączkowska Z (1999) Slope dynamics in the periglacial zone of the Tatra Mountains. Biul Peryglac 38:127–133
Rączkowska Z (2006) Recent geomorphic hazards in the Tatra Mountains. Studia Geomorphol Carpath Balcanic 40:45–60
Rączkowska Z (2007) Współczesna rzeźba peryglacjalna wysokich gór Europy (Present-day periglacial relief in the high mountains of Europe). Pr Geogr Inst Geogr Przestrz Zagosp PAN 212: 252 p
Starkel L (1980) Altitudinal zones in mountain with continental climates. Pr Geogr Inst Geogr Przestrz Zagosp PAN 136:91–102
Wiśliński (1996) Nowe mapy płatów firnu i lodu w Tatrach Polskich (New map of firn and ice patches in the Polish Tatra Mountains). In: Przyroda Tatrzańskiego Parku Narodowego a Człowiek, 1, Nauki o Ziemi, Kraków-Zakopane, pp 126–127

Chapter 15
Landslide Hazards in the Polish Flysch Carpathians: Example of Łososina Dolna Commune

Elżbieta Gorczyca, Dominika Wrońska-Wałach, and Michał Długosz

Abstract Lithology and tectonics (jointing, faulting) combined with relative relief and steep slopes induce slope failures in the Polish Flysch Carpathians. Therefore, landslides are frequent within inhabited areas of the Polish Carpathians and a major problem for local communes. This chapter presents a case study from a rural commune, which is located on the borderline between the Beskid Wyspowy Mountains and the Carpathian Foothills. The local geology makes that area extremely susceptible to landslides. A recent episode of landslide reactivation occurred in May and June of 2010 there, as a result of the clustering of continuous and heavy rainfalls, which appear to be the most important factor capable of triggering diverse types of mass movement. The analysis was based on the field-work conducted in 2010–2011 in the Łososina Dolna Commune and the research methods established by Polish National Geological Institute for the SOPO Landslide Protection Program. A total of 572 landslides were identified and documented in the study area, which occupies 17.2% of Łososina Dolna Commune. This contribution demonstrates that mass movements are significant processes which limit human activities.

Keywords Landslide hazard • Heavy rainfalls • SOPO • Polish Flysch Carpathians

E. Gorczyca (✉) • D. Wrońska-Wałach
Institute of Geography and Spatial Management, Jagiellonian University,
ul. Gronostajowa 7, 30-387 Cracow, Poland
e-mail: e.gorczyca@geo.uj.edu.pl; dominika.wronska-walach@uj.edu.pl; d.wronska@gmail.com

M. Długosz
Department of Geoenvironmental Research, Institute of Geography and Spatial Organisation,
Polish Academy of Sciences, str. Św. Jana 22, 31-018 Cracow, Poland
e-mail: dlugosz@zg.pan.krakow.pl

D. Lóczy (ed.), *Geomorphological impacts of extreme weather: Case studies from central and eastern Europe*, Springer Geography, DOI 10.1007/978-94-007-6301-2_15,

15.1 Introduction

Slope instability can be due to natural and anthropogenic factors. Instability on natural slopes is a complex process, which usually requires long-term slope evolution (Crozier 1986). On the other hand, in areas affected by human impact, slope instability may arise in a matter of hours. J. Corominas (1996) described the most common elements of *human impact* leading to mass movements: housing development in areas not suited to construction (e.g., areas of old landslides), poorly executed earthworks prior to housing development, poor drainage of the construction site, and excessive undercutting of slopes during road construction. In addition, shallow niches and small depressions resulting from shallow landslides on slopes with weathering mantles are not regarded as inappropriate sites in housing and other types of construction. Landforms of this type point to future landslide activity, and housing development in such areas should be considered a planning mistake.

Landslide hazard has increased substantially worldwide over the last 100 years. This is associated with growing population numbers and more and more properties located in landslide-prone areas (Crozier 1986). There appears to be a difference in this realm between developed nations and developing nations. In developing nations, landslides tend to threaten human life, while in developed nations, they only endanger property.

Landslides are frequent in the Carpathians and constitute a problem for local communities. About 20,000 landslides occur in the region and extend over almost 20% of the area (Chowaniec et al. 1975; Mrozek et al. 2000), including more than 7,000 km^2 in the Polish Carpathians (36% of the total area – Długosz 2009, 2011). Our study area is the commune of Łososina Dolna – one of the most active landslide areas, where large-scale landslides occurred following intense precipitation in 2010.

15.2 Research on Landslide Hazards in the Polish Carpathians

Contemporary landslide research in the Polish Flysch Carpathians is focused on geographical and physical differences between landslides. The research is conducted by the Carpathian Division of the National Geological Institute in Kraków and has produced a *landslide map* of the Polish Flysch Carpathians (scale, 1:200,000; Bober 1985) and a monograph on Carpathian landslides (Bober 1990). One of the most important works on landslides in recent years was published by L. Zabuski et al. (1999), which is a summary of landslide research in the Polish part of the Flysch Carpathians, focusing on the relationships between the geological structure of selected nappes and landslides as well as slope evolution and slope stability.

Landslide hazards, the negative impacts of landslides, and the associated economic damage estimates are rarely presented in literature, mostly only considered in the case of major construction projects (Bober 1975; Wójcik and Rączkowski 2001). Several papers on rainfall and flood damage were published after 1997 (Oszczypko

et al. 2002; Poprawa and Rączkowski 2003; Gorczyca 2004; Wrońska 2004–2005; Rączkowski 2007). The single comprehensive paper on landslide risk in the Polish Carpathians was prepared by T. Mrozek (2008), who introduced a consistent terminology and a number of research methods previously not used in the Carpathians.

The landslides in Łososina Dolna were first mapped in the 1930s (Sokołowski 1935). Between 1967 and 1970, the National Geological Institute catalogued landslides in the commune. Landslide processes were studied in detail in the Rożnowskie Foothills by Ziętara (1973, 1974), who noted that landslides had occurred in the study area seven times in the period 1934–1974 (1934, 1940, 1948, 1958, 1960, 1970, 1972). Ziętara (1973) also noted that the Rożnowski Reservoir had affected landslide activity in the area. Łososina Dolna experienced a catastrophic rainfall and flooding in 1997, which generated landslides, analyzed by Poprawa et al. (1997) and Gorczyca (2004).

15.3 Study Area

Łososina Dolna Commune is located in the Outer Carpathian geological unit, which consists of the Cretaceous and Paleogene flysch rocks of the Magura Nappe, Grybów unit, Silesian Nappe, and Michalczów zone (Burtan and Skoczylas-Ciszewska 1964; Cieszkowski 1992; Burtan et al. 1991; Paul 1997). The Magura Nappe and the Grybów unit coincide with the mountainous part of the commune (ca 49.5% of area). The foothill part of the commune is built of rocks of the Silesian unit (ca. 35%) and Michalczów zone rocks (15.5%) (Cieszkowski 1992 – Fig. 15.1).

Łososina Dolna Commune is found on the borderline between the Beskid Wyspowy Mountains (highest point: Jaworz, 921 m) and the Carpathian Foothills (Wieliczka Foothills, Ostra Góra, 455 m – Starkel 1972) (Fig. 15.1). The Beskid Wyspowy are low and middle mountains and middle foothills (Starkel 1972) with slope gradients ranging from 10° to 35° and elevations from 300 to 340 m in the mountainous part and 140 and 180 m in the foothills. Here slope lengths range from 0.6 to 1 km, while they are between 5° and 25° at elevations of 120–150 m in the foothills.

Łososina Dolna Commune lies next to the Rożnowskie Reservoir, which was built in the 1930s on the Dunajec River. The smaller part of the commune is drained by the Łososina River. The area is largely deforested and experiences a high rate of throughflow and short flood wave concentration times (Starkel 1991).

Łososina Dolna is a rural commune (area, ca. 84 km^2; population, 10,175; population density, 120 people per km^2 (2010 data – www.stat.gov.pl)). The part of the commune close to the Rożnowskie Reservoir grew rather rapidly in terms of population between 1978 and 1988 (more than 1% per year – Soja 2008). In the mostly agricultural (54%) commune, forests occupy 26%. Due to its attractive landscape and

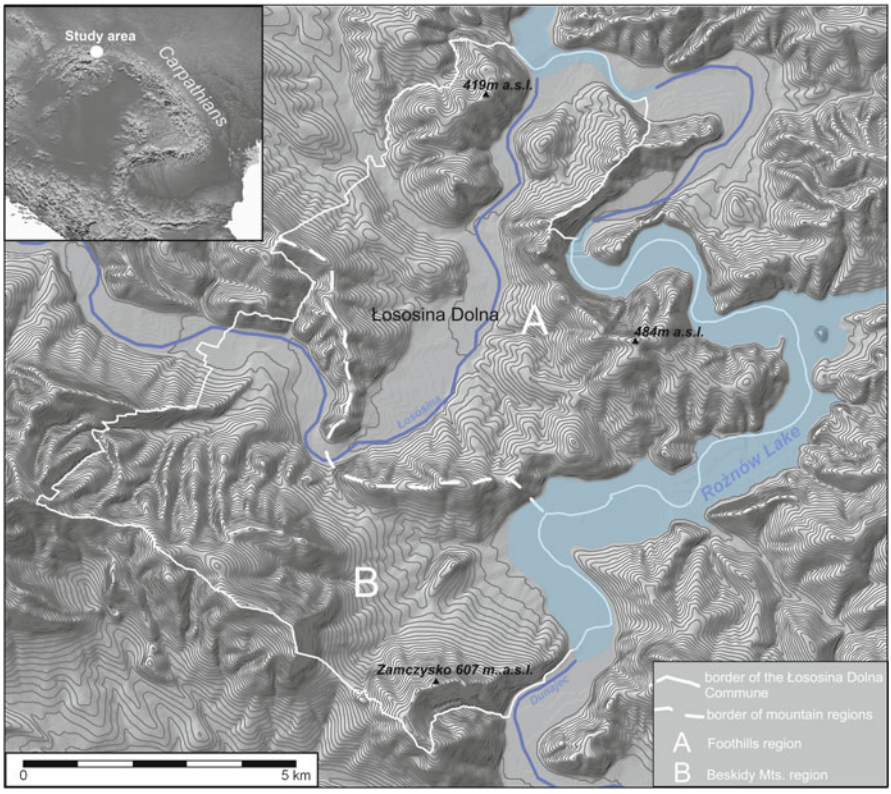

Fig. 15.1 Location of the study area

recreational opportunities, Łososina Dolna is popular with tourists. Recreational activities are centered on the Rożnowskie Reservoir. Residential areas are scattered but more compact built-up areas are found in valleys and single homesteads at high elevations (750 m) on slopes, forest clearings, and drainage divides.

15.4 Methods

For the research, methods approved by the Polish National Geological Institute for the SOPO Landslide Protection Program (Grabowski et al. 2008) were used. Fieldwork was done in 2010–2011 and topographic maps (at 1:10,000 scale) were produced on their basis. Fieldwork and laboratory data were represented on the map of areas of existing landslides and of those threatened by landslides. This involved the identification and documentation of landslides through detailed geomorphological/geological analyses, the assessment of activity and landslide development potential, and risk assessment for local residential buildings and commune infrastructure.

15.5 Results and Discussion

15.5.1 Landslide Activation Factors

Most of the landslides in Łososina Dolna Commune were probably triggered by natural causes. It may be assumed that, along with favorable rock stratification, infiltrating rainwater and snowmelt contributed to their activation. The Magura overthrust and numerous tectonic weakness zones may have also contributed to landslide activation. Other important triggers include river erosion undercutting slopes, reservoir construction on the Dunajec River, and, to a lesser extent, abundant springs on slopes and in cones of depression. Today *human impact* (shocks and vibration deriving from road traffic, terracing of slopes housing development, and improper drainage of slopes) may also play a role in triggering landslides.

In the summer of 2010, the activation of landslides in the Carpathians was the result of high and frequent precipitation in May and June. Precipitation in the Carpathians between April and September of 2010 was much higher than the 1971–2000 average (IMIGW Bulletin of Polish Climate Monitoring). Two precipitation periods of several days each were the most important in the activation of landslides in 2010. The first spell occurred from 15 May to 20 May and was associated with a rain-bearing low moving along track Vb from the Adriatic Sea to the Balkans and the Carpathians. The highest precipitation (in excess of 300 mm) was recorded in the Western Carpathians. The second spell of May 31–June 4 was due to another low pressure system moving from the Atlantic Ocean to southern Germany and then to the Carpathians in Romania. The highest precipitation – above 150 mm day^{-1} – was recorded across the Beskid Wyspowy Mountains and the Nowosadecka Basin.

Enduring rainfalls of variable intensity may trigger landslides. Continuous precipitation in the Flysch Carpathians (cumulative rainfall amount, 50–400 mm over the course of 2–5 days) is capable of inducing mudslides and debris slides (Starkel 1996; Gil 1997), while for deep rockslides long-lasting continuous precipitation totaling 100–500 mm per month is necessary. The requirements were met in Łososina Dolna Commune in May and June 2010, when shallow mudslides and debris slides as well as rock and debris slides were generated.

15.5.2 Landslide Development on Slopes

Research done as part of the SOPO Landslide Protection Program in Łososina Dolna commune made it possible to identify and document 572 landslides in 2010 with a total area of 1,280 ha. This included 298 fully active landslides, 69 partially active landslides, and 205 inactive landslides (Fig. 15.2). More than half of the documented landslides were small in area – 325 had an area of less than 1 ha (total area, 102.5 ha), 185 had an area of 1–5 ha (total area, 425.9 ha), 33 had an area of

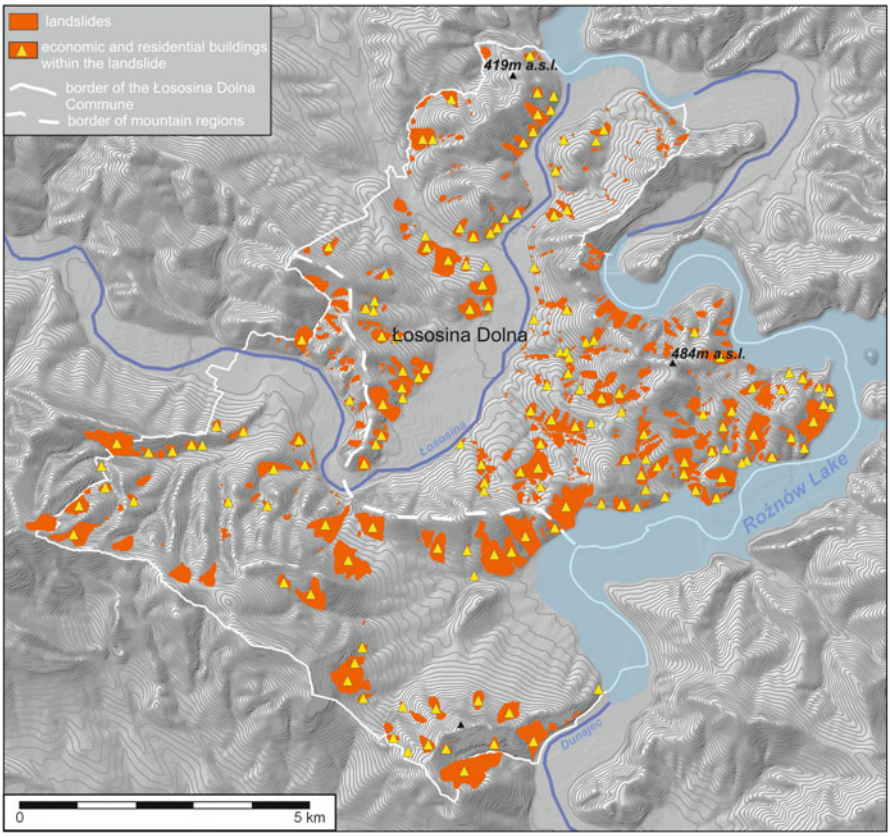

Fig. 15.2 Location of landslides in Łososina Dolna Commune

5–10 ha (total area, 223.46 ha), and 29 had an area of more than 10 ha (total area, 525.43 ha). Large inactive landslides were usually found in the Beskid Wyspowy part of the commune: in woodland areas, on upper slope segments, and in cones of depression. The area most prone to landslide activity is directly adjacent to the Rożanowski Reservoir. The mean size of the analyzed landslides is 2.3 ha, and maximum size is 45 ha.

The *landslide surface density index Op* was calculated for the study area using Bober's formula (1984). The index measures the relationship between the total landslide area (*Po*) in a given region and the surface area (*Pr*) (without valley bottom and terraces) of that region. The *Op* index for Łososina Dolna Commune is 17.2%, with a *Pr* value of 74.91 km^2. A second index was also calculated for the study area – the *landslide density index G*, which is the relationship between the number of landslides (*n*) in a given region and the surface area of the given region (*Pr*). The *G* index for Łososina Dolna Commune is 8 landslides per km^2. Most of the landslides in the study area are (translational, rotational, or combined) rock-debris slides or typical debris slides.

Table 15.1 Characteristics of and losses/damage from landslide in Łososina Dolna Commune

	Beskid Wyspowy mountains	Foothills
Percentage of commune area	47	53
Number of landslides	178	395
Surface area of landslides (ha)	570	710
Number of active landslides	108	190
Surface area of active landslides (ha)	253	290
Number of partially active landslides	12	54
Surface area of partially active landslides (ha)	118	175
Landslides causing damage to buildings	23	26
Destroyed and damaged houses	38	32
Destroyed and damaged farm buildings	40	32
Landslides causing damage to roads	19	26
Landslides causing damage to power lines	15	16
Landslides causing damage to field crops	14	12
Landslides causing damage to orchards	11	7

The following *landslide classification* is based on a division of Łososina Dolna Commune into a Beskid Wyspowy part (47% of area) and a foothill part (53%) with respect to the principal tectonic units. A total of 178 landslides (31% of all landslides) were identified in the Beskid Wyspowy (Magura, Grybów, partly Silesian units) with a total area of 570.1 ha (44.5% of the area of all the landslides in the commune). Landslides in the Beskid Wyspowy part of the commune were found mostly in cones of depression as well as covering entire slopes or on lower parts of slopes. The main scarps of these landslides are usually 3–6 m, exceptionally 10 m high, and scarp gradients are about 35°. Secondary scarps are quite common in large landslides along with accumulation thresholds, colluvial hills, mid-landslide depressions, rock formations, and debris crevices. Most of the landslides documented in this area had a toe front up to 3 m high. The scarps lead down to valley floors or river terraces. The colluvial material is mainly composed of weathering debris, clay with debris, silt, and pure clay.

Landslides on upper slope segments and in cones of depression tend to be overgrown with trees, and most of them did not activate in 2010. Most landslides which were active in 2010 were found on lower slopes and in smaller valleys, on open terrain (abandoned or still cultivated arable land or meadows).

The majority of landslides are fully active (108 instances with an area of 253 ha) or partially active (12; 118 ha), presenting a major problem for transportation and construction (Table 15.1). About 80 buildings were destroyed or damaged by 23 landslides (Fig. 15.3). Roads, including a national highway, were seriously damaged by 19 landslides, power transmission lines by 15, arable crops by 14, and orchards by 11 landslides.

The Magura nappe strata are the most prone to sliding, especially when in contact with the hieroglyphic beds containing variegated shales. The dip of the strata is generally to the south and southwest; dip angles range from 15° to 60°. The major landslides, primarily found on north-facing slopes, tend to be complex

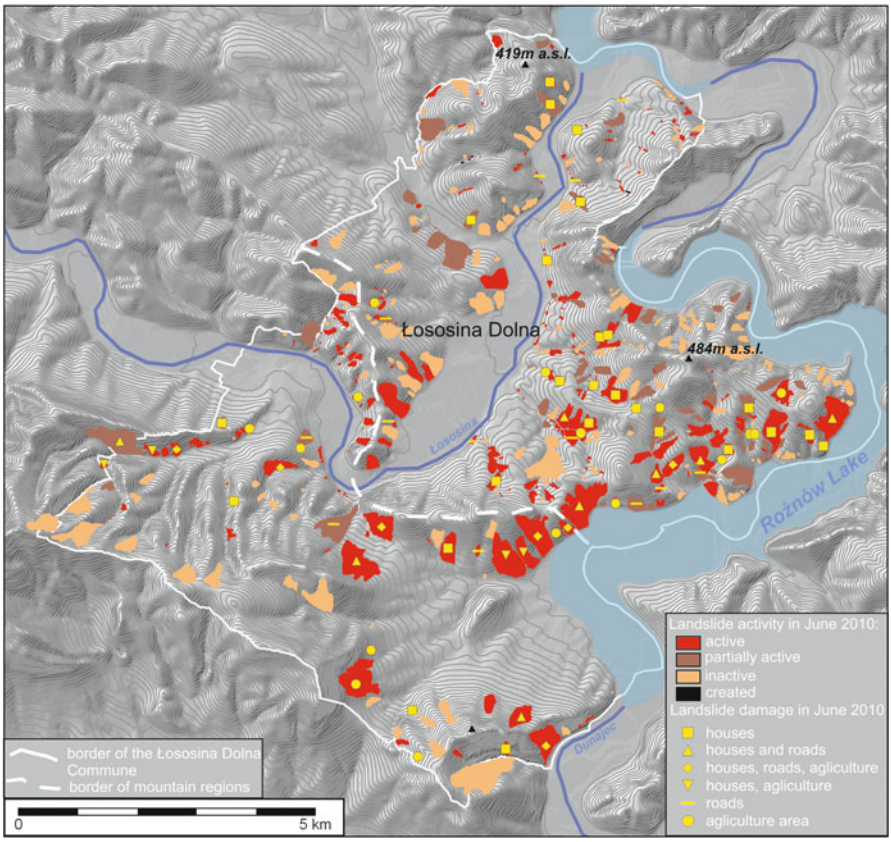

Fig. 15.3 Location of landslides reactivated in June 2010

landforms, while those on south-facing slopes tend to be insequent or subsequent features. Consequent landslides are quite rare. The landslides formed in sandstone and shale facies or in sandstone in contact with shale and marl generally face towards the southwest, and their gradient ranges from 30° to 60°.

In the Silesian unit and the Michalczów zone of the foothills, a total of 395 landslides (69% of all movements) were identified with a total area of 710.5 ha (55.5%). The largest number of landslides can be found in the middle and eastern parts, in the Dunajec River catchment along the Rożnowski Reservoir, mainly on lower slopes. Eight landslides were more than 10 ha in area. The total area of 178 minor landslides was 141 ha. Most landslides show clearly defined boundaries – particularly those activated in 2010. The main head scarps are usually 3 m high, for major features 6–10 m. Most scarp gradients are ca. 20°. Landslides larger than 5 ha feature accumulation thresholds, colluvial hills, and mid-landslide depressions.

Nearly half of the landslides in the area are fully *active* (190; 290 ha). There are also 54 partially active landforms (total area, 175 ha). Together they are a major

threat to transportation infrastructure and built-up areas (Table 15.1; Fig. 15.3). Buildings and roads were destroyed or damaged by 26 landslides. Sixty homes and other buildings as well as 26 road sections were affected. Sixteen landslides damaged transmission lines. Field crops were substantially damaged by 12 landslides, and orchards were damaged by 7 landslides.

Landslides found in the Silesian unit sandstone in contact with variegated shales and hieroglyphic beds generally dipping towards the south have gradients between 10° and 60°. Major (complex insequent) landslides are mainly found next to the Rożnowski Reservoir. The Silesian unit also includes the unique Michalczów zone of NW–SE strike, the sandstones and shales (30–70° SSE dip) of which are extremely prone to landslides.

15.5.3 Threats to Infrastructure

Landslides in Łososina Dolna Commune are found on meadows, pastures, orchards, and arable land. Forests and bushes are rather rare, except in the Beskid Wyspowy and also at higher elevations and in cones of depression. In the foothills, forests cover steep slopes of valleys and those of the Rożnowski Reservoir. Residential houses, commercial buildings, and roads are found on 160 landslides, and 468 homes and 432 commercial buildings are on active and inactive landslides in 2010 on nearly 100 active landslides. Severe damage to property has been recorded on 49 landslides – almost 140 destroyed or damaged buildings (Fig. 15.4). Active landslides (in 45 instances) also threaten roads. Road surfaces and embankments were damaged in many parts of the commune. Many roads only suffered minor cracking, but national highway no. 75 is threatened by nine active landslides and ten periodically active and inactive landslides. The highway suffered major damage at some locations in 2010 (Fig. 15.4).

The large number of new and old buildings situated atop landslides is the result of inadequate landslide identification and the lack of local zoning laws. *Flat terrains* appear to be naturally suited for development (Fig. 15.5). Large packet-type landslides consisting of rocks and weathering material and formed in the Magura and sub-Magura units show numerous flat surfaces, particularly in the Beskid Wyspowy. Mass movements have been found to exert a positive effect on human settlement patterns. Margielewski (2000) states that past landslides offered an opportunity to settle at higher elevations, especially in the Beskids. Landslides reduced slope gradients, which made human settlement more likely. Other favorable features of landslide areas include springs, relatively deep soils, and a locally milder mountain climate promoting agriculture and animal husbandry.

Two examples of the above landslides are given below, with buildings found in landslide niches, on colluvial ridges, or on small flat colluvial surfaces:

1. The Łyczanka landslide is a large rock–regolith movement with an area of 17 ha, active in the entire area. The landslide has been substantially altered by cultivation. The landslide reactivated and its upper portion extended in 2010,

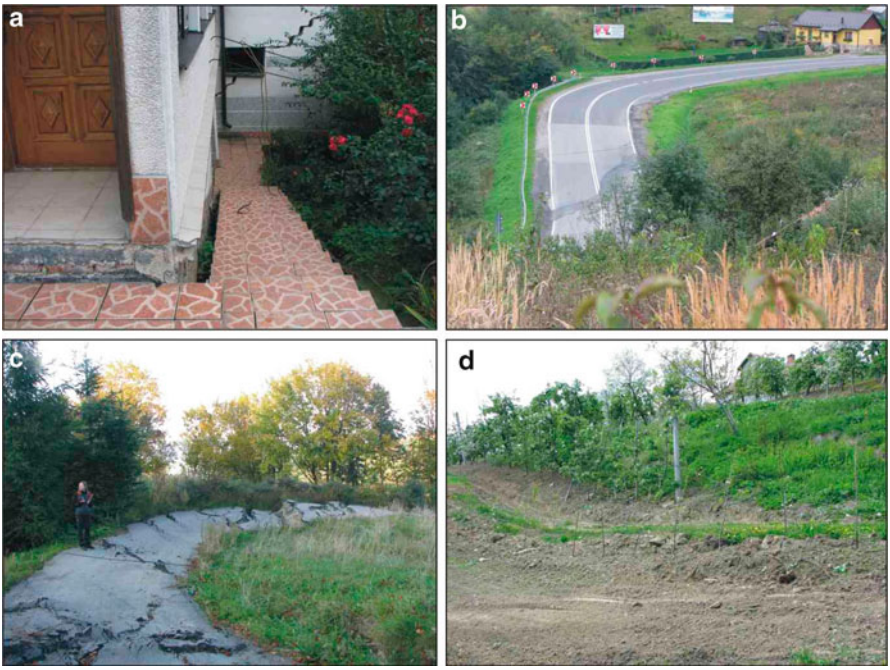

Fig. 15.4 Examples of landslides damage in Łososina Dolna Commune. (**a**) Damaged house; (**b**) damaged national highway; (**c**) damaged local road; (**d**) damaged orchard

Fig. 15.5 Examples of houses located in landslide niches

destroying or damaging six buildings in the northwestern part. Roads and transmission lines were also damaged. Further activity of the landslide will threaten all buildings and roads situated across the landform (Fig. 15.6).

2. The Tęgoborze-Struga landslide has an area of 35 ha and consists of several movements scattered across the slopes of the Dunajec River (today the Rożnowski Reservoir). Head scarp heights range from 1 to 18 m, and there are

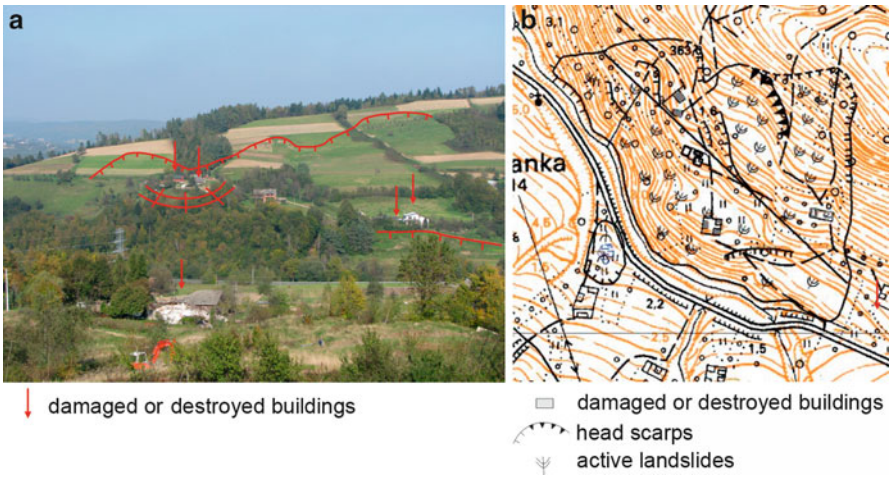

Fig. 15.6 The Łyczanka landslide. (**a**) location of damage; (**b**) diagram of landslide

numerous secondary scarps and sagging hollows. The landslide is active over almost 90% of its area. Further activity may inflict immense damage to a large number of residential and farm buildings (15 houses, 8 farm buildings, 20 summer homes). In 2010 six buildings suffered minor damage (cracked walls). Paved roads (at eight locations) and unsurfaced roads were also affected.

15.6 Conclusions

1. The large-scale activation of landslides in Łososina Dolna Commune was caused by the *clustering* of two precipitation *events*. The intensity of precipitation and large precipitation amounts promoted the activation of shallow landslides, mudslides, and deep rockslides.
2. The immediate causes of extreme landslide damage to buildings and roads in Łososina Dolna Commune are the location of *buildings atop old landslides* and *poor drainage* of landslide slopes. Indirect causes included the scattering of housing across large areas and a high population density.
3. The areas most prone to landslides are those built of *sandstones* and *shales*. All landslides located on variegated shales also became activated.
4. A comparison of relief changes caused by landslides in all of Łososina Dolna Commune makes it possible to outline the following trends:
   - The number of landslides in the foothills is double that in the Beskid Wyspowy.

- The surface area occupied by landslides is comparable for both parts of the commune; the total landslide area in the Beskid Wyspowy is more extensive than in the foothills.
- Differences in the parameters of the investigated landslides are the result of variations in geological structure, relative relief, and land use (share of forests and farmlands).
- The large landslides found on woodland slopes in the Beskid Wyspowy did not activate in 2010.
- The extent of physical damage to buildings and roads is similar for both parts of the commune.

5. Given favorable hydrometeorological conditions, further landslide activity (of both active and inactive landslides in 2010) is quite possible in Łososina Dolna Commune. Landslides remain a threat to structures.
6. Landslide hazard here is due to exceptionally favorable natural conditions for mass movements (relative relief, lithology, tectonics, and hydrometeorological factors). Other factors that favor landslides in the commune include construction at inappropriate sites and other mistakes made by infrastructure planners following World War II.
7. Landslide hazard is substantially greater in its foothill part of the commune, where numerous active landslides developed in weathering material, population density is higher, and intensive agricultural cultivation is widespread.

References

Bober L (1975) Metody rozpoznawania budowy geologicznej zboczy osuwiskowych w Lipowicy, Kotelnicy i Dobczycach (Methods of surveying of geological conditions of landslide slopes in Lipowica, Kotelnica and Dobczyce communities). Materiały badawcze IMGW, Seria specjalna 4:113–135 (in Polish)

Bober L (1984) Rejony osuwiskowe w polskich Karpatach fliszowych i ich związek z budową geologiczną regionu (Landslide areas in the Polish Flysch Carpathians and their connection with the geological structure of the region). Biul Inst Geolog 340:115–158 (in Polish)

Bober L (1985) Mapa osuwiskowości polskich Karpat fliszowych – skala 1: 200 000 (Map of landslides in the Polish Carpathians – scale 1:200,000). Manuscript. Instytut Geologiczny Oddział Karpacki, Kraków

Bober L (1990) Monografia osuwisk karpackich (Monograph of Carpathian landslides). Manuscript Państwowy Instytut Geologiczny, Oddział Karpacki, Kraków (in Polish)

Burtan J, Skoczylas-Ciszewska K (1964) Szczegółowa Mapa Geologiczna Polski 1:50,000, arkusz Męcina (bez utworów czwartorzędowych) (Detailed geological map of Poland – 1:50,000, sheet Męcina (without Quaternary)). WG, Warszawa

Burtan J, Cieszkowski M, Ślączka A, Zuchiewicz W (1991) Szczegółowa Mapa Geologiczna Polski w skali 1:50,000, arkusz Męcina (1018) (Detailed map of the Polish Geological Survey at 1:50,000 scale sheet Męcina (1018)). Central. Arch. Geolog. PIG-PIB, Warszawa (in Polish)

Chowaniec J, Gierat-Nawrocka D, Kolasa K, Witek K, Wykowski A (1975) Katalog osuwisk województwa krakowskiego (Catalogue of landslides in the Cracow voivodeship). CAG – Archiwum Oddział Karpacki PIG-PIB, Kraków (in Polish)

Cieszkowski M (1992) Płaszczowina magurska i jej podłoże na północ od Kotliny Sądeckiej (Magura Nappe and its substrate north of the Nowy Sącz Basin). Przegląd Geologiczny 7:410–416 (in Polish with English summary)

Corominas J (1996) Debris slide. In: Dikau R, Brunsden D, Schrott L, Ibsen ML (eds) Landslide recognition. Identification, movement, and causes. Wiley, Chichester, pp 97–102

Crozier MJ (1986) Landslides: causes, consequences, and environment. Croom Helm, London, 252 p

Długosz M (2009) Landslide susceptibility zoning in the Polish Flysch Carpathians. Z Geomorpholo 53(Supplementary Issue 3):41–48

Długosz M (2011) Podatność stoków na osuwanie w polskich Karpatach fliszowych (Landslide susceptibility in the Polish Carpathians). Prace Geograficzne 230:112 p (in Polish with English summary)

Gil E (1997) Meteorological and hydrological conditions of landslides, Polish Flysch Carpathians. Studia Geomorphol Carpath Balcanic 31:143–158

Gorczyca E (2004) Przekształcenie stoków fliszowych przez procesy masowe podczas katastrofalnych opadów (dorzecze Łososiny) (The transformation of flysch slopes by catastrophic rainfall-induced mass processes (Łososina River catchment basin)). Wydawnictwo Uniwersytetu Jagiellońskiego, Kraków, 101 p (in Polish with English summary)

Grabowski D, Marciniec P, Mrozek T, Nescieruk P, Rączkowski W, Wójcik A, Zimnal Z (2008) Instrukcja opracowania mapy osuwisk i terenów zagrożonych ruchami masowymi (Manual for mapping landslides and areas threatened by mass movenents). PIG, Warszawa, 92 p (in Polish)

Margielewski W (2000) Gospodarcze znaczenie osuwisk Beskidu Makowskiego (Economic effects of the landslides in the Beskid Makowski Mts.). Problemy Zagospodarowania Ziem Górskich 46:15–34 (in Polish with English summary)

Mrozek T (2008) Ocena zagrożenia osuwiskowego i związanego z nim ryzyka przy wykorzystaniu metod GIS na przykładzie okolic Szymbarku, Beskid Niski (Landslide hazards and risk assessment using GIS methods: a case study from Szymbark region, Beskid Niski Mountains). Manuscript PhD thesis. National Geological Institute, Kraków, 186 p (in Polish)

Mrozek T, Rączkowski W, Limanówka D (2000) Recent landslides and triggering climatic conditions in Laskowa and Pleśna regions, Polish Carpathians. Studia Geomorphol Carpath Balcanic 34:89–109

Oszczypko N, Golonko J, Zuchiewicz W (2002) Osuwisko w Lachowicach (Beskidy Zachodnie): skutki powodzi z 2001r. (The landslide at Lachowice (Western Outer Carpathians, Poland): effects of catastrophic flood in 2001). Przegląd Geologiczny 50(10/1):893–898 (in Polish with English summary)

Paul Z (1997) Szczegółowa Mapa Geologiczna Polski w skali 1:50 000, arkusz Męcina (Polish Geological Map at a scale of 1:50 000, sheet Męcina). Central Arch Geolog. PIG-PIB, Warszawa (in Polish)

Poprawa D, Rączkowski W (2003) Osuwiska Karpat (Carpathian landslides (southern Poland) Przegląd Geologiczny 51(8):685–692 (in Polish)

Poprawa D, Rączkowski W, Dziopak P, Kopciowski R, Mrozek T, Niescieruk P, Zimnal Z (1997) Rejestracja osuwisk i innych zjawisk geodynamicznych na terenie województwa nowosądeckiego i tarnowskiego, powstałych w wyniku katastrofalnych opadów i powodzi 1997 r. (Inventory of landslides and other geodynamic phenomena caused by catastrophic rainfalls and flooding in the Nowy Sącz and Tarnów Regions in 1997). Manuscript. CAG—Archiwum OK PIG, Kraków, 1600 p (in Polish)

Rączkowski W (2007) Landslide hazard in the Polish Flysch Carpathians. Studia Geomorphol Carpath Balcanic 41:61–76

Soja M (2008) Cykle rozwoju ludności Karpat Polskich w XIX I XX wieku (Population growth cycles in the Polish Carpathian Mountains during the19th and 20th centuries). Wyd. IGiGP UJ, Kraków, 141 p (in Polish with English summary)

Sokołowski S (1935) Geologia doliny Dunajca miedzy Kurowem a Tropiem (Geology of Dunajec Valley between Kurów and Tropie). Kosmos 60:49–63 (in Polish)

Starkel L (1972) Charakterystyka rzeźby Polskich Karpat (i jej znaczenie dla gospodarki ludzkiej) (An outline of the relief of the Polish Carpathians and its economic importance). Problemy Zagospodarowania Ziem Górskich 10:57–150 (in Polish with English summary)

Starkel L (1991) Rzeźba terenu (Relief). In: Dynowska I, Maciejewski M (eds) Dorzecze górnej Wisły I. PWN, Warszawa–Kraków, pp 42–54 (in Polish)

Starkel L (1996) Geomorphic role of extreme rainfalls in the Polish Carpathians. Studia Geomorphol Carpath Balcanic 30:21–28

Wójcik A, Rączkowski W (2001) Osuwiska w dolinie Wisłoki na terenie projektowanego zbiornika w Kątach (Beskid Niski) (Landslides in the Wisłoka valley in the neighbourhood of projected reservoir at Kąty (Beskid Niski Mountains, Southern Poland). Przegląd Geologiczny 49:389–394 (in Polish with English summary)

Wrońska D (2004–2005) Wpływ procesów osuwiskowych na działalność człowieka oraz szatę roślinną Magurskiego Parku Narodowego (The influence of landsliding on human activity and vegetation cover in Magura National Park). Folia Geographica, Series Geographica–Physica 35–36:31–52 (in Polish with English summary)

Zabuski L, Thiel K, Bober L (1999) Osuwiska we fliszu Karpat polskich (Landslides in the flysch of the Polish Carpathians). Wydawnictwo Instytutu Budownictwa Wodnego, PAN, Gdańsk, 171 p

Ziętara T (1973) Obszary osuwiskowe w dolinie Dunajca nad Jeziorem Rożnowskim (Landslide areas on the Rożnowskie Water Reservoir (the Dunajec River Valley). Rocznik Sądecki 14:685–712 (in Polish)

Ziętara T (1974) Rola osuwisk w modelowaniu Pogórza Rożnowskiego (Role of landslides in modelling of the Rożnowskie Foothills). Studia Geomorphologica Carpatho–Balcanica 9:115–130 (in Polish)

Chapter 16
Landslides in the Romanian Curvature Carpathians in 2010

Mihai Micu, Dan Bălteanu, Dana Micu, Răzvan Zarea, and Ruţă Raluca

Abstract Similarly to many European countries, 2010 was a year of temperature and precipitation extremes in Romania. The spring showers that overlapped in numerous areas with snowmelt; the intense, torrential rainfalls in the summer; and the long-lasting autumn rains had either direct or indirect effects on the occurrence of numerous riverine floods, flash floods, and low-to-high-magnitude landslides. The Curvature area of the Romanian Carpathians was severely affected by flash floods and landslides, which caused damage to the extent of several millions of Euros. Through a series of case studies, this chapter presents the effects of spring and summer rains on landslide morphodynamics in Buzău County, manifested in either shallow earthslides, first-time failures, mudflow pulsations, or the reactivation of some deep-seated slides.

Keywords Landslides • Pulsating mudflow • Flash floods • Geomorphological mapping • Buzău County • Curvature Carpathians • Romania

16.1 Introduction

Following a longer series of extremely humid years (2002, 2005, 2006), 2010 was marked by precipitations high above the multiannual mean values throughout the Danube Basin. Due to synoptic conditions that basically involved pressure lows and front systems moving along a SE–NW trajectory from the Mediterranean and

M. Micu (✉) • D. Bălteanu • D. Micu
Institute of Geography, Romanian Academy of Sciences, Dimitrie Racoviţă 12, Sect. 2, 023993 Bucharest, Romania
e-mail: mikkutu@yahoo.com; igar@geoinst.ro

R. Zarea • R. Raluca
Romanian Waters Company, Buzău-Ialomiţa Branch, Bucegi 20 bis, Buzău, Romania
e-mail: razvan.zarea@daib.rowater.ro

D. Lóczy (ed.), *Geomorphological impacts of extreme weather: Case studies from central and eastern Europe*, Springer Geography, DOI 10.1007/978-94-007-6301-2_16,

Black Seas towards Central Europe and in west to east direction from the Atlantic Ocean to Eastern Europe, almost the entire Central and Eastern Europe was subject to severe flood and (sometimes related) slope instability events (ICPDR/IKSD 2012).

In Romania, the damage caused by floods and related processes in 2010 exceeded €870 million. Over 3,900 houses were affected, of which 863 destroyed; 110,000 ha of agricultural land flooded; 707 river bridges and 2,729 small bridges collapsed; 87 schools, 3 hospitals, and 33 churches damaged; and more than 5,000 km roads affected.

16.2 The Year 2010 in Romania: Hydrometeorological Situation

According to the Annual Environmental Report of the Ministry of Environment (2010), in Romania annual mean temperature was 0.7 °C higher than the multi-annual average (Fig. 16.1). Due to a rainy winter (January to March) and a very humid late autumn and winter (October to December), annual average precipitation (Fig. 16.2) (846.3 mm) exceeded by 33% the climatic normal. This weather did not only affect Romania but in the meantime extended over the entire Danubian region. According to the cited report (ICPDR/IKSD 2012), the deep snowpack and the overlapping spring showers registered in the basin sometimes twofold exceeded the multiannual mean value for the 1961–1990 reference interval – an absolute record for the period of instrumental meteorological observation. Intense pluvial and fluvial floods (inducing intensified lateral erosion and several landslides along rivers) started in winter (January) and continued into the spring and early summer.

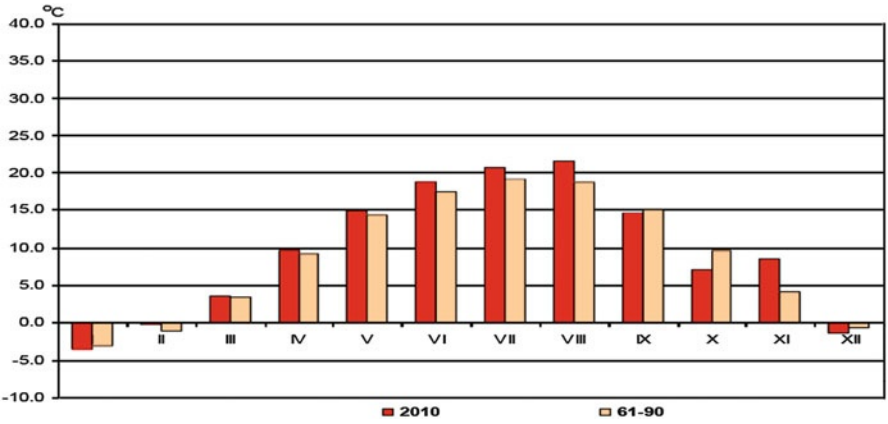

Fig. 16.1 Monthly mean temperatures (°C) in Romania in 2010, compared to mean multiannual values (1961–1990) (*Source*: Ministry of Environment 2010)

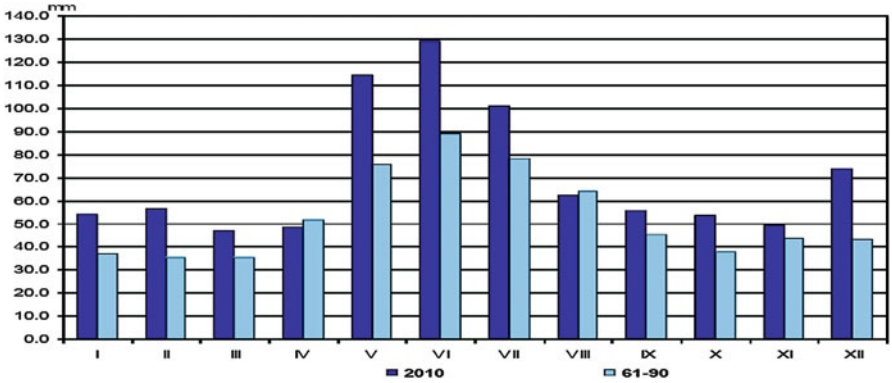

Fig. 16.2 Monthly mean precipitation (mm) in Romania in 2010, compared with mean multiannual values (1961–1990) (Ministry of Environment 2010)

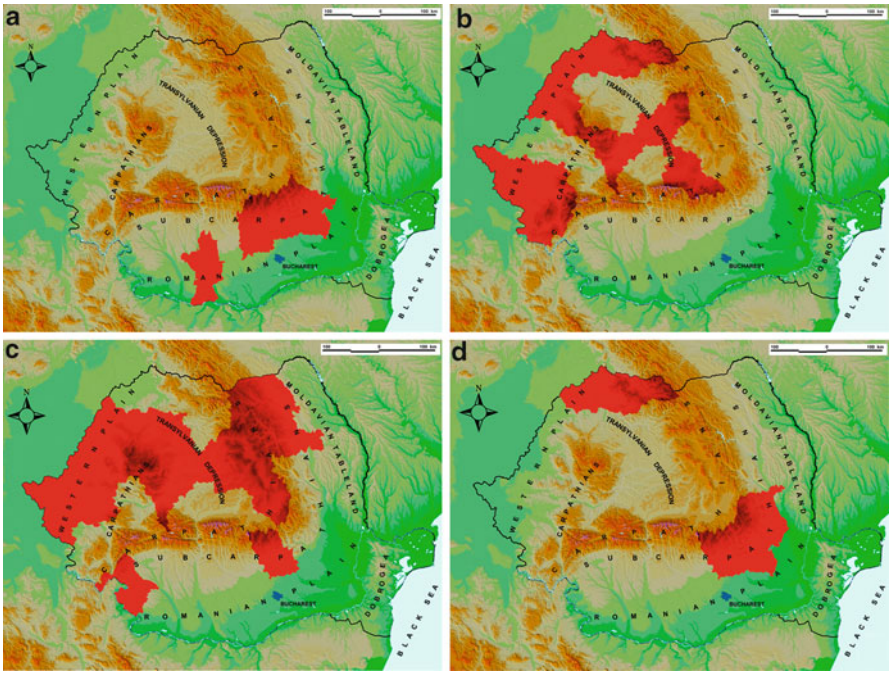

Fig. 16.3 Areas affected by riverine floods, flash floods, and landslides. (**a**) February–March, (**b**) May–June, (**c**) July, (**d**) November–December

In *Romania* diverse spatial and temporal *weather patterns* are typical (Fig. 16.3). The interval of 6–12 January was warm with above-zero temperatures, which generated snowmelt, and temperatures in February and March were also above the average in the regions outside the Carpathian Arc, especially in the south and

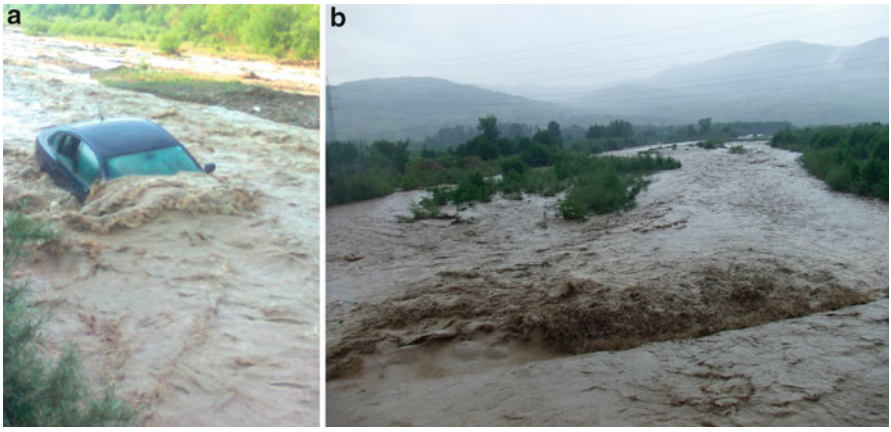

Fig. 16.4 Effects of the 16 May flash flood on the Bâsca Chiojdului catchment (**a**) Lera village, (**b**) Corbu village (Photo by R. Zarea)

southeast (in Olt, Dâmboviţa, Prahova, and Buzău counties). The months May and June were characterized by heavy precipitation in the western half of the country, due to an eastward extension of the same low that caused major floods in Austria, Slovakia, Hungary, and southwestern Ukraine (see Chap. 1 by Bartholy, Pongrácz, this volume). Also in June–July, numerous episodes of intense rainfall followed, exceeding 100 mm on the majority of Romanian territory. In the northeast monthly amounts up to 300 mm were recorded (annual average, 500–600 mm), first of all in the counties of Alba, Arad, Bihor, Cluj, Mehedinţi, Mureş, Neamţ, Sălaj, Suceava, and Timiş (Fig. 16.3). The floods affected 656 localities, causing the death of 24 persons, completely destroying 753 and severely damaging 9,769 households, and covering with water 100,000 ha of arable land. Along rivers like Siret, Prut (see Chap. 7 by Romanescu, this volume), Olt, Mureş, Someş, and Tisa, floods and numerous riparian landslides occurred, while flash floods in Harghita, Covasna, Suceava, and Prahova counties also caused severe damage (Figs. 16.4 and 16.5).

Towards the end of the year (in November and December), temperatures increased again (sometimes 3–6°C exceeding the monthly average), and several intense and long-lasting rainfalls (even downpours in December) advanced from the west, after causing severe floods in the Middle Danube Basin. Numerous landslides resulted from relatively high temperatures which delayed the freezing of the soil and from rainwater which could not infiltrate into the already saturated soil.

16.3 Study Area: Buzău County

With almost 6,100 km^2 area, half of which being mountainous and hilly, Buzău County is situated 110 km northeast of Bucharest (Fig. 16.6), in the heart of the Vrancea seismic region, which includes the Curvature sector of the Southeast

Fig. 16.5 The flash flood of July 2010 on the Drajna catchment (Ceraşu, Prahova County) overpassed bank protections by 2 m (**a**), damaging 18 households and causing numerous riparian landslides (**b**) through lateral erosion (Photo by M. Micu)

Romanian Carpathians, considered to be the most *active seismic region* with subcrustal earthquakes (at 80–160 km depths) in Europe (Lungu and Saito 2001). In this region of continental collision area, three or four major events ($M_w > 7$) occur per century.

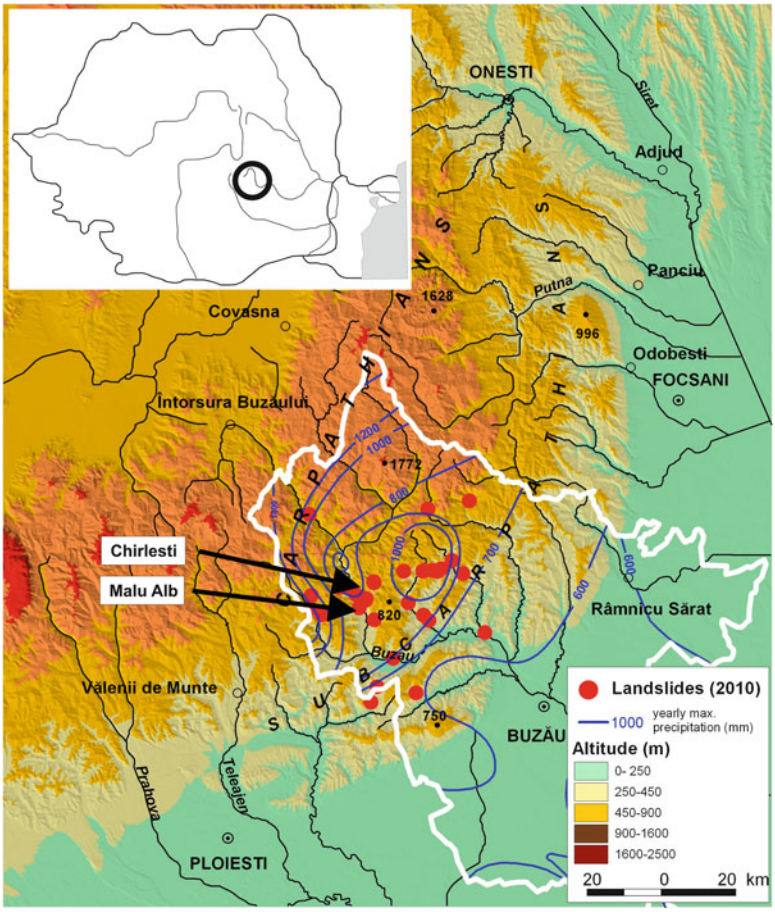

Fig. 16.6 Location of the study area (*in white*: the borders of Buzău County)

The northwestern half of the county belongs to the Buzău Carpathians and Subcarpathians and the southeastern half to the Romanian Plain. The mountain area is subdivided into two regions with different morphology, morphometry, and morphodynamic patterns. The interior is represented by the Carpathian Mountains, built of resistant Cretaceous and Paleogene flysch sediments, while the exterior consists of the hills and depressions of the Subcarpathians, corresponding to the less cohesive and heterogeneous Mio-Pliocene molasse formations. In addition to favorable lithology and structure, the neotectonic parameters (uplift rates of 5 mm year^{-1} in the mountain sector and 3–4 mm year^{-1} in the Subcarpathian hills – Zugrăvescu et al. 1998) and high seismicity make the area even more vulnerable to slope processes (Micu and Bălteanu 2009; Micu et al. 2010). The low-to-mid-altitude Carpathians, up to 1,300–1,700 m elevation, have 500–800 m relative relief, 8–10 km km^{-2} drainage density, and usual slope inclinations of 30–45°. The

Subcarpathians, with up to 900 m elevation, are featuring the morphometrical properties typical of loose molasse deposits (dominated by schistose marls and clays) with relative relief of 300–500 m; drainage density, 3–8 km km^{-2}; and slope inclinations, 30–45°.

The *climate* is of a moderate temperate hill and low-to-middle mountain type, marked by the Carpathian orographic barrier and a high foehn frequency (Sandu and Bălteanu 2005). The precipitation has a torrential character during the summer (frequently 80–100 mm in 24 h) and is often overlapping with the snowmelt of late spring. The annual amount ranges from 550 mm along the outer border of the Subcarpathians to 900–1,000 mm in the highest mountains. Monthly values peak at 70–150 mm in June, dropping to the minimum of 25–40 mm in February and March. This is reflected in mean slope denudation rates of 4–5 t ha^{-1} $year^{-1}$ in the mountains and over 13 t ha^{-1} $year^{-1}$ in the Subcarpathian hills (Moţoc 1983).

The favorable conditions of life (accessible relief, mild climate, the presence of salt deposits, the mountain–plain contact propitious to intense trade relations) have long allowed and encouraged *human activities*. Presently, the average population density of 90 inhabitants per km^2 rises to 150 inhabitants per km^2 along the valleys of the Buzău, Slănic, and Râmnic rivers. The direct result of population growth has been *land degradation* by overloading the slopes, changing the drainage pattern, and overgrazing (although the number of animals decreased in the last two decades) – encouraged by changes in land administration and ownership, especially after 1989.

Being one of the densest populated regions of Romania, with a developed network of villages spread along a dense river system, the region is heavily affected by *multiple hazards*, among which landslides, floods, and earthquakes are the most important. The presence of numerous elements at risk (villages, isolated households and a dense road network) requires appropriate hazard assessment and mapping for risk management and governance.

16.4 Methods

Throughout 2010, several field *geomorphological mapping* campaigns were launched to outline the places of occurrence and the morphometric changes of landslides. DGPS (Thales MobileMapper) measurements were performed at Malu Alb and Chirleşti (1 and 4 km north, respectively, of the Pătârlagele Natural Hazards Research Center, where daily temperature and precipitation data were recorded). The typology of landslides, the study of their spatial distribution, and the description of their morphodynamic behavior through case studies were meant to help understand the significance of weather extremes (here above-average temperatures and precipitations) in the generation of slope and channel processes.

16.5 Landslides in Buzău County

In 2010 the territory of Buzău County was affected by a large number of landslides, prolonging a previous time interval with intense activity of processes which lasted throughout the 2004–2006 period. The landslides occurred in February (due to temperature rise), March (showers overlapping with snowmelt), June–July (torrential rainfalls), and November–December (showers). Their occurrence is either directly related with external factors (temperature or precipitation) or indirectly resulted due to enhanced lateral erosion during flash flood events (riparian landslides, representing the majority in terms of frequency). Shallow *mudslides* occurred during the spring (at Pătârlagele, Pănătău, Colţi, Sibiciu de Jos, Scorţoasa, Odăile, Pârscov, Bisoca), while the main period of activity for *mudflows* was the summer (at Pătârlagele, Scorţoasa, Pănătău). Both movements particularly affected the Subcarpathian area, while local lithologic conditions contributed to rockslides (at Siriu, Lopătari). There were no deep-seated landslides registered, especially in the absence of high antecedent precipitation. According to Buzau's Prefecture primary estimations, the costs of damage from landslides and floods reached €20 million in the county (Table 16.1).

Table 16.1 Total damage caused by floods and landslides in Buzău County in June–July, 2010

	Element at risk		
No.	Category	Subcategory	Affected in June–July 2010
1	Flood control	Dikes	7.1 km
		Bank protection	6.8 km
		Dams	6
2	Roads and bridges	National	11.1 km
		County	1.35 km
		Commune	72.2 km
		Streets	51.1 km
		Bridges	43
		Railroads	–
3	Utility networks	Water	3 km
		Wells	61
		Sewage	–
		Electricity	1.8
		Natural gases	–
		Communication (cable, optic fiber)	–
4	Land use	Agriculture	107 ha
		Forestry (access roads)	25 km
5	Buildings	Damaged houses	1
		Destroyed houses	1
		Damaged annexes	16
		Destroyed annexes	–
		Other structures	–

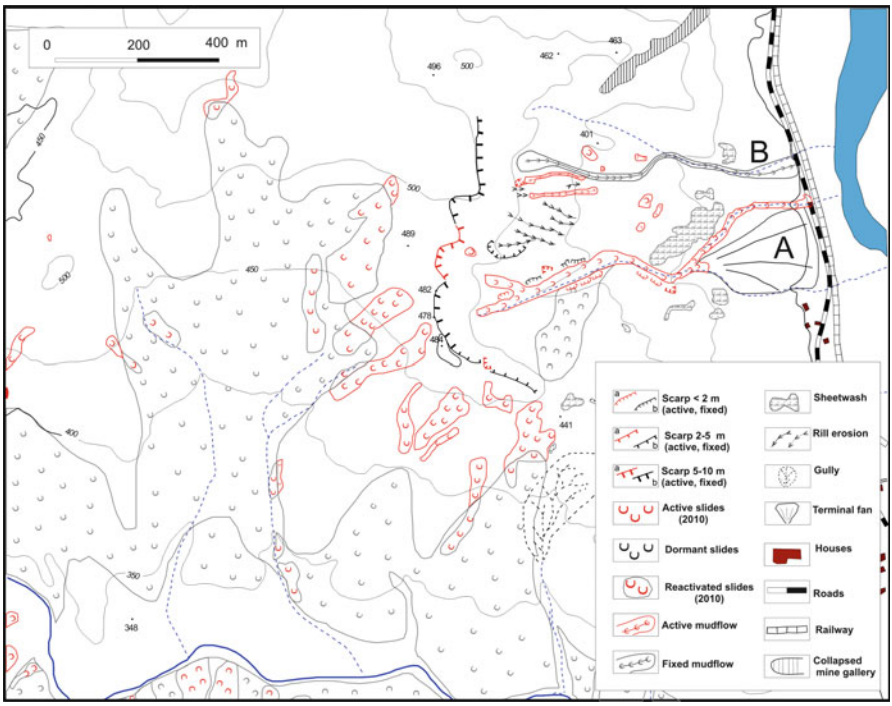

Fig. 16.7 Geomorphological sketch of the Malu Alb landslide, with features and processes originated in 2010

16.5.1 Case Study 1: The Malu Alb Complex Landslide

The observation site at Malul Alb (0.6 km^2) is situated on the right bank of the Buzău River (1 km north of the town of Pătârlagele), at the contact between the Neogene molasse and the Paleogene flysch (Fig. 16.7). It comprises two small catchments, 85% of which are affected by mass movements. Investigations started in 1968 and involved large-scale geomorphological mapping, topographic surveys, and measurements of profiles.

Basin A consists of a *mudflow* 990 m long, 15–20 m wide, with 1–3 m deep colluvium and an average slope of 10°. The accumulation fan is 250 m long with a maximum width of 200 m, 5–10 m thickness, and ca. 250,000 m^3 total volume of high-plasticity (20–42%) clay (angle of internal friction 9° and cohesion 0.43 daN cm^{-2}).

Basin B corresponds to a valley landslide (600 m long, 10–71 m wide, average slope 12°). The mobilized material is (ca 3–10 m deep) clayey–sandy colluvium of very high plasticity (27–45%) and low consistency (0.50–0.65), with angle of internal friction of 22° and cohesion of 0.15 daN cm^{-2}. Boreholes revealed the presence of *three* major stages of *reactivation* and several slip planes located at different depths.

The upper part of the two basins appears from large amphitheaters with steep slopes, where many shallow mudslides and mudflows were recorded (in 2005, 2006, and 2010). Due to the structure and lithology (an alternation of folded Miocene strata of schistose clays and marls with sands and gravels), rainwater usually accumulates on different steps and flows under pressure, generating intense subsurface erosion, reducing slope stability. In the rainy period between 1974 and 1978, progressive accentuation of slope instability happened, culminating in May 1981, when movements reached rates of 30–40 m day^{-1}. In 1982, for stabilizing the slope, excess water was drained and the road protected by a concrete parapet. Unfortunately, the system is not working properly anymore, and, as a result, in February 2010, the Buzău–Braşov national road was completely blocked by a mudflow.

The most important date of landslide reactivation was February 2010, when large surfaces within the perimeter were affected by a complexity of processes (especially slides and flows, but to some extent also sheet wash or rill erosion – Fig. 16.7). Since February is generally a dry and cold month in the region (Sandu and Bălteanu 2005), in 2010 unusual weather (rapid warming caused by a Mediterranean frontal air mass, moving northwards and crossing the Curvature Carpathians) was the primary trigger of movements. As a result of constant temperature growth (mean daily temperatures rising from –3 and –6 °C in the first decade to +2– + 7 °C by 18–21 February and maximum temperatures rising from –0.2 to 18.9 °C), the snow cover melted completely and very quickly, causing – since the vegetation was still in hibernation stage – the oversaturation of soil and regolith. Numerous *lateral source areas* (of 10^2–10^3 m^2 size – Fig. 16.8) emerged, from where the soil and sometimes also the upper part of the regolith were removed. Despite their low magnitude, numerous lateral sources developed (seven along 50 m of flow track) and channeled flows of some thousands of m^3 volume merged to form a 800-m-long *mudflow* (Fig. 16.8), moving with rates of some 20–30 m h^{-1}, which blocked the road completely for 1 day until local authorities (the Pătârlagele town administration) cleared it from the accumulated material by two bulldozers.

16.5.2 Case Study 2: The Chirleşti Mudflow

The Chirleşti mudflow (Fig. 16.9) affects the right-bank slope of the Buzău River valley in the Buzău Mountains, close to the confluence of the Cătiaşu Stream. The flow extends along a northeast-oriented valley, cut in Paleogene flysch deposits (sandstone intercalated with schists and clays). It is 1,350 m long, located between 330 and 615 m elevation, and consists of a main source area, a flow channel, and an accumulation fan (lobe). First reported in the spring of 1953 (Badea and Posea 1953), the movement was triggered in 1953 by rainfall simultaneous with snowmelt on a substrate saturated by the abundant precipitation of autumn 1952.

The main *source area* (3.36 ha) is elongated in shape and separated from the flow track by a deluvial accumulation usually above a structural step formed of

Fig. 16.8 Lateral source areas (**a**) reactivated during January–February 2010 nourished an 800-m-long mudflow (**b**) which blocked DN 10 (national road) (Photo by M. Micu)

more resistant rocks (schistose sandstone). This lithologic barrier is periodically overlain by the material accumulated from all over the surface of the circular scarp (540 m long, 5–15 m high, and 40–50° steep) marked by strong backward regression nearly all along its length. The *flow channel* is 750 m long and originates from

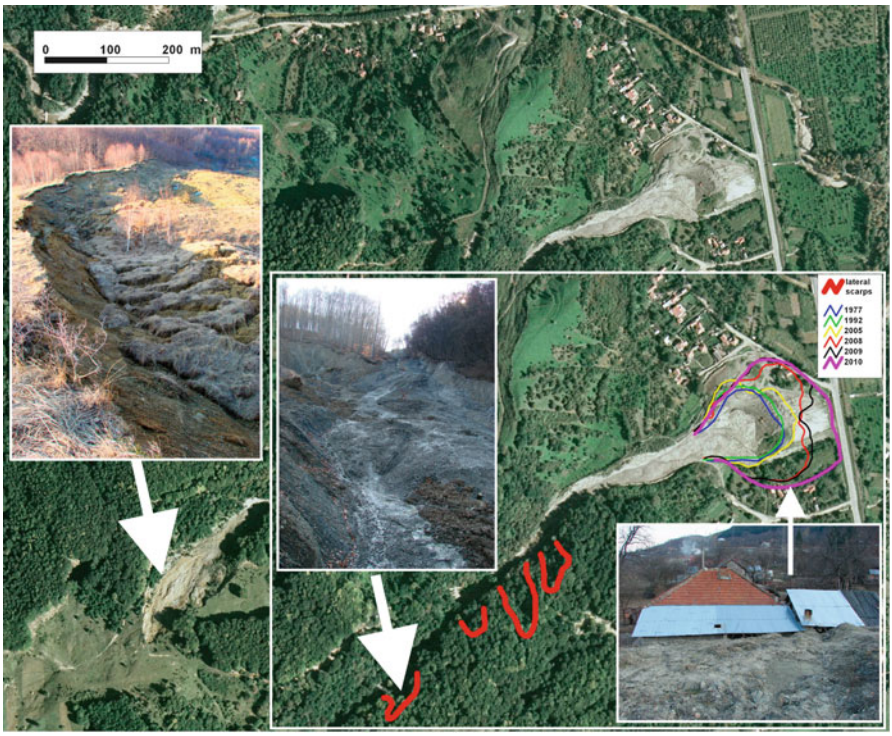

Fig. 16.9 The Chirleşti mudflow. The activity of the main source and the reactivation of several lateral (secondary) sources made the accumulation fan expand 5,000 m^2 in area, destroying one house and blocking one communal and one national road

a narrowing sector situated right below the lithologic step that limits the source area. In this sector the mudflow is no wider than 5–15 m, with high (1–2 m) lateral *pressure ridges* bordering it throughout its length. The 2–3-m-thick material consists of a sandy–marly matrix, in which menilites, disodiles, and schistose sandstone fragments (10–15%) of up to 20–30 cm diameter are embedded. The *accumulation fan*, the last and most important sector in terms of direct effects, covers 1.67 ha and consists of the virgation of several accumulation stages overlying the low terrace of the Buzău River. Its maximum width is 130–140 m and its 2–5-m-high front shows sheet and rill erosion features. In 1953 ten houses were damaged here, in 2006 here was another, and the national road and railway were also threatened.

Spring and summer are the seasons with stronger dynamics both for scarp regression and expansion and thickening of accumulation in the terminal fan sector. The end of summer and the autumn months witness largely the consolidation of lateral pressure ridges and temporary accumulations along the flow track.

Over time major changes were noticed in the source area and the scarp, which slightly shifted from north to south, following the steepest slopes. The scarp

regression of June–July 2006 involved the sliding of 28,616 m^3 of material from 5,731 m^2 area. The years 2005 and 2010 were, after 1975, the second and third rainiest in the region. The large amounts of daily precipitation (69 mm at Pătârlagele, 78% of the multiannual mean) between the end of spring and all through the summer months of 2005, combined with rainfalls in 2006, induced the biggest changes recorded: enlarged the main source area by some 11,000 m^2 and the accumulation fan by 5,500 m^2. In the meantime, the flow track incised deep (sometimes by 1–2 m). After the 2005–2006 humid period, the years 2007–2009, with low-to-average precipitation, were of relative stability. One of the direct results was that the channel remained emptied of material and, as previously described, deepened. This caused the lack of support for some slope deposits previously accumulated as dormant sliding/flowing masses at confluences. During February 2010, due to abruptly rising temperatures, the rapid water infiltration all across the main source area caused *pulsation*, and the flowing mass generated intense lateral erosion all along the flow track. In the lower third of the channel, the effect was reactivation (and afterwards, throughout 2010, retrogressive evolution) of the dormant deposits. Presently, there are two major (area, 400–500 m^2; volume, 500–1,500 m^3) and two minor (200–400 m^2 and 200–800 m^3) sectors in which the narrow track is widened by regressing secondary scarp areas. The material yielded increased the volume, mass, and sliding rate of the material originating from the source area. Therefore, the year 2010 may be considered crucial for the morphodynamics and future behavior of the mudflow. In addition to viscous–plastic rheology, a switch from a single source area to *multiple source areas* should be taken into account in further dynamic modeling of the mudflow.

16.6 Conclusions

The year 2010, even though with somewhat less precipitation than in 2005 (at least in Romania), provided an important insight into the significance of precipitation and temperature in landslide occurrence. One major trigger, winter–spring temperature rise, could be clearly identified. In the Curvature Carpathians, mid-February was marked by a sudden increase in temperature, rapid snowmelt, intensified infiltration, and oversaturation of soils and regolith, which led to both first-time failures and the reactivation of numerous shallow earthslides and mudflows in the oncoming period (March to April), when precipitation amounts were below monthly averages. In the meantime, due to the convective character of many summer rainfalls, landslides were also generated by riverine and flash floods also in areas with no precipitation records. This fact underlines the importance of full understanding of *multi-hazard assessments* with the objective of implementing proper risk mitigation.

References

Badea L, Posea GR (1953) Torentul noroios de la Chirleşti (The mud torrent of Chirleşti). Natura 5(3):109–112 (in Romanian)

ICPDR/IKSD (2012) 2010 Floods in the Danube River Basin. Brief overview of key events and lessons learned International Commission for the Protection of the Danube River, Vienna, 17 p http://www.icpdr.org/main/publications/preliminary-flood-risk-assessment-in-the-danube-river-basin

Lungu D, Saito T (2001) Earthquake hazard and countermeasures for existing fragile buildings. contributions from JICA International Seminar, Bucharest, Romania, 23–24 Nov 2000

Micu M, Bălteanu D (2009) Landslide hazard assessment in the Bend Carpathians and Subcarpathians, Romania. Z Geomorphol 53(Supplement 3):49–64

Micu M, Sima M, Bălteanu D, Micu D, Dragotă C, Chendeş V (2010) A multi-hazard assessment in the Curvature Carpathians of Romania. In: Malet J-P, Glade T, Casagli N (eds) Mountain risks: bringing science to society. CERG Edition, Strasbourg, pp 11–18

Ministry of Environment (2010) Raport anual privind Starea Mediului în România pe anul 2010 (Annual report on state of the environment in Romania for 2010). Ministry of Environment, Bucharest. http://www.anpm.ro/Mediu/raport_privind_starea_mediului_in_romania-15

Moţoc M (1983) Participarea proceselor de eroziune şi a folosinţelor terenurilor la diferenţierea transportului de aluviuni în suspensie pe râurile României (The role of erosion and land use in differentiating suspended load transport on Romanian rivers). Buletin Informativ, Academia de Ştiinţe agricole şi silvice, Nr. 13. Bucureşti (in Romanian)

Sandu M, Bălteanu D (eds) (2005) Hazardele naturale din Carpaţii şi Subcarpaţii dintre Buzău şi Teleajen. Studiu geografic (Natural hazards in the Trotus-Teleajen Carpathians and Subcarpathians. Geographical study). Edit. Ars Docendi, Bucuresti, 384 p (in Romanian)

Zugrăvescu D, Polonic G, Horomnea M, Dragomir V (1998) Recent vertical movements on the Romanian territory, major tectonic compartments and their relative dynamics. Revue Roumaine de Géophysique, seria Geofizică 42:3–14

Chapter 17
Landslides in the Republic of Macedonia Triggered by Extreme Events in 2010

Milorad Jovanovski, Ivica Milevski, Jovan Br. Papić, Igor Peševski, and Blagoja Markoski

Abstract The territory of the Republic of Macedonia is vulnerable to various types of natural disasters (landslides, rockfalls, earthquakes, floods, torrential floods, and excessive soil erosion). Mass movements are controlled by topography, engineering–geological properties of soils and rocks, runoff and infiltration conditions, human influences, and other factors. In this chapter some historical data on major landslides are presented with special regard to extreme landslide events in 2009 and 2010, a period with deep snowpack and intense rainfalls. It is observed, however, that almost all new or reactivated slides developed along the existing road network. The chapter describes to what extent the influence of extreme weather can be detected in landslide occurrences. The concepts of improved analytical methodology for landslide hazard mapping are also tackled, with the objective to outline the general directions for landslide prevention in the future and land use planning in Macedonia.

Keywords Landslides • Rockfall • Hazard mapping • Risk assessment • Zonation • Macedonia

M. Jovanovski • J.B. Papić • I. Peševski
Faculty of Civil Engineering, University Ss. Cyril and Methodius, blvd. Partizanski odredi No. 24, 1000 Skopje, Republic of Macedonia
e-mail: jovanovski@gf.ukim.edu.mk; papic@gf.ukim.edu.mk; pesevski@gf.ukim.edu.mk

I. Milevski (✉) • B. Markoski
Institute of Geography, Faculty of Natural Sciences, University Ss. Cyril and Methodius, Gazi Baba bb, 1000 Skopje, Republic of Macedonia
e-mail: ivica@iunona.pmf.ukim.edu.mk; blagojamarkoski@gmail.com

D. Lóczy (ed.), *Geomorphological impacts of extreme weather: Case studies from central and eastern Europe*, Springer Geography, DOI 10.1007/978-94-007-6301-2_17,

17.1 Introduction

The Republic of Macedonia, in the southern part of Balkan Peninsula (area: 25,713 km^2), is a mountainous country (mean elevation, 832 m), where hills and mountains cover 79%, plains and valleys 19.1%, and water surfaces 1.9% of the territory. With large areas of erodible soils, crystalline rocks (gneiss, mica-schists, other schists), sandstones, lacustrine and fluvial deposits, steep slopes (39.5% of the area above 15°), semiarid climate (annual precipitation: 500–700 mm; Lazarevski 1993), and sparse vegetation, hillslope processes are very intensive in Macedonia (Milevski 2007).

Frequent storms with heavy or prolonged rains in wet seasons contribute to excess runoff and, in combination with human influence, the intensification of weathering and hillslope processes. Landslides, slumps, and soil creep are especially common on the basin margins, where Neogene lacustrine sands and sandstones overlie inclined clay or schists layers. In more compact weathered rocks (igneous, limestones, marbles), especially in the western mountains, rockfalls, rockslides, debris flows, and other phenomena occur.

In addition to natural factors, human action (road and other constructions on sloping terrain) is a significant trigger of landslides with serious economic damage and casualties in Macedonia (Dragičević and Milevski 2010).

In Macedonia moderate *slopes* (10–30°) dominate (49.5% of area – Table 17.1). If other factors are favorable, landslides frequently occur on such slopes. Terrains with gentler slopes (3–10°; 26.2%) are usually affected by small rotational landslides, while flat depositional areas (0–3°) cover 17.2%. Steep slopes (above 30°; 7.1%) are potential sites for rockfalls, topples, and debris avalanches. The elevation/slope plots (Fig. 17.1a, b) show how slopes in Macedonia tend to rise with elevation.

DEM analyses show that, as a consequence of the Dinaric strike, WSW (26.4%) and ENE (26.1%) *slope aspects* prevail in Macedonia. Terrains with southern aspect (24.8%) cover larger areas than northern slopes (21.9%), and western (27.4%) slightly prevail over eastern (25.8%) slopes. Rockfalls are far more common on southern slopes, while the distribution of landslides by aspect is more random. However, the largest landslides in Macedonia were recorded on northern slopes.

Table 17.1 Inclination of slopes in the Republic of Macedonia

	Area	
Slope (°)	km^2	%
0–3	4,413.7	17.2
3–5	1,904.1	7.4
5–10	4,844.3	18.8
10–20	8,089.8	31.5
20–30	4,625.1	18.0
30–40	1,554.3	6.0
>40	281.7	1.1
Total	25,713.0	100.0

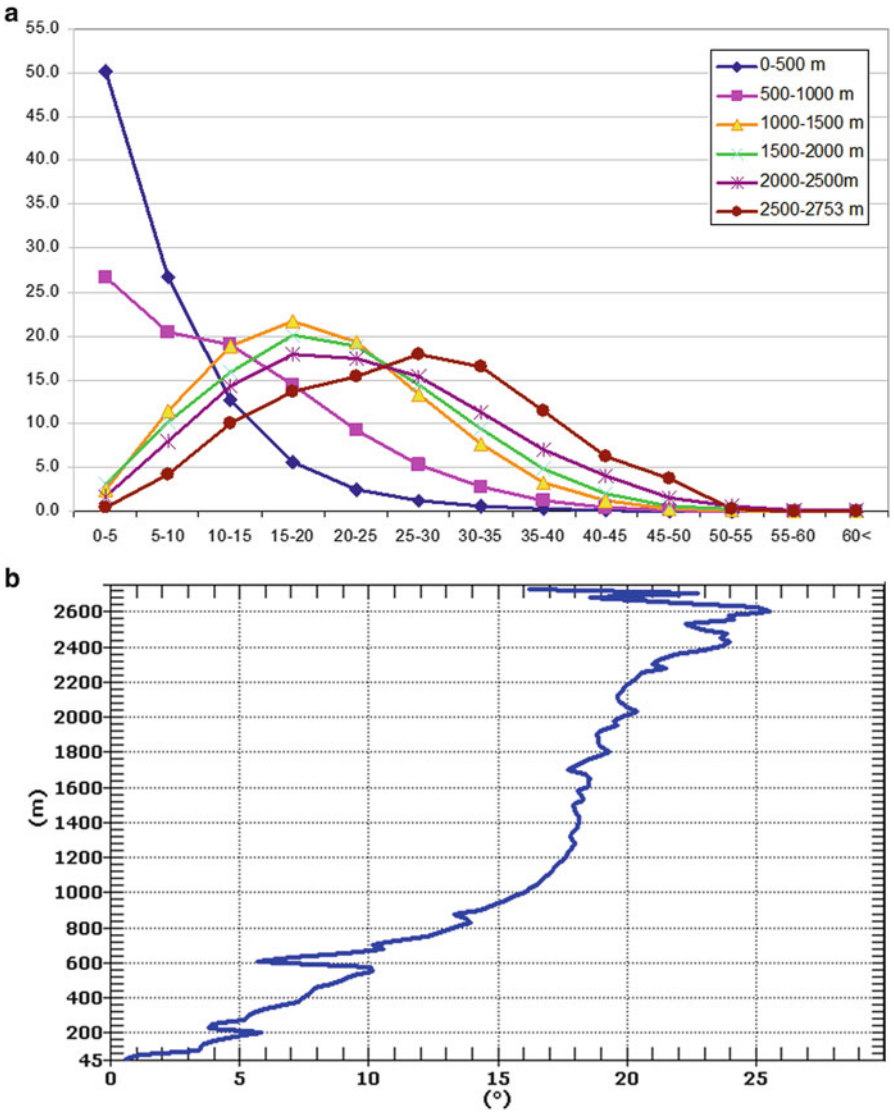

Fig. 17.1 Elevation/slope plots of elevation zones of 500 m interval in percentage (**a**); mean slope plotted against elevation (**b**)

17.2 Historical Landslides

Landslides and *rockfalls* in Macedonia are generally associated with the following rock zones:

- Hard rocks (Jovanovski 2010) (limestone, volcanic rocks, schists): rockfalls of structural origin

Table 17.2 Major landslides in Macedonia

Map symbol	Site	Year	Main negative impact
A	Surnati Ridoi	–	Threat to the regional irrigation canal
10	Sasa–Kosevica	–	Ruined houses and structures, traffic blocked
B	Jelovlane	–	Ruined houses in rural area
11	Crnik	1904–	Ruined houses and local road
2a	Velebrdo	1930–	Ruined houses, traffic blocked between several villages
C	Gradot	1956	Death toll, artificial lake ponded
D	Ramina	1963–	Ruined houses in urban area
E	Timjanik	1994	Ruined irrigation canal and local road, devastated vineyards
2	Rock avalanche Radika	2010	Traffic blocked for a month
5	Gjavato	2010	Traffic blocked during remedial works for 6 months

- Mixed hard and soft rocks (flysch, diabases): complex slope failures (structural preformation and weathering) and local rockfalls
- Soft rocks (soils, clays, fluvial glacial deposits): complex and deep-seated landslides (Milevski 2008)

More than one hundred larger landslides are known and described in literature (Manaković 1960; Manakoviќ 1974; Andonovski 1982; Andonovski and Vasileski 1996; Milevski 2004; Jovanovski et al. 2005). Some major landslides and rockfalls caused casualties and serious economic losses (Table 17.2).

At the *Gradot landslide*, near the town Kavadarci, the western slope of a hill failed at a speed of 6 km h^{-1} in 1956. Landslide width was 800 m, length 400 m, relative height 200 m, and the total mass moved ca 20,000,000 m^3 (landslide *C* in Fig. 17.5). A river valley was covered by 70-m-deep water (Fig. 17.2). Fatalities included 11 people and many animals. Infiltrating waters caused the piping of sand grains in overloaded tuff and generated creep at ca. 15 mm $year^{-1}$ long before the movement.

Several kilometers to the northeast, near the village *Timjanik*, heavy rainfall on 26 September 1994, activated a landslide of 250 m in length and 150 m in width (landslide *E* in Fig. 17.5). The sliding mass was 10–15 m deep and its total volume ca. 400,000 m^3. Here Pliocene sands overlie clay beds, and interesting landforms, marked earth pillars, and pyramids were created (Fig. 17.3). Damage included destroyed vineyards, local roads, and 200-m-long modern irrigation canals.

On the north-eastern part of the *Suvodol* coal mine, near Bitola, there is a landslide of huge dimensions (length: ca 1,500 m; maximum width: 880 m; maximum depth: 55 m; total volume: ca 30,000,000 m^3) (also landslide No. 7 in Fig. 17.5) (Manasiev et al. 2002). Judging from the very long displacement and large mass, it originated at least 20 years ago, due to a tectonic event. Its development is a special combination of natural and man-made causes. It blocked eight million tons of *coal* at the toe. Spontaneous combustion ensued, polluting the environment. Above the main scarp, there is a 1-km-long earth-fill dam raising groundwater levels and reducing slope stability.

Fig. 17.2 Scar of the Gradot landslide with impounded river (Photo by B. Markoski)

Fig. 17.3 Timjanik landslide with earth pyramids in 1994 (Photo by I. Milevski)

North of the town Bitola, on the eastern slope of Oblakovo Mountain, the huge landslide known as '*Surnati Ridoi*' (slided hills) has a length of ca 500 m, width of 300 m, maximum height 180–200 m, and total volume exceeding 1,000,000 m^3 (landslide *A* in Fig. 17.5). Today this landslide is mostly inactive, but even small reactivation can damage the main irrigation canal system Streževo. Complex hydrotechnical preventive measures are required (Andonovski 1982).

Fig. 17.4 View from the top of the Ramina landslide onto the built-up area (**a**) and on the main scarp (**b**) (Photos by M. Jovanovski)

A major landslide occurred in *Veles* (landslide *D* in Fig. 17.5) in 1999 and 2002 on an illegally settled hill called *Ramina* and caused widespread damage to houses and infrastructure (Fig. 17.4). The landslide is ca 320 m long, average width is

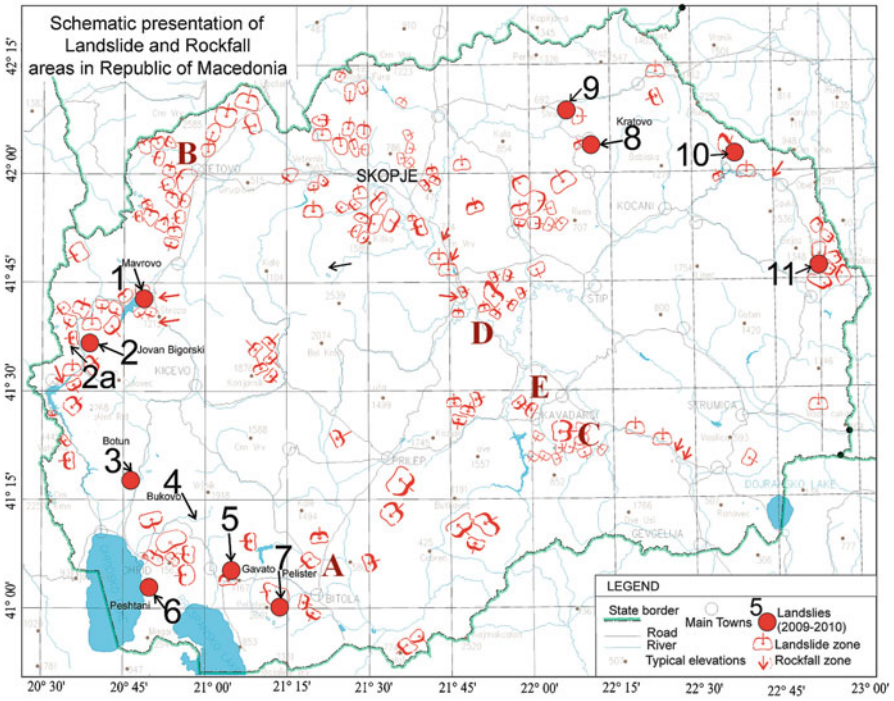

Fig. 17.5 Sites of landslides and rockfalls in Macedonia with major occurrences in 2009 and 2010

85 m, depth is up to 20 m, and volume is ca 400,000 m^3. Geotechnical investigations indicate that the main slip plane was formed on the contact between the clay soil of middle to low plasticity and the Paleozoic amphibolitic schists bedrock, highly foliated, faulted, and locally weathered. The triggering effect was rising groundwater table.

Several large landslides are found in the Radika River valley (Western Macedonia), generated on steep valley sides with rock debris by high precipitations as well as direct and indirect human impact (deforestation, road construction, etc.). The largest of them (with volume of several millions m^3), at the village of *Velebrdo* (landslide No. 2a in Fig. 17.5), is located on river terraces built up by schists and sandstones with fossilized alluvial fan deposits, which, when saturated, start to slide towards the valley bottom (Manakoviḱ 1974). Since the 1930s the slide has been repeatedly reactivated, particularly during favorable weather conditions.

The large landslide near the village *Crnik* (Eastern Macedonia) is found in the southern valley side (320 m long, 100–150 m wide, 15–20 m deep, with up to 700,000 m^3 volume). Pliocene sands move above inclined clay beds towards the Crnička River, which undercuts the toe, especially during torrential flows. The rate of movement usually does not exceed several meters a year – except during heavy or prolonged rains like in early 2010 (landslide No. 11 in Fig. 17.5). There is also high risk of large mass falling in the river valley and making a natural dam like as of

Gradot landslide. Most probably, the cause of this landslide activation is the catastrophic Pehčevo–Kresna earthquake of $M = 7.8$ occurred in 1904 (Milevski 2004, 2011).

Numerous landslides are recorded in the valley of the Kamenička River, where erodible schists and clastic sediments are exposed on steep slopes (landslide No. 10 in Fig. 17.5). A huge system of landslides (total estimated volume, 5,000,000 m^3) endangers the village *Kosevica* (Milevski 2011; Milevski et al. 2008). Along with other recorded movements, it considerably contributes to the rate of sedimentation from the Kalimanci reservoir through the Bregalnica River (Blinkov 1998). Some landslides have been reactivated recently by direct human impact, mostly by road construction (Petkovski 2002).

17.3 Landslides Caused by Extreme Weather in 2010

Under continental and Mediterranean climatic influence, the 500–700 mm annual precipitation in Macedonia is *unequally distributed* through space and time: dry summers and autumns are followed by short wet spells from October to December and between March and May. Extremely warm or wet/dry years may occur as it happened in the period 2007–2009 (Table 17.3). Average annual precipitation in the Skopje area for this period was 526.6 mm. Excessive rain and snowfalls in 2009 were followed by similarly high precipitation in early 2010 (Table 17.4).

As a result, extreme water levels in rivers and lakes (locally almost up to the 100-year level) as well as static and hydrodynamic levels of *groundwater* were registered. One of the key variables for the intensity of hillslope processes and mass movement is weather conditions since surplus water increases both loading and pore pressure and, at the same time, decreases shear strength. Through rising groundwater levels, major landslides were generated in Macedonia in 2009 and 2010 (Fig. 17.5).

A *stone–soil–tree–snow* mixed *avalanche*, similar to those described from Switzerland, Canada, and other countries with extreme actions of snow and ice, happened in western Macedonia (landslide No. 2 in Fig. 17.5) in early 2010. The national road between the important ski centers Mavrovo and Debar was blocked for about a month after a mudflow of hundreds of meters length and almost 10 m depth. Meanwhile, some parts of slided mass moved downwards, occupying part of the picturesque river Radika (Fig. 17.6). Luckily, it demanded no victims.

Table 17.3 Monthly and annual precipitation (mm) for Skopje, 2007–2009

Year	J	F	M	A	M	J	J	A	S	O	N	D	Annual
2007	29.5	21.0	14.1	7.8	86.2	35.0	1.2	52.7	27.2	140.0	69.4	14.6	198.7
2008	7.7	0.5	29.8	18.7	40.7	46.9	57.8	24.8	78.5	27.3	37.5	68.3	438.5
2009	72.8	12.2	68.6	65.3	70.2	104.3	10.2	50.2	11.1	52.9	56.1	68.7	642.6
Average	36.7	11.2	37.5	30.6	65.7	62.1	23.1	42.6	38.9	73.4	54.3	50.5	526.6

Table 17.4 Monthly precipitations (mm) for several stations in Macedonia in early 2010 compared to multiannual averages

City		Months				Total
		J	F	M	A	
Skopje	Precipitation in 2010	28.2	63.7	68.6	63.8	704.1
	Average precipitation	25.1	31.4	26.9	40.7	441.2
	Difference	3.1	32.3	41.7	23.1	262.9
Prilep	Precipitation in 2010	27.9	71.3	55.2	52.2	747.6
	Average precipitation	29.8	34.8	37.1	47.6	517.3
	Difference	−1.9	36.5	18.1	4.6	230.3
Demir Kapija	Precipitation in 2010	22.5	82.8	71.4	32.2	654.0
	Average precipitation	43.4	47.8	49.6	53.8	536.2
	Difference	−20.9	35	25.9	−17.4	117.8
Štip	Precipitation in 2010	14.5	58.1	61.3	55.9	623.3
	Average precipitation	23.0	27.3	31.0	40.6	460.1
	Difference	−8.5	30.8	30.3	15.3	163.2
Gevgelija	Precipitation in 2010	32.6	168	67.6	30.5	970.9
	Average precipitation	49.5	61.2	57.8	54.3	649.6
	Difference	−16.9	106.8	9.8	−23.8	321.3
Ohrid	Precipitation in 2010	123.8	187.9	74.5	94.7	1143.8
	Average precipitation	72.5	42.7	77.4	49.0	650.4
	Difference	51.3	145.2	−2.9	45.7	493.4

Source: Statistical Yearbook of the Republic of Macedonia

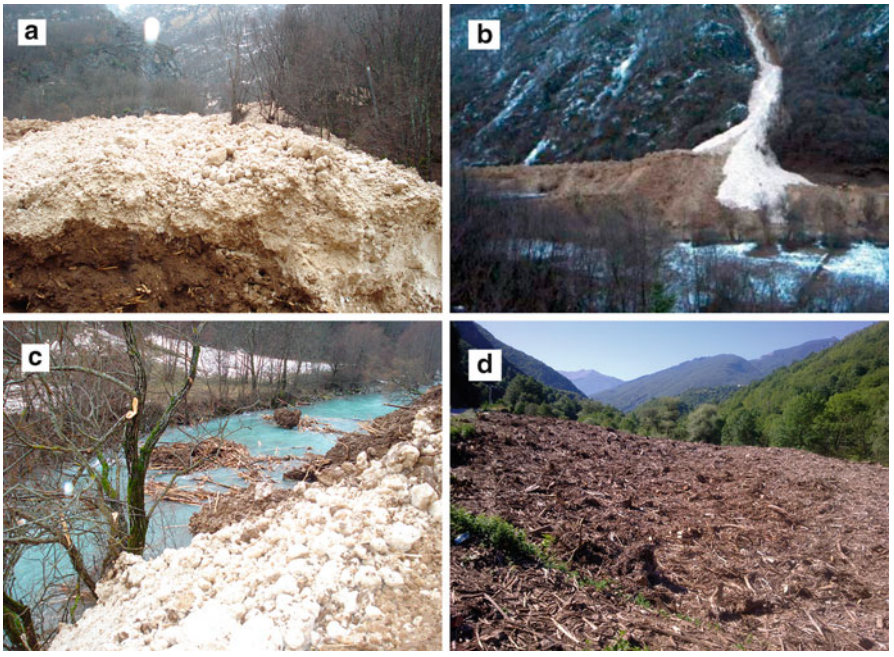

Fig. 17.6 Stone–soil–tree–snow avalanche on the Mavrovo–Debar road. (**a**) View of avalanche; (**b**) part of the slid mass; (**c**) toe on the valley bottom; (**d**) dried avalanche surface with trees (Photos by M. Jovanovski)

Fig. 17.7 Repairing the national road M5 between Resen and Bitola (south-western Macedonia): unloading the slided mass, stabilization with gabions, and reinforced soil surface (Photo by A. Strašeski)

From the autumn of 2009 to the spring of 2010, masses on the road between Bitola and Resen (towards the UNESCO Cultural Heritage city Ohrid) moved downslope along a length of 50 m (landslide No. 5 in Fig. 17.5). Several solutions had been proposed until technical and economical analyses persuaded the designers to decide on gabions and geotextiles (Fig. 17.7).

In 2010 many existing *landslides* were *reactivated* or intensified, including the already mentioned complex of landslides between Bituše, Velebrdo, and Rostuše (landslide No. 2a in Fig. 17.5). From February to April 2010, these landslides were highly active, damaging local roads between the villages, several houses, and other buildings. Some fields slipped down tens of meters. The cleaning of roads or reparation of structures proved to be no lasting solution.

One of the largest landslides reactivated in 2010 is at Crnik (landslide No. 11 in Fig. 17.5). The rate of movement was estimated to ca. 0.5–2 m day^{-1} in contrast to the 'normal' 3–5 m year^{-1}, reflected in many new longitudinal and perpendicular cracks (Fig. 17.8). A dirt road was totally destroyed and large amounts of debris reached the Crnička River. A major earthfall had threatened the village Crnik before the movement considerably slowed down by July.

Fig. 17.8 Cracks on the Crnik landslide and mass movement towards the Crnička River in May 2010 (Photo by I. Milevski)

In the same period, a highly active landslide occurred on the Stracin pass along Corridor 8 towards Bulgaria (landslide No. 9 in Fig. 17.5), where the road is cut 10–12 m deep for several hundred meters into stratified volcanic tuffs mixed with clay. A field survey in May 2010 showed that the Stracin landslide was 85 m long and active along 54 m, indicated by progressive falls of debris upon the road. Many new scars gave a stairlike shape to the landslide mass (Fig. 17.9). During the peak of activity in March 2010, most of the road was covered with debris, slowing down traffic.

In addition to these large landslides, some smaller were also generated (e.g. at Kriva Palanka town), and some were reactivated (e.g. above the administrative building of the hydroelectrical power plant Tikveš near Kavadarci, in the hills above Strumica town). The embankments next to abutments of several bridges on the Skopje–Veles highway were eroded. At the southern exit of Skopje, on the eastern slopes of Vodno Mountain, the small but deep and wide landslide of Sopište village endanger, and for some period even blocked, the traffic on the road. Also near Skopje the access road arch dam of St. Petka under construction was often exposed to *rockfalls*, which intensified in 2009/2010 and also demanded death toll among workers and civil engineers. In the winter 2010, a landslide was also registered on the road to the Kneževo dam (Eastern Macedonia).

Fig. 17.9 The Stracin landslide on the international road Corridor 8, highly active in early 2010 (Photo by I. Milevski)

17.4 Climatic Factors in Landslide Hazard

While there is a definite relationship between slope stability and climate, the consequences of *climate change* on the rates, dimensions, and frequency of movements are hardly predictable because they depend on a range of variables (Schmidt and Dikau 2004). Higher temperatures and increased temperature range induce more intensive rock weathering and slope instability. Although at a first glimpse, lower precipitation would imply reduced erosion and transport rate, in reality the situation is much more complicated. *Seasonal variations in rainfall* would reduce vegetation cover and density (Donevska 2006; MEPP 2008), and more severe storm events would cause flash floods, soil erosion, and landslides. In addition, the indirect impact of climate change on landslide is observed through alterations in vegetation cover, soils, biota, and human activities. In 2007, 2010, and 2012, the number of *forest fires* and the size of the area burned have significantly increased, influencing vegetation quality and density, runoff, overland flow, oversaturation, accelerated erosion, and landslides. With lower precipitation and diminished water resources, more water will be extracted from groundwater, river channels, and reservoirs, promoting *ground subsidence*. Over recent decades several landslides occurred on the shores of reservoirs because of large water level range (the largest was the Pralenik landslide on the shore of the Debar reservoir – Andonovski and Vasileski 1996).

According to the *climatic scenario* for Macedonia based on direct GCM output (Bergant 2006), a mean temperature increase of 1.9 °C is expected for 2050 and 3.8 °C for 2100, with −5% precipitation decrease by 2050 and −13% by 2100 and significant seasonal variations in temperature and precipitation. The highest temperature rise for the entire country and precipitation decrease are foreseen for the summer. Thus, temperature will increase by 2.5 °C until 2050 and by 5.4 °C until 2100 compared to 1990. On the other hand, a drastic drop in summer precipitation is predicted (−17% in 2050 and −37% in 2100). In autumn, mean daily temperatures will increase by 1.7 °C until 2050 and by 4.2 °C until 2100 in respect to 1990, while mean precipitation will drop by −4% by 2050 and by −13% by 2100. Winter mean daily temperature increase may reach 1.7 °C by 2050 and 3.0 °C by 2100, with no major change in winter precipitation. In spring, mean daily temperatures are forecast to rise by 1.5 °C until 2050 and by 3.2 °C until 2100 compared to 1990. Precipitation will change by −6% by 2050 and −13% by 2100. Higher temperatures are expected in the northwestern and southern regions (ca 8.5 °C), while a major drop in precipitation will occur in the central and southern regions (−26 to −27% by 2100, compared to 1990) (Bergant 2006).

In terms of landsliding, rainfall has been proved to be an important triggering factor, and modeling has shown that responses to rainfall vary at different *timescales*. On shorter timescales (minutes to hours and days), heavy rainfall events can result in severe erosion, landslide triggering, and flash flooding. Both freeze–thaw action and alternation of wet/dry spells on seasonal timescales can greatly exaggerate mechanical weathering (Abele 1997). The role of temperature also varies over time, and extreme events, such as the hot summers of 2007 and 2012, highlight more recent increased variability. The extreme snowmelt of early 2010 illustrates how a short-term *temperature* rise can induce widespread slope instability. Another indirect impact is that if summers are hotter in the cities, more and more people build summer houses in the mountains reducing natural slope stability.

Precipitation also has a destabilizing effect on slopes, although in a more complex way than temperature: involving increased load, pore water pressure, and reduction of shear strength. During periods of high variability of monthly to seasonal precipitation or those with high storm intensity, landslide frequency, and magnitude will grow (Iverson 2000). However, in recent years the contrast between hot and dry summers and cold, snowy, or rainy winters and springs in Macedonia has been increasing, leading to more and larger landslides. In this respect, some years like 2010 are very representative. A national strategy for landslide and other natural hazards prevention and protection is urgently needed.

17.5 Conclusions

The extreme climate events in 2009 and 2010 with high precipitations as opposed to the preceding mostly dry seasons, significantly increased hillslope processes in Macedonia causing activation or reactivation of more than hundred landslides and

rockfalls. The situation was even more dramatic because of sharp increase of the temperature and rapid snowmelt in January and February 2010. Because of such circumstances, the *Crisis Management Center* of the Republic of Macedonia was permanently active in the mentioned period providing relevant information, forecasts, and measures for maximal risks and damages preventions. However, total material damage is estimated to more than €5 million, mostly as a result of roads cleaning, restoration, traffic delay, ruined houses, and damaged infrastructural and other objects. Moreover, several casualties and even two deaths occurred.

Although weather conditions (as a crucial input parameter) could be forecast on the short term, there is no way to predict other important influencing factors (shear strength or hydraulic permeability) or control them. Nevertheless, the activation of some of the mentioned landslides could have been avoided by employing surface or subsurface drainage measures. According to the climate scenarios (Bergant 2006) and research findings from all around the world, further increase of extreme geomorphological events in Macedonia can be expected (excess erosion, landslides, rockfalls, floods, etc.). In that sense, to prevent the reactivation of old and the generation of new landslides, *maps of hazard zonation* are proposed to be prepared. There are currently two working approaches: one based on interpolation (Djordevic et al. 1993) and second based on cluster classification of landslide factors (Milevski et al. 2009). The assessment of the degree of exposure to risk in the analyzed area will be correlated with the safety factor, a conventional measure of slope stability. The forthcoming climate/weather variations and accompanying precipitation will test the usefulness of the approach.

References

Abele G (1997) Influence of glacier and climatic variation on rockslide activity in the Alps. In: Matthews JA, Brunsden D, Frenzel B, Gläser B, Weiß MM (eds) Rapid mass movement as a source of climatic evidence for the Holocene, Paläoklimaforschung-Palaeoclimate Research, 19. Gustav Fischer Verlag, Stuttgart, pp 1–6

Andonovski T (1982) Landsliding in the area of Surnati Ridoi. Geogr Rev Skopje 20:45–52 (in Macedonian)

Andonovski T, Vasileski D (1996) Sliding (slump) of earth near village Pralenik in Debarska Župa. Geogr Rev Skopje 31:11–21 (in Macedonian)

Bergant K (2006) Climate change scenarios for Macedonia – review of methodology and results. University of Nova Gorica, Centre for Atmospheric Research, Nova Gorica, Slovenia, 50 p

Blinkov I (1998) Influence of the rains on the intensity of soil erosion in the Bregalnica watershed up to the profile "Kalimanci Dam". Manuscript doctoral thesis. Faculty of Forestry, Skopje, 127 p (in Macedonian)

Djordjevic M, Trendafilov A, Jelic D, Georgievski S, Popovski A (1993) Erosion map of the Republic of Macedonia. Memoir. Water Development Institute, Skopje, 89 p (in Macedonian)

Donevska K (2006) Vulnerability assessment and adaptation for water resources sector. In: Report on second communication on climate and climate changes and adaptation in the Republic of Macedonia. Ministry of Environment and Physical Planning, Skopje, 128 p

Dragičević S, Milevski I (2010) Human impact on the landscape – examples from Serbia and Macedonia. In: Zlatic M (ed) Global change – challenges for soil management, Advances in geoecology 41. Catena Verlag, Reiskirchen, pp 298–309

Iverson RM (2000) Landslide triggering by rain infiltration. Water Resour Res 36:1897–1910

Jovanovski M (2010) Landslide and rock fall occurrences and processes in R. Macedonia, Croatia–Japan Project on Risk Identification and land-use planning for disaster mitigation of landslides and floods in Croatia, Dubrovnik, Croatia

Jovanovski M, Gjorgevski S, Josifovski J, Dolenec-Včkova K (2005) A landslide in town Veles, from a natural hazard to prevention. In: Proceedings of the international symposium on latest natural disasters – new challenges for engineering geology, geotechnics and civil protection, Sofia, Bulgaria, 5–8 Sept 2005

Lazarevski A (1993) Climate of the Republic of Macedonia. Kultura, Skopje (in Macedonian)

Manaković D (1960) Landslide of Gradot hill. Ann Serbian Acad Sci, Belgrade 17:119–128 (in Serbian)

Manakoviќ D (1974) Landslide in the village Bituša. Ann FNSM Skopje 20:37–46 (in Macedonian)

Manasiev J, Jovanovski M, Gapkovski M, Novacevski T, Petreski Lj (2002) Landslide on the NE part of the coal mine "Suvodol": phenomenology of the event and experiences. In: Proceedings of 1st symposium of the Macedonian association for geotechnics, Ohrid, 2002, pp 68–77 (in Macedonian)

Milevski I (2004) Soil erosion in the Želevica catchment. Bull Phys Geogr Skopje 1:59–75 (in Macedonian)

Milevski I (2007) Morphometric elements of terrain morphology in the Republic of Macedonia and their influence on soil erosion. In: Proceedings from international conference "Erosion 2007", Belgrade, 2007, 10 p

Milevski I (2008) Fossil glacial landforms and periglacial phenomena on the Osogovo Mountain massif. Ann Inst Geogr Skopje 37:25–49

Milevski I (2011) Factors, forms, assessment and human impact on excess erosion and deposition in upper Bregalnica watershed (Republic of Macedonia). Z Geomorphol 55(Supplementary issue 1):77–94

Milevski I, Blinkov I, Trendafilov A (2008) Soil erosion processes and modelling in the upper Bregalnica catchment. In: Proceedings of the 24th conference of the Danubian countries on the hydrological forecasting and hydrological bases of water management, Bled, Slovenia, http://ksh.fgg.uni-lj.si/bled2008/cd_2008/index.htm

Milevski I, Markoski B, Gorin S, Jovanovski M (2009) Application of remote sensing and GIS in detection of potential landslide areas. In: Proceedings of the international symposium geography and sustainable development, Ohrid, 2009, pp 453–463

Ministry of Environment and Physical Planning of the Republic of Macedonia (2008) Second national communication on climate change. Project strategy ed. by M. Adzievska. Skopje, 118 p

Petkovski R (2002) Possible damages of the construction objects because of unequal soil settlements. In: Proceedings of 1st symposium of the Macedonian association for geotechnics, Ohrid, 2002, pp 427–435 (in Macedonian)

Schmidt J, Dikau R (2004) Modelling historical climate variability and slope stability. Geomorphology 60:433–447

Chapter 18
Debris Flows in the Middle Struma Valley, Southwest Bulgaria

Rositza Kenderova, Ahinora Baltakova, and Georgi Ratchev

Abstract In this chapter, we analyze seven events of debris flow in the tributary network of the middle Struma River Valley. Features and sediments resulting from debris flows and the hydrometeorological background of their activation are described. In order to define the type of the debris flow, we have used sedimentological analyses, generalized in cumulative curves and tables. Data from laboratory analyses showed the predominance of coarse materials (gravels and sands up to 90%). In May 2010, debris flows were triggered by a weather situation typical of the region: an invasion of a cold front combined with a warm, moist, and unstable air mass arriving from the southwest. We have made a general assessment of the mitigation activities and found that its best solution is by using gabions, which support large blocks and, at the same time, allow water and fine fractions to pass through.

Keywords Debris flow • Sedimentological analyses • Meteorological situation • Stream channelization • SW Bulgaria

18.1 Introduction

We have investigated the valley of the Middle Struma River and tributaries south of the Blagoevgrad Basin to the Bulgarian–Greek border, which is affected by active debris flows and torrents every year causing floods on the main river and damage to the international highway E79. In addition to blocking traffic, they also inflict serious damages to nearby settlements, agricultural lands, and protected areas.

R. Kenderova • A. Baltakova (✉) • G. Ratchev
Department of Climatology, Hydrology and Geomorphology, Faculty of Geology and Geography, St. Kliment Ohridski University, 15 Tsar Osvoboditel Blvd, 1504 Sofia, Bulgaria
e-mail: rosica@gea.uni-sofia.bg; abaltakova@gea.uni-sofia.bg; ratchev@gea.uni-sofia.bg

D. Lóczy (ed.), *Geomorphological impacts of extreme weather: Case studies from central and eastern Europe*, Springer Geography, DOI 10.1007/978-94-007-6301-2_18,

The catastrophic character of debris flows here was first recognized by Glovnja (1958), who studied the geomorphology of the Rila Mountain (the highest on the Balkan Peninsula) and described debris flows from the Blagoevgradska Bistritsa catchment. Until the next publication on a similar subject 40 years passed (Kenderova and Vassilev 1997). The present authors have studied these processes to determine flow type, climatic conditions, and partly their mitigation over the past 10 years (Kenderova and Vassilev 2000; Kenderova et al. 2012). In the last 5 years, this team was involved in a bilateral project with the Republic of Macedonia and in another coordinated at the University of Sofia.

18.2 Selected Debris Flows

In this chapter, some selected debris flow events are analyzed:

- The event on 2 July 1954, affecting the Kovachitsa River with its tributaries Babkite, Argachka, and Svetetsa (on the left bank of the Struma, site L1). The debris flow deposited its load into the Blagoevgradska Bistritsa riverbed and temporarily impounded it for 10–12 h. The Blagoevgradska Bistritsa overflowed its banks and flooded agricultural land, roads, villages, and parts of Blagoevgrad town with a death toll of six people.
- On September 20, 1994, a debris flow on two minor tributaries (site L2) destroyed the E79 highway. It caused the redirection of international traffic and underlined the necessity of building a new bridge across and barrages in the river bed of the tributaries.
- On May 18, 2009, and on December 3–5, 2010, the Klisurska River and its tributary Gabrovska (and also other minor tributaries) were affected by debris flows (site R1).
- On May 24, 2009, at the entrance of the Kresna Gorge (site R3), a debris flow accumulated deposits on the highway E79, closed for over 24 h.
- Also on May 24, 2009, and again on December 3–5, 2010, the river Potoka (key site R2) was flooded 2.9 km north of site R3.

In addition debris flows on the eastern slope of Maleshevo Mountain (key site R4) and on the west slope of Pirin Mountain (key site L3) are also studied. The primary goals of investigations were:

– To analyze debris flow features, deposits, and types and assess mitigation opportunities
– To analyze weather conditions which trigger debris flow activity and climatic conditions which lead to reactivation

18.3 Physical Geographical Setting

The Struma River, with the third largest catchment area in Bulgaria, issues in Vitosha Mountain at 2,210 m elevation and runs to the southwest (Fig. 18.1). The Middle Struma Valley is located in the western part of the Rila–Rhodopes Mountains between the eastern fault slopes of the Osogovo–Belasitsa mountain group and western fault slopes of the Rila, Pirin, and Slavyanka Mountains. The valley is an elongated graben with broader and narrower sections (Kanev 1989). Most of the gorges of the Middle Struma are conceived as epigenetic (Radev 1933; Velchev 1994). The section investigated here includes the morphostructural units of the Blagoevgrad Basin, Oranovski (Zheleznishki) Gorge, Simitli–Krupnik Basin, Kresna Gorge, and Sandanski Basin (Kanev 1989).

Site L1 is located along the tributaries of the lower Blagoevgradska Bistritsa River with small mountainous watersheds (elevation: 800–1,200 m). Site L2 is on the catchments of two small unnamed tributaries in low-mountain and hill environments (elevation 420–800 m). Site L3 is consisted of the basins of the Potoka River (L3_1, 19.212 km^2) and Melnishka River (L3_2, 99.662 km^2), located in both high mountains and lowlands. Site R1 is on the catchment of the Gabrovska River (area 30.044 km^2) in belts above 1,200 m and 420–800 m. Site R2 is in the Sushishka River basin (86.152 km^2), mostly higher than 1,200 m, but 290 m at its lowest point. Site R3

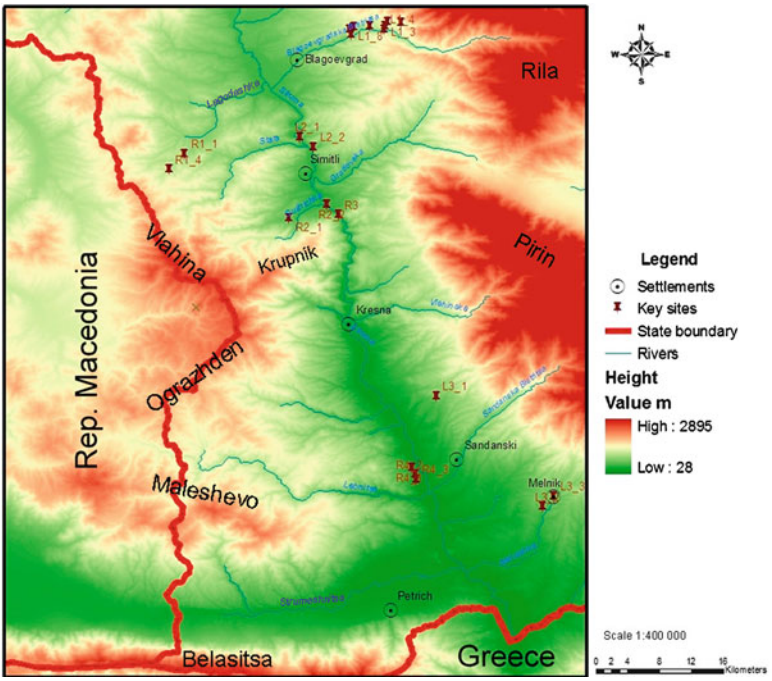

Fig. 18.1 Map of the study area

is a small watershed on the right bank of the Struma River with elevations between 200 and 800 m. Site R4 involves three unnamed streams with basin elevations below 800 m. Asymmetric topography is manifested in better developed left-bank tributaries (longer rivers, larger basins at higher elevations).

The sites are located in the following petrographic provinces L1, L2, and R4: Precambrian gneiss–migmatite complex; L3 and R2: Neogene sandstones and conglomerates; R1: Paleogene sandstones and conglomerates; and R2: Precambrian crystalline rocks. No major difference in rock composition is observed between the left and the right-bank valleys. Mountain foothills are built up of Neogene and Paleogene sediments, while higher catchment parts are on gneisses and migmatites.

The study area embraces two *climatic zones* (Ratchev and Nikolova 2009): north of the Kresna River continental, and south of it continental-Mediterranean climate prevails. Streams with sources close to 1,000 m elevation are influenced by the mountain climate of Rila, Pirin, Vlahina, and Maleshevo Mountains.

18.4 Methods

Streams are classified by order (Strahler 1952), and watershed parameters like topography (hypsographic curves), shape (Shchukin 1960; Filosofov 1960), and size are defined. We used SRTM DEM of 90 · 90 m resolution, improved to 30 · 30 m by digitizing topographic maps at M 1:50,000 and 1:25,000 scales as well as GPS coordinates. As extraction from the DEM was not sufficiently accurate, river courses were digitized and classified by order from the topographic maps.

Riverbed sediments are defined by *grain size*, *shape*, *roundness*, *and petrographic properties*, and cumulative curves were drawn for sand sorting based on the 75th and 25th percentiles (Pettijohn et al. 1972, 1987; Serebrjannij 1980). Catastrophic events were reviewed based on literature, press reports, and personal observations over the past 10 years to identify the conditions which promote torrential flow and debris flow development.

18.5 Discussion

18.5.1 Left Valley Sites

In *key site L1* several locations associated with the 1954 Blagoevgradska Bistritsa flood (Fig. 18.2) were selected based on data of the National Institute of Meteorology and Hydrology (NIMH) and literature (Glovnja 1958; Kanev 1989; Baltakov 2003). In the sources two incidents are mentioned: the blocking of the Bistritsa

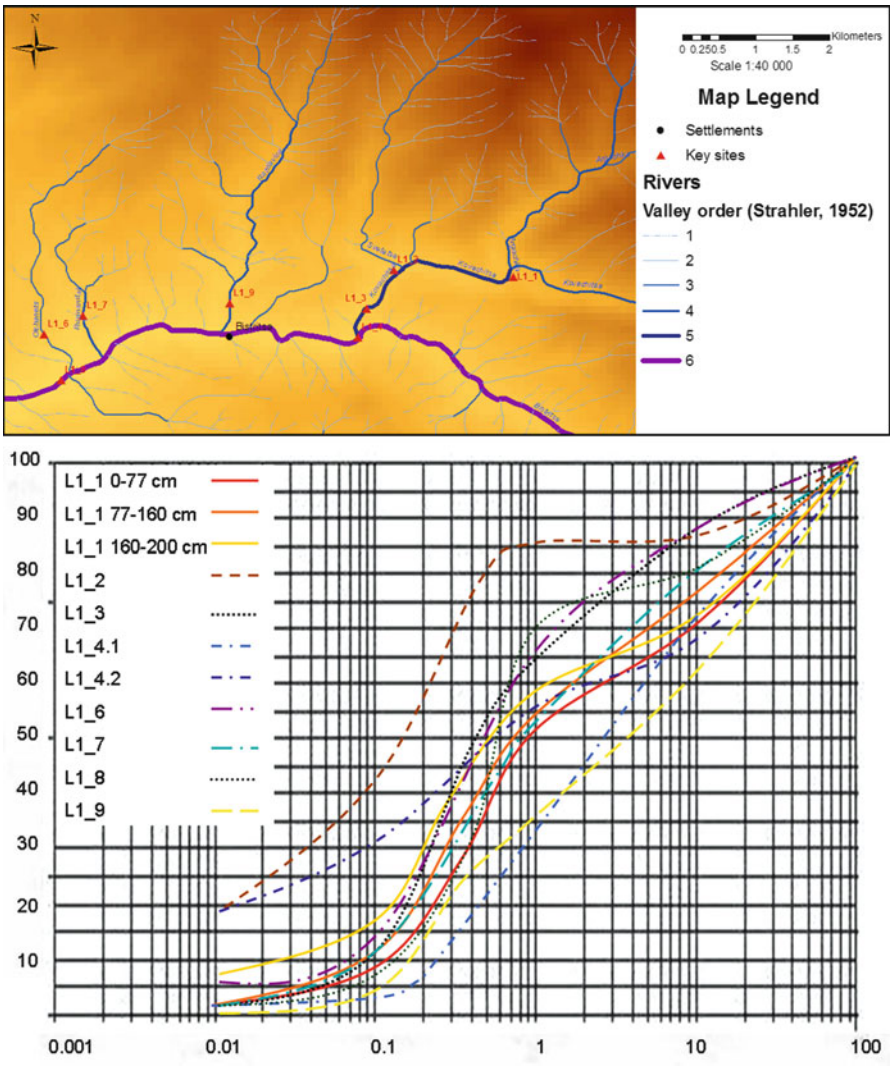

Fig. 18.2 Location of samples and results presented with cumulative curves of deposits in key site L1

River channel by sediments from the Kovachitsa fan and the deposition by tributaries downstream of the Bistritsa.

Our field studies showed that all the right tributaries of Blagoevgradska Bistritsa from Kovachitsa River to Blagoevgrad town acted like *paths for debris flows*. They formed separated levees and banks of incoherent heterogeneous material, left on spots above the contemporary channels (from 2 to 3.5 m); rocky terraces (to 16 m in

diameter) in the lower and flat sections of the floodplain, containing pavement of gravels and with fragments of older fans in the confluence areas. On the poorly developed floodplain, remains of marshes are preserved. These features are the same in all the tributaries in this area, but their dimensions are different, the largest being in the sections of the drainage network of the Argachka and Babkite Rivers.

Laboratory data proved that the largest overflow from July 1954 was of incoherent type, mixture of boulders and silt with predomination of silt (L1_4.2, L1_1), but in spots it was of boulders and predominantly of sand (Fig. 18.2). The main mass came from the Kovachitsa and Argachka Rivers, which blocked the Blagoevgradska Bistritsa River channel. The material was (and remained) slope debris from *rockfalls* and *tali* mixed with alluvium. It is possible that part of it is of fluvioglacial origin because the headwaters of these streams are in the zone of the Pleistocene *glacier tongues* (Glovnja 1958; Kanev 1989). Most of the debris was transported by traction. From a petrographic aspect gneisses predominate and the quartz is most resistant to roundness by water. Downstream the size of the particles decreases.

Key site L2 (Fig. 18.3) was observed during the flood of two unnamed left-bank tributaries of Struma River on 20 September 1994, in the area of the Zheleznik Gorge of the Struma River when the E79 highway was closed. The synoptic picture of the day was characterized by Kenderova and Vassilev (1997). Only in Blagoevgrad town did rainfall (over 44 mm) show a torrential character. The streams begin as *ravines* at an elevation of 680 m (L2_1) and 720 m (L2_2). They acted like paths for an incoherent debris flow of predominantly coarse material. They formed temporary and small features of erosion (ravines, steps, and evorsion potholes (up to 1 m diameter)) and accumulations (levees (to 4–5 m in height)), containing heterogeneous material and fans at their foot. Transportation of the coarse particles was by traction (43–92%) and the finer particles by saltation. Sample No L2_1_1 characterizes a profile in the fan of the river mouth, formed after 1994, and sample Nos L2_1_2, L2_1_3, and L2_1_4 represent accumulative features formed on September 20, 1994. The second stream (L2_2) is characterized by samples from its upper, middle, and downstream sections (L2_2_2 is from 1994 and the others from 2012). The data from the particle size analysis showed that in 1994 the stream had an incoherent character with predomination of the coarse fractions. The samples from 2012 do not differ in character from the previous deposits.

The rivers (Potoka, Melnishka, and Sushishka) in *key site L3* (Fig. 18.4) were described as debris flows in literature (Marinov 1984; Zakov 2001; Bruchev et al. 2001), but they did not present such character over the last 20 years. Their type is different from the others described here on grounds of geological conditions (Neogene sediments: breccias/conglomerates, conglomerates, sandstones, aleurolites, and clays). The higher roundness and percentage of broken pieces also point to their *Pliocene lacustrine origin*. The forms from their erosion and accumulation activity are newly formed ravines in the upper and the middle sections, thresholds in the channel profiles, levees of heterogeneous material in the floodplains, and fans in the mouth parts. There is alternation of *gorges and embayments* along the valleys of

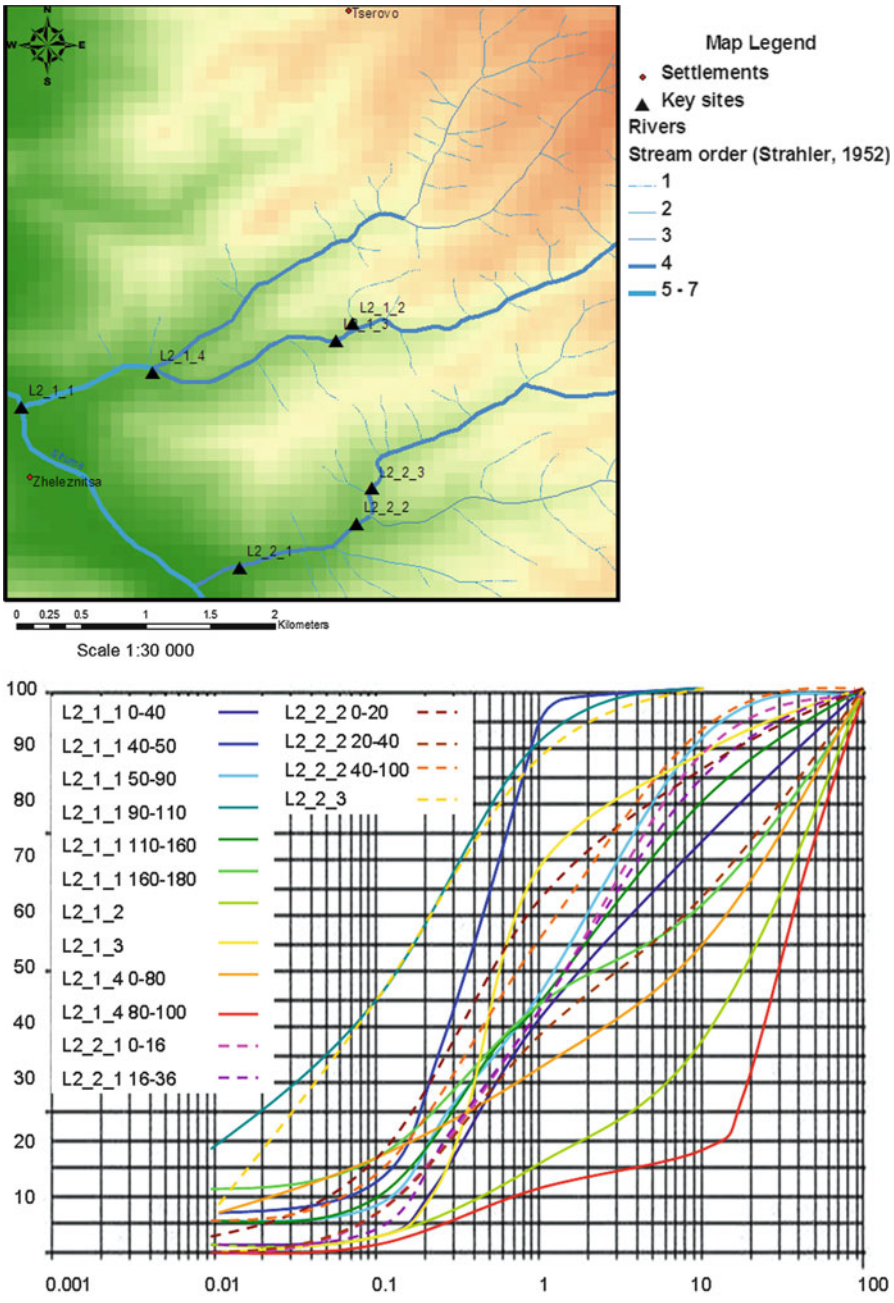

Fig. 18.3 Location of samples and results presented with cumulative curves of deposits in key site L2

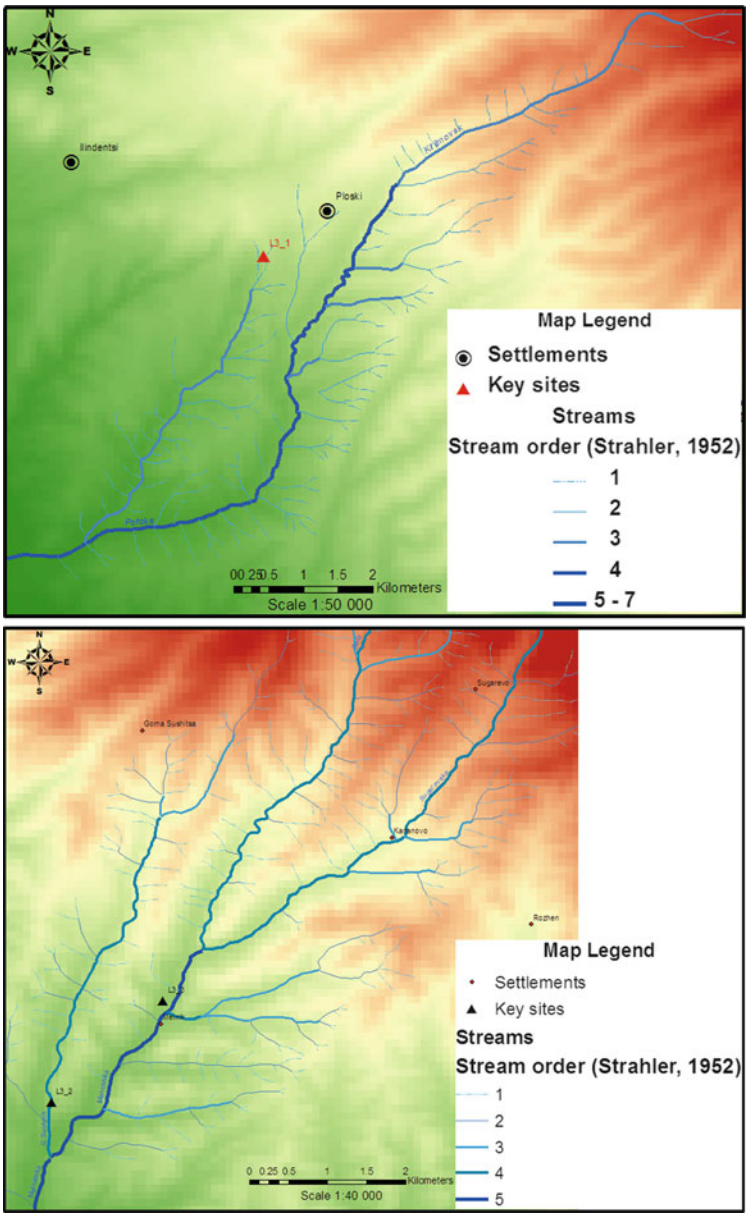

Fig. 18.4 Location of samples and results presented with cumulative curves of deposits in key site L3

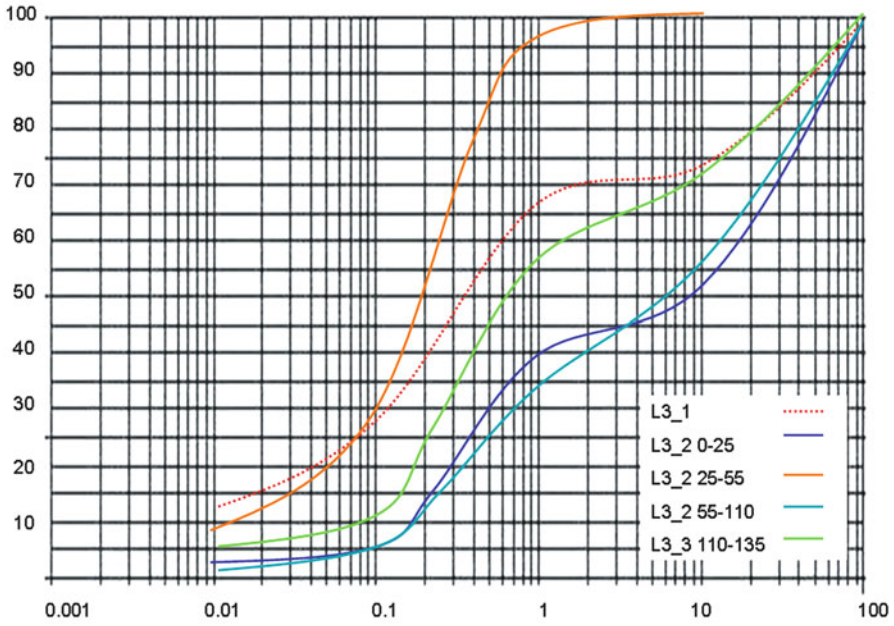

Fig. 18.4 (continued)

Melnishka and Sushishka Rivers because of differences in rock conditions and tectonics.

Laboratory data showed that all the rivers have *incoherent* materials. Transportation of the pieces was by traction and saltation.

18.5.2 Right Valley Sites

Key site R1 (Fig. 18.5) is in the valley of Gabrovska River (a tributary of Klisurska and Lagodashka Rivers). Its sources are located at 1,300 m in various petrographic provinces. Our observations showed that on May 18, 2009, and December 3–5, 2010, precipitations activated several debris flows on the tributaries and induced flooding of the Klisurska River. The weather situation on May 18, 2009, was similar to that of May 24, 2009 (see R3): in most places, the amount of rainfall was very low; in isolated sites, however, short but intense showers were recorded. This underlines the sporadic nature of summer rainfall as a rule, even when the events result from pronounced frontal activities. During the intense rain in December 2010, the Klisurska River suffered again a debris flow along its upper section, but the recently built concrete barrages and weirs withheld it.

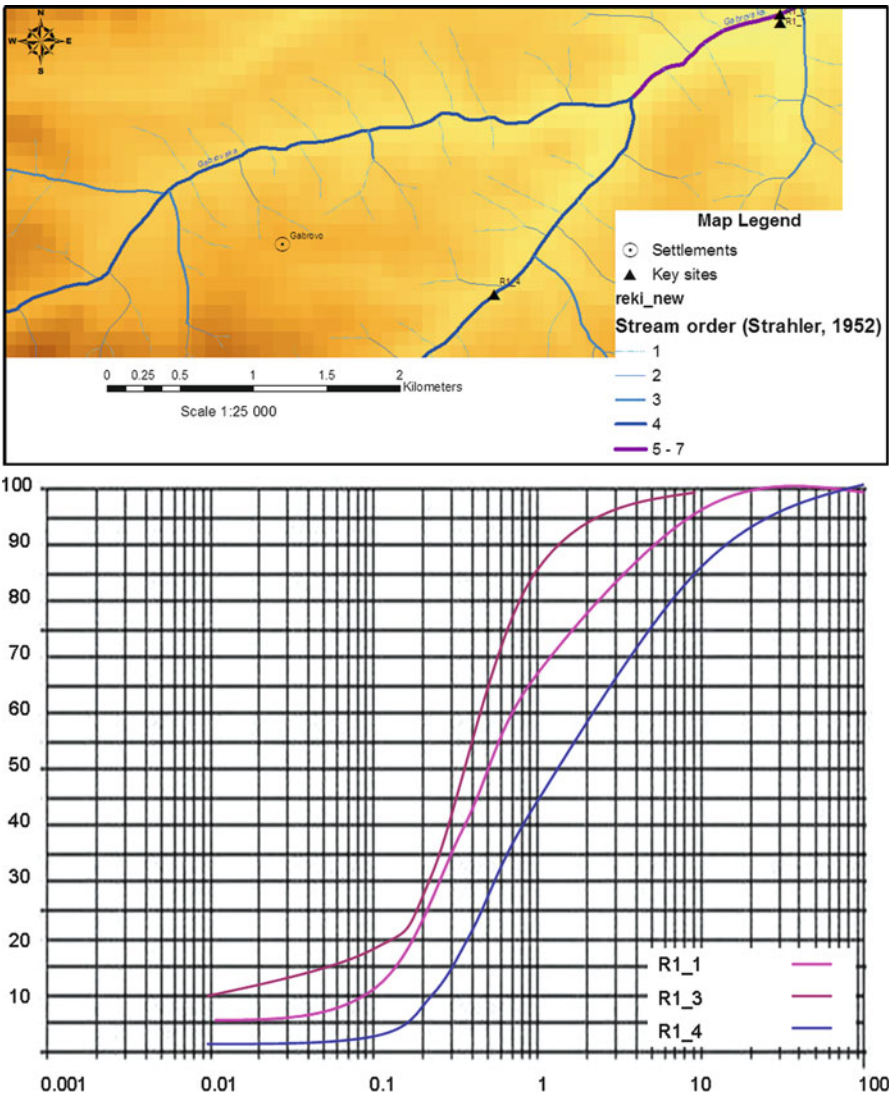

Fig. 18.5 Location of samples and results presented with cumulative curves of deposits in key site R1

Key site R2 (Fig. 18.6) represents the middle part and the mouth of the Potoka River on the western slopes of Vlahina Mountain. A *Mediterranean cyclone* was the reason why rainfall in northwestern Bulgaria and the high valleys of western Bulgaria exceeded the monthly average in the period December 3–5, 2010. *Rainfall* was most *abundant* in the area of the northern tributaries of the Struma River and prolonged with high intensity: on December 4, 2010, in Sofia 37.5 mm was measured, in Kyustendil 30.2 mm, in Riltsi 45 mm, in Boboshevo 52.5 mm,

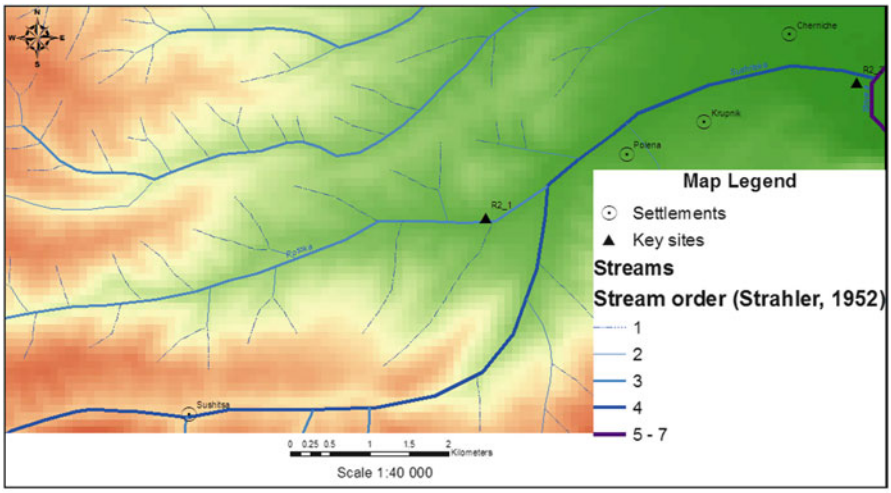

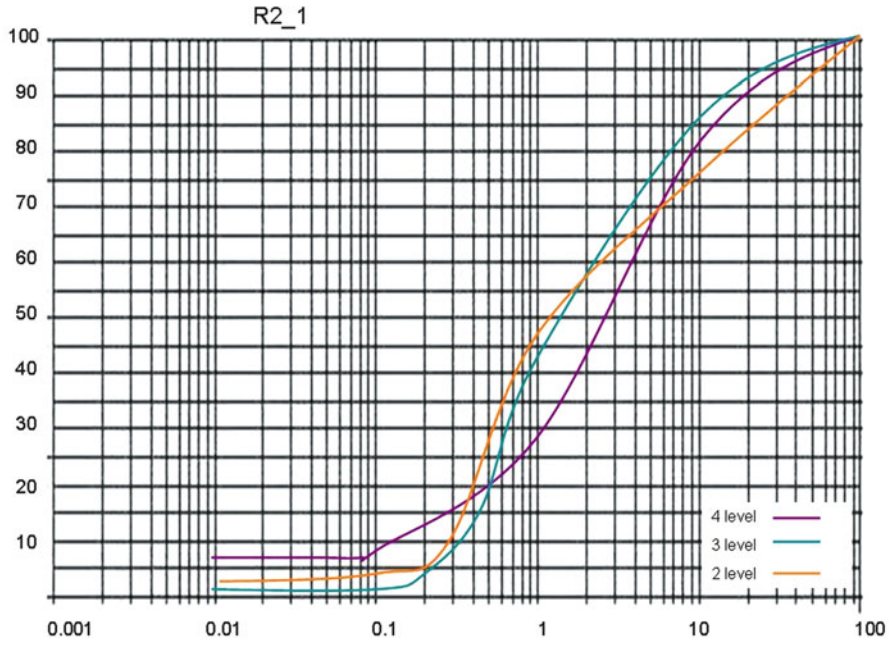

Fig. 18.6 Location of samples and results presented with cumulative curves of deposits in key site R2

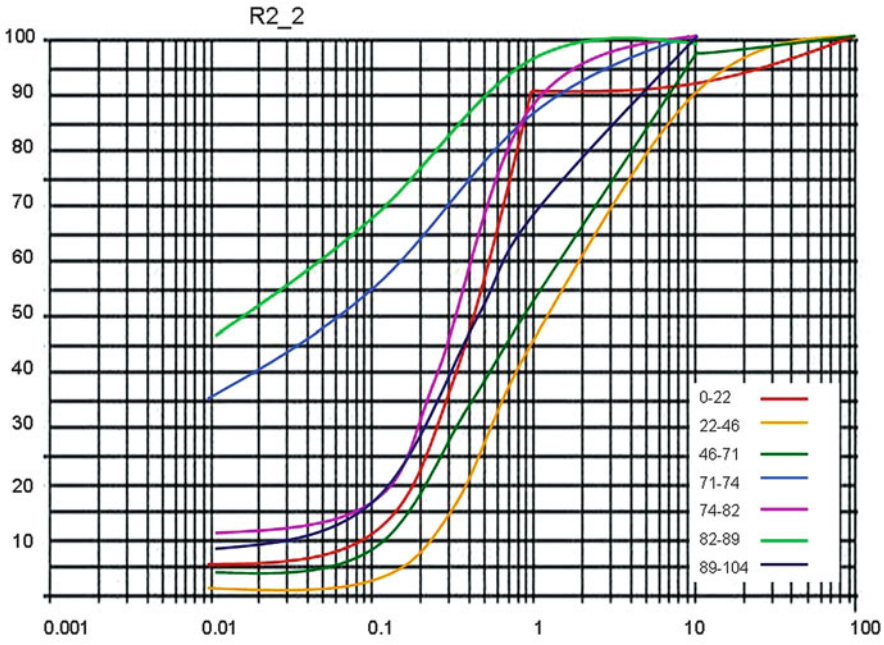

Fig. 18.6 (continued)

and in Dupnitsa 58.8 mm. Along with the rainfall of December 2 and 3, the amounts reached extraordinarily high values: in Sofia 73.8 mm, in Kyustendil 52.6 mm, in Riltsi 66.2 mm, in Boboshevo 78.5 mm, and in Dupnitsa 121.2 mm. The *synoptic situation*, which induced the rainfalls in the studied part of Bulgaria, was typical for this time of the year. In the middle section (R2_1), the river deposited on its floodplain levees of heterogeneous mixed material. The largest blocks lie upon small fragments and there is a significant amount of broken gravel grains. At its mouth, the Potoka River (R2_2) forms a large *alluvial fan* with various features: oxbow, sand bars, levees, etc. The analysis of the levees deriving from the debris flow (mostly aligned transverse to the flow direction) showed that they were deposited by incoherent flows carrying coarse debris (Fig. 18.3).

Key site R3 (Fig. 18.7) is a little stream, which runs 1.9 km south of R2 at the entrance of the Kresna Gorge. On May 24, 2009, it channeled a debris flow, carried sediments on the *road* of E-79, and, *blocking* it, led to its *closing* for more than 24 h. In its channel concrete *check dams* and *gabions* were installed.

The analysis of the ground synoptic situation leading to the occurrence of this debris flow shows a well-defined *cold front* that came over Bulgaria from west–northwest. The synoptic situation over Europe was characterized by a multicentered depression of parallel ridges of high pressure deriving from the Azores high. In the early hours of May 24 near Osogovo–Belasitsa mountain group and in particular over Krupnik

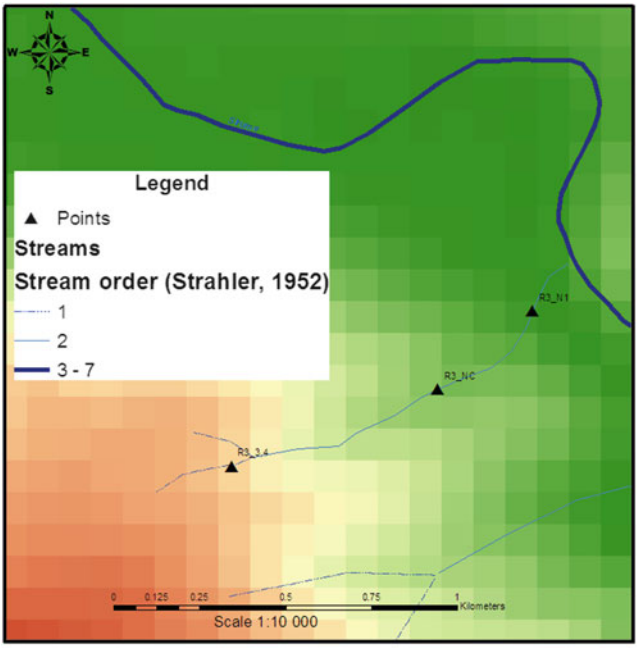

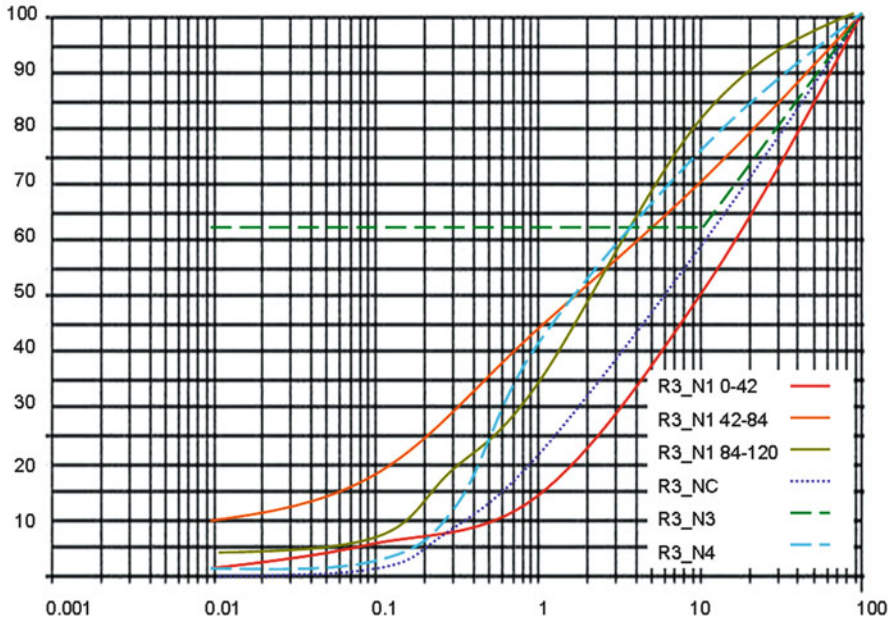

Fig. 18.7 Location of samples and results presented with cumulative curves of deposits in key site R3

Mountain, powerful cumulonimbus clouds had been developed. Many of the meteorological stations in southwestern Bulgaria, Eastern Macedonia, and northern Greece recorded *thunderstorms* and intense rainfalls. For the interval between 15 and 23 h on May 24, precipitation amounts were around 6 mm between Kyustendil and Sandanski towns. In some areas affected by the cold front, however, where water flow and orography, combined with an influx of warm, moist air from the southwest, created favorable conditions for the formation of expressed *cumulonimbus cells* bringing heavy and intense rainfall. We believe that such a cell caused the debris flow. Only rainfall in the range of 25–30 mm for the period from 17.30 to 18.30 h on May 24, 2009, could form a stream with a flow volume of 3,000 m^3 and deposition on the road in 1.5–2 m.

The catchment area of the stream is composed of porphyric biotite granites of Paleozoic age (Zagorchev 1990). Field observations and the laboratory data (Fig. 18.7) allowed us to divide the flow into *three sections*:

- Upper section: downstream of the confluence of two first-order tributaries, the stream runs as debris flow; in the main channel rock steps, evorsion potholes, small levees, and talus fans formed.
- Middle section: where the channel is developed in profile and there is a considerable variety of forms (temporary islands, levees, rocky thresholds, and talus fans), with various mechanical compositions.
- Lower section: characterized by a steep channel profile, with alluvial fan, rock steps and narrow reaches, and voluminous sediment accumulations.

Laboratory analyses (Fig. 18.7) from different reaches show incoherent sediments, although downstream the size of large pieces is reducing.

Key site R4 is located at the western foot of Ograzhden Mountain (Fig. 18.8). It includes three second- and third-order streams. Their channelization was in connection with the construction of a secondary road. In the observed period, they did not cause flooding and destruction. The main *features* are bedrock cuts and the formation of U-shaped valleys, small potholes, rock scarps with waterfalls, talus cones at the footslopes, levees of accumulated material, and stepped alluvial cones. Sorting in all the sections is very poor, which is a sign of their torrential character.

18.6 Conclusions

The data obtained from field observations and morphometric and laboratory analyses showed that on both sides of the Middle Struma Valley, *active incoherent debris flows* are restricted to certain first- to fourth-order tributaries, which vary for length, size of watershed, and elevation. A complex of erosional (potholes, rock thresholds and narrow gorges) and accumulational forms (transverse floodplain levees and alluvial fans at confluences) is observed with tali and rockfalls on valley

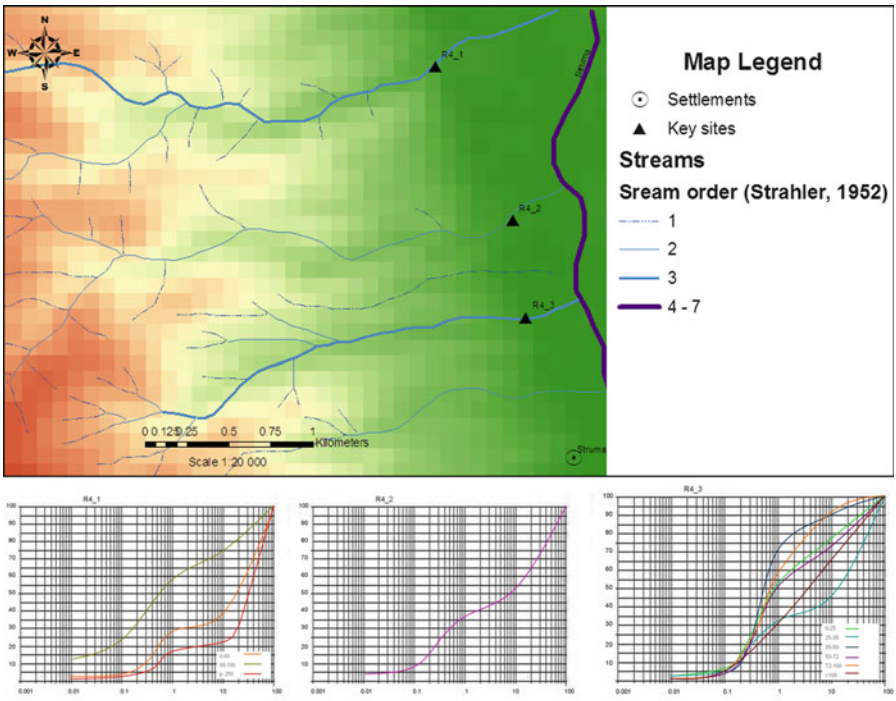

Fig. 18.8 Location of samples and results presented with cumulative curves of deposits in key site R4

slopes. Slope material is mixed with fluvial deposits in the channels. Debris flows impound trunk valleys and induce floods.

The typical *weather situation* triggering debris flow in the region is invasion of cold air into a warm and unstable air mass in cyclonic pressure fields with huge cumulonimbus clouds resulting in intense rainfall (25–30 mm day^{-1}) over a small watershed.

The analysis of synoptic weather situations underlined the random and spontaneous occurrence of debris flows in the region under study, proportional to rainfall intensity and soil moisture from previous rainfall events. Forecasting is made extremely difficult by the inability to predict the intensity and spatial distribution of precipitation.

Data from laboratory analyses showed the predominance of *coarse materials* (gravels and sands) up to 90%, while grain sizes below 0.02 mm diameter rarely reached 10%. Grains are angular and moved by saltation (at higher levels) and traction (close to the bottom). The amount of broken fragments is between 13 and 73%. Petrographic composition includes rocks of different ages and sustainability: granite granodiorite, migmatites, amphibolites, diorite, gneiss, etc. All the streams are from incoherent type and with predomination of the coarse fractions. Exceptions are those that occur in the southwestern foothills of Pirin Mountain of Neogene

sediments (conglomerates, sandstones, and sands). They increase the amount of sand (above 30%) and sediments of 0.1–0.02 mm grain size (20%), making the flow coherent. All studied tributaries of Struma River are fortified with flood defense, some of them not only once, by building of gabions, check dams, and concrete weirs.

The best way of *mitigation* (Biolchev 1966; Zakov 2001) is by using *gabions* which hold large blocks back and allow water and fine fractions to pass through. Our observations underline that the worst possible way of preventing debris flows is to build concrete *check dams* in the riverbed. Check dams cannot withhold sediment flow if gravels amount to an 80% share in load and sedimentation makes them inefficient within 10 years. There is a cumulative increase of transported sediment beyond each dam. Thus, future debris flows will cause even greater damages.

We believe that for the prevention of disasters, continuous monitoring of concrete structures along roads, slope stabilization by afforestation in the upper and middle watersheds, and the construction of gabions in the middle and lower sections are necessary.

References

Baltakov G (2003) Балтаков Г (2003) Неогенска и кватернерна скулптурна геоморфогенеза на източните части на Балканския полуостров (Neogene and Quaternary sculptural geomorphogenesis in the eastern Balkan Peninsula). Manuscript habilitation thesis, Sofia, 477 p. (in Bulgarian)

Biolchev A (1966) Биолчев А (1966) Ерозията и борбата с нея (Erosion and its control). Zemizdat, Sofia, 459 p (in Bulgarian)

Bruchev Il, Frangov G, Varbanov R, Ivanov P (2001) Geological hazards in the Western Periphery of the Rhodope Region. In: Proceedings of the international conference "Geodynamic hazards, late alpine tectonics in the Rhodope Region", Sofia, pp 17–27

Filosofov VP (1960) Философов ВП (1960) Краткое руководство по морфометрическому методу поисков тектонических структур (Short manual of morphometric methods in studying tectonic structures). Saratov University Press, Saratov, 94 p (in Russian)

Glovnja M (1958) Гловня М (1958) Геоморфоложки проучвания в Югозападния дял на Рила планина (Geomorphologic study of western part of Rila Mountain). In: Yearbook of the University of Sofia "St. Kliment Ohridski". Faculty of Biology and Geography, Geography 55(2):66–84 (in Bulgarian)

Kanev D (1989) Канев Д (1989) Геоморфология на България (Geomorphology of Bulgaria). University Press "St. Kl. Ohridski", Sofia, 322 p (in Bulgarian)

Kenderova R., Vassilev I (1997) Кендерова Р, Василев И (1997) Характеристика на селевия поток на 20.09.1994 г в Железнишкия пролом на р. Струма (Characteristics of the debris flow from 20.09.1994 in Zheleznik gorge of Struma River). In: Yearbook of the University of Sofia "St. Kliment Ohridski". Faculty of Geology and Geography, Geography 88(2):29–50 (in Bulgarian)

Kenderova R, Vassilev I (2000) Кендерова Р, Василев И (2000) Климатичните проблеми в България – причина за активизирането на селевите потоци (Climatic problems in Bulgaria – cause of debris flow activation). Geography Issues 1–4 (in Bulgarian)

Kenderova R, Ratchev G, Baltakova A (2012) Кендерова Р, Рачев Г, Балтакова А (2012) Формиране и проява на селеви потоци в долината на Средна Струма (3–5.12.2010) (Debris flow development and evidence in Middle Struma Valley (3–5.12.2010)). In: Yearbook of the

University of Sofia “St. Kliment Ohridski”. Faculty of Geology and Geography, Geography 105(2) (in print) (in Bulgarian)
Marinov ITs (1984) Маринов ИЦ (1984) Ерозията и борбата с нея във водосбора на р. Мелнишка (Erosion and its control in Melniska River catchment area). Manuscript habilitation thesis, Sofia (in Bulgarian)
Pettijohn J, Potter P, Siever R (1972, 1987) Sand and sandstone. Springer, New York, 553 p
Radev Zh (1933) Радев Ж (1933) Епигенетичните проломи по долината на р. Струма (Epigenetic gorges in the Struma valley). Bulg Geogr Soc News 1:305–336
Ratchev G, Nikolova N (2009) Рачев Ж, Николова Н (2009) Климатът на България (Climate of Bulgaria). In: Yearbook of the University of Sofia “St. Kliment Ohridski”, Faculty of Geology and Geography, Geography 101(2):17–29 (in Bulgarian)
Serebrjannij L (1980) Серебрянный Л (1980) Лабораторный анализ в геоморфологи и четвертичной палеогеографии (Laboratory analyses in geomorphology and Quaternary paleogeography). VINITI, Geomorphology series 6 (in Russian)
Shchukin IS (1960) Щукин ИС (1960) Общая геоморфология (General geomorphology), vol. 1. Moscow University Press, Moscow, 614 p
Strahler AN (1952) Hypsometric (area-altitude) analysis of erosional topography. Bull Geol Soc Am 63:1117–1142
Velchev A (1994) Велчев А (1994) Формиране и еволюция на съвременните ландшафти в Югозападна България (Formation and evolution of the present-day landscape of Southwest-Bulgaria). Manuscript habilitation thesis, Sofia, 388 p (in Bulgarian)
Zagorchev I (ed) (1990) Загорчев И (ред.) (1990) Геоложка карта на България (Geological map of Bulgaria) Scale 1:100 000. sheet Razlog; sheet Petrich
Zakov D (2001) Зъков Д (2001) Ерозия (Erosion). Martilen Ltd., Sofia, 243 p (in Bulgarian)

Web Links

http://www.wabd.bg/bg/docs/plans/PORN/DOKLAD_2.pdf
http://webcache.googleusercontent.com/search?q=cache:_Vm_HlYwoS4J:www.vesti.bg/index.phtml%3Ftid%3D40%26oid%3D3456251+&cd=8&hl=bg&ct=clnk&gl=bg&client=firefox-a
http://www.google.bg/url?sa=t&rct=j&q=&esrc=s&source=web&cd=5&ved=0CDcQFjAE&url=http%3A%2F%2Fwww.wabd.bg%2Fbg%2Fdocs%2Fplans%2FStruma%2FRazdel%2520I-STRUMAl.doc&ei=C907UMDxLI2LswbB6IGACg&usg=AFQjCNHWvGkPWh04PJmYn3_E6sh3XSd0bg
http://www.wabd.bg/bg/docs/plans/OB/RAZD/RBMP_OBI.pdf
http://www.wabd.bg/bg/docs/plans/PORN/porn2012/Pril_1_12.doc

Part IV
Other Impacts

Chapter 19
The Effects of Flash Floods on Gully Erosion and Alluvial Fan Accumulation in the Kőszeg Mountains

Márton Veress, István Németh, and Roland Schläffer

Abstract Along the Hungarian-Austrian border the rainfalls of 2009 and 2010 have reached intensities of 100 mm day^{-1}. The events have caused flash floods along watercourses and had remarkable geomorphological impacts: accelerated the evolution of existing erosional and depositional landforms (headwater channels, rills, gullies, gorges, minor alluvial fans, and sediment veneers) and generated new features in the Kőszeg Mountains, Western Hungary, of metamorphic rocks, and a deep weathering mantle. In addition to the rainfall properties, we found that the most influential conditions on the rate of erosional processes and the extent of damage in foothill settlements were the high density of roads, the depths of surface deposits, and the slope inclinations on watersheds. Gullies and alluvial fans are classified by their origin and response to disastrous hydrometeorological events.

Keywords Intense rainfall • Channel incision • Cross sections • Gullies • Alluvial fans • Sediment veneer • Hungary

19.1 Introduction

Heavy rainfalls may induce sheet wash, rill, and gully erosion if the environmental setting is suitable for these processes (Czigány and Lovász 2005). Through the concentration of runoff and removal of sediment from headwater areas of mountain streams during the resulting flash floods, landforms are modified, while accumulations in the foothills generate new landforms and threaten densely populated areas. The disastrous events may not only change the course geomorphic evolution but also have an effect on vegetation, drainage network, man-made structures (railways, roads, buildings), and agricultural production.

M. Veress (✉) • I. Németh • R. Schläffer
Department of Physical Geography, University of West-Hungary, Károlyi Gáspár tér 4, 9700 Szombathely, Hungary
e-mail: vmarton@ttk.nyme.hu; inemeth@ttk.nyme.hu; sroland@ttk.nyme.hu

D. Lóczy (ed.), *Geomorphological impacts of extreme weather: Case studies from central and eastern Europe*, Springer Geography, DOI 10.1007/978-94-007-6301-2_19,

19.2 Study Area

Part of the Eastern Alps, the Kőszeg Mountains is a geological "fenster," where the Penninicum Nappe built up of metamorphic rocks (quartz phyllite, calcareous phyllite, black lead phyllite and metaconglomerate) is exposed due to uplift dated to 15.1–18.5 Ma (Demény and Dunkl 1991) and subsequent denudation. The southern part of the mountains, studied in this chapter (Fig. 19.1), is constituted by an anticline structure with a southern dip of strata and, for geomorphology, a main ridge and adjoining ridges aligned in west to east direction. The ridges result from the regression and valley incision of the tributaries of the Gyöngyös stream towards the main ridge and the dissection of the mountain surface into a range of interfluvial ridges between the valleys.

The stream valley selected for the analysis of the geomorphological impacts of intense rainfalls, the Bozsok Valley, has been carved by the outflow channel of the Szénégető Spring, 50 m upstream (Fig. 19.1). Along this section of 300 m length weathering mantle is rather thin, and the valley floor is flat and wide. Adjoining to the

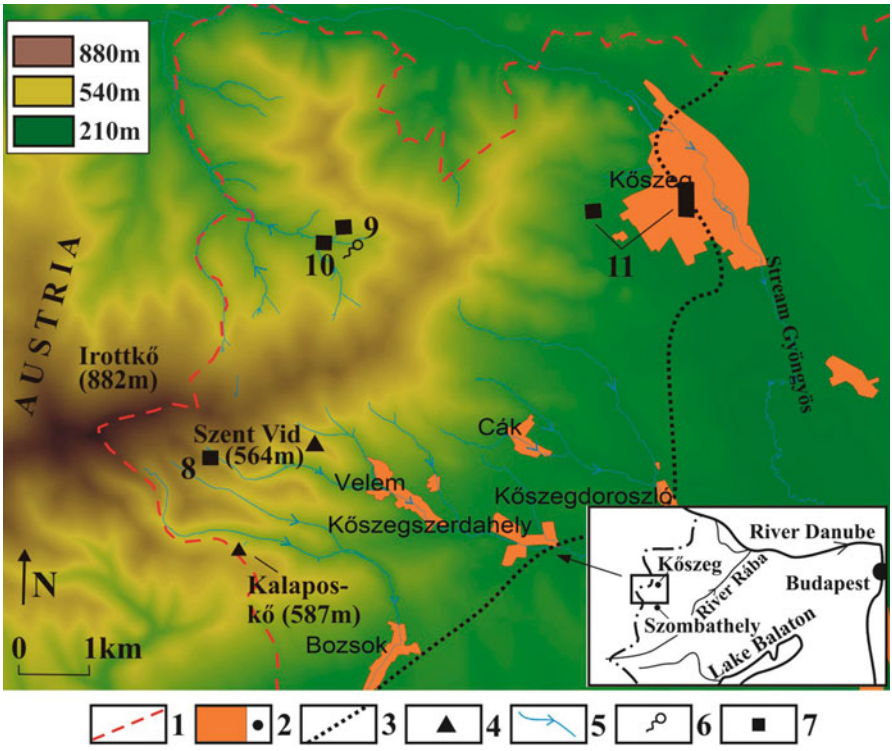

Fig. 19.1 Location of measurement sites in the southern Kőszeg Mountains. *1*, national border, *2*, settlement, *3*, important peak, *4*, borderof the Kőszeg Mountains, *5*, stream, *6*, spring, *7*, measurement sites

drainage network, *hollow roads* (abandoned carriage tracks in the weathering mantle) are important routes of runoff in the mountains. Their origin is related to forest clearance intensified significantly towards the end of the twentieth century.

19.3 Objectives and Methods

In order to reveal the impact of the intensive rainfalls of 24 June 2009 (with intensity of 100 mm day^{-1}), and in 2010 (rainfall amount on June 2, 50 mm; on June 18, 37 mm; and on 15 July 2010, 45 mm; cumulative amount for 20–26 September 2010: 113 mm) on the channel, *cross sections* of the stream channel in the Bozsok valley were surveyed at three sites in the post-precipitation period, on 20 October 2009 (Fig. 19.1). Channel depths were recorded at 20 cm intervals along a profile perpendicular to the thalweg, and the measurements were repeated three times (on 13 September, 30 September, and 6 October 2010). Cross-section changes were established through the superimposition of profiles upon one another.

The cross sections before 24 June 2009 were reconstructed from floor remnants and the extent of *channel incision* established from the difference between the position of the old channel floor and that of the channel floor existing at the time of measurement (Fig. 19.2).

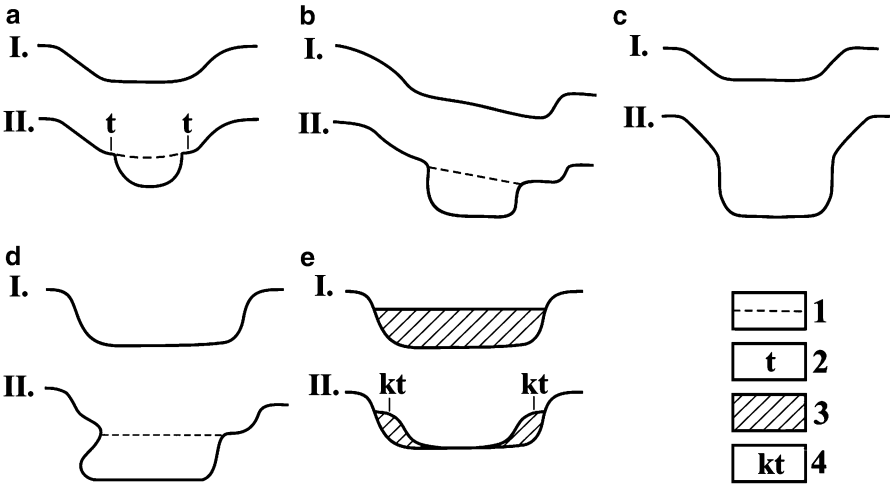

Fig. 19.2 Reconstructing former channel shape from morphology. *1* – Former channel floor, *2* – Floor remnant, *3* – channel fill, *4* – floor remnant in channel fill. *I* – Previous channel shape, *II* – Channel shape after development of a younger channel. (**a**) Symmetrical floor remnants developed through the partial destruction of the channel floor, (**b**) symmetrical floor remnants at various altitudes developed through the destruction of a slanting channel floor, (**c**) no floor remnant (channel floor completely destroyed), (**d**) asymmetrical floor remnant and overhanging side developed through thalweg shift, (**e**) symmetrical channel fill remnants developed through the partial destruction of channel fill

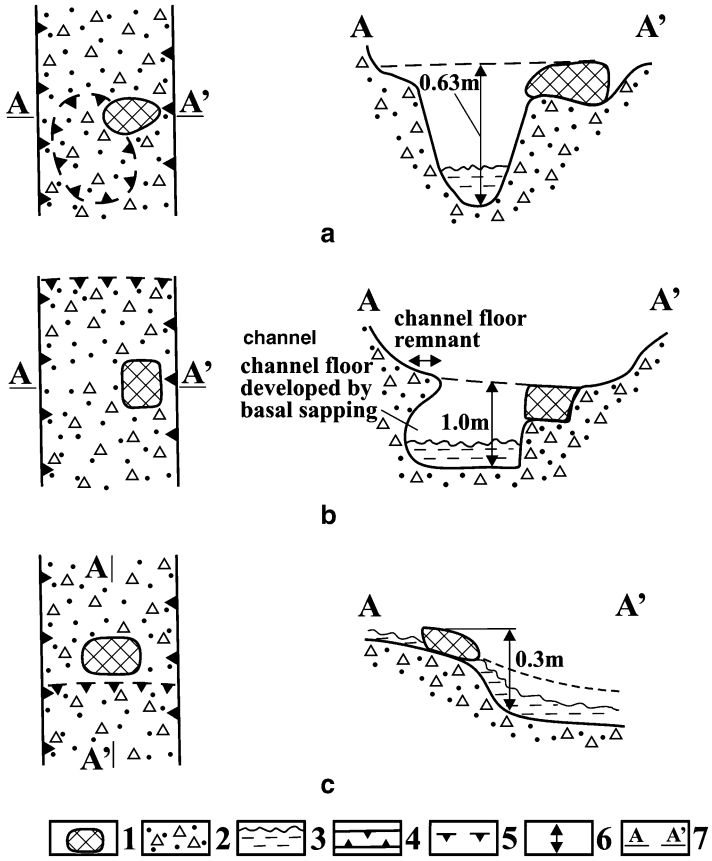

Fig. 19.3 Channel scouring processes downstream of the Szikla Spring (surveyed on 2 October 2009). (**a**) Channel scouring near the boulder, (**b**) scouring all around the boulder, (**c**) scouring only downstream of the boulder. *1* – Boulder. *2* – Sediment accumulation. *3* – Channel flow. *4* – Stream bed. *5* – Step and pool developed by incision on 24 June 2009. *6* – Extent of incision (m). *7* – Site of profile

The end points of channel incision by reaches and the extension of alluvial fans were related to a fixed point. The process of *channel scouring* was reconstructed from observations on the stream of the Szikla Spring (Fig. 19.1). Scouring around and downstream of large boulders were studied (Fig. 19.3).

Rill and *gully development* was monitored along the same stream below the Szikla Spring. The gullies developed during the intensive rainfall and flash flood of 24 June 2009, were counted and their dimensions surveyed (see in detail Veress et al. 2012).

The expansion and thickness of *sediment veneer* accumulated by 24 June 2009, flash flood at the town of Kőszeg was recorded at ten sites and represented on a map. As most of the sediments had already been cleared away at the time of observation, the highest mark on the surrounding houses was taken as the guiding point to

estimate the thickness of accumulated sediment, visualized employing DigiTerra Map GIS software (Veress et al. 2012).

19.4 Results

The *channel* of the Bozsok Valley has significantly *incised* in the wake of the 2009 flash flood. At the profile marked B-4, the extent of incision was ca 0.5 m (Fig. 19.4a), while at profile B-5 it was 1.25 m (Fig. 19.4b). The channel also deepened at profile B-3. Channel cross sections were modified into complex shapes through the remobilization and redeposition of channel fill (Fig. 19.5).

Dense networks of *rills* also developed in both 2009 and 2010, mostly along forest and hollow roads (now unused). Gullies may be distinguished according to their cross sections and their longitudinal profiles (Leopold and Miller 1956). The sections of discontinuous gullies have different floor gradients or are separated by alluvial fans. Although the majority of the gullies in the mountains had developed before 2009, we observed that they expanded significantly due to intensive rainfall and runoff. A series of minor gullies developed on the floor of the stream rising near Szikla Spring (Fig. 19.6).

Renewed incision began during the intensive rainfalls in 2010, and *secondary internal channels* developed on the older channel floors, producing *complex channels* (Fig. 19.7). Large boulders protect fine-grained deposits from entrainment by the stream flow (Fig. 19.3). Several-meter high steps emerged on the channel floors, where boulders were exposed above scour pools. Previously formed step-and-pool series were often buried under flash flood deposits, and new steps were created during the next high-water event. *Channel regression* has also been observed: the steep heads of the internal channels carved within older channels in 2009 retreated further in 2010 (Fig. 19.7).

Observation concerning the influence of artificial structures, like *culverts*, could also be made (Fig. 19.8). Some concrete rings withstood the flood, while others were displaced. Sediment deposition upstream of the culvert was followed by scouring beyond it, where channel slope increased. Intensive channel incision (exceeding 3 m) on the floor of the Bozsok Valley happened downstream of *bridges* in at least three sites in 2009.

Hollow roads developed into *gorges* with dense rills on their floors since 2009, and alluvial fans accumulated at their outlets to terrains of lower slope.

In 2009 and 2010 *mass movements* (translational slides, topples) also appeared on steeper slopes – mostly the sides of valleys and gorges, often developed on south-dipping bedding planes and, on the opposite side, heads of beds. The roots of trees can intrude to a smaller depth into the rock on the bedding planes than on the heads of beds. Therefore, trees are more easily uprooted by *creep* on the bedding planes, particularly during major storms.

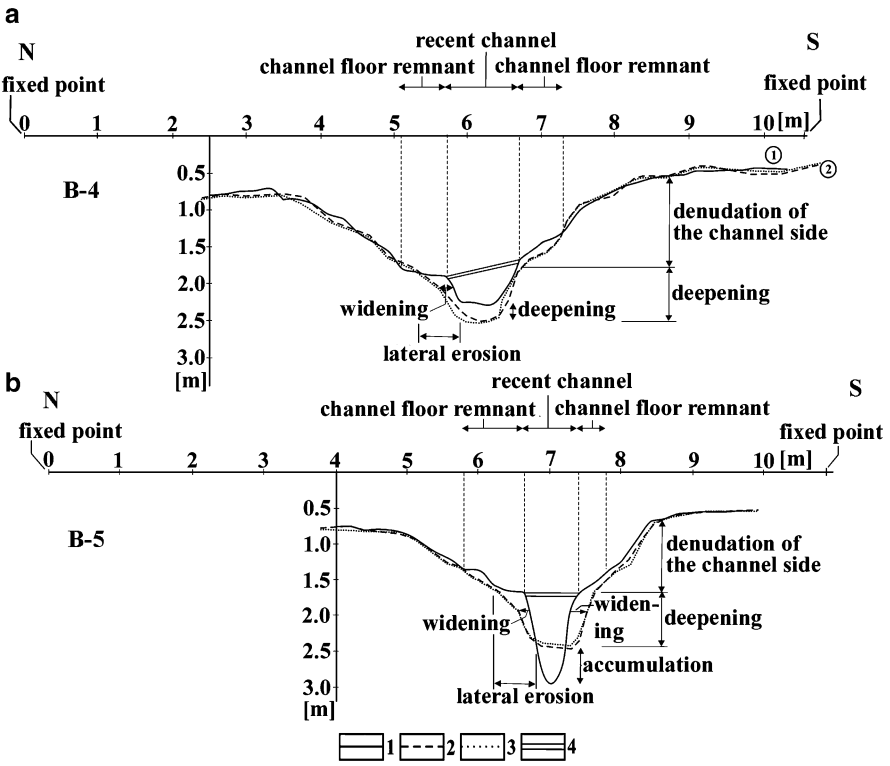

Fig. 19.4 Two channel profiles in the Bozsok Valley. (**a**) Profile B-4. (**b**) Profile B-5. *1* – Channel as measured on 20 October 2009. *2* – Channel as measured on 13 September 2010. *3* – Channel as measured on 30 September 2010 and/or 6 October 2010. *4* – Channel floor before 24 June 2009

Coarser stream sediments accumulated on *alluvial fans* within the valleys (Fig. 19.9a) or along the mountain margins (Fig. 19.9b). Avulsions, junctions, and braided channels are characteristic of them. The material in alluvial fans is well sorted, with buried channels filled by gravel, and their structure is cross-bedded and truncated by erosion surfaces. *Sediment veneers* may originate directly from rills or deposited by streams.

19.5 Discussion

The channels of the mountain valleys have undergone considerable changes since 2009: they incised along their whole length or dissected into reaches with or without scour and fill. Erosion worked periodically on the floor of discontinuous gullies. Gully erosion due to the increased runoff from intense storms did not generally cut through the soil mantle by incision. Such features are regarded

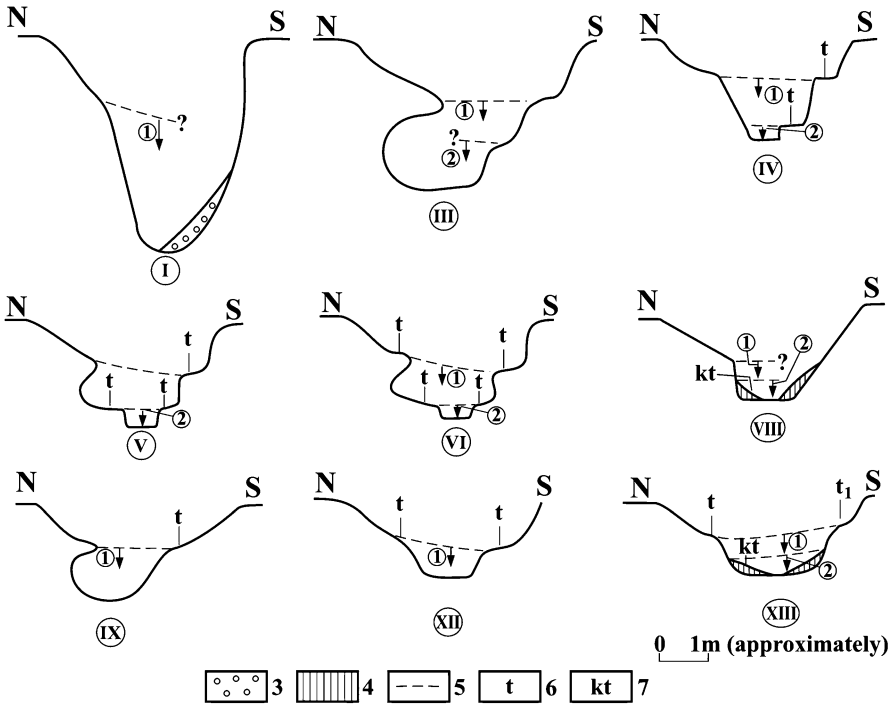

Fig. 19.5 Channel profiles (nos I to XIII) across the stream channel of the Bozsok Valley. *1* – Collapsed sediment. *2* – former channel fill. *3* – Former channel floor. *4* – Channel floor remnant. *5* – Channel floor in the fill. *6* – Channel section created on June 24, 2009. *7* – Channel section created after June 24, 2009

embryonic gullies and common in the sides of the Bozsok Valley. Rainwater channeled into hollow roads may alleviate gully development.

Gullies and *gorges* channeled overland flow and contributed to the development of other landforms. For instance, a gully at the head of the Bozsok Valley has emptied onto a deep-cut hollow road, which incised intensively both in 2009 and 2010.

In the mountains alluvial fans developed in 2009 fall into two classes: inside the channels (internal fans – Fig. 19.9a) or outside the channels (external fans – Fig. 19.9b). The external alluvial fans are larger than the valleys from where their material derives. During the intensive rainfalls of 2009, primarily *internal alluvial fans* formed in the mountains, the shape of which was controlled by the bearing channels of elongated platform. The size of the alluvial fans may be several tens of meters along the axis of the channel with a width of a few meters. Internal alluvial fans are small in size and have a steep front (up to 70°); their material is non-sorted and comprise soil and plant debris (branches, trunks). A series of alluvial fans developed along some channel sections. The above characteristics prove that internal alluvial fans consist of the deposits of a single flood.

Alluvial fans may be *dry* or *wet*. Wet alluvial fans are accumulated by permanent streams and wet fans by gullies, gorges, and hollow roads. Wet fans were typical of

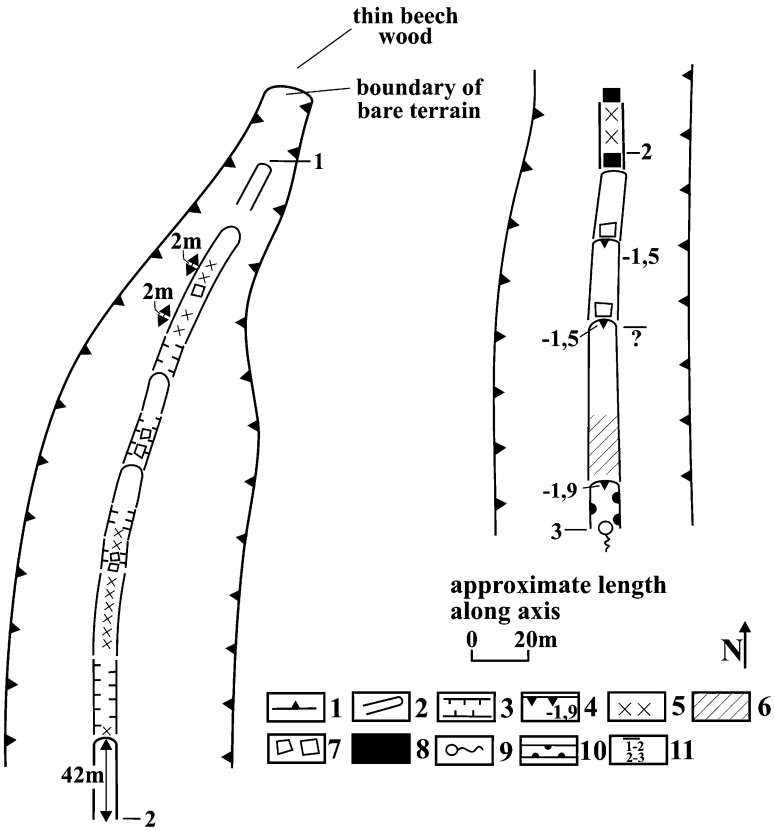

Fig. 19.6 Ephemer and embryonic gullies developed in 2009 on the floor of the intermittent stream channel above Szikla Spring (measured on October 20, 2009). *1* – Creek margin, *2* – gully developed in 2009 (depth 0.2–1 m), *3* – embryonic gully in 2009 (depth 0.1–0.2 m), *4* – step (depth in m), *5* – partly filled channel developed in 2009, *6* – section of completely filled channel developed in 2009, *7* – boulders, *8* – bedrock, *9* – spring, *10* – channel, *11* – the two figures parts show two various sections of the same creek

the floods in 2009. Preexisting alluvial fans expanded considerably during the events of 2010. The internal alluvial fans probably extended along their lower margins and were destroyed at their apex. Incisions were observed all over the external alluvial fans in 2009 and 2010. Alluvial fans often formed above obstructions (e.g., bridges or large woody debris), and channel accumulations occurred upstream of exposed boulders (causing scour and fill) in the Kőszeg Mountains as the effect of the flash floods various accumulation features developed not only in the valleys of the mountain but also at the margin of the mountain (Fig. 19.10).

Fine-grained deposits accumulated in the form of *sediment veneers* in the administrative area of Kőszeg town, manifested in the plugging of culverts, instability of various structures in and next to channels, and damage to roads (e.g., the road between Velem and Szent Vid was destroyed, and on Pintér-tető 24 rills cut into the forest roads during the 2009 event).

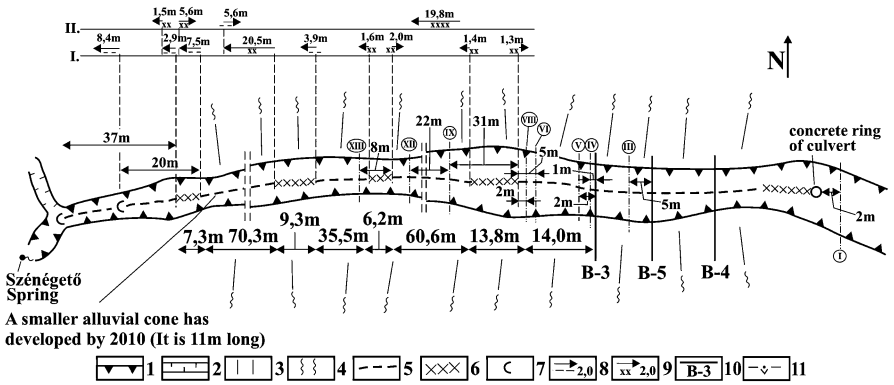

Fig. 19.7 Sketch of channel incision and alluvial fan development in the Bozsok Valley (without scale). *1* – Channel predating the June 24, 2009 event. *2* – Gully. *3* – Valley floor. *4* – Valley gradient. *5* – Channel reach developed during rainfall. *6* – Wet alluvial fan developed during June 24, 2009, rainfall. *7* – Head of channel. *8* – Channel growth (arrow shows regression, length in m). *9* – Alluvial fan growth (arrow shows the direction of expansion, length in m). *10* – Site of profile. *11* – Code. I – Data from measurements on September 19, 2010, II – Data from measurements on September 30, 2010. The sites of channel profiles (I–XIII) in Fig. 19.5 are indicated

Fig. 19.8 Culvert in the Bozsok Valley on October 30, 2010. *1* – Valley floor. *2* – Channel. *3* – Caved-in channel side. *4* – Displaced concrete ring. *5* – Stable concrete ring

Fig. 19.9 Accumulation landforms in the Bozsok Valley (Photos taken on October 30, 2010). *1* – slope of Bozsoki valley, *2* – floor of Bozsoki valley, *3* – floor channel, *4* – alluvial fan which developed on June 24, 2009, *5* – channel on the alluvial fan, which developed after June 24, 2009, *6*-new channel which developed after June 24, 2010

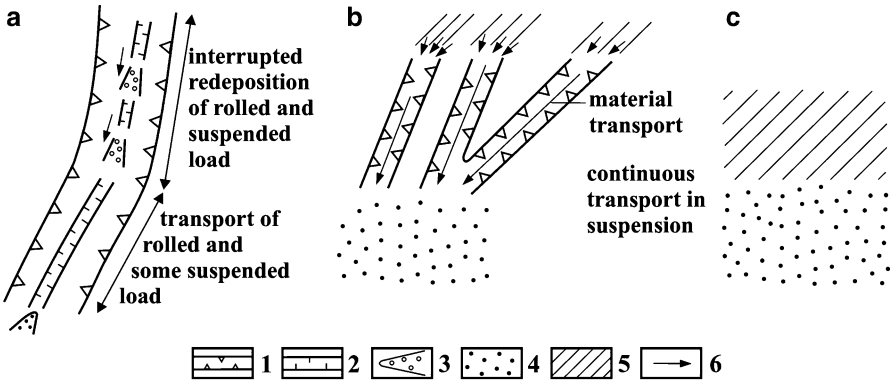

Fig. 19.10 Genetic types of accumulation features in the Kőszeg Mountains. (**a**) Alluvial fans on the floor and at the valley mouth. (**b**) Sediment veneer due to sediment transport in the valley. (**c**) Sediment veneer deposited from the sediment transported by rills. *1* – Valley, *2* – stream channel or gully, *3* – alluvial fan, *4* – sediment veneer, *5* – zone of rills, *6* – redeposition of sediment

19.6 Conclusions

The impact of the intensive rainfalls in the 2-year period was manifested in channel incision, alluvial fan expansion (in valleys and at their outlets), gully and rill development, and sediment veneer accumulation. Overall channel incision is estimated at 0.7 m for a rainfall amount of 100 mm. The longitudinal axes of the alluvial fans in the Bozsok Valley changed (increased or decreased) by 2–6 m at the expense of the incised channel sections. The lengths of incised channel sections increased by 2–10 m during the study period. At the same time there were channel sections which decreased as some alluvial fans expanded.

If rainfalls with intensity and frequency similar to those in 2009 and 2010 happen in the future, even *badland formation* may take place in some parts of the Kőszeg Mountains. Badlands can preferably develop on valley sides where the heads of slate beds are overgrown by trees.

The proportion of *forests* among land use classes have decreased by the year of 2008 compared to that of the 1900s on the catchment of the valleys leading to the town, while clear-cut surfaces and arable land have grown. The length of forest roads has increased from 23.86 to 61.19 km. The spreading of summer houses also contributed to increasing road density, which induced rill formation and sediment transport. Sediment transport may happen either periodically or continuously during intensive rainfall and endanger human structures and agricultural land.

Acknowledgement The research was supported by the EU under Grant No. TÁMOP-4.2.2-08/1-2008-0020.

References

Czigány Sz, Lovász Gy (2005) A várható klímaváltozás és hatása hazánk néhány jelenkori geomorfológiai folyamatára (Predictable climate change and its impact on recent geomorphic processes in Hungary). In: Debreceni Földrajz Disputa, Természetföldrajzi és Geoinformatikai Tanszék, Debreceni Egyetem, Debrecen, pp 97–111 (in Hungarian)

Demény A, Dunkl I (1991) Preliminary zircon fission-track results in the Kőszeg Penninic Unit, W-Hungary. Acta Miner Petrogr 32:43–47

Leopold LB, Miller JPC (1956) Ephemeral streams: hydraulic factors and their relation to the drainage net, Professional papers 282-A. US Geological Survey, Reston

Veress M, Németh I, Schläffer R (2012) The effects of intensive rainfalls (flash floods) on the development on the landforms in the Kőszeg Mountains (Hungary). Cent Eur J Geosci 4(1):47–66

Chapter 20
Weather Extremities and Soil Processes: Impact of Excess Water on Soil Structure in the Southern Great Hungarian Plain

Norbert Gál and Andrea Farsang

Abstract With global climate change, the frequency of extreme weather events, which also affect soil properties, has increased. Hungarian agriculture was stricken with drought in the 1990s, whereas inland excess water has caused damages in 2000, 2006 and again in 2010. According to multivariable correlation tests, in addition to hydrometeorological, geological and topographical factors, soil properties also influence the formation of excess water, which can, in turn, modify soils (bring about hydromorphic characteristics or physical degradation). The aim of the present study is to reveal the interactions between inland excess water and soil properties illustrated by a case study carried out on a fertile chernozem soil after the extensive excess water coverage of 2010. Three excess water patches were identified for analysis from multitemporal Landsat images in the study area and were connected in a southwest-west–northeast-east aligned, 700-m-long, catena. In July 2011, topsoil samples were collected along this catena at 50-m intervals from three depths, to compare the particle-size distribution and agronomical structure of soils of temporary excess water with those not affected by it. In order to create a multilayer map from soil compaction data, penetration resistance and relative soil moisture were measured at a depth of 60 cm at 117 points in the 45-ha study field using a 3 T System hand penetrometer. The results call attention both to the physical soil degradation caused by excess water and to the risk of erosion due to inadequate tillage or cultivation practices.

Keywords Excess water • Inundation • Soil structure • Penetration resistance • Chernozem • Hungary

N. Gál (✉) • A. Farsang
Department of Physical Geography and Geoinformatics,
University of Szeged, Egyetem u. 2, 6722 Szeged, Hungary
e-mail: galnorbert@geo.u-szeged.hu; farsang@geo.u-szeged.hu

D. Lóczy (ed.), *Geomorphological impacts of extreme weather: Case studies from central and eastern Europe*, Springer Geography, DOI 10.1007/978-94-007-6301-2_20,

20.1 Global Climate Change and Inland Excess Water

Precipitation is one of the most important natural factors influencing the formation of inland excess water or groundwater flooding (Salamin 1966; Pálfai 2011), and its spatial and temporal distribution are becoming more and more extreme and unsettled due to global climate change (OMSz 2005, 2012). The area stricken by excess water surpassed 250,000 ha several times in the last decade (in 1999, 2000, 2006 and 2010, (Fig. 20.1)) (Vízügy 2011; Pálfai 2011).

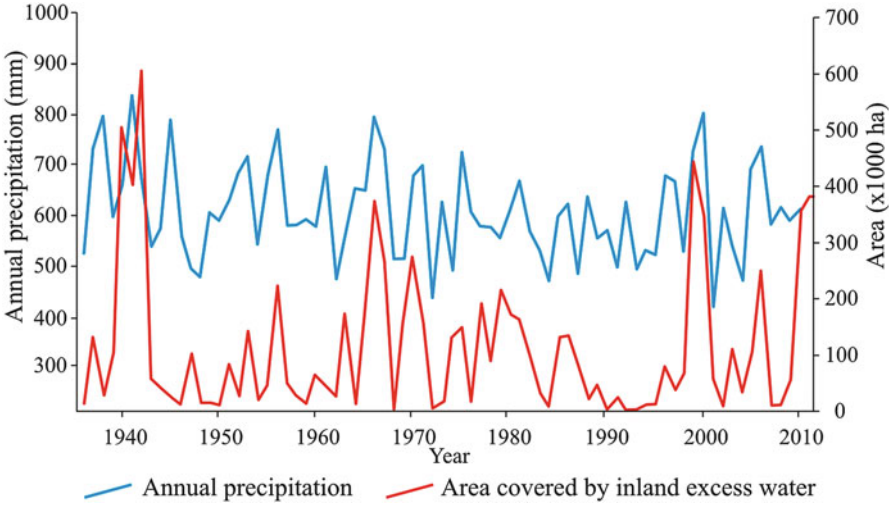

Fig. 20.1 Annual precipitation and area flooded by inland excess water in Hungary, 1935–2011 (After Pálfai 2011 and OMSz 2005, 2012)

Fig. 20.2 Inland excess water and soil properties on an arable field in South Hungary (Photo by authors)

The direct and indirect causes of *excess water* have often been analysed (Salamin 1966; Rakonczai et al. 2003; Pálfai 2004; Várallyay 2005; Bozán et al. 2008; Körösparti et al. 2009). The conclusion of researchers is that this phenomenon is a compound system with several key factors, including hydrometeorology, relief, soil, geology, groundwater, land use and technical influences. According to multivariate correlation analysis, the decisive elements are soil properties (Fig. 20.2) (Körösparti et al. 2009).

20.2 Concepts for Excess Water Assessment

20.2.1 Definitions

Several disciplines have proposed *definitions* for excess water (Török 1997; Pálfai 2001). As a *traditional*, non-process-oriented aspect of water management, this term can be used when continuous ponds and inundations appear, ground and surface water flow is slow and water level increases notably in the drainage system. From the *biological* perspective, excess water occurs when inundation by high levels of groundwater or saturated soil encumbers – or even totally inhibits – life. According to this definition, no open water surface is needed for excess water. The *economic* view considers the damages excess water causes, for instance, to crops or real estates. (In the case of agriculture, excess water occurs when the expenses are higher due to inundation or saturated soil than the surplus income of the unaffected areas.)

According to the *physical geographical* approach, water resources can be divided into groundwater and surface water, despite – as different approaches have shown – the fact that inland excess water is temporary and can be considered as ground and surface water at the same time. One of the most recent definitions conceives excess water as surplus water in the soil, which renders the upper soil saturated on the one hand and results in continuous inundation of areas with no runoff on the other, creating surface water on a larger scale (Kozák 2006).

20.2.2 Classes of Excess Water

To mitigate or prevent the stress caused by inland excess water, it is essential to know the relationships between first causes and influencing factors. Three different genetic types of inland excess water can be distinguished (Fig. 20.3) (Rakonczai et al. 2011).

Horizontal or *accumulative excess water* originates in precipitation and geomorphology. As this type of excess water precipitation can neither evaporate from nor infiltrate into the soil, a large amount of water appears and accumulates in local depressions (Fig. 20.3a). On a plain with a gentle slope, there is no appreciable

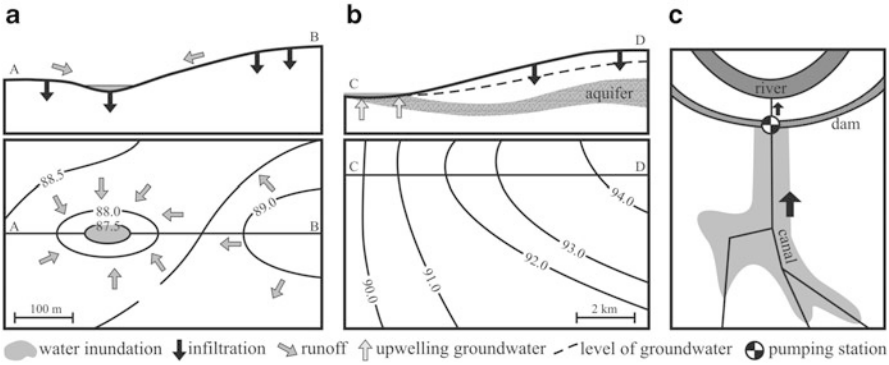

Fig. 20.3 Formation of three categories of inland excess water. (**a**) Horizontal or accumulative type; (**b**) vertical or upwelling type and (**c**) 'queuing up' type (After Rakonczai et al. 2011)

runoff or horizontal transport of water, so the formation of excess water is principally influenced by soil and hydrometeorological factors (e.g. frost).

The *vertical* or *upwelling type* derives from the upward push of groundwater. Groundwater flows from higher areas towards lower areas, and pressure conditions make groundwater appear on the surface. This type is common in alluvial fans, where the coarse-grained sediments of buried former riverbeds enable horizontal groundwater flow, and in former floodplains protected by dykes, where water can percolate below the dyke (Fig. 20.3b).

The third type, '*queuing up*' *excess water*, is of anthropogenic origin: it is related to the insufficient capacity of canals leading to a pumping station, where the water is pumped into a main river. The rate of the water conduction is determined not by the rate of excess water accumulation but by the capacity of the pumping station (Vágás 1989). If this capacity is not sufficient, water will flood the fields next to the canals (Fig. 20.3c).

20.2.3 Conditions for the Occurrence of Excess Water

Excess water formation can be influenced by hydrometeorological (frequent precipitation, water accumulation, e.g. as snow or ice, reduced evaporation, frozen soil), geomorphologic and topographic reasons (local depressions, edge of alluvial fans), hydrogeological agents (positions of impermeable strata and aquifers) and soil properties as *natural factors*. *Human factors* include water management structures (drainage systems, dykes), land use (built-up areas, railways, highways), irresponsible cultivation and lack of modern agrotechnics.

20.3 Excess Water and Soil Properties

In the process of excess water formation, soil properties are influential in the following ways (Fig. 20.4) (Rakonczai et al. 2011):

1. The soil is *not degraded* but the *infiltration rate* is lower than the *precipitation intensity*. The formation of excess water is influenced by soil depth and plasticity. Soils with high values of Arany's plasticity index (above 42, hygroscopicity higher than 3.5) have low infiltration capacities.
2. *Saturated* (*biphase*) *soil* has a limited infiltration capacity (saturated with water from previous precipitation or melting snow).
3. Infiltration is prevented by *frozen topsoil* in late winter.
4. A *compact impermeable layer* forms on the surface or in the topsoil due to permanent external pressure (from agricultural vehicles, animals, etc.). Compaction can affect any type of soil and can also be due to low amounts of precipitation.
5. Soils with a compact (clayey) soil horizon near the surface (*plough pan*) caused by improper land use and tillage in the same depth (monoculture, irrigation and compaction by vehicles) (Pálfai 1988; Gyuricza 2001). In wet periods, tillage causes compaction of the soil at a depth of 25–35 cm, which thickens upwards and downwards if not remedied. The depth of the new ploughing decreases due to the high penetration; hence, less water can be stored in the topsoil. Compaction can be expressed as bulk density (higher than 1.5 g cm^{-3}), porosity (less than 40%) and penetration resistance (above 3.0 MPa by the relative moisture content of field capacity) (Farkas and Gyuricza 2006; Jury and Horton 2004).
6. Soils with an *extreme moisture regime* due to *crusting* (cemented by ironstone, calcium carbonate or gypsum).
7. Soils with *extremely unfavourable water budget* due to high *salinity/sodicity* and/or *clay accumulation* in the B horizon. As Na^+ ions induce large-scale swelling, these soils are also crusted.

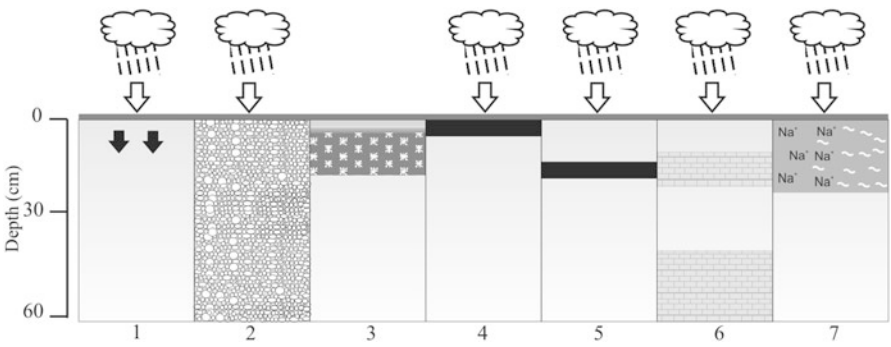

Fig. 20.4 Pedological reasons for the formation of inland excess water – for explanation, see text (After Rakonczai et al. 2011)

20.4 Case Study: Southern Great Hungarian Plain

20.4.1 Objectives

The impacts of inland excess water on the physical structure were studied in a degradation-free chernozem soil in the field and in the laboratory. *Chernozems* are the most fertile soil in Hungary, characterised by humus accumulation, crumb structure and calcium saturation (Stefanovits 1999). Chernozem areas are used mostly for farming, hence the risk of inland excess water does not only involve ecological but also economic damages.

20.4.2 Methods

Based on a multitemporal analysis of *Landsat TM* images (for April 2000, June 2006 and July 2010), a study area temporarily covered by excess water was selected (on the southern Great Hungarian Plain). In this process, the chernozem class of soil as identified on the *AGROTOPO maps* (scale: 1:100,000, MTA TAKI 1990), the soil maps of Kreybig's survey (Kreybig et al. 1938; scale: 1:25000, 1933–1951), the recharge zones on the regional hydraulic regime map by Almási (2001), excess water inundation maps by Pálfai (2000) and Corine Land Cover 50 database were all considered (Fig. 20.5).

Therefore, as a study area, a 45-ha Calcic Chernozem, frequently inundated arable land was delimited in Békés County, South Hungary. This area with infusion (wetland) loess is characterised by extremely low relief (1 m km^{-2}), an annual mean temperature of 10.6 °C and an annual precipitation of 570 mm (Dövényi 2010). Three major inland excess water patches were appointed, and a 700-m-long catena was fitted on them. In July 2011, soil samples were collected along this catena at 50-m intervals from depths of 0–5, 10–15 and 20–25 cm. Particle-size distribution was measured according to MSZ-08-0205:1978 Hungarian Standard (Buzás 1990), and agronomic structure was identified with dry sieving – 9 classes of structural aggregates were separated (>20, 20–10, 10–5, 5–3.15, 3.15–2, 2–1, 1–0.5, 0.5–0.25 and <0.25 mm). Agronomic structure was expressed as *mean weight diameter* (*MWD*), calculated from the mean size of the aggregate-fractions (D_x) according to their weight ratios (weight %) (Kézdi 1974; Filep 1999).

$$\mathrm{MWD\,(mm)} = \frac{(\mathrm{weight\%})_1}{100} \times \mathrm{D_1} + \frac{(\mathrm{weight\%})_2}{100} \times \mathrm{D_2} + \cdots + \frac{(\mathrm{weight\%})_9}{100} \times \mathrm{D_9}$$

To detect soil compaction caused by inland inundation, *penetration resistance* (MPa) and relative soil moisture (expressed in volume percentage of a moisture state of field capacity [2.5 pF]) were determined at a depth of 60 cm with three repeats at defined points ($n = 117$) on a 25 × 25-m grid over the 45 ha of study

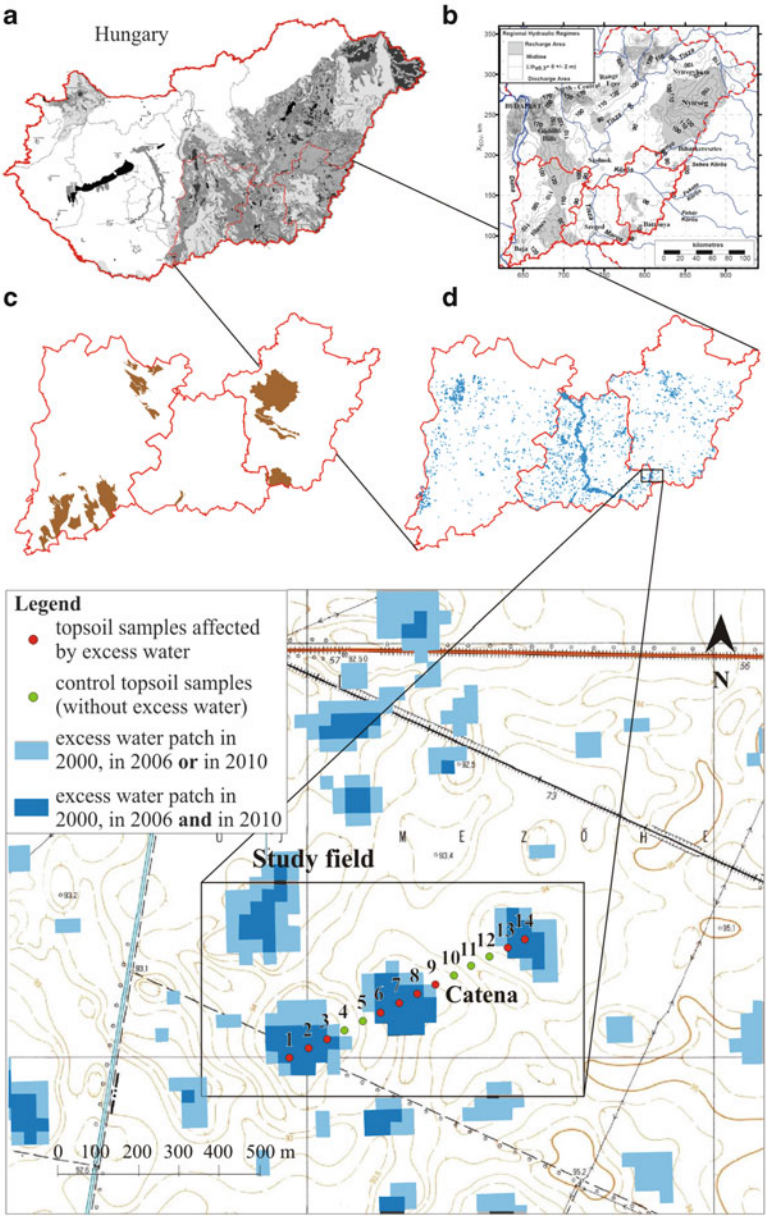

Fig. 20.5 Steps in defining the boundaries of the study area considering (**a**) inland excess water frequency maps by Pálfai; (**b**) regional hydraulic regimes by Almási; (**c**) chernozem soil category from agrotopographic map; (**d**) excess water pattern derived from Landsat images

field using a 3 T System hand penetrometer. The mean was calculated for the measured 21,060 data pairs in each 5 cm. Extreme values and data from depths of 0–5 and 55–60 cm were removed from the analysis. The data were visualised as *multilayer maps of soil compaction*.

20.4.3 Results

Two classes were derived from the soil samples: samples affected by excess water (Nos 1, 2, 3, 6, 7, 8, 9, 13, 14) and unaffected reference samples (Nos 4, 5, 10, 11, 12). The results were evaluated from the smallest particle to the largest aggregate. At each sampling point, the particle-size distribution (the proportion of clay, silt and sand fractions) was determined for three depths. The mean of each depth was calculated for the entire sampling point, resulting in a mean proportion of silt, sand and clay (Table 20.1).

The samples from inundated areas were characterised by a higher proportion of clay (26.16–45.47%) compared to the non-inundated reference areas (21.02–33.49%), while the proportion of sand fraction was lower. Both on the area covered and not covered by excess water, the particle-size distribution of the soil samples was characterised by an *increase* in the proportion of *clay with increasing depth* (Table 20.2). This increase, however, was larger in the case of soils affected by inland excess water (ca. 6%). A similar proportion, but with the inverse trend, was observed for the sand fraction, while no significant change (1.5%) was found for the silt fraction. The texture group of excess water soils, derived from the proportions of clay (<0.002 mm), silt (0.002–0.05 mm) and sand (>0.05 mm), was silty clayic loam, while the reference soil samples had a silty loam texture.

The agronomic structure, i.e. the means of the MWD indices (Fig. 20.6) for soils with excess water were higher than those of control samples, and reciprocity can be seen in the changes of the MWD indices in soils with excess water compared to control samples. The aggregate size of water-affected samples was greatest at a depth of 0–5 cm depth (mean 12.36 mm), while this parameter was 5.86 mm in the case of control samples, and the value was only 7.83 mm at a depth of 20–25 cm. The greatest differences were observed in the maximum values of the MWD indices: the MWDs of samples covered by water (23 and 16 mm) show massive *crusting*, while the maximum MWDs of control points (9.88, 7.49 and 9.26 mm, respectively) indicate a more favourable, *crumb structure*.

To detect changes in soil structure induced by excess water coverage, 117 points were measured by 3 T System hand penetrometer and classified either as ‘covered by excess water’ ($n = 40$), ‘sampled from the edge of excess water patches’ ($n = 25$) or ‘non-affected (control)’ ($n = 52$). From the vertical profiles, *relative moisture variation* of 17% (volume) could be observed between the points covered

Table 20.1 Average particle-size distributions of inundated and control soil samples

Soil samples	Fraction	Mean (%)	Maximum (%)	Minimum (%)	Standard deviation
Inundated ($n = 27$)	Clay	34.57	45.47	26.16	4.17
	Silt	33.95	50.43	30.10	4.12
	Sand	31.48	42.24	4.10	6.76
Control ($n = 15$)	Clay	27.43	33.49	21.02	3.74
	Silt	36.98	41.33	29.58	3.20
	Sand	35.59	41.38	32.45	2.34

Table 20.2 Vertical changes in particle-size distribution of soil samples

Soil samples	Depth (cm)	Clay (%)	Silt (%)	Sand (%)
Inundated ($n = 9$)	0–5	32.64	34.12	33.24
	10–15	35.61	32.56	31.84
	20–25	34.36	33.18	32.46
Control ($n = 5$)	0–5	24.04	37.88	38.07
	10–15	28.09	36.63	35.28
	20–25	30.15	36.42	33.43

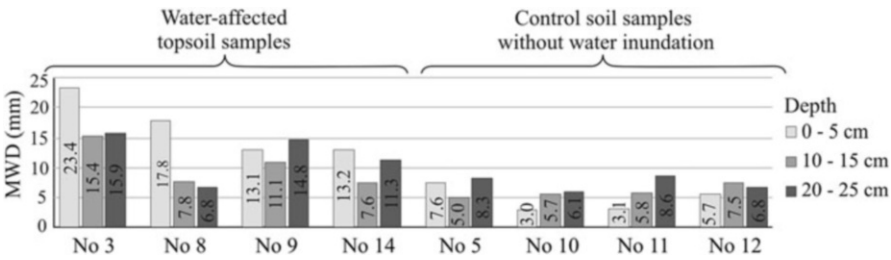

Fig. 20.6 Vertical change of agronomic structure expressed by MWD indices for some topsoil samples

by excess water and control points (Fig. 20.7a). The same difference applies for penetration resistance, which was 0.2 MPa lower for points affected by excess water (Fig. 20.7b), and its profile showed higher values at two depths: 15–20 and 40–45 cm (above 3.0 MPa), indicating soil compaction (Birkás 2008).

On the *multilayer interpolation maps* areas with higher moisture content coincided with the excess water patches delimited earlier by remote sensing methods (Fig. 20.8). Moisture content reached field capacity (2.5 pF) at a depth of 40 cm; hence the hand penetrometer did not differentiate in relative soil moisture content of beyond this depth, showing a maximum (99 vol %) value. Soil compaction first appeared at a depth of 15–20 cm in the maps of penetration resistance. Maximum compaction was measured at 40 cm depth (Fig. 20.9).

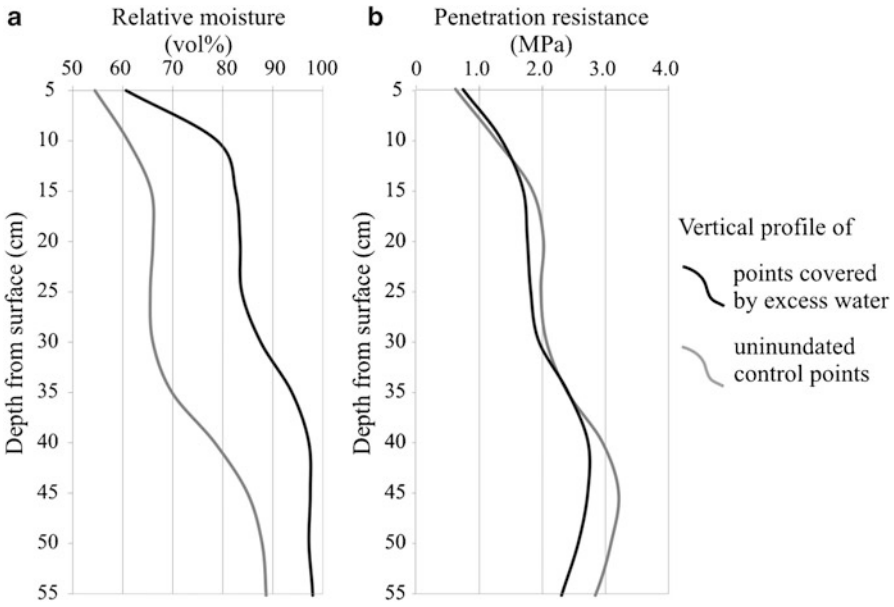

Fig. 20.7 Vertical profiles of relative moisture content (vol%) (**a**) and penetration resistance (MPa) (**b**) in two categories of sampling points

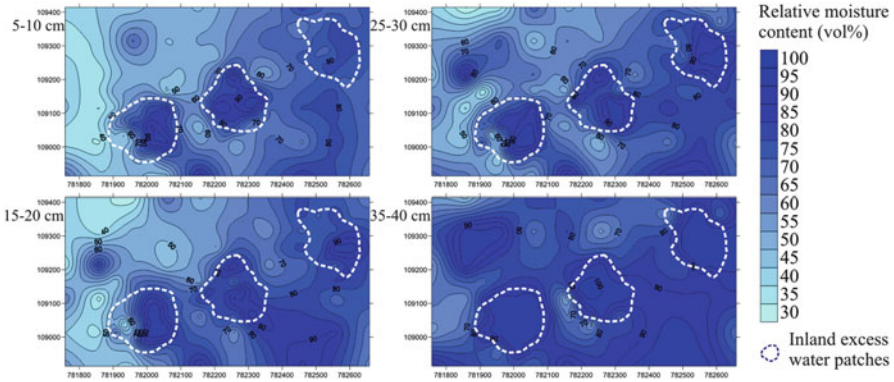

Fig. 20.8 Multilayer interpolation maps of relative moisture content in four different depths

20.4.4 Conclusions

Inland excess water is a complex phenomenon, and physical soil parameters and characteristics play a major role in its formation. It may even affect soil types of high quality and fertility if water infiltration is hindered by high clay content,

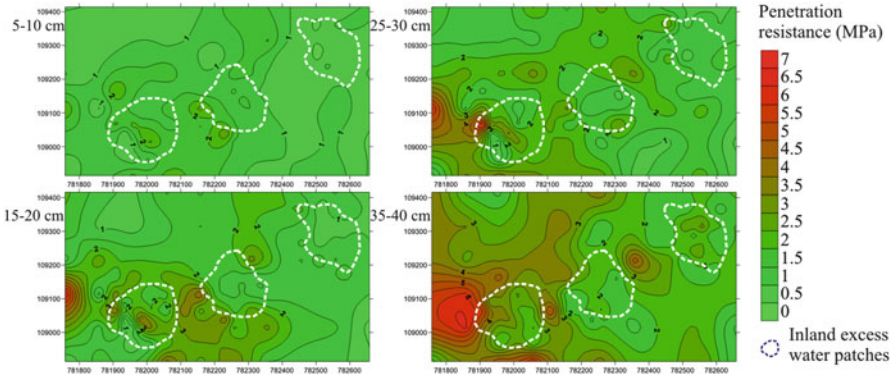

Fig. 20.9 Multilayer interpolation maps of penetration resistance at four different depths

Fig. 20.10 Road course had to be changed after water inundation at the study site in Békés County, Hungary (Photo by authors)

slight compaction, plough pan and other conditions. Furthermore, physical soil degradation (e.g. in soil structure) can be conceived as an indication of inland excess water and temporary water coverage.

Soil particle distributions change over the long term. Therefore, the differences between excess water covered and uncovered (control, reference) samples do not derive from inundation. Soil particle-size distribution is one of the agents responsible for the formation of the phenomenon. The soil samples from the inundated areas have higher clay and lower sand contents which hinder the infiltration of water into the soil.

In addition to hydrometeorological, geological and topographical factors, through positive feedback mechanisms, soil properties also influence the formation of excess water, and excess water can, in turn, modify soils (bring about hydromorphic characteristics or physical degradation).

Studying the results of vertical penetration resistance, plough hard pans can be identified at depths of 15–20 and 40–50 cm. Higher penetration resistance measured at the edges of the inundated patches can be explained by the observation that vehicles have to make a detour around such patches. Therefore, the higher moisture content in their neighbourhood is associated with the compaction by vehicles (Fig. 20.10).

Inland excess water as a direct consequence of weather extremities decreases the adaptability of soils to further extreme weather events. In addition, it is not only increasing the sensitivity of soils but generates higher frequency of excess water.

References

Almási I (2001) Petroleum hydrogeology of the Great Hungarian Plain, Eastern Pannonian Basin, Hungary. University of Alberta, Edmonton, 624 p

Birkás M (2008) Environmentally-sound adaptable tillage. Akadémiai Kiadó, Budapest, 356 p

Bozán Cs, Bakacsi Zs, Szabó J, Pásztor L, Pálfai I, Körösparti J, Tamás J (2008) A belvíz-veszélyeztetettség talajtani összefüggései a Békés-Csanádi löszháton (Excess water hazard based on soil factors in the Békés-Csanád Loess Plateau). Talajvédelem – Különszám, Talajvédelmi Alapítvány, Bessenyei György Könyvkiadó, Nyíregyháza, pp 43–52 (in Hungarian)

Buzás I (1990) Talaj és agrokémiai vizsgálati módszerkönyv 1. (Methods of agrochemical and soil analysis 1). INDA 4231 Kiadó, Budapest, 358 p (in Hungarian)

Dövényi Z (2010) Magyarország kistájainak katasztere (The Cadastre of the Microregions of Hungary). Hungarian Academy of Sciences, Geographical Institute, Budapest, 876 p (in Hungarian)

Farkas Cs, Gyuricza Cs (2006) A talaj szerkezete és állapota (Soil structure and condition). In: Birkás M (ed) Földművelés és földhasználat (Land use and cultivation). Mezőgazda Kiadó, Budapest, pp 42–54 (in Hungarian)

Filep Gy (1999) A talaj fizikai tulajdonságai (Physical soil properties). In: Stefanovits P (ed) Talajtan (Soil science). Mezőgazda Kiadó, Budapest, pp 131–190 (in Hungarian)

Gyuricza Cs (2001) A szántóföldi talajhasználat alapjai (Bases of arable land use). Szent István Egyetem, Gödöllő, 197 p (in Hungarian)

Jury WA, Horton R (2004) Soil physics, 6th edn. Wiley, Hoboken, 370 p

Kézdi Á (1974) Handbook of soil mechanics. Soil physics, vol 1. Akadémiai Kiadó, Budapest, 294 p

Körösparti J, Bozán Cs, Pásztor L, Kozák P, Kuti L, Pálfai I (2009) GIS alapú belvíz-veszélyeztetettségi térképezés a Dél-Alföldön (Applicability of GIS techniques in excess water hazard mapping on the South Great Hungarian Plain). In: Hungarian hydrological society, 27th national meeting, Baja, 1–3 July 2009. http://www.hidrologia.hu/vandorgyules/27/dolgozatok/04korosparti_janos.htm (in Hungarian)

Kozák P (2006) A belvízjárás összefüggéseinek vizsgálata az Alföld délkeleti részén, a vízgazdálkodás európai elvárásainak tükrében (Inland excess water regime on the SE Hungarian Great Plain in context of the European water management requirements). Manuscript Ph.D. thesis, University of Szeged, Szeged, 86 p (in Hungarian)

Kreybig L, Sík K, Schmidt E (1938) Magyarázatok Magyarország geológiai és talajismereti térképeihez (General memoir to the soil maps of Hungary). Mezőhegyes 5465/4. 1:25.000. Stádium Sajtóvállalat Rt., Budapest, 52 p (in Hungarian)
MSZ-08-0205:1978. Determination of physical and hydrophysical properties of soils. Laboratory tests. Hungarian Standard Association, Budapest
MTA TAKI (1990) AGROTOPO Map Digital Data Base, 1:100 000. Hungarian Academy of Sciences, Research Institute for Soil Sciences and Agrochemistry
OMSz (2005) Some characteristics of the climate of Hungary since 1901. National Meteorological Service, Paletta Press Ltd., Budakeszi, 12 p
OMSz (2012) Magyarország éghajlata, Csapadék (Climate of Hungary, precipitation). National Meteorological Service, Budapest. http://www.met.hu/eghajlat/magyarorszag_eghajlata/altalanos_eghajlati_jellemzes/csapadek/ (in Hungarian)
Pálfai I (1988) A mértékadó belvízhozam számítási módszerei (Methods for calculation of standard excess water discharge). Vízügyi Műszaki Gazdasági Tájékoztató 165. Budapest, 155 p (in Hungarian)
Pálfai I (2000) Az Alföld belvízi veszélyeztetettsége és az aszályérzékenysége (Excess water risk and drought sensitivity of the Hungarian Plain). In: Pálfai I (ed) A víz szerepe és jelentősége az Alföldön (The role and importance of water on the Hungarian Great Plain). Nagyalföld Alapítvány 6, Békéscsaba, pp 85–95(in Hungarian)
Pálfai I (2001) A belvíz definíciói (Definitions of inland excess water). Vízügyi Közl 83 (3):376–391 (in Hungarian)
Pálfai I (2004) Belvizek és aszályok Magyarországon. Hidrológiai Tanulmányok (Inland excess water and drought in Hungary. Hydrological papers). Vízügyi Közl 86(1–2):318–320 (in Hungarian)
Pálfai I (2011) A csapadékviszonyok szerepe a belvízképződésben (Precipitation conditions and excess water formation). In: Hungarian hydrological society, 29th national meeting, Eger, 6–8 July 2011. http://www.hidrologia.hu/vandorgyules/29/dolgozatok/palfai_imre.html (in Hungarian)
Rakonczai J, Csató Sz, Mucsi L, Kovács F, Szatmári J (2003) Az 1999. és 2000. évi alföldi belvíz-elöntések kiértékelésének gyakorlati tapasztalatai (Practical experience of evaluation of the inland excess water inundations in 1999 and 2000). Vízügyi Közlemények 1998–2001 Special Issue 4:317–336 (in Hungarian)
Rakonczai J, Farsang A, Mezősi G, Gál N (2011) A belvízképződés elméleti háttere (Conceptual background to the formation of inland excess water). Földrajzi Köz 135(4):339–349 (in Hungarian)
Salamin P (1966) Vízrendezések (Water regulation). Institute for engineer further training publication M 166. Tankönyvkiadó, Budapest, 283 p (in Hungarian)
Stefanovits P (1999) Talajok osztályozása (Soil classification). In: Stefanovits P (ed) Talajtan (Soil science). Mezőgazda Kiadó, Budapest, pp 239–320 (in Hungarian)
Török IGy (1997) "Eszmetöredékek" a belvíz fogalmának korszerű értelmezése és a belvízvédekezés gazdaságossága tárgyában (Thoughts on the modern interpretation of the definition and rentability of protection against excess water). In: Hungarian hydrological society, 15th national meeting, Kaposvár, 9–11 July 1997 (in Hungarian)
Vágás I (1989) A belvíz elvezetése (Drainage of inland excess water). Hidrológiai Közlöny 2:77–82 (in Hungarian)
Várallyay Gy (2005) A talaj vízgazdálkodása és a környezet (Soil water budger and the environment). In: Németh T (ed) A talaj vízgazdálkodása és a környezet. Research Institute for Soils Science and Agrochemisty, Hungarian Academy of Sciences, Budapest, pp 15–30 (in Hungarian)
Vízügy (2011) Tájékoztató a 2010–2011 évi belvízi helyzetről (Information on the 2010–2011 excess water situation). http://www.vizugy.hu/print.php?webdokumentumid=280 (in Hungarian)

Chapter 21
Intense Rainfall and Karst Doline Evolution

Márton Veress

Abstract The impacts of the rainfall events of 2010 were analyzed on dolines in some karst regions of Hungary (primarily on those in the eastern part of the Bakony Mountains, on the Tés Plateau). In order to detect change, the depths of dolines were repeatedly measured and for one doline mapping was repeated. Between 2004 and 2010 deepening (by maximum 120 cm) and accumulation (by maximum 32 cm) of variable degree could equally be observed. Repeated survey and mapping revealed changes in shape governed by numerous factors (such as catchment area, sediment cover, topographical setting). Assessing changes in shape and depths jointly over the period 2004–2010, the sediment budget of 15 dolines was estimated. For six dolines sediment influx exceeded sediment loss, while eight dolines showed the opposite balance. No change was found in the case of one doline.

Keywords Intense rainfall • Cryptokarst • Dolines • Doline deepening/infilling • Sediment budget • Hungary

21.1 Introduction

As a corollary of climate change, extreme weather may equally include the increasing frequency of intense rainfall and higher amounts of precipitation per event. The geomorphological impacts could be the accelerated evolution, modification or growing density of landforms (Büdel 1977; Bremer 2002; Czigány and Lovász 2005). This could also apply to karst landforms.

M. Veress (✉)
Department of Physical Geography, University of West-Hungary,
Károlyi Gáspár tér 4, 9700 Szombathely, Hungary
e-mail: vmarton@ttk.nyme.hu

D. Lóczy (ed.), *Geomorphological impacts of extreme weather: Case studies from central and eastern Europe*, Springer Geography, DOI 10.1007/978-94-007-6301-2_21,

Table 21.1 Precipitation amounts measured between 1 January and 8 October 2010

Rainfall period	Rainfall amount (mm)	Rainfall period	Rainfall amount (mm)	Rainfall period	Rainfall amount (mm)
2 January	0.1	4–5 April	34	20 July	0.1
5–9 January	30.2	10–15 April	68.1	24–27 July	16
17–21 January	9.1	18 April	4	29–31 July	23
23 January	0.1	20–21 April	0.2	3 August	34
29–30 January	5	2 May	1	5–6 August	27
6 February	6	4–5 May	20	8–9 August	2
10–12 February	17.1	8 May	0.1	13–18 August	13.2
19–20 February	15.1	12–16 May	152	27–28 August	9
23 February	2	20–21 May	4	30 August–4 September	36.3
26 February	14	24–27 May	29.1	7–8 September	12
28 February	0.1	30 May–4 June	90.1	10–12 September	21.1
2 March	0.1	13–22 June	102.2	16–19 September	57
10–11 March	6	26 June	0.1	25–26 September	68
15–16 March	0.2	6 July	4	29 September	0.1
22 March	2	15 July	3	4–5 October	18.1
30 March–1 April	8	17 July	26		

The impacts of intense rainfalls on the dolines of the Tés Plateau (Bakony Mountains, western Hungary) were investigated during the period 2004–2010. As opposed to 2008 (632.3 mm) or 2009 (666.8 mm), in 2010 record amounts were registered (1,146.1 mm) and therefore, for this year daily values are also shown until the end of observations (8 October 2010) (Table 21.1). Between 1 January and 8 October, 989.9 mm precipitation fell on the Tés Plateau. Precipitation amounts were particularly high in the months of May (237 mm) and September (158 mm) (Table 21.1). It has been even more influential on doline evolution that in some periods (especially in that between 12 and 16 May), daily amounts were well above 10 mm (on 12 May, 13 mm; on 13 May, 25 mm; on 14 May, only 1 mm, but on 15 May, 64 mm, and on 16 May, 49 mm).

In karst areas intense rainfalls are expected to affect stream caves (as floods), karst springs (as increased yield – Jakucs 1956), ponors (as ponding – Veress 1987) and *covered karst* features. In the evolution of a covered karst type (cryptokarst, where the cover sediments are permeable), high-intensity rainfalls can be particularly efficient. Here typical features are subsidence, or dolines with ponor (of dropout or suffosion subtypes – Williams 2003) and depressions in cover sediment. Formed by the compaction or redeposition of the cover sediment above a karst chimney, suffosion dolines have gentle slopes. *Dropout dolines* result from caving in of the slightly cohesive cover sediment in the case of sufficient deficit of support. Collapse is more probable if the cover sediment is

coarse-grained (gravels, till) or the material deficit is generated very rapidly. Both subtypes are created to compensate for material deficit in the limestone, but formed by complex processes. It is not probable that they are directly associated with material deficit and chimney formation (Veress 2005), but rather indirectly (removal of chimney fill – Veress 2009). If the depression forms as a consequence of material deficit in the cover sediment, the chimney is continued in a passage of the cover sediment (Veress 2009).

Depressions in cover sediment are mostly extensive features which enclose suffosion and dropout dolines as well as ponors. Their fills are transported into the karst hollows through passages (Veress 2009).

21.2 Types of Rainfall Impact

In the case of covered karsts (cryptokarsts), intense rainfalls may lead to the following:

- Modified doline functioning
- Sedimentation from inflow
- Formation of partial features
- Changes in dimensions of depressions

21.2.1 Modified Doline Functioning

The increased inflow into dolines and other depressions as sheetflow, gully, gorge or valley flow may cause ponding in the karst (Fig. 21.1). The flood ponds may be ephemeral, enduring (surviving the inflow period and the ensuing period without inflow) or long term (lasting longer than the rainy period) (Veress 1987). *Ephemeral ponds* are drained rapidly with sinking water levels; *enduring ponds* show level fluctuations (rising during inflow and falling in periods without inflow), while the level *long-term ponds* present a slow lowering trend in the rainy period because of evaporation. Flood ponding is preconditioned by intensive rainfalls and the degree to which the depression is filled (which determines the type of pond). The deeper is the fill, the longer ponding lasts with rainfalls of the same intensity. The overflow of flood ponds over the rim of the depression is also possible.

Inflow into and ponding of dropout dolines depends on several additional factors: soil saturation and frozen conditions, *vegetation* cover etc. In 1980 over the vegetation-free environs of dolines in agricultural fields, a 2-h rainfall of 13.4 mm amount resulted in intensive inflow (1987). On 7 November 1982, at Hárskút (Bakony Mountains) 13 mm of rainfall produced inflow in subsidence dolines of grassland environment and no inflow in those found on arable fields.

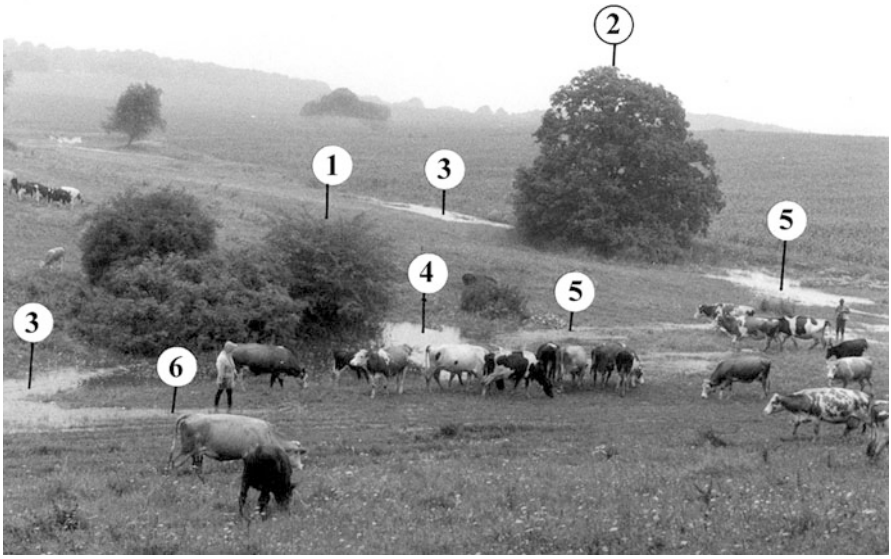

Fig. 21.1 Flood ponding in 1984 (Hárskút Basin, Bakony Mountains). *1*, doline G-9; *2*, twin dolines K-2 and K-3; *3*, water inflow on valley floor; *4*, flood pond; *5*, overflow; *6*, water loss next to doline G-9

21.2.2 Sedimentation from Inflow

If cover sediments are of uniform grain size and refining from bottom to top, the passage below the doline or the chimney is gradually more and more plugged (by the suspended material deposited during ponding). Therefore, the increasing proportion of fine sediments in the fill indicates the ever decelerating water level lowering of the intermittent doline pond. Less and less sediment is transported from the doline or the passage into the deeper karst. As the doline is filling up, the dip of the accumulating fine sediments is reducing which indicates growing inflow (from heavy rains or because of the lack of vegetation on the catchment). *Plant residues* in the accumulated sediment point to farming and soil particles to soil erosion (Veress 1986). Plant residues forming a continuous layer attest to an ephemeral pond, while striped layering and/or annual colloid crusting on tree trunks is an indication of water level fluctuations (an enduring pond). The termination of inflow generates charcoal accumulation (Veress 1995). Limonite forms during groundwater accumulation (no inflow from the cover sediments to the limestone – Veress 1995).

21.2.3 Formation of Partial Features

The *doline* is transformed if its *sediment budget* (influx, transport and internal redeposition) changes (Fig. 21.2a). If influx is less than transport to the deeper

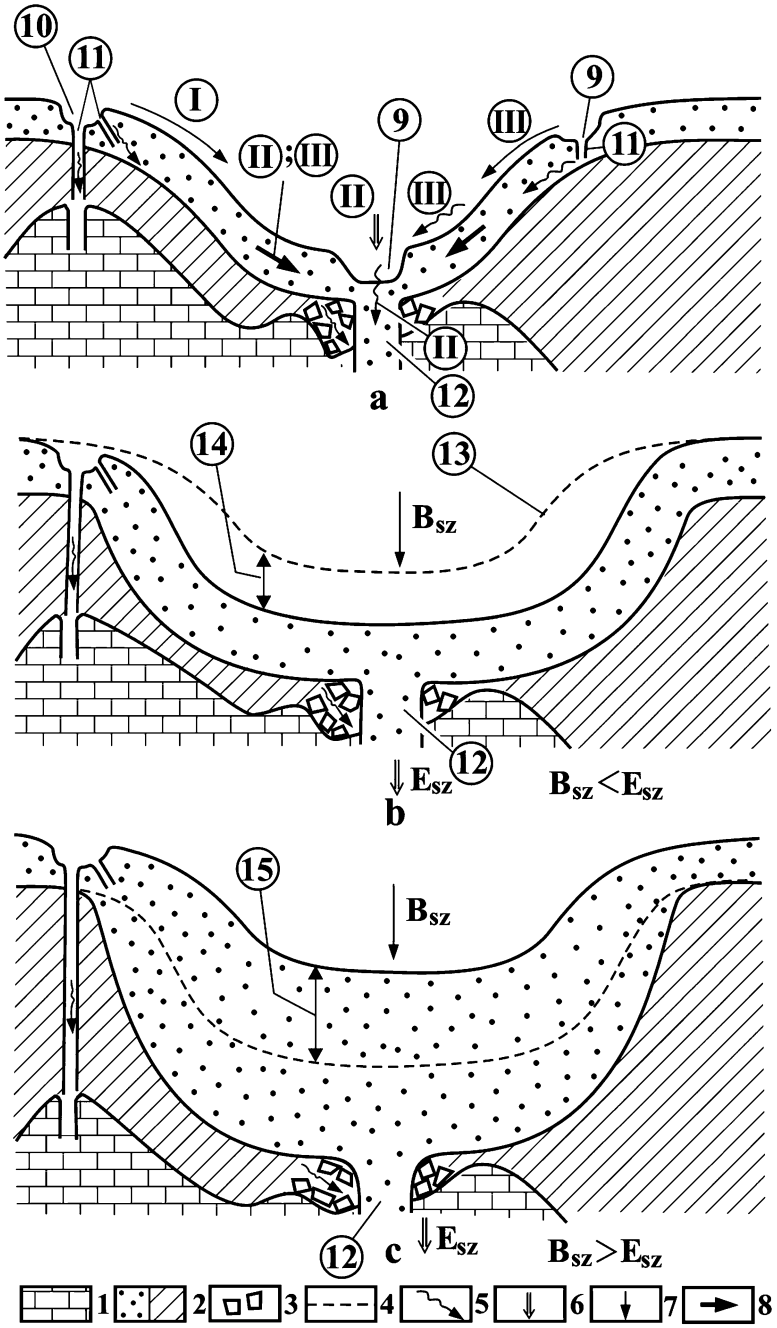

Fig. 21.2 Sediment budget (**a**), deepening (**b**) and infilling (**c**) of a subsidence doline. *1*, limestone; *2*, cover sediment; *3*, limestone fall mound; *4*, former surface; *5*, piping; *6*, fall in cover sediment; *7*, slide; *8*, soil and regolith creep; *9*, partial depression; *10*, marginal depression; *11*, passage; *12*, chimney; *13*, original floor; *14*, deepening; *15*, infilling; B_{sz}, amount of sediment input; E_{sz}, amount of sediment transport; *I*, input; *II*, sediment transport from the doline; *III*, internal sediment redeposition

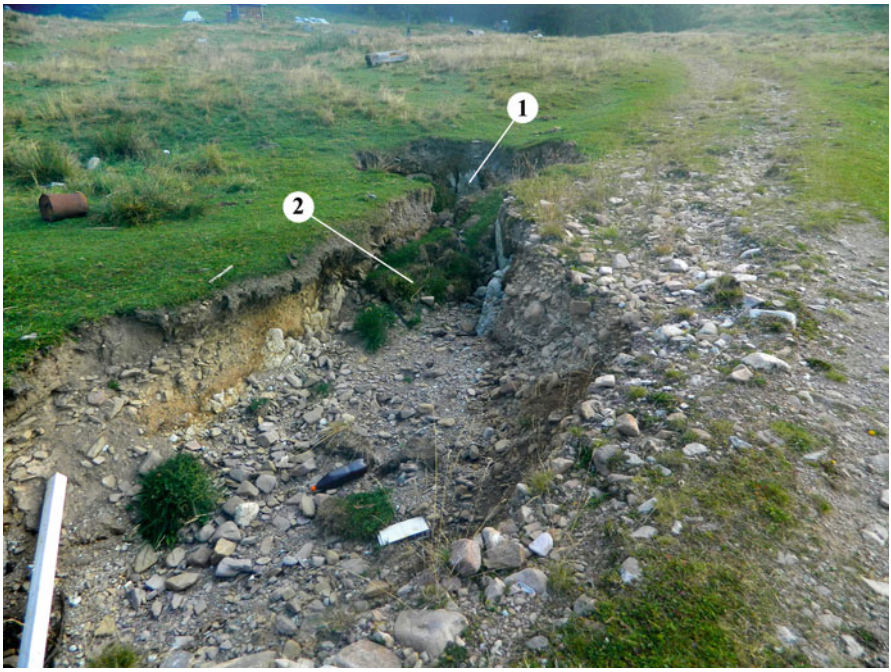

Fig. 21.3 Dropout doline developed in thin sediment cover (Padis Plateau, Romania, in 2011). *1*, limestone; *2*, grass and plant spots indicating recent fall

karst, the depression deepens and degradational features develop; if transport is less, it fills up and aggradational features develop (Fig. 21.2b, c). Sediment influx can happen through water inflow or mass movements (falls, slides, creep). The accumulation from creep may reach 0.5–6 cm per decade for some subsidence dolines (Veress 2000). Transport into the karst may also take the form of mass movements (fall), solifluction or by water flow. Falls, deriving from material deficit or overloading by accumulation, occur in chimneys or passages without being manifested on the surface.

The development and further evolution of covered karst dolines may be rapid and complex (Veress 1986, 1987, 1995; Ford and Williams 2007). The *partial features* of subsidence dolines may be non-karstic (fall and slide scars and accumulations, rills, gullies and gorges with their accumulations) or karstic (minor depressions in cover sediment generated by falls and passages – Veress 2000). Minor depressions (Veress 2000) are closed features of some meters in diameter and maximum 1–2 m deep with steep slopes. Asymmetric on the sides of dolines, they may widen through falls and flatten through sheetwash, often forming hanging features along the doline rim. Passages may open up by falls or be reshaped by the action of water run-off into tunnels of some centimeters across in the soil. Accumulation produces flat surfaces in the partial depressions or over the entire doline floor. The sediment derives from rills, gullies or gorges on the doline side or on the catchment.

If the sediment cover is shallow (less than 3.5 m), the material deficit of the underlying strata is directly inherited over the cover (Vererss 2008, 2009 – Fig. 21.3). With a sediment cover deeper than 3.5 m (Vererss 2008, 2009), a blind

Fig. 21.4 Features attesting to recent and rapid development in a dropout doline (Padis Plateau, Romania, in 2012). *1*, steep surface in sediment cover; *2*, plant 'beard' due to fall; *3*, caved-in cover; *4*, spots of living plants fallen in

passage develops in the sediment cover (Veress 2009), caves in and opens up to the surface. There is no direct cause-and-effect relationship between rainfall and collapsing. The latter happens when overloading exceeds support – caused by a single rainfall event or more probably several consecutive events, which are, however, not immediate triggers. Variable time span separates rainfall and collapsing in the case of different dolines and even of different collapsing events of the same doline. A single rainfall may be responsible for accumulation linear erosion features (rills, gullies), but not for depression formation, which is preceded by a series of rainfalls increasing material deficit to a threshold value. Both types of landform, however, indicate intensive rainfall – particularly, if their origin (date of occurrence) is documented.

Collapsed features are young (some months old) if their walls are (sub)vertical, vegetation-free with traces of sod or grain crops on their floors (Fig. 21.4); failure fronts are fresh, the rim is sharp (Fig. 21.5), and collapse mounds are not yet destroyed or dissected by rilling. Plant residues, tilted or uprooted trees, displacements or upward wedging crack-like passages show rapid development. Short-term and recent accumulation is indicated by buried trees and human utensils (e.g. cans, tires – Fig. 21.6, Table 21.2). Serial collapses can also be documented (Fig. 21.7).

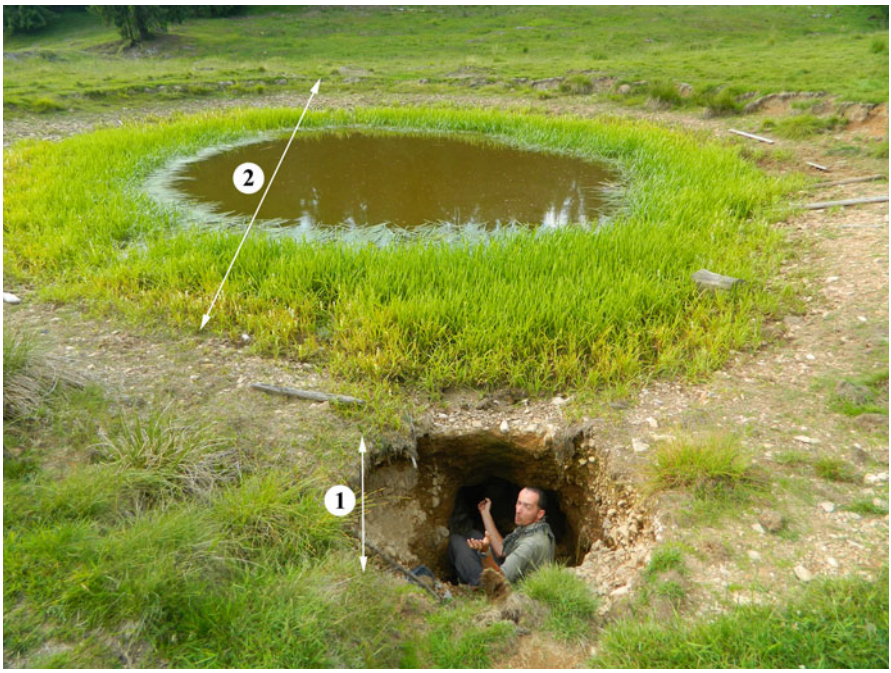

Fig. 21.5 Opening formed between 31 August 2011 and 5 June 2012 (Padis Plateau). *1*, opening; *2*, infilled ponded doline

Fig. 21.6 Intensively infilling doline (Durmitor Mountains, Montenegro, in 2012). *1*, buried tire; *2*, deposits on tire

Table 21.2 Duration and start of development of some partial features of dolines

Feature	Formation process	Duration of development	Determination method	Start of development related to observation	Determination method
Plant 'beard'	Fall	1–2 s	Estimation	Less than 1 year	In the growing season
Vertical surface in sediment cover	Fall	1–2 s	Estimation	Less than 1 year	No raindrop impact
Collapse mound	Fall	1–2 s	Estimation	Less than 1 year	No raindrop impact
Plant residue or soil on doline floor	Fall	1–2 s	Estimation	Less than 1 year	In the growing season
Tilted or uprooted (dead) tree	Series of falls/ slides	From 1–2 days to several years	Estimation	Maximum age of the tree	Tree ring counting
Partially buried tree trunk	Infilling	From 1–2 days to several decades	Tree ring counting	Maximum age of the tree	Tree ring counting
Buried object	Infilling	From 1–2 days to several decades	At earliest date of manufacture	From 1–2 days to several decades	At earliest date of manufacture

21.2.4 Changes in Dimensions of Depressions

During deepening depth and diameter may increase or decrease parallelly. The direction of change depends on the sediment budget of the doline. With negative influx/transport balance (Fig. 21.2b), the doline deepens and expands, while with a positive balance, both depth and diameter decrease (Fig. 21.2c).

21.3 Study Area: The Tés Plateau

21.3.1 Geographical Setting and Study Dolines

The Tés Plateau (eastern Bakony Mountains, central western Hungary) is elongated in NE to SW direction. Its area is ca 59 km^2 and elevation is 400–480 m above sea level and 200–300 m above its surroundings. It is mostly built up of Mesozoic

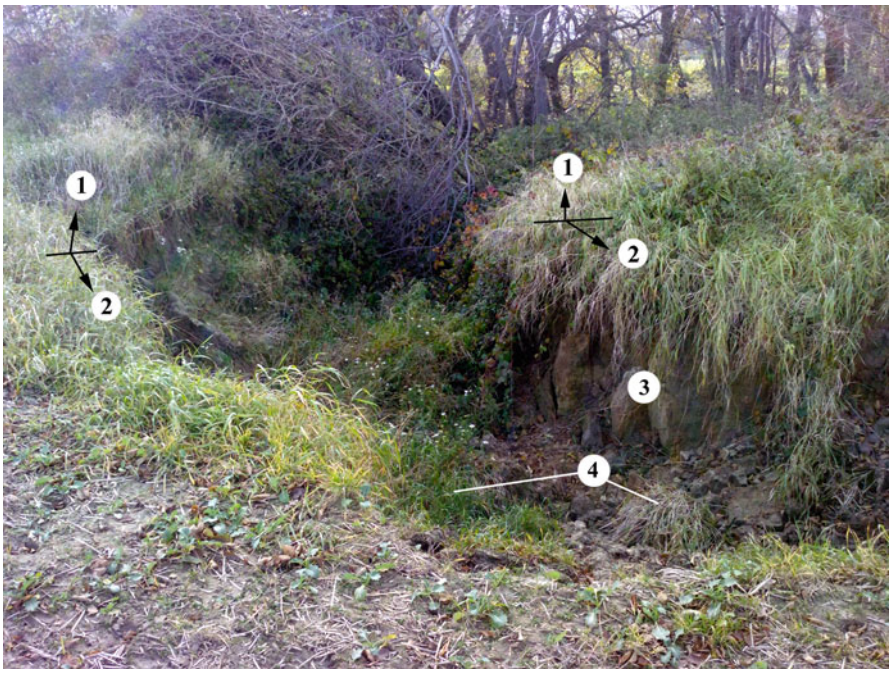

Fig. 21.7 Marginal depression developed in the I-12 system of the Háromkürtő shaft (Tés Plateau, 2010). *1*, section of partial depression formed before 2010; *2*, section formed after July 2010; *3*, scarp created by falls; *4*, plant remains removed by falls

limestones mantled by loess and spots of clay. The plateau is dissected by NW to SE running epigenetic valleys.

The investigated karst features are located in and around the Tábla Valley (Fig. 21.8). In the area Tés-1 (Veress 2006), two depressions with sediment cover were studied: D-1 (with dolines I-32, 32 L and I-33) lies on the floor of the Tábla Valley, while D-2 (with doline I-31) is on the valley wall (Fig. 21.9). Doline I-29 is also found on the valley floor. The dolines have elevations of 460–464 m. The cover sediments of up to 18 m thickness are (clayey) Jurassic limestone debris, (clayey) loess and clay (with loess and/or limestone debris).

The area Tés-2 (Veress 2005) lies some hundred meters to the NW. Six of the dolines are on the floor of a tributary to the Tábla Valley, in the depression with sediment cover D-4, at 442–458 m elevation. The sediment cover is 0–10 m deep. Three dolines are outside the valley, on almost flat terrain at 457–458 m elevation, with 0–10 m cover thickness (Fig. 21.10). Area Tés-2 is built up of Jurassic limestone with (clayey) limestone debris, (clayey) loess, clay (with loess and limestone debris) and (sandy) loess (with limestone debris).

Among the dolines of the area Tés-3 (Veress 2006), three are found in the depression with sediment cover D-3 and one outside the depression (Fig. 21.11) at 436–442 m elevation. Jurassic limestone is covered by maximum 15 m of (clayey) limestone debris, sandy or clayey loess, loess with limestone debris and clay (with loess, limestone debris).

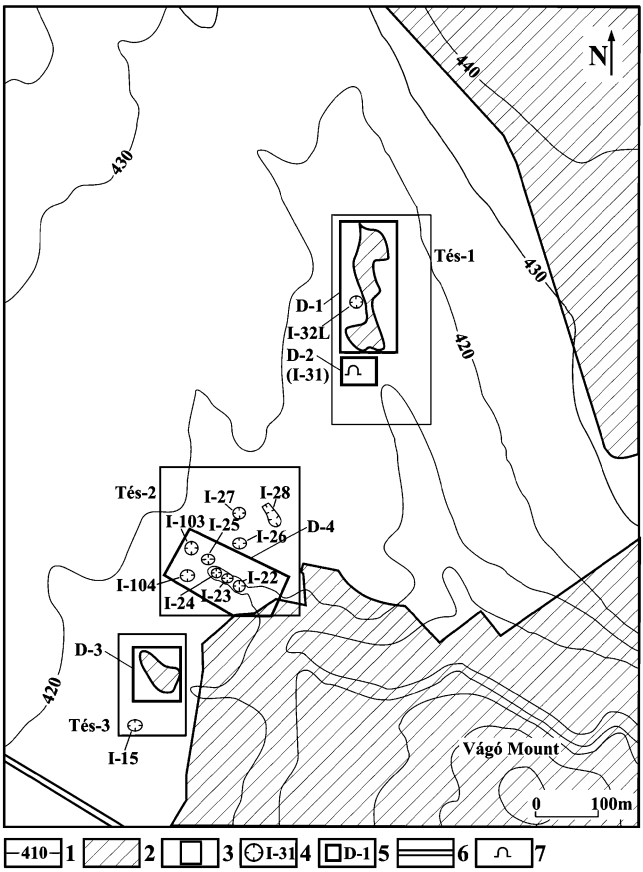

Fig. 21.8 Overview map of the eastern part of the Tés Plateau. *1*, contour; *2*, forest; *3*, study area; *4*, doline; *5*, depression with code; *6*, road; *7*, cave

21.3.2 Methods

In 2004 the depressions and dolines were surveyed in detail and represented on a *geomorphological map*. The data were annually updated between 2004 and 2009 and revisited on 8 October 2010, when the changes were documented (Table 21.3).

In 2010 the maximum depth of the dolines surveyed in 2004 was measured again by GPS, the changes in depth (deepening or infilling) between 2004 and 2010 were recorded, and the rates of change were calculated Table 21.4. Comparisons were made with the alterations of dolines in other karst areas of Hungary.

For depression I-31 the detailed survey was repeated in 2010 and the difference between the contours (0.3 m interval) of the 2010 and 2004 surveys was calculated. The map of changes in the shape of the depression (if the depth of 2010 is larger: deepening; if the depth data of 2010 is smaller: in filling) (Fig. 21.12).

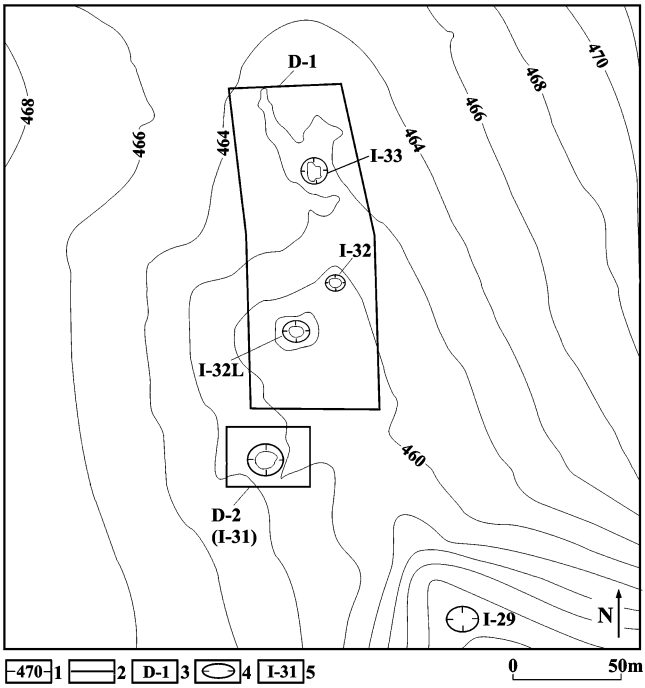

Fig. 21.9 The area Tés-1. *1*, contour; *2*, approximate rim of depression; *3*, depression code; *4*, doline; *5*, doline code

21.3.3 Discussion

It was observed that in the karst regions of Hungary under study, solution dolines (of the Aggtelek Karst, NE Hungary) were infilled to the largest extent between 2004 (2006) and 2010. For the subsidence dolines, the *rate of infilling* (1.3 cm year^{-1}) is 33% of that of the solution dolines (3.9 cm year^{-1}). The sediment of solution dolines is not forwarded into the karst, while 67% of the fill of subsidence dolines reaches the deeper karst.

Making comparisons by the vegetation cover of the catchment, the mean rate of infilling between 2004 and 2010 for the collapse dolines with grassed catchments (2006–2010 for the dolines of the Nagy-mező, Bükk Mountains, NE Hungary) was 0.8 cm year^{-1}, and for those with forested catchments (2003–2010 for the Homód-árok, Bakony Mountains), it was 1.2 cm year^{-1}, while for those in agricultural environment (2004–2010 for the Tés Plateau), it was 2.0 cm year^{-1}. The rate of infilling for covered karst features in agricultural environment is double of that calculated for grassland and forested catchments. Infilling can be most probably dated for the wet year of 2010, when the rate could be higher than the calculated average. In subsidence dolines in agricultural environment, seasonally lacking

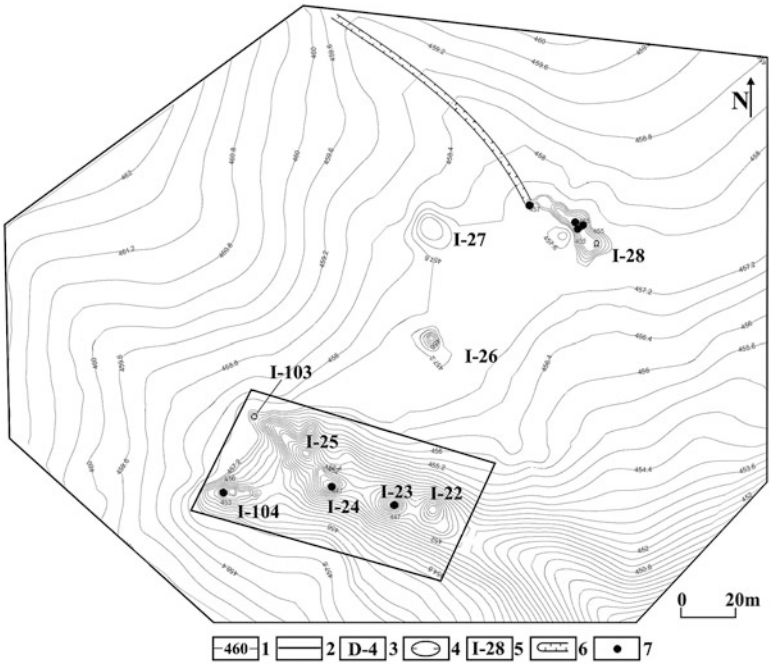

Fig. 21.10 The area Tés-2. *1*, contour; *2*, approximate rim of depression; *3*, depression code; *4*, doline; *5*, doline code; *6*, erosion gully; *7*, limestone exposure

vegetation cover, the predicted growth in the frequency of intense rainfalls will involve accelerated infilling.

The depth of the doline I-15 in agricultural environment (Tés-1 area) has decreased without morphological changes. Both dolines of the D-3 depression in extreme positions (I-17 and I-19) showed depth reduction, while the depth of the doline in central position (I-19) has increased. The differences are explained by the following setting: the dolines in extreme positions received sediment recharge from the arable fields, while the central doline was 'sheltered' from that. At the same time, *sediment transport* was detected from the dolines I-18 and I-19.

The depression D-4 lies in a forest, but the part of its catchment is agricultural. The marginal doline (I-104) receives significant run-off from arable land and, therefore, shows major morphological changes. (Unfortunately, no depth data are available.) The eastern part is totally filled up and the western shows features of sediment transport. With the exception of doline I-22 (of unchanged depth), doline depths have grown. There are dolines (I-25 and I-23) with indications of deepening or accumulation (I-24).

Among the *doline*s of the flat Tés-2 area, I-26 shows *deepening* and I-28 became much shallower because a channel of several 100 m is attached to it. Sediment transport is attested by the deep shaft in its interior. The doline I-27, filled up even

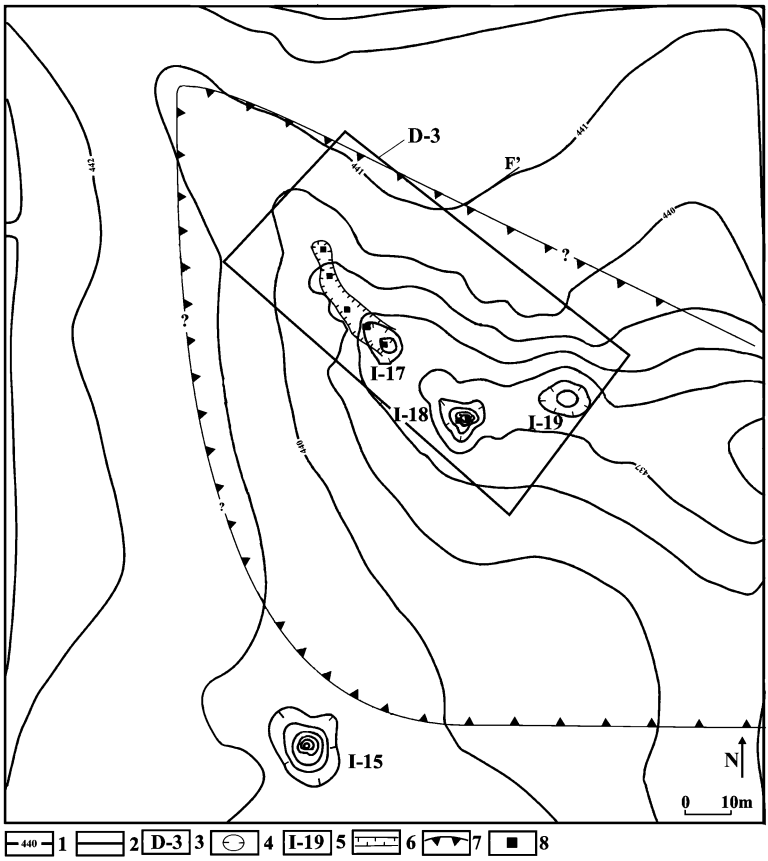

Fig. 21.11 The area Tés-3. *1*, contour; *2*, approximate rim of depression; *3*, depression code; *4*, doline; *5*, doline code; *6*, erosion gully; *7*, valley; *8*, limestone exposed

before 2004, contained a partial feature indicating sediment transport. Here the rainfalls of 2010 were able to reactivate a partially fossilized doline.

Changes of the largest scale were observed in depression D-2 (doline I-31) with 120 cm deepening over 7 years (Fig. 21.9). The partial depression of its eastern margin (or doline) had filled up completely by 2010, while a new depression developed on the western margin and was connected to the main doline in 2010. Here intensively deepening features (Fig. 21.12) contribute to sediment transport. The significant changes are probably explained by the existence of a major and less explored cave below (the Táblavölgy dripstone cave) and its sediment input through an artificial well. Sediment transport and deepening are indicated by the relative position of the rims of well casing.

Table 21.3 Partial features of dolines developed in 2010 (observed on 8 October 2010)

Doline code	Feature	How many?	Process	Area	Setting
I-15	No	0	–	Tés-3	Flat terrain
I-17	No	0	–	Tés-3	In depression D-3
I-18	Passage	1	Opening by fall	Tés-3	
I-19	Passage	2	Opening by fall	Tés-3	
I-22	No	0	–	Tés-2	In depression D-4 on valley floor
I-23	Partial depression	1	Fall	Tés-2	
I-24	Flat floor	1	Filling of cleaned shaft	Tés-2	
I-25	1. Flat floor in partial depression	2	1. Infilling	Tés-2	
	2. Passage		2. Opening by fall		
I-104 E	Flat floor	0	Infilling	Tés-2[a]	
I-104 W	1. Passage	1	1. Opening by fall	Tés-2	
	2. Partial depression	1	2. Fall		
	3. Channels	5	3. Rill/gully erosion		
I-26	No	0	–	Tés-2	Flat terrain
I-27	Partial depression	1	Fall	Tés-2	Flat terrain
I-28	Passage	ca 10–15	Water percolation	Tés-2	Flat terrain
I-29	1. Flat floor in partial depr.	3–5	1. Infilling	Tés-1	On the floor of Tábla Valley
	2. 3–5 passages in margins		2. Water percolation		
I-31	1. Channel	1	1. Rill/gully erosion	Tés-1	In the depression D-2 in the side of Tábla Valley
	2. Broadening of partial depr.	1	2. Induced by fall		
	3. Passage in partial depr.	1	3. Opening by fall		
I-32	1. Passage		1. Opening by fall	Tés-1	In the depression D-1 on the floor of Tábla Valley floor
	2. Flat floor		2. Infilling		
I-32 L	No	0	–	Tés-1	
I-33	No	0	–	Tés-1	

[a]Ceased to show depression character

Notice: the observation of the data in the table is 08.10.2010 former observations between 2004 and 2009

Table 21.4 Infilling or deepening of karst depressions in the 2000s

Tés Plateau (Bakony Mountains), measured from April 2004 to June 2010					Homód-árok (Bakony Mountains), measured from June 2003 to July 2010				
Code	Change in depth (cm)	Rate (cm year^{-1})	Catchment vegetation	Genetic type	Code	Change in depth (cm)	Rate (cm year^{-1})	Catchment vegetation	Genetic type
I-33	+16	2.3	Arable	F_1	Ho-1	−20	2.5	Forest	F_1
I-32	+10?	1.4	Arable	F_1	Ho-2/a	0	0	Forest	F_1
I-32_L	+13	1.6	Arable	F_1	Ho-2/b	−22	2.7	Forest	F_1
I-31	−120	17.1	Arable	F_2	Ho-3	−30	3.7	Forest	F_1
I-22	0	0	Forest	F_1	Ho-4	0	0	Forest	F_1
I-23	−25	3.6	Forest	F_1	Ho-6	+19	2.4	Forest	F_1
I-24	−14	2.0	Forest	F_1	Ho-7	+22	2.7	Forest	F_1
I-25	−10	1.4	Forest	F_1	Ho-8	+23	2.9	Forest	F_1
I-26	−17	2.4	Arable	F_1	Ho-9	0	0	Forest	F_1
I-28	+21	3.0	Arable	F_1	Ho-10	+29	3.6	Forest	F_1
I-15	+16	2.3	Arable	F_1	Ho-11	+12	1.5	Forest	F_1
I-17	+21	3.0	Arable	F_1	Ho-12	0	0	Forest	F_1
I-18	−32	4.6	Arable	F_2	Ho-13	+16	2.0	Forest	F_1
I-19	+16	2.3	Arable	F_1	Ho-14	0	0	Forest	F_1
I-27	+13	1.9	Arable	F_3	Ho-15	+10	1.2	Forest	F_1
Nagy-mező (Bükk Mountains), measured from July 2006 to July 2010					Ho-16/A	−39	4.9	Forest	F_1
N-1	−19	3.8	Grassland	F_1	Ho-16/B	−12	1.5	Forest	F_1
N-3	+10	2.0	Grassland	F_1	Ho-17	0	0	Forest	F_1
N-8	0	0	Grassland	F_1	Ho-20	0	0	Forest	F_1
N-6	+6?	1.2	Grassland	F_1	Ho-21	0	0	Forest	F_1
N-4	0	0	Grassland	F_1	Ho-22	+10	1.2	Forest	F_1
N-9	+13	2.6	Grassland	F_1					
N-5	0	0	Grassland	F_1					
N-2	0	0	Grassland	F_1					
Aggtelek Karst, measured from July 2006 to July 2010									
A-1	+32	6.4	Forest	O					
A-2	+21	4.2	Forest	O					
A-3	+25	5.0	Forest	O					
A-4	0	0	Forest	O					

O solution doline, *F* subsidence doline, F_1 suffosion doline, F_2 dropout doline, F_3 fossil suffosion doline

Notice: time of measurements Tés (Bakony): 04, 2004/06, 2010; Homód Valley (Bakony): 06, 2003/07, 2010; Aggtelek: 07, 2006/07, 2010; Bükk: 07, 2006/07, 2010

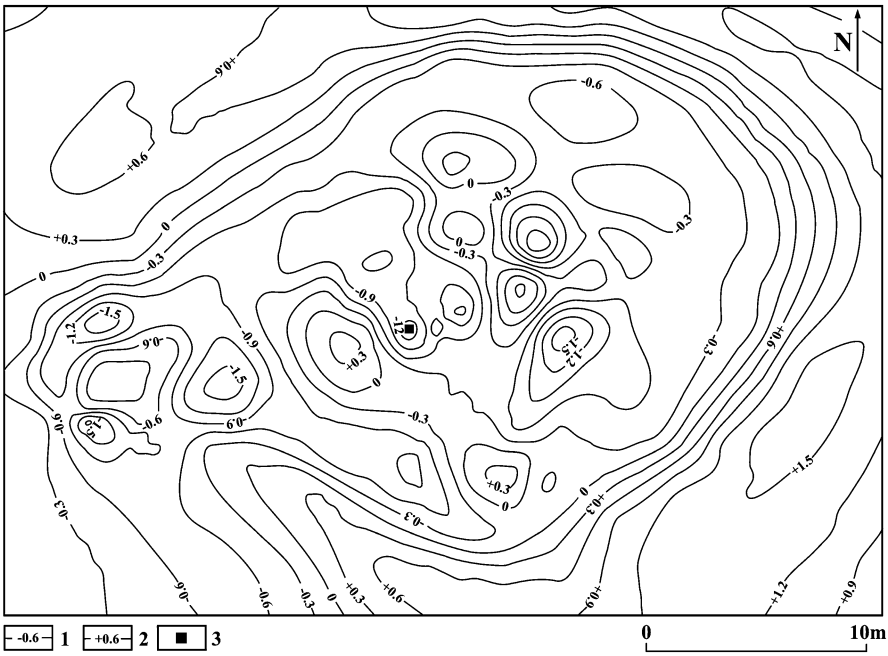

Fig. 21.12 Map of morphological changes for depression D-2 (doline I-31). *1*, deepening (dm); *2*, infilling (dm); *3*, chimney (cave) of depression with well casing

21.4 Conclusions

Doline sediment budgets in a rainy period can be estimated from the joint assessment of the features developed and the changes of depth observed. According to sediment budget type, features of sediment input and transport may develop both in deepening and infilling dolines (Table 21.3).

Deepening dolines fall into several *classes*:

A, no feature developed on floor, but deepening and sediment transport without sediment input

B_1, degradational features, deepening and sediment input at a lower rate than sediment transport; input preceding transport

B_2, aggradational features, deepening and sediment input at a lower rate than sediment transport; transport preceding input

Infilling dolines are classified as follows:

C, aggradational features (or no morphological change), reduced depth, sediment input without remarkable transport to deeper karst

D, degradational features, reduced depth, sediment transport rate lower than input

E, no depth or morphological change, no sediment input or transport

Table 21.5 Sediment budgets, depth changes and morphology of dolines

Doline code	Depth change (cm)	Features	Sediment budget type
I-15	+16	x	C
I-17	+21	x	C
I-18	−32	m	B_1
I-19	+16	m	D
I-22	0	x	E
I-23	−25	m	B_1
I-24	−14	a	B_2
I-25	−10	m, a	B_1
I-26	−17	x	A
I-27	+13	m	D
I-28	+21	m	D
I-29	?	m, a	?
I-31	−120	m	B_1
I-32	+10	m, a	D
I-32 L	+13	x	C
I-33	+16	x	C
I-104 E	?	a	?
I-104 W	?	m	?

+ infilling, − deepening, *m* feature indicating sediment transport, *x* no morphological change, *a* infilling, E_{sz} sediment transport into deeper karst, B_{sz} sediment input into doline (For the explanation of A, B_1, B_2, C, D and E, see text)

The morphological changes of dolines are associated with several factors: vegetation cover of the catchment, slope conditions, relative position to other dolines and the cleaning or sediment-free conditions of passages. Doline infilling is highly dependent on the vegetation cover of the catchment – and the significance of this controlling factor will increase in the future. Extreme rainfalls will primarily result in the intensive infilling of subsidence dolines on arable fields and solution dolines (even if they are in forests or in the case of thin sediment cover).

Doline sediment budgets (Table 21.5) show that in the case of six out of 15 dolines, the rate of sediment transport exceeds input, while for eight dolines input surpassed transport. One doline was neither affected by input nor transport. The map of doline floor depth indicates that the response to heavy rainfall is more variable: sections of subsidence and accumulation alternate as a result of internal redeposition or the development of several chimneys on the doline floor, which vary in their intensity of sediment transport.

References

Bremer HC (2002) Tropical weathering, landforms and geomorphological processes, field work and laboratory analysis. Z Geomorphol 46:273–291

Büdel J (1977) Klima-Geomorphologie. Gebrüder Borntraeger, Berlin, 304 p

Czigány Sz, Lovász Gy (2005) A várható klímaváltozás és hatása hazánk néhány jelenkori geomorfológiai folyamatára (Predictable climate change and its impact on geomorphic processes in Hungary). Debrecen Geographical Disputes. Department of Physical Geography and Geoinformatics, University of Debrecen, Debrecen, pp 97–111 (in Hungarian)

Ford DC, Williams PW (2007) Karst hydrogeology and geomorphology. Wiley, Chichester, 561 p

Jakucs L (1956) A barlangi árvizekről (On cave floods). Földrajzi Közlemények 80(4):281–403

Veress M (1986) Feltárás előrejelzése a karsztos üledékek vizsgálatával (Forecasting exposure by investigating karst sediments). Karszt és Barlang 2:95–104 (in Hungarian)

Veress M (1987) Karsztos mélyedések működése bakonyi fedett karsztokon (Karst depression functioning on the covered karst of the Bakony Mountains). Földrajzi Értesítő 36(1–2):91–114 (in Hungarian)

Veress M (1995) Fosszilizálódó karsztos formák és környezetük fejlődésének értelmezése kitöltő üledékeikkel (Interpretation of fossilizing karst features and their environs from their fills). Karszt- és Barlangkutatás 10:225–236 (in Hungarian)

Veress M (2000) Covered Karst Evolution in the Northern Bakony Mountains, W-Hungary. Resultationes Investigationam Rerum Naturaliam Montium Bakony, Zirc XXIII. 167 p

Veress M (2005) Adalékok a Tábla-völgyi-dülő (Tési-fennsík) fedett karsztosodásához (On covered karst formation on the Tés Plateau) Karsztfejlődés X. Department of Physical Geography, Berzsenyi Dániel College, Szombathely, pp 267–291 (in Hungarian)

Veress M (2006) Adatok a Tési-fennsík két térszínrészletének fedett karsztosodásához (On covered karst formation in two areas of the Tés Plateau). Karsztfejlődés XI. Department of Physical Geography, Berzsenyi Dániel College, Szombathely, pp 171–184 (in Hungarian)

Veress M (2008) A mészkőfekü morfológiájának hatása a fedett karsztosodásra az Északi-Bakonyban (Impact of the limestone morphology on covered karst formation in the Northern Bakony Mountains). Karszt és Barlang 2004–2005:33–54 (in Hungarian)

Veress M (2009) Investigation of covered karst form development using geophysical measurements. Z Geomorphol 53(4):469–486

Williams PW (2003) Dolines. In: Gunn J (ed) Encyclopedia of caves and Karst science. Fitzrey-Dearborn, New York/London, pp 304–310

Chapter 22
Urban Geomorphological Processes in Pécs, Southwest-Hungary, Triggered by Extreme Weather in May and June 2010

Levente Ronczyk and Szabolcs Czigány

Abstract In urban areas with increased surface runoff, high-intensity rainfalls may inflict serious damages to various structures. Authors analyze extreme precipitation events with the purpose of compiling an urban geomorphological hazard map for Pécs, drawing on the experience gathered from the May to June events in 2010. DEM and digitized cadastral maps were employed to survey the spatial distribution of the extraordinary events, their impacts on geomorphic processes and the resultant damages. The findings confirm that the incorporation of stormwater management into the urban hydrologic master plan could be highly beneficial for Pécs and many other municipalities. This way localized flooding could be avoided or reduced to manageable levels.

Keywords Urban geomorphology • Extreme rainfall • Urban runoff • Damage classification • Stormwater management • Pécs

22.1 Introduction

Although in the 21st century more people live in urban settlements than in rural areas, while only 3% of the Earth surface is occupied by towns, urban geomorphology is still an evolving discipline (Gamba and Herold 2009). Torrential rainfalls and other extreme weather phenomena may involve infrastructural damages to roads, stormwater sewers, ditches, culverts, retaining walls, levees, dikes,

L. Ronczyk (✉)
Institute of Geography, University of Pécs, Ifjúság útja 6, 7624 Pécs, Hungary
e-mail: hidrogen@gamma.ttk.pte.hu

S. Czigány
Institute of Environmental Sciences, University of Pécs, Ifjúság útja 6, 7624 Pécs, Hungary
e-mail: sczigany@gamma.ttk.pte.hu

D. Lóczy (ed.), *Geomorphological impacts of extreme weather: Case studies from central and eastern Europe*, Springer Geography, DOI 10.1007/978-94-007-6301-2_22,

embankments, bridges and enforced stream banks, the proper maintenance of which is an essential task in stormwater management (Douglas 2005).

The town of Pécs, SW Hungary, is a fine example for sealed urban surfaces of high relief are especially prone to catastrophic flooding (Czigány et al. 2010). Pécs has been affected repeatedly by excess stormwater runoff causing severe losses to infrastructure (Lóczy and Gyenizse 2010), most of which directly resulted from the poor maintenance of urban infrastructure. In addition, pollutants (Pb, Zn, Cu, pesticides, PAHs and alkylphenols) originated from human activities and carried with stormwater runoff (Kovács et al. 2006) often caused ecological problems in the surface and subsurface water bodies of Pécs.

The main goal of our study is to prepare an *urban geomorphological hazard map* for Pécs, based on the impacts of torrential rainfalls focusing on the series of events from 29 May to 4 June 2010.

22.2 Study Area

The city Pécs is located in the Pécs Basin, Southwest Hungary (Fig. 22.1). The majority of the urban area belongs to the upper, urbanized, watershed of the Pécsi-víz Stream (Ronczyk and Lóczy 2006). Although completely channelized in the last two centuries, due to the diverse watershed topography, stormwater management, flood prevention and slope stabilization remain as problems. The headwaters of the Pécsi-víz, within the administrative borders of the city, are traditionally divided into 13 subcatchments (Buchberger 1994): eleven of them are on the steep, urbanized slopes of the Mecsek Hills, while the remaining two are found on the gently sloping Southern Baranya Hills, south of the Pécs Basin. The current study primarily focuses on the mountainous, northern part, the core area of urban development, and where most of the damages occurred during the heavy rainfalls in 2010.

22.3 Methods

The grid-based *Digital Elevation Model* (DEM) was used to analyze slope and relief conditions and to delineate watersheds. A second group of vector-based datasets is derived from the *cadastral maps* of urban geomorphological relevance: the location of retaining walls, storm sewers, sealed riverbeds, culverts etc. Land use and land cover data (LULC) were taken from the digital database of the European Environmental Agency developed in 2009 (EEA 2010). Daily total rainfall was recorded by the University of Pécs rain gage network at five locations in Pécs. For comparative purposes, additional precipitation data (Pogány and Nagyárpád automated rain gages) were also obtained from the Hungarian

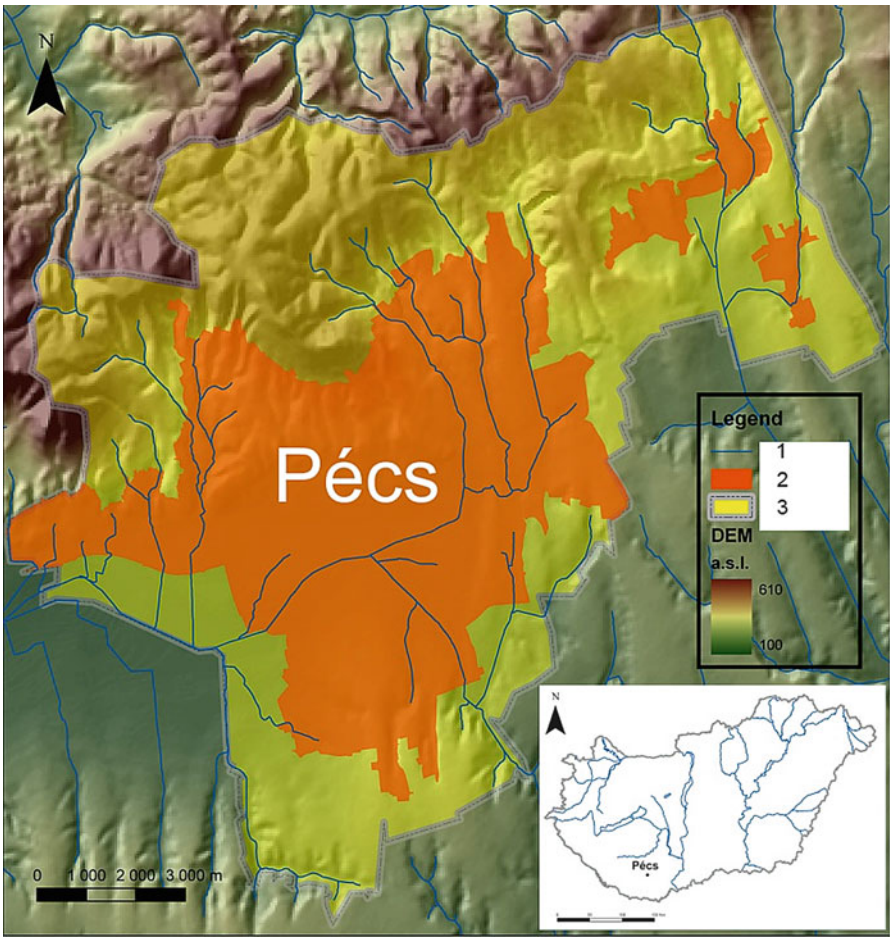

Fig. 22.1 Location and topographic setting of Pécs. *1*, watercourses; *2*, built-up area; *3*, administrative area

Meteorological Services (OMSz). Data on reported and recorded damages to slope-stabilizing and hydrologic structures used for disaster prevention were provided by the mayor's office of Pécs for the period of May and June 2010.

The datasets were analyzed in ArcGIS 9.3 software environment. The delineation of the individual subcatchments was carried out using ArcHydro, an ArcGIS hydrologic tool. Data were summarized in *analytical tables*, which were used for damage assessment. The spatial correlation between the damages triggered by extreme weather and the urban geomorphological character of the subcatchments were determined with overlay functions of ArcGIS 9.3.

22.4 Results and Discussion

22.4.1 Rainfall Characteristics of May and June 2010

The observed precipitation for the environs of Pécs in May 2010 considerably exceeded the long-term mean value. Extreme precipitation triggered by a Mediterranean cyclone (called Zsófia in Hungary) in mid-May 2010 induced the largest flood wave in 2010 and the second highest for the period 2001–2010 (see Chap. 1 by Bartholy and Pongrácz, this volume). This unusually long-lived cyclone transported air masses of extremely high humidity from above the Mediterranean Sea northwards, accompanied by continuous cloud formation and updrafts. One of the high-precipitation cores of the cyclone stayed over Southwest Hungary centered on the Mecsek Mountains, while a second maximum area was in the Bakony Mountains (cumulative precipitation above 250 mm between 15 and 18 May 2010).

Mean rainfall intensity remained low throughout the 4-day rainfall event, averaging a value of 0.367 mm in 10 min (Fig. 22.2), and, despite the high moisture contents of the atmosphere, few thunderstorms were reported. Total cumulative rainfall exceeded 150 mm in Pécs at four (and reached 202 mm at one) out of the five rain gages used for the present study (Table 22.1), showing a pronounced orographic effect (Fig. 22.3).

A second, also larger-than-average, Mediterranean cyclone (called Angéla in Hungary) between 29 May and 4 June once again brought heavy rains of typical return period of 10 years (Bozó et al. 2010) to the area (Table 22.1) – although smaller amounts than in the previous period. Due to the high antecedent soil moisture content, however, the second cyclone also triggered significant excess runoff and increased flow equally reflecting an orographic effect in distribution (total rainfall: 129–161 mm between 29 May and 4 June 2010 – Fig. 22.3).

22.4.2 Classification of Damages

Extreme weather phenomena significantly contribute to the increased rate of surface (and subsurface) geomorphic processes (Szabó 2010). In urban planning it is of foremost importance to reduce, or at least mitigate, the undesired impacts of geomorphological processes (Gyenizse and Ronczyk 2010). Despite considerable advances in urban planning and engineering, unmanaged urban challenges, rooted in the complex physical, social and economic environment of urban development, still exist. In most cases, human impact on the landscape is responsible for excess runoff. The emergent disharmonies need to be compensated by appropriate engineering structures: drainage ditches, canal systems, bridges, culverts, dikes, levees, retaining walls and sink fills which are meant to maintain a balance between the exogenic geomorphic processes and the man-made environment and to mitigate damage. Temporary stabilized sealed surfaces require continuous maintenance or subsequent

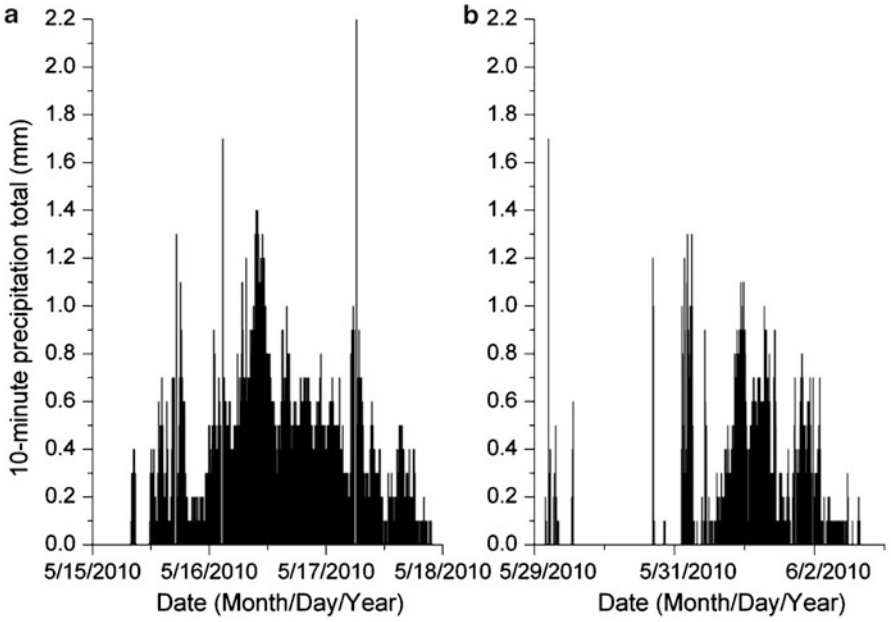

Fig. 22.2 10-min rainfall totals for the period of (**a**) 15–18 May and (**b**) 29 May–3 June observed at the rain gage of the Ifjúság Street campus, University of Pécs

Table 22.1 Daily precipitations in Pécs for the 15–18 May 2010 and the 29 May–4 June 2010 precipitation events

	Daily precipitation (mm)				
Rain gage	Tettye	Erdész street	Jegenyés street	Újhegy	Ifjúság street
15 May 2010	34	84	19.1	62	32.1
16 May 2010	92	89	83.5	91	94.6
17 May 2010	13	26	67.6	24	36.1
18 May 2010	2.9	3	4.9	5	2.5
Total	141.9	202	175.1	182	165.3
29 May 2010	1.6	5	3.7	1	6.7
30 May 2010	16	8	22.9	10	29.2
21 May 2010	50	63	72.7	59	68.7
1 June 2010	52.5	45	23.8	56	31.6
2 June 2010	4.7	27	0	5	0.6
3 June 2010	3	13	0	3	4.9
4 June 2010	3.2	0	5.9	3	0
Total	131	161	129	137	141.7

development and upgrading at the available level of technology and planning practice. In the present study we systematically refer geomorphological damages observed during the May and June extensive rainfalls into classes according to their spatial impact on the surface and subsurface (Table 22.2).

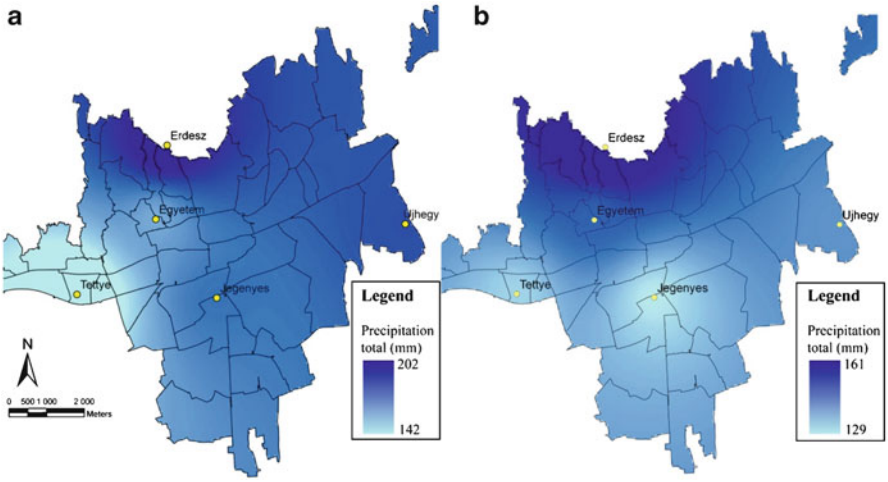

Fig. 22.3 Interpolated map of cumulative precipitation amounts in Pécs for 15–18 May 2010 (**a**) and 29 May–4 June, 2010 (**b**)

Table 22.2 Definitions of types of storm water-related damages in Pécs

	Description
Surface	
Bank erosion	Heavily undercut and eroded stream banks and ditches (both paved and unpaved)
Flooding/inundation	Coverage with surface water during excess runoff
Ponding	Surface water accumulation behind levees and dikes due to hindered drainage
Sediment accumulation	Deposition and accumulation of sediments and debris due to decreased velocity and energy of running water/floodwater
Pavement damage/ scouring	Roads/sidewalks/driveways made impassable through excessive destruction to their surfaces
Damage to bridges	Collapse of bridges or serious damage to the base
Subsurface	
Damage to retaining walls	Undercutting and collapse of retaining walls
Boils/temporary springs	Water upwelling due to excessive hydraulic pressure during floods, primarily along dikes
Collapse of underground structures	Collapse of cellars, scouring, collapse of tunnels with distant heating pipelines

22.4.3 Damages in Pécs in May and June 2010

The various kinds of damage reported from Pécs between 16 May and 5 June 2010, which required immediate actions, are undoubtedly associated with the observed extreme weather phenomena in this period. The majority of losses occurred in the high-elevation watersheds of the city of rugged terrain (Fig. 22.4). Only losses

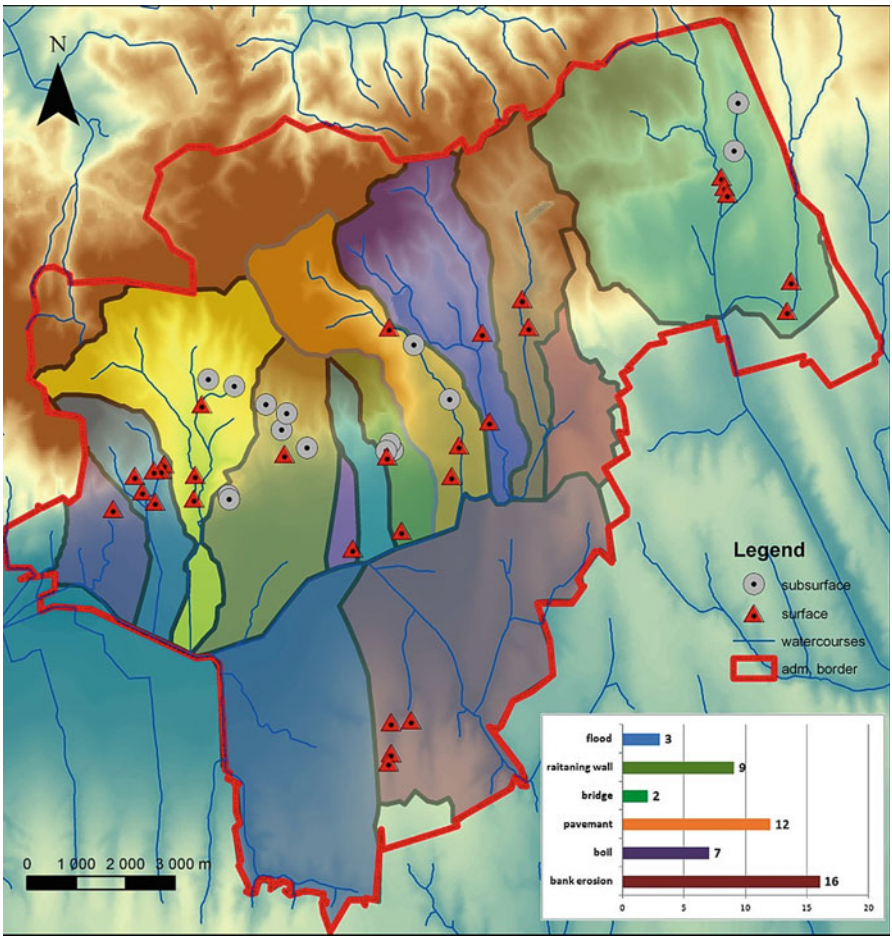

Fig. 22.4 Types and location of reported losses during the flood events of May and June 2010

officially classified as weather-related *vis major* disasters by the Pécs Holding Company (the predecessor of the current city management company, BIOKOM Ltd) were considered. The list includes 49 disasters, out of which nine events generated great economic losses and restoration costs, covered from the national *vis major* financial fund. Among the types of damages, *bank erosion* and the related severe erosion of *retaining walls* dominated (16 cases), with the consequence that local watercourses overflew their channels at multiple locations. The second most common type was the *erosion of paved and sealed surfaces* (12 cases). Several gravel and stone-paved and dirt roads became impassable (Fig. 22.5). Nine retaining walls were severely affected, getting close to complete collapse and requiring instantaneous restoration works. In seven cases new *upwellings* and *springs* were observed. In three cases significant *ponding* was reported, calling for intense pumping. According to field reports and

Fig. 22.5 Various types of flood impacts in Pécs and vicinity during 15–18 May. The photos (**a**–**c**) were taken in Pécs, while (**d**) was taken in Sásd, about 30 km to the north (Photos by L. Ronczyk)

records, two bridges became unusable. Even though peak discharges occurred during early morning hours, the most intense and devastating flash floods in the city fortunately did not demand a death toll.

Reviewing the analytical tables with geomorphological and land use parameters and data on the damages which arose during the discussed period (Tables 22.3 and 22.4), we found no significant correlations among the geomorphological parameters, land use data and the damages caused by the extreme weather events. The length of the human infrastructure is raised together with the ratio of the urban fabric percentage in land use, but this obvious relationship is not necessary to interpret. Further multivariate statistic is essential to employ to highlight the deeper coherence between the different types of database.

22.4.4 Flash Flood Impact

Flash floods, primarily due to poor infrastructural maintenance and improper engineering, caused the most severe problems within the city, especially in the Vince and Május 1 Streets. In the Vince Street in central Pécs, drainage-hindering factors (i.e. clogged drainage filters) had ever been present, but, with neglected

Table 22.3 Selected geomorphological parameters and types of damage in the subcatchments of Pécs

	Geomorphological parameters							Damage (instances)					
								Surface				Subsurface	
Subcatchment	Area (km^2)	Average elevation (m)	Maximum elevation (m)	Absolute relief (m)	Average slope	Average relief (100 m)	Max. relief (100 m)	Bank erosion	Flooding	Pavement souring	Bridge	Boil	Retaining wall
Disznóhizlalda stream	3.4	183	542	436	6.1	12	42	1	–	–	–	–	–
Patacs stream	4.6	257	577	463	7	17	46	**3**	–	**3**	–	–	–
Magyarürög stream	**14.1**	306	**610**	**496**	10.4	**21**	71	2	–	2	–	2	–
Új Füzes stream	9.6	201	576	462	5.8	12	53	1	–	–	–	2	**4**
Hunyadi út sewer	2	239	529	410	7	14	49	–	1	–	–	–	–
Új Tettye ditch	2.3	258	529	408	7.7	16	59	–	1	1	1	1	3
Lámpás stream	8.5	**335**	**610**	483	**10.7**	**21**	105	**3**	–	1	–	1	1
Meszes stream	11	282	482	336	8	17	70	1	–	–	1	–	–
Szabolcs stream	8.7	280	412	246	7.6	15	**110**	2	–	–	–	–	–
Vasas-Belvárad stream	55	289	454	293	5.9	12	97	**3**	–	1	1	**2**	1
Nagyárpád stream	30.6	171	226	106	3	6,4	34	–	1	**3**	–	–	–

Bold numbers indicate extreme values

Table 22.4 Land use types and selected infrastructural parameters in the subcatchments of Pécs

	Land use (%)					Human infrastructure length (m)					
Subcatchment	Forest	Agricultural	Urban	Industrial and commercial	Roads, railways	Retaining walls	Dike	Bridge (number)	Sewer	Stream/ ditch	Sealed stream
Disznóhizlalda stream	14	**44**	23	12	5	5,581	2,479	44	1,948	5,218	1,023
Patacs stream	40	24	24	6	4	1,537	5,393	48	3,391	6,630	1,129
Magyarürög stream	**54**	11	30	< 1	3	26,466	6,055	95	627	10,436	1,834
Új Füzes stream	10	17	**44**	17	8	**57,896**	9,636	36	**42,158**	7,923	**7,207**
Hunyadi út sewer	19	1	30	**35**	**10**	21,367	–	5	7,097	617	6
Új Tettye ditch	38	3	27	18	8	18,618	–	26	5,111	2,668	1,558
Lámpás stream	48	17	22	7	4	26,333	728	51	5,537	9,095	1,477
Meszes stream	53	8	18	6	3	10,374	–	**102**	5,377	14,492	–
Szabolcs stream	51	17	19	6	4	17,444	1,483	92	4,465	9,514	154
Vasas-Belvárad stream	49	33	10	2	2	8,153	34	41	1,926	**35,382**	2,101
Nagyárpád stream	15	49	15	14	4	6,855	**9,823**	65	6,639	21,051	2,930

Bold numbers indicate extreme values

Fig. 22.6 Damages in the Vince Street on 17 May 2010. (**a**) Clogged drainage filter at the northern end of the street; (**b**, **c**) damaged road surfaces; (**d**) accumulation of deposits at the southern end of the street and on Ágoston Square (Photos by L. Ronczyk)

maintenance, the severity of the May and June 2010 events triggered exceptionally intense flooding there. The undrained surface runoff heavily eroded and scoured the road surface and deposited a ca 50 cm deep layer of sediment at the lower and of the street on Ágoston Square (Fig. 22.6). These undesired processes necessitated the immediate restoration of the drainage passages in order to prevent death toll and excessive damages to houses.

Another example of urban flash floods triggered by fundamental land use change (coal mining activities) occurred in the eastern part of the city, in Május 1 Street. Active mining affected the headwaters of the Meszes Stream, which flows along Május 1 Street. A dike was built along the street with a road on top. Here a culvert of 100-cm diameter conveys the water underneath the dike. By 15 May, 2010, the culvert completely clogged up with debris;, various communal waste and tree branches and a hydraulic head of 20 m formed behind the dike. The high hydraulic head unplugged the culvert and allowed water flow through. Ca half million m^3 water inundated Május 1 Street causing losses around two million Euros. The water damaged houses and, pedestrian bridges, overtopped several cars, destroyed retaining walls and seven properties became inaccessible. The street itself became impassable for any vehicle, including fire trucks and ambulance cars (Fig. 22.7).

Fig. 22.7 Damages in Május 1 Street on 17 May 2010

22.5 Conclusions

The current study points out the need for systematic data collection and data exploration to highlight major urban geomorphological impacts of torrential rainfalls. We identified topographic, land use and infrastructural factors which may play a crucial role in damage-related urban geomorphology. Inappropriate maintenance of infrastructure could be one of the core components of deleterious hydrologic and geomorphic processes. To avoid, or at least mitigate, losses, new urban design techniques inevitably need to be introduced, while, at the same time, city authorities should map stream reaches and urban watersheds to locate potential risk. A complex

mapping would require a profound GIS-based analysis of factors contributing to excess runoff and flooding and responsible for infrastructural losses.

One way to reduce or mitigate urban excess runoff would be the widespread application of sustainable *stormwater management* approaches: the introduction and maintenance of *soft engineering* solutions conformable with natural drainage systems and processes. Such facilities would use permeable surfaces, including soil and vegetation, to filter, absorb, and moderate runoff. Such *low-impact development* (LID) techniques would also reduce pollution of watercourses and localized flooding as well as providing amenity and biodiversity benefits (Hinman 2005). Green roofs, bioretention swales, and permeable pavements are the most common techniques of controlling stormwater in urban areas.

The prevention of the negative impacts associated with excess stormwater involves complex tasks for urban development planners. On the long run, the incorporation of stormwater management into the urban hydrologic master plan could be highly beneficial for Pécs and many other municipalities. This way localized flooding could be avoided or mitigated. Achieving increased accuracy of rainfall-runoff models, urban flood guidance systems will acquire a more solid scientific foundation.

Acknowledgements Research was funded by the "TÁMOP 4.2.1.B-10/2/KONV-2010-0002" Project (Developing Competitiveness of Universities in the South Transdanubian Region). Authors are indebted to the BIOKOM Ltd, Pécs, and Pécs Municipality for providing data.

References

Bozó L, Horváth Á, Zsikla Á, Hadvári M, Kovács A (2010) Szélsőséges meteorológiai helyzetek 2010 május-júniusban (Extreme meteorological situations in May and June, 2010). "Klíma-21" füzetek 63:7–15 (in Hungarian)

Buchberger (1994) Pécs város vízkárelhárítás (Hydrologic masterplan of Pécs). Manuscript report, Buchberger Mérnöki Iroda Kft., Pécs, 111 p (in Hungarian)

Czigány S, Pirkhoffer E, Nagyváradi L, Szebényi A, Vass P, Geresdi I (2010) Potential areas of flood impoundment in human environments, Bükkösd Valley, Southwest-Hungary. Géomorphol Relief Process Environ 3:301–310

Douglas I (2005) Urban geomorphology. In: Fookes PG, Lee EM, Milligan G (eds) Geomorphology for engineers. Whittles Publishing & CRC Press, Boca Raton, pp 757–781

EEA (2010) GMSE – mapping guide for European Urban Atlas. European Environmental Agency, Copenhagen, 36 p

Gamba P, Herold M (2009) Global mapping of human settlements. CRC Press, New York, 374 p

Gyenizse P, Ronczyk L (2010) A természeti környezet változásának térképezése Pécsen és környékén (Mapping of changes in the Physical Environment in Pécs and in its vicinity). In: Szilassi P, Henits L (eds) Tájváltozás értékelési módszerei a XXI. században. Szegedi Tudományegyetem TTK Természeti Földrajzi Tanszék, Szeged, (Földrajzi Tanulmányok V), pp 127–139 (in Hungarian)

Hinman C (2005) Low impact development – technical guidance manual for Puget Sound. Puget Sound Action Team, Washington State University, Olympia, http://www.psat.wa.gov/Publications/LID_tech_manual05/lid_index.htm

Kovács A, Ronczyk L, Czigány S (2006) The water quality of the Pécsi-víz, 1996–2005. Publ Inst Geogr Univ Tartu 101:128–137

Lóczy D, Gyenizse P (2010) Human impact on topography in an urbanized mining area: Pécs, Southwest-Hungary. Géomorphol Relief Process Environ 3:287–300

Ronczyk L, Lóczy D (2006) Alternative stormwater management in Pécs, Hungary. Publ Inst Geogr Univ Tartu 101:113–121

Szabó J (2010) Anthropogenic geomorphology: subject and system. In: Szabó J, Dávid L, Lóczy D (eds) Anthropogenic geomorphology. Springer, Dordrecht, pp 3–12

Part V
Conclusions

Chapter 23
Evaluation of Geomorphological Impact

Dénes Lóczy

With climate change, weather conditions will become even more important controls on the operation of geomorphic processes. In this respect extreme precipitation events are of great significance. According to the most recent definition (IPCC SREX 2012), a *climatic extreme* is 'the occurrence of a value of a weather or climate variable above (or below) a threshold value near the upper (or lower) ends of the range of the observed values of the variable'. The case studies also present examples of *compound events*, when precipitation events are clustered or combined with extreme values of other variables (e.g. extraordinary temperature and wind conditions). The precise interpretations and environmental impacts of climatic extremes, however, vary with climatic regions.

As it is cited by Mustafić and co-workers in this volume (Chap. 11), in Central Europe there is an ongoing *redistribution of precipitation* from summer/autumn to winter/spring. Extreme events in winter and spring are on the increase: 13% growth per decade as opposed to 8% of decrease per decade in the summer period (Zolina et al. 2008). For the geomorphic evolution of hillslopes, it means that in lack of tree foliage interception is reduced, snowmelt may induce soil saturation (or directly runoff), and on soils of lower water retention capacity runoff intensifies. Therefore, intensive spring downpours deriving from cyclonic intrusions are of enhanced erosive power.

On the other hand, ensemble modeling projects more intense *summer drought* for the entire twenty-first century in Slovenia, Slovakia, Hungary, and Romania, likely to accelerate towards the end of the century. An average 30% precipitation decrease in summer is estimated for the eastern Central European region (e.g. a−37 mm drop in summer precipitation for central and southern Macedonia – Jovanovski et al., Chap. 17). Summer drought will particularly hardly hit Romania (Bartholy, Pongrácz – Chap. 1) and involve intense convective showers of high erosivity.

D. Lóczy (✉)
Institute of Environmental Sciences, University of Pécs,
Ifjúság útja 6, 7624 Pécs, Hungary
e-mail: loczyd@gamma.ttk.pte.hu

D. Lóczy (ed.), *Geomorphological impacts of extreme weather: Case studies from central and eastern Europe*, Springer Geography, DOI 10.1007/978-94-007-6301-2_23,

Global climate change would not only be manifested in shifts of mean precipitation but in the increasing *frequency* and/or *intensity of* various climatic *extremes*, the manifestations of instabilities in climate during a transitional period (as pointed out, e.g. for northeastern Romania by Romanescu – Chap. 7). The mentioned special report of the Intergovernmental Panel on Climate Change on extreme weather phenomena (IPCC SREX 2012) predicts more warm days and more high-precipitation days for Central Europe. The extreme daily precipitations which are of once in 20 years return period now would have a return period of 10–15 years (between 2046 and 2065) and of 8–16 years (between 2081 and 2100). Although that is below the rate of temperature growth, compound events may lead to extreme consequences. The numbers of *very wet days* (*RR20*) generally tend to increase in the future, particularly in winter, even more significantly towards the end of the century (in Hungary, by 175%; Slovakia, 107%; Romania, 102%). The frequency of torrential rains, for instance, shows an undoubtedly rising trend for most of the territory of Bulgaria. A growing number of days with precipitations above 10% of the annual total are observed in Bulgaria for the period 1901–2004 with summer and autumn maxima (Nikolova et al. – Chap. 12). In the Carpathian (Middle Danubian) Basin, investigations (Pálfai 2012) have indicated that in the time series 1983–2012 as many as 21 out of 30 years proved to be extraordinary, either too dry or too wet, as evidenced by insurance costs related to material damage of natural origin.

The *thresholds of precipitation* amount which generate dangerous soil erosion and efficient geomorphic evolution differ with the regional environment. In Western Europe hourly intensities have been preferred: previously a critical intensity of 10 mm h^{-1} was identified for England, 6 mm h^{-1} for Germany, and 1 mm h^{-1} for Belgium (Morgan 2004). Analyses in Serbia pointed out that for flash floods it is 25 mm day^{-1} (Milanović 2006), whereas 30 mm day^{-1} has been regarded as a threshold for excessive erosion (Dragićević 2007). In Bulgaria, in the case of complete soil saturation, it is estimated to lie between 18 and 38 mm h^{-1} (Nikolova et al. – Chap. 12) and the number of days with precipitation above 20 mm (RR20) is growing in the Stara planina (Balkan Mountains). In Hungary, also assuming saturated soils, flash flood hazard is associated with 30 mm of daily rainfall (Lóczy et al. 2011). In Slovakia, up to 150 mm rainfall over an extensive area resulted in a 100-year flood on the Ondava River in June 2010 (Lehotský et al. – Chap. 3).

Thresholds are also established for efficient *sediment transport* of rivers. In Serbia, on the Nišava River, for instance, a change in the manner of suspended load transport is associated with the classes of runoff above the 20 L s^{-1} km^{-2}-specific runoff threshold (Mustafić et al. – Chap. 11).

The various *geomorphological impacts* of climate change, including those induced by the growing frequency (and perhaps also magnitude) of climatic extremes, are more and more intensively studied (e.g. McInnes et al. 2007). Some authors are concerned with *historical floods* and their return periods. The EM-DAT database includes 13 major floods in Bulgaria for 1900–2011. Eleven of them occurred between 2000 and 2009, 1.2 cases per year, a significant increase compared to the average number of 0.1 cases for the past 111 years (Nikolova et al. – Chap. 12). This was mainly due to the year 2005, which was extremely wet in

several countries of the Carpatho-Balkan-Dinaric region. Over the past decade in Romania, floods occurred in 2004, 2005, 2006, 2008, and 2010 – they have become a kind of 'norm' for hydrologists (Romanescu – Chap.7).

The events of the spring and summer (and in the lower Danube Basin in winter) of 2010 brought *flood hazard* into the fore again. The rainfall amounts in May were really extraordinary. In many localities of the Czech Republic, precipitations more than threefold surpassed the corresponding monthly means for 1961–2000 (Pánek et al. – Chap. 13), and resulting peak river flows corresponded to discharges of 50–100-year return period (Brázdil et al. 2012). In Southwest Hungary cumulative rainfall in May and June locally reached 300 mm. Compared to torrential thunderstorms, however, mean rainfall intensity remained relatively low, 0.33 mm h^{-1} (as described by Lóczy et al. (2011) and Czigány et al. – Chap. 5). As most of the precipitation was transported by southerly winds, Kiss et al. (Chap. 6) claim that the most abundant rainfall amounts were observed on watersheds opening to the south. On several rivers of North Hungary (e.g. Zagyva, Sajó, Hernád), record maximum flood levels were measured, while in the southwest the Drava River, the border river between Hungary and Croatia, the basin of which opens to the east, was spared from flooding. In Croatia 2010 was an extremely wet, very wet, or wet year for 99% of the territory. In addition to spring rainfall, the sudden snowmelt in late December 2009 and in the beginning of January 2010 also played a significant part in the formation of two major flood waves (ICPDR 2012; Biondić et al. – Chap. 9). In Slovenia destructive flash, lowland (riverine), and urban floods equally occurred. In the opinion of Komac and Zorn (Chap. 8), flood damage was aggravated by the fact the most of the urban residents were unaware of their exposure to flood risk. In Serbia too two major flood waves (in February and May) occurred with extreme suspended load concentrations (Mustafić et al. – Chap. 11). In the Nišava River – in the driest region of Serbia – 62% of the annual runoff was observed in 4 months of 2010, while suspended sediment transport was 2.1-fold higher than the average for the period of 50 years. Out of the total annual sediment transport, 90.7% was moved in the period from February to May. Complex sediment dynamics were usually intensified by the rapid alternation of dry and wet periods. Mustafić and co-workers (Chap. 11) prove a long-term *hysteresis effect* from the analysis of the relationship between mean monthly concentration of suspended load and specific runoff. On the Nišava River basin, peak discharge is usually followed by maximum suspended load transport with a certain time lag. In May 2010, however, heavy rainfall and high river flow overlapped, and maximum suspended load coincided with peak discharge.

Although the 2010 precipitation events affected huge areas, fortunately, it applies to all countries of the region that simultaneous floods on the trunk river and all the tributaries of a river system were not observed (see also Fig. 1 in the Introduction).

Authors often underline that flood hazard is not simply a function of precipitation amounts and intensity, but heavily depends on *landscape factors*. This makes flood hazard a truly geographical topic. Lehotský et al. (Chap. 3) claim that the

geomorphological responses of different river systems to high specific runoff and discharge are governed by a combination of 'global' laws and 'local' spatial and/or temporal factors (different settings and scales) – as evidenced by several chapters in this volume. The orographic effect is emphasized in the case of the Polish Carpathians (Gorczyca et al. – Chap. 2) and Bulgaria, where flood waves are often associated with orographic occlusion (Nikolova et al. – Chap. 12). In another case study Dragićević et al. (Chap. 10) describe the Kolubara River as 'ideal' for the generation of large-scale floods: it has a high watershed shape coefficient, high relief, orientation towards the northwest, where humid air masses arrive from, extensive surfaces cleared of forests, tributaries of torrential properties, rocks and soils with poor water retention capacity coupled with human activities.

Excess water inundations resulting from the groundwater table rising to the surface occur in spring months throughout the lowlands and broad valleys of the region. In addition to the immediate loss of yields or a complete devastation of winter wheat and other crops over hundreds of thousands of hectares, excess water may even modify the properties of *soils* of high quality and fertility (e.g. their infiltration capacity through siltation and compaction) (Gál, Farsang – Chap. 20). In turn, combined with hydrometeorological, geological, and topographical factors, soil properties are also of decisive importance for the formation of excess water patches. Groundwater flooding seems to have a 'memory': lands once affected will have a good chance to be subject to it again in the future. In hills and mountains soil saturation is an important component of riverine and *flash flood hazards* (Czigány et al. – Chap. 5).

Floods particularly accelerated *bank retreat* along sections where bank height is low and bank material has low resistance. (Kiss et al. revealed high values along the Hernád, Tisza, and Drava Rivers in Hungary – Chap. 6). In the case of high bluffs, undercutting and the removal of slump toes during floods resulted in *bank failure*. In Romania the highest impact on channel processes was observed during the 2005 floods: at Cosmeşti village on the Siret River, the concave bank was eroded in more than 50 m width, while at Piscu an accumulation strip of 100 m length emerged as new dry land (Romanescu – Chap. 7).

The vulnerability to floods is particularly high in urbanized areas. A single chapter is devoted to *urban floods* generated by climatic extremes: a case study on the southwestern Hungarian town of Pécs (Ronczyk, Czigány – Chap. 22), which has no river, but where local characteristics (e.g. an extensive network of cellars, steep lanes following the alignment of one-time watercourses) are also influential. The message is made clear: inappropriate maintenance of infrastructure could aggravate the impact of heavy rainfall and may lead to intensive geomorphic processes and severe damage. In May 2010 the undrained surface runoff heavily eroded and scoured road surfaces and deposited a ca 50 cm deep layer of sediment. In the same month similar kinds of damage have been reported from cities on major rivers like the Vistula (at Tarnobrzeg, Nowy Sącz, Wrocławek) and the Oder (Görlitz) and in December from the Sava (Šabac) and Drina (Gorazde) and many others.

Among the most common consequences of extreme rainfall events is intensified *soil erosion*. Its features (headwater channels, rills, gullies, hollow roads, gorges, minor alluvial fans, and sediment veneers) were studied by Veress and co-workers

(Chap. 19) in mountains of metamorphic rocks and a deep weathering mantle. They found that pre-existing gullies and hollow roads considerably incised (at a rate of 0.7 m in response to a rainfall event of 100 mm day^{-1} intensity) and alluvial fans expanded during the 2010 events. The dense network of forest roads has also accelerated erosion processes. With suitable lithological and vegetation conditions, even incipient badlands have emerged.

Mass movements constitute the other group of processes which are closely associated with extreme climatic events. Abundant water supply combined with high groundwater level and soils saturated in the preceding winter and spring brought about by both flooding and landsliding in the Carpathians and their foreland, where ca 20,000 landslides have been inventoried to date.

In the Polish Outer Carpathians, the wet summer of 2010 (from May to September) led to the activation of more than 2,000 *landslides*. In 2010 – as opposed to a previous major period of landsliding in 1997 (Kotarba 1997) – damage was mostly recorded in material goods, and no fatalities directly caused by landsliding were reported. Because the rate of motion was generally low (not more than some meters per day), local residents could be evacuated in time. Although 2,300 inventoried rapid *debris flows* and equally numerous avalanches model slopes in the High Tatra (Kotarba et al. – Chap. 14), in 2010 no debris flow occurred. *Threshold* precipitation amounts have also been identified for mass movements. In the summer of 2010 precipitation amounts were sufficiently large (in 5 days 220 mm in June and 200 mm in July), but mostly in the form of snow and rain which fell upon an almost continuous snow cover – particularly at higher elevations. That explains why rainfalls did not trigger debris flows. In other respects, however, the geomorphological impact of rainy weather cannot be ignored: it has significantly intensified *slope evolution* (e.g. gully and alluvial fan formation – Kijowska 2011). Debris flows in turn were triggered by the 41.4 mm rain lasting 1.5 h on 23 August 2011 (Kotarba et al. – Chap. 14).

Landslide hazard – as described in one of the case studies (Gorczyca et al. – Chap. 15) – is due to natural conditions (relative relief, lithology, tectonics, and hydrometeorological factors) usually conducive to mass movements, coupled with irrational developments at inappropriate foothill sites and other mistakes made by infrastructure planners.

In Tatra Massif rainfall thresholds necessary to trigger debris flows vary with landscape factors, including lithology and topography (Kotarba et al. – Chap. 14). Kotarba and co-workers claim that the debris flows which extend over the full length of the debris slope are triggered by rainfalls of 35–40 mm h^{-1} intensity of or at least 80–100 mm day^{-1} (10% probability) with instantaneous intensity of 1.3–1.7 mm min^{-1}. In the cryonival domain above the upper forest line at 1,290–2,390 m elevations of the High Tatra, shorter hillslope debris flows can follow 30 mm rainfall, while in the Western Tatra 20 mm of rainfall is sufficient. In Bulgaria the typical synoptic situation which can trigger gravel-sand debris flows is the invasion of cold air into a warm and unstable air mass in cyclones, with the precipitation threshold of 25–30 mm day^{-1} (Kenderova et al. – Chap. 18). The Bulgarian authors, however, do not forget to emphasize the influence of various landscape factors either.

During the period 15–25 May 2010, more than 150 landslides originated in the Outer Western Carpathians and their foredeep (Pánek et al. – Chap. 13) in a quite uniform spatial distribution. Also here precipitation was the main trigger, but in different amounts: four precipitation intervals (81–120, 121–160, 161–200, and 201–240 mm) involve 19, 15, 19, and 18% of all investigated landslides, respectively. On the other hand, 65% of all recorded landsliding took place in areas where May totals more than threefold exceeded the monthly mean for 1961–2000. The Girová Mountain translational rockslide of long runout (length: 1,150 m), reactivated in May 2010, stands out not only in the Czech Republic but for the entire Carpathians. It demonstrates that large-scale movements may also develop under favorable circumstances even in settings which are of low hazard viewed purely from a topographic aspect (slope angles: up to 20° and local relief: up to 200 m) (Pánek et al. – Chap. 13).

In the Curvature Carpathians of Romania, spring (rapid temperature rise and snowmelt) and summer are the seasons with stronger dynamics both for scarp regression and intensive toe accumulation (Micu et al. – Chap. 16). From the end of summer, lateral pressure ridges tend to be fixed and only temporary accumulations occur along the flow track. In 2010 maximum daily temperatures rose constantly from −0.2 to 18.9 °C between 18 and 21 February. Pulsating flow along the main track eroded valley sides and generated both first time failures and the reactivation of numerous shallow *earthslides* and *mudflows* in the oncoming period (March to April), when precipitation amounts were already below monthly averages. This observation raises similar time lag issues as in the case of precipitation and floods (see above: Mustafić et al. – Chap. 11). Also a dense network of linear drainage elements in the Tatra Mountains is accompanied with a network of numerous slides, sometimes in the form of turbid flow, i.e. transitional processes between stream flow and debris flow (Gorczyca et al. – Chap. 2).

The Republic of Macedonia is particularly interesting for landslides as it is the country of the highest average elevation (832 m) in the region. In January and February 2010, a long dry period was followed by heavy rainfalls, their impact also intensified by an abrupt temperature rise and rapid snowmelt. More than a 100 *movements of various types* were brought about (or renewed): landslides, earthfalls, rockfalls, topples, and debris avalanches (Jovanovski et al. – Chap. 17). The significance of the local environment (including human action) is particularly well discernible in the case of landslides in Macedonia and the Ukrainian Transcarpathians (Kovalchuk et al. – Chap. 4). Both freeze-thaw action and alternation of wet/dry spells can exaggerate the mechanical weathering of the great *variety of rocks*. Both in Macedonia and Bulgaria large amounts of coarse rock fragments are stored along mountain streams, liable to be mobilized by debris flows. It is increasingly recognized that check dams are unrewarding approaches of mitigation (Kenderova et al. – Chap. 18). In the broad flysch zone of the northern and northeastern section of the Carpathian arc, the interbedding of clays in sandstone sequences is often responsible for plastic flow (Gorczyca et al. – Chap. 15 and Kovalchuk et al. – Chap. 4).

The case studies of the book do not at all prove that all damage can be attributed to natural processes intensified by climate change. Societal impact, insufficient knowledge and awareness, as well as human negligence in planning, implementation, and maintenance may be equally important contributing factors of disasters (Visser and Petersen 2012). Recommendations for damage mitigation are included in most of the chapters. Nevertheless, the assessment of the predictable regional and local impacts of future climate change is a proper task for all geomorphologists. Examples like the landslide inventories in Poland, Slovakia, and Romania pave the road to *multihazard assessments* (Micu et al. 2010), comprehensive surveys of unified methodology for the entire eastern Central European region. In the future, in addition to strategies for climate change (also incorporating geomorphological impact), *maps of natural hazards* (like the one prepared by Dragićević et al. (2011) for Serbia) are badly needed in other countries too.

Although partly understandable under the conditions of the enduring economic crisis in Europe, it is not correct thinking by politicians and the authorities responsible for disaster prevention to focus attention and concentrate financial resources exclusively on avoiding immediate damage – let it originate from floods, droughts, or landslide events. Mitigation policies designed for a single interval between parliamentary elections seldom lead to real achievements. Recently enlivened research activities – of which the present volume only gives a selection – may provide better scientific foundations for longer-term and more coordinated action in water and hillslope management. The contributions from various countries clearly illustrate that proper management involves tasks which could be only fulfilled in international cooperation equally embracing research, preventive, and emergency action.

References

Brázdil R, Reznícková L, Havlícekand M, Ellender L (2012) Floods in the Czech Republic. In: Kundzewicz ZW (ed) Changes in flood risk in Europe. CRC Press, London, pp 178–198

Dragićević S (2007) Dominant processes of erosion in the Kolubara Basin. Jantar grupa, Beograd, 245 p

Dragićević S, Novković I, Carević I, Živković N, Tošić R (2011) Geohazard assessment in Eastern Serbia. Forum Geogr 10(1):10–19

ICPDR (2012) 2010 floods in the Danube river basin: brief overview of key events and lessons learned. International Commission for the Protection of the Danube River, Vienna, 20 p. http://www.icpdr.org/main/publications. Accessed on 15 Nov 2012

IPCC SREX (2012) Managing the risks of extreme events and disasters to advance climate change adaptation. Intergovernmental panel of climate change, special report. Cambridge University Press, Cambridge, UK/New York, 582 p

Kijowska M (2011) The role of downpours in transformation of slopes in the Polish Carpathian foothills. Studia Geomorphol Carpath Balc 45:69–87

Kotarba A (1997) Formation of high-mountain talus slopes related to debris-flow activity in the high Tatra Mountains. Permafr Periglac Process 8:191–204

Lóczy D, Czigány S, Pirkhoffer E (2011) Flash flood hazards. In: Kumarasamy M (ed) Studies on water management issues. InTech Publications, Rijeka, pp 27–52

McInnes R, Jakeways J, Fairbank H, Mathie E (eds) (2007) Landslides and climate change: challenges and solutions. Taylor & Francis, Abington/Oxfordshire, 514 p

Micu M, Sima M, Bălteanu D, Micu D, Dragotă C, Chendeş V (2010) A multi-hazard assessment in the Curvature Carpathians of Romania. In: Malet J-P, Glade T, Casagli N (eds) Mountain risks: bringing science to society. CERG Edition, Strasbourg, pp 11–18

Milanović A (2006) Hydrological forecast of maximal water level in Lepenica river basin and flood control measures. Bull Serbian Geogr Soc 86(1):47–54

Morgan RPC (2004) Soil erosion and conservation, 3rd edn. Wiley/Blackwell, Chichester/Oxford, 320 p

Pálfai I (2012) Vízháztartási szélsőségek a Kárpát-medencében (Extreme water budget in the Carpathian Basin). In: International conference "Environmental problems in the Carpathian Basin II", Pécs, 30 November 2012 (in Hungarian)

Visser H, Petersen AC (2012) Inferences on weather extremes and weather-related disasters: a review of statistical methods. Clim Past 8:265–286

Zolina O, Simmer C, Bachner S, Gulev S, Maechel H (2008) Seasonally dependent changes of precipitation extremes over Germany since 1950 from a very dense observational network. J Geophys Res 113:1–17

Index

D. Lóczy (ed.), *Geomorphological impacts of extreme weather: Case studies from central and eastern Europe*, Springer Geography, DOI 10.1007/978-94-007-6301-2,